The Sword in the Stone:

Lithic Raw Material Exploitation in the Middle Stone Age at Pinnacle Point Site 5-6, Southern Cape, South Africa

by

Kyle S. Brown

Thesis Presented for the Degree of
Doctor of Philosophy
Faculty of Science
University of Cape Town
November, 2011

Department of Archaeology
Dr. David Braun
Dr. Judith Sealy

The Sword in the Stone:

Lithic Raw Material Exploitation in the Middle Stone Age at Pinnacle Point Site 5-6, Southern Cape, South Africa

"Among environmental factors which may greatly affect the kinds of artifacts produced, the nature of the materials available to the artisan is of primary importance." (Goodman 1944)

"Change in raw material coincided with some changes in technology but alteration of the biome still has to be recognized." (Clark 1980:53)

by

Kyle S. Brown

Thesis Presented for the Degree of
Doctor of Philosophy
Faculty of Science
University of Cape Town
November, 2011

Department of Archaeology
Dr. David Braun
Dr. Judith Sealy

Abstract

Sites along the southernmost coast of Africa preserve the best known record of the behaviour of early modern humans. Until recently, there has been only one relatively well-described long-sequence site, Klasies River, which has been taken as the reference sequence for the MSA. The bulk of the excavations at Klasies were carried out in the 1960s. This thesis presents a description and analysis of the lithic artefacts from the recently excavated site of Pinnacle Point 5-6, Mossel Bay, from a sequence dating between ~50-85ka. PP5-6 has been excavated to the highest contemporary standards, enabling a more detailed analysis of the lithics than is possible for Klasies. Although the PP5-6 lithic sequence conforms with the overall trends of MSA artifact manufacture, a number of differences from other sites are identified here for the first time - a significant step towards understanding behavioral variability and complexity among early modern humans.

The increased use of fine-grained raw materials at Pinnacle Point Site 5-6 (PP5-6) and other stratified coastal southern African Middle Stone Age (MSA) sites is contemporary with the widespread appearance of material culture often cited as evidence for the early expression of behavioral modernity in southern Africa. The observed patterning in raw material use (typically silcrete and quartzite), which also corresponds with a period of extreme climate instability, has led to differing interpretations of the behavioral complexity of raw material selection in the MSA.

The PP5-6 assemblage is unique in that it is well-dated and is currently the only coastal MSA site that has a complementary stable carbon and oxygen isotopic record and coastline model that provides detailed local paleoenvironmental context. The methodology for this study includes a survey of raw materials in the Mossel Bay region and the formulation and testing of a new model that predicts how paleoenvironmental change may have affected raw material availability and technological organization at Pinnacle Point. The PP5-6 assemblage is described in detail and then a focused technological analysis examines raw material procurement patterns, lithic heat treatment, and aspects of raw material economy for the predominant stone materials used in the assemblage.

The results of this dissertation demonstrate that there are consistent technological differences in patterns of procurement, preparation, debitage size, and conservation

between silcrete and quartzite lithics at PP5-6 that establishes a record of complexity in raw material use well in advance of the proliferation of fine-grained raw materials and formal tool production commonly observed at MSA sites between c. 60-75ka. The technological variability at PP5-6 is partially correlated with changes in the paleoenvironment, but tool production may be viewed as a parallel strategy where the choice in material selection considered the costs and functional advantages of each raw material balanced by the opportunities or constraints imposed by the dynamic paleolandscape. Heat treatment of silcrete has been demonstrated in this thesis to occur early in the PP5-6 sequence at approximately 85ka. Fire-assisted engineering of materials is a technological innovation that signals an elevated ability for advanced planning and supports an increasingly early origin for technological complexity in the MSA of southern Africa.

Acknowledgments

I would like to thank my supervisors, David Braun and Judith Sealy, who put a lot of trust in my ability to make progress while spending most of my time working away from UCT in Mossel Bay. I could not have finished without their guidance, encouragement and advice. I also appreciate the very helpful comments and insight provided by the external examiners. This dissertation was immeasurably improved by their suggestions.

I would also like to acknowledge the support of the Institute for Human Origins at Arizona State University during the four years that I was living and conducting research in Mossel Bay. The intellectual interaction with SACP4 project members and other visiting scientists during field seasons stimulated many of the ideas presented in this dissertation. In particular I would like to thank the personal and professional guidance of Curtis Marean, a friend and mentor who gave me the opportunity to direct excavations at PP5-6 and the freedom to study the Pinnacle Point collections. A special thanks to Zenobia Jacobs for permission to use unpublished OSL ages, and to Erich Fisher and Mira Bar-Matthews for leading the research efforts that provided most of the environmental context for the research presented here.

The MAPCRM team at the Dias Museum, headed by Betina du Plessis, deserves a lot of credit for making sure that the collections are always well managed and ready for analysis. Lwando Magxidolo meticulously organized the PP5-6 lithics in preparation for this study. Benjamin Schoville, Simen Oestmo, Jocelyn Bernatchez, and Amy Rector assisted in raw material collection and heat treatment experiments.

Finally, I would like to express my deepest appreciation to my family for their encouragement and support, and particularly to my wife Kathy, who patiently shouldered the load during my physical and often mental absence from family responsibilities while conducting research and writing.

Table of Contents

List of Tables

List of Figures

Note: Crevice Cave carbon isotope curve and satellite imagery in location maps used by permission from the SACP4 project. All other figures, tables and photographic images were produced by the author

1.0 Introduction

Many southern African Middle Stone Age (MSA) lithic assemblages exhibit traits that were once considered to be unique to the European Upper Paleolithic. These features include the regular use of blade technology (McBrearty and Brooks 2000), the refinement of bifacial technology (Brooks et al. 2006), the production of standardized and specialized tool types (Mellars 1989), complex hafting technology (Wadley et al. 2009), bone tools (Brooks el al. 1995; Henshilwood et al. 2001a; Yellen et al. 1995), lithic heat treatment (Brown et al. 2009), and more complex use of raw materials selected for tool production (Kuhn 2004; Féblot-Augustins 1997). These and other features, including regular ochre use (Watts 2002), ornamentation (Henshilwood et al. 2004) and early exploitation of marine resources (Marean et al. 2007), are frequently cited as evidence for the early appearance of modern human behavior or cognition in southern Africa.

Paleoanthropological research has now moved beyond the "revolution that wasn't" (McBrearty and Brooks 2000), the traditional view that behavioral modernity originated in Europe around 40,000 years ago (ka). Overwhelming evidence from Africa has fueled a consensus view that some so-called indicators of behavioral modernity are found at least sporadically across coastal southern Africa during the MSA (Klein 2008; Marean and Assefa 2005) and as early as 164ka at Pinnacle Point (Marean et al. 2007). The current challenge is to develop the context to explain early expressions of so-called modernity and behavioral variability as adaptive strategies that express human uniqueness (Shea 2011).

Intermittently during the MSA, early modern humans appear to have invested in the production of technologies with derived features not found in Eurasia until some 30,000 to 40,000 years later. In combination with these new developments, it seems likely that EMH tool makers would have also invested in the selection of raw materials that would satisfy the requirements of more specialized or complex technology. Between ~72 and 79ka, the lithic sequence from Pinnacle Point Site 5-6 (PP5-6), a recently excavated and well-stratified MSA site in the southern Cape of South Africa (Figs. 1-2), shows a transition from quartzite to silcrete as the predominant raw material used for stone tool production. A similar shift in raw material patterning has been observed at other coastal southern African MSA sites within a similar time interval, and is usually

associated with the production of so-called advanced or modern appearing Howiesons Poort (HP) backed blades and Still Bay (SB) bifaces (Henshilwood 2008).

No consensus exists on whether the raw material pattern observed from coastal MSA sites results from the deliberate human selection of lithic raw materials for their physical properties or from changes in availability (Minichillo 2006). Researchers have proposed that the shift in raw material use may be associated with climate-induced changes in human mobility (Ambrose and Lorenz 1990; McCall 2006), reciprocal exchange (H.J. Deacon 1989; Wurz 1999), and functional demands imposed by adaptive technology (Mackay 2008a). These models have been difficult to test because they are based on lithic assemblages that are poorly or incompletely dated and are difficult to directly link to a paleoclimate record (Chase 2010).

PP5-6 is unique in that it has been carefully excavated, extensively sampled for optically stimulated luminescence (OSL) dating, and is currently the only site in southern Africa that has a complementary local terrestrial isotopic climate record (Bar-Matthews et al. 2010) and coastline model (Fisher et al. 2010) to provide paleoenvironmental context for examining technological variability in the PP5-6 sequence. The lithic assemblage at PP5-6 is also ideal for studying what is referred to here as the Cape MSA Raw Material Pattern (CMRMP) (Ch. 3) because the shift in stone use is pronounced when compared to other coastal sites. The change in raw material use at PP5-6 occurs at approximately the same time that widespread evidence exists for symbolic behavior (Henshilwood et al. 2001a) and ability for abstract planning (Brown et al. 2009).

The goal of this research approach is to investigate a link between the dynamic PP5-6 raw material and lithic sequence and the local paleoenvironmental record. This is done in order to assess the relative contributions of deliberate raw material selective behavior for functional reasons on the one hand and paleoenvironmental landscape changes that may have dictated raw material availability on the other hand. Existing models are reviewed and a new model is proposed and evaluated. The methodology presented here includes: 1) background on raw material selection focused on the southern African record; 2) review of existing raw material models and proposal of the Site Context Model; 3) field surveys and literature review to generate testable hypotheses for source locations of major PP5-6 raw material types; 4) a high-resolution spatial analysis of raw material patterning throughout the PP5-6 sequence; 5) a descriptive analysis of the PP5-6 lithic sequence; 6) a study of raw material preparation and silcrete heat treatment to identify some of the hidden costs of material selection; and 7) a technological analysis

aimed at identifying differences in the way that stone materials were flaked across raw material categories.

The results of the analysis demonstrate that between 90-48ka quantifiable differences exist in how raw materials were selected, prepared, and flaked through the 11 meter PP5-6 stratigraphic sequence analyzed in this dissertation. The shift in raw material use at PP5-6 coincides with perceptible changes in local environment and coastline, and it is contemporary with an early appearance at PP5-6 of backed blade tools in the MSA archaeological record. The exaggerated raw material patterning at PP5-6 may be associated with three primary variables: 1) distance to coastline, 2) changing landscape and vegetation, and 3) preferential selection of materials for their mechanical properties. The raw material pattern—with respect to the stone types exploited (predominantly quartzite and silcrete)—can be viewed in terms of a flexible dual strategy that varied according to the site's position with respect to the coastline and its environmental context. The apparent static nature of the earlier MSA may actually be the result of occupation gaps and limited sampling of the diversity of possible site contexts rather than the limited cognitive ability of early MSA tool makers.

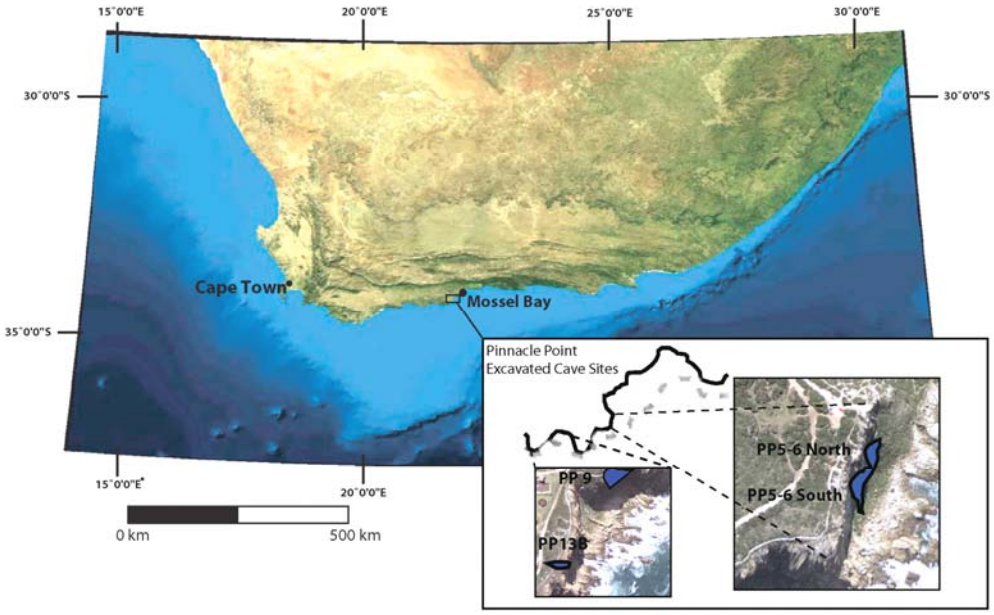

Figure 1. Location of Pinnacle Point and PP5-6

Figure 2. PP5-6 view north from present coastline

2.0 Literature Review

This dissertation is directed at understanding the role of lithic raw material selection within broader patterns of technological change observed in the Middle Stone Age at PP5-6 and other sites in the southern Cape. Raw material selection has figured prominently in studies of hominid technological variability in Africa where there is a greater diversity of stone materials available for flaking in comparison to Western Europe (Clark 1980). Intra-assemblage changes in lithic raw materials have been hypothesized to co-vary with mobility (Ambrose and Lorenz 1990), procurement patterns (Kuhn 2004), or changes in demography (Clark 1980). It has also been argued that intra-assemblage variability in proportions of raw materials used for flaking represents longer duration of site occupation (Noll 2000). The consensus view that early hominid raw material selective ability was limited to stone that was immediately available on the landscape has been challenged in recent years by findings that suggest Oldowan hominids had the capacity to select and transport raw materials up to 10km away (Stout et al. 2005, Noll 2000, Braun et al. 2009). The term "raw material" used in this dissertation refers to all material collected and used by ancient hominins to make stone artefacts and is not intended to convey information about the level of heat treatment associated with the rock.

The following literature review summarizes recent models developed to explain why past technologies changed in correspondence with variations in the behavioral and environmental context. These models are usually based on a body of theory developed through ethnographic observation (Shott 1986), and are typically employed to explain patterns of technological change identified in the archaeological record (Kelly 1992). This review is not exhaustive but is meant to provide a theoretical background for the approach taken in this study in order to understand variability in lithic raw material use at PP5-6.

Many lithic studies have sought to explain technological variability and raw material use in consideration of the mobility and settlement patterns of prehistoric hunter gatherers (Kelly 1988; Henry 1989; Bamforth 1990, Roth and Dibble 1998; Kuhn 1994) The theoretical foundation for most of this research can be traced to Binford's comparative models on settlement patterns and material culture (Jeske 1996). In particular Binford set up a series of heuristic dichotomies for conceptualizing a range of different technological strategies to cope with problems presented by the environment and the distribution of subsistence resources. Binford's observations are worth

summarizing because they still form a common thread in efforts to understand prehistoric technological adaptations.

Binford (1977) outlined some preliminary expectations for the technological composition of archaeological assemblages based on his ethnographic observations of gear that Nunamiut hunters transported on trips. Binford (1977) argued that Nunamiut have technology that is "highly organized curatorially" (p.34). His observations documented that tools transported on the trips very seldom failed to return to the residential camp, even when they were broken during the journey. The tools that didn't return were either purposefully cached or unintentionally dropped. The gear that remained at the task-specific sites tended to reflect the byproducts of the work. This conclusion led Binford to make predictions on the technological composition of archaeological assemblages based on the hypothetical extremes of 'curated' versus 'non-curated' (or 'expedient') technology but without regard to procurement strategy.

Binford (1979) made a distinction between what he called *household* and *personal* gear, classified as objects made for an anticipated or scheduled task, and *situational* gear, which may be made or used by unanticipated necessity. The distinction is important for two reasons. First, household/personal items are likely to be made from materials that are deliberately selected for that purpose, meaning raw material with properties suited for the task. He also argued that personal gear was more likely to be curated. By contrast, situational items were more likely to have been made expediently from any material on hand; either that which was immediately available on the landscape or materials that may have been cached for another purpose altogether. Second, the distinction is important because it explains to Binford how intra-assemblage variation might be partially explained by convergence. Planned tools and those that are made more expediently may be used for the same purposes but have very different production paths.

Binford's fieldwork led him to develop the idea that raw material procurement was in almost all cases embedded in other scheduled subsistence activities. He argued that raw material acquisition would rarely, if ever, occur as logistical forays devoted primarily to collecting stone.

> My experience with the Eskimo, and a limited but enlightening experience with the Alyawara of the central desert of Australia, has convinced me that variability in the proportions of raw materials found at a given site is primarily a function of the scale of the habitat which was exploited from the site location, possibly coupled with a founder effect resulting from discard on the site of items which had been manufactured previously at some other location. (Binford 1979:7)

Binford (1979) stated that in the case of the Nunamiut, raw materials would always be collected when encountered. Surplus materials would be cached for later use at locations that had a high likelihood of being visited again during regularly scheduled activities.

In another classic publication, Binford (1980) outlined endpoints in a hypothetical continuum of mobility patterns typified by foragers versus collectors, and described the probable archaeological signatures of each strategy. Foragers gather food daily in an encounter based strategy and return to a residential base at the end of day. There is typically no food storage. The number of residential moves is determined by resource distribution and group size. The archaeological visibility of residential mobility would depend on the group size and duration of stay and any seasonal component of the camps. *Localities*, which are sites of resource extraction, should have low densities of archaeological residues.

Collectors on the other hand, may also exhibit residential mobility but they typically store food and obtain resources through special trips. These logistical trips occur when the group is located away from one or more critical resources and it is not practical or possible to move the group from one place to another. Food and other resources obtained through logistic trips were known commodities and were often predictable on the landscape and seasonally abundant. Binford (1980) argued that in situations where seasonality temporally restricts access to food resources, hunter gatherers would have a need for obtaining a greater number of critical resources in a shorter period of time. Scheduling conflicts should lead to greater logistical mobility. Archaeological residues may show the reuse resource extraction sites and may reflect similar or repetitive site function over many visits through time.

Binford's models were not always well received (Gould 1985; Sackett 1986; Gould and Yellen 1991), but his publications did promote debate that is still relevant to the modeling of raw material acquisition. Gould and Saggers (1985) were critical of what they considered to be Binford's inflexible embedded procurement strategy model, and they noted that some of Gould's own ethnographic observations, as well as archaeological site patterning, provided clear evidence for the direct procurement of raw materials. At James Creek East, non-local materials were predominantly selected for adze production, and actualistic experiments demonstrated these materials to be superior for woodworking over locally available stone (Gould and Saggers 1985). At James Creek West, the local materials were better suited for specific purposes, and their preferential selection was reflected in that sequence. They attempted to demonstrate that factors

beyond an encounter-based strategy could explain raw material preference at many sites although they agreed with Binford that many examples of so-called “exotic” stone materials could be explained by collection during other activities.

Research on the organization of technological systems stemming from Binford’s synthesis of ethnographic settlement patterns and associated material cultural has advanced in a number of directions. Some of the more influential studies described below have focused on technological optimization (Bleed 1986), time stress (Torrence 1983) or risk amelioration (Torrence 1989; Bousman 1993; Bamforth and Bleed 1997). Other studies have emphasized technology strategies associated with settlement systems (Kuhn 1991, 2004) or have expanded on Binford’s curated and expedient technologies (Nelson 1991; Bousman 1993). Most have attempted to take a cost/benefit or risk avoidance approach to understanding why prehistoric technological strategies changed, although understanding the evolutionary implications of technological change in the strict Darwinian terms of the fitness of the individual is extremely complex (Bamforth and Bleed 1997).

Torrence (1983) hypothesized that subsistence technology should vary according to the “severity and character of time stress” (p. 12). She argued that technological variability should be influenced by the scheduling of tool making considered with respect to the overall requirements for subsistence activities. She cited Binford’s embedded procurement as the prime example where time scheduled for tool making and maintenance is built into other activities. Diversity and complexity in the tool assemblage should be inversely correlated with the time available to accomplish tasks because specialized tools perform tasks more efficiently. Complex or modular tools may represent forward investment in the production of compound or modular tools so that replacement parts are quickly substituted when time is at a minimum.

Torrence (1983) then ranked time stress encountered by ethnographic hunter gatherers according to latitude and seasonality as a proxy for time stress, using ethnographic data from Oswalt (1973, 1976). Torrence found significant linear relationships in tool diversity and complexity (both in number of components per tool, and per toolkit) with increasing latitude and argued that time stress and conflicts in scheduling in the higher latitudes, with more seasonal availability of resources, was at least partially responsible for the level of investment in technology reflected by the ethnographic data.

Bleed (1986) applied principles of modern engineering to predict the most efficient or optimal design of ethnographic hunting weapons that would be expected within the framework of Binford's (1979) forager versus collector dichotomy. Bleed defines efficiency as the output of a technology divided by its cost. He makes a distinction between tools that are *reliable* and those that are *maintainable*. Reliable tools are designed to always work when they are needed. Maintainable tools are designed to be easily repaired or retooled for a different use.

Reliable systems tend to be overbuilt to avoid failure and function below their maximum capacity. They have redundant components and typically have built in backup systems. Maintenance is scheduled in advance of use and is done by specialists with a tool kit that is designed to be able to handle all situations that arise during repair. Collectors are more likely to adopt reliable technology because they have scheduled resource acquisition where food needs to be acquired in bulk during narrow and predictable time windows and thus there is also predictable downtime for scheduling maintenance.

Bleed (1986), citing Binford's data, argued that Nunamiut hunters use more reliable extractive technological practices particularly in terms of maintenance where preparation occurs well in advance of hunting. There are periods of more intensive gear preparation activities immediately prior to hunts. The Nunamiut carry multiple rifles for their hunting which is scheduled during the caribou run. The extra bulk of this redundant technology is offset by transportation technology which is presumably subjected to the same rigorous maintenance. Repair kits tend to incorporate elements for a wide range of probabilities. Similarly, Eskimo seal hunters have harpoons that are overbuilt and designed to always function when they are needed.

Maintainable systems are simpler in design and construction than reliable systems and typically incorporate fewer parts (Bleed 1986). If one part fails then the whole system fails. The repair kit incorporates spares for parts that might be expected to fail. The repair kit is more specialized and includes modular replacement parts. Maintainable systems may still work even when compromised and can easily be adapted for another unanticipated use. Maintainable systems are repaired by the user as they break and not typically during scheduled times.

Bleed (1986) proposed that the ethnographic! Kung and Yanamano, groups considered to be foragers, had technology that fit the maintainable design model. The hunting kits from both groups are simple and lightweight. They include both hunting

technology and repair kits that include modular parts. There is no redundancy in design. The Yanomano have some specialized tips but arrows need to be repaired after each shot to be used again. Bleed (1986) proposed then that the scheduling of tool use and the cost of failure are the best means for evaluating the efficiency in design of hunting technology. In some situations, design elements of both reliability and maintainability may be incorporated into a single system but reliable systems are typically very costly to make and transport. Bleed argues that reliability is most important when the cost of failure is high. Maintainable tools are less costly to manufacture and transport and may be more appropriate when failure does not carry a significant cost. Bleed cautions that not all higher latitude hunting systems would be considered reliable. The Central Eskimo kit is very similar to those of the !Kung and Yanamano, and is designed for spontaneous hunting opportunities. Therefore cultural tradition or latitude change (*cf.* Torrence 1983) cannot necessarily be used to predict what design strategy may have been adopted in the past. Instead Bleed argues that technological variables were altered to reach an "optimal solution to environmental problems" (p.745).

In contrast to Bleed (1986), Torrence (1989) made the case for treating reliability and maintainability as separate variables rather than as a continuum, and argued that the choice of technological strategy has less to do with human mobility and should be more closely associated with frequency of tool use and the mobility and temporal and spatial availability of prey. When the risk of failure is high, hunter gatherers will invest in technology and will have a greater diversity of specialized tools. Hunter gatherers with broad diet breadths are under less stress as they typically have plant food options and show less investment in specialized tools. Torrence argued that plant gathering tools are least complex, and technology for mobile prey is most complex. She noted that some of the most complex tools are what Oswalt (1973) defined as untended facilities, which are technologies for trapping or disabling prey that may have limited archaeological visibility. Wadley (2010), however, has made a case, based on faunal assemblages from the HP and post-HP MSA levels at Sibudu Cave (Clark and Plug 2008), that the use of snares for smaller bodied animals should not be ruled out in archaeological contexts.

Torrence (1989) observed in discussing technological change, that tool complexity is not a linear trend in time. She cites a number of examples where more recent Stone Age assemblages show replacement of formal tool assemblages by what might be considered expedient technologies made from low quality raw materials. She argues that the investment in technology is conditioned by risk and the severity of loss

which in turn may be assessed by looking at the abundance of alternative resources, typically stationary plant foods. Risk arises when there is dependence on mobile prey which may only be seasonally available. Some tools are better at minimizing resource variation in space and others are better for coping with temporal variability.

In terms of raw material selection, Torrence argued that hunter gatherers would have chosen the least costly raw materials suitable for the intended task. For example, maintainable technologies may require stone that is more amenable to tool recycling. She argued against the influence of raw material availability on raw material selection and also cautions against considering raw material choice independent of tool use arguing for the technological system as a whole as being a solution to a problem.

Ugan et al. (2003) proposed a technological investment model that treats intensification of technology as a series of decisions related to artifact use and how additional time and energy expended on technology affects searching and handling times for food resources. They caution that in decision making, the costs associated with the investment in technology are as important to consider as the realized benefits. They note that at some point, there are diminishing returns for continued investment in a technology. The assumption of their model is that the goal of foraging is to maximize the return rate of food resources in the most efficient way possible.

They argued that there is a critical balance between search and handling times for procuring food resources, and the time spent on improving technology, which Ugan et al. suggest are mutually exclusive activities. How is this balance achieved? They use tangent lines on a gain function based on manufacture time (x-axis) and energy yield from foraging (y-axis) to predict the point at which technological investment should occur. They argue that investment in technology should increase with the amount of time spent handling a resource. However, investment in technology comes at a cost of reducing the available search times. They argue that for mobile hunter gatherers the available foraging time is affected by an artifact's use life.

Ugan et al. (2003) proposed that technological investment can manifest in a number of ways. Design strategies can include decisions to invest in high quality material and construction so that the artifact lasts for a longer period of time, or the investment can take the form of relatively expedient construction with most of the time spent in the maintenance of the technology to extend its use life, or one can adopt a strategy of regularly replacing the artifact entirely. Ugan et al. noted that one of the most effective ways of reducing the cost in the investment of a technology is to embed these costs in

other activities. An example of this would be the collection of lithic raw materials while collecting food resources.

Bettinger et al. (2006) contend that the Ugan et al. (2003) model does not accurately explain how technological investment occurs. They cautioned against using a single gain curve in comparing rates of procurement functions between technologies that are not a direct replacement for one another. They proposed an alternative model of technological intensification that uses points and lines to connect between different curve functions of gain and manufacture time to predict when there should be a switch to more expensive technologies. They maintain that it would never make sense to invest in a technology that has a lower return rate than a cheaper technology and conversely one should continue to use a technology if a more expensive option does not have a higher return rate. Their model also predicts that in situations where diffusion or transmission of ideas introduces a new technology that significantly improves yield, existing technologies, if retained, should revert to cheaper and more simple forms.

Bousman (1993) sought to unite foraging theory with technological organization. He noted the lack of a uniform body of theory by archaeologists to explain why past technology changed and that patch and prey foraging models do not typically include the input of technology. He argued for the inclusion of technology in resource search and handling costs because most human foraging activities require tools. Returns are modeled as gains from food. He postulated that hunter gatherer diet breadth may increase if technology costs are minimized but may decrease with more expensive technologies.

Bousman (1993) argued that resource structure could be characterized by abundance, temporal availability, and dispersion of food resources. The predictability of food resources can be viewed in terms of *constancy* and *contingency*. Constancy is when resources are found in the same place at the same time year round. Contingency is when resources are predictable but seasonal. He uses the example of shellfish as having some degree of constancy. Seasonal fish runs have contingency. Some resources have low predictability due to low constancy and low contingency.

Bousman summarizes the expected technological patterns adopted by Binford's foragers versus collectors. His findings in this respect are similar to those of Bleed (1986). Foragers favor extending use life of extractive technology but work to reduce production and maintenance costs of associated repair tools. Foragers are time minimizers. Alternatively, collectors invest more time in extractive and repair tools. The collector pattern is tied to predictable resource structure. The forager pattern is associated

with wider but less predictable resources. Collector and forager patterns may alternate depending on changing resource structure and may coexist.

Risk (used by Bousman to describe both risk and uncertainty) is mainly assessed based on the outcome of food collection but the costs and benefits of technology can be manipulated in many different ways. Bousman (1993) outlines four primary strategies by which tool makers can increase their efficiency in terms of time allocation and handling costs:

1. Quicker production time by making expedient tools defined by minimal alteration or shaping. If the expedient strategy is planned, (in the sense of Nelson 1991) then Bousman argues it is necessary to have raw materials readily available.

2. Increased use life in the form of maintainable tools as defined by Bleed (1986). The use life of maintainable tools is extended by repair or resharpening. Tool maintenance reduces the cost of raw material acquisition.

3. Increased effectiveness through the strategy of producing reliable tools as outlined by Bleed (1986). Reliable tools may be useful when risk of failure is high and also perhaps when food resource package size is high and can be gained in bulk. Reliable tools are costly and require great amount of planning. Bousman postulates that southern African MSA HP segments may be some of the first reliable tools.

4. Increased production volume can result in more efficient tools. Efficient technologies increase the yield of tools from a given amount of raw material. This strategy decreases the cost of raw material acquisition.

Bousman (1993) suggests that the dichotomy between curated and expedient tools should be modified by subdividing curated technology into maintainable and reliable tools. He then expands the characteristics of curated tools to include tools planned in advance of use, and those that are; transported, maintained, flexible, reshaped, and tools that have been cached. Thus maintainable, reliable, and expedient technologies are three points on a hypothetical triangle and do not necessarily represent mutually exclusive strategies. He argues that tool use-life and curation rates may be greatly influenced by the type of stone used. Raw material availability is suggested to be a function of mobility range size and material exchange.

Risk and the potential cost of failure is the conceptual framework used by Bamforth and Bleed (1997) to balance the decisions made by hunter-gatherers with respect to raw material procurement, tool production, and tool use. The cost of failure can be high or low in each phase. They argue that technological strategies should be avoided

when the cost of failure is unacceptably high. High failure cost situations should thus select for solutions that minimize failure.

In practice, Bamforth and Bleed use technological diversity (number of tools) and number of parts in tools (technological complexity) to define how ethnographic groups managed risk. Similar to Torrence (1983) they argue, from a cross-cultural comparison of ethnographic hunter-gatherers, that risk and the cost of failure increases towards higher latitudes because of a lack of alternative sources of food. If alternative foods are taken into account when hunting mobile prey, then increasing latitude leads to greater toolkit diversity but not necessarily toolkit complexity.

Bamforth and Bleed (1997) highlight the role of raw material selection in technological organization. The raw material procurement stage is critical because it sets the range of possibilities for the later tool production and tool application. With respect to risk, if suitable stone is not available when needed, then scheduled tool production may not be possible and the intended activity may not happen. Special efforts to obtain stone may be costly and impinge upon other activities. These costs may be necessary in situations where high failure rates in production require access to substantial amounts of raw materials and greater efforts in procurement. Bamforth and Bleed (1997) argue that even the most complex flaked stone tools can be made by a skilled worker in about one hour once raw materials have been acquired.

Consideration of the role of raw material availability and distance to source is a common theme in modeling past technological variability (Goodyear 1989; Kuhn 1991; Andrefsky 1994). The concept of distance decay (see Blumenschine 2008 for a recent review of the distance-decay concept) holds that raw materials that come from farther away or that are more costly to obtain will be represented in lower frequencies than local materials (Renfrew 1969). Raw material imported from distant sources could be expected to show more evidence for conservation than local materials (Bamforth 1990; Neeley and Barton 1994), and items that are made on non-local raw materials might be found in smaller size (Ambrose 2002) and in more finished form than local raw materials (Geneste 1985).

Bamforth (1986) used two test cases to examine the relationship between curation, raw material availability and assemblage variation. In his first archaeological example taken from sites on the Santa Barbara, California coastline, he notes a change in prehistoric settlement patterns from foraging to collecting sometime around 1500BP. These changes in subsistence at the California sites were not associated with any

observed changes in proxy indicators of curation, although Bamforth notes that the special use sites where there was a lack of available raw materials, exhibit evidence for maintenance and recycling of hunting tools.

Bamforth's second archaeological test case was a Paleoindian lithic assemblage from Lubbock Lake, Texas, with tools made from both local and non-local lithic raw materials. Bamforth found significant differences between tools made from categorically different raw materials in the degree of retouch, discard patterns and tool use and interpreted data from the Texas assemblage to support curation based on proximity to sources and tool use rather than mobility. He concluded that raw material availability and intended tool use need to be considered as factors in discussing technological variability in addition to mobility and time stress.

Andrefsky (1994) also stressed the importance of raw material availability in determining the technological organization of a lithic assemblage. He hypothesized that it was the relative abundance and quality of the available lithic material—and not the settlement system—that determined the formal vs. informal nature of an archaeological assemblage. Andrefsky (1994) used three archaeological test cases in the western United States with examples of both sedentary and mobile site occupations to show that raw material availability and abundance was more important in determining assemblage composition than human mobility.

Andrefsky (1994) defined raw material quality in terms of flakeability, or the suitability of a stone to facilitate the production of formal tools that require skill and craftsmanship. Stone that meets these requirements is described as being more fine-grained. In situations where raw materials, regardless of quality, were locally abundant, then the majority of tools would be made on the local materials, although formal tools were more common with higher quality materials. In situations where local materials were scarce and of relatively low quality (more coarse-grained), then the majority of tools represented were imported as formal tools and the local inferior quality raw materials were used to make expedient tools. When raw materials were scarce, Andrefsky argued, that they would be conserved by producing and maintaining formal tools (on non-local stone) that could be resharpened and used again for a variety of tasks.

In his dissertation, J-M Geneste (1985) examined Middle Paleolithic assemblages from sites in the Perigord region of France. He conducted extensive refitting of Levallois debitage and constructed a technological typology that organized core reduction and tool production into four stages. These include; acquisition and retrieval of lithic materials

(Phase 0), initial core preparation (Phase 1), core exploitation (Phase 2), and tool retouch and resharpening (Phase 3). A slightly modified version of Geneste's techno-typology is used in this dissertation for presenting assemblage inventories from PP5-6 by stratigraphic sample. Geneste demonstrated that locally available raw materials tended to be represented by all phases of reduction whereas non-local raw materials were recovered as finished and discarded tools. He concluded that Mousterian technology incorporated a dual strategy of provisioning places with local raw materials which were used more expediently, and provisioning the individual with curated tools made from non-local raw materials.

Féblot-Augustins (1997) examined published evidence for the movement of lithic raw materials across the Europe in the late Middle and Upper Paleolithic periods. Movement of raw materials is described in terms of 'transfer distance' when the mode of movement is not clear (i.e. direct procurement or obtained through trade networks). She notes that the Late Middle Paleolithic western European transfer distances rarely exceed 100km, but eastern European late Middle Paleolithic transfer distances may occur as far as 200-300km. The western European transfers occur within geographically delimited basins, whereas the eastern Europe transfers usually cross geographic boundaries and may be the result of more seasonable mobility. The Middle Paleolithic sites show evidence for distance-decay in that the longer transfer distances are typically made with less volume of material and include more finished products as the transfer package.

The Upper Paleolithic pattern includes longer distance transport of raw materials with occurrences over the Middle Paleolithic 300km threshold being common. The Middle Paleolithic pattern of greater transfer distance seen in the Late Middle Paleolithic in eastern Europe continues in the Upper Paleolithic. Also, the pattern of the confinement of transfer distances within geographic entities in western Europe holds true. Féblot-Augustins (1997) hypothesizes that continuity observed between the MP and UP could be related to the environmental characteristics of the eastern or western European regions under study.

Upper Paleolithic sites provide good evidence for long distance transport of complete nodules but there is more variability as a whole across eastern and western Europe than the late Middle Paleolithic. Féblot-Augustins observed that the "pace of change" and variability in raw material use is the most notable difference in comparing Middle and Upper Paleolithic assemblage. In summarizing Upper Paleolithic raw material use, she noted that in the Aurignacian, a wider range of raw materials was

tolerated as long as the stone was amenable to the production of large blades. In the Gravettian, large quantities of unmodified fine-grained stone were transported for the production of thin and slender blades. The transportation of unreduced nodules is not consistent with the distance-decay seen in the later Middle Paleolithic. The Epigravettian is variable in tool production and in raw material requirements. The Magdalenian has Gravettian-like blades but raw material use is variable and more like the Aurignacian.

Féblot-Augustins postulated that synchronic change in raw material may result from trade in some cases, especially where other trade goods such as shell are lacking, but may be linked to mobility in other cases where large migratory animals are part of the faunal assemblage. She noted that where large quantities of materials are required, trade networks may be too much of a supply risk. She argued for embedded procurement with some examples of special purpose trips for shorter distances. The staging of supplies along path of seasonal mobility may represent an increased level of planning in the UP above that in the MP, or alternatively the technological demands required a more steady supply of higher quality materials.

The studies by Geneste (1985), Bamforth (1986), and Andrefsky (1994) are versions of distance-decay models that make the case for the importance of geographic setting and distance to source in interpreting assemblage variability. In the following studies, constraints on availability were not found to explain technological variability on the assemblage scale (Kuhn 1991; Milliken 1998). Kuhn (2004) identified cases where procurement strategies may have been designed to overcome supply constraints. Brantingham (2003) proposed a mathematical model that documents the development of that distance-decay patterning even in the absence of preferential selection of raw materials.

Kuhn (1991) examined the intensity of lithic reduction at Guattari and Sant' Augostino, two Pontinian Mousterian sites in Italy, both based on the use of small flint pebbles which limited the size of debitage and use of the Levallois reduction technique. Guattari has unworked pebbles in the vicinity of the cave but Sant' Augostino does not. Kuhn's test hypothesis was that decisions to reuse or economize stone materials should relate to the cost of raw material acquisition. He used indices of core size, frequency of multiple edged tools, ratio of unretouched to retouched flakes, and scraper reduction to estimate the intensity of core reduction and tool maintenance.

Kuhn found that the Guattari site showed the expected pattern of greater intensity of core reduction but not in tool reduction. He concludes that the intensity of core

reduction may be associated with raw material availability but not tool reduction and concludes that the differential conservation of “exotic” raw materials may have more to do with mobility and extended tool use than with cost of raw material acquisition. He argues that sites with longer duration of occupation are more amenable to lowering costs by stockpiling of raw material during the performance of other activities (embedded procurement). In that case, non-local raw materials may actually be used more expediently than might be expected by a simple distance decay model.

Kuhn (2004) then focused on provisioning strategies to explain changes in raw material use at the Upper Paleolithic site of Űçağızlı in Turkey. He described continuity in the types of raw material used throughout the sequence. Change occurred with a steady increase in the use of flint from secondary to primary sources (based on cortex) and increased transfer distances that occurred alongside a shift from more episodic to more intensive occupation of the cave at 12,000BP. Similar to his previous research in the Middle Paleolithic, Kuhn (2004) identified a relationship in the Upper Paleolithic that runs counter to the premise of distance decay models. Scrapers made from materials that come from greater distances to the cave, and are found in the more intensive occupations, actually seem to be less exhausted than those that are made from local materials in the more ephemeral occupations in the base of the deposit.

Kuhn (2004) outlined three potential provisioning strategies. The first is described as provisioning the individual with finished transportable (formal) tools and would be appropriate for more mobile populations that need to keep weight at a minimum. Provisioning the location is another strategy for more frequent use of the cave and more sedentary occupation where it would make sense to keep lithic raw materials in ready supply. Kuhn referred to the third strategy as the unplanned provisioning of activities, which would basically entail making tools as the need arises. Kuhn argued that the provisioning strategy at Űçağızlı changed from being primarily focused on provisioning the individual in the less intensively occupied layers to provisioning the location in the more intensive occupation. This shift would be accompanied by fewer restrictions on conserving raw material and thus there was less need to maintain or prolong the use-life of endscrapers. Kuhn proposed that raw material economy may change with corresponding change on settlement systems and provisioning strategies.

Milliken (1998) compared lithics from Late Paleolithic sites in two regions of Italy. Sites located in the Gargano Promontory are located near chert sources and sites on the Salento Peninsula located over 250km from sources. She expected that the Salento

sites would show more evidence for economizing behavior due to a scarcity of materials. Her comparison included variables associated with the laminar nature of each assemblage, indexes of maintenance, recycling, breakage, curation, intensity of core reduction, and use of alternative lower quality raw materials. Milliken concluded that only certain classes of tools were supported by distance decay and argues that the degree of curation and expediency had more to do with land use and activities at the site rather than distance to source. She was critical of what she called "single conditioners of technology" including raw material availability, time stress, risk, or mobility and argued for looking at multiple variables within a larger settlement system.

Brantingham (2003) used an agent-based computer simulation to show that most of the patterning observed in raw material use where distance decay models have been employed can be explained randomly by his neutral model. In Brantingham's simulation, raw material sources are randomly distributed in space. The agent uses up an increment of raw material for each random movement. The raw material supply carried by the agent is limited and is renewed each time a new source is encountered.

Brantingham's simulation yielded three important results. First, the observed assemblage richness in raw materials should always be less than the available range of materials on the landscape. Second, the neutral model predicts that the mobile tool kit will mostly consist of raw materials that occur in proximity to the observation location. Conversely raw materials from distant sources should be minimally represented in an assemblage. As a result, Brantingham argues that in order to demonstrate the deliberate selection of raw materials, patterning must be shown to be different than the results of the neutral model. It will be demonstrated in Chapter 6 that the patterning at Pinnacle Point is different from Brantingham's (2003) neutral model.

In summary, many of the studies discussed above have attempted to model technological adaptations alongside human mobility as strategies for risk avoidance. Risk may take the form of time stress and scheduling conflict, or can be modeled in terms of the failure to procure food. In either case it would seem that the measure of success for a given technological option is whether it maximizes food obtaining opportunities when the need arises. The cost of failure can be assessed by the number of alternative or fallback food resources.

The preceding literature review also shows that there is disagreement over the role or importance of raw material within the larger technological strategy employed. The 'righteous rocks debate' of Binford and Stone (1985) and Gould and Saggers (1985)

highlights the importance of understanding the degree to which raw material use can be explained by an encounter-based strategy or random walk (Brantingham 2003), or whether there was deliberate selection of raw materials for their physical properties. It is useful in this context to understand why certain raw materials might have been selected over others in the past.

Quality is the characteristic most often cited by archaeologists in considering aspects of raw material selection (Brantingham et al. 2000). Stone quality is often ranked by modern knappers and lithic analysts according to texture, or grain size (i.e. "fine-grained"), and the perceived ease and control of flaking. Goodyear (1989) defined quality based on stone grain size, and he stated that the advantages associated with the use of fine-grained raw materials include the increased control over core reduction and a reliable isotropic fracture. Fine-grained stone has the quality of "plasticity" in that these materials can be reduced with minimal, undesired breakage (Goodyear 1989).

Andrefsky (1994) defined raw material quality based on how easily material can be shaped and reduced. Fine-grained raw material gives the knapper greater control over the reduction processes compared to coarse-grained materials, which are more difficult to shape (Andrefsky 1994). For example, glass became the preferred raw material for bifacial projectile point production by Ishi, a Yahi California Native American and skilled tool maker, because of its superior workability (Nelson 1916). Package size may also play a part in the consideration of raw material quality as nodule size or configuration may constrain the technological approach to core reduction (Kuhn 1991, Brantingham et al. 2000, Hiscock et al. 2009).

In reality, the materials chosen in prehistoric times and by ethnographic subjects were not always the materials that were easiest to flake (Braun et al. 2009). Stone was also chosen for edge strength and durability among other properties. This bias toward ease of flaking as the direct measure of quality likely stems from the observation that most modern knappers have the goal of replicating the appearance of formal tool specimens rather than producing tools that they might need for their fitness or survival (Luedtke 1992; Magne 2001). More recent ethnographic research highlights how subjects with traditional stone tool making knowledge define raw material quality.

Binford and O'Connell (1984) described a day of stone quarrying with Alywaran tool makers in the Australian Central Desert. Their subjects began the process of making men's knives (carefully crafted bifacial tools considered to be sacred objects). They investigated the flaking properties of the quartzite materials in their quarry area, looked at

previously knapped waste products, and struck test flakes from larger blocks. Informants made reference to “purity of color” and “smooth texture,” when asked about what properties they were seeking in their stone. Raw materials exposed on the ground surface were considered to be “rotten” because they would not fracture predictably. The authors also stressed the point that the Alywarans did not rush through quarrying activities; they took time for the deliberate selection and preparation of materials.

Stout (2002) described ethnographic research with Irian Jaya adze makers in Indonesia. The raw material includes metamorphosed basalt and andesitic basalt, which were quarried by groups of men often during a period of several days led by expert craftsmen. Stout noted that the selection of the proper “high quality” materials was one of the most important steps in the process. The entire quarry party evaluates prospective raw material source cobbles and boulders according to crystalline structure, grain size, and internal flaws.

Boulders are often broken up by the use of large hammerstones and also by heating with fire, a process that can take most of a day (Stout 2002). The work group may remain at the quarry area for several days sharing cores and flake blanks. “Roughed out” adzes are stockpiled and then wrapped in leaves and carried back to the village. They are then finished through a combination of knapping and grinding, all done in a group setting.

Stout (2002) noted that the Irian Jaya had a complex vocabulary for describing and teaching the adze making process with a structured way of identifying the desired properties of potential nodules prior to core preparation. The actual name of the raw material was seldom agreed upon, which suggests that the classification of the material was less important than the critical identification of the material’s physical and even aesthetic properties. A similar observation was made by Heider (1967) for the Dugum Dani of the West New Guinea highlands. There was some preference for harder black stone over softer speckled stone for ground stone axe and adze heads but no specific names by the Dani for what archaeologists would likely classify as different raw material types.

Arthur (2010) studied the tool making practices of Konso Ethiopian women hideworkers who still use stone in addition to glass to produce hide scrapers. The Konso tool makers were traditionally selective with raw material and often travelled a distance of 25km to get their preferred chalcedony because it was homogeneous and easy to flake. When possible, they avoided stone that “falls into too many pieces when you break it”

(Arthur 2010:232). Arthur noted that chalcedony was most often selected at the height of the Konso hide trade in the 1970s. But since the practice shifted to a part-time activity, glass and more local quartz and quartz crystal have been increasingly used although the traditional raw material preferences are still taught to young apprentices.

The ethnographic observations of raw material selective behavior indicate that raw material quality is considered primarily with respect to both flaking properties and suitability for the intended task. Although the previous ethnographic observations identify preferences associated with non-functional stone properties, this deliberation often occurred after mechanical properties were evaluated. The stone traits considered to be important by modern knappers, including homogeneity, fracture predictability, and edge durability, are grounded in fracture mechanics theory and can be measured and quantified in actualistic experiments and standardized laboratory tests.

An early ground-breaking study involving the mechanical testing of lithic stone properties identified two of the major hurdles in quantifying the fracture properties of a raw material (Goodman 1944). First, archaeologists and geologists do not often identify and describe stone in the same way. Second, tests that attempt to rank materials according to physical properties should be designed to mimic conditions of human flaking and tool use. Goodman's research addressed the observation that materials chosen in prehistoric times and by ethnographic subjects were not always the easiest to flake. She also stated that a variety of variables need to be addressed to accurately describe the range of properties desirable to prehistoric tool maker/user. Goodman used a battery of tests to rank flint, obsidian, quartzite, fossilized wood, and tuff, according to density, hardness, toughness, and resiliency.

Stone hardness and toughness are still commonly used along with abrasion, uniformity, elasticity, and stiffness in comparing the physical properties of raw materials (Domanski et al. 1994). All of these characteristics evaluate a material's resistance to applied pressure usually given in units of pound-force per square inch (PSI) or in megapascals (MPa), but the manner or directionality of the applied force simulates different aspects of tool manufacture and/or use. Unfortunately the results of the tests generally show much variability within similar lithologies and may be useful only for statistical comparison across materials from a given locality or region (Luedtke 1992). Domanski et al. (1994) noted, for example, that mechanical properties of chert can vary greatly when comparing samples that originated in volcanic versus sedimentary formation processes.

Mechanical properties are also controlled by a sample's homogeneity, grain size, and isotropism (Cotterel and Kamminga 1990). Uniformity studies seek to quantify the frequency or encounter rate of flaws in a given mass of stone. Domanski et al. (1994) ranked stone according to the number of samples that failed during preparation. Brantingham et al. (2000) tabulated visible flaws and crystal impurities in calculating an impurity encounter rate to rank raw material quality at Tsagaan Agui Cave in Mongolia.

It has been argued that fracture toughness and rebound hardness are two tests that most closely track lithic "flakeability," meaning the ease with which a stone can be fractured (Domanski et al. 1992). Fracture toughness is the resistance of a material to fracture propagation (Domanski et al.1994), which is tested by notching one end of a cylinder core and applying and measuring the force required to pull apart the notched sides and completely fracture the specimen. Low fracture toughness values approach those of glass or obsidian and indicate that the stone is relatively easy to initiate fracture.

Rebound hardness, commonly measured with a Schmidt Hammer (Goudie 2006), is an estimate of the resistance of a material to strain and deformation, and it is heavily influenced by the homogeneity and purity of the stone, thus representing a measure of fracture predictability (Braun et al. 2009). Rebound hardness is correlated with other measures of hardness and elasticity, but it does not appear to be as tightly linked to tests of resistance to abrasion (Braun et al. 2009). Rocks that have higher rebound values (R) are considered to be stiffer (Noll 2000) and thus fracture more easily and predictably (Braun et al. 2009). Importantly, rebound hardness is influenced by stone moisture content, particularly with sampled southern African sandstones and quartzite (Sumner and Nell 2002).

Young's Modulus measures material resistance to deformation under a gradually increased compressive load until the point of failure is reached (Domanski et al. 1994). Young's Modulus (given in MPa) is calculated from stress curves and is essentially a measure of material stiffness, which can be an important variable for evaluating performance in blade manufacture (Domanski et al. 1994). High values of Young's Modulus are indicative of greater material stiffness. Heat treatment of certain lithologies can increase their overall stiffness, resulting in greater ease of flaking (Domanski and Webb 1992; Brown et al. 2009). Compressive strength, usually assessed through uniaxial compression tests, appears to be closely aligned with Young's Modulus, and testing is generally performed the same way. Measurement is taken by dividing the amount of the compressive load required to fracture the material by the cross-sectional area of the

sample core (Domanski et al. 1994). The compressive strength does not change consistently during lithic heat treatment.

Abrasion tests are designed to simulate strain on materials associated with tool use rather than tool manufacture. The Los Angeles and Taber Abrasion tests are two commonly used methods in which blocks of material are subjected to a controlled amount of abrasive force. The blocks are then measured to determine the percentage of material lost during the tests. Greater percentage values mean that the material is less resistant to abrasion (Noll 2000). The Los Angeles Abrasion Test may correlate with the compressive strength if the formation processes and porosity are taken into account (Kahraman and Fener 2007), but Braun et al. (2009) demonstrated that abrasion (simulating durability) and rebound hardness are not directly correlated. This distinction is important because it means that lithic materials having high rebound hardness (and thus flake more easily) are not always the most durable.

Properties quantified by mechanical studies essentially mirror the ethnographic observations. Fundamental and quantifiable differences can occur in the flaking and performance qualities of raw materials that suggest stone was often selected because of its suitability for planned tasks (Stout 2002; Arthur 2010). Mechanical properties were known and taught to apprentices by the ethnographic tool makers and were critical in decisions made during the first stage of tool production. In the case of the Irian Jaya, they might not have been able to "name" the material, but they could readily come to a consensus on the suitability of the material based on an agreed upon set of criteria.

Of course it is important to caution against drawing concrete conclusions about prehistoric raw material use from 20th century hunter-gatherers. Their original settlement and technology systems have been significantly altered by more sedentary living patterns sometimes associated with a breakdown in more traditional mobile economies, although many modern hunter gatherers may be extremely mobile from the use of motor vehicles. Unlike most modern knappers, however, subjects reported in ethnographies either regularly used stone tools themselves or had been taught traditional knowledge. From a strictly functional perspective, mechanical studies of properties, such as hardness, elasticity, and durability from a range of raw material classes found in a given region, should be useful in predicting which materials would be best suited for given tasks. In reality, raw material selective behavior will also be limited by the range of materials available on the landscape and local knowledge concerning source locations.

In summary, the concept of stone quality is subjective and depends upon the intended use of the tool. A balance exists between ease of flaking and edge durability (Braun et al. 2009). Materials can be ranked based upon mechanical properties, including hardness, elasticity, and edge durability (Domanski et al. 1994; Noll 2000). Factors unrelated to mechanical aspects of stone quality that might influence raw material selection include preference for appearance or color (Stout 2002), symbolic value (Gould et al.1971; Wurz 1999), trade networks (Torrence 1986), and style (Sackett 1982; Close 2002; Mackay 2011).

It is likely that many of the factors reviewed here contribute to the actual patterning observed in the archaeological record. The dichotomy between mobility-dependent and deliberate selection typified by the "righteous rocks" debate of Binford and Gould is useful for analytical purposes and is a common theme in African archaeological research where great regional diversity occurs in lithic raw materials found on the landscape (Clark 1980). The key points of this debate which centered on embedded versus logistical acquisition of materials will be seen to have heavily influenced models that were later constructed to explain Middle Stone Age raw material patterning. For example, Ambrose and Lorenz (1990) model raw material acquisition in the HP MSA occurring as an encounter-based strategy during increased episodes of mobility associated with hunting but Mackay (2008a) argues that fine-grained raw materials were deliberately sought because these materials allow for greater recovery of cutting edge per mass unit of material.

2.1 Early Stone Age

The African Stone Age is divided into the Early Stone Age (ESA), Middle Stone Age (MSA), Later Stone Age (LSA), which are distinguished at the most general level by the presence of large core tools (ESA), flakes and blades produced on prepared cores (MSA), and various microlith, scraper, and flake tool assemblages (LSA). Obviously there are exceptions to these trends, but the overall pattern in the African Stone Age is a long and punctuated progression from larger to smaller tools, as well as for increased complexity in core reduction and an implied elevation in the level of planning involved in tool making (Clark 1992; Ambrose 2001; Foley and Lahr 2003). An apparent trend can also be seen in raw material preferences from tougher more durable materials through the ESA and much of the MSA toward an increased use of what has often been described as

higher quality or more finer-grained raw materials in microlithic late MSA and early LSA assemblages (Ambrose 2002). Sections 2.1 and 2.2 provide a brief summary of the ESA and LSA in order to provide context for developments in raw material use and technological organization that occur in the MSA (Section 2.3).

The ESA lasts from approximately 2.6 million to perhaps 250,000 years ago and was possibly produced by at least four different hominid species. It is traditionally classified as a core-tool-focused technology although microwear studies indicate that the flake removals in core-tool-based assemblages were also utilized (Keeley and Toth 1981). The ESA is divided into two major periods, the Oldowan (2.5-1.6ma) and Acheulian (1.7ma-c. 300ka). Although these periods are often considered to be simple or static technological complexes that persist to the rise of archaic Homo sapiens, they do offer some subtle clues to cognition and early material selection behavior.

The Oldowan is characterized by the production of simple flaked pieces (FPs) and detached pieces (DPs) usually made from river cobbles of volcanic origin (Isaac 1981). The Oldowan is found mainly in East Africa and perhaps also at Sterkfontein and Swartkrans in southern Africa (Kuman 1994). The Oldowan was originally viewed as being typologically diverse with some degree of specialization in tool forms (Leakey 1971). But it is now generally acknowledged that most flaked pieces can be viewed as stages in a continuum (Toth 1985), and it has been argued that much of the variability in the Oldowan can be attributed to the morphology of the raw material "package" form and degree of reduction (Potts 1991).

While Oldowan tool forms may not offer much evidence for cognitive complexity (Ambrose 2001), research has indicated that at least some Oldowan assemblages show evidence for deliberate selection and preferential transport of stone materials (Braun et al. 2008; Harmand 2009; Goldman-Neuman and Hovers 2009; Stout et al. 2005). Schick and Toth (1993) observed that knappers at Koobi Fora were able to select materials that were free of flaws and weathering. Early Oldowan sites at Gona appear to show a preference for felsic and aphanitic rocks in greater frequency than would be found in the local gravels, leading Stout et al. (2005) to argue for the deliberate selection by Oldowan knappers of finer-grained, more easily flaked materials. Braun et al. (2008) geo-chemically sourced raw materials used in the vicinity of the Kanjera South site (Kenya) and found that local materials were not proportionally represented in the Kanjera assemblage. They investigated two raw material mechanical properties (fracture predictability and edge durability) to demonstrate that raw materials were preferentially

selected on the basis of resistance to abrasion rather than fracture predictability or local availability, with some material transported as far as 10km away.

The Acheulian follows the Oldowan period and spans approximately 1.6 million to c. 250,000 years ago (Marean and Assefa (2005); Klein 2000). It is generally considered to be the technology made by H. erectus/ergaster and archaic H. sapiens. The Acheulian marks the introduction of true bifacial shaping technology. The classic recognizable tool form is the handaxe or cleaver core tool, but the Acheulian also includes flake tools and unmodified flakes and scrapers. Raw material studies have figured prominently in an effort to understand Acheulian inter-assemblage variability Sharon 2008. Handaxes have been offered as evidence for more advanced cognition in planning and tool making (Delagnes and Roche 2005), as they appear to come in more standardized shapes. Early Acheulian researchers (and lithic research in general) often assumed that tool diversity reflected cultural tradition and reflected chronological change from cruder to more refined forms (Isaac 1975; Noll 2000). Isaac (1986) advocated residual analysis to try and remove the effects of raw material on the finished tool form before discussing the cultural implications of differing biface shape and form. Similarly, Clark (1980) proposed to identify aspects of the Acheulian that could be easily tested (raw material primary form, distance and quantity on landscape, nature of collection area, material texture or fabric, constraints of the primary form, retouch attributes) from those material-linked aspects that could not (range of variability expected within and between groups of people, mental templates, task specific demands, technical or stylistic preferences dictated by the environment).

Early experimental archaeology attempted to address the relationship between raw material diversity and edge characteristics. Jones (1979) found that experimentally replicated quartzite bifaces were well-suited for butchery because the edges were not easily dulled, but quartzite flaking qualities did not allow for careful retouch. He argued that retouch—necessary for maintaining the edge on finer-grained materials—led archaeologists to classify them as being “more refined” when in fact they took the same level of skill as those seemingly cruder bifaces made on coarser materials.

Noll (2000) used Taber abrasion, rebound hardness, and uniaxial compressive strength tests to rate mechanical properties of igneous stone available surrounding the Acheulian site of Olorgesaile, Kenya, in an application of Isaac’s (1986) residual analysis approach to investigate the contribution of raw material mechanical properties to handaxe variability. He found that raw material frequency had a significant effect on measurable

artifact attributes including tool thickness, scar stepping, and edge angle, and that cutting edge seemed to be more important than symmetry. Noll concluded that large cutting tools were intended to provide long cutting edges and that raw material was selected for hardness and strength. Thus, hominid tool makers at Olorgesaile were aware of the mechanical properties of the stones they were flaking.

In a sweeping survey of the Acheulian of Africa and western Asia, Sharon (2008) also found an overwhelming preference for tougher, more durable materials for the production of handaxes and particularly for cleavers, supporting an earlier claim for the limited distribution of the latter based on raw material availability (Clark 1980). Research indicates that at least some ESA Oldowan and Acheulian assemblages show a deliberate preference for more durable raw materials even when materials that fracture more predictably were available (see Stout et al. 2005; Braun et al. 2009). Also, early evidence shows long distance transport of raw materials (Clark and Kurashina 1979). The important implication of this research is that the ability to preferentially select materials for their mechanical properties is likely a behavior trait shared by all hominin tool makers.

2.2 Later Stone Age

The following review of the Later Stone Age (LSA) focuses on southern Africa. It is important to note that the LSA of East Africa looks very different from southern Africa and seems to show fewer gaps in sequence and more continuity in the tool forms (particularly in backed blades and segments) across the transition from the MSA (McBrearty and Brooks 2000; Ambrose 2002). The oldest, well-defined LSA entity in southern Africa is the Robberg Industry, dating from 22 to 12ka (J. Deacon 1978). The Robberg is characterized by unretouched microlithic bladelets from blade cores and a small number of backed tools and scrapers. The three major Robberg sites are Nelson Bay Cave in Plettenberg Bay, Rose Cottage Cave in the Free State (Wadley 1996), and Sehonghong in Lesotho (Mitchell 1995; 1996). At Nelson Bay Cave, quartz is the predominant raw material used (Fig. 4) in the Robberg Industry followed by quartzite and less commonly silcrete, except in layer YSL (Deacon 1978). In Lesotho and Free State, opalines are used throughout the sequences (Mitchell 1995). Mitchell (1995) noted the presence of crested blades in the Robberg, arguing for standardized blade reduction

process and H.J. Deacon (1995) postulated that the small blades are similar to the HP in that both appear to have been produced by indirect percussion (punch).

The Oakhurst, named for a rockshelter near Wilderness, occurs from 12 to 8ka years ago and was formerly known as the Smithfield A (Mitchell 2002). The Oakhurst is characterized by round endscrapers and "duck bill" scrapers, and also contains polished bone and few or no "backed pieces." Tools are made from more "coarse-grained" raw material than the preceding and following assemblages (Deacon 1978; Mitchell 2002). Regional variants include the Albany in the southern Cape (NBC) and Lockshoek in the Karoo. At NBC, more than 90% of Albany artifacts were made on quartzite (Fig. 4), and the quartz-dominated LSA sequence at Boomplaas shows the highest jump in quartzite during the Albany layers (Deacon 1978; Mitchell 2002).

The Wilton Industry applies to mid to late Holocene microlithic assemblages that can be subdivided into the Mid-Holocene (Classic Wilton) dating from 8000 to 4500BP and the Late Holocene Wilton (formerly Smithfield C) during the last 4500 years (also termed "Interior Wilton," "Late Wilton," "Post-Classic Wilton"). The Wilton has a wide range of microliths, borers, small scrapers (less than 25mm), double scrapers, ornaments and polished bone tools. The Late Holocene Wilton has fewer segments and an increase in bladelets. At the type site, the predominant raw materials across all categories are silcrete, chalcedony, and quartz (J. Deacon 1972). Quartzite was most commonly selected at Nelson Bay Cave (J. Deacon 1978), and opaline was used throughout the Wilton at Rose Cottage Cave (Wadley 2000).

The term "Smithfield" (i.e., Late LSA) used to apply to a number of mainly scraper-based assemblages, but it is now used to describe late LSA (last 1000 years) scraper-dominated assemblages in the Karoo. Preceding and contemporary to the Smithfield (within the last 3000 years) on the South Coast is material loosely termed "macrolithic," consisting of large unretouched flakes. This late informal technology could be due to changes in activity (Deacon and Deacon 1999), or perhaps territory constraints imposed by expanding pastoralists (Jerardino 2007).

The southern African Later Stone Age shows trends in raw material use and is useful for comparative purposes because LSA tools were made by tool makers from an unquestionably modern behavioral context (Barut 1994). In the coastal Robberg at NBC, quartz is the preferred material for bladelet production although an increase occurs in silcrete use in Layer YSL. Opaline is used throughout the LSA in Lesotho and Free State. Quartzite is most commonly used in the Albany variant of the Oakhurst for making large

scrapers. The use of fine-grained materials for tool making may have been substituted or replaced by the many bone tools found in Oakhurst assemblages. In the following Wilton, a shift again occurs to microlithic tools and use of fine-grained materials and quartz (J. Deacon 1972).

There is a lot of variability in post-Wilton LSA assemblages in terms of artifact size and raw material use (Orton 2008). The most recent LSA lithics at some sites on the West Coast appear to show a decrease in percentage of formal tools and reduced diversity in raw material use perhaps because these were the more expedient tools of herders (Schrire and Deacon 1989) or maybe due to the marginalization of hunters by herders (Smith et al. 1991) and a breakdown in the supply of non-local raw materials. Dunefield midden near Elands Bay preserves an LSA microlithic bipolar quartz technology with segments between 900-600BP (Orton 2002). On the South Coast, Nelson Bay Cave has Wilton-like segments up to 3200BP and then a less formal younger assemblage with quartzite tools, and Boomplaas has small scrapers and backed blades made from fine-grained stone associated with herding (Deacon and Deacon 1999).

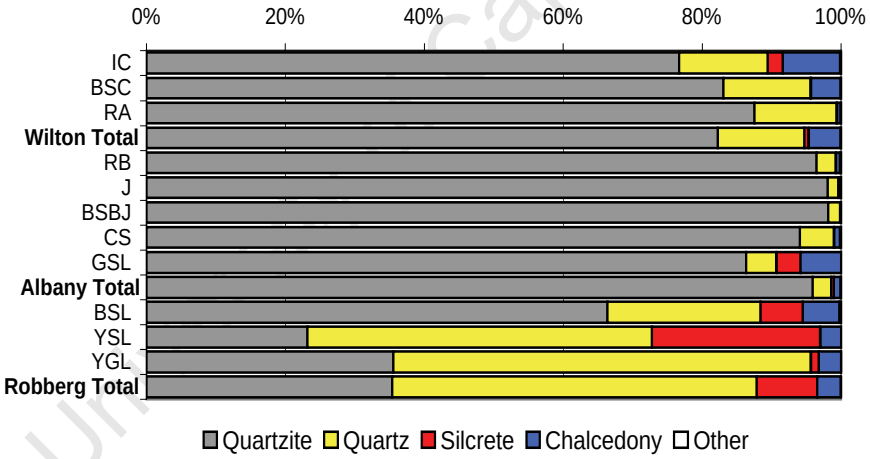

Figure 3. Raw material percentages for LSA layers at Nelson Bay Cave (Deacon 1978)

2.3 Southern African MSA

The following background on the southern African MSA describes archaeological sequences from stratified MSA sites that have been excavated with relatively modern techniques, documentation, and dating (in most cases). This particular section focuses on both technology and raw material selection from sites that provide complementary records from coastal and inland contexts for comparison with PP5-6. It will be

demonstrated in the following analysis that PP5-6 is broadly similar to other coastal MSA sequences although some important differences occur. Each site sequence is described under its own heading.

Klasies River

Modern technological studies of southern African MSA lithics have their origins in the studies published from the excavations by Singer and Wymer (1982) at the site of Klasies River on the Tsitsikamma Coast. Artifact samples from the deep series of deposits at Klasies River stimulated the development of a new way to describe the southern African MSA lithic sequence. But other pioneering efforts contributed terminology and conventions that are still in use (Goodwin and van Riet Lowe 1929; Sampson 1974). The excavations at Klasies River resolved some long-standing issues concerning the cultural stratigraphic sequence of the MSA. An effort was made to tie the cultural sequence at Klasies River to the global climate record (Shackleton 1982) which promoted efforts to link environmental change with MSA lithic technology (H.J. Deacon 1983). The MSA lithic assemblage from the Singer and Wymer excavations was divided into five stages, based on stratigraphy and typology (Singer and Wymer 1982). From the oldest to more recent deposits, these excavations included the MSA I, MSA II, HP, MSA III, and MSA IV.

The MSA I was characterized by long blades, “flake-blades” (elongated flakes that may or may not have a length of twice their width. Many of the flake-blades are thin, with platforms that were reduced or trimmed before the flake was struck from the core. The thinned platforms led Wymer to believe that some of the blades were produced by indirect percussion (Singer and Wymer 1982:112). Only rarely were convergent products retouched into denticulates and points. The majority of cores are of single and double platform type. The MSA II was defined by a higher frequency of convergent flake-blades and a lower percentage of worked points. Single platform cores continue to be well represented, but more irregular cores exist.

The HP Industry at Klasies River was described as being “radically different” than the overlying and underlying MSA stages (Singer and Wymer 1982:112). Flake-blades are smaller and are much less frequent. Unlike the type assemblage from Howiesons Poort Rockshelter, retouched points are rare. Backed blades, including crescents, trapezes, and triangles, are common, along with obliquely blunted points, which are all made on blade segments. Due to the small striking platforms and diffuse

bulbs seen on the flakes, Wymer believed that indirect percussion was also used to produce blades of the HP. Gravers and scrapers are also present in the HP. While quartzite continues to be the dominant raw material chosen for blade production, a marked increase occurs in the use of fine-grained silcrete. The increase in use of fine-grained raw material is a pattern that has become synonymous with the HP in southern Africa (Ambrose 2002). On the basis of core types represented, Singer and Wymer argued that all raw material classes appear to have been worked in the same manner (Singer and Wymer 1982:114). The Klasies River excavations clearly placed the HP stratified within the MSA. The HP includes assemblages that were previously termed "Magosian" (Clark 1959), "Modderpoort" (Malan 1949), or "Epi-Pietersburg" (Beaumont et al. 1978) and were once considered transitional from the MSA to the LSA.

The MSA III is described as being very similar to the MSA II with many convergent flake-blades, a few examples of small unifacial points, and also backed flake-blade "knives" (Singer and Wymer 1982:114). In the MSA IV, which only occurs as a small sample in Cave 1, fewer flake-blades are present than in previous MSA stages. Convergent flake-blades are more numerous. In general, flake-blades are smaller with fewer retouched pieces. Few tools are made on non-quartzite stone. The majority of cores are irregular and undeveloped, followed in frequency by single and double platform cores (Singer and Wymer 1982:114).

Volman (1981; 1984) modified and expanded Singer and Wymer's (1982) MSA sequence from Klasies River to include assemblages from sites that were believed to be older and located outside of the southern Cape. Volman examined lithics from most of the southern African MSA assemblages available for study at the time, with particular attention to Klasies River, Boomplaas, Die Kelders Cave 1, Border Cave, and Apollo XI. Volman used his data to develop an informal and flexible way to characterize the MSA sequence south of the Limpopo River. Volman also synthesized available chronological evidence in an attempt to link the entire sequence to an isotopic climate record (1984). It is noteworthy that Volman's classification did not include the SB, an original MSA Industry, defined by Goodwin and van Riet Lowe 1929, that has been demonstrated to be 6 to 7ka older than HP occupations in sites where both occur (Jacobs et al. 2008). Prior to the excavations at Blombos Cave, the position and age of the SB was largely misunderstood (Jolly 1948). Volman (1981) used standard rather than Roman numerals to describe his comparative sequence but most other researchers that have worked on

Klasies River materials (Thackeray and Kelly 1988; Wurz 1999; Villa et al. 2010) continue to use Roman numerals to describe the sequence.

Volman's (1981) MSA 1 included assemblages from Duinefontein 2, Peers Cave, Elands Bay Cave, and possibly Bushman Rockshelter. The Duinefontein 2 assemblage is now considered to be Acheulean (Klein et al. 1999). The MSA 1 is characterized by a high percentage of convergent-flaked cores. Flakes are small, broad, and rarely show evidence for platform preparation. Denticulates make up the majority of the few retouched tools present. Retouched points are absent, and scraper retouch is rare. Volman (1984) assigned the MSA 1 to OIS 6 based on archaic forms of fauna, sediment sequence, and infinite radiocarbon dates taken from more recent levels above these assemblages.

The MSA 2 includes characteristic tools previously assigned to MSA I and MSA II of Singer and Wymer's (1982) Klasies River chronology. Volman (1981) divided the MSA into an earlier stage2a and later stage 2b. The MSA 2 consists of large, narrow flakes and blades that decrease in average length from MSA 2a through MSA 2b. The abundance and number of retouched types increase from MSA 2a to MSA 2b. Denticulates are common in MSA 2a and retouched points are common in MSA 2b. Volman (1981) suggested some possible overlap between MSA 2a occurrences and OIS 6, but believed most MSA 2 assemblages were associated with OIS 5e-5c.

HP assemblages are defined by a higher percentage of retouched tools in the form of crescents, segments, trapezoids, and similar backed or truncated pieces. Flakes from the HP are not usually facetted, and they are smaller and broader than those of the MSA 2. Many HP assemblages are associated with an increase in the use of fine-grained raw material, which may be less common in the preceding or following layers. Most HP assemblages contain scrapers, but variable quantities are present of unifacial and bifacial points. Volman (1984) placed the HP somewhere between OIS 5b, and OIS 4, indicating a trend toward colder, drier temperatures.

The MSA 3 includes assemblages that overlie the HP. The MSA 3 contains the same artifacts as MSA 2, and looks very similar to MSA 2b. This final stage shows a trend toward larger flake-blades. Volman believed that the MSA 3 ranges from OIS 5a-3, implying that the latest MSA 3 assemblages lie within the range of radiocarbon dating (Volman 1984:209).

Volman's (1981;1984) typological classification provided the first useful way of characterizing and comparing southern African MSA sequences although sites with SB

assemblages and site outside of the cape do not necessarily fit the Klasies pattern. Differentiating the MSA stages continued to be difficult because in many collections the similarities were usually more obvious than differences (Singer and Wymer 1982). Unfortunately the early excavations at Klasies River were also selectively biased in the collection of artifacts, leading to difficulties in applying the sequence to other sites (Thompson and Marean 2008).

The H.J. Deacon 1984-1988 excavations at Klasies River main site refined the stratigraphic sequence (Deacon and Geleijense 1988) and created an unselected lithic sample from controlled stratigraphic contexts. The following description is summarized from Wurz (2002). The MSA I is at the base of Cave 1 and Cave 1A (centered at c. 8masl) and may date from approximately 90 to 110ka. The MSA II in Cave 1A comes from the SAS Upper and Lower members and may include ~15m of sediment. Volman's division of the MSA 2 is now referred to as MSA II Lower and MSAII Upper (Wurz 1999). The RF and Upper members of Cave 1A and Cave 2 were recently and systematically OSL dated (Jacobs et al. 2008; Jacobs and Roberts 2008). Their OSL ages for the RF (rockfall) Member/Layer 22 at 72k.1 ± 3.4 and 71.6 ± 2.9 provide a minimum age for the top of the SAS member (upper MSA II). The overlying HP is OSL dated from 63.4 ± 2.6 to 65.5 ± 2.3 and the MSA III above the HP at 57.9 ± 2.3.

Studies of lithics from H.J. Deacon's 1984-1988 excavations at Klasies River have mainly focused on variability in shape and size of MSA points and blades through time. Thackeray and Kelly (1988) argued that only subtle changes occur in the long MSA II sequence, indicating technological continuity through time. Thackeray (1989) conducted a study of Klasies River lithics from the 1984 to 1988 excavations. Her analysis validated Singer and Wymer's division of the sequence into MSA stages, but she argued for technological continuity throughout the sequence particularly with respect to the production of quartzite points and blades through the entire sequence. Wurz also conducted a technological analysis of the entire Klasies River sequence focusing on materials from the Deacon excavations. Her results are described in more detail alongside those of PP5-6 in Ch. 7.8 but as with Thackeray (1989), she found significant metric change between the MSA stages (Wurz 2000; 2002; 2003). Wurz (1999) found that no technological differences seemed to exist in how raw materials were used despite the inflated percentages of fine-grained raw materials in the HP.

Die Kelders Cave 1

The Die Kelders cave complex is situated just above mean sea level on the Walker Bay coast of the southern Cape. Schweitzer (1979) conducted the first excavations of Die Kelders Cave 1 from 1969 to 1973. Schweitzer was mainly concerned with the LSA material, and he was surprised to find MSA lithics beneath the sterile occupation level that signaled the end of the LSA sequence (Schweitzer, 1979).

Volman summarized the entire MSA lithic sequence from Schweitzer's excavations of Die Kelders (Volman 1981; Grine, Klein, and Volman 1991). Most of the MSA tools come from the "occupation layers" (4, 6, 8, 10, 12, 14) that are separated by layers that contain few artifacts (Layers 5, 7, 9, 11, 13). Centripetal cores occur throughout the MSA sequence. Few cores are large enough to account for the elongated, parallel, sub-parallel, and convergent flakes that are common in all levels. Volman suggested that the longer flakes could have been produced on single and double platform cores, which were subsequently reconfigured centripetally as they approached exhaustion (Grine, Klein, and Volman 1991:368). Retouched pieces are very rare and usually take the form of notches or edge-damaged pieces. Quartzite flakes in the earlier and later MSA tend to be long and narrow, whereas in the middle levels they are shorter and broader.

Quartzite, quartz, and silcrete were the only raw materials utilized at Die Kelders. In general, quartzite is used throughout the sequence, but in levels 11 and 12, the majority of debitage was produced on silcrete (Volman 1981; Thackeray 2000; Brown 1999). The pattern of raw material utilization at Die Kelders is interesting because unlike many other MSA sites in southern Africa, the shift to finer-grained raw material does not correspond to the production of retouched blade tools characteristic of the HP. Assigning a date to the Die Kelders Middle Stone Age sequence using Volman's typological system is difficult. Depending on how one interprets the raw material pattern previously described, the MSA levels could predate the HP MSA from other sites, suggesting a correlation with the MSA II. If the silcrete dominated assemblage from level 12 is related to or synchronous with the HP, overlying levels could be assigned to the MSA 3 (OIS 5a-OIS 3) (Grine, Klein, and Volman 1991:370). ESR dates are in suggested to be in the range of 60-80ka for the Die Kelders Cave I MSA (Avery et al. 1997).

Additional excavations of the MSA deposits at Die Kelders were conducted from 1991 to 1995 (Marean et al. 2000). Thackeray (2000) compared the artifact samples from the recent excavations to those described in Grine, Klein, and Volman (1991). In general,

the samples are comparable, but with some notable differences. Based on artifact counts, the percentage of silcrete in layer 12 is 34% in the recent excavations, compared to 61% from the Schweitzer collection. The discrepancy in raw material counts likely results from the high frequency of quartzite roofspall found in the assemblage which was excluded in the Volman analysis (Brown 1999). This brings up the point that raw material percentages for MSA assemblages are typically presented based on artifact counts. That convention is followed for many of the analyses in this study but raw material mass is also provided for each analytical sample in Chapter 5 and is used in Chapters 10 as a proxy measure for the cost of transporting raw material to site. A comparison of raw material percentages by count versus by total mass for Die Kelders Cave I is shown in Figure 4, based on a reanalysis of Layers 10, 12, and 14 (Brown 1999). In this case, the overall patterning does not change very much but the contribution of non-quartzite raw materials may be overemphasized.

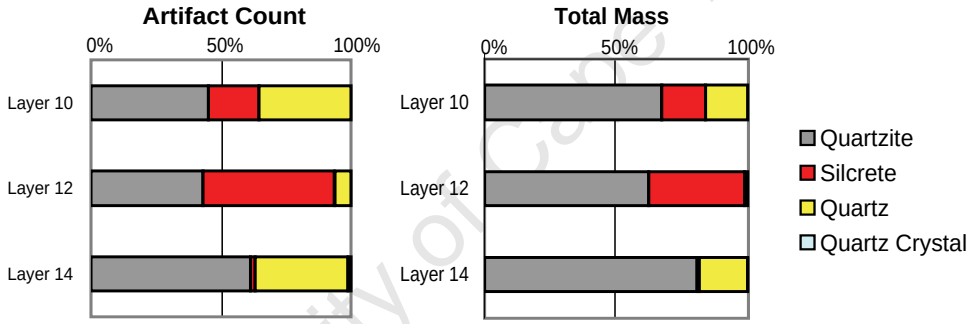

Figure 4. Comparison of Die Kelders Cave I raw material percentages from Layers 10, 12, and 14 by artifact count (left) and total mass (right). Data from Brown (1999)

Volman (1991) noted that all raw materials appeared to be reduced in the same way, but Thackeray found that most of the silcrete blades are smaller than the quartzite blades, which, she argued, was the result of differences in the size of the available nodule. Silcrete cores are small and are irregularly or centripetally prepared. In the Schweitzer collection, the majority of quartzite cores are centripetally prepared, but in the more recent sample, some quartzite cores show evidence of flake and flake-blade removal. Examples are present of single, multiple, and opposed platform cores, as well as single-removal prepared cores. Thus, more variability may exist in the method of flake production than was previously thought.

A focused study of the Schweitzer Collection lithics from layers 10 to 14 suggests that there are quantifiable differences in the conservation of raw materials at Die Kelders Cave I (Brown 1999). A study of cutting edge to mass ratios on quartzite and silcrete

flakes showed that MSA tool makers employed a flake production strategy that attempted to recover the maximum amount of cutting edge on silcrete. Quartzite flakes and blades have larger surface areas in relationship to thickness and less edge length per mass unit of raw material. A similar trend has been documented for the HP of Klein Kliphuis (Mackay 2008a) and for PP5-6 (Ch. 11).

Montagu Cave

Montagu Cave is located approximately 180 km E, northeast of Cape Town and west of the Little Karoo near the town of Montagu. Haughton, Barnard and Tucker first excavated the site in 1919 (Keller 1973). Charles Keller was interested in looking at the Acheulian tools in his 1964-1965 excavation of Montagu. He uncovered a sequence from the Acheulian to the LSA that included MSA horizons. He identified all surfaces in Layer 2 as being representative of the HP. Volman (1981) re-examined the collection from Montagu Cave and argued on a typological basis (a lack of backed blade segments) that the most recent MSA surfaces in Level 2 should be assigned to a post-HP MSA (Surface 1-Surface 6) (Volman 1981). The sample from Horizon 6-7 and Surface 7 is representative of the HP, based on the criteria defined in the published description of the type site (Stapleton and Hewitt 1927;1928).

Quartzite, silcrete, quartz, and a variety of fine-grained raw materials were utilized at Montagu Cave to produce flakes, flake-blades, and blades of all sizes and shapes. No trends appear in the use of raw material between levels, but all the characteristic HP retouched blade tools at Montagu were produced using the fine-grained raw materials (Volman 1981). Centripetal cores are predominant throughout Level 2, but amorphous cores, single and double platform cores, and discoid cores are also common (Keller 1973). With the exception of the backed pieces of the HP, few retouched tools appear in the Middle Stone Age at Montagu Cave (Volman 1981, Brown 1999). Sidescrapers make up a small percentage of the collection. Volman's HP sample contains rare examples of unifacial points and a single bifacial point.

Nelson Bay Cave

Nelson Bay Cave is located on the Robberg Peninsula in the southern Cape. The site was excavated by Ray Inskeep in 1964-5, 1965-6, 1970-1 and 1979, and by Richard Klein in 1970 and 1971. The cultural deposits begin with pre-HP MSA (levels 10-7), followed by HP (Level 7 to Crust Layer), and after a sterile occupation gap, followed by

the Robberg, Albany, and Wilton LSA. Volman (1981) described the Middle Stone Age lithics from Klein's excavation and noted a number of trends in flake production.

Quartzite is the most abundant raw material, followed by quartz, silcrete, and other fine-grained raw materials, including chert, chalcedony, and silicified shale. The frequency in the use of quartzite is high throughout all levels (usually above 90%), but a moderate increase is seen in the use of silcrete, quartz, and other fine-grained stone in the HP. Unlike the pattern seen at Montagu Cave, backed tools in the Nelson Bay Cave HP were made from quartzite and fine-grained raw material in similar proportions (Volman 1981:208). A few strangled and multiple notched pieces occur on silcrete and chert. All other formal tools were made using quartzite.

Volman (1981) noted a low ratio of primary cortical flakes to cores within the Nelson Bay Cave MSA, although the percentage of cortical products and the criteria for identifying a primary flake was not defined. He suggested that primary reduction occurred outside of the cave, and only successfully prepared cores were transported into the cave. Most cores are highly reduced with an absence of single-removal prepared cores, suggesting that once a core was prepared, it was reduced until the core was nearly exhausted. The majority of cores are centripetal cores with single and multiple platform cores for the production of parallel and sub-parallel flakes. Flakes in the HP levels are generally small, whereas flakes in the pre-HP MSA are long and narrow. Few "simple" (unifacial) points are present overall, and most are found in the pre-HP layers. Retouched tools in the HP are characterized by segments, triangles, trapezoids, other backed pieces, as well as denticulate endscrapers. Multiple-notched and strangulated pieces are confined to the HP, and retouched points and sidescrapers are only found in the pre-HP.

Volman (1981) described the pre-HP MSA Level 8 as MSA 2b, and Levels 9 and 10 as MSA 2a. On the basis of Butzer's (1973) study of Nelson Bay Cave sediment, Volman (1981) suggested that the MSA sequence began around 110ka in OIS 5d, continued through the HP, and ended at 83ka in OIS 5a. The Nelson Bay Cave sequence has not been dated, but the recent OSL study by Jacobs et al. (2008) indicates an age of 65-60ka for the upper MSA levels by association with other dated HP sites.

Border Cave

Border Cave is located in KwaZulu-Natal (KZN) on the border of Swaziland. The site is important because it contains a deeply stratified MSA sequence that was originally claimed to date to 195ka (Butzer et al. 1978). The site represents an inland sequence for

comparison with Klasies River. The Border Cave sequence has not been published and the major source for data is Beaumont's 1978 unpublished dissertation. The base of the sequence (levels BACO.D-1GBS.UP) was described in a conference paper by Beaumont (1979) as an MSA Phase 2 entity, comparable to the Pietersburg Industry of Cave of Hearths. Volman (1984) divided the lower Border Cave sequence into MSA 2a and MSA 2b. The MSA 2a level has few retouched pieces with more triangular shaped flakes than in the rest of the overlying sequence. The upper MSA 2b has retouched points, scrapers, and a few core reduced pieces (outils ecaillés). Quartzite and rhyolite were used throughout the Border Cave MSA. The following levels (3BS-1RGBS.B) were originally described as MSA Phase 2, comparable to Epi-Pietersburg. Volman (1984) placed them in the HP because of segments, trapezoids, and other backed segments and a few retouched points, scrapers, or scaled pieces. An increase in the use of cryptocrystalline raw material appears in the HP. The rest of the MSA sequence at Border Cave was grouped by Volman (1984) into MSA 3, which is characterized by the presence of scaled pieces, unifacial and bifacial points, a few endscrapers, and rare backed pieces.

It was first argued that the base of the Border Cave sequence dated to early OIS 6 (Butzer et al. 1978). This date was based upon the extrapolation of the rate of sedimentation from the radiocarbon sequence and was contested (Volman 1981; Parkington 1989). Volman (1981, 1984) argued that the Border Cave MSA archaeological sequence should be viewed as being contemporary with the similar sequence from Klasies River Mouth. Revised ESR ages continue to indicate an early age for the MSA spanning to at least 195ka (Grün and Beaumont 2001).

Rose Cottage Cave

Rose Cottage Cave is located near Ladybrand in the Free State province of South Africa. The site was first excavated by B.D. Malan between 1943 and 1946. Beaumont conducted further excavations in 1962. Wadley and Harper (1989) analyzed the unpublished lithics from Malan's excavations and then re-excavated the LSA and Final MSA. The Rose Cottage Cave sequence is divided into the Pre-HP MSA, HP, and Post-HP (Wadley and Harper 1989; Soriano et al. 2007).

The Pre-HP lithics sample (layers LEN, KUB, and KUA) is produced on tuff, siltstone, and opaline. Disc, blade, flat bladelet, core reduced, and irregular cores are common throughout the entire MSA sequence with numerous unifacial points, large flakes, and large parallel-sided flake-blades. These layers also contain a few "partly

bifacial" points (retouch occurs on both sides of a lateral edge, but is not invasive like retouch on SB points), as well as unretouched convergent points. Wadley and Harper (1989) associated their pre-HP with Volman's MSA 2b.

The HP at Rose Cottage (EMD, MAS) is characterized by the increased use of opaline and the almost exclusive production of small blades. Blade production in the Rose Cottage Cave HP is argued to be similar to that of the European Upper Paleolithic (Soriano et al. 2007). Blades were generally initiated on a natural ridge in the raw material with little preparation although crested blades do occur in the HP assemblage. The blades are suggested to have been struck from the core using soft hammer percussion in a marginal flaking motion (Soriano et al. 2007). The formal tool assemblage consists of backed blades and obliquely backed blades (equivalent to Singer and Wymer's obliquely backed points). Points and scrapers are rare. The Rose Cottage Cave HP has been OSL dated from c. 65 to 63ka (Jacobs et al. 2008).

The Rose Cottage Cave Post-HP includes Layers BYR, THO, ELA, LYN, and KAR. The Post-HP dates to 56 ± 2.6ka (Jacobs et al. 2008). Soriano et al. (2007) propose a more gradual shift away from the traits that define the HP at Rose Cottage. The pattern of opaline use continues in layers that immediately follow the HP and then there is a gradual transition to the use of tuff which corresponds with a shift away from small blades and backed pieces to an emphasis on scrapers, points, and knives. Flakes are small and blades are irregular. The transition from the HP to the MSA III at Klasies River has been demonstrated to be similar to that of the HP to Post-HP at Rose Cottage with gradual change away from marginal soft hammer blade production (Villa et al. 2010).

Blombos Cave

Blombos Cave is located near the town of Still Bay in the southern Cape. Early excavations at Blombos resulted in the recovery of what were considered at the time to be unique and unusual finds, including worked bone (Henshilwood and Sealy 1997; Henshilwood and d'Errico 2007), shell beads (Henshilwood et al. 2004), and engraved ochre (Henshilwood et al. 2002). Excavations also revealed a large sample of retouched stone tools, including complete and fragmentary bifacial points made predominantly from silcrete and quartz (Villa et al. 2009). The high frequency of bifacial finds at Blombos has led to increased interest in Goodwin's original "Still Bay Industry." Blombos Cave does not have an HP and lithics from levels below the SB have not been described.

The SB at Blombos Cave is separated from the LSA by a layer of dune sand that has been dated to ~70ka (Jacobs et al. 2003a; 2003b). A thick layer of dune sand dated to ~69ka is stratified within the PP5-6 sequence as well (Brown et al. 2009). The SB layers at Blombos Cave were originally grouped into four units from oldest to most recent: BBC3, BBC2, BBC1B, BBC1A. Silcrete is the most common raw material in debitage from all but BBC2 which is rich in quartz (Henshilwood et al. 2001b). Quartzite varies from 9% to 18%. Points are either lanceolate or elliptical in shape and are represented by a number of production phases (Villa et al. 2009). The preliminary analysis of debitage was suggestive of hard hammer production (Henshilwood et al. 2001b), but a recent replication study it was proposed that that SB points were first roughed out, heat-treated, and then finished by pressure flaking (Mourre et al. 2010). The overall high percentage of silcrete used in the SB levels at Blombos Cave offers supporting evidence that heat treatment was part of the biface production process because raw silcrete of the type available in this region cannot be efficiently used to produce refined bifaces similar to those found in the SB (Brown et al. 2009; Section 8.3, this dissertation).

Systematic OSL dating of other sites with stratified SB has indicated that SB occupations center at ~71ka and may represent a very short duration (Jacobs and Roberts 2008). The SB at Blombos Cave is capped by a ~70ka dune that constrains the upper age. The base of the Blombos Cave SB sequence is now argued to extend to 78ka (Mourre et al. 2010), which would significantly expand its time duration when compared with other sites. Resolution of the antiquity of the SB is important, especially given the recent excavations at Soutfontein, which is an open air SB site in southern Namaqualand, South Africa (Mackay et al. 2010).

Diepkloof Rock Shelter

Diepkloof Rock Shelter is located on the west coast of South Africa, approximately 200km north of Cape Town. The site is not actually located on the coastline but occurs 18km inland on the Verlorenvlei River, which eventually drains into Elands Bay. Diepkloof has been excavated intermittently since 1973 by John Parkington and Cedric Poggenpoel of UCT and a joint UCT/University of Bordeaux team since 1999.

The ~ 4m archaeological section at Diepkloof has been claimed to span from c. 45 to 130ka, based on TL dates (Tribolo et al. 2009; Texier et al. 2010) although OSL age estimates place the MSA sequence between 48 and 92ka (Jacobs et al. 2008). The DRS

sequence is divided into six complexes. The complex numbering system differs between publications and therefore the system presented in the most recent Diepkloof publication (Texier et al. 2010) is given here. Archaeological layers were assigned to common personal names with the first letter of each name providing a relative indication of its stratigraphic placement. The "Ante-Still Bay" occurs at the base of the excavated sequence, and is described as "Complex 6" ("Neva" to "Laureen").

Complex 5 is the Diepkloof SB ("Lynn" through "Jess" and "Kerry," "Kate," "Kim," and "Larry") which has not yet been published. Thirty-five complete and fragmentary bifacial points are reported to have been recovered, associated with bifacial production debitage (Tribolo et al. 2009).

Complex 4 is an HP sequence that has few backed pieces ("Jack" including "John" and "Orange black Complex 5" to "Governor"), along with the recently described "Jeff" assemblage (Porraz et al. 2008). "Jeff" is summarized in Section 10.10 in comparison to Pre-HP layers at PP5-6.

Complex 3 is the "conventional" HP (Porraz et al.2008). Complex 3 HP ("Orange black Complex 4-1" and "Fiona" to "Debbie") is suggested to contain mainly silcrete debitage and two modes of production: one based on blades and bladelets and the other based on flakes. Formal tools include backed blades, notches, and denticulates (Texier et al. 2009). Jacobs et al. (2008) OSL dated the DRS HP at 63.3 ± 2.1 to 58.9 ± 1.9. The Complex 5/Complex 4 transition (beginning of HP) is TL dated to 93±8 and the Complex 4/Complex 3 interface is TL dated to 61 ± 4 ka (Tribolo et al. 2009). Complex 3/2 transition has no TL dates.

Complex 2 (Danny to Claude) is noted to contain unifacial points and convergent scrapers (Porraz et al. 2008). Two OSL samples from Complex 2 provide ages of 55.4 ± 2 and 47.7 ± 1.7 (Jacobs et al. 2008).

With the exception of "Jeff." the Diepkloof Rock Shelter lithic sequence has not been described in detail. The DRS HP has received recent attention for a series of engraved ostrich eggshell fragments from the HP (Texier et al. 2010). The lithic sequence is noteworthy for having relatively high percentages of silcrete even though the nearest silcrete sources may occur as far as 10 to 40km away (Porraz et al. 2008).

Mackay (2008b) studied blades and backed pieces from the HP levels of Diepkloof to attempt to understand the relationship between blade production and the morphology of blanks that were actually selected for backed blade production. He found that at least 25% of the backed blades were actually produced on flake blanks. A high

percentage of blades made in the Diepkloof HP were too short to have functioned as blanks for backed blades, and these shorter blades seem to represent the final removals in core reduction. Mackay (2008b) concluded that small elongated blades were the most efficient way of recovering cutting edge from cores nearing the end of their effective use life. The trade off in conservation of raw material is the diminishing size of the small blades which would not have been useful as blanks for curation or formal tool production. The fact that blade production continued past the point where blanks were useful for formal tools suggested to Mackay (2008b) that the small unretouched blades had an intended function as well.

Sibudu Cave

Sibudu Cave is located in KwaZulu-Natal on the Tongati River approximately 15km from the present coastline (Wadley and Jacobs 2006). It has been excavated intermittently by a team from the University of Witwatersrand led by Lyn Wadley since 1998. The Sibudu sequence is noteworthy for being well-published and systematically dated and having multiple Post-HP occupations. Sibudu is one of the few well-excavated sites that have both stratified SB and HP. The system for describing the cultural stratigraphy at Sibudu, which was also used at RCC, has come into favor in recent publications. This is in part due to the redating of HP and SB occurrences across southern Africa that allows for tighter correlations of MSA site sequences (Jacobs et al. 2008).

Sibudu Cave lithics are made from a different group of raw materials than those of PP5-6, including course-grained igneous dolerite and more fine-grained hornfels along with quartz (Delagnes et al. 2006). Dolerite is available locally in primary context as tabular nodules and as rounded cobbles in the Tongati River in front of the cave. Hornfels exposures and quartz occur within 20km of site and may have been available as nodules in the Tongati River. Dolerite is more coarse-grained in comparison to the hornfels that was used at Sibudu.

The Sibudu sequence begins with the Pre-SB which has been OSL dated to ~77 to 72.5ka (Jacobs et al. 2008). The Pre-SB, which sits either on bedrock or a layer of rockfall, has not yet been described in publication but lithics include unifacial points (Wadley and Jacobs 2006). The SB at Sibudu occurs in the RGS and RGS2 layers and is dated to 70.5ka (Wadley 2007; Jacobs et al. 2008). Most of the SB retouched tools are made on dolerite but with reduced proportions of dolerite elevated percentages of hornfels in comparison to the overall debitage sample (Wadley 2007). Most of the

retouched tools are bifacial points (the majority of which are fragmentary) with rounded or pointed bases. It has been argued that the bifacial points may have been used as knives based on microwear residue analysis, although several point fragments are suggested to have been used as hunting weapons based on spin-off fractures and blood/animal fat residues on the tips (Lombard 2006). Debitage is described as consisting mainly of flakes with few blades. Several unifacial points and backed pieces are present in the Sibudu SB.

The SB is followed by an occupation hiatus and then the HP (c. 62-65ka), which occurs in layers PGS, GS2, GS, GR, and GR2. The HP layers are reported to have blades and a large sample of backed pieces, which are made more frequently on fine-grained hornfels (n=53) in comparison to dolerite (n=29) and quartz (n=14) (Delagnes et al. 2006; Wadley 2008).

Wadley and Mohapi (2008) noted size differences in the backed pieces made on the three predominant raw material types. Dolerite segments have the highest measurements in length, width, and thickness, quartz segments are short and narrow, and hornfels segments fall in between. They also noted a change in size through time associated with raw material use with the youngest HP segments being the largest and made mainly from dolerite, and segments from the oldest made on hornfels and quartz. Different hafting and function are suggested for the smaller quartz backed pieces, perhaps as projectiles or other armatures, based on their apparent standardized size in terms of length/breadth, although nearly all backed pieces are argued to have had the potential to be components of hunting weapons (Wadley and Mohapi 2008).

Three occupations occur above the HP at Sibudu. The first is the Post-HP at ~60ka (Cochrane 2006). Dolerite is the most commonly used raw material in the Post-HP, although quartz and quartzite are briefly predominant in layers immediately following the HP. The quartz and quartzite, which co-occur with ground stone and an anvil, are suggested to function as a temporary replacement for the dolerite and hornfels used throughout the rest of the sequence. The few cores present are suggested to be heavily reduced. Debitage is generally small and variable with some prepared core products. Blades and bladelets occur in low frequencies. Formal tools include retouched unifacial points and a variety of scraper forms with three backed pieces.

The RSP Layer at Sibudu is described as “Late MSA” and occurs at c. 53ka (Villa et al. 2005). Unifacial and unretouched points, as well as two bifacial points, make up the largest category of formal tools in the RSP layer, which also includes broken point tips, scrapers, burins, scaled pieces, denticulates, and other miscellaneous forms. Hornfels was

favored for retouched tools (70%). Villa et al. (2005) noted a low percentage of cortical products, suggesting that cores were initially reduced elsewhere. The most recent MSA occupation at Sibudu is described as the "final MSA" and is OSL dated to ~37ka (Wadley 2005). The final MSA continues to have pointed forms with bifacial and unifacial points. A few examples of hollow-based points and several large backed segments are present. The complete debitage assemblage consists mainly of flakes and low percentages of blades and bladelets. Raw material percentages favor hornfels across most categories although the small core sample was made primarily on quartz.

Overall, the entire Sibudu Cave assemblage appears to show an emphasis on pointed tool forms, many of which were unifacially or bifacially worked. Dolerite and hornfels are used throughout the sequence with a brief period between the HP and Post-HP where quartz and quartzite use peaks. Hornfels is more fine-grained than dolerite, and it appears to have been preferentially selected for making retouched tools. There is diversity in HP segment size that can be related to raw material. The smallest and most standardized backed pieces are made on quartz.

Apollo XI

Apollo XI cave is located in southern Namibia. W.E. Wendt excavated the cave from 1968 to 1972. Like Klasies River, Border Cave, and Rose Cottage Cave, Apollo XI has HP stratified within the Middle Stone Age. A brief description of the lithics from Apollo XI is summarized here from Wendt (1976). The basal Middle Stone Age layer (Layer H) rests on bedrock. The assemblage consists of several large points and flake-blades with some medium to small sized true blades and a few notches and denticulates also present. No radiocarbon dates were sampled from Layer H. This basal layer correlates with the MSA 2a (Volman 1984:196).

Layer G is stratified above Layer H. The assemblage from Layer G is characterized by large blades with retouched blades and flakes, a few burins, and unifacial and bifacial points. Eleven radiocarbon dates for Layer G suggest dates greater than 47,500 BP. Layer G corresponds to MSA 2b (Volman 1984:196)

Layer F is a "facies of blade industries still assigned to the Middle Stone Age" (Wendt 1976:7). The assemblage contains many small snapped blades with burins, backed blades, backed points, a few large crescents, and unifacial points. Wendt noted that a few worked ostrich eggshell fragments, pigments, and a few fragments of shell were also found. He believed that Layer F shares "certain affinities with the 'Howiesons

Poort' (Wendt 1976:7). Layer F has a single radiocarbon date of >48,000. Layer F is convincingly HP. The Apollo XI HP now has an OSL age of 63.2 ± 2.2ka (Jacobs et al. 2008).

Layer E represents the top of the MSA sequence. This layer consists of several stratigraphic horizons. Artifacts were relatively scarce. The uppermost horizon contains blades that belong to the Middle Stone Age. Wendt (1976) noted that one edge-damaged blade shows traces of mastic around its base. The upper horizon is also where three painted slabs were recovered. The upper horizon of Layer E produced radiocarbon dates of 26,300 BP, 26,700 BP, and 28, 400 BP. A single radiocarbon date from near the base of Layer E produced a date of 46,400 BP. Dates from the middle of Layer E range from 21,600 BP to 39,800 BP. Based on these dates, the painted slabs and blade with mastic found near the top of the level are probably associated with the overlying LSA (Layer D). Volman placed Layer E into MSA 3 (Volman 1984:196), and this most recent MSA is OSL dated to 57.9 ± 2.6ka (Jacobs et al. 2008).

Summary

On the basis of the stratified sites previously described, some generalizations about the Middle Stone Age sequence in southern Africa can be made. In the southern Cape, quartzite is the most commonly used raw material, though in some locations silcrete becomes an important lithic resource. Outside of the Cape, other raw materials including dolerite, hornfels, and opaline were used in varying frequencies throughout the sequences. Raw material use at many stratified MSA sites is compared in more detail in the following chapter.

The method of flake production varies widely between sites and assemblages. Common formal core types include centripetal cores, single and multiple platform cores for the production of parallel, semi-parallel, and convergent flakes, flake-blades, and true blades. Retouched tools generally occur in low frequencies except in HP and SB assemblages. Retouched points are also common at Border Cave and Rose Cottage Cave. At Montagu Cave, most of the formal retouched tools are produced on silcrete. The raw material distributions from many of the southern African stratified MSA sites are discussed in the following chapter.

3.0 The Cape MSA Raw Material Pattern

At many well-stratified MSA sites on the south coast there is a recognized shift in raw material use from predominantly quartzite utilized in the MSA II for making points and blades to an increase in the use of more fine-grained lithic raw materials, and especially silcrete, between ~75 and 65ka. This shift toward the use of silcrete and other non-quartzite stone, described here as the "Cape MSA Raw Material Pattern" (CMRMP), is most commonly cited in association with the appearance of the HP (Deacon and Deacon 1999) and SB (Minichillo 2006) MSA Industries. Quartzite frequencies increase again in post-HP occurrences at some coastal sites (Volman 1981; Wurz 2002).

Until recently, few absolute dates would allow for the raw material sequences from these coastal MSA sites to be compared to verify that the raw material shifts are synchronous. The comprehensive OSL dating study by Jacobs et al. (2008) allows for correlation between portions of the PP5-6 and Klasies River sequences and indirect correlation with Nelson Bay Cave and Diepkloof Rockshelter, using the presence of HP occupations from c. 65 to 60ka as stratigraphic markers (Jacobs et al. 2008). It is important to note that most sites (including PP5-6) have significant gaps in their occupation sequences (Jacobs et al. 2008). Diepkloof Rockshelter is located approximately 18km from the present coastline, but it has a stratified sequence that shows some interesting similarities with PP5-6 and is included for comparative purposes. Only Diepkloof and Sibudu Cave have both SB and HP occurrences; Die Kelders Cave 1 would appear to have neither SB nor HP.

PP5-6 shows the most exaggerated raw material pattern of all coastal sites if the depth of sequence is considered (Fig. 5). The shift from quartzite to silcrete and other non-quartzite stone use begins between 76 and 79ka, with pronounced peaks from 71 to 72ka and 60-65ka. Increased quartz use is also a clear feature of the CMRMP. Quartzite use at PP5-6 (by percentage of lithic artifact count) only returns to greater than 50% during the immediately post-HP occupations. The Klasies River sequence shows a less pronounced shift away from quartzite, but as with PP5-6, increased percentages of non-quartzite materials occur around 72ka and c. 60-64ka. In fact, peaks occur prior to the HP at PP5-6 (SADBS), Diepkloof (Jeff), and Klasies River (Layer 22). At PP5-6 and Klasies River, this pre-HP shift is dated to c. 72ka at both sites (Jacobs et al. 2008; Brown et al. 2009). The initial peak at Diepkloof occurs between the SB and the early HP. At Die

Kelders Cave 1, the frequency of silcrete artifacts peaks in Level 12 but is not associated with retouched formal tools (Volman 1984; Brown 1999; Thackeray 2000). Currently, no published OSL dates and no SB or HP markers at Die Kelders allow for direct comparison.

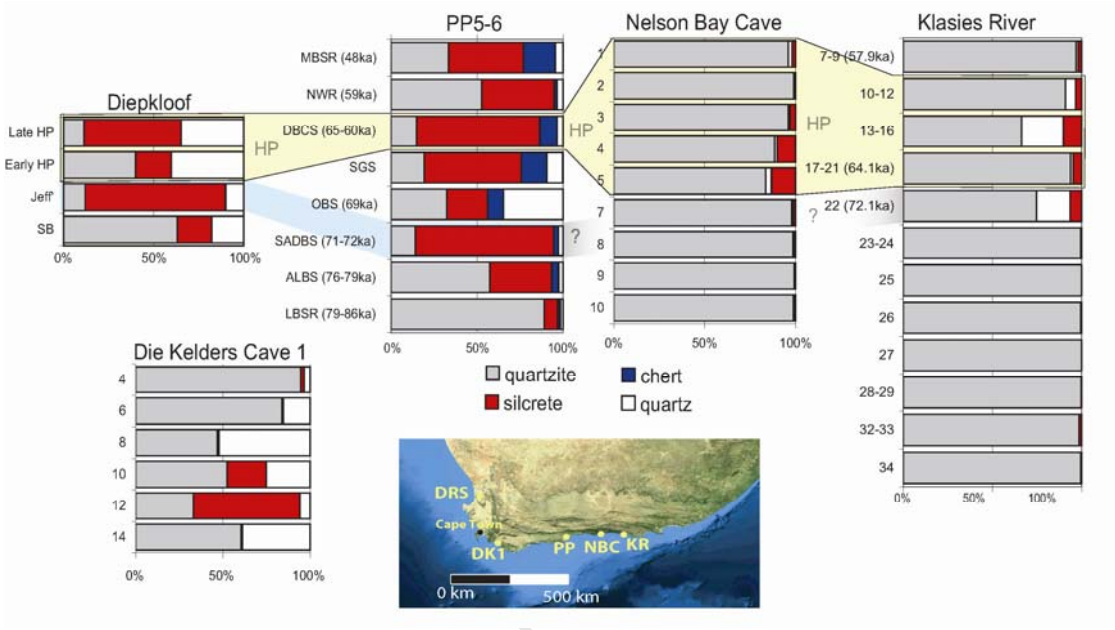

Figure 5. Raw material percentages from stratified coastal MSA sites. The stratigraphic position of the HP is shown with yellow shading and the pre-HP increase in silcrete and quartz use is shaded in blue. Diepkloof from Mackay (2008a) except for Layer Jeff from Porraz et al. (2008); Nelson Bay Cave from (Volman 1981); Klasies River from Singer and Wymer (1982). Silcrete was combined with other fine-grained raw materials by Volman for Nelson Bay Cave

The TL or OSL samples do not appear to have been taken strictly from Diepkloof layer Jeff, but an OSL sample taken from the John/Jeff interface provided an age of 63.3 ± 2.1. Diepkloof layer Kate/Kerry, which occurs approximately 30cm below Jeff and is characterized as SB, has an age estimate of 70 ± 2.3ka (Jacobs et al. 2008, but see Tribolo et al. 2009). At present, it would appear that the raw material peaks associated with PP5-6 SADBS and Klasies River layer 22 could be contemporary with the SB (but are clearly not SB), and the DRS Jeff peak occurs between the SB and early HP, and may be chronologically separated from pre-HP peaks at the other two sites by c. 2000 years.

This pre-HP increase in silcrete use is noteworthy in light of the consensus association between the HP and use of fine-grained raw materials (McBrearty and Brooks 2000). In fact, the early jump in silcrete use occurs at most sites prior to the HP, and is

associated with relatively small blade technology and rare formal retouched tools. Thus, the pattern of inflated silcrete and quartz may appear prior to the HP at some sites (Ambrose 2002). At PP5-6 and Diepkloof Rockshelter, the pre-HP silcrete frequencies are actually greater than in the following HP. The general association between the HP and silcrete use therefore holds true but the pattern is set prior to 65ka.

At the coastal stratified sites, silcrete is not always the predominant raw material used to make backed pieces (Fig. 6), but nearly every site shows inflated silcrete percentages when compared to pre- and post-HP assemblages. Coastal sites with SB occupations also show a preference for silcrete in the production of SB bifaces from approximately 70 to 72ka (Minichillo 2006; Villa et al. 2009), but raw material frequency from pre- and post-SB levels at these sites has not yet been published.

Change in raw material use is less dramatic at stratified inland MSA sites (Henshilwood 2008), but more "fine-grained" or "sharp-edged" materials were still preferentially selected for the production of retouched tools (Fig. 7). Montagu Cave exhibits an even representation of silcrete and quartzite in the early HP layers and then quartzite remains at 60% to 70% for the remainder of the HP and post-HP sequence (Volman 1981). At Rose Cottage Cave, raw material percentages remain fairly constant through the sequence but there is a slight decrease in the percentage of opaline from the bottom to the top of the sequence at the expense of "tuff," but backed pieces were made almost exclusively on opaline (Soriano et al. 2007). Border Cave also shows a more even representation of raw materials across the sequence with a slight elevation of chalcedony during the HP except in HP layer 3BS+3WA where chalcedony jumps to almost 40% (Fig. 21) (Beaumont 1979). Raw material percentages for the complete Sibudu sequence are in preparation (Lyn Wadley pers. comm.), but they are not currently available for this analysis.

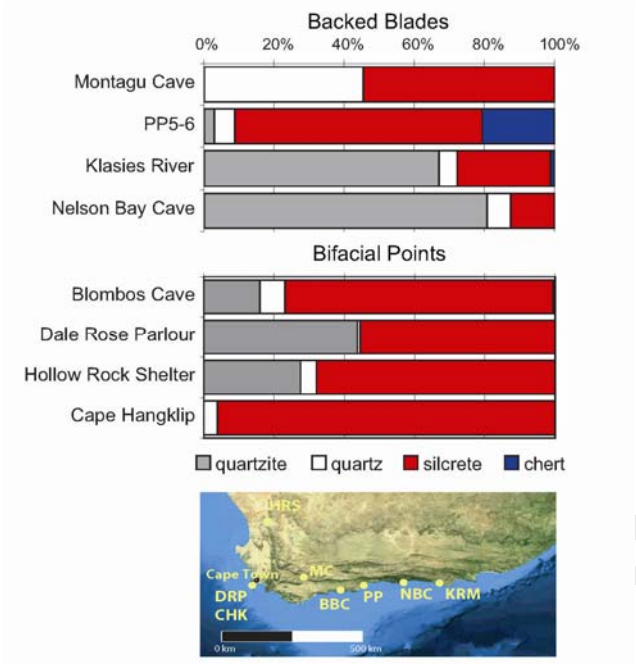

Figure 6. Raw material percentages used for making backed blades and bifacial points at selected MSA sites. Montagu Cave from Keller (1973) and Nelson Bay Cave from Volman (1981); Klasies River from Singer and Wymer (1982); Blombos from Henshilwood et al. (2001b); Dale Rose Parlour, Hollow Rock Shelter and Cape Hangklip from Minichillo (2005)

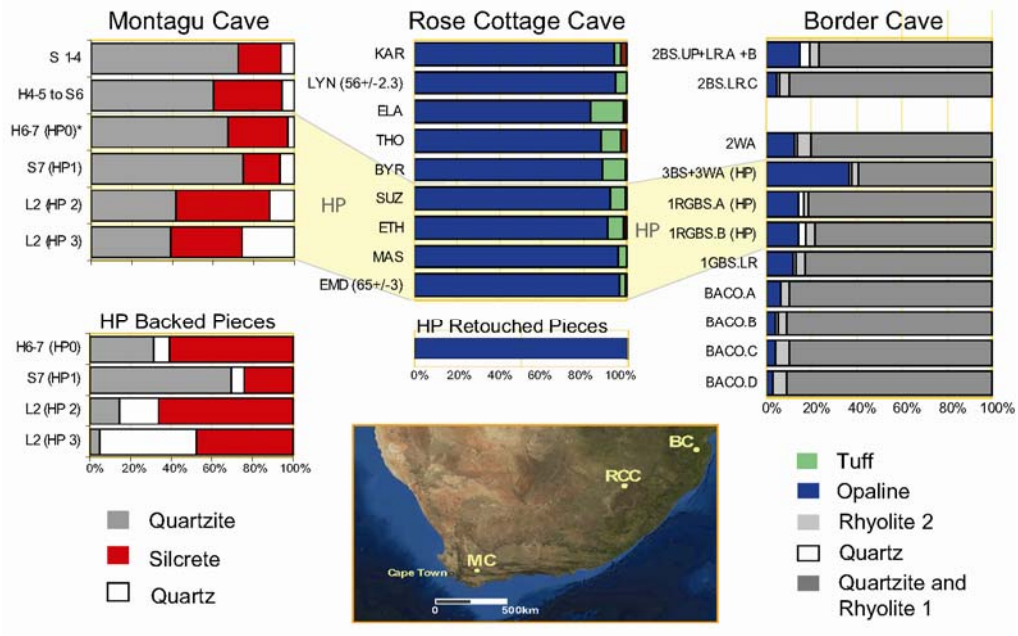

Figure 7. Raw material percentages from stratified inland MSA sites. Montagu Cave from Volman (1981) except Horizon 6-7 from Brown (1999); Rose Cottage Cave from Soriano et al. (2007); Border cave from Beaumont (1979)

3.1 Existing Models

Three primary models have been put forward during the past two decades to explain the increase in fine-grained raw material use that occurs in MIS 4 and the corresponding appearance and subsequent decline of associated backed blade tools and bifaces. Ambrose and Lorenz (1990) portrayed raw material selection as a side effect of changing mobility patterns, resulting from climate and resource base change. Minichillo (2006) challenged Ambrose and Lorenz's assumptions of raw material availability. H.J. Deacon (1989) argued that the increase in use of fine-grained "exotic" stone was evidence for reciprocal exchange similar to that seen in modern ethnographic groups to cope with environmental stress. In support of H.J. Deacon (1989), Wurz (1999) found no technological differences in how Klasies materials were flaked in the HP. Mackay (2008a) did find technological differences in the conservation of raw materials at Klein Kliphuis and Diepkloof Rockshelter (EL/M), and he argued for economic advantages associated with fine-grained material use during harsher climates to explain the raw material shift.

Ambrose and Lorenz (1990) proposed an inverse relationship with exotic raw materials and resource abundance and predictability. In their model, technological change was presented as the product of change in human foraging range size, degree of information sharing, and territoriality. These changes were argued to be in response to fluctuation in the abundance and predictability of resources (Ambrose and Lorenz 1990). Ambrose and Lorenz inferred that HP assemblages occur toward the end of the last interglacial, when the climate became cooler and drier. They argued that faunal remains appear to demonstrate a shift to more open grassland. Thus, the resource base is less predictable and abundant, mobility increases, and a corresponding increase occurred in the frequency of non-local raw material encountered on the landscape. This argument is essentially an application of Binford's (1979) embedded procurement strategy model that suggests all raw materials are obtained during other subsistence activities. Ambrose and Lorenz concluded that HP populations were not able to adapt to changing conditions in the same way as LSA populations. They rejected the alternative explanation that raw material procurement patterns changed as a result of technological change.

The competing hypothesis proposed by H.J. Deacon (1989) argued that the selection of exotic raw material in the HP results from the reciprocal exchange of hunting equipment similar to that observed in ethnographic research with San hunter gatherers.

For Deacon, reciprocal exchange was viewed as a means for coping with environmental stress brought on by the colder climates of MIS 4. Deacon used this aspect of raw material selection to support his contention that anatomically modern humans in the Middle Stone Age were behaviorally modern.

Wurz (1999) provided supporting evidence for H.J. Deacon's (1989) theory by performing a comparative metric analysis of backed artifacts from Deacon's more recent excavations of Klasies River. She found only marginal differences in size between backed artifacts across raw material categories. While Wurz (1999) believed that the overall pattern of increased use of non-local raw materials was deliberate and significant, she found no functional difference in the way that local and non-local materials were used. The advantage implied in the use of non-local materials was then interpreted as being symbolic or provided by the artifact maker.

Mackay (2008a) argued that the climate conditions of OIS 4 and the HP MSA pressured tool makers to maximize the economic recovery of edge length from a given mass of raw material. MSA tool makers gradually intensified their efforts to locate raw materials that would satisfy the need for flake production that maximized cutting edge and reduced mass. As the selective pressures eased toward the end of OIS 4, the requirements for fine-grained raw materials diminished. In contrast to the Mobility Model, Mackay argued that at Diepkloof Rockshelter and Klein Kliphuis, raw material selection was not a function of distance to source but rather a need for materials that allowed for the production of thin flake blanks. These flake blanks would maximize core life by conserving core volume.

Each model makes use of a different theoretical mechanism to explain the raw material patterning, and all can be examined in light of the main theme brought out by the Binford-Gould ethnography debate. The Ambrose and Lorenz (1990) model is an example of embedded procurement (McBrearty and Brooks 2000) where fine-grained raw material is selected because increased human mobility is hypothesized to have brought people closer to non-quartzite raw materials as they ranged on the landscape. Raw materials were flaked the same way, regardless of type or source. The H.J. Deacon (1989) and Wurz (1999) model can be regarded as an example of non-functional selection. Stone or backed tools produced on non-local materials have an abstract value unrelated to its physical properties (except color), and all raw materials were still flaked in the same manner. The Mackay (2008a) model would be most closely aligned with the Gould and Saggers (1985) argument that lithic material patterning in the archaeological

record represents evidence for the deliberate selection of specific raw materials because of functional properties that make one stone better than another for a specific task.

In reality, the behavior behind the CMRMP may include aspects of each of the previous models in that change in mobility and symbolic and functional selections of raw material should all have some effect on the technological strategy employed at a given time. However, all assume a link between fine-grained material use and "cold" or "harsh" climates of MIS 4 without the benefit of a regional high-resolution terrestrial climate record. The effects of Pleistocene glaciation on the Northern Hemisphere do not necessarily apply to the expression and duration of MIS 4 in southern Africa, which has an extremely variable climate signature (Chase 2010; Bar-Matthews et al. 2010).

An additional shortcoming is that the above models do not address the apparent differences in raw material patterns between the coastal and inland sites (Henshilwood 2008). Lithic assemblages from coastal sites typically show an increase in non-quartzite raw materials that occurs within a similar time range in MIS 4. Changes in raw materials at inland sites are more subtle. Most sites with an HP assemblage, regardless of location, show some preference for fine-grained raw materials for the production of backed pieces. Models need to account for what was happening on the coast that seems to have exaggerated the shift in raw material use that either did not occur at the inland sites or were more subtle in expression.

The Pinnacle Point speleothem record indicates that weather patterns and vegetation regimes fluctuated quite dramatically in MIS 4 (Bar-Mathews et al. 2010), and the coastline was dynamic (Fisher et al. 2010). Changes in coastline should have influenced distance to raw material source, as well as site use patterns (Marean 2010a). Changes in landscape should have influenced aspects of tool design and use and thus the functional requirements of raw materials.

3.2 PP5-6 Site Context Model

Two recent publications complement the archaeological record at PP5-6, and provide a novel way for developing the paleoenvironmental context of the archaeological sequence. These papers are the product of interdisciplinary research initiated by the SACP4 project directed by Curtis Marean of Arizona State University and are summarized here. Bar-Matthews et al. (2010) provided a local terrestrial, speleothem-based carbon and oxygen isotope record that complements the PP5-6 sequence

chronology. Fisher et al. (2010) developed a paleoscape model that estimates the position of the coastline in 1500-year increments for the past 420,000 years for the Mossel Bay region of South Africa. The output of these research projects provides a means for investigating ancient weather patterns, vegetation regime, and paleoenvironmental context for each PP5-6 stratigraphic aggregate (to be covered in other publications). For the purposes of this project, such a foundation allows for the construction of more detailed modeling of raw material availability with respect to the dynamic paleoscape (i.e., distance to coastline for cobbles, open/closed nature of vegetation for silcrete collection).

The following is summarized from Bar-Matthews et al. (2010), who analyzed multiple overlapping speleothems that formed in Crevice Cave at Pinnacle Point, located approximately 150m from PP5-6. The speleothem samples were U-Th dated from 53-90ka (PP5-6 sequence described in this thesis spans c. 48-85ka) at a time when Crevice Cave was sealed by a dune. Approximately 152 growth laminae were sampled, providing extremely high-resolution $\delta^{18}O$ and $\delta^{13}C$ isotopic curves. Changes in $\delta^{18}O$ are posited to represent variations in summer and winter rainfall regimes, as compared with an analysis of systematically collected modern rainfall samples from Mossel Bay. The $\delta^{13}C$ is interpreted to represent fluctuations in the proportions of C3 shrubby vegetation and C3 grasses, which have relatively depleted $\delta^{13}C$, perhaps similar to the modern Proteoid and Restiod Fynbos communities, and the influx of C4 grasses which are more enriched in $\delta^{13}C$, and may be representative of more open Grassy Fynbos or Thicket vegetation.

The Crevice Cave speleothem is compared against a Holocene $\delta^{13}C$ record from Pinnacle Point and a mixed C3/C4 signal from Cango Cave speleothem (Talma and Vogel 1992). The Crevice $\delta^{18}O$ and $\delta^{13}C$ curves are correlated, suggesting that low $\delta^{18}O$ values, indicative of more winter rainfall, correlate with an increase in C3 vegetation and higher $\delta^{18}O$ values from increased summer rainfall correlates with an increase in C4 grasses. The implications of the Crevice Cave isotopic record for human behavior are that the late MIS 5 interglacial period at Pinnacle Point is characterized by more winter rainfall and shrubby fynbos vegetation and the onset of MIS 4 glacial conditions produce increased summer rainfall and an increase in C4 grasses at Pinnacle Point. Importantly there is also a significant global climate excursion documented in the Crevice Record at c. 72ka which may have led to extreme unpredictability in global and local climate conditions as expressed in rainfall patterns and vegetation (Bar-Matthews et al. 2010).

Fisher et al. (2010) developed a GIS-based sea level curve for the southern African coastline that takes into account the topography of the submerged and gently sloping Agulhas Bank and the sea cliffs at Pinnacle Point. This approach is a major advance over outdated 2-dimensional models that calculate distance to coast using vertical sea height and distance from a single point on the coastline. The Fisher et al. model is dynamic in that it provides estimates of coastline at 1500-year increments. It is tested using strontium isotopes from Pinnacle Point speleothem (as an independent proxy for distance to coastline) and shellfish abundance at PP13B and Blombos Cave (intersection of coastline and hunter gatherer daily foraging range). In this study, data from the Fisher et al. (2010) model will be used to estimate relative distance to dynamic sources of lithic raw materials (beach cobbles) from PP5-6, and to make general predictions on the extractive technology required for a given site context (inland vs. coastal resource base).

An alternative hypothesis for explaining change in raw material use is proposed here, utilizing the new paleoenvironmental data for Pinnacle Point. The "Site Context Model" postulates that differential use of quartzite and fine-grained lithic raw materials may be linked to the position of PP5-6 on the landscape relative to the coastline for a given time interval during the late Pleistocene. The distinction made here is that where Ambrose and Lorenz argued that *people* were increasing their movements, here it is the relative context of the site on the landscape that is also argued to be 'moving'. At one extreme, during global warm periods, the site is located directly adjacent to the coastline with an implied emphasis by cave inhabitants on coastal and fynbos resources. At the other extreme, during global cold periods, the cave may have been located as far as 30 to 40km inland (Fisher et al. 2010).

During coastal occupations at PP5-6 (coastline similar to today), MSA tool makers were more likely to gather locally available quartzite beach cobbles, accentuating the quartzite-dominated pattern seen at PP5-6 and perhaps at other coastal sites, particularly during MIS 5 occupations. Active beaches are dynamic, and ocean swell, tidal activity, and storm surges act to reshuffle and replenish beach cobbles and provide regular access to new material. Other secondary context raw materials, including silcrete and hornfels, may have also been collected in lower frequencies as encountered on beaches creating a raw material pattern generated from a selection of materials locally available in secondary context.

During periods of coastline regression and more inland occupations of PP5-6, knappers would still have had access to cobbles, but the more easily accessible higher quality stone cobbles would have been quickly depleted without an active energy source to replenish materials. As distance to secondary context raw materials increased, other terrestrial stone resources became more attractive. Improvement in flaking quality of more locally available silcrete through heat treatment may have been one strategy to reduce search costs during these inland occupations (Brown et al. 2009).

An association between raw material use at PP5-6 and fluctuations in the $\delta^{13}C$ record at Crevice Cave have been discussed elsewhere (Bar-Matthews et al. 2010), but is investigated in greater detail here. The Crevice Cave speleothem record tracks vegetation change and fluctuation from 53 to 90ka. It has been argued that fynbos occurs along a coastal strip that moves along with changes in the coastline (Bar-Matthews et al. 2010; Marean 2010a). During coastline retreat, the predominantly fynbos vegetation, with a strong C3 signature, retreats out on the Agulhas Bank and is replaced with a mixed or mosaic C3/C4 vegetation regime. The fynbos and C3 signature is also argued to be associated with a predominantly winter rainfall regime plus mixed C3/C4 signature, with C4 grasses and increased summer rainfall (Bar-Matthews et al. 2010).

The model introduced here uses modern raw material availability as a baseline to evaluate the relative contributions of landscape change and functional demand as explanations for the raw material shift. In other words, the model evaluation attempts to identify whether or not some of the coastal MSA raw material patterning can be explained primarily by changes in the coastline and fluctuations in the geographic distribution of cobble beach sources. The Site Context Model is not proposed as a direct explanation for the appearance and disappearance of the SB and HP, which occur at a number of sites (Sibudu Cave and Montagu Cave for example) where raw material availability would not have been directly affected by coastline movement.

The current challenge in linking the PP5-6 archaeological sequence with the paleoenvironmental data and coastline models is that the temporal resolution of the data occurs at different scales. The published and unpublished OSL dates for PP5-6, kindly provided by Zenobia Jacobs of Wollongong University, Australia, have a resolution of approximately ± 3000 years. The coastline model is scaled at a resolution of 1500-year increments (Fisher et al. 2010), and the isotopic data from the Crevice Cave speleothem is accurate to the century or even decade level (Bar-Matthews 2010).

3.3 Model Evaluation Methodology

The primary goal of this research project is to investigate the association between the dynamic PP5-6 raw material sequence and the local paleoenvironmental record. This is done to assess the relative contribution of deliberate selective behavior of raw materials for functional reasons on the one hand, and paleoenvironmental landscape changes that may have constrained raw material availability on the other hand. Several of the models developed to explain the CMRMP have failed to find any significant technological differences across raw material categories that would support deliberate selective behavior of raw materials for functional reasons (Ambrose and Lorenz 1990; H.J. Deacon 1989; Wurz 1999). PP5-6 is a good test case for these models because the raw material patterning is exaggerated in comparison to the other sites discussed here. The results of this analysis will be used to evaluate the Site Context Model and other published models, and also to develop a series of assumptions and hypotheses concerning raw material availability and use that can be investigated and tested in the next phase of Pinnacle Point research.

The model evaluation is phased in the following way. A regional literature review and field survey was conducted to develop test hypotheses concerning the availability and distance to source of raw materials found at PP5-6 (Ch. 5). Expectations for raw material use, based on distance to coastline, are developed. The PP5-6 raw materials sequence is then dissected in high-resolution to see if micro-patterning in raw material can be associated with the coastline model and proxy indicators of climate change (Ch. 6).

A descriptive analysis of the PP5-6 lithic sequence is presented in Chapter 7 following the raw material analysis. Then focused technological analyses will target attributes that have been experimentally linked to raw material economy and how economy relates to the knapper's decision-making process from material preparation to tool production. A recent study (Brown et al. 2009) demonstrated that many silcrete artifacts from PP5-6 were heat-treated to improve flaking properties. Heat treatment, if differentially applied to raw materials, already indicates important technological and economic differences between raw materials, and represents a significant investment in preparation time. Silcrete artifacts were examined for the presence of characteristic heat treatment luster (Luedtke 1992; Brown et al. 2009) using a gloss meter (Ch. 8).

The analysis of core primary form and cortex characteristics (Ch. 9) will provide an indication of the origin for each raw material class (primary or secondary). Analysis of cortex and core attributes will determine the form or "package" in which the materials were transported to the site. The quantification of cortex abundance (Ch. 10) attempts to provide an estimate of which stages of manufacture are occurring on the site for a given stratigraphic aggregate and raw material, using a volumetric approach to estimating expected amount of cortex for each raw material class (Dibble et al. 2005).

Braun (2005) and Mackay (2008) demonstrated the effectiveness of using the ratio of edge length to mass to track material conservation. A flintknapper wishing to control flake morphology can alter the flake platform angle and size (Dibble 1997) and thus control the length of cutting edge produced from a given mass of material. It is expected that there would have been an effort to conserve mass during flake production when raw materials were transported to site over greater distances. The ratios of cutting edge to mass (CE/M) are compared across raw material categories through the PP5-6 sequence (Ch. 11).

The dependence of the test variables and distance to coastline are evaluated against the predictions of the Site Context Model using Kendall's Tau test of rank correlation. This non-parametric test is used because many of the sample sizes are very small and not normally distributed and thus subject to extreme levels of homoscedasticity that would invalidate the assumptions of parametric measurements of association. Test variables based on raw material ratios were often logarithmically transformed in order to better visualize the data and adjust for different scales of measurement. In situations where the logarithmic transformation would have resulted in a negative number, a constant (1.0) was added to avoid the calculation of a logarithm of zero which is undefined. The test variables for each stratigraphic assemblage are then compared with distance to coastline calculated by using the mean of the average distance to coastline in Fisher et al. (2010) Supporting Online Material (SOM) adjusted to the mean OSL age of each stratigraphic assemblage including the full range of the OSL error bars (Table 3). The statistical evaluation of each test variable is detailed individually in Chapters 8-11.

3.4 Summary of Model Expectations and Assumptions

Expectations and assumptions for the following detailed analyses are presented here and summarized in Table 1. In some cases, it will be demonstrated that small sample

sizes make conclusive statistical comparison impossible at present, but the conclusions presented can be tested with larger samples from planned excavations at PP5-6 in 2011 and from other sites. Some of the test expectations will require higher level statistical modeling with the Crevice Cave isotopic record and coastline model as well as additional sampling and finalized dates for the PP5-6 OSL chronology. This modeling will occur as part of a collaborative effort prior to the publication of the more qualitative results presented in this dissertation. Major assumptions are explicitly presented so that they may be revisited and tested as new field studies are initiated. The results are summarized at the conclusion of each chapter and then the Site Context Model is evaluated in total in Chapter 12.

1. Raw Material Availability Expectations: Transport costs are lower for local materials. When cobble beaches were close to PP5-6, MSA knappers at the shelter would have used quartzite cobbles in greater frequency than material from distant sources. Conversely, when cobble beaches moved farther away from site during coastline regression, MSA knappers at PP5-6 would have turned to inland sources and most notably silcrete for the supply of raw materials.

    Evaluation Methodology: A chi-square goodness-of-fit analysis will be performed on major raw material classes to test whether the raw material proportions for each assemblage are significantly different than what might be expected by chance. The ratio of quartzite to silcrete (by assemblage weight) is then compared against the Pinnacle Point mean distance to coastline data presented in Fisher et al. (2010) for each assemblage using a non-parametric test of correlation.

    Assumptions: MSA knappers would have preferred cobbles from active beaches rather than raised beaches or alluvial deposits. High-energy beaches would have provided a constantly replenished or reshuffled supply of material in a context where raw material quality could be easily assessed by visual and mechanical criteria. Cobble beaches in the past provided low frequencies of non-quartzite cobbles, in similar proportions that they are found today. Silcrete deposits do not occur on the submerged Agulhas Bank within a few kilometers of site (Ch. 5.1).

2. Cortex Type: Expectations for cortex are similar to those for raw material in (1) above. In occupations where cobble beaches are close to the site, cortical lithics should exhibit higher percentages of beach cobble cortex. Conversely, when the coastline is modeled to be farther away, primary context (outcrop) cortex should be more common.

    Evaluation Methodology: The mean distance to coastline for PP5-6 raw material classes is compared against the ratio of cobble to primary outcrop cortex. The ratio should be highest when the coastline is modeled to bring cobble beaches close to site and decrease during coastline regression.

    Assumptions: The coastline around Mossel Bay today has stretches of sandy, rocky, and cobble-strewn beaches. The assumption is that cobble beaches would always be present along the coastline regardless of its geographic position relative to PP5-6.

3. Raw Material Preparation Expectations:

    1. It is hypothesized that heat treatment is an important stage in the reduction process for the systematic use of silcrete (Brown et al. 2009). PP5-6 analytical samples with high percentages of silcrete are expected to show higher frequencies of heat treatment tracked by gloss analysis.
    2. It is expected that silcrete collected from cobble beaches would have been used more like the other materials collected from secondary contexts, including hornfels and quartzite, which are not amenable to heat treatment. Gloss distributions from occupations—where beaches are proposed to be a major source of raw materials—are expected to have lower maximum gloss distributions than those occupations where primary outcrop silcrete is the predominant raw material used.

4. Cortex Abundance: It is expected that transport costs of raw material would increase with distance to source. Materials transported to site from greater distances should have less cortex present than occupations occurring in proximity to cobble beaches.

Evaluation Methodology: The hypothesized distance to source for PP5-6 raw material classes in each assemblage is compared against the Cortex Ratio of total observed versus expected cortical surface area (Dibble et al. 2005).

Assumptions: The coastline around Mossel Bay today has stretches of sandy, rocky, and cobble beaches. The assumption is that the coastline would have always had some cobble beaches present regardless of its location for a given time period.

5. Debitage Metrics: As noted above, weight would have been a consideration in transporting materials to site. It is expected that materials transported over longer distances would be smaller and lighter than those available in the immediate vicinity of the site.

   Evaluation Methodology: Comparison of mean dimensions and maximum dimensions for debitage and core size for complete debitage for each analytical sample. Mean flake length is compared against distance to coastline for each assemblage using a non-parametric test of correlation.

6. Raw Material Conservation: Materials with higher transportation and processing costs are more likely to have been conserved in comparison to raw materials available in the vicinity of site.

Evaluation Methodology: The ratio of cutting edge to mass (CE/M) is a measure of the amount of cutting edge recovered from a given volume of raw material. It is expected that materials transported over longer distances would have higher cutting edge/mass values than raw materials available more locally. Mean CE/M is compared against distance to coastline for each assemblage using a non-parametric test of correlation.

Table 1. Site Context Model analysis test expectations

Analysis	Test Expectations	
	Coastline Near	***Coastline Far Away***
Raw Material	Greater use of local quartzite	Increase in materials from inland
Cortex	More beach cobble cortex	More primary cortex
Heat Treatment	Lower percentage of heated silcrete	Higher percentage of heated silcrete
Cortical Reduction	More cortical products	Less cortical products
Debitage Metrics	Larger products	Smaller products
Cutting Edge/Mass	Lower ratio of cutting edge to mass	Higher ratio of cutting edge to mass

4.0 Introduction to PP5-6

PP5-6, located at -34.205954°S and 22.091380°E (Google Earth V.5), consists of two locales which were originally documented as separate sites (PP5 and PP6). They have since been grouped under one name and excavation permit because they may be stratigraphically linked. The southernmost locale, PP5-6 South (formerly PP6), is a large sea cave formed from the wave-erosion of a fault breccia seam in Table Mountain Sandstone (TMS) layers. The exposed or immediately accessible surface area of the cave measures approximately 40m N-S and 21m E-W and sits at an average of 13 meters above mean sea level (AMSL). However, a small opening at the back of the cave reveals a much larger cavern that extends some 15 meters to the west that can be accessed by crawling through a narrow passageway.

PP5-6 South has been adversely affected by surface erosion, with an incised gulley that dissects the cave mouth from the northwest to the southeast. The eroded sections of the PP5-6 South gulley exposed a seemingly intact MSA shell midden resting on a thick dune. Excavations in 2006 targeted this area (designated EG for Erosion Gulley) to assess the integrity of the shell midden. Results were disappointing and revealed significant post-depositional mixing with modern plastic and trash stratified at the base of the midden deposit. Due to their disturbed context, lithics from the PP5-6 South erosion gulley excavations were not analyzed, and this locale is not described in more detail for this dissertation.

PP5-6 North is a rockshelter located along the same rock face as PP5-6 South, centered at -34.205527°S and 22.091595°E (Google Earth V.5). The two locales are separated by a slightly protruding angle or corner in the TMS cliff face, which gives the rockshelter opening a more easterly orientation and a view across Eden Bay. PP5-6 North measures c. 37m N-S and 18m E-W with an elevation of 27.35m (AMSL) at the northern end of the site and 14.25m at the southern end. The protruding ledge above PP5-6 North, which provides a partial roof over the shelter, probably extended farther out to the east but gradual erosion of several fault breccia seams has occurred in the rock face above the site (Fig. 8). Over time, that erosion has resulted in the retreat of the overhang and several rockfall events which are captured in the archaeological sections.

As with most cave sites, PP5-6 North has a complicated formation process that is a challenge to model and interpret. This locale is unique because prehistoric erosion by

surface runoff over time has cut a profile that reveals a deep and intricately layered stratigraphic sequence. This sequence was only partially visible beneath a modern dune prior to any archaeological investigations at the site. The cleaning, sampling, and dating of this c. 11m truncated section (the "Long Section" or LS), has been the focus of seven archaeological excavation seasons from October 2006 to December 2010 (Fig. 9). Hereafter, the excavated area of PP5-6 North will simply be described as either PP5-6 or the Long Section. This author has served as site director at PP5-6 for all excavations except those in 2010 during preparation of this dissertation.

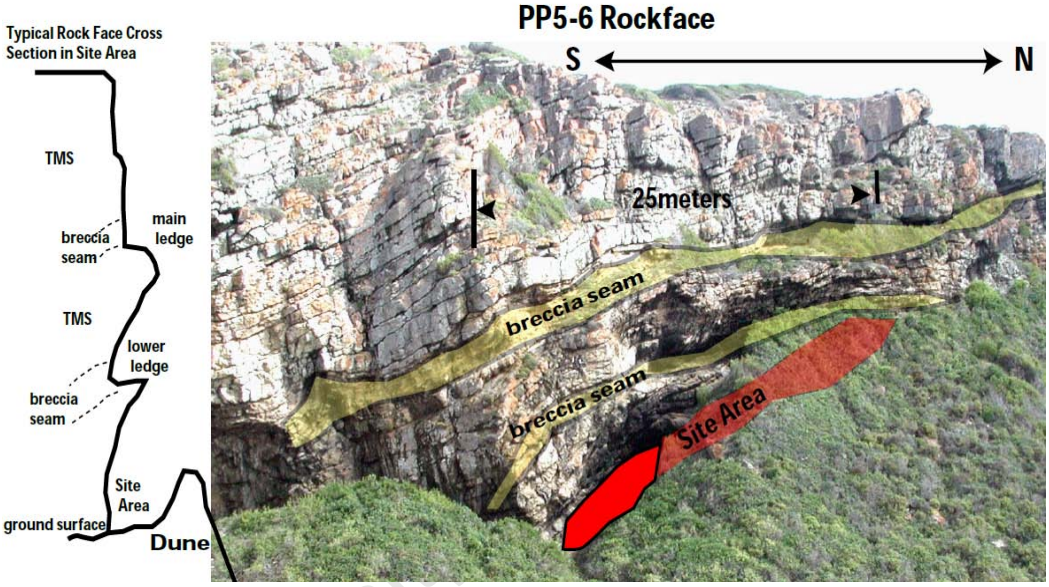

Figure 8. PP5-6 cliff face showing the site area and location of fault breccia seams that contributed to cave roof collapse

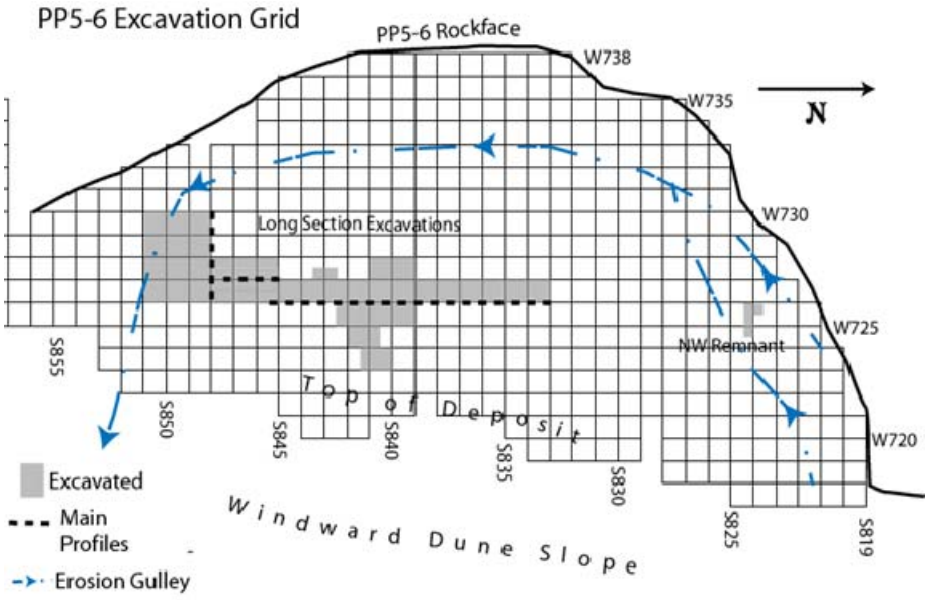

Figure 9. Plan view of PP5-6 excavations aligned to the South African National Grid

4.1 PP5-6 Site Formation Model

The following is a preliminary and simplified model of site formation that is subject to revision prior to publication. The sea caves at Pinnacle Point formed during an interglacial prior to MIS 11 (Karkanas and Goldberg 2010) with a high sea stand that eroded away softer fault breccia seams within the TMS, leaving the cave open for occupation (Fig. 10A). A number of episodes of sediment infilling and washout from subsequent sea level regression/transgression episodes has likely occurred and the basal sediment of the Long Section began accumulating at least by MIS 5c/b prior to 90ka (Z. Jacobs, pers. comm.).

Anthropogenic and geogenic sediment input eventually filled the rockshelter so that sometime after 48ka the cave was no longer open for occupation (Fig. 10B). No LSA occurs in the PP5-6 deposit, perhaps indicating that these caves were not open again until a more recent erosion event truncated the deposit (Fig. 10C). Eventually a remnant column or cone of stratified sediment was left standing in front of the rockshelter and perhaps also between PP5-6 North and PP5-6 South (Fig. 10D), which was then covered by Holocene dune sand and colluvial material from the cliffs above (Fig. 10E). It then stabilized with fynbos vegetation to its modern pre-excavation condition (Fig. 10F).

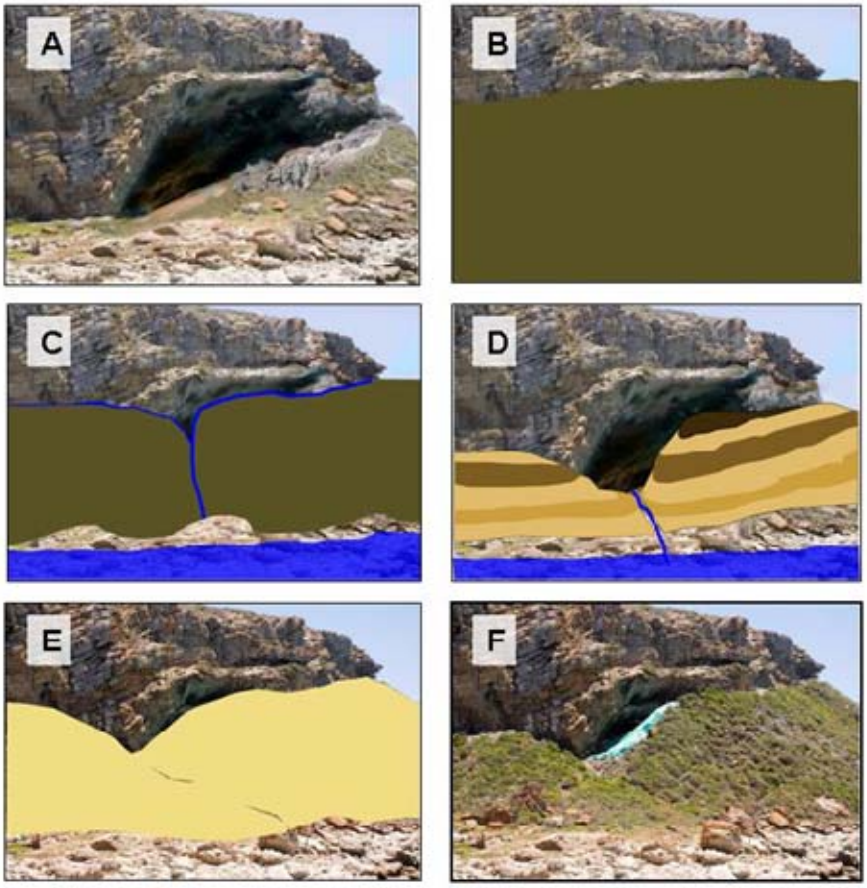

Figure 10. Simplified PP5-6 formation sequence: A) cave is carved out by high sea and is available for occupation; B) anthropogenic and geogenic sediment builds up until the cave is sealed to occupation; C) high sea stands erode the base of the deposit and an erosion gulley forms along between deposit and rock face and begins to carve an eroded profile; D) erosion continues leaving a stratified cone or column of sediment deposit; E) the remnant deposit is covered by a dune sequence; F) modern condition with vegetated dune

4.2 PP5-6 Excavation Strategies

Excavations at PP5-6 began in October 2006, with a planned strategy to start at the very top of the Long Section sediment "cone" and excavate down through the sequence proceeding layer-by-layer. A three-person team was also positioned at the northwest corner of the site where a small remnant triangle of sediment had been isolated by erosion ("Northwest Remnant"). An excavation platform was designed and used for the first two field seasons on the Long Section to provide a safe workplace on the steeply-angled surface (Appendix 1, Fig. 1). The platform, which was cabled to two long steel anchoring pins on the ocean-side of the sediment cone, could be adjusted by adding sections of chain onto the cables, allowing it to be dropped as excavation proceeded to

the base of the eroded section. Excavators were attached by a climbing harness to a separate safety cable to prevent injury by falling.

It became obvious in May 2007 that a change in excavation strategy would be needed at PP5-6 to allow for the placement of additional team members in order to accelerate progress. We were able to add work areas in what became known as the "Upper," "Middle," and "Lower" Long Sections, accommodating up to 15 excavators working at one time using platforms built from stacked sandbags and a temporary shelter (Appendix 1, Fig. 2). From May 2007 to July 2009 (four seasons), the focus of fieldwork was to achieve a continuous and clean excavated section to provide a sample of artifacts from each stratigraphic unit, OSL ages, micromorphology, and other samples for project specialists.

The stepped, erosion-truncated section at PP5-6 allowed for relatively easy access for excavation during the first five seasons and a continuous cleaned profile was achieved in early May and June 2009. The latest phase of excavation has been focused on defining the upper and lower boundaries of the Long Section sequence and has required the removal of modern overburden consisting of rockfall, colluvium, slopewash, and modern sterile dune sand. Connecting the upper portion of the Long Section to the Northwest Remnant will require the controlled excavation of a long strip (ongoing) to link the stratigraphy. Cleaning the base of the PP5-6 erosion-cut section requires a stepped pit approach more typical of other cave excavations.

4.3 Excavation Methods

Excavation methods for the SACP4 project were developed jointly by Dr. Curtis Marean and Dr. Peter Nilssen (Marean et al. 2004). The approach simulates a lab setting in the field where all provenience information is recorded to a database and checked for errors during excavation. Spatial control on the site was first obtained through differential GPS by Dr. Marean using a Trimble FC100 handheld and two Topcon HiperXT receivers that permit sub-centimeter accuracy. Permanent stainless bolts were set as control points in the rocks below the caves where good satellite reception for GPS static sessions was possible. Topcon total stations were then used to traverse from these control points to new points drilled into the PP5-6 rock face. Elevations were transferred from benchmark survey points above the cliff face.

The excavation grid at PP5-6 was established following 1-meter intervals of the South African National Grid Coordinate System (Fig. 9). Through resection function

from three known points, a total station can be used to tie into the existing South African Grid accurately and without the need for hanging grids, arbitrary datum, or string lines. An additional advantage to this system is that the archaeological grid at PP5-6 can be easily re-established in the future without the need for guesswork. Excavation squares are named by the last three digits of the northing and easting coordinates for the northeast (NE) corner of the square. However, we use the prefix "S" to identify a north-south (N-S) gridline and "W" to describe an east-west (E-W) gridline to denote the direction that the number sequence is increasing. Thus a square, whose NE corner has South African National Grid coordinates of -3786839.0 (northing) and -83726.0 (easting), would be called S839W726. Each 1 x 1m square is then excavated in 50cm quadrants named by their location within the square: NE, NW, SE, and SW.

Excavation proceeds vertically by following natural stratigraphic units, which are called "StratUnits." StratUnits include what can be variously described as geogenic sediments (i.e., aeolian sand), anthropogenic sediment layers (i.e., shell midden layers), features such as pits and hearths, as well as disturbances such as tuber cavities and burrows. All similar archaeological sediments are carefully excavated using small hand tools (mini-trowels, dental tools or bamboo skewers) as one StratUnit or as StratUnit spits for thick layers. StratUnits are named and tagged in profile for their locale, year of excavation, and a running letter sequence. All materials collected from a given StratUnit and quadrant are coded with the same lot number, and therefore this is the minimum unit of provenience for excavated materials.

All finds observed by the excavator, regardless of size, are plotted in three dimensions (X, Y, Z) using a Topcon total station and handheld computer. The handheld associates the StratUnit lot number with a unique plotted find identification number, and links these to the coordinates of each plotted object. In essence, a basic database of all plotted finds and their provenience is constructed simultaneously as excavators plot their finds. Specialist samples, StratUnit topography, GIS-rectified photography, and section drawing are also plotted by total station for the almost seamless layering of digital data. All sediment is bagged according to lot number and is wet-sieved (using freshwater) through nested 10, 3, and 1.5mm screens, and is then sorted and catalogued in the project field lab by MAPCRM staff at the Dias Museum in Mossel Bay between field seasons.

4.4 PP5-6 Stratigraphy/Context of Lithic Samples

The PP5-6 stratigraphy is described in a hierarchical classification system of stratigraphic aggregates (StratAggs), sub-aggregates (SubAggs), and stratigraphic units (StratUnits). StratUnits, as previously noted, are the individual sediment layers identified by the excavator. StratUnits can be extremely small, a smudge of ash for example, or quite large when excavating a homogeneous layer of dune sand. StratUnits greater than 5cm in thickness are broken into spits in the field for recording purposes (i.e., LS9C, LS9C1, LS9C2 etc.). SubAggs can be described as a grouping of one or more contiguous StratUnits with similar sediment and/or artifact composition. SubAggs are named according to first names of project members, participants, or other individuals. StratAggs consist of multiple contiguous SubAggs that have shared features that distinguish them from what comes above or below. The Long Section StratAggs are shown in Figure 11. As a general rule at PP5-6, StratAggs are usually differentiated by observed changes in sediment composition whereas SubAggs are usually defined by artifact density and presence or absence of anthropogenic sediment.

The following outline of PP5-6 stratigraphy proceeds from bottom to top of the site by StratAgg, starting with the base of the Long Section and ending at the Northwest Remnant. StratAgg names will be presented in italics and SubAgg names in single quotations to avoid confusion with other acronyms. A future publication will cover stratigraphy in greater detail but this description is intended to describe the context and ages for the excavated lithic samples, and provides justification for the sample analytical units that are compared for analysis. All isotopic data presented below is inferred from the Bar-Matthews et al. (2010) study of Crevice Cave and PP5-6 mean distance to coastline from Fisher et al. (2010).

Light Brown Sand and Roofspall

The Light Brown Sand and Roofspall (*LBSR*) is composed of at least 6 meters of layered sediment at the base of the Long Section (Fig. 11) from 14.2 to 19.8masl. Excavations at PP5-6 have not yet reached the bottom of the *LBSR*. Sediment input consists primarily of TMS roofspall and fault breccia that have eroded out of the rock face wall and a small contribution from windblown sand, giving the sediment a rough texture. Few large blocks of roofspall (>10cm) are present. The *LBSR* is characterized by alternating layers of occupation and abandonment. Occupations are visible in profile as

dark organic-rich bands of sediment with abundant shellfish remains and combustion features (Fig. 12). It appears that shellfish collection was the focus of these occupations. In between the darker shellfish-rich layers are mostly sterile bands of light brown roofspall and breccia. Each alternating light/dark *LBSR* layer was assigned a unique SubAgg name in the field.

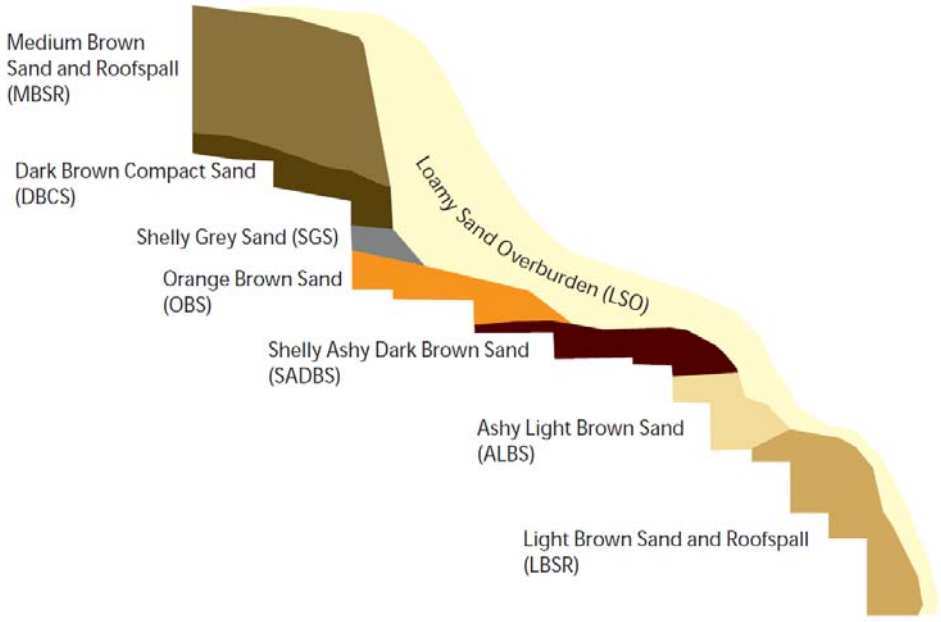

Figure 11. Schematic diagram of the PP5-6 Long Section east profile (north is to the left). The *LBSR* StratAgg continues in depth below what is depicted here.

The *LBSR* has been OSL dated from 79 ± 3ka at the top to 86 ± 3ka (Fig. 13b) at the base of the October-November 2008 excavations (Brown et al. 2009). Currently, 4.5m of exposed *LBSR* eroded profile are beneath the lowest calculated age; additional OSL samples were taken in May-June 2009. The OSL ages place the exposed *LBSR* within MIS 5b (Martinson et al. 1987; Shackleton et al. 1990). The Crevice Cave $\delta^{13}C$ curve (Fig. 13a) suggests a relatively stable vegetation regime at this time (Bar Matthews et al. 2010) and the distance to the coastline (Fig. 13c) was similar to the present (1-2km of the site).

Figure 12. Upper LBSR Sequence view north: The tagged profiles have been excavated, and the untagged profile is the cleaned and unexcavated eroded section

Ashy Light Brown Sand

The Ashy Light Brown Sand (*ALBS*) occurs directly above the *LBSR* at 19.8 to 20.6masl. This StratAgg marks a transition from the roofspall/breccia-dominated sediment of the *LBSR* to sediment composed primarily of aeolian dune sand, which characterizes the middle Long Section as a whole. In the *ALBS*, the sandy sediment brackets a layer of rockfall. Several low-density occupation layers are located within the otherwise sterile *ALBS* dune sand, which indicate a focus on shellfish collection. The *ALBS* is OSL dated to 76 ± 3 to 79 ± 3ka (Brown et al. 2009). These ages place the *ALBS* as approximately synchronous with MIS 5a (Martinson et al. 1987; Shackleton et al. 1990) with a more variable but still strongly C3 vegetation signal and slight coastline regression.

Shelly Ashy Dark Brown Sand

The Shelly Ashy Dark Brown Sand (*SADBS*) is stratigraphically above the *ALBS* at 20.6 to 21.2masl. Sediment consists of aeolian sand with significant anthropogenic contribution of ash and organics. This StratAgg has a high density of plotted finds and is rich in shellfish, lithics, and fauna. The *SADBS* has OSL ages of 71-72 ± 3ka, placing it within MIS 4, but additional OSL samples have been taken. The *SADBS* has a highly variable C3/C4 signature and coastline modeled to be in regression although abundant shellfish remains are still present.

Orange Brown Sand

The Orange Brown Sand (*OBS*) is a massive wedge of dune sand that rests on top of the *SADBS* from 21.2 to 21.9masl. Several layers within the *OBS* are rich in shellfish, indicating some occupation of the site during the accumulation of this dune. Few combustion features are present, and the sand between occupation layers is mostly sterile. The *OBS* is OSL dated at 69 ± 4ka (Brown et al. 2009) in MIS 4, with a significant contribution from C4 vegetation. The coastline was likely in regression; however shellfish remains are still present in the associated sediments.

Shelly Grey Sand

The Shelly Grey Sand (*SGS*) occurs at an elevation between 21.9 and 22.5masl above the *OBS*. A small sample has been excavated from the *SGS* (less than a single 50cm quadrant) that includes three SubAggs in order from bottom to top: 'Jinga', 'Zuri', and 'Tamu'. The eastern profile of the trench, which began in May-June 2009 to connect the Long Section with the Northwest Remnant, shows that the *SGS* might be a thicker and more significant StratAgg farther to the north. This StratAgg is laterally discontinuous and it pinches out near the location where it was excavated in October-November 2008. No OSL dates have been taken directly from the *SGS* profile; however, ages from aggregates above and below constrain the range from 65 ± 3 to 69 ± 4ka.

Dark Brown Compact Sand

The Dark Brown Compact Sand (*DBCS*) sediment consists primarily of aeolian sand with significant anthropogenic contributions of charcoal and organics. The *DBCS* occurs at 22.5 to 22.9masl, but as with the SGS, the eastern profile of the NWR trench

indicates that the *DBCS* is thicker and denser in artifact content to the north. While the *DBCS* is rich in organics, there is an almost complete absence of shellfish remains. The *DBCS* is OSL dated from 60 ± 2 to 65 ± 3ka (Brown et al. 2009) at the transition of MIS 4-3 (Shackleton and Opdyke 1973), with significant contribution from C4 grasses. The coastline was likely in a transgressive phase at this time. The ages and the lithic artifact content indicate that the *DBCS* is associated with the HP Industry.

Medium Brown Sand and Roofspall

The Medium Brown Sand and Roofspall (*MBSR*) StratAgg represents a rapid buildup of geogenic sediment from c. 23 to 25masl, including fault breccia and roofspall similar to the *LBSR*, with an increase in aeolian sand near the surface of the deposit. The excavated portion of the *MBSR* shows evidence for significant erosion with intrusive runnels visible in profile. Artifacts occur sporadically throughout the *MBSR*, but a relatively dense layer of lithics and fauna (SubAgg 'Takis') occurs midway through the *MBSR* at c. 24.5m. This assemblage was selected for analysis because it appears to be layered horizontally, and may occur in association with a paleosol that appears to extend beyond the PP5-6 boundary. Multiple OSL samples place the age of the deposits at 47 ± 3 to 49 ± 3 (Brown et al. 2009) and within MIS 3. The *MBSR* does not overlap with the Crevice Cave speleothem, but the Fisher et al. (2010) coastline model predicts a mean distance to coastline of approximately 15km.

Northwest Remnant

The Northwest Remnant (*NWR*) (26.8-27.5masl) is not yet stratigraphically connected to the Long Section. Stratigraphic correlation and micromorphology allow for reasonable correspondence between the two site areas. The *NWR* (OSL dated at 59 ± 3ka), likely rests directly on top of the *OBS* (Z. Jacobs, pers. comm.), and therefore the Long Section *SGS* and *DBCS* do not appear to extend to the northern boundary of the site. The *NWR* sediment looks similar to that of the *DBCS*, with continuing absence of shellfish, but the sand content is finer in texture. Fisher et al. (2010) predicted a mean distance of 7.6km to the coastline from PP5-6 and the Bar-Matthews et al. (2010) $\delta^{13}C$ curve predicts a mostly C3 signature.

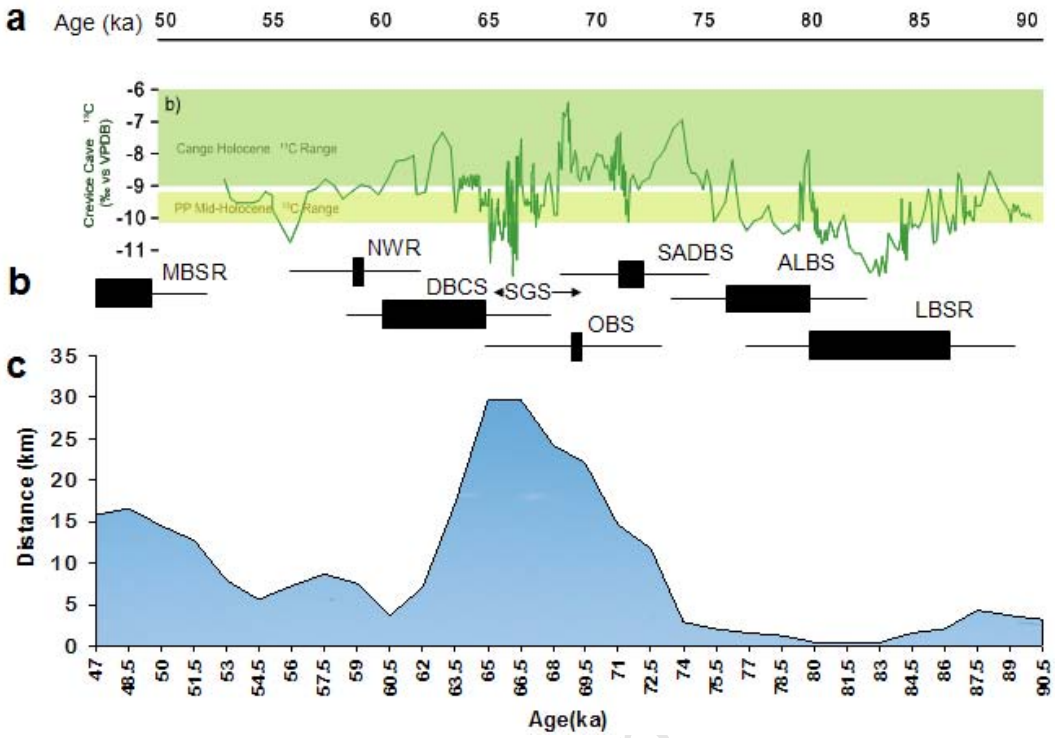

Figure 13. The PP5-6 paleoenvironmental context and age: a) $\delta^{13}C$ climate curve (Bar-Matthews et al. 2010); b) PP5-6 OSL ages (Brown et al. 2009; Z. Jacobs, pers. comm.); c) mean distance to coastline (Fisher et al. 2010). Crevice Cave carbon curve figure used in this study by permission of the SACP4 project. Coastline curve recreated from data published in supporting online material (SOM) from Fisher et al. (2010).

5.0 Lithic Raw Material Distributions

Evaluation of the models discussed in Chapter 3 requires at least an elementary understanding of the probable primary and secondary source locations for materials used for lithic production at PP5-6. A long-term study of raw material would consist of at least three parts. The first stage, initiated here, required an intensive field survey and literature review to create a geo-referenced database of 'likely' source locations and to collect material samples. The second stage, laboratory analysis, which is not a component of this dissertation, will attempt to compare the geo-chemical signature of the modern samples with the PP5-6 archaeological samples to assign a probability for source location matches. The ultimate goal is to create source probability maps for a variety of artifact classes (ochre, charcoal-wood fuels, plant resins, and other resources) to develop better test expectations for understanding the technological variability observed at PP5-6.

The geology of the Mossel Bay region is well studied and well described, due in part to the development of the offshore natural gas fields and associated PetroSA refinery, located just west of Pinnacle Point. This section is intended to discuss the regional geology as it relates to the availability of materials suitable for stone tool making. Sources were identified through this author's field surveys in various locations throughout the southern Cape and also from a geological literature search conducted from a knapper's perspective. The goal was to establish a framework that included a wide range of potential sources that could be further investigated by field survey and eventually sampled for a comprehensive lithic geo-chemical sourcing program tied to the Pinnacle Point sites. It is rarely possible to positively identify a specific location in space from which materials found in an archaeological context originated, therefore it is necessary to assign a probability to a source area or region (Shackley 1998). Here potential source materials are discussed in terms of their geological distributions and general proximity to Pinnacle Point.

5.1 Primary Context Lithologies

Quartzite

The primary context (*in situ*) bedrock exposures in the Mossel Bay area are predominantly elements of the Cape Supergroup, which formed as a thick wedge in a deep trough associated with the breakup of Gondwana (Malan and Viljoen 2008). The Cape Supergroup, which may be up to 10km thick and dates from 330 to 500ma (Thamm and Johnson 2006), is divided into the Table Mountain, Bokkeveld, and Witteburg Groups, of which only the former two are represented in the Mossel Bay Area (CGS 1:50k series *Mossel Bay* and *Hartenbo*s geology maps). The Table Mountain Group is dominated by sheets of sandstone with some alternating beds of shale and conglomerates (Thamm and Johnson 2006).

In the vicinity of Pinnacle Point, the Table Mountain Group is well represented by the Skurweburg and Baviaanskloof Formations of the Nardouw Subgroup and also by the Ceres Subgroup which, due to inclination, are expressed as linear east-west trending exposures that roughly parallel the N2/R102 highways from the Gouritz River to Mossel Bay. The Pinnacle Point Caves occur in Skurweburg quartzitic sandstones. In general, the Nardouw and Ceres Subgroups can be described as occurring in thick cross-bedded layers, which are composed of former marine and fluvial sediments (Thamm and Johnson 2006). The overlying Bokkeveld Group consists of alternating sandstone and mud/silt stone layers. These layers were deposited during episodes of coastline transgression and regression that shifted deposition from lower energy deltaic environments to more high-energy, wave-influenced marine environments (Thamm and Johnson 2006).

Sandstones of the Table Mountain Group (commonly referred to as “TMS”) outcrop throughout the Mossel Bay area, but most of this material is coarse-grained, cross-bedded, and does not fracture conchoidally. The Table Mountain Group provides vein quartz in some local exposures (Thompson et al. 2010). Less than a dozen lithics from PP5-6 can be attributed to the local cave wall Skurweburg quartzite, which at Pinnacle Point is yellowish-grey to light brown in color and crumbly and coarse in texture. Conversely, sandstones of the Robberg Formation in the more recent Uitenhage Group (Cretaceous, 145-65ma) have been noted for being highly indurated (Shone 2006), and have therefore been hardened by heat or the introduction of cementing siliceous material (“induration” *McGraw-Hill Dictionary of Geology and Mineralogy* 1994).

Robberg quartzite exposures occur at the base of Cape St. Blaize Cave at the Mossel Bay Point, and also occur along the eastern end of the nearby Cape St. Blaize hiking trail. These quartzites are distinctive for being fine-grained in which individual sand grains are not often visible without magnification. Color is generally light and ranges from brown to red and grey, but exposures below Cape St. Blaize Cave exhibit distinctive dark red and grey "leopard spots."

Based on cortex type present in the assemblage, primary exposure Robberg quartzite appears to have been preferentially selected over secondary context beach cobbles in the MSA of nearby Cape St Blaize Cave (Thompson and Marean 2008). Indeed, surface scatters of MSA artifacts along Cape St. Blaize Trail also seem to be concentrated near outcrops of Robberg quartzite. This lithic material was found to be well suited for the experimental production of flakes and blades (Schoville and Brown 2010).

Silcrete

As with quartzite, silcrete formation and distribution is largely linked to the morphology of land surfaces that developed as a consequence of the breakup of Gondwana (Partridge et al. 2006). After rifting, the land surfaces above and below the Great Escarpment experienced parallel erosion due to Cretaceous warm and wet conditions, resulting in more or less continuous and flat surfaces on the seaward and inland sides of the escarpment. This has been referred to as the "African Surface" (King 1948). Drainage was characterized by relatively large, slow meandering river systems. Sometime following the late Cretaceous, the African Surface was cemented over or capped by ferricrete, calcrete, and most extensively by silcrete (Grahamstown Formation) along the southern coast (Partridge et al. 2006).

The African Surface may be the product of multiple erosional episodes that created a non-uniform or multi-level topography (Marker and McFarlane 1997). This silcrete-capped surface reaches a maximum elevation in the Riversdale-Albertinia area of 300m in the north and slopes to the south and east to less than 120m (Summerfield 1981). But silcrete appears to have formed at several different elevations (Fig. 14), and may have different formation ages (Marker and McFarlane 1997; Roberts 2003).

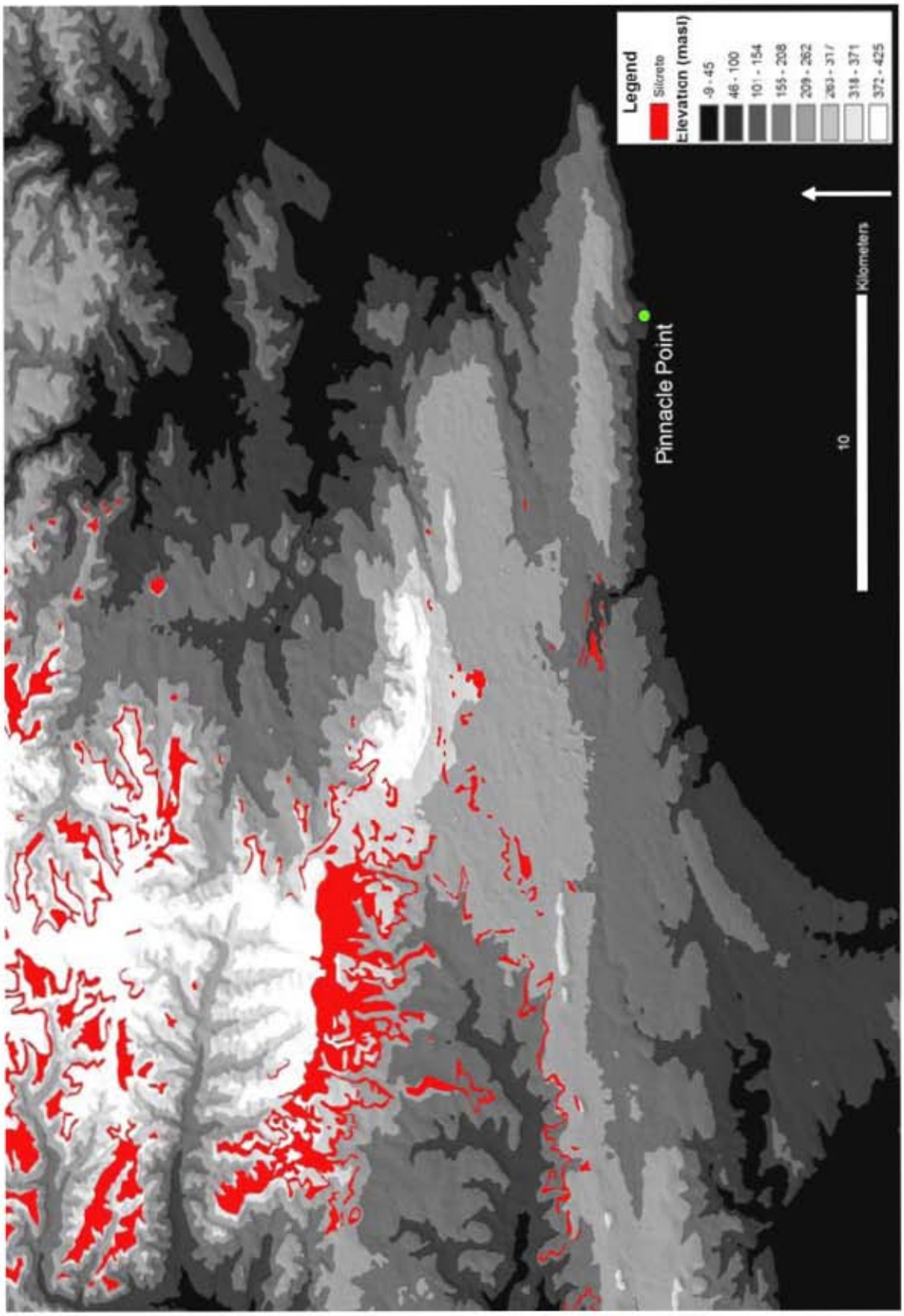

Figure 14. Digital elevation model (DEM) of Mossel Bay region with silcrete outcrops digitized from the CGS Mossel Bay and Hartenbos 1:50,000 series geology maps

The environmental conditions, mechanism, and timing of the processes which led to silcrete formation near the southern Cape coastline are not well understood. Challenges to research on silcrete formation include; 1) a lack of analogous modern silcrete formation (Roberts 2003); 2) knowledge that silcrete will precipitate at low or high soil pH leading to competing hypotheses of formation (Partridge et al. 2006); and 3) a lack of published absolute dates for southern African weathering profile silcretes (Roberts 2003). Summerfield (1983) proposed a model of silcrete formation during low pH environments, based on the apparent co-precipitation of silica and titanium. He argued for a humid, well vegetated tropical environment at the time of precipitation. An alternative view is that cooler temperatures and increased aridity in the late Cretaceous could have raised soil pH and caused silica precipitation (Partridge and Maud 1987). The consensus seems to be that silcrete formed, probably at multiple times during warm humid environments, aided by increased ground water and dense vegetation that lowered soil pH and facilitated silica precipitation (Roberts 2003). Most researchers agree on a Miocene/Pliocene age for coastal belt silcretes (Summerfield 1981).

The term "silcrete" describes the eventual outcome of widespread pedogenic processes, formed in association with degraded bedrock (termed "weathering profile silcrete"). The parent geology therefore heavily influences the physical property of the silcrete stone (Summerfield 1981; Roberts 2003). Summerfield noted that in the southern coastal belt, silcretes generally occur in association with weathered Bokkeveld clay/silt profiles, which is consistent with the exposures that occur closest to Mossel Bay. The Bokkeveld formation is also a good source for angular quartz nodules. Farther to the north, silcretes also occur in the Uitenhage Group- Buffelskloof Formation sandstone/conglomerates (CGS 1:50k series *Mossel Bay* and *Hartenbo*s geology maps), in Kirkwood Formation silt and mudstone, and even within weathered profiles of the Cape Granite Suite.

Summerfield (1981) followed Frankel (1952) in characterizing silcrete deposits as being either "globular" (occurring as rounded masses surrounded by uncemented sediment), "conglomerate" (consisting of cemented silcrete and quartz pebbles), or "massive." It is the massive silcretes that are noteworthy here because they tend to be the most homogeneous, fine-grained, and hardest of the silcrete types (Summerfield 1981). Summerfield noted that massive silcretes often contain a lighter more "powdery" material occurring with darker grey silcrete that is harder and fractures more predictably (based on

Schmidt hammer tests). The powdery material, described in this study as “rind,” is undesirable for experimental flaking and is removed as a secondary cortical surface to access the harder micro/macro-crystalline silcrete within. Silcretes can also be classified based on petrographic thin sections according to “fabric.” Summerfield (1981) defined four silcrete fabrics: “grain-supported” (GS), “matrix supported” (M), “floating” (F), and “conglomerate” (C). This classification is based on the relative proportion of cementing silica matrix (M fabric), inclusive quartz grains (F fabric), and presence or absence of pre-existing (usually quartzitic) structure (GS fabric), and the inclusion of previously cemented materials (C-fabric).

The parent geology controls the fabric of the silcrete, but does not heavily influence the mineralogy (Summerfield 1981). Silcretes are composed predominantly of silica dioxide with minor percentages of titanium, iron (goethite or hematite), and assorted trace elements. The challenge for geochemically fingerprinting archaeological silcrete is that multiple samples from a single weathering profile may show more variability in trace element composition than samples analyzed from widely separated exposures of differing geology (Corkill 1999).

Figure 15. Zuurvlagtke silcrete profile between Mossel Bay and Herbertsdale

Silcrete from a variety of parent geological formations are available and abundant northwest of the Pinnacle Point project area (Fig 14). Silcretes derived from the Bokkeveld and Kirkwood Formations and the Cape Granite Suite were sampled for the published study of silcrete heat treatment (Brown et al. 2009). Almost all of the silcrete exposures sampled for the study, regardless of parent geology, yielded material of

sufficient quality (once prepared by heating) for flaking although some locations required more search time than others to locate suitable nodules. The important point for this analysis is that unlike many other MSA sites where the source locations for the silcrete used to produce the lithics are not known and are assumed to be non-local or "exotic" in origin, silcrete would have been abundantly available and recognizable to MSA tool makers as close as 8.5km from Pinnacle Point (Fig. 15).

It is not known whether there are submerged silcrete exposures in the vicinity of Pinnacle Point on the Agulhas Bank that would have been accessible during periods of lower sea levels in the Pleistocene. Several lines of evidence suggest that this would not be the case. First, the Agulhas Bank would have been submerged during the post-Cretaceous periods when silcrete on the higher land surfaces formed. Second, terracing from more recent Pleistocene sea level transgressions would very likely have planed off any southern extension of the deep weathered profiles on which the silcretes formed (D. Roberts, pers comm.). In support of Roberts's argument, no silcrete exposures occur below 140m in the Mossel Bay region (Fig. 14). There is no evidence, based on the elevations of known silcrete exposures, to suggest that coastline movement during the Pleistocene would have produced overlap between the coastline and silcrete deposits (in effect creating silcrete-rich cobble beaches). The assumption that no submerged silcrete exposures occur within 8 to 10km of PP5-6 is a key point of the model presented here and will be discussed later.

Crystalline quartz and other semi-precious minerals are known to form in South Africa in pegmatites of the Cape Granite Suite (Walker and Mathias 1946). Crystalline quartz is rare but occurs in trace amounts in the PP5-6 sequence. Where cortex still exists, crystalline plains are unweathered with sharp edges, perhaps suggesting direct acquisition from primary sources. The closest Cape Granite Suite formation with pegmatite occurs c. 21km from Pinnacle Point near George (Ferré and Améglio 2000), which could set a minimum radius for the direct procurement or transfer of raw materials in the PP5-6 sequence.

5.2 Secondary Context Materials

Secondary sources for lithic materials often get overlooked in discussions of raw material availability (Shackley 1998), leading to potentially erroneous statements regarding the so-called "exotic" nature of the source lithologies for tool manufacture

(Minichillo 2006). A number of potential secondary sources of stone cobbles would have been available on the southern coastline during the Pleistocene. These secondary sources include nodules from active cobble beaches and river drainages, static fossil river/beach terraces, and ancient alluvial gravels occurring in stratified geological formations.

Coastal Cobble Beaches

Modern coastal cobble beaches with nodules suitable for lithic reduction occur at the following locations: Kanon Beach near the Gouritz River Mouth (c. 28km); Mossel Bay Point (9km east of PP5-6); Eden Bay (directly adjacent to the Pinnacle Point sites); and Dana Bay (5km west of PP). This stretch of coastline has been surveyed on foot via the historic Cape St. Blaize Trail without locating any other significant modern cobble beaches—although more may exist. The Eden Bay beach adjacent to PP5-6 is dominated by the local Skurweburg quartzite cobbles, which do not tend to fracture with any degree of predictability. Better quartzite cobbles can be found by canvassing the beach and testing a large number of nodules. The Mossel Bay Point provides relatively homogeneous materials that appear to derive from the locally outcropping Robberg quartzite. Most nodules found on the beach or in the intertidal zone are semi-angular, probably representing more recent detachment from the Robberg exposures that make up Mossel Bay Point.

The cobble beach at Dana Bay consistently provides the most uniform, rounded and homogeneous fine-grained cobbles of any secondary source sampled in the area. During a period of almost four years, this author has visited the same beach locality at Dana Bay (First Beach) to collect cobbles for experimental MSA point and blade production (Fig. 16). During two collection outings with crew members of MAPCRM (each lasting about an hour), 91 total cobbles were collected after testing many more. These included 86 fine quartzite nodules (95%), 4 hornfels cobbles (4%), and 1 silcrete nodule (1%). Silcrete is available on the Dana Bay beaches but only in unpredictable quantities. It will be demonstrated that these raw material frequencies are similar to those found in the lower assemblage from PP5-6 (LBSR). It is interesting to note that during each subsequent visit to the beach (three to four times), tested nodules were still encountered from the original two visits, but sufficient turnover or reshuffling of cobbles between visits provided a supply of new cobbles. While the materials here are of relatively good flaking quality, they are not always available as they occur at or slightly below mean sea level and are frequently covered by 0.5-1m of beach sand. The

movement of the covering beach sand does not seem to be predictably linked to tides, seasons, or storm surges. A systematic study of cobble availability at Dana Bay was planned, but the beach was entirely covered by sand from 2008 to 2010. It is not known whether intertidal sand movement would have been a limiting factor to beach cobble availability during the Pleistocene but source locations may have been unpredictable.

Figure 16. First Beach at Dana Bay with cobbles and covering sand

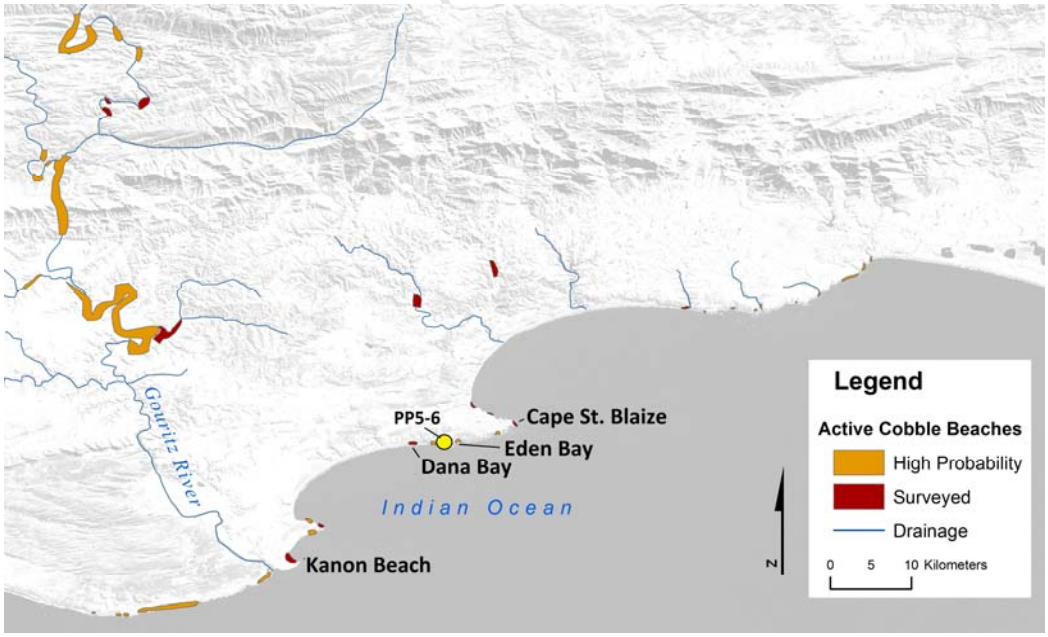

Figure 17. Known (dark red) and high probability (orange) locations for active cobble beaches based on previous surveys and Google Earth satellite imagery. Locations discussed in text are identified.

Gouritz River

It has not been difficult to find modern primary and secondary sources for silcrete, hornfels, quartz, and quartzite. Other lithic materials found in the archaeological sequence at Pinnacle Point have been a challenge to locate on the landscape. These materials include opaline, chert, and various silicified silt/mudstones, commonly referred to by archaeologists as "CCS" (cryptocrystalline silicates). The similarity in appearance and flaking properties of many of these silicate minerals has led archaeologists to form their own classification schemes. Similarly, archaeologists often use the terms "flint" and "chert" synonymously or to differentiate between color, geographic distribution (Old World vs. New World), or by formation process (Crabtree 1967; Luedtke 1992). Geologists are quick to point out that many of these silicates formed under different geo-chemical processes (Lowe and Nocita 1999), and proper geological classification can be accomplished only by thin-section petrography. Following the more recent geological convention, the term "chert" will be used here to describe all crypto- and microcrystalline silicates with conchoidal fracture (not including silcrete) found at PP5-6.

Cherts form either by silicification through low temperature interaction of sediment and water on the sea floor or as precipitates from highly saturated silica solutions that may sometimes precipitate through contact with cold upwelling water or warm subsurface volcanic vent systems (Lowe and Nocita 1999). Chert is not known to occur in any of the geological formations in the Mossel Bay region. Archaeological examples of chert cortical specimens exhibit pebble or cobble cortex, indicating that they have been water transported over great distances from non-local geological formations. While several smaller drainage systems are present in the region, including the Hartenbos, Little Brak, and Great Brak Rivers, only the Gouritz extends north of the Cape Super Group in the present day.

The Gouritz River and its tributaries form a massive drainage system that extends over 250km inland and cuts through at least six major geological entities (Figs. 17-18). Preliminary survey work at points along the Gouritz system has been unsuccessful in identifying unmodified chert cobbles from the modern drainage, but there remain good reasons to focus here. The Gouritz River Mouth has an extensive cobble and boulder beach, but the majority of materials are coated with marine algae and nodules are not identifiable to stone type without systematic cleaning. The lower Gouritz riverbed and terraces are currently lined with fine sand and silt that may obscure cobble beds, which might have been available after high-water volume scouring of the drainage.

Investigations farther upriver in the Little Karoo identified MSA primary lithic reduction areas on cobble-rich Gouritz River terraces. These lithic reduction areas contained chert artifacts with rolled cobble cortex, indicating a high probability that these materials would have been available within the drainage in prehistoric times. Perhaps the relatively low volume of water flow, due to damming, irrigation, and invasive hydrophilic plant species in modern drainages has significantly reduced the transport of chert materials from the Karoo in historic times.

The Gouritz River cuts through the southern facies of the Prince Albert Formation of the Ecca Group in the southern Karoo Basin, which is a sedimentary formation containing dark colored chert and phosphatic minerals, argued to have formed in marine mud around areas of cold water upwelling (Johnson et al. 1996). The Abrahamskraal Formation of the Beaufort Group, also drained by the Gouritz in the southwestern Karoo Basin, is known to have massive greenish-grey or purplish chert layers ranging up to 2m in thickness (Catuneanu et al. 2005; Johnson et al. 2006). As with the abundant chert formations that occur in the Barberton Supergroup in Swaziland (Lowe 1999), the Abrahamskraal chert may occur in association with siliceous volcanic ash (Martini 1974).

It is clear from the survey that the Gouritz River transports a wide variety of raw materials in cobble form from the interior to the coastline. It is also evident that in the Karoo, MSA knappers made use of extensive river terrace deposits as sources of stone for tool manufacture. It is not known whether Pinnacle Point MSA knappers would have expended the energy to procure lithic materials directly from the Gouritz River drainage, which would have required a 60km round trip. Alternatively, they could have waited for the materials to be transported down the coastline.

A study conducted on the high-energy, west-facing Oregon Coast of the United States employed radio transmitters to track basalt gravel and cobble (4-256mm diameter) movement along the coastline (Allan et al. 2006). Here, the wave direction is seasonal with weaker summer swells coming from the northwest and stronger winter swells from the southwest. They found a strong tendency for the northward movement of nearly all tracked cobbles and gravel driven by the stronger winter wave action from the southwest. Several cobbles travelled farther than 285 meters in 8 months. They also noted that gravel and cobble movement required seasonal scouring of the sandy foreshore to facilitate cobble movement. Larger cobbles tended to travel faster because smaller particles got locked in place between larger particles.

Swell direction of the Agulhas Current off the southern Cape is predominantly from the southwest (Lavrenov 1998). If cobbles from the Gouritz River Mouth and other drainages to the west of Mossel Bay are subjected to similar high energy wave transport, then it seems probable that the cobble beaches in the vicinity of Pinnacle Point should have offered at least a sample of materials transported from the interior via the Gouritz River drainage and then by wave action farther east along the coastline. Indeed a one-hour survey of Kanon Beach, located 2km east of the Gouritz River Mouth, yielded six small chert pebbles (Fig. 19) of sufficient size to produce the cores found in the SGS and SADBS (Section 9.0). The modern limited availability of silcrete cobbles on First Beach in Dana Bay would also tend to support this hypothesis.

Conglomerates

Cobble beds also occur in several conglomerate formations found in the Mossel Bay area and in the vicinity of Pinnacle Point (Fig. 20). These conglomerates are a possible source for raw materials where they are exposed in eroded profiles. But they also may have been an additional source of beach cobbles where sea level transgressions could have churned up the formations. These conglomerate formations have not yet been found to contain materials that derive from outside of the Cape Super Group (Shone 2006), and they therefore are an unlikely source for non-quartzite materials.

The Enon Formation of the Uitenhage Group is approximately contemporary to the Robberg Formation previously discussed (Shone 2006). This formation can be found in thick beds in the Mossel Bay, Knysna, and Oudtshoorn areas and locally near Dana Bay. The Enon Formation consists of quartzite and slate pebbles and cobbles that occur in an iron-rich limonite matrix, giving exposures a bright red appearance. In most contexts, cobbles are coated with limonite which, if noted on cobble cortex on artifacts found at the site, could give some evidence for the extraction of Enon cobbles for tool-making if not mistaken for ochre staining. The Enon Formation, which does not appear to be continuous across the region, is modeled as having formed in alluvial fans (Shone 2006).

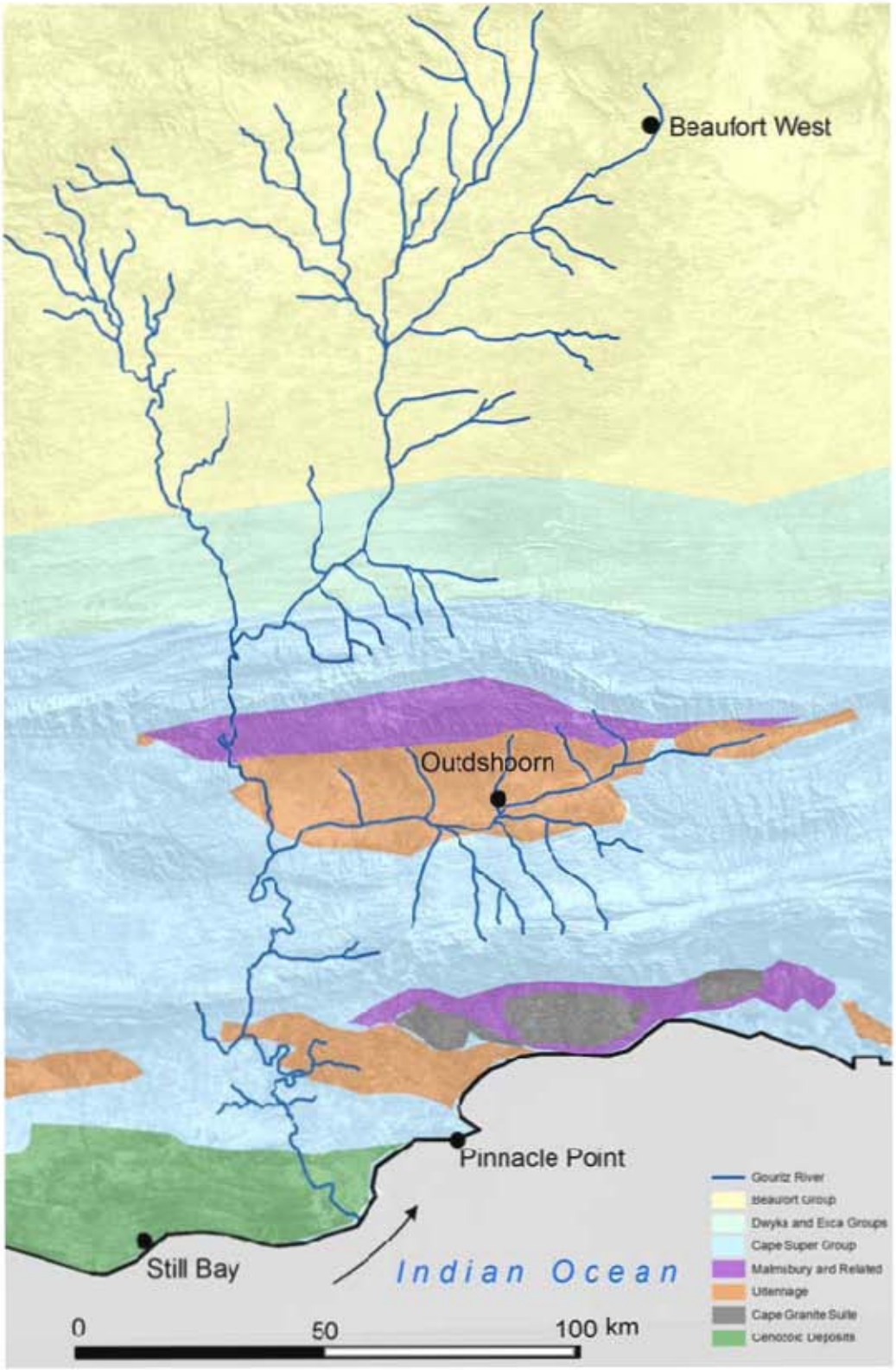

Figure 18. Gouritz River drainage and major geological entities within the catchment. Map digitized from Vorster (2003). Arrow shows the prevailing direction of ocean swell in the present day

Figure 19. Chert pebbles collected from Kanon Beach

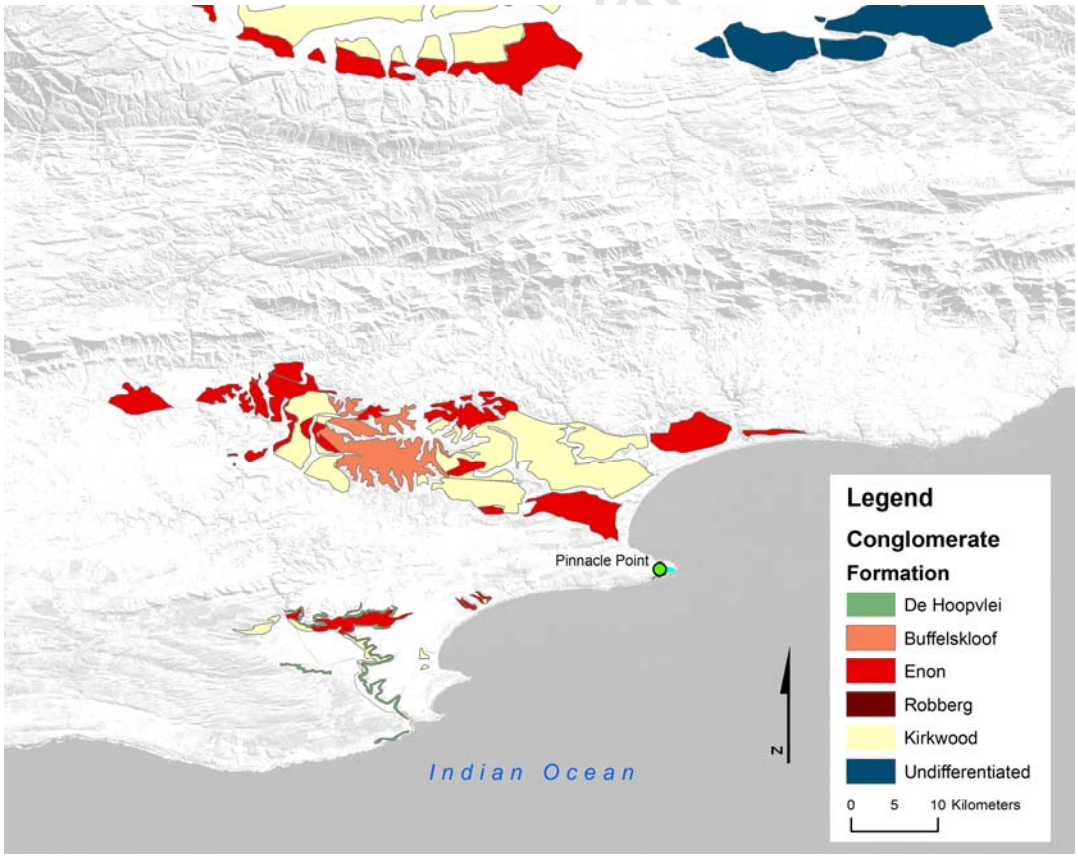

Figure 20. Conglomerate formations digitized from the CGS Ladismith, Riversdale and Outdshoorn 1:250,000 series geology maps showing potential static sources of secondary context raw materials in the Mossel Bay region

An additional conglomerate source is the Early Pliocene De Hoopvlei Formation of the Bredasdorp Group (Roberts et al. 2006). This formation is localized compared to the Enon Formation, but it is of interest because one of the few exposures in the area occurs along the Cape St. Blaize trail midway between Pinnacle Point and Mossel Bay Point. This conglomerate, with well-cemented clasts, appears to have been utilized as a source for quartzite at various times in the past, based on the large number of debitage pieces on the ground surface in this area.

5.3 Raw Material Distribution Summary

The source locations and distances to the site proposed in text and in Table 2 are meant to provide relative proxy measure for cost of acquisition. Cost path analysis, which takes into account slope, terrain, watercourses, and other impediments to movement, was not conducted for the purposes of this analysis. Most of the estimated distances to source locations are relatively short, occur on flat or moderately sloped terraces, and could be walked round trip within a day depending on the density of vegetation. These distances in some cases are assumptions that can be tested and reevaluated by future raw material survey work.

Sources for silcrete and quartzite were relatively easy to find (especially when aided by maps and a vehicle) during surveys conducted to gather materials for experimental biface manufacture and MSA point production. The closest known silcrete source to Pinnacle Point (Rietvlei near the N2 Total Station) is located 8.5km away. Additional sources are abundant and easily recognizable as flat hilltop terraces farther to the north and east. Silcrete and hornfels cobbles have also been regularly found at Dana Bay. Flakeable quartzite is available in cobble form locally (but not in abundance) at Eden Bay, which is adjacent to the cave sites and is periodically available in greater frequency at nearby Dana Bay (5.4km from PP). A variety of conglomerates provide a static (not replenished) supply of quartzite cobbles located from 5.5km and beyond. The nearest source for primary outcrop quartzite, with similar appearance and homogeneity as that found at PP5-6, occurs at Cape St. Blaize (Mossel Bay Point), located at a distance of 6.4 to 8.0km from the site.

Table 2. Summary of raw materials available in modern contexts

Source	Type	Formation	Context	Modern Distance (km)	Quartzite	Silcrete	Hornfels	Chert	Quartz	Quartz Crystal
Eden Bay	Cobble Beach		Secondary	200-500m	x					
Dana Bay	Cobble Beach		Secondary	5.4	x	x	x	?		
Cape St. Blaize	Conglomerate	De Hoopvlei	Primary/Secondary	5.5	x					
Cape St. Blaize	Exposure	Robberg	Primary	6.4-8.0	x					
Cape St. Blaize	Cobble Beach		Secondary	8.2						
Rietvlei+Various	Exposure	Grahamstown	Primary	8.5 and beyond		x			x	
Dana Bay	Conglomerate	Enon	Primary/Secondary	14	x					
Unknown	Exposure?	Cape Granite Suite	Primary	21						x
Kanon Beach	Cobble Beach		Secondary	28	x	x	x	x	x	
Gouritz Rover	River Drainage		Secondary	30	x	x		?	x	

Quartz, chert, and crystalline quartz have been more difficult to locate on the landscape. Angular quartz nodules usually occur in association with silcrete formed on Bokkeveld shale. Quartz is also found in cobble form in the upper Gouritz River drainage and on Kanon Beach east of the Gouritz River Mouth. Quartz cobbles have not yet been located on the beaches at Dana Bay. Chert has been very challenging to locate except as cobble cortical debitage along the Gouritz River and as pebbles on Kanon Beach. The extensive Gouritz River drainage system appears to be the most likely source for chert cobbles. As noted in Section 6.2, ocean currents may act as a conveyor, bringing materials from the Gouritz River closer to PP5-6 than the c. 30km distance required to access the drainage directly.

Crystalline quartz does not occur in great frequency, but it could be the best evidence for the distance procurement of raw materials. Quartz crystals are known to form within the Cape Granite Suite, with the nearest formation occurring 21km away. All but one cortical crystalline fragment exhibit sharp crystalline edges that have not been rounded or polished by water transport and were likely collected from a primary source.

5.4 Raw Material Availability and the Site Context Model

The major assumption of the Site Context Model is that primary sources of raw materials are not expected to have changed position on the landscape since the MSA. Dynamic cobble beaches, which are hypothesized here to be a major source of quartzite cobbles for MSA tool production, are expected to move closer or farther away from the site as the coastline shifts during Pleistocene sea transgression/regression cycles. Tool makers may have used locally available quartzite cobbles during coastal occupations at PP5-6. Coastal occupations occur when the coastline is in a position similar to the present day, and cobble beaches are located within approximately 0 to 5 km from the site. When

the coastline regresses from the site and increases the distance from the cave to the dynamic cobble beaches, it is hypothesized that inland raw materials may have been less costly to procure.

The Site Context Model also assumes that raw materials are chosen based on distance as a proxy measure for cost of procurement. The estimates of distance to source in Table 2 are calculated as if PP5-6 is the center of settlement and mobility and that procurement would require logistical forays to access resources. The Site Context Model also assumes that all raw materials have equal value and were selected based strictly on the cost of procurement. It should be emphasized that the Site Context Model links the selection of silcrete with changes in distance to secondary sources of quartzite. The distance to primary sources of silcrete does not change with movement of the coastline (given the caveat that there are no submerged sources of silcrete). These assumptions are made for the purposes of first evaluating the potential baseline effects of coastline movement on lithic raw materials. Some of the effects of functional variability in raw material, human mobility and site use patterns on raw material selection at PP5-6 are developed in Chapter 12. This discussion will show that the costs and benefits of selecting silcrete and quartzite can be viewed independently.

Figures 21 and 22 illustrate how the Site Context Model would apply to Late Pleistocene fluctuating coastlines at Pinnacle Point. Figure 21 shows the coastline (dashed line) in the Mossel Bay region as it occurs today with modern sources of raw material plotted on the map. Cobble beaches occur directly adjacent to PP5-6 and within 5km of PP5-6 to the west in Dana Bay. These are the sources that are most likely to have been accessed for tool manufacture on the site.

Figure 22 depicts a hypothetical coastline at a distance of 10km from PP5-6. Any cobble beaches on the coastline are then located at a distance of at least 10km from the site. They occur outside of the 8.5km distance set by the intersection of the radius with the Rietvlei silcrete primary outcrop. Robberg Formation primary outcrop quartzite also occurs within this 8.5km radius and might have become attractive for quarrying. As the radius increases to 20km, this distance begins to intersect silcrete rich zones to the north and east. At 30km, the radius intersects the Gouritz River Mouth and very abundant inland silcrete terraces.

The 8.5km distance from PP5-6 to coastline for the hypothetical transition from coastal cobble quartzite sources to primary silcrete and other material sources is depicted in Figure 23 as a dashed line. The intersection of the dashed lines and the coastline curve

(Fisher et al. 2010) provides zones (shaded in red for silcrete and grey for quartzite) where the Site Context Model would predict change in the relative proportions of primary versus secondary context raw materials. Change is predicted based on distance to source alone. Specifically, it is predicted that in the grey areas, PP5-6 knappers would have been more likely to use quartzite cobbles as the main source of raw material for tool making because the coastline was near to the site. Silcrete and other non-quartzitic raw materials would be expected to occur in greater frequency in the red zones where the coastline is farther from the site.

It should be noted prior to the raw material analysis, that the chronology of the coastline model has not yet been globally tuned so that the coastline curve in Figure 29 is an estimate that is subject to adjustment (Fisher et al. 2010). Similarly, the OSL dates used to place the SubAggs on the coastline and Crevice $\delta^{13}C$ curves have error bars of 2 to 9ka, as indicated by horizontal lines on the figures. Portions of the speleothem curve have decade-level accuracy, and the OSL and sea level models may have millennium-level standard errors. The refinement of the coastline model, an additional set of OSL dates sampled in 2009, and completion of ongoing studies of micromammals, shellfish, and sediment chemistry should allow for the refinement and more rigorous statistical modeling of the SubAgg-level patterning presented in Figure 23.

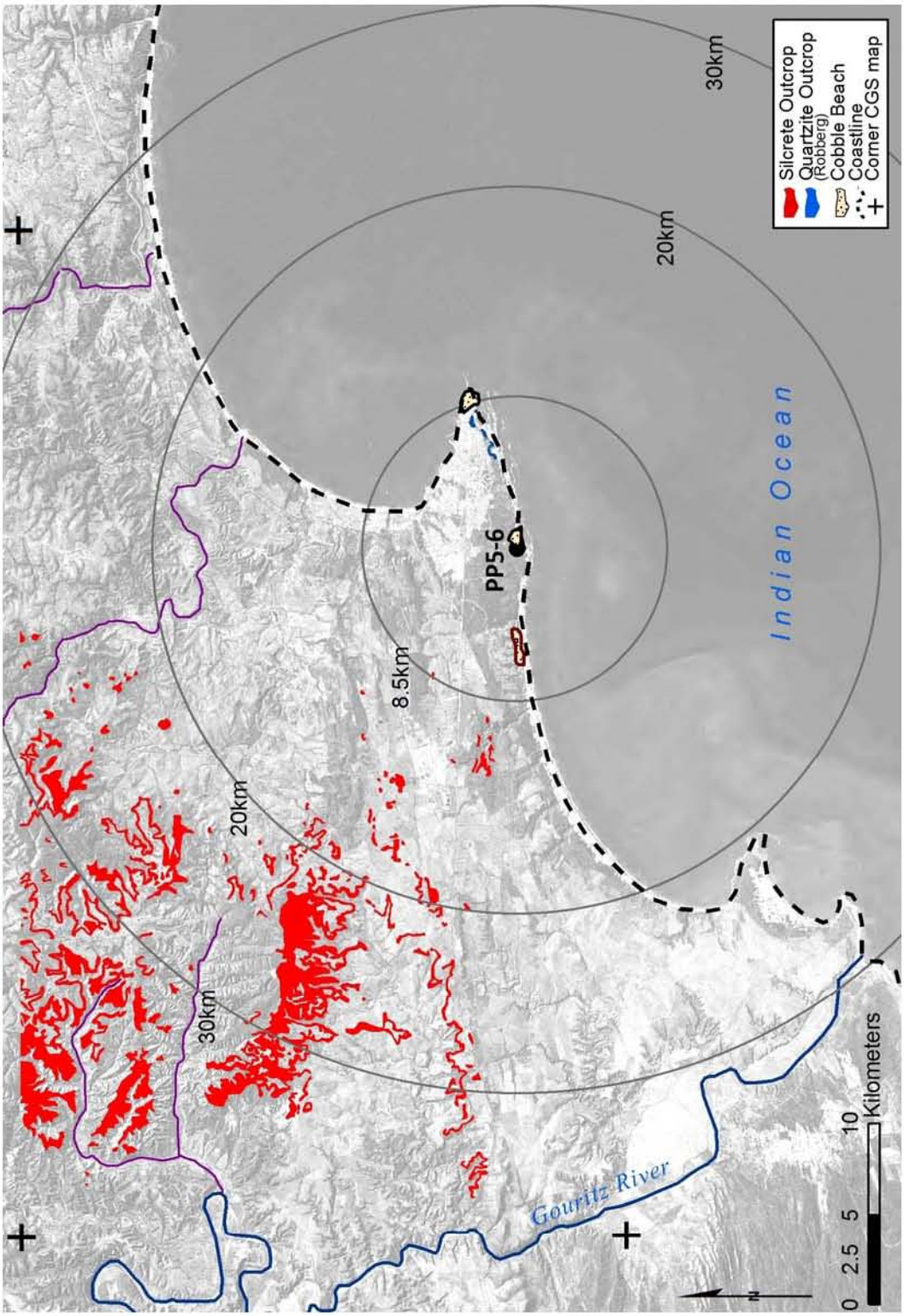

Figure 21. Modern coastline and distribution of silcrete sources, Robberg formation quartzite, and cobble beaches. Graticules mark the extent of the Council for Geosciences 1:50,000 series Mossel Bay and Herbertsdale maps.

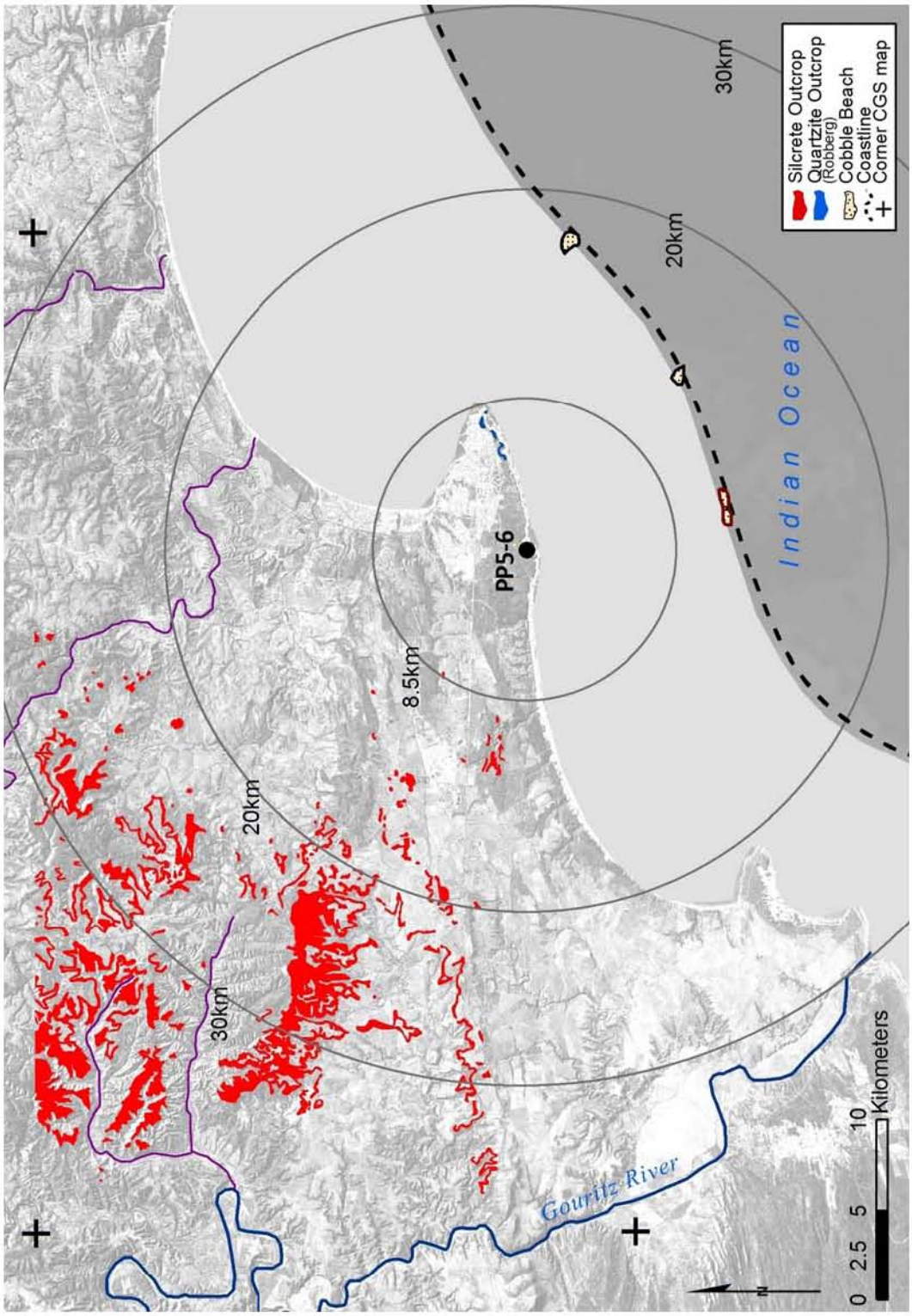

Figure 22. Hypothetical coastline at 8km distance from Pinnacle Point showing movement of active cobble beaches away from PP5-6.

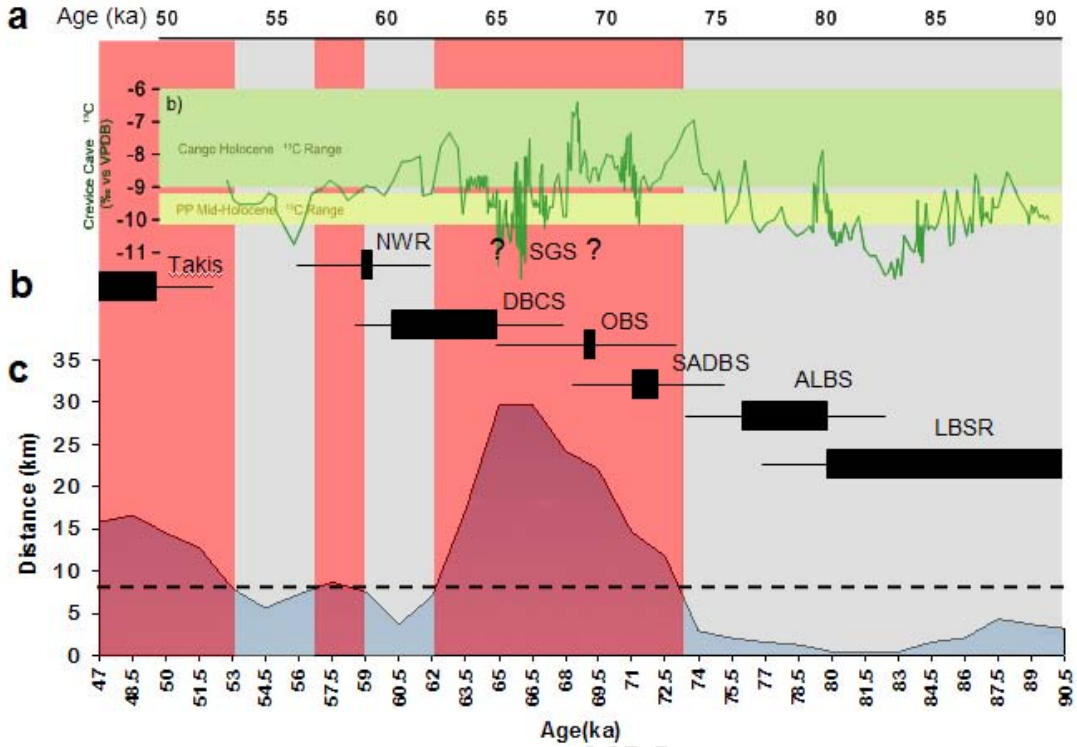

Figure 23. Raw material predictions based on a transition from secondary to primary sources at 8.5km coastline. Red areas predict predominantly silcrete collection, and grey areas predict quartzite cobble collection. Graph a is the Crevice Cave $\delta^{13}C$ Curve from Bar-Matthews et al. (2010); Graph b is PP5-6 StratAgg chronology, based on OSL ages (Brown et al. 2009); Graph c is the mean distance to the coastline from Fisher et al. (2010).

6.0 GIS Analysis of PP5-6 Raw Material Patterning

The raw material proportions observed from PP5-6 in Figure 24 and similar graphs from other coastal MSA site sequences may be considered macro-level patterning in that raw material percentages are taken from director/excavator-assigned block layers, which are in turn, composed of smaller occupation units. Because these bulk stratigraphic divisions are not usually well dated, it is not always clear how much time has been captured in each layer and gaps in occupation certainly have occurred. It is therefore almost impossible to provide an accurate chronology for patterning in the artifact assemblage, and it is difficult to create a direct link to paleoclimate records to know how abrupt or gradual changes in raw material use occur (Mackay 2008a).

Attempts to correlate macro-stratigraphy with global or local climate records are complicated by the issue that proxy climate curves are often displayed as smoothed graphs, resulting in averaged values over a given time. The resulting record may conceal dramatic changes that can occur over a very short period. The emerging chronology of PP5-6 indicates that portions of some relatively thick or dense stratigraphic aggregates (particularly the LBSR) could represent fairly short occupation periods within rapid sediment deposition regimes. The PP5-6 sequence also offers the possibility of examining micro-level patterning in raw material selection and technology that can be dated and placed in environmental context.

One goal of the GIS analysis is to examine the PP5-6 lithic and raw material sequence at a very high resolution as it occurs at the site rather than strictly as an output in a table or graph which is subject to bias according to how the analyst lumps or splits stratigraphic samples. The surrounding sediment and non-lithic artifacts are virtually removed, revealing the actual three-dimensional distributions of the plotted finds as they occur in the PP5-6 deposits. The display of coded artifact plots allows the viewer to see subtle spatial patterning that might not otherwise be visible when stratigraphy is lumped without considering artifact plots. At this time, the GIS analysis was also used as an aid in identifying discrete samples for the graphic presentation of raw material patterning, as well as the technological analyses in Chapters 8.0 to 11.0. The display of OSL dating sample locations was useful to avoid the lumping of samples that may be separated by long occupation gaps. An additional advantage of this analysis is that the plots can

identify where excavators may have inadvertently split an artifact concentration at the horizontal interface of a StratUnit.

The GIS accepts the coded lithic database and allows for the display of multiple variables by a combination of colors and symbols. In this chapter, the raw materials analysis is limited to the distribution of raw material and cortex type because these variables directly relate to lithic package type and source area. Virtually any analyzed database field can be examined at this level of detail. Some additional GIS-based technological patterning is presented in Chapter 12.

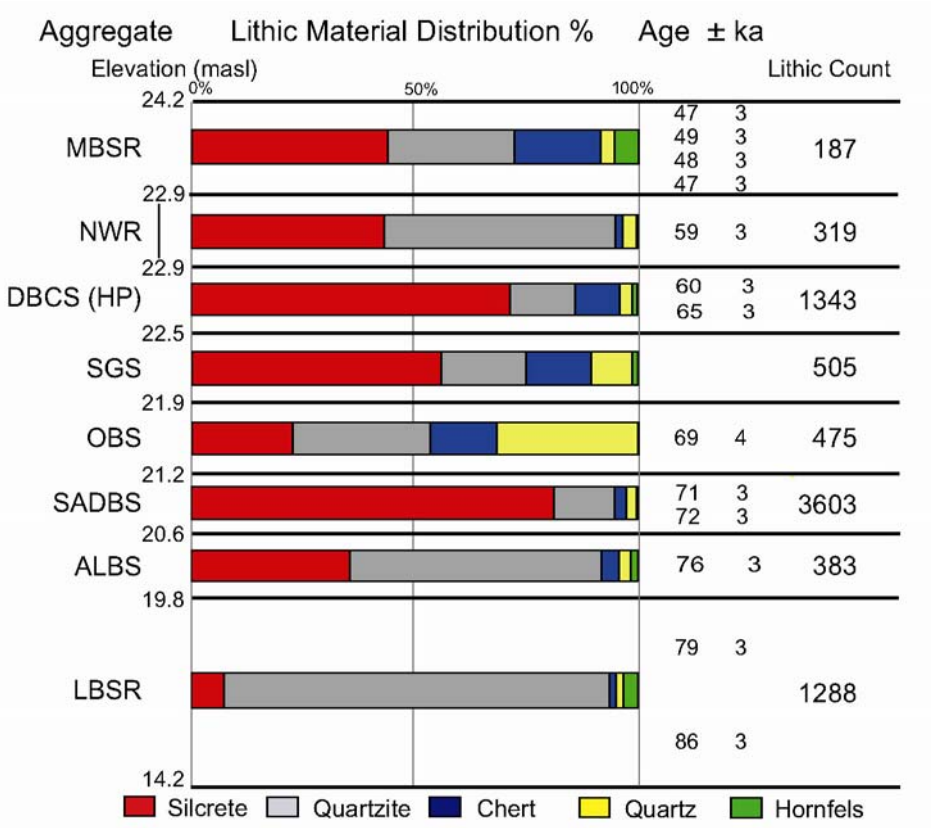

Figure 24. Raw material percentages for PP5-6 stratigraphic aggregates (StratAggs) based on artifact counts. Note that the NWR is not stratigraphically connected to the Long Section. OSL ages from Brown et al. (2009)

6.1 GIS Methodology

The SACP4 excavation strategy requires that all artifacts observed by excavators, regardless of size, are piece plotted by total station within the South Africa National Survey Grid to sub-cm accuracy in x, y, and z dimensions. To date, the six excavation seasons at PP5-6 have resulted in the logging and collection of more than 150,000 piece-

plotted artifacts distributed stratigraphically across 11 vertical meters, 8 stratigraphic aggregates, and over 1,000 distinct sediment layers or features. Twenty-five OSL ages have been obtained from PP5-6, 23 of which are internally consistent in that the ages conform to the order of stratigraphy. Permission to use unpublished OSL ages from PP5-6 was generously granted by Zenobia Jacobs of Wollongong University.

Lithics from PP5-6 were prepared for GIS analysis according to the following system. All plotted lithic artifacts that had been collected and catalogued by May 1, 2010, using standard non-residue protocol (collected without gloves and special plastic tools), were examined for this project. Each lithic specimen was assigned a unique plotted find number in the field, and was then catalogued by the staff of MAPCRM. Artifacts were then examined to record raw material and technological data (described in Chapter 7).

The coded MS Access lithics database was joined with South African National Grid X,Y, and Z coordinate data for the c. 8200 lithic plotted finds, and was then imported into ArcGIS 9.3 as a database format (.dbf) table. The table was displayed by assigning X and Y values to the coordinate easting and northing, respectively, and was then converted to a shapefile. The shapefile was transformed to three-dimensional format by using the conversion feature in 3D Analyst that brings in the elevation field in meters above sea level (MASL) as the Z value. This three-dimensional shapefile was manipulated in ArcScene, a 3D viewer that allows the artifact plots to be rotated and viewed from any angle. The sequence was examined in 3D in ArcScene and then exported in 2D from ArcMap, which is poor for 3D viewing but produces a higher resolution image output with data labeling functionality.

6.2 Raw Material Distribution and Sample Identification

Figures 25-32 display exported artifact plots for the upper and lower PP5-6 sequence. The figures are split up to cover the sequence in three panels. Each Upper and Lower Long Section panel has three figures. The first figure provides background graphics of all plotted finds to show the SubAggs (Figs. 25-26). These are followed by figures with lithics color coded by raw material (Figs. 27-28), and then cortex type by raw material (Figs. 29-30). The smaller points displayed in the background give an indication of orientation and density of non-lithic finds (shell in most cases). The *NWR* plots are provided in Figures 31-32. It is best to view the plots across the shortest axes to prevent densely aligned plots from obscuring those that occur behind. The two-

dimensional exported images show the upper half of the sequence view from east to west and the lower half of the sequence from the south facing north, with inset maps to provide more detail for the *SGS* and *DBCS* StratAggs. The names of SubAggs are presented in single quotation. Analytical samples that will be used to describe the lithic samples discussed for the remainder of this paper are introduced below with double quotations the first time they are presented in text. With the exception of lithics from the *LBSR*, the majority of analytical samples take the name of the SubAgg from which they come. Summary information for each analytical sample described below is provided in Table 3.

LBSR

Lithics in the lower *LBSR* sequence occur at relatively low densities (Table 3) and they tend to cluster within shellfish-rich layers (Fig. 27). The base of the analyzed sequence from 'Cobus Shell' to 'Bijou Sand and Roofspall' consists primarily of quartzite artifacts with some quartz (mainly in 'Leba Shell'), chert, hornfels, and few silcrete lithics. This portion of the sequence lies below the 86 ± 3ka OSL sample taken from 'Adrian SR'. The quartzite-favored 'Leba Shell' appears to be the only tight cluster of lithics in this group. It will be identified as "Leba Quartzite" during analysis. The majority of cortical pieces are derived from cobbles, but one quartzite lithic is derived from 'Cobus Shell' and one silcrete lithic from 'Leba Shell' with outcrop cortex (Fig. 29). 'Cobus Shell' has a single piece of quartz crystal.

A discrete silcrete-dominated layer occurs above 'Bijou SR', mainly within 'Kyle Shell', but it includes lithics from the top of 'Adrian SR' and the base of 'Kyle SR' (centered at 18.25m). This layer occurs between OSL dates of 81 ± 9ka and 86 ± 3ka. This sample, termed "AK Silcrete," demonstrates some fine-grained patterning of silcrete raw materials that occur within the quartzite-dominated *LBSR* StratAgg. Cortical silcrete lithics cluster on the eastern side of the quadrant and reflect primary outcrop origin except for one silcrete lithic with cobble cortex. Two quartzite lithics with cobble cortex occur in AK Silcrete. Lower *LBSR* SubAgg layers are very sparse, and clusters of cortical specimens, such as these, could all derive from a small number of core reductions. An attempt was made to refit these lithics during technological analysis (Chapter 7.2.3). The AK Silcrete sample may align with the coastline regression 'bump' (Fig. 23) at 87.5ka, subject to revision with the forthcoming OSL ages that target this area.

Few lithics occur between 'Kyle Shell' and 'Katharine SR' in almost one meter of sediment. At this location, two OSL samples provide an age estimate of 80 ± 3ka. The OSL samples from 'Katharine Shell' up to 'Ludumo SR' are relatively consistent with ages clustering around 80 to 81ka, but one anomalous OSL age of 66 ± 2ka occurs from 'Lwando SR' that we strongly suspect contained a mixture of more recent sand grains. An estimate of 80 to 81ka places this portion of the sequence within a grey zone of Figure 29 where the Site Context Model would predict greater acquisition of quartzite cobbles for tool making. These OSL ages appear to show a relatively rapid accumulation of sediment in the *LBSR* sequence and may predict an occupation hiatus of several thousand years, perhaps within 'Kyle SR'.

'Aaron Shell' contains a cluster of 12 lithics with some diversity of raw materials. The overlying sample from 'Lwando Shell' is larger and consists mostly of quartzite, with all cortical pieces deriving from cobbles. 'Lwando Shell' includes a thin quartzite-dominated layer termed "Lwando Quartzite."

'Hope Red', along with four flakes from the base of the overlying 'Martin Sand and Roofspall', consists of a thin, silcrete-dominated layer with hornfels and quartzite. "HM Silcrete/Hornfels" is interesting because all cortical specimens, regardless of material, exhibit cobble cortex. This is unlike the silcrete rich sample represented by AK Silcrete, which derives from primary outcrops. This sample might also be suggestive of focused selection of less common materials from a cobble source.

'Martin Red' is a combustion layer rich in charcoal and ash, which has reddened sediment from the hearth-induced thermal alteration of goethite to hematite in the TMS roofspall breccia matrix (Herries and Fisher 2010). A thin layer of quartzite was plotted in 'Martin Red' and the base of the overlying 'Ludumo SR' totaling 23 artifacts. Three lithics from the sample have cobble cortex. This layer anticipates the strong predominant quartzite patterning that occurs above. 'Martin Red' and 'Ludumo SR' occur between OSL dates of 80 ± 4ka below and 81 ± 4ka above.

'Ludumo Red' is another combustion layer that occurs at approximately 19.6m and has also yielded mostly quartzite, with several pieces of hornfels, silcrete, and a single quartz flake (Ch. 7.2.6). All cortical pieces, including hornfels, exhibit cobble cortex. An OSL sample taken from 'Jed SR' above 'Ludumo Red' provides an age of 79 ± 3ka.

'Jed' and 'Jed Red' occur at c. 19.75 to 20m as a thick, dense layer of quartzite debitage that marks the top of the LBSR sequence. 'Jed Red' is a dark combustion feature

that grades into ‘Jed’ from west to east and is almost certainly part of the same occupation. The western quadrant of ‘Jed Red’ was excavated using residue protocol; it was not analyzed for this project. The artifacts observed during excavation are entirely consistent with those analyzed here. “Jed/JR Quartzite” is a large sample dominated by quartzite. Cortical specimens strongly hint of significant primary or secondary cortical reduction occurring on-site. The vast majority of cortical specimens of all materials in Jed/JR Quartzite exhibit cobble cortex. The OSL dates above and below ‘Jed’ and ‘Jed Red’ are in concordance at 79 ± 3ka.

The Jed/JR Quartzite sample produces the quartzite-dominated pattern of the LBSR due to its very large sample size in comparison to the rest of the *LBSR* layers. When *LBSR* SubAggs are grouped together (as in Fig. 34a), then Jed/JR Quartzite ‘swamps’ the other thin layers and obscures the small AK Silcrete and HM Silcrete samples. If Jed/JR Quartzite represents a discrete occupation at 79 ± 3ka, then this dense layer is not representative of the remaining sampled *LBSR* sequence, depending on how the samples are differentiated.

Jed/JR Quartzite occurs temporally at or near the minimum distance to the coastline between ~48-90ka as depicted in Figure 23. Jed/JR Quartzite is a critical sample for this analysis because it represents one extreme of the PP5-6 assemblage in that the quartzite is derived from beach cobbles, and it sits near the transition to the opposite extreme of the silcrete-dominated pattern. Jed/JR Quartzite fits the predictions of the Site Context Model. Unlike the other *LBSR* samples identified for analysis, Jed/JR Quartzite has a relatively large sample size.

ALBS

The *ALBS* sequence begins with ‘Conrad Shell’, which occurs stratigraphically above ‘Jed’ and ‘Jed Red’. The contact between ‘Jed’ and ‘Conrad Shell’ is difficult to discern from the artifact plots because several large roof fall boulders from ‘Conrad Cobble and Sand’ distort the stratigraphy. The “Conrad Series” sample, which includes ‘Conrad Shell’, ‘Conrad Cobble and Sand’ and ‘Conrad’, are all sandy layers with sparse lithics in comparison to layers above and below.

ALBS ‘Jocelyn’ occurs stratigraphically above ‘Conrad’ at c. 20.4m. ‘Jocelyn’ is one of the more interesting samples because it looks to be transitional between the quartzite-dominated pattern of Jed/JR Quartzite and the silcrete-weighted pattern of the overlying ‘Erich’ and *SADBS* layers. Similar proportions of silcrete (n=53) versus

quartzite (n=49), and cobble (n=10) versus outcrop (n=13) cortex types, are present in the 'Jocelyn' sample. An additional set of OSL samples have been taken from the *ALBS* with two samples taken from 'Jocelyn' to have a better age estimate for this transitional sample.

'Erich' is located at 20.5m in elevation and has an OSL date of 76 ± 3ka. The raw material proportions from 'Erich' are much the same as in the overlying *SADBS*, thus setting the silcrete-dominant pattern in the middle Long Section. Although 'Erich' is rich in silcrete, the cortex pattern shows approximately equal proportions of cobbles and primary context materials similar to 'Jocelyn'.

Most of the *ALBS* raw material and cortical traits of the *ALBS* fit technologically as well as physically between the *LBSR* and *SADBS*. Due to the importance of the ALBS SubAgg samples with respect to the transition from silcrete to quartzite use, they are addressed separately when possible and combined when sample size is an issue for analysis.

SADBS

The *SADBS* includes SubAggs 'Thandesizwe' through 'Joanne' (20.6-21.3masl). The OSL dates place the sequence from 71-72 ± 3ka and perhaps as old as 76ka pending additional OSL dates for the transition from the *ALBS* to the *SADBS*. The raw material patterning of the *SADBS* represents the opposite extreme to the quartzite-dominant Jed/JR Quartzite sample. The *SADBS* exhibits low percentages of non-silcrete materials, especially in 'Thandesizwe' and 'Sydney'. Silcrete percentages remain constant throughout the *SADBS*, but the percentage of cobble cortical silcrete diminishes from 'Thandesizwe' (20%) through 'Joanne' (3%). Quartzite cobble cortex, though scarce, never completely disappears from the *SADBS* sequence. Quartz and chert lithics begin to appear with some frequency in the Upper *SADBS* ('Enrico', 'Pit Fill', and 'Joanne'), which is a trend that continues in the overlying *OBS*. Quartz crystal begins to be used in small proportions in the *SADBS* whereas only a single example is present from the base of the analyzed *LBSR* sequence ('Cobus SR'). The *SADBS* SubAggs are not analyzed individually because all appear similar with respect to raw material and there is no clear break in plotted finds or stratigraphy.

OBS

The *OBS* consists of the 'Celeste', 'Peter' and 'Lizelle' SubAggs, located at approximately 21.3 to 22.1masl. Two OSL dates provide an estimate of 69 ± 3ka and 69 ± 4ka for the base of 'Celeste'. The OSL ages for the top of 'Lizelle' are not yet available. The *OBS* represents a thick and probably rapid accumulation of dune sand with some MSA occupation. Lithic counts drop off from 'Celeste' through 'Peter' to 'Lizelle', but the raw material proportions are fairly similar. The quartzite frequency in the *OBS* is elevated in comparison to the *SADBS*, but the major difference in raw materials is that silcrete percentages are greatly reduced at the expense of quartz and chert. This pattern is interesting because it suggests that so-called fine-grained materials are still sought out over quartzite, but silcrete is no longer the predominant material collected. Silcrete is still acquired mainly from primary outcrops, but most other cortical materials have cobble surfaces. Quartz crystal continues to be present in the sequence. The Site Context Model would place the *OBS* closer to the MIS 4 peak of the coastline model at approximately 20km distance from the caves. The diversity of materials utilized would seem to fit the model but the elevated percentage of cobble cortex observed within the chert and quartz cortical lithic does not support the model. *OBS* SubAgg samples are addressed separately when possible and combined when larger sample size is required for analysis.

SGS

The *SGS* is above the *OBS* and includes the steeply pitched 'Jinga', 'Zuri', and 'Tamu' SubAggs from c. 22.1 to 22.6 masl. The *SGS* represents a return to the exaggerated silcrete pattern of the *SADBS*, but quartz still occurs in some frequency, and chert counts peak at the top of the *SGS* in 'Tamu' (Ch. 7.4). A slight linear clustering of chert is visible in the 'Tamu' artifact plots (inset-Figure 28). Non-silcrete cortical lithics derive almost entirely from cobbles (a continuation of the same pattern from the *OBS*). Silcrete exhibits mostly primary outcrop cortex but with some cobble silcrete specimens present. The *SGS* ages are not currently available, but samples have been taken from the profile. At present, the ages are constrained by the 69 ± 4ka date from the base of the *OBS* and the 65 ± 3ka from the base of the overlying *DBCS*. The *SGS* would line up with the peak of the coastline model if OSL dates prove to fall within that chronological range. The *SGS* sequence is more expansive to the north, and any conclusions reached in this study regarding the *SGS* are preliminary. All *SGS* SubAggs were grouped for analysis.

DBCS

The *DBCS* consists of 'Quinn' (65 ± 3ka), 'Coco', 'Sorel' (63 ± 4ka), and 'Miller' (60 ± 2ka) SubAggs. The *DBCS* is one area that has been targeted for residue analysis because of its cultural assignment to the HP. Large portions of the sample, particularly 'Coco' and 'Quinn', are not yet available for study. The *DBCS* raw material percentages are similar to those of the *SGS*, strongly favoring silcrete and the continued utilization of moderate percentages of chert, some quartz, and a few lithics made from quartz crystal. Raw materials collectively show similar proportions of outcrop and cobble sourced materials (62 and 60 pieces, respectively), but cortical silcrete exhibits mainly outcrop cortex. Quartzite, chert, and quartz are from cobbles. The *DBCS* analytical sample includes the two largest SubAgg samples ('Miller' and 'Sorel') and several combined 'Miller/Sorel' StratUnits that could not be differentiated during excavation. 'Coco and Quinn' will be analyzed when larger samples are available after the completion of a residue/edge-wear analysis.

NWR

The Northwest Remnant (Figs. 31-32) has three SubAggs: 'Coarse-Grained Dark Brown Sand (CGDBS)', 'Compact Brown and Red Sand (CBRS)', and 'Dark Brown Silty Sand (DBSS)'. Although the *NWR* is not yet stratigraphically connected to the Long Section, an OSL sample provides an age of 59 ± 3ka. The largest sample of *NWR* lithics derives from the 'DBSS'. The 'DBSS' and 'CBRS' raw material percentages are close to 60% quartzite and 35% silcrete. The small 'CGDBS' sample has only 10 pieces. The 'DBSS' and 'CBRS' have few quartz and chert artifacts. All silcrete cortical specimens are from primary outcrops, and quartzite cortical lithics were made mainly from cobbles with a few pieces that have outcrop cortex. One quartz lithic with cobble cortex was plotted in the 'CGDBS'. Due to the apparent similarities in raw material and cobble attributes, *NWR* lithics will be grouped as one sample for analysis, and they represent the only quartzite-majority sample (by artifact count) to follow Jed/JR Quartzite in the PP5-6 sequence. The *NWR* is positioned at the edge of the grey quartzite zone centered at 60.5ka in Figure 23.

MBSR-Takis

'Takis' is the only discrete cultural layer that was identified within the apparent rapid accumulation of sediment in the *MBSR* StratAgg that occurred around 48ka (Figs. 28 and 30). The analytical sample will be referred to as "Takis." Most artifacts are made from silcrete, but quartzite and chert are relatively common. Several hornfels and quartz lithics were also recovered. Half of the silcrete cortical specimens and the majority of chert and quartzite cortical lithics were made from cobbles creating a complete sample pattern that favors secondary context sources. The raw material percentages for Takis fit the Site Context Model, but the elevated percentages of cobble cortex do not.

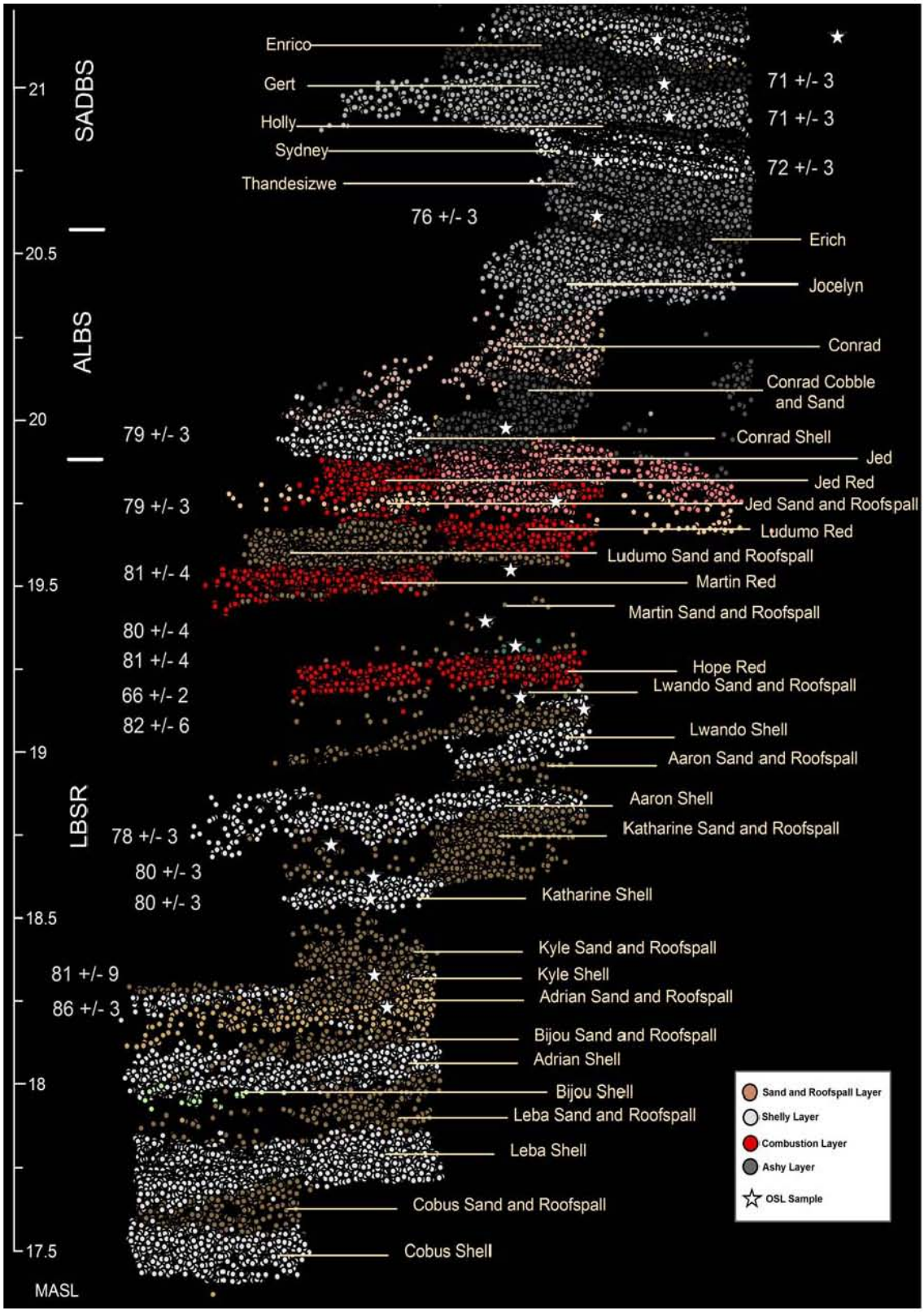

Figure 25. SubAgg sequence for the north profile of the lower Long Section. Figure includes all plotted finds excavated from October 2006 to December 2009 that could be assigned to SubAgg

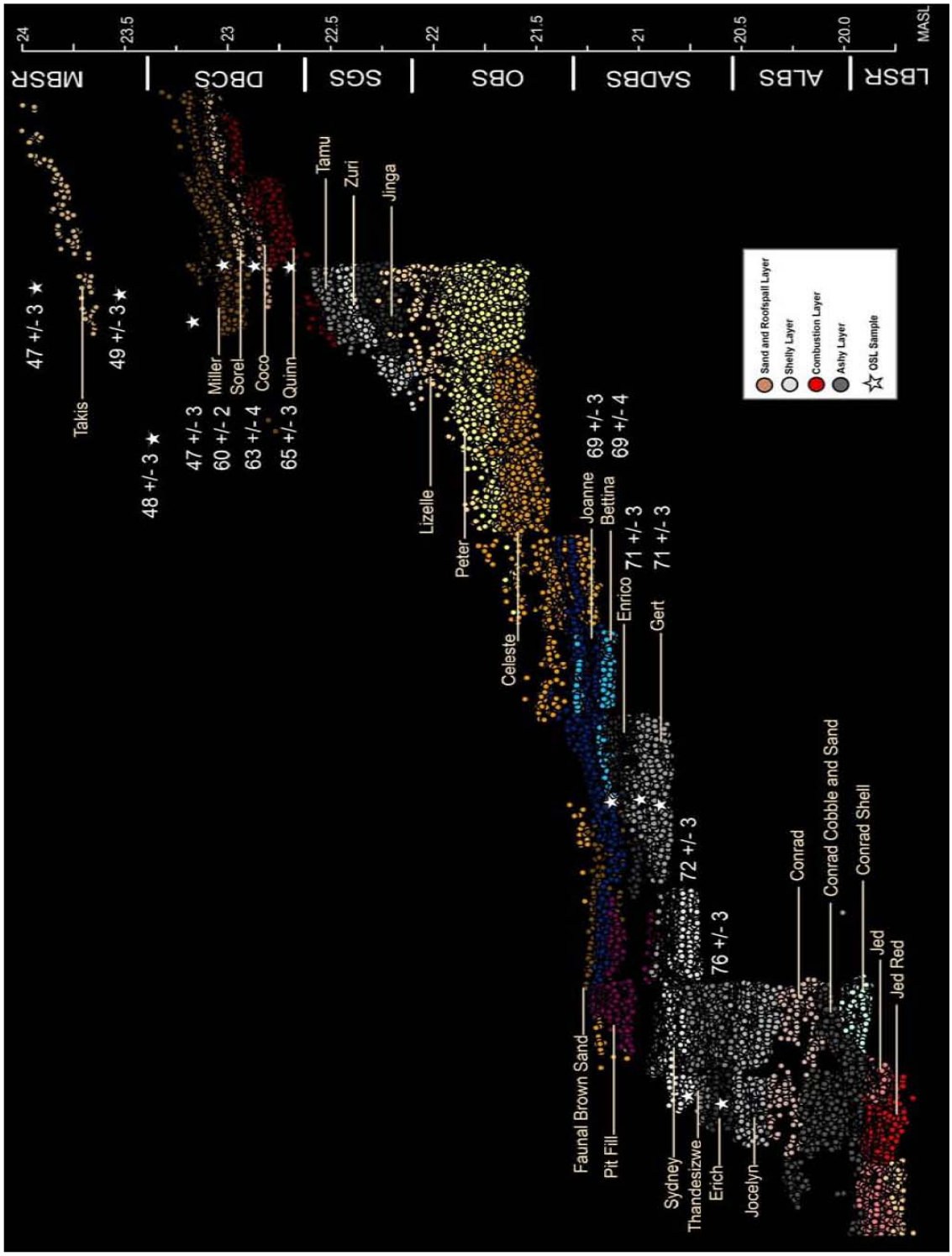

Figure 26. SubAgg sequence for the west profile of the upper Long Section. Blue plots mark the top of the SADBS sequence

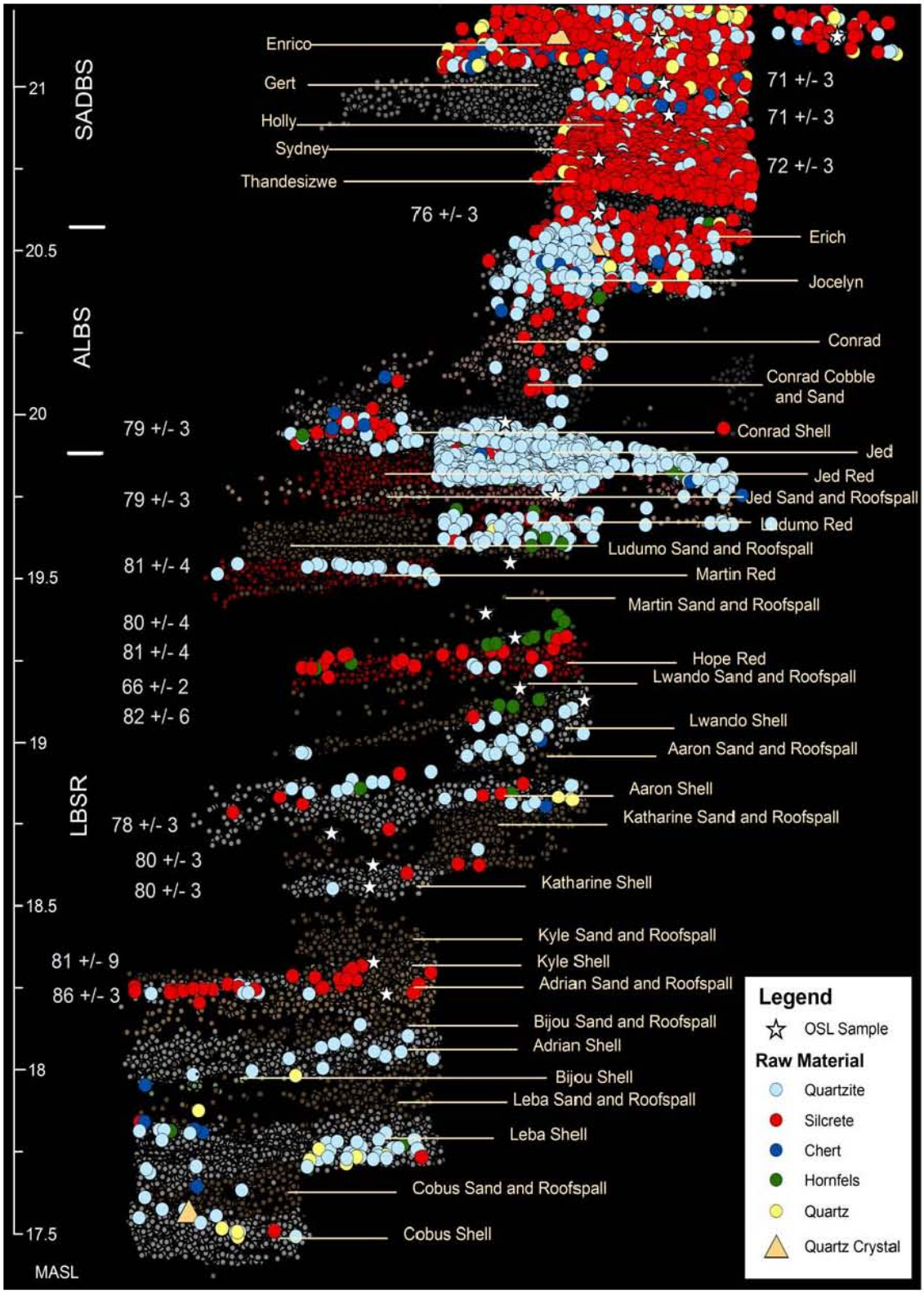

Figure 27. Lithic plots showing color-coded raw materials—north profile of lower Long Section. The smaller plots in the background represent all other plotted finds including shell, fauna, and ochre, to provide an indication of artifact density.

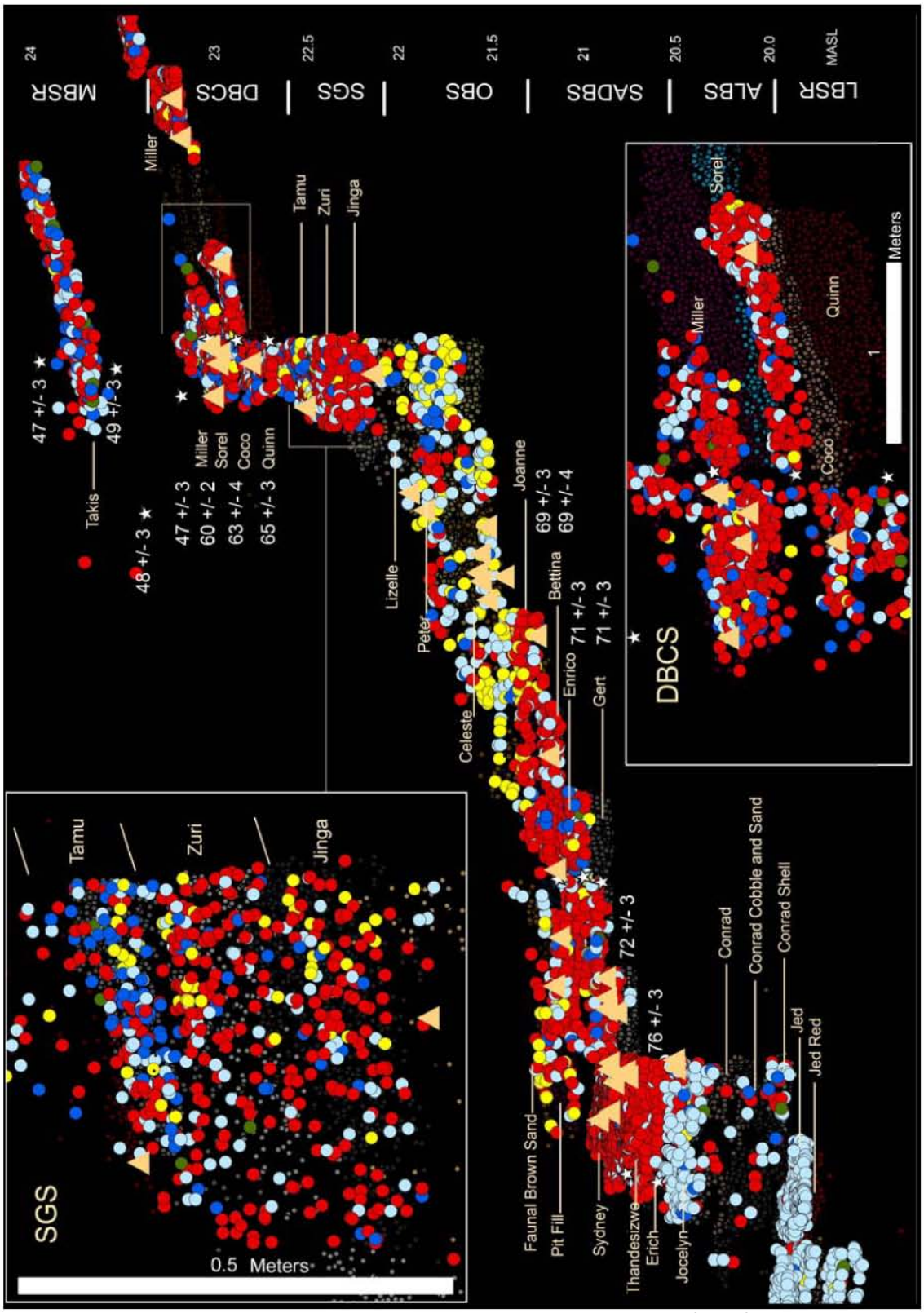

Figure 28. Lithic plots showing color-coded raw materials—west profile of the upper Long Section. Color scheme is the same as presented in the Figure 29 legend

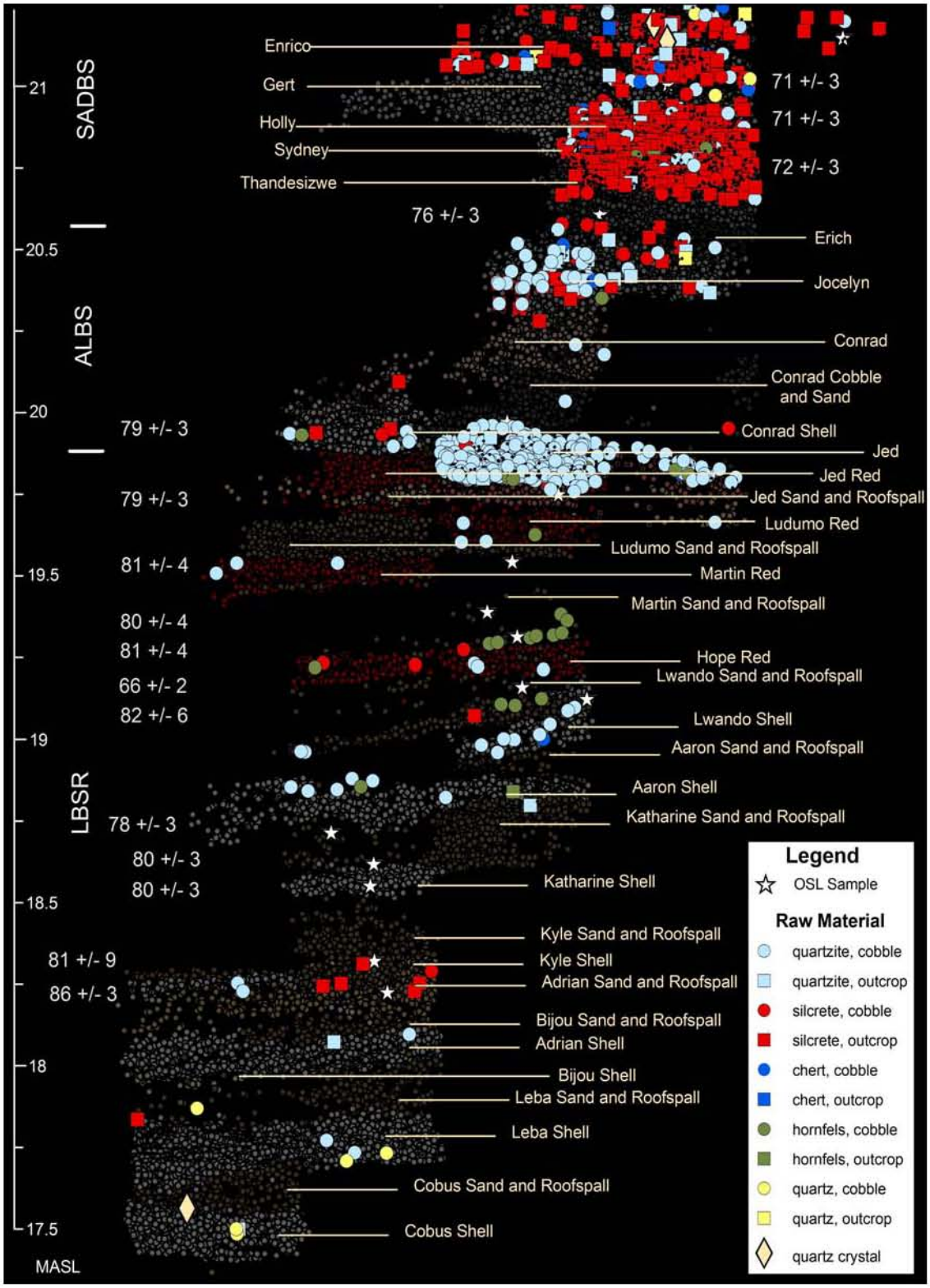

Figure 29. Lithic plots limited to specimens that have cortex. Figure shows color-coded raw materials and cortex type—north profile lower Long Section

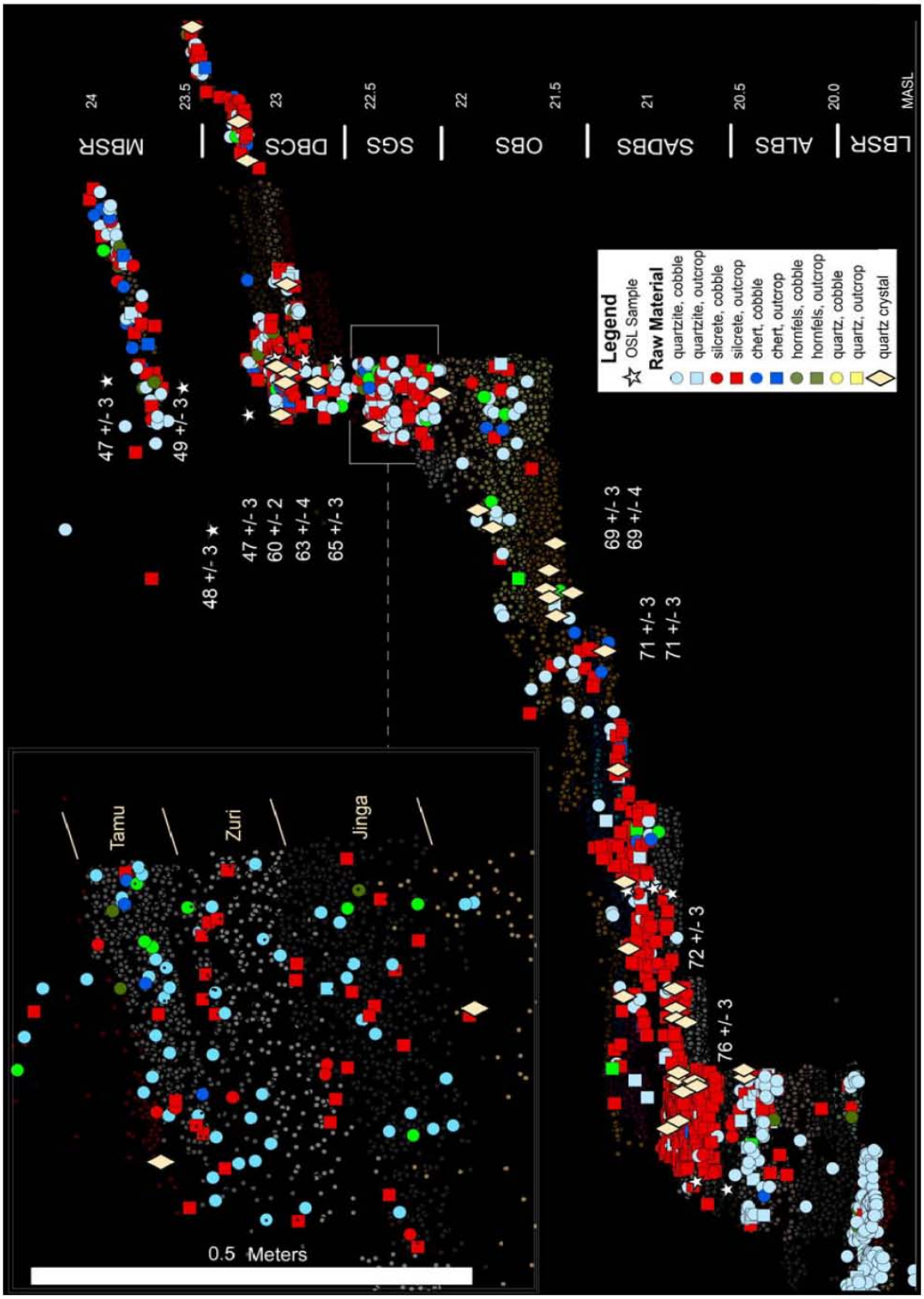

Figure 30. Lithic plots limited to specimens that have cortex. Figure shows color-coded raw materials and cortex type —west view upper Long Section

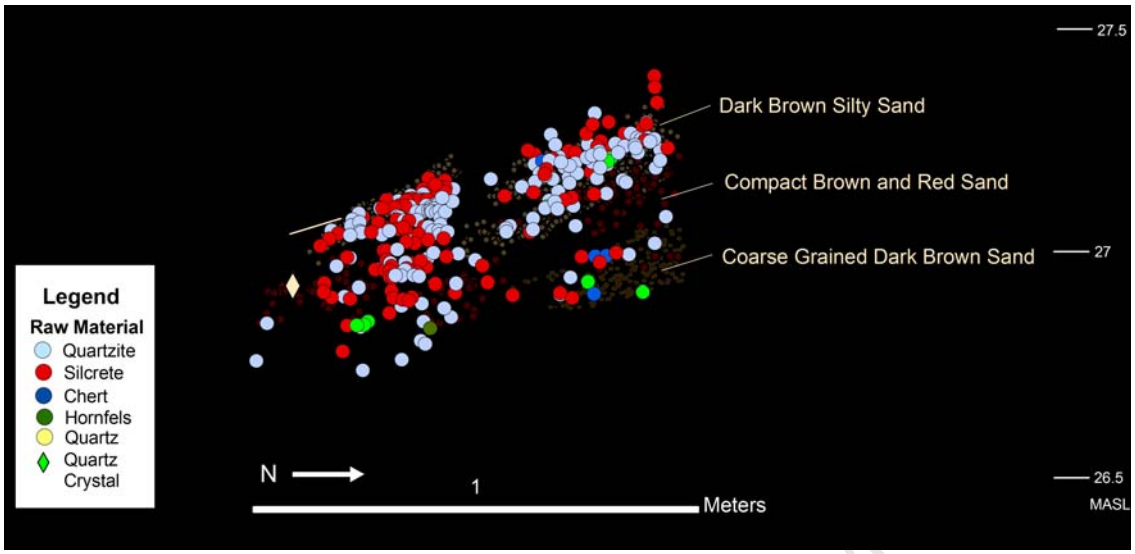

Figure 31. Lithic plots showing color coded raw materials- Northwest Remnant (*NWR*)

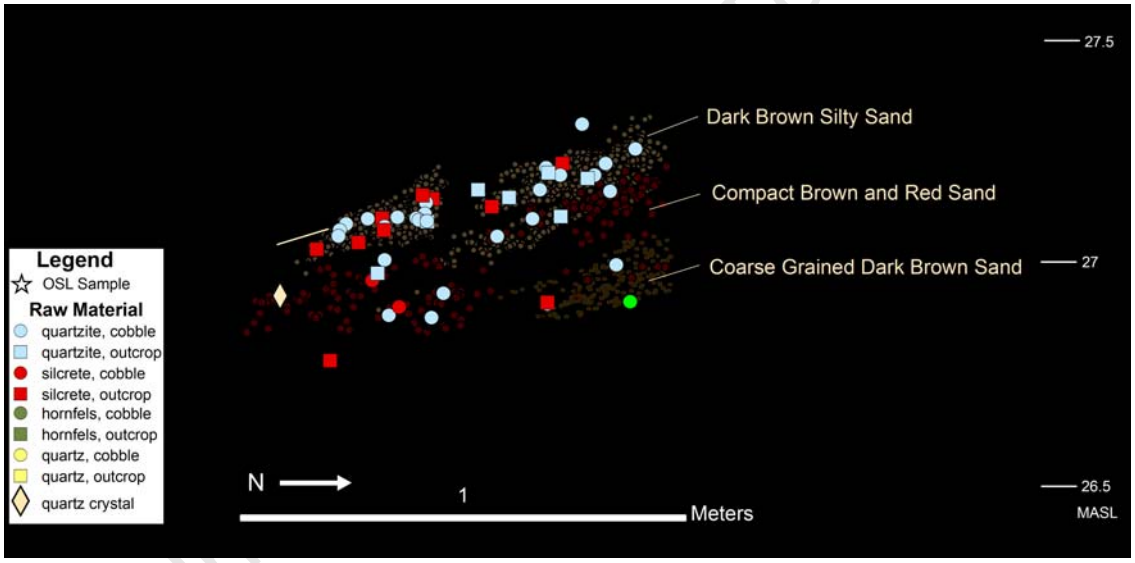

Figure 32. Lithic plots limited to specimens that have cortex. Figure shows color-coded raw materials and cortex type —*NWR*

Table 3. Analytical samples selected for detailed technological analysis. Ages from Brown et al. (2009) and Z. Jacobs (pers comm.); distance to coastline from Fisher et al. (2010); carbon isotope data from Bar-Matthews et al. (2010). Analytical subsamples used in the analyses presented in this dissertation are indented and in smaller font and are listed below the respective SubAgg sample from which they originate (e.g. Miller and Sorel are two subsamples of the *DBCS*).

Sample	Agg	Subagg(s)	Predominant Raw Material	Age (ka)	Age Min/ Max (ka)	OIS	Mean Distance to Coastline	$\delta^{13}C$	Excavated Sediment m^3	Lithic Count	Sample Mass (kg)	Lithic Density (kg/m3)	Lithic Density (n/m^3)
Takis	MBSR	Takis	Silcrete	47-49 ± 3	44-52	3	14.9	unknown	0.06	187	1.0	16.7	3106.3
NWR	NWR	CGDBS, CBRS,CGDBS	Quartzite/ Silcrete	59 ± 3	56-62	3	6.4	C3	0.19	313	1.9	10.3	1653.5
DBCS	**DBCS**	Miller, Sorel	Silcrete	60-63 ± 4	58-76	3	14.4	C4	0.16	1356	2.8	17.5	8475.0
Miller	DBCS	Miller	Silcrete	60 ± 2	58-64	3	8.5	C4	0.06	613	2.1	34.4	9927.1
Sorel	DBCS	Sorel	Silcrete	63 ± 4	59-67	3	15.8	C4	0.01	217	0.4	49.0	25529.4
SGS	SGS	Jinga, Zuri, Tamu	Silcrete	65 ± 3 to 69 ± 3	62-68	4	21.3	Highly Variable	0.04	510	1.2	29.4	12750.0
OBS	OBS	Celeste, Peter, Lizelle	Quartz	69 ± 4	65-73	4	22.0	C4	0.74	486	2.1	2.9	656.8
SADBS	SADBS	Thandesizwe, Sydney, Holley, Gert, Enrico,Betina, Pit Fill, Joanne	Silcrete (80%)	71 ± 3 to 72 ± 3	67-75	4	13.0	C4	0.77	3556	5.3	6.9	4618.2
ALBS	**ALBS**	Erich, Jocelyn,Conrad Shell, Conrad CS, Conrad	Quartzite/ Silcrete	76 ± 3 to 79 ± 3	73-81	5a	3.0	C3	0.28	384	2.2	7.8	1371.4
Erich	ALBS	Erich	Silcrete	76 ± 3	73-79	5a	3.9	C3	0.01	76	0.2	24.7	10482.8
Jocelyn	ALBS	Jocelyn	Quartzite/Silcrete	76 ± 3 to 79 ± 3	73-81	5a	3.0	C3	0.06	177	1.2	21.2	3064.9
Conrad Series	ALBS	Conrad Shell, Conrad CS, Conrad	Quartzite	76 ± 3 to 79 ± 3	73-81	5a	3.0	C3	0.19	131	0.8	4.2	697.7
Jed/JR Quartzite	LBSR	Jed, Jed Red	Quartzite >90%	79 ± 3	76-81	5a/5 b	1.2	C3	0.06	925	7.9	140.4	16357.2
Ludumo Quartzite	LBSR	Ludumo Red	Quartzite	79 ± 3 to 81 ± 4	76-81	5a/5 b	1.2	C3	0.06	65	0.5	8.8	1140.4
HM Silcrete/ Hornfels	LBSR	Hope Red, Martin SR	Silcrete/ Hornfels	81 ± 4 to 82 ± 6	76-81	5b	1.2	C3	0.07	52	0.4	5.5	786.7
Lwando Quartzite	LBSR	Lwando Shell, Lwando Shell/Aaron SR	Quartzite	82 ± 6 to 78 ± 3	76-81	5b	1.2	C3	0.05	50	0.6	12.8	1105.0
AK Silcrete	LBSR	Adrian SR, Kyle Shell, Kyle SR	Silcrete	81 ± 9 to 86 ± 3	81-89ka	5b	2.2	C3	0.02	41	0.1	5.1	1855.2
Leba Quartzite	LBSR	Leba Shell	Quartzite		83-?	5b	unknown	C3	0.04	52	0.6	14.1	1304.9

6.3 Summary of Raw Material and Cortex Patterns

Three patterns emerge from the detailed examination of the raw material profiles:

1. The shift from quartzite to silcrete in the PP5-6 sequence occurs in a relatively short time interval.

The two extremes of the PP5-6 raw material pattern, Jed/JR Quartzite and *SADBS* (particularly the 'Thandesizwe' and 'Sydney' SubAggs) are separated only by the *ALBS* and perhaps 3,000 years. The *ALBS* raw material and cobble patterning seem to be transitional when taken as a whole, but a visible change is present from *ALBS* 'Jocelyn' (~30% silcrete) to 'Erich' (~75% silcrete) (Fig. 27). 'Erich' contains a thin sandy layer that may be indicative of a hiatus. A temporal gap may exist between *ALBS* 'Erich' (76 ± 3ka) and *SADBS* 'Sydney'/'Thandesizwe' (72 ± 3ka). Supplemental micromorphology and OSL samples have recently been taken in the *ALBS*/*SADBS* interface and should provide more information about the nature of this stratigraphic transition. It is also clear that the seemingly intensive occupation of *LBSR* Jed/JR Quartzite, dated to 79 ± 3ka is the impetus behind what originally looked like a quartzite-dominated pattern for the entire *LBSR* (Fig. 24). Other thin occupation layers beneath Jed/JR Quartzite show more variability in raw material use with some intriguing silcrete and hornfels patterning (investigated in more detail in Ch. 7.2).

2. Starting in the *SADBS*, along with intensive silcrete use, the procurement strategy changed.

Most of the silcrete at PP5-6 comes from primary sources and quartzite from secondary sources (Fig. 33). A contingency table analyses was performed to assess the degree of independence between silcrete and outcrop cortex, and quartzite with cobble cortex. The results show significant dependence between silcrete and outcrop cortex, and quartzite with cobble cortex for the SADBS (X^2=109.54, 1 d.f., p <.001) and also for the entire PP5-6 assemblage (X^2=789.34, 1 d.f., p <.001).

The shift from quartzite to silcrete then corresponds with changes in landscape use, as indicated by the shift in raw material procurement patterns. If the assumption is correct that submerged silcrete sources do not exist, then most of the silcrete used at PP5-6 came from at least 8.5km away and was transported to the site. Alternatively, if

currently submerged silcrete sources were available during periods of coastline regression, then the coastline model would predict that these sources could be located relatively close to PP5-6. Outcrop silcrete appears in the record before and after Jed/JR Quartzite when the coastline is modeled to be approximately 2km away from PP5-6 (Fig. 23). However, for about 85% of the time period sampled at PP5-6 in this study, the coastline is modeled to be farther than 2km away. This means that the same hypothetical sources that were available during occupations that were rich in silcrete (*SADBS* and *DBCS*), should have been accessible during time periods that show less reliance on silcrete (*NWR* and Takis occupations).

3. The PP5-6 sequence has parallel production strategies by predominant raw material type.

Quartzite cobble use, which peaks in Jed/JR Quartzite at 79ka, never completely disappears from the PP5-6 record. Silcrete is also present in the *LBSR* sequence and in some frequency in AK Silcrete. The HM Silcrete/Hornfels is exceptional in that all cortex comes from beach cobbles. Refitting of HM Silcrete/Hornfels debitage (discussed later in Ch. 7.2.5) demonstrates that much of this material originates from a single hornfels cobble reduction. Most of the chert, hornfels, and quartz tools throughout the PP5-6 sequence also derive from cobbles.

Quartz only occurs in trace amounts in the PP5-6 sequence once the coastline is modeled to be farther than 2-3km away. Quartz use is highest in the *OBS* and *SGS* near the peak of the coastline curve at 25 to 30km distance from the site. Quartz seems to take the place of silcrete, which dips in frequency in the *OBS* and *SGS* layers. Cortical quartz debitage exhibits mainly cobble surfaces, which are counter to the predictions of the Site Context Model. During the *OBS*, the coastline is modeled to be at or near the MIS 4 maximum distance from the site.

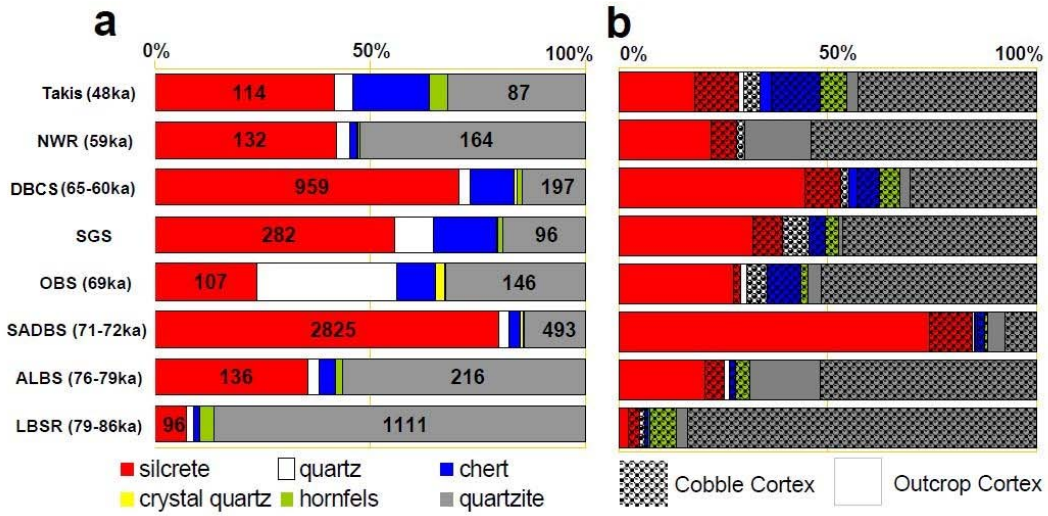

Figure 33. Raw material percentages on the left (a) and cortex type on the right (b) for PP5-6 StratAggs. Textured bars indicate cobble cortex and solid bars depict outcrop cortex. Indeterminate cortical specimens were not included

6.4 Spatial Analysis Results and the Site Context Model

A chi-square goodness-of-fit analysis tested the observed raw material counts for each analytical sample against expected values calculated from the mean of the sum of raw material counts for all PP5-6 analytical samples (Quartzite-30.0%; Silcrete 58.5%; Quartz-4.3%). Except for the OBS, which is quartz dominant, the analysis only included quartzite and silcrete artifact counts for all analytical samples because other raw materials occur in such small frequencies for most stratigraphic samples that their inclusion would have greatly increased the risk of a Type I error (Howell 1999). Similarly raw material proportions from Leba Quartzite and Ludumo Quartzite were not tested at all because silcrete counts are lower than five, which is a generally accepted cutoff for the use of the chi-square test due to the increased risk for Type I errors (Howell 1999).

The results of the chi-square analysis show that the proportions of quartzite and silcrete raw materials for the majority of samples cannot be explained by chance based on the expectation of mean percentages values for the entire site (Table 4). The Jed/JR Quartzite and *SADBS* samples in particular had very high chi-square values resulting from the respective predominance of quartzite and silcrete in these samples. The chi-square tests were not significantly different than mean values for HM Silcrete/Hornfels, which has a relatively small total sample size (n=33). A more comprehensive analysis in the future might take into account the distribution of raw materials on the landscape to test observed raw material percentages against expected values based on the frequency

that the materials are modeled to occur on the landscape (Duke and Steele 2010). A linear model was performed on quartzite and silcrete counts for the PP5-6 analytical samples in order to first test if there is correlation between quartzite and silcrete counts, and second to use the residuals from the analysis as a method of estimating the deviation of each analytical sample from the linear model. Figure 34 is a plot of quartzite (x-axis) and silcrete (y-axis) counts for each PP5-6 analytical sample. This model uses a Reduced Major Axis (RMA) algorithm to minimize error on both axes when fitting the regression line. The red shading above the fitted line indicates samples that have higher than predicted counts of silcrete and the grey shading designates samples that have higher quartzite counts. The result of Pearson's r correlation between quartzite and silcrete (r 0.37, p 0.219) shows no significant relationship between quartzite and silcrete counts for the tested samples.

Table 5 provides the output of residual values from the linear model. Analytical samples are presented in ascending order of distance from predicted quartzite values and descending order of distance from predicted silcrete values. Figure 34 and Table 5 show that the *SADBS*, Jed/JR Quartzite, and *DBCS* deviate the most from the linear model, which is also consistent with the high chi-square values for these same samples (Table 4). The chi-square analysis and linear model presented here demonstrates that the proportion of raw materials on either end of the transition from quartzite to silcrete use represented by the Jed/JR Quartzite and *SADBS* samples is highly unlikely to have resulted from random chance. The prediction of the Site Context Model is that the raw material transition between Jed/JR Quartzite through the *ALBS* to the *SADBS* occurs during the onset of the MIS 4 coastline regression.

The raw material and cortex patterning can be seen to fit the Site Context Model in terms of the overall shape of the curves and alignment of the two most prominent samples, which define the raw material patterning at PP5-6 (Figs. 35c,d). The 8.5 km threshold was clearly set too high. Jed/JR Quartzite (~79ka) occurs close to the modeled minimum distance to the coastline between 80 and 83ka (Fisher et al. 2010). Jed/JR Quartzite is dominated by quartzite and beach cobble cortical products. Distance to the coastline increases on either side of Jed/JR Quartzite. PP5-6 assemblages with distances modeled to be greater than 2km from the coastline begin to show increased percentages of silcrete and primary outcrop cortex. The small AK Silcrete sample may date to 87.5ka when the distance to the coastline is modeled to have increased to c. 5km. The *ALBS*

sample, which occurs after Jed/JR Quartzite, still favors quartzite (Table 4) but shows a trend toward increased silcrete use from primary outcrops.

Table 4. Results of chi-square goodness-of-fit analysis on predominant raw material proportions from PP5-6 analytical samples against mean raw material percentages for the combined analytical samples

H_0:observed raw material counts for each sample do not differ significantly from the mean percentage values for the entire site

Sample	Quartzite		Silcrete		Quartz		X^2	d.f.	P	Result
	Observed	Expected	Observed	Expected	Observed	Expected				
Takis	53	56	82	110			7.288	1	0.00694	reject null hypothesis
NWR	165	96	138	187			62.43	1	<.001	reject null hypothesis
DBCS	159	356	865	694			151.15	1	<.001	reject null hypothesis
SGS	96	153	282	298			22.09	1	<.001	reject null hypothesis
OBS	146	146	107	285	150	23	812.43	2	<.001	reject null hypothesis
SADBS	491	1079	2896	2103			619.45	1	<.001	reject null hypothesis
ALBS	216	115	136	224			123.28	1	<.001	reject null hypothesis
Jed/JR Quartzite	882	277	19	540			1824.10	1	<.001	reject null hypothesis
Ludumo Quartzite*	55	19	2	37						
HM Silcrete/Hornfels	11	15	22	30			3.20	1	0.0736	fail to reject null hypothesis
Lwando Quartzite	37	14	5	27			55.70	1	<.001	reject null hypothesis
AK Silcrete	7	12	32	23			5.60	1	0.017	reject null hypothesis
Leba Quartzite*	36	15	3	30						

samples tested using PAST v. 2.08 with 'sample vs. expected' and 'one constraint' to account for proper degrees of freedom for goodness-of-fit test.

*test not performed because silcrete frequencies are lower than five with inflated risk of Type I error (Howell 1999)

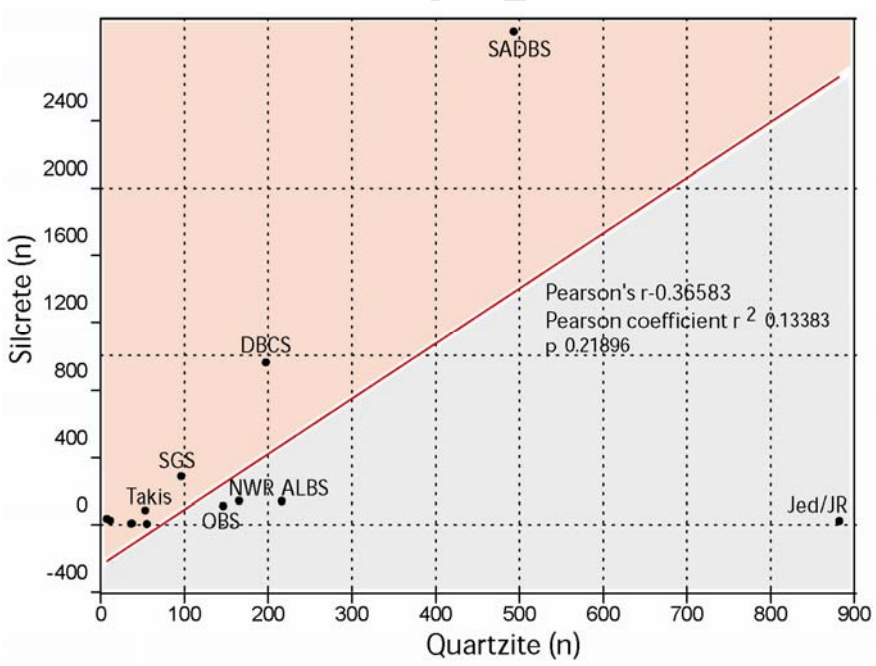

Figure 34. Linear model of fit between quartzite (x-axis) and silcrete (y-axis) counts for PP5-6 analytical samples. The red shading indicates samples that have higher than predicted counts of silcrete and the grey shading designates samples that have higher quartzite counts. The Pearson's Correlation between quartzite and silcrete is not significant (*r* 0.37, p 0.21896). The linear alignment of unlabeled points along the y-axis, near the origin is ordered from left to right: AK Silcrete; HM Silcrete/Hornfels; Leba Quartzite, Lwando Quartzite; Ludumo Quartzite.

Table 5. Table of residual values from linear model (Fig. 34) of correlation between quartzite and silcrete counts from PP5-6 analytical samples. Analytical samples are presented in ascending order of distance from predicted quartzite values and descending order of distance from predicted silcrete values.

	Sample	Count		Residuals	
		Quartzite	Silcrete	Quartzite	Silcrete
Silcrete Rich ↑	SADBS	493	2923	-1822.6	2189.7
	DBCS	197	959	-483.83	581.26
	SGS	96	282	-21.308	25.599
	AK Silcrete	7	32	97.786	-117.48
	Takis	53	82	102.17	-122.74
	HM Silcrete/Hornfels	11	22	110.11	-132.28
	Lwando Quartzite	37	5	150.26	-180.52
	Leba Quartzite	36	3	150.93	-181.32
	NWR	165	138	167.55	-201.3
	Ludumo Quartzite	55	2	170.76	-205.14
	OBS	146	107	174.36	-209.47
	ALBS	216	136	220.22	-264.57
↓ Quartzite Rich	Jed/JR Quartzite	882	19	983.61	-1181.7

The dense *SADBS* sample occurs when the coastline is in regression (c. 10-15km distance from PP5-6), and lithic samples are dominated by silcrete from primary outcrops. An upward trend in the sampled raw material and cortex between Jed/JR Quartzite and the *SADBS* tracks the coastline regression. The *SADBS* and Jed/JR Quartzite samples can be seen as having inverse raw material and cortex patterning.

The *OBS* and *SGS* samples that are stratigraphically above the *SADBS* are interesting because they still show elevated silcrete and primary outcrop cortex in comparison to Jed/JR Quartzite. These values are, however, reduced in comparison to the *SADBS*, even though the *OBS* and *SGS* date to a time when the distance to coastline is modeled to be at an MIS 4 maximum of c. 30km away. The *OBS* has the highest percentage of quartz at PP5-6 and the majority of cortical pieces have cobble cortex. The *SGS* shows an increase in silcrete in comparison to the *OBS*, but the *SGS* also has increased quartz and chert percentages. The *OBS* and *SGS* have similar cortex percentages indicating that cobbles were the most common primary form collected in raw materials other than silcrete. The *OBS* values for silcrete raw material and outcrop cortex are still many times higher than those of the Jed/JR Quartzite sample, but they are lower than would be expected for a peak maximum coastline distance.

The *DBCS* occurs toward the end of a modeled coastline transgression from c. 60 to 65ka. The *DBCS* raw material percentages are similar to those of the *SADBS* and the cortex percentages favor primary outcrops as the source of materials. But the percentage of cobble cortex is higher than in the *SADBS* sample. It is interesting that the richest

silcrete samples occur on the regressive (*SADBS*) and transgressive (*DBCS*) slopes of the MIS 4 coastline curve but not on the peak; a pattern that offers one of the strongest challenges to the Site Context Model and is repeated with other tested variables in the chapters to follow.

The *NWR* shows reduced percentages of silcrete and primary outcrop materials in comparison to the *DBCS*, and is modeled to occur within approximately 1,500 years of the minimum coastline marked by the MIS 4/3 transition at 3.6km (Fisher et al. 2010). It will be interesting to see if future refinement of the coastline model brings the *NWR* in alignment with this minimum coastline, given the increase in use of quartzite beach cobbles.

The raw material and cortex percentages for Takis are similar to those of the *OBS* and *SGS*. As with the *OBS* and *SGS*, Takis occurs near a coastline regression maximum at a 15km peak in distance from Pinnacle Point. The Takis silcrete percentages are higher than those of Jed/JR Quartzite, but the Site Context Model predicts that all other samples should have reduced percentages of quartzite materials and cobble cortex in comparison to Jed/JR Quartzite.

6.5 Test of Site Context Model Expectations

Raw Material

It was expected that quartzite use would be more common when the coastline was near and, silcrete use to be more common when the coastline was farther away (Ch. 3.3). This prediction was tested by correlation between log transformed values of the ratio of quartzite to silcrete (Q/S) based on weight and distance to coastline for each analytical sample (Fig. 37a). Variables were log transformed to adjust for different scales of measurement. A constant (1.0) was added to Q/S to avoid the calculation of an undefined logarithm of zero. This comparison shows the expected relationship of lower quartzite to silcrete ratios with increased distance to coastline. The correlation is not significant however (Kendall's Tau -0.5, p .083) because the *ALBS* and *SADBS* values are higher than expected and consequently the silcrete raw material use peaks well before the MIS 4 peak in distance to coastline (Fig. 35c). When the *SADBS* and *ALBS* are removed, there is a significant correlation in the quartzite to silcrete ratio (Kendall's Tau -0.73, p .039).

Cortex Type

The Site Context Model predicted that in occupations where cobble beaches are modeled to be close to the site, cortical lithics should exhibit higher percentages of beach cobble cortex. The comparison of the log transformed values of Cobble/Outcrop cortex ratio with distance to coastline is one of the least significant correlations observed in this dissertation (Kendall's Tau -0.07, p .80) which essentially shows no dependence at all (Fig. 37b). This outcome is interesting given that there was a highly significant relationship observed between primary outcrop cortex with silcrete, and cobble cortex with quartzite (Ch. 6.3). The plots show that the *SADBS* and *ALBS* have ratios of outcrop to cobble cortex that are too low for samples that occur during regression prior to the peak distance in coastline. The opposite is true of the *OBS*, *SGS*, and Takis samples which have higher cobble ratios than would be expected for their positions on the coastline curve. This is almost certainly associated with the increased use of quartz and chert in these samples which typically have cobble cortex (Fig. 33b, Fig. 35d). An interesting feature of chert and quartz in the *OBS*, *SGS*, and Takis is that they appear to have been collected as very small pebbles in comparison to the larger quartzite cobbles (Ch.9) and occur infrequently in assemblages prior to the upper *SADBS* (Figs 27-28).

6.6 Discussion

A general association between the raw material patterning and coastline change exists even though the relationship is not significant. The two quartzite-dominated assemblages occur at PP5-6 when the coastline is modeled to be at the minimum distances for late MIS 5 through early MIS 3. All other samples have higher non-quartzite raw material percentages and lower percentages of cobble cortex in comparison to the Jed/JR Quartzite assemblage, which is hypothesized to have been flaked on-site at PP5-6 when the coastline was very close. The raw material predictive 'zones' generated for the 8.5km coastline (Figs. 23 and 35) however, do not accurately predict raw material patterning for the entire sequence.

The model is more parsimonious when the hypothetical distance threshold for the change in use from beach cobble quartzite to inland primary outcrops is reduced to 4km (Fig. 36). Four kilometers is not a particularly long distance for the transfer of raw materials and is well within the foraging radius that hunter gatherers might be expected to cover from Pinnacle Point in a day (Kelly 1995). Gould and Saggers (1985) provide

ethnographic evidence of 40km for direct procurement of lithic materials and there is archaeological evidence for direct procurement of 18km in the European Middle Paleolithic (Feblot-Augustines 1997), although it has been noted that raw material conservation may occur even when sites are located only a few kilometers from a lithic source (Marks et al. 1991).

Several scenarios can be invoked to explain why the Site Context Model does not account for the higher percentages of cobble cortex for the *OBS*, *SGS*, and Takis samples. First, it is possible that there may have been one or more rapid regression/transgression cycles of the coastline during or near the OBS/SGS occupations which are not picked up by the 1,500-year resolution of the coastline model. A second explanation for the *SGS*/*OBS*/Takis cortex pattern is that secondary sources may have existed, including raised beaches, conglomerates, and alluvial materials closer to the site than those predicted in Chapter 5.2. These sources could have been regularly visited even when the coastline was far away. Another possibility is that some secondary context materials (particularly the chert) may have been coming from the Gouritz River drainage located approximately 30km from PP5-6.

The *OBS*, *SGS*, and Takis samples occur near or within episodes of intensive dune formation at PP5-6. It is also possible that the landscape changes or perhaps even territorial constraints at this time restricted access to primary outcrop sources. In support of this idea, the percentage of non-quartzite raw materials actually remains fairly constant between analytical samples even though the percentage of primary source materials is reduced. The quartzite to silcrete ratio (Q/S) tested above focused on the two major classes of raw materials represented throughout the PP5-6 sequence. The chert and quartz in the *OBS*, *SGS*, and Takis samples may represent substitutes for silcrete if access to silcrete outcrops was hindered by dunes or other environmental barriers. The substitute of one fine-grained material for others could indicate that these materials were being selected for functional reasons. In order to test this idea, a second index defined by the ratio of quartzite to non-quartzite raw materials (Q/NQ) was then plotted against distance to coastline (Fig. 37c). This ratio takes into account the increase in use of quartz and chert in the *OBS* and *SGS*, which effectively adjusts for the reduced percentages of silcrete in these samples. Again, variables were log transformed and a constant (1.0) was added. There is a significant correlation between distance to coastline and quartzite use when the ratio of quartzite to non-quartzite raw materials is tested (Kendall's Tau -0.57, p .048).

The raw material and cortex percentages for the PP5-6 sequence are more similar in appearance to the bimodal patterning in the δ^{13}C carbon isotopes rather than the coastline curve (Fig. 35). The highest peaks in silcrete use (*SADBS* and *DBCS*) occur close to modeled spikes in C4 vegetation on the smoothed Crevice Cave δ^{13}C curve (Bar-Matthews et al. 2010). As discussed above, silcrete and primary outcrop cortex show a dip near the OBS and SGS samples which corresponds with a return to more C3 conditions in the carbon record (Fig 35a). Silcrete percentages and the ratio of cobble/outcrop cortex were compared against Crevice Cave δ^{13}C values calculated by taking the mean of δ^{13}C published measurements from Bar-Matthews et al. (2010) across the full range of the OSL error bars for each analytical sample (Table 3). The Takis sample was omitted because the Crevice Cave speleothem record does not span beyond 53ka.

The correlation between silcrete percentage (by weight) and δ^{13}C is highly significant (Kendall's Tau 1.0 p .002)(Fig. 38a). As noted in Chapter 4. the Crevice Cave δ^{13}C is interpreted to represent fluctuations in the proportions of C3 and C4 vegetation, as compared with a Holocene C3 curve at Pinnacle Point and a mixed C3/C4 record from Cango Cave speleothem. The Crevice Cave speleothem record tracks vegetation change and fluctuation from 90 to 53ka. Shrubby fynbos vegetation occurs along a coastal strip that likely follows changes in the coastline (Bar-Matthews et al. 2010; Marean 2010a). During coastline regression, the strongly C3 fynbos vegetation retreats out on the Agulhas Bank and is replaced with a mixed or mosaic C3/C4 vegetation regime. The correlation between silcrete use and an increase in C4 vegetation may indicate that during the SADBS and DBCS in particular, the site is positioned to take advantage of interior resources. The peaks in silcrete use may be the result of increased encounter rates with silcrete outcrops during foraging of interior resources or the change in context of the site may create a scenario where the lithic assemblage is sampling what was already happening in the interior away from the coastline. The link between the Crevice Cave isotopic record and variability in the PP5-6 lithic sequence is discussed in more detail in Chapter 12.

The correlation between the ratio of Cobble/Outcrop cortex and δ^{13}C mean values for the analytical samples is also significant (Kendall's Tau -0.71 p .02)(Fig. 38b). The better fit between the cobble/outcrop cortex ratio and δ^{13}carbon record as compared to the coastline model does support the possibility that there may have been a short duration

coastline transgression that occurred in the time period overlapping with the *OBS* and *SGS* occupations producing a variable carbon isotope signature from c. 65-68ka (Fig. 35a) which may be indicative of the temporary return of the coastal fynbos strip between the *SADBS* and *DBCS* occupations. It is also possible that the quartz and chert pebbles that elevate the percentage of secondary context cortex in the OBS and SGS may have been collected from distant sources if mobility increased with more open C4 environments (Ch. 12.3).

The post-hoc analyses of raw material and cortex have identified three significant relationships. Quartzite proportions when compared as a ratio to non-quartzite raw materials is significantly correlated with distance to coastline. Silcrete percentages on the other hand are significantly correlated with changes in the $\delta^{13}C$ record and silcrete use is highest in periods where C4 vegetation is modeled to be most common (Bar-Matthews et al 2010). The ratio of Cobble/Outcrop cortex is also significantly correlated with $\delta^{13}C$. Distance to coastline influences the percentage of quartzite at PP5-6, but the highest peaks in silcrete use may be driven by climate and landscape change.

It should be noted that the chronology of the coastline model has not yet been globally tuned so that the coastline curve (Figs. 23, 35 and 36) is an estimate that is subject to adjustment (Fisher et al. 2010). Similarly, the OSL dates used to place the SubAggs on the coastline and Crevice $\delta^{13}C$ curves typically have error bars of ±3ka, as indicated by horizontal lines on those same figures. Portions of the speleothem curve have decade-level resolution (Bar-Matthews et al. 2010) and the OSL (Brown et al. 2009) and sea level models (Fisher et al. 2010) have millennium-level standard errors. The refinement of the coastline model, an additional set of OSL dates sampled in 2010 and 2011, and completion of ongoing studies of micromammals, shellfish, and sediment chemistry should allow for better anchor points and more rigorous testing of the patterning evaluated here.

6.7 Summary of Findings

- Raw Material Availability Expectations: In periods where the coastline was near to PP5-6, cobble beaches were used as the major source of stone producing raw material patterns dominated by quartzite. During periods of coastline regression, where active cobble beaches were located at a greater distance from site, increased transport costs of quartzite cobbles may have led MSA tool makers to increase their use of more predictable primary sources of silcrete.

  Analysis Results: Quartzite percentage is highest in the Jed/JR Quartzite occupation (~79ka) which is modeled to be very close to the coastline. Silcrete percentages rise with increased distance to the coastline. Silcrete use remains in proportions at or above 50% for all other MIS 4 samples except for the *OBS* and *NWR*. The AK Silcrete sample may be associated with a slight coastline regression around 87.5ka, and the *NWR* may be associated with a coastline transgression at around 60.5ka.

  Conclusion: The predicted positive relationship between the ratio of quartzite to silcrete (Q/S) and increasing distance to coastline exists but the correlation is not significant. The ALBS and SADBS have higher Q/S than would be expected prior to the peak in MIS 4 coastline regression. The post-hoc test of correlation between the ratio of quartzite to non-quartzite raw materials (Q/NQ) and distance to coastline is significant. The post-hoc correlation between silcrete percentages and the Crevice Cave $\delta^{13}C$ record is also significant.

- Cortex Expectations: In occupations where cobble beaches are close to the site, cortical lithics should exhibit higher percentages of beach cobble cortex. Conversely, when the coastline is modeled to be farther away, primary context (outcrop) cortex should be more common.

  Analysis Results: Cobble cortex percentages are highest in Jed/JR Quartzite, which is modeled to be close to the coastline. Primary outcrop cortical materials increase between Jed/JR Quartzite and the *SADBS*

samples as the distance to the coastline increases. The plots show that the *SADBS* and *ALBS* have more outcrop cortex than would be expected for samples that occur during regression prior to the peak distance in coastline. The opposite is true of the *OBS, SGS,* and Takis samples which have more cobble cortex than would be expected for the coastline peak Cobble cortex decreases to less than 50% in the silcrete-rich *DBCS* and then again increases to above 50% in the *NWR* and Takis samples. Primary outcrop sources are elevated in the small AK Silcrete sample, but not in the HM Silcrete/Hornfels sample.

Conclusion: The correlation between the ratio of outcrop to cobble cortex and distance to coastline for the PP5-6 analytical samples was not significant and did not support the predictions of the Site Context Model. The post-hoc correlation between the Cobble/Outcrop ratio and the Crevice Cave $\delta^{13}C$ record is significant.

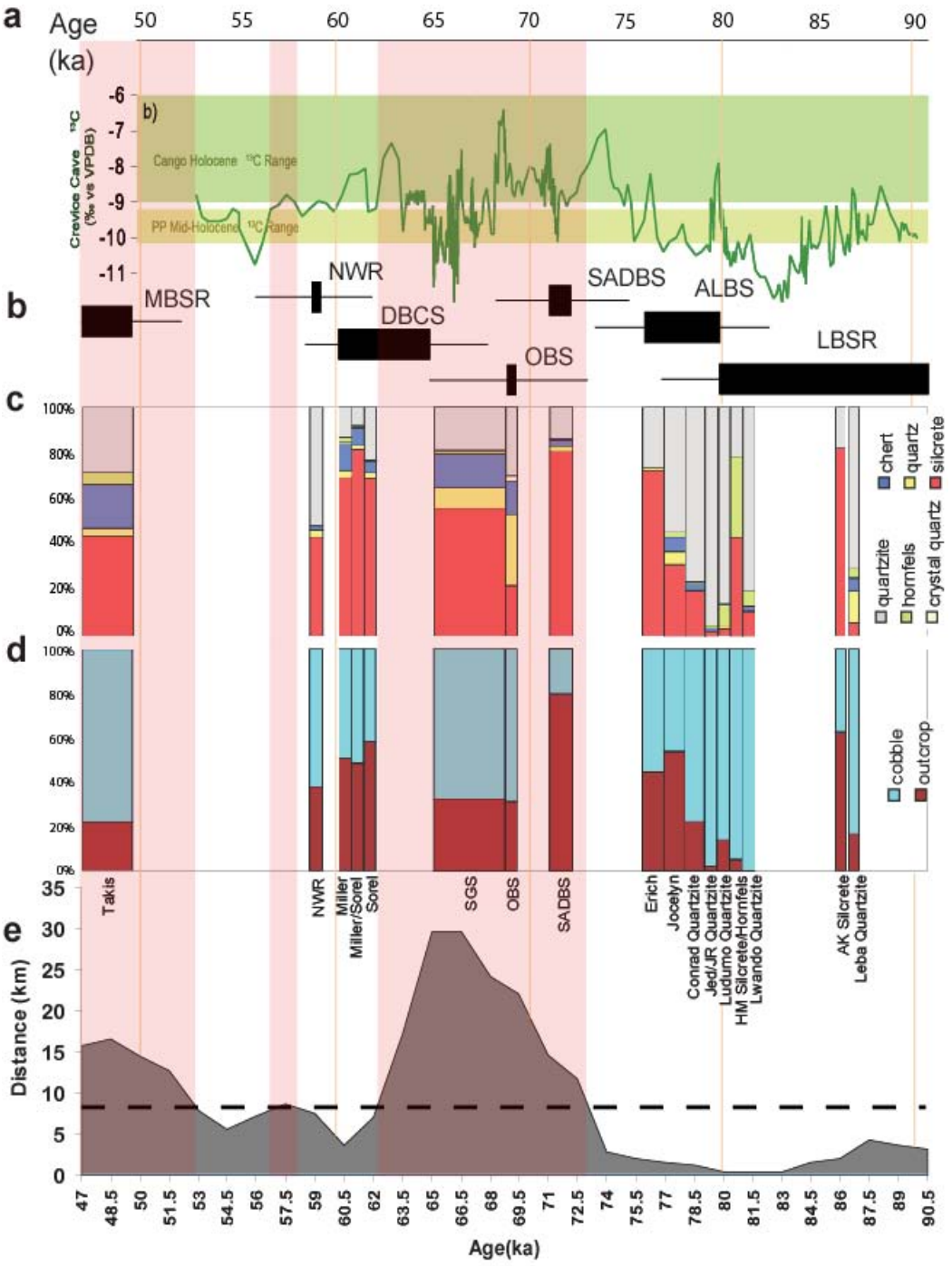

Figure 35. Raw material predictions based, on a transition from secondary to primary sources at 8.5km coastline (equal distance between the coastline and closest source of silcrete). Red zones indicate preference for primary outcrop materials and white zones for beach cobble materials. a) is the Crevice Cave $\delta^{13}C$ Curve from Bar-Matthews et al. (2010); b) PP5-6 StratAgg chronology based on OSL ages (Brown et al. 2009); c) raw material percentage by analytical sample; d) percentage cortex type; e) mean distance to the coastline from Fisher et al. (2010)

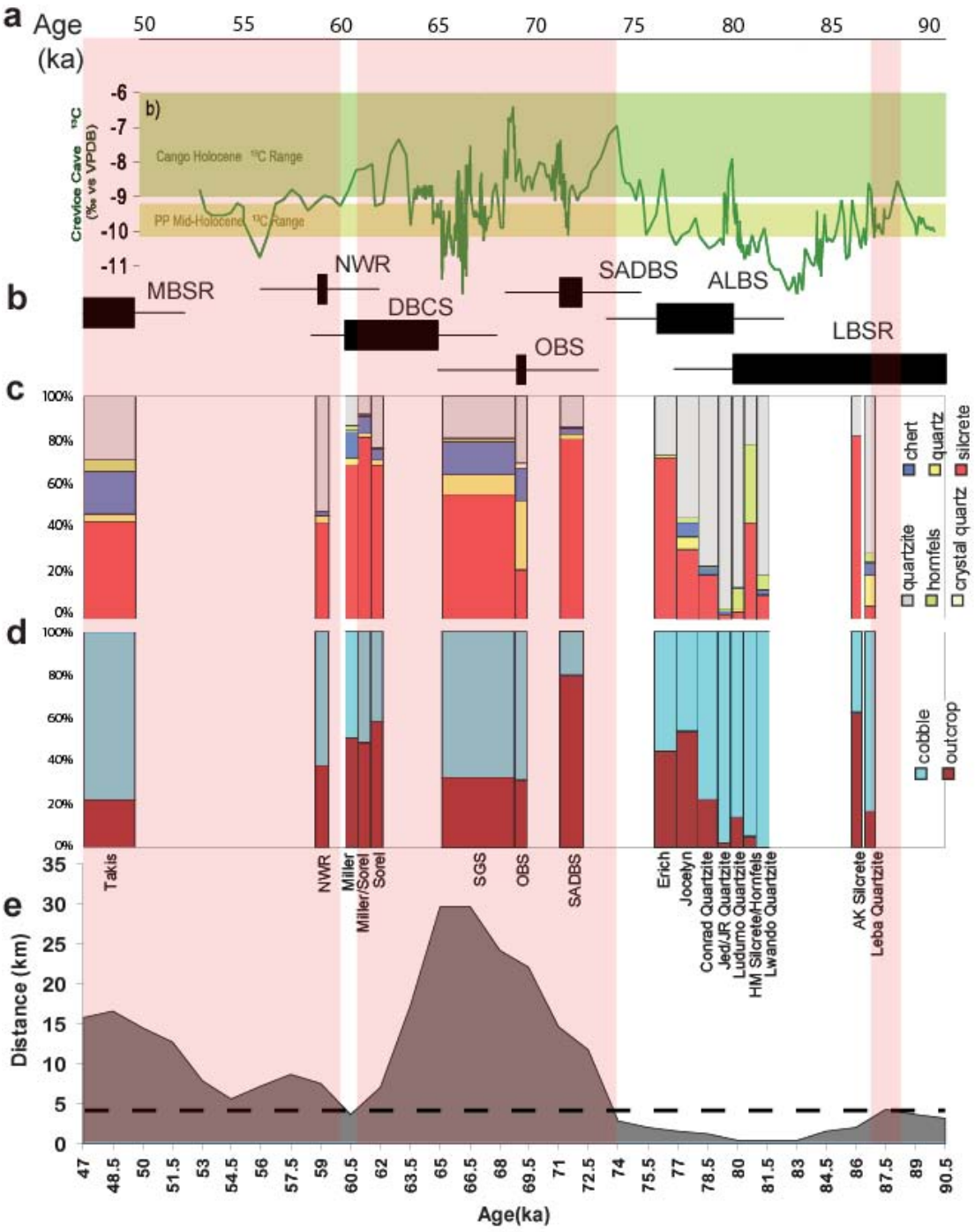

Figure 36. Raw material predictions, based on a transition from secondary to primary sources at 4.25km coastline (half the distance to the closest source of silcrete). Red zones indicate preference for primary outcrop materials and white zones for beach cobble materials. a) is the Crevice Cave $\delta^{13}C$ Curve from Bar-Matthews et al. (2010); b) PP5-6 StratAgg chronology based on OSL ages (Brown et al. 2009); c) raw material percentage by analytical sample; d) percentage cortex type; e) mean distance to the coastline from Fisher et al. (2010)

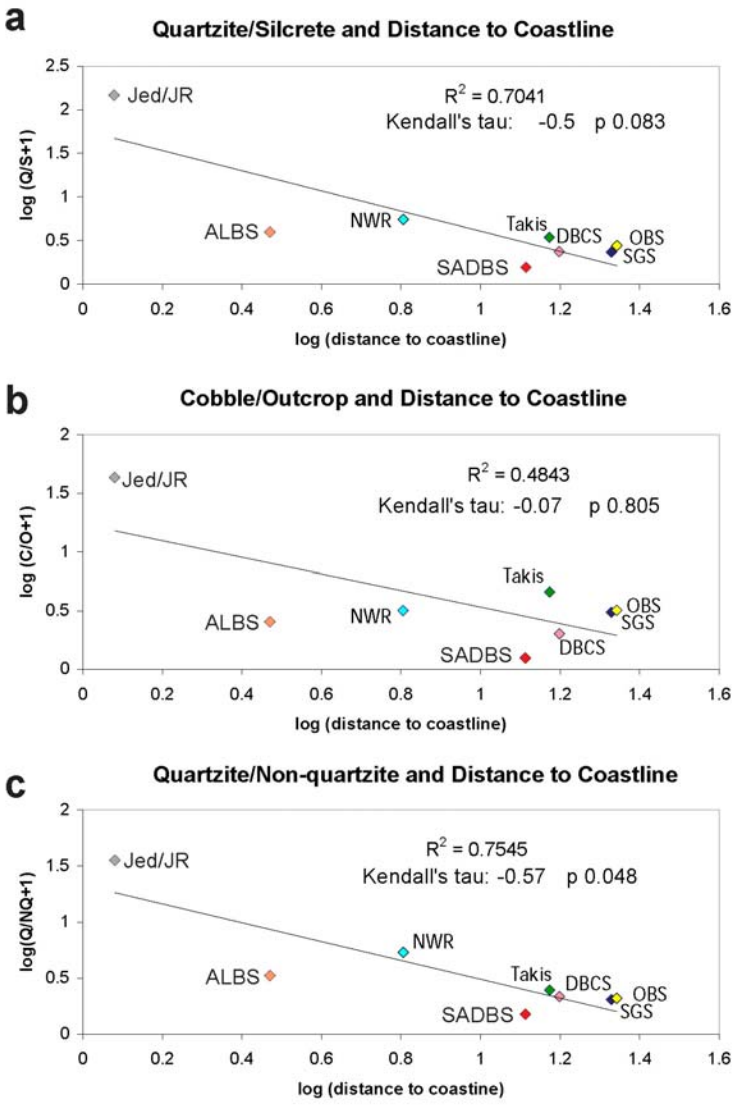

Figure 37. Scatterplot comparisons of log transformed PP5-6 analytical sample raw material test variables and the results of Kendall's Tau rank correlation tests. a) correlation between distance to coastline and ratio of quartzite/silcrete (Q/S) (weight); b) distance to coastline and ratio of cobble/outcrop (C/O) counts for cortical specimens by analytical sample; c) distance to coastline and ratio of quartzite/non-quartzite (Q/NQ) raw materials.

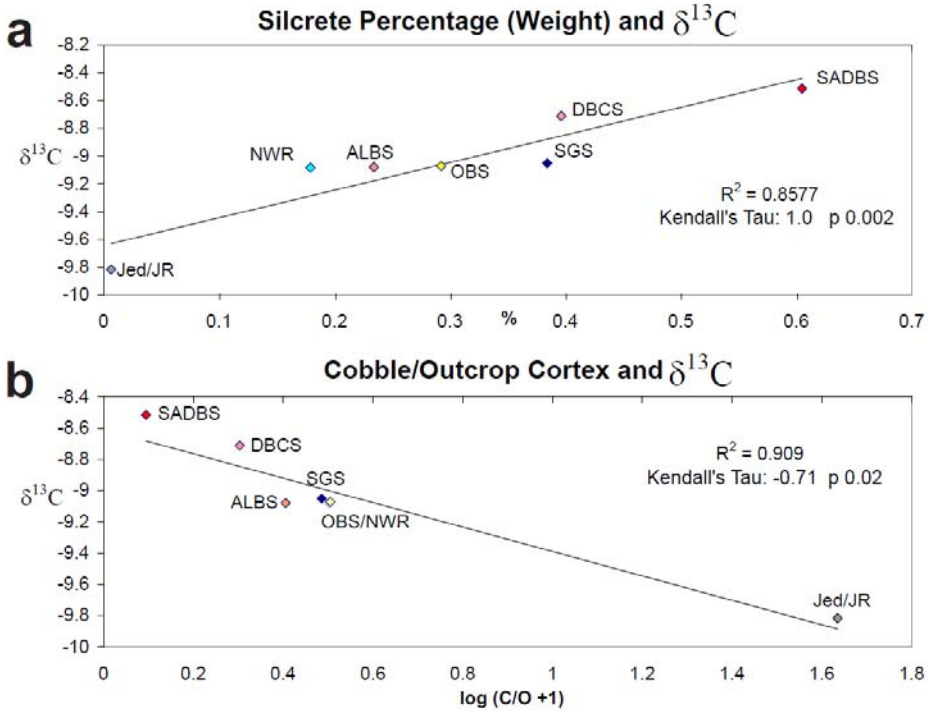

Figure 38. a) Correlation between mean Crevice Cave δ13C from Bar-Matthews et al. (2010) and: a) silcrete percentages (based on mass) for each analytical sample; b) log transformed ratio of cobble/outcrop cortex for each analytical sample. The Takis sample was omitted because the Chronology for the Crevice Cave $\delta^{13}C$ record ends at 53ka.

7.0 Descriptive Analysis of PP5-6 Lithics

The following analysis provides a summary of the PP5-6 lithic sequence in order to provide context for the more detailed analyses to follow. Many of the PP5-6 analytical samples have low artifact counts and are given less attention in this chapter than the larger Jed/JR Quartzite, *SADBS*, and *DBCS* stratigraphic samples. The conclusions reached here will be updated with samples from future excavation seasons and with sieved materials, and should thus be considered preliminary.

A common criticism of southern African MSA lithics is that variation in descriptive terminology may hinder regional comparison (Villa et al. 2005; Cochrane 2006). The methodology followed here has been used at other Pinnacle Point sites (Marean et al. 2004; Thompson et al. 2010), but an effort was made to adapt terminology and technological variables from other MSA studies when appropriate. Artifact images for the majority of cores, points, and formal tools are provided in Appendix 4 to give other researchers an opportunity for direct visual comparison of PP5-6 artifacts with those of their own assemblages. The lithics from PP5-6 are described in context with the well-known Klasies River sequence in Chapter 7.8.

7.1 Lithic Analysis Methods and Materials

The total sample of lithics analyzed for this dissertation consists of 8,322 pieces. This includes all Long Section and Northwest Remnant plotted artifacts from undisturbed stratigraphic contexts that were catalogued up to May 1, 2010, and a very small sample of 10mm sieved material from key lot numbers in the *LBSR*. Lithics from PP5-6 were processed and analyzed according to the following system. Each lithic specimen was assigned a unique plotted find number in the field. The artifacts were then catalogued by the staff of MAPCRM. Each lithic collected with non-residue protocol was washed using an ultrasonic cleaner in a solution of Calgon, following the protocol in Evans and Donahue (2005) in order to minimize damage to microwear and residues.

Every find was examined under magnification with an attempt to identify distinguishing features (bulb, platform, hackle marks, flake scar ripples, etc.) that would allow for orientation of the fragment with respect to the former complete specimen. These fragments are thus classified as having either orientation (proximal, medial, distal, or lateral) or as indeterminate fragments. For analysis of categorical data, “almost complete”

specimens (missing an estimated 2-3mm of distal end) are grouped with complete artifacts. Only complete specimens were included for metric analysis,

Following the methodology of Brown (in Marean et al. 2004), artifact samples were coded by raw material and then organized according to primary technological class, including debitage (flakes, flake fragments and chunks), cores, and retouched artifacts. The samples were assigned to a modified version of Geneste's (1985) techno-typology created for classifying European Middle Paleolithic assemblages. The difference between the Geneste's typology and the tables presented here are that the word 'Levallois' has simply been replaced with 'prepared' and here, fragments were also classified when possible although only complete and nearly complete specimens are presented in the tables. The advantage of using this system is that it allows one to characterize an assemblage according to reduction stage. These phases are organized with respect to tool manufacture in the following way: Phase 0- Acquisition/Retrieval of Material; Phase 1- Initial Core Preparation; Phase 2- Core Reduction; and Phase 3- Retouch/Resharpening (Geneste 1985).

Continuous and discrete variables were recorded for all complete flakes. A list and description of coded attributes can be found in Appendix 2 and screen captures of the Access debitage and core data entry forms in Appendix 3. Continuous measurements include weight (g) and maximum dimension (mm) for all artifacts, and then technological length, maximum width, width at flake midpoint, thickness at flake midpoint, and length of cutting edge (all in mm) for complete and almost complete (missing estimated 1-3mm of distal tip) flakes. Cutting edge does not include the flake platform or relict edges. Complete flakes and retouched flakes were measured to quantify flake exterior platform angle (when possible), platform width and platform thickness (measurements made according to Dibble [1997]).

Discrete variables recorded for all flakes and flake fragments include cortex coverage, flake termination type, scar count, scar pattern, platform type, platform shape, and flake completeness. Dorsal cortex coverage was estimated as a percentage of total dorsal surface area in 20% increments for the analysis of cortex abundance (Ch. 10). In this study, primary cortical debitage describes artifacts with more than 60% cortex coverage. Residual cortical debitage has less than or equal to 60% coverage. The term 'residual cortical' is from Geneste (1985) who used 50% as a cutoff. Complete blades and bladelets were also coded according to a slightly simplified version of the blade techno-typology in Soriano et al. (2007).

Retouched and edge-modified artifacts were also coded according to location of modification, characteristics, and retouch angle (when possible). Core measurements include weight, maximum length, maximum width, maximum thickness, and cortex coverage. Core type (Volman 1981), scar pattern, and scar count were recorded as discrete variables for each complete core.

The three largest excavated samples from PP5-6 come from the Long Section *SADBS*, *DBCS*, and *LBSR* aggregates. The vast majority of the lithic artifacts in all aggregates are classified as debitage; flakes, flake fragments, and chunks/block shatter make up approximately 98% of the entire sample. The PP5-6 assemblage is highly fragmentary and sample sizes, except for the *SADBS* and Jed/JR Quartzite, are relatively small. An effort was therefore made to maximize the amount of information that could be extracted from all complete and fragmentary pieces. The artifact sample counts presented in text, figures and tables presented in this and following chapters may vary by analysis. Samples sizes are dependent upon which analytical samples and raw material categories are selected for comparison. On some specimens it was also not possible to code every attribute (for example on specimens with damaged or concreted surfaces) and therefore the exact sample size counts may not be identical from chapter to chapter. Unless otherwise noted, there is no cutoff size for the following descriptive analysis which includes all plotted artifacts identified by the excavators. The cutoff size for the more detailed analyses to follow is discussed in Chapter 9.

The descriptive analysis is presented in stratigraphic order of the StratAggs from the base to the top of the PP5-6 sequence according to the analytical samples identified and discussed during the GIS analysis of raw materials in Chapter 7.2 and summarized in Table 3.

7.2 PP5-6 LBSR

The analyzed *LBSR* sequence spans from approximately 85ka from the 'Leba Shell' SubAgg (Z. Jacobs pers. comm.) to the 'Jed' SubAgg at ~79ka. The *LBSR* represents a long time span but the majority of analyzed LBSR lithics (72%) derive from the LBSR Jed/JR Quartzite lithic sample (Table 6). Jed/JR Quartzite appears to represent a relatively narrow time span for occupation based on the statistically similar OSL ages that bracket the sample (79 ± 3ka). The Jed/JR Quartzite sample is described out of stratigraphic sequence first below. Five smaller samples (in terms of artifact counts) were

also differentiated for the *LBSR* during the spatial analysis of lithic artifact plots presented in Chapter 6. Three of these samples favor quartzite raw materials, including Leba Quartzite (71% quartzite), Lwando Quartzite (81% quartzite), and Ludumo Quartzite (86% quartzite). Two samples (AK Silcrete and HM Silcrete/Hornfels) are of interest because the raw material patterning from these excavated layers stands out against the predominantly quartzite background of the LBSR (Fig. 39). The research question addressed in this section is whether these layers represent a departure from the large point and blade-based *LBSR* general pattern or represent deliberate selection of non-quartzite raw materials that anticipates the small blade production in some of the silcrete-rich PP5-6 MIS 4 samples.

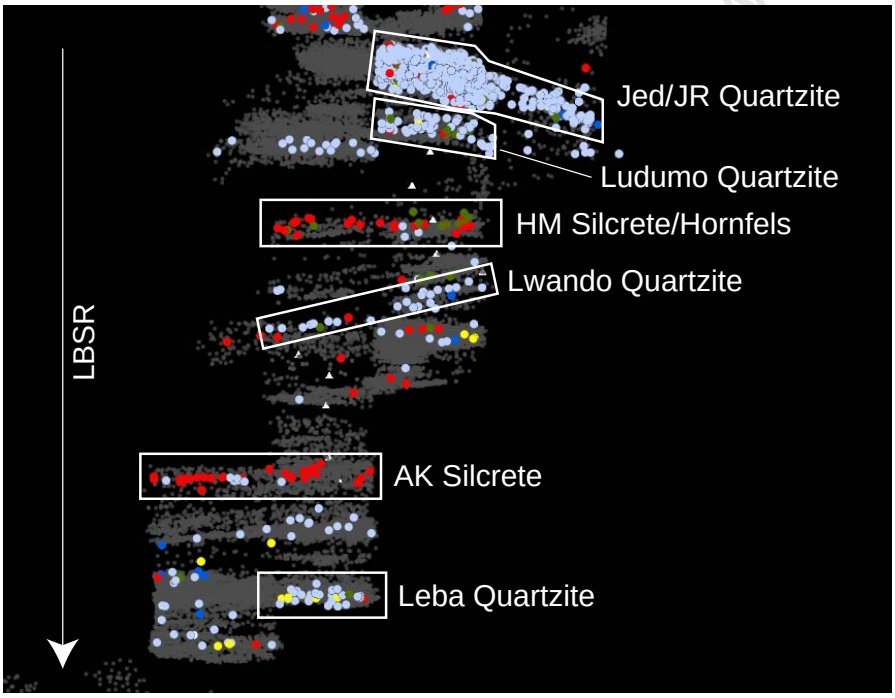

Figure 39. Lithic raw material plots showing the stratigraphic relationship between the *LBSR* analytical samples; view facing north of E-W profile.

Table 6. *LBSR* raw material counts by analytical sample

LBSR Sample	Silcrete	Quartzite	Quartz	Chert	Hornfels	Other	Total
Jed/JR Quartzite	19	882	2	12	10		925
Ludumo Quartzite	56	1		6			63
HM Silcrete/Hornfels	23	11			18		52
Lwando Quartzite	5	40	0	1	3		49
AK Silcrete	33	7				1	41
Leba Quartzite	3	37	7	3	2		52
Total	**139**	**978**	**9**	**22**	**33**	**1**	**1182**

7.2.1 Jed/JR Quartzite

The Jed/JR Quartzite sample consists of over 900 plotted lithics, and most were made from quartzite (Table 6). The analysis of cortex presented in Chapter 7 demonstrates that the majority of the Jed/JR Quartzite cortical debitage exhibits beach cobble cortex (Fig. 40). It is not surprising that most cores (where primary form can be discerned) also have cobble cortex (Table 8).

Wurz (2000) identified blade and point core reduction as being the two primary methods for blank production at Klasies River, where the majority of raw materials also derive from cobbles. She argued that blade production most commonly occurred on conical cores where the flaking surface could maximize use of exploitable core volume to create laminar products, a feature more typical of upper Paleolithic blade production (Inizan et al. 1992). Many blade cores are then reduced to the point where the flaking surface is almost flat or even to an exhausted state where the original production method is no longer discernable.

Wurz argues that point cores more closely follow Levallois point production with an active flaking surface and passive undersurface that may or may not be shaped. In many MSA I and II cores, the base of the core opposite to the flaking surface is minimally exploited and often retains cobble cortex (Wurz 2002). Core convexity is created and maintained through the use of laminar core edge flakes that provide convergent and sub-parallel guiding flake scar ridges. The term 'core edge' is used throughout this dissertation and is equivalent to Wurz's "bordering flake" which is a "long triangular-sectioned blade" (Wurz 2002:65) removed from either or both core margins to create lateral convexity and establish ridges for point removal. Core edge flakes may or may not retain cortex. Wurz notes that point core reduction was more typical of the MSA II, but suggests that point cores may represent a later stage in blade core life.

The analyzed PP5-6 LBSR core sample is small (n=14), and the majority of cores are discoid in organization (Table 9). Three single platform cores from Jed/JR Quartzite (Appendix 4, Section 1: Find Numbers 107398, 156523, and 158317) fit Wurz's (2002) point core definition. The remaining LBSR cores give the impression of being randomly or opportunistically flaked using large flake blanks or of representing the intensive centripetal reduction of more formal point cores into discoid cores. There are no blade

cores in the LBSR sample examined for this dissertation. Core attribute data for all PP5-6 cores and photo images for most cores can be found in Appendix 4, Section 1.

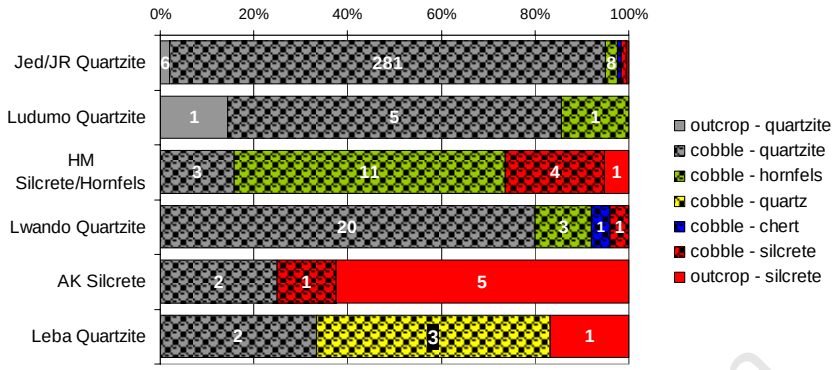

Figure 40. Cortex type across raw material categories by *LBSR* analytical sample. Textured bars indicate cobble cortex and solid bars represent outcrop cortex

Table 7. *LBSR* Jed/JR Quartzite artifact counts by type and raw material

Production Phase	Modified Geneste Techno-Typology	Quartzite	Silcrete	Quartz	Chert	Hornfels	Total	%
0	Manuport	1					1	3
	Primary Cortical (>60% cortex)	21			1	1	23	
1	Residual Cortical (<61% cortex)	60	2		2	1	65	8
	Naturally Backed Flake/Blade	9				1	10	
2	Plain Platform Flakes	115	3				118	22
	Plain Platform Blade	9	1				10	
	Cortical point,flake, or blade with facetted platform	9				1	10	
	Facetted flake	21					21	
	Blade with facetted platform	8					8	
	Point with facetted platform	23					23	
	Core-edge or crested flake/blade	7				1	8	
	Facetted core-edge flake/blade	3					3	
	Thinning Flake	1					1	
	Discoid core	1					1	1
	Single platform core	3					3	
	Core on a flake				1		1	
	Minimal core	1					1	
	Change of orientation core	1					1	
	Indeterminate core fragment	2					2	
various	Block shatter and flake fragments of indeterminate orientation	201	6	1	5	1	214	66
	Flake fragments with orientation (proximal,medial,distal)	370	6	1	2	4	383	
	Small Production Debris (<15mm max dimension)	16	1		1		18	
Total		**882**	**19**	**2**	**12**	**10**	**925**	100

Table 8. Core primary form by raw material and analytical sample

Raw Material	Quartzite					Silcrete						Quartz			Chert				Hornfels	Crystal Quartz	Grand Total
Primary Form / Sample	flake	tabular nodule	cobble	indeterminate	total	flake	tabular nodule	cobble	thermal spall	indeterminate	total	cobble	indeterminate	total	flake	cobble	indeterminate	total	cobble	cobble	
Takis								1		2	3					2	2	4			7
NWR	2			1	3	1					1										4
Miller			2		2	3	1			4	8					1	2	3			13
Miller/Sorel	1				1	4				2	6						1	1			8
SGS										1	1					1	2	3			4
OBS				1	1	1				2	3	1	3	4			2	2		1	11
SADBS			4	1	5	2	2		1	22	27		1	1			2	2			35
Jocelyn						1				2	3		1	1			2	2	1		7
Conrad Series						1		1			2								1		3
Jed/JR Quartzite			5	1	6										1			1			7
Ludumo Quartzite			1		1																1
HM Silcrete Hornfels						1					1										1
Lwando Quartzite			3		3																3
AK Silcrete										1	1										1
Leba Quartzite		1			1																1
Grand Total	3	1	15	4	23	14	3	2	1	36	56	1	5	6	1	4	13	18	2	1	106

Table 9. PP5-6 Core Type after Volman (1981) by analytical sample

SubAgg	Sample / Core Type	single platform	adjacent platform	opposed platform	other double platform	change of orientation	core on a flake	cylinder	discoid	minimal	bipolar	Total
MBSR	Takis		1	4	1				1			7
NWR	NWR	1		2			1					4
DBCS	Miller	1		4	2		1		4	1		13
	Miller/Sorel	2					5		1			8
SGS	SGS			2	1	1						4
OBS	OBS	2		2		4	1		1		1	11
SADBS	SADBS	5	4	10	2	4	3		6	2		36
ALBS	Jocelyn	2		2	1	1			2			8
	Conrad Series	2						1				3
LBSR	Jed/JR Quartzite	3				1	1		1	1		7
	Ludumo Quartzite								1			1
	HM Silcrete Hornfels						1					1
	Lwando Quartzite								3			3
	AK Silcrete					1						1
	Leba Quartzite									1		1
Total		**18**	**5**	**26**	**7**	**12**	**13**	**1**	**20**	**5**	**1**	**108**

Flake Scar Patterning and Platform Preparation: Debitage

Analysis of flake dorsal scar patterning can show how core reduction was organized to provide scar ridges to guide the production of desired flake blanks. The PP5-6 assemblage as a whole, regardless of raw material composition and stratigraphic sample, is blade or point oriented, and flake dorsal scars are typically parallel and convergent. Tables 10-11 provide the scar patterning and directionality of complete/almost complete debitage grouped according to the modified Geneste (1985) techno-typology production phases outlined in Chapter 7.1. Scar patterning refers to the alignment of flake scars with respect to other adjacent scars, and scar directionality addresses the direction from which flakes were struck from the core.

Scar patterning and directionality analysis of primary cortical debitage (production phase 0) indicate that the general pattern of cortical flake removal from all stratigraphic samples was usually initiated from a single platform core (unidirectional). Scars exhibit unidirectional and parallel alignment, meaning that ridges formed from previous removals were used to guide the next sequential flake removals. Not surprisingly, dorsal scar count is low for primary debitage, with most specimens exhibiting entirely cortical dorsal surfaces or a single scar from a previous removal (Table 12).

Platform preparation is also minimal and most primary flakes have cortical or plain platforms (Table 13). Residual cortical debitage (production phase 1) products continue to show mainly parallel unidirectional dorsal flake scars, but with a slight increase in the number of flakes with convergent scars and in bidirectional scars from opposed platforms. Dorsal scar density increases in comparison with primary debitage, with most secondary debitage across all stratigraphic samples having 2 to 3 dorsal scars. Most of the complete/almost complete residual cortical flakes have plain platforms, but in Jed/JR Quartzite, an increase occurs in faceting preparation. Naturally backed core border flakes for creating core lateral convexities are present in some frequency in the Jed/JR Quartzite sample (n=14) (Table 7).

Dorsal scars from non-cortical debitage (production phase 2), indicative of more advanced core reduction (typically 2-3 dorsal scars), still show an emphasis in all samples for parallel flaking from a single direction (when compared with cortical debitage), but with an increase in the percentage of bidirectional flake scars. A higher percentage of

flakes with convergent flake scars occur in Jed/JR Quartzite and the LBSR as a whole; a pattern that is almost certainly associated with the production of points.

An increase in the frequency of flake platform preparation exists in the non-cortical Jed/JR debitage (n=74, 41%) sample in comparison to residual cortical flakes (n=12, 17%). Non-cortical facetted flakes (n=74) occur in slightly greater frequency than plain platform flakes (n=99). The presence of platform abrasion (equivalent to Wurz's [2002] "crushing and abrasion") was recorded similar to the manner described in Soriano et al. (2007) as being "slight" (only visible under magnification), "moderate" (visible without magnification), and "heavy" (abrasion actually alters the exterior platform angle). Platform abrasion occurs infrequently in the Jed/JR Quartzite residual cortical (n=6, 9%) and non-cortical debitage (n=27, 15%) (Table 14).

Few flakes are present from the entire PP5-6 assemblage that exhibit dorsal scar patterning and directionality consistent with centripetal flaking (n=31). A discrepancy exists when flake dorsal scar patterning and directionality are compared with core scar patterning and directionality (Tables 15-16). A relatively high percentage of cores, particularly from the LBSR exhibit centripetal and multidirectional (change of orientation) flaking (Table 9). The over-representation of centripetally flaked discoid cores is likely the result of core mass having been intensively exploited to maximize the yield of cutting edge. The PP5-6 cores are probably not an accurate predictor of core reduction strategy during preferential phases of core reduction because they were discarded at the very end of use-life. Traces of previous removals have been erased by final opportunistic flaking.

Table 10. Dorsal scar patterning for all complete and almost complete PP5-6 debitage by analytical sample

Production Phase	0					1						2					Grand Total
Flake Scar Pattern / Sample	cortical	perpendicular	parallel	convergent	total	cortical	perpendicular	parallel	convergent	centripetal	total	perpendicular	parallel	convergent	centripetal	total	
Takis	4		1		5		2	6			8	1	30	6	2	39	52
NWR	1				1	1		6	3		10	9	29	13		51	62
DBCS	1		1		2	2	5	23			30	13	48	17	3	81	113
Miller			1		1	2	4	15			21	9	32	8	3	52	74
Miller/Sorel								2			2	1	5	1		7	9
Sorel	1				1		1	6			7	3	11	8		22	30
SGS	2				2	1	2	5	3		11	3	25	12	1	41	54
OBS	2		1		3		3	11	2	2	18	7	28	24	2	61	82
SADBS	26	2	9	1	38	5	7	98	16	3	129	53	215	93	13	374	541
ALBS	2		2		4		1	11	1		13	6	32	14		52	69
Erich								1			1		5	2		7	8
Jocelyn	2		2		4			4	1		5	3	16	8		27	36
ConradSeries							1	6			7	3	11	4		18	25
LBSR	13	2	6		21	1	9	32	8		50	22	71	56	7	156	227
Jed/JR Quartzite	8	2	6		16	1	6	27	7		41	17	53	43	5	118	175
Ludumo Quartzite	3				3							1	2	2		5	8
HM Silcrete/Hornfels	1				1		1	3	1		5		8	2	1	11	17
Lwando Quartzite							2	2			4	1	2		1	4	8
AK Silcrete	1				1							1	1			2	3
Leba Quartzite												2	5	9		16	16
Grand Total	**51**	**4**	**20**	**1**	**76**	**10**	**29**	**192**	**33**	**5**	**269**	**114**	**478**	**235**	**28**	**856**	**1200**

Table 11. Dorsal scar direction for all complete and almost complete PP5-6 debitage by analytical sample

Production Phase	0			1				2				Grand Total
Sample / Flake Scar Directionality	unidirectional	bidirectional	total	unidirectional	bidirectional	centripetal	total	unidirectional	bidirectional	centripetal	total	
Takis	1		1	4	4		8	28	7	2	37	46
NWR	1		1	4	4		8	24	18		42	51
DBCS	2		2	19	9		28	40	23	3	66	96
Miller	2		2	11	8		19	26	17	3	46	67
Miller/Sorel				2			2	3	1		4	6
Sorel				6	1		7	11	5		16	23
SGS				7	4		11	23	12	1	36	47
OBS	1		1	11	6	2	19	36	14	2	52	72
SADBS	15	3	18	101	21	3	125	204	94	13	311	454
ALBS	2		2	9	4		13	27	16		43	58
Erich				1			1	5	1		6	7
Jocelyn	2		2	3	1		4	12	11		23	29
ConradSeries				5	3		8	10	4		14	22
LBSR	7	2	9	43	15		58	82	38	7	127	194
Jed/JR Quartzite	7	2	9	38	11		49	65	29	5	99	157
Ludumo Quartzite									1		1	1
HM Silcrete/Hornfels				3	2		5	6	2	1	9	14
Lwando Quartzite				2	2		4	2	2	1	5	9
AK Silcrete								1	1		2	2
Leba Quartzite								8	3		11	11
Total	**29**	**5**	**34**	**198**	**67**	**5**	**270**	**464**	**222**	**28**	**714**	**1018**

Table 12. Scar count for all complete and almost complete PP5-6 debitage by analytical sample

Production Phase		0					1								2							Grand Total
Sample	Dorsal Scar Count	Cortical/No Scars	1	2	3	4	total	Cortical/No Scars	1	2	3	4	5	>5	indeterminate	total	Cortical/No Scars	1	2	3	4	5	>5	indeterminate	total	
Takis		3	1				4	2	2	3	2	1				10	1	2	16	13	9	2	1		44	58
NWR		2	1				3	1	1	6	2	1	1			12		4	14	17	12	7	2	1	57	72
DBCS		1	3	1			5	2	9	17	8	6	1	1		44	4	10	25	29	15	9	6		98	147
	Miller		3	1			4	2	6	11	5	4	1	1		30	3	9	16	20	8	8	5		69	103
	Miller/Sorel								2	1		1				4			1	1	4				6	10
	Sorel	1					1		1	5	3	1				10	1	1	8	8	3	1	1		23	34
SGS		3					3		6	7	5	3				21	1	4	17	14	12	3	3	5	59	83
OBS		1			1	1	3		4	6	6	4	2			22	2	8	27	25	13	4	4		83	108
SADBS		20	19	4	1		44	2	33	68	36	11	6	2	3	161	17	58	131	145	62	31	12	7	463	668
ALBS		2	2				4		3	6	3	3	1		2	18	1	6	27	19	8	5	1	4	71	93
	Erich									1					1	2		1	5	2					8	10
	Jocelyn	2	2				4		1	5		1			1	8	1	4	10	9	6	4			34	46
	ConradSeries								2		3	2	1			8		1	12	8	2	1	1	4	29	37
LBSR		17	9	2	1		29	1	16	27	20	9	2	1	2	78	15	33	62	64	25	13	5		217	324
	Jed/JR Quartzite	11	8	2	1		22	1	12	23	17	7	2	1	2	65	10	29	46	50	17	9	5		166	253
	Ludumo Quartzite	3					3										1		1	4		1			7	10
	HM Silcrete/Hornfels	2					2		1	2	2	1				6	1	2	3	2	4	1			13	21
	Lwando Quartzite		1				1		1	2	1	1				5	1	1	3	2	1	1			9	15
	AK Silcrete	1					1		2							2			1	1					2	5
	Leba Quartzite																2	1	8	5	3	1			20	20
Total		**49**	**35**	**7**	**3**	**1**	**95**	**8**	**74**	**140**	**82**	**38**	**13**	**4**	**7**	**366**	**41**	**125**	**319**	**326**	**156**	**74**	**34**	**17**	**1092**	**1553**

Table 13. Platform types for all complete and almost complete PP5-6 debitage by analytical sample

Production Phase	0								1										2								Grand Total
Flake Platform Type	cortical	plain	facetted	residual facetted	punctiform	crushed/shattered	total		cortical	plain	facetted	residual facetted	punctiform	irregular	crushed/shattered	unknown/indeterminate	total		cortical	plain	facetted	residual facetted	punctiform	irregular	crushed/shattered	unknown/indeterminate	total	
Sample																												
Takis	1	3				1	5		6	2	1	1			1		11		6	19	9	2	1		5	1	43	59
NWR		1	1				2			5	5				1		11		1	24	21	6	2		6		60	73
DBCS	1	1	1		2	1	6		6	27	2	6	1	1	4		47		3	48	37	6	10		7		111	164
Miller	1	1	1		2		5		5	17	1	3	1	1	4		32		3	36	27	2	6		5		79	116
Miller/Sorel										4							4			4	2		2				8	12
Sorel						1	1		1	6	1	3					11			8	8	4	2		2		24	36
SGS	1					1	2		1	13	1	1	4		3		23		14	21	12	4	8		3		62	87
OBS		2		1			3		3	14	2	1	1			1	23		7	46	27	4	5		3		92	118
SADBS	15	20	5	3	2	7	52		16	78	16	20	11		21	5	167		30	256	91	24	43		41	2	487	706
ALBS		3	1				4		1	13	1	1	2		1		19		7	43	17	4	3		1	1	76	99
Erich										1	1	1					3		1	4	3					1	9	12
Jocelyn		3	1				4			8							8		3	20	8	2	2		1		36	48
ConradSeries									1	4			2				8		3	19	6	2	1				31	39
LBSR		20	4	2		1	27		4	51	14	3	2		8		82		13	89	98	16	6	1	9	3	235	344
Jed/JR Quartzite		17	3	2			22		2	44	12	2	2		7		69		8	69	74	15	3	1	7	2	179	270
Ludumo Quartzite		2	1				3												1	2	5				1		9	12
HM Silcrete/Hornfels									2	2	1				1		6		1	6	4		1		1		13	19
Lwando Quartzite						1	1			4		1					5		2	3	4	1					10	16
AK Silcrete		1					1			1	1						2			1	1						2	5
Leba Quartzite																			1	8	10		2			1	22	22
Total	**18**	**50**	**12**	**6**	**4**	**11**	**101**		**37**	**203**	**41**	**33**	**22**	**1**	**40**	**6**	**383**		**81**	**546**	**312**	**66**	**78**	**1**	**75**	**7**	**1166**	**1650**

Table 14. Platform abrasion for all complete and almost complete PP5-6 debitage by analytical sample

Production Phase	0					1					2					Grand Total
Flake Platform Edge Abrasion	slight	moderate	none	indeterminate	total	slight	moderate	high	none	indeterminate	total	slight	moderate	high	none	indeterminate	total	
Sample																		
Takis	2		2		4	3	1		6		10	8	2	1	30	1	42	56
NWR			2		2	3			8		11	12	6		38	1	57	70
DBCS	1		5		6	12	4		27		43	31	13	2	60		106	155
Miller	1		4		5	6	3		19		28	23	9		43		75	108
Miller/Sorel						1	1		2		4	3	3		2		8	12
Sorel			1		1	5	1		6		11	5	1	2	15		23	35
SGS	1		1	1	3	5	1		15	1	22	17	9		33	2	61	86
OBS			3		3	3	1		18		22	16	5	1	71		93	118
SADBS	6		41	2	49	36	28	3	90	6	163	148	51	2	265	10	476	688
ALBS			3		3	5	2		6		13	14	3		36	1	54	70
Erich						1			1		2				5	1	6	8
Jocelyn			3		3	2	1		4		7	9	3		22		34	44
ConradSeries						2	1		1		4	5			9		14	18
LBSR		2	24		26	7	1		69	3	80	23	8	1	195	3	230	336
Jed/JR Quartzite		2	20		22	5	1		59	3	68	19	7	1	147	2	176	266
Ludumo Quartzite			3		3							1			6	1	8	11
HM Silcrete/Hornfels						1			4		5				12		12	17
Lwando Quartzite						1			4		5	1			9		10	15
AK Silcrete			1		1				2		2				2		2	5
Leba Quartzite												2	1		19		22	22
Total	**10**	**2**	**81**	**3**	**96**	**74**	**38**	**3**	**239**	**10**	**364**	**269**	**97**	**7**	**728**	**18**	**1119**	**1579**

Table 15. Core flake scar patterning by analytical sample

Sample	Core Scar Pattern					Grand Total
	Parallel	Convergent	Perpendicular	Multi-directional	Centripetal	
Takis	6		1	1	1	9
NWR	3	1				4
Miller	7	2			4	13
Miller/Sorel	5				1	6
SGS	2	1	1			4
OBS	4	1		3	2	10
SADBS	19	1	1	5	8	34
Jocelyn	4	1		1	2	8
Conrad Series	2	1		1		4
Jed/JR	2	3		1	2	8
Ludumo Quartzite					1	1
Lwando Quartzite					3	3
AK Silcrete				1		1
Total	**54**	**11**	**3**	**13**	**24**	**105**

Table 16. Core flake scar directionality by analytical sample

Sample	Core Scar Directionality				Grand Total
	Unidirectional	Bidirectional	Multi-directional	Centripetal	
Takis	2	5	1	1	9
NWR	1	3			4
Miller	4	5		4	13
Miller/Sorel	4	1		1	6
SGS	2	2			4
OBS	3	2	3	2	10
SADBS	7	15	5	8	35
Jocelyn	2	3	1	2	8
Conrad Series	3		1		4
Jed/JR	4	1	1	2	8
Ludumo Quartzite				1	1
Lwando Quartzite				3	3
AK Silcrete			1		1
Total	**32**	**37**	**13**	**24**	**106**

Jed/JR Quartzite End Products

The following terms are adopted from Wurz (2002) and are applied to cobble-based quartzite dominated samples from PP5-6. “End products” (p. 1004) refer to lithics that usually have facetted platforms, are symmetrical in plan, and have dorsal scar ridge patterning organized to predetermine the final shape of the intended flake. The PP5-6 “points” or “points with facetted platform” are equivalent to Wurz’s “points” and are end products, which include convergent blades and flakes that are triangular and symmetric in plan view with central guiding ridges and facetted platforms (Wurz 2000). “Blades with facetted platforms” are equivalent to Wurz’s “blades,” and are end products that adhere to the typical archaeological classification of having length of at least twice their width. The strict distinction between flakes and blades is an analytical construct, but the classification allows for comparison with other MSA collections. The functional difference between flakes and blades is probably better addressed by an assemblage-wide analysis of edge-damage patterning to identify if these end products were differentially utilized (Schoville 2010).

The majority of complete LBSR points (10 of 17) and all of the LBSR facetted blades (6 complete and 2 fragments) are found in the Jed/JR sample (Table 17). Point size is compared across the PP5-6 sequence and with those of Klasies River in Chapter 7.8, and it will be demonstrated that the points from Jed/JR Quartzite are variable in size but are generally short and broad. The tip cross-sectional area (TCSA) index (*max width* $*$ *max thickness* $*$ *0.5*) has been argued to be a useful way of characterizing the potential use and delivery system for stone-tipped projectiles (Shea 2006; Sisk and Shea 2009). The points from Jed/JR Quartzite have a mean TCSA value of 175.7mm^2 (Table 18), placing them within the range of values calculated as being optimal for modern experimental thrusting spears based on point survival rate during calibrated crossbow experiments (Shea et al. 2001). The PP5-6 points are far too large to have been used as armatures on distance projectiles. The mean TCSA value for the small sample of Jed/JR points is also similar to those calculated for a sample of Klasies River MSA II (upper) points (mean TCSA-170, SD-79) (Shea 2006). Edge modification on PP5-6 end products is currently being studied in a more systematic way by Benjamin Schoville of ASU using GIS methodology developed by Bird et al. (2007).

Table 17. Jed/JR Quartzite complete end product mean dimension and summary statistics. The total LBSR total sample is included for comparison. All *LBSR* facetted blades occur in the Jed/JR Quartzite sample

	Points		Blades
	Jed/JR	LBSR	Jed/JR
Mean Length	47.4	50.3	58.2
SD	14.3	15.7	7.6
count	10	17	6
95% CI	8.9	7.5	6.1
Mean Width	31.4	32	26.2
SD	6.2	6.4	3.8
count	10	17	6
95% CI	3.8	3.0	3
Mean Thickness	10.8	11.4	8
SD	2.9	3.3	2.1
count	10	17	6
95% CI	1.8	1.6	1.7
Mean Plat Width/Plat thickness	3.3	3.2	3.2
SD	0.6	1.4	0.3
count	10	17	6
95% CI	0.4	0.7	0.2

Table 18. Jed/JR Quartzite tip cross-sectional area (TCSA) summary statistics for quartzite points

Jed/JR Point TCSA	
Mean	175.7
Median	186
Standard Deviation	74.9
Sample Variance	5614.7
Range	231.5
Minimum	80.5
Maximum	312
Count	10
Confidence Level(95.0%)	53.6

Informal Retouch

There are few examples of retouched tools at PP5-6 with repetitive or standardized forms, apart from the backed pieces that occur in the upper Long Section sequence. Many specimens have edge modification consistent with deliberate retouch or damage incurred from use or post-depositional processes. These other unstandardized retouched or edge-modified tools are categorized here as being “informal” following Wurz (2000). “Abrasion” and “blunting” describe the crushing or rounding of tool edges

either through use or deliberate abrasion or grinding. Pieces with abrasion or blunting do not have the systematic and regular modification exhibited by typical backed pieces such as crescents. “Single scar notches” are approximately equivalent to “break-out notches” in Wurz (2000:88), and they appear to be the result of use or post-depositional damage rather than as deliberate retouch to create a concave working edge as in the “notched” tools of the DBCS discussed below. “Denticulates” have multiple single scar notches that create a saw-like edge. Lithics with “burination” scars are not necessarily considered to be deliberately made formal burins unless specifically noted. “Steep” retouch denotes tools with scraper-like retouch. “Marginal” retouch is very small irregular modification that is often not visible without magnification.

There are few informal retouched tools from the entire LBSR (n=23) and a total of 10 modified pieces from Jed/JR Quartzite (Table 19). All Jed/JR pieces occur on quartzite and most are classified as single flake notches (n=6) or pieces with marginal retouch (n=2) (Table 20). Half of the Jed/JR sample modification occurs on lateral left (n=3) and distal dorsal surfaces (n=2) and the remainder on ventral laterals or multiple locations (Table 21).

Table 19. Counts of informal retouched pieces by raw material and analytical sample

Sample	Silcrete	Quartzite	Chert	Quartz	Hornfels	Quartz Crystal	Other	Total
MBSR	6	2	2					10
NWR	6	14	1					21
DBCS	59	10	11			1		81
Miller	31	7	7					45
Miller/Sorel	20	1	4			1		26
Sorel	8	2						10
SGS	9		1	1			1	12
OBS	13	6	2	1				22
SADBS	114	14	10	1	1			140
ALBS	5	12	3					20
Erich		3						3
Jocelyn	5	7	1					13
ConradSeries		2	2					4
LBSR	3	19			1			23
Jed/JR Quartzite		10						10
Ludumo Quartzite		1						1
HM Silcrete/Hornfels		1			1			2
Lwando Quartzite	1							1
AK Silcrete	1	1						2
Leba Quartzite	1	6						7
Grand Total	**215**	**77**	**30**	**3**	**2**	**1**	**1**	**329**

Table 20. PP5-6 informal retouched pieces by analytical sample and modification type

Sample	Abrasion	Blunting	Burination	Denticulate	Marginal	Single Scar Notch	Steep	Total
MBSR			1	1	7		1	10
NWR		1	1	2	13	2	2	21
DBCS	13	7		2	36	16	7	81
Miller	3	4		2	19	13	4	45
Miller/Sorel	10	3			10	2	1	26
Sorel					7	1	2	10
SGS	1	1			4	4	2	12
OBS				1	8	8	5	22
SADBS	6	12	1	3	80	15	22	139
ALBS			1	1	9	7	2	20
Erich					2	1		3
Jocelyn			1	1	5	4	2	13
ConradSeries					2	2		4
LBSR		1			10	10	2	23
Jed/JR Quartzite		1			2	6	1	10
Ludumo Quartzite					1			1
HM Silcrete/Hornfels					2			2
Lwando Quartzite						1		1
AK Silcrete					1		1	2
Leba Quartzite					4	3		7
Grand Total	20	22	4	10	167	62	43	328

Table 21. Location of informal retouch by analytical sample

Sample / Location	lateral left dorsal	lateral left ventral	lateral left bifacial	lateral right dorsal	lateral right ventral	lateral right bifacial	both laterals	distal ventral	distal dorsal	distal bifacial	proximal bulbar	proximal dorsal	other multiple location	other bifacial	entire cutting edge	indeterminate	Total
Takis	3	1		1	1		1		2		1						10
NWR	3	3	1	3	1		7	1	1							2	22
DBCS	20	8	1	16	1	2	11		13	1		2			2	3	80
Miller	13	6	1	8		1	5		7			1			1	2	45
Miller/Sorel	4	2		6	1		6		3	1		1			1		25
Sorel	3			2		1			3							1	10
SGS	1	1		4	1		1		3							1	12
OBS	6			3	1	2	7						2		1		22
SADBS	36	7		24	9	4	14	1	29	1			7		1	9	141
ALBS	2	1	1	4	2	3		1	2				1	1			19
Erich				2		1											3
Jocelyn	2	1		2	2	1		1	2					1			13
ConradSeries			1			1							1				3
LBSR	6	1	3	2	1		4		3				1		1	1	23
Jed/JR Quartzite	3	1			1		1		2				1			1	10
Ludumo Quartzite									1								1
HM Silcrete/Hornfels			1												1		2
Lwando Quartzite	1																1
AK Silcrete	1		1														2
Leba Quartzite	1		1	2			3										7
Grand Total	**77**	**22**	**6**	**57**	**17**	**11**	**45**	**3**	**53**	**2**	**1**	**2**	**11**	**1**	**5**	**16**	**329**

Jed/JR Quartzite Summary

The analysis of core primary form and debitage cortex type indicates that Jed/JR Quartzite cores were made predominantly from quartzite secondary context beach cobbles. The small sample of Jed/JR Quartzite end products includes facetted points and blades from single platform cores. The Jed/JR points are typically short and thick. The PP5-6 LBSR cores were flaked centripetally before discard and were more likely to be abandoned in a small size and in discoid form. A small percentage of LBSR lithics show evidence for edge modification (2%), although it should be cautioned that lack of visible damage does not rule out the possibility of tool use given that most lithics are made from quartzite which is considered to provide a durable edge that is resistant to damage in comparison to other more brittle raw materials (Wurz 2000).

7.2.2 Leba Quartzite

Leba Quartzite is a small (n=52) quartzite dominant sample (71%) (Table 22) that represents the base of the PP5-6 analyzed lithics and occurs at approximately 86ka (Fig. 39). Leba Quartzite lithics have a relatively high percentage of products from production stage 2 (44%) and no primary cortical debitage. The few examples of quartzite and quartz residual cortical lithics exhibit cobble cortex except for one outcrop silcrete specimen. Both stage 2 cortical lithics have facetted platforms. Points are well represented (n=5, 10%) given the small size of the sample. Leba Quartzite appears to be an end product (point) dominated sample with few early stage products perhaps indicating that many of the primary cortical pieces were either produced elsewhere on site or were discarded elsewhere on the landscape.

Table 22. *LBSR* Leba Quartzite artifact counts by raw material

Production Phase	Modified Geneste Techno-Typology	Silcrete	Quartzite	Quartz	Chert	Hornfels	Quartz Crystal	Other	Total	%
2	Plain Platform Blade	1	2		1				4	44
	Plain Platform Flakes		9	2					11	
	Point with facetted platform		5						5	
	Cortical point,flake, or blade with facetted platform		2						2	
	Minimal core		1						1	
various	Block shatter and flake fragments of indeterminate orientation		3		1	2			6	56
	Small Production Debris (<1.5mm max dimension)				1				1	
	Flake fragments with orientation (proximal,medial,distal)	2	14	4					20	
	Other/Indeterminate		1	1					2	
Total		**3**	**37**	**7**	**3**	**2**			**52**	**100**

7.2.3 AK Silcrete

AK Silcrete occurs stratigraphically above Leba Quartzite at ~86ka (Fig. 39). This sample has 41 plotted lithics, 33 of which are silcrete (80%)(Table 23). The majority of the sample consists of small fragmentary debitage, with one primary flake and two secondary cortical flakes and one small silcrete core (Find Number 134600). The three cortical flakes have outcrop cortex. Quartzite lithics are limited to several small flake fragments and the proximal ends of two larger end products (Find Numbers 141096 and 141111 with facetted platforms and convergent flake scars). Find Number 139450 is a silcrete distal convergent blade fragment with bifacial edge damage on the left margin that may represent a fragment of a larger preferential removal. It is not clear whether this blade is more like the larger facetted quartzite proximal fragments found in this sample, or if the complete blank would have resembled the smaller plain platform bladelets of the *SADBS* discussed below.

The entire lithic sample weighs just over 100g and gives the appearance of having been opportunistically flaked from at least five individual small silcrete nodules, based on differential color, texture, and cortex of the debitage (Fig. 41). Refitting was attempted for the AK Silcrete sample but only a single conjoin of a small bladelet was found (specimens 139429 and 139479). The lack of refits likely results from the very small excavated horizontal area (0.02m^2: Table 3) and diversity of silcrete materials (a few pieces each from a relatively large number of nodules).

The presence of primary outcrop cortex and heat treatment gloss observed on most of the sampled silcrete (including gloss on early stage products) are features that AK Silcrete has in common with the silcrete-dominant *SADBS* assemblages that occur ~20ka later in the PP5-6 sequence (discussed in Ch. 8). The strategy for the use of primary outcrop silcrete and heat treatment preparation was already in place well before the major MIS 4 raw material transition from quartzite to silcrete. The presence of silcrete from at least five different nodules indicates that the raw material proportions in this layer are not skewed due to a single silcrete core reduction. In terms of core reduction, the AK Silcrete debitage is mainly reflective of small production waste and the silcrete core is in a near-exhausted stage of exploitation. The utilized silcrete convergent distal blade fragment indicates that there is some silcrete blade production at this time but there are few intermediate (production stage 2) blade products in AK Silcrete that fit between the small core and discarded distal blade to know if silcrete blade production was happening on site at that time. The presence of quartzite end products indicate that the occupation(s) that

produced the AK Silcrete sample was still tied to the broader *LBSR* quartzite blade and point production system.

Table 23. *LBSR* AK Silcrete artifact counts by raw material

Production Phase	Modified Geneste Techno-Typology	Silcrete	Quartzite	Quartz	Chert	Hornfels	Quartz Crystal	Other	Total	%
0	Primary Cortical (>60% cortex)	1							1	2
1	Residual Cortical (<61% cortex)	2							2	5
2	Plain Platform Flakes	1							1	7
	Cortical point,flake, or blade with facetted platform	1							1	
	Change of orientation core	1							1	
various	Block shatter and flake fragments of indeterminate orientation	10	1					1	12	85
	Flake fragments with orientation (proximal,medial,distal)	13	5						18	
	Small Production Debris (<15mm max dimension)	3	1						4	
	Other/Indeterminate	1							1	
Total		**33**	**7**					**1**	**41**	**99**

Figure 41. AK Silcrete lithic sample arranged to approximate the actual horizontal spatial distribution of the plotted finds

7.2.4 Lwando Quartzite

Lwando Quartzite is a sparse scatter of mostly quartzite debitage (n=50: Table 24). Approximately half of the sample exhibits cobble cortex (26 complete or fragmentary pieces). There are three heavily reduced discoid cores in the sample and all have cobble cortical bases and a convergent flake proximal fragment of what was probably an asymmetric facetted point. There is also a complete large quartzite cobble (Fig. 42) that exhibits some thermal damage in the form of potlidding and cortical exfoliation. The cobble weighs 1611g and measures 148mm in length, 105mm width, and 72mm thickness. The cobble does not exhibit any hammerstone battering.

Figure 42. Lwando Quartzite lithic sample and manuport cobble

The large number of cobble cortical pieces indicates some focus on secondary cortex removal of beach cobbles on site. There are five pieces of silcrete but only one has an MG value over the 2.7 gloss unit (GU) heat treatment threshold (Ch. 8.4). An effort was made to refit the Lwando Quartzite sample but only one conjoin was found (Find Numbers 121782 and 120698). Only a few quartzite pieces appear to come from the same nodule. Lwando Quartzite is primarily representative of early stage reduction of quartzite cobbles but the three discoid cores also suggest that there was more opportunistic flake production happening as well.

Table 24. *LBSR* Lwando Quartzite artifact counts by raw material

Production Phase	Modified Geneste Techno-Typology	Silcrete	Quartzite	Quartz	Chert	Hornfels	Quartz Crystal	Other	Total	%
0	Manuport		1						1	4
	Primary Cortical (>60% cortex)	1							1	
1	Residual Cortical (<61% cortex)		4						4	10
	Naturally Backed Flake/Blade				1				1	
2	Plain platform flakes		6						6	28
	Flake with facetted platform	1	2						3	
	Cortical point,flake, or blade with facetted platform		1						1	
	Bipolar Flake		1						1	
	Discoid core		3						3	
various	Block shatter and flake fragments of indeterminate orientation		3						3	58
	Flake fragments with orientation (proximal,medial,distal)	3	17			3			23	
	Other/Indeterminate		3						3	
Total		**5**	**40**	**0**	**1**	**3**	**0**	**0**	**50**	**100**

7.2.5 HM Silcrete/Hornfels

HM (Hope, Martin) Silcrete/Hornfels occurs stratigraphically above Lwando Quartzite at ~81-82ka. This sample represents a second thin occupation layer with a small sample of lithics made mostly from non-quartzite raw materials including silcrete and hornfels. Silcrete occurs across both excavated quadrants of the layer but hornfels was mainly plotted in the eastern-most quadrant (right side of Fig. 39). The HM Silcrete/Hornfels sample (n=52) is similar in sample size to that of the underlying Lwando Quartzite (n=50) and has a slightly lower percentage of complete and fragmentary cortical products (42%) most of which are from cobbles. There is one quartzite facetted point and one small silcrete core made from a flake.

HM Silcrete/Hornfels has the largest hornfels plotted find count (n=18) of any PP5-6 sample and the obvious question is whether this sample represents an occupation where raw material procurement deliberately targeted hornfels or if the distribution of artifacts was overrepresented by a single core reduction. To answer this question, an attempt was made to refit the silcrete and hornfels lithics. No refits were found within the silcrete debitage, and similar to the AK Silcrete sample, the HM Silcrete/Hornfels sample silcrete artifacts appears to come from several individual nodules.

It was possible to refit nine hornfels specimens from a single cobble nodule back together (three of these are from the 10mm sieved material) along with three conjoins from the same reduction (Figure 43a,b). Two other pairs of conjoins were made between hornfels lithics (Fig 43c- Find Numbers 119097 and 257663; Find Numbers 120626.2 and 257669) that can't be directly associated with the same cobble as the larger refitted sample. The larger refitted sample represents secondary cortical reduction debitage (no primary flakes were recovered) where the dorsal scar ridges created by a previous cortical removal were used to guide the next removal in sequence along the cobble platform. Three of the six sequential flake removals split along the long axis of the flake and one flake snapped transversely. There is a percussion mark on one flake (119094) indicating that this was probably a hard hammer reduction. The refits, which were spread out over an area of approximately 75 x 25cm (Fig. 44), are indicative of good stratigraphic integrity and show that cortical reduction of cobbles was happening on site.

The majority of HM Silcrete/Hornfels cortical lithics across all raw material categories derive from beach cobbles which is different than the AK Silcrete sample

which exhibited silcrete cortical lithics from primary outcrops. In HM Silcrete/Hornfels the cobble-based acquisition strategy is more similar to the LBSR sample as a whole. The HM Silcrete/Hornfels sample demonstrates that the higher hornfels count is inflated by a single or limited number of core reductions and might not be representative of the preferential selection of hornfels within the occupation that created this sample. The refitting of this sample points out the strong points and weaknesses of the PP5-6 vertical excavations. The excavated samples appear to come from minimally disturbed stratigraphic contexts which may offer the opportunity of documenting some discrete activities through the sequence. The small horizontal extent of the excavations will bias the behavioral interpretations of many layers having low artifact counts to what was happening in a very limited area.

Table 25. *LBSR* HM Silcrete/Hornfels artifact counts by raw material

LBSR-HM Silcrete/Hornfels

Production Phase	Modified Geneste Techno-Typology	Silcrete	Quartzite	Quartz	Chert	Hornfels	Quartz Crystal	Other	Total	%
0	Primary Cortical (>60% cortex)	1				1			2	4
1	Residual Cortical (<61% cortex)	1	1			2			4	12
	Naturally Backed Flake/Blade	1				1			2	
2	Plain Platform Flakes	5	3			1			9	31
	Plain Platform Blade	2							2	
	Flake with facetted platform					1			1	
	Point with facetted platform		1						1	
	Core-edge or crested flake/blade	1							1	
	Facetted core-edge flake/blade	1							1	
	Core on a flake	1							1	
various	Block shatter and flake fragments of indeterminate orientation	2	1			5			8	54
	Flake fragments with orientation (proximal,medial,distal)	6	5			7			18	
	Thermal Spall	1							1	
	Other/Indeterminate	1							1	
Total		**23**	**11**			**18**			**52**	**101**

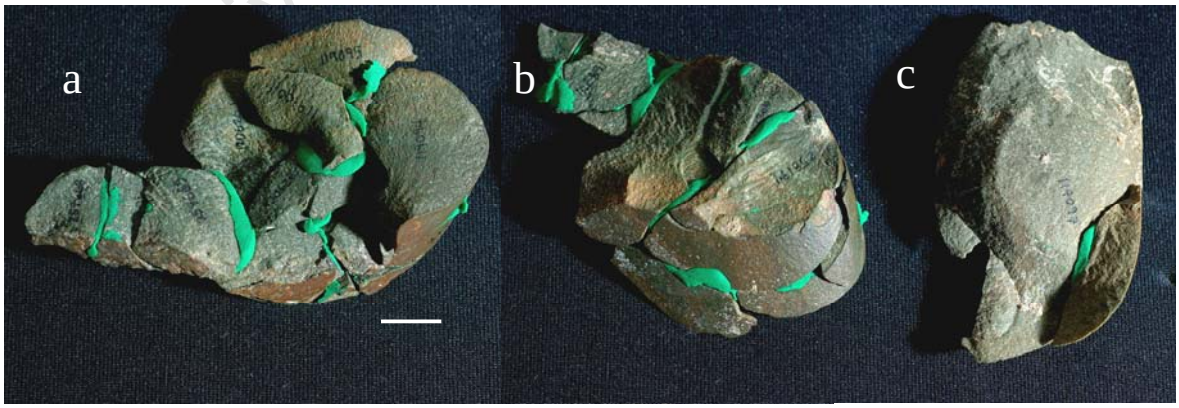

Figure 43. HM Silcrete/Hornfels partial cobble refit of residual cortical flakes. Images a) and b) are interior and exterior views of the same refit sequence and c) are conjoins from a different cobble nodule

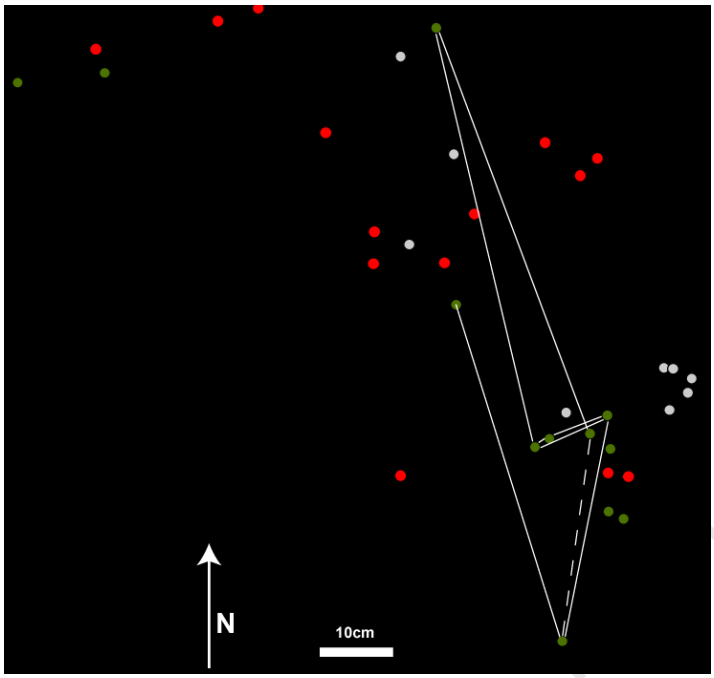

Figure 44. Plan view of HM Silcrete/Hornfels refits. Solid lines indicate refits and the dashed line is a conjoin

7.2.6 Ludumo Quartzite

Ludumo Quartzite occurs above HM Silcrete/Hornfels and is separated from the overlying thick Jed/JR Quartzite by a layer of sand and roofspall that likely represents an occupation hiatus. Ludumo Quartzite dates to ~79-81ka. This sample has a low artifact count (n=64), is highly fragmentary (32% complete specimens), and contains only nine non-quartzite lithics (Table 26). The complete flake sample includes five cortical flakes, 11 plain platform flakes and one facetted point (Appendix 4, Section 2-Find Number 119985). There is one discoid core with centripetal flake scars (Appendix 4, Section 1-Find Number 120722). Ludumo quartzite has fewer cortical specimens (n=8) than the other thin quartzite dominant layers (n=8) and all but one came from beach cobbles.

Table 26. *LBSR* Ludumo Quartzite artifact counts by raw material

Production Phase	Modified Geneste Techno-Typology	Silcrete	Quartzite	Quartz	Chert	Hornfels	Quartz Crystal	Other	Total	%
0	Primary Cortical (>60% cortex)		4						4	6
1	Residual Cortical (<61% cortex)		1						1	2
2	Plain Platform Flakes	1	10						11	25
	Plain Platform Blade		1						1	
	Flake with facetted platform	1	2						3	
	Point with facetted platform		1						1	
	Discoid Core		1						1	
various	Block shatter and flake fragments of indeterminate orientation		13			1			14	67
	Flake fragments with orientation (proximal,medial,distal)		22	1		5			28	
	Other/Indeterminate		1						1	
Total		**2**	**56**	**1**		**6**			**65**	**100**

7.3 ALBS

The *ALBS* represents one of the most interesting and important samples with respect to the subject matter of this dissertation because of its position between the quartzite-dominated upper *LBSR* sequence and the silcrete-favored *SADBS*. The underlying occupation of Jed/JR Quartzite is dated to 79 ± 3ka and the top of the *ALBS* is dated to 76 ± 3. There are three subsamples within the *ALBS* including (from bottom to top) the Conrad Series, 'Jocelyn', and 'Erich' samples. In terms of raw material use, Conrad Series lithics look more like the *LBSR* in favoring quartzite. 'Erich' lithics look more like the *SADBS*, and 'Jocelyn' has affinities with both. The *ALBS* currently has a single calculated OSL age of 76 ± 3 taken from 'Erich', (although several more OSL samples have been selected from this area). There may be as much as 7000 years represented by the *ALBS* 'transition' with potentially significant occupation gaps represented by aeolian sediment buildup on either side of 'Erich.'

ALBS raw material counts favor quartzite overall but there is a shift from quartzite to silcrete that occurs between 'Jocelyn' and 'Erich' (Table 27). Micromorphology and OSL samples have been positioned to target this interface in order to understand the rate of technological change between the *LBSR* and *SADBS*.

Table 27. *ALBS* raw material counts by analytical sample

Sample	quartzite	silcrete	chert	quartz	hornfels	other	Total
Erich	20	55			1		76
Jocelyn	96	55	11	10	4	1	177
Conrad Series	100	26	4	0	1	0	131
Conrad	3	9	2				14
Conrad Cobble and Sand	85	6					91
Conrad Shell	12	11	2		1		26
Total	**216**	**136**	**15**	**10**	**6**	**1**	**384**

The lithic sample from the Conrad Series assemblage consists of 134 total pieces (Table 28). There are two quartzite cores (single platform and cylinder type) and one core fragment (Appendix 4, Section 1). Debitage is fragmentary (n=91, 67%) and there are few complete/almost complete silcrete flakes (n=5). The quartzite debitage sample consists mainly of complete plain platform flakes (n=18) and plain platform blades (n=5). There are few facetted flakes (n=5) and non-cortical points are absent. Flake scars are mainly parallel and unidirectional (Tables 10-11).

Table 28. *ALBS* Conrad Series artifact counts by raw material

Production Phase	Modified Geneste Techno-Typology	Quartzite	Silcrete	Quartz	Chert	Hornfels	Quartz Crystal	Other	Total	%
1	Residual Cortical (<61% cortex)	4	3						7	5
	Naturally Backed Flake/Blade	2							2	
2	Plain Platform Flakes	18	1						19	26
	Plain Platform Blade	5	1		1				7	
	Cortical point,flake, or blade with facetted platform	2							2	
	Facetted flake	2							2	
	Blade with facetted platform	1							1	
	Single platform core	1				1			2	
	Core fragment	1							1	
	Cylinder core	1							1	
various	Block shatter and flake fragments of indeterminate orientation	22	5						27	67
	Small Production Debris (<15mm max dimension)	2	2		1				5	
	Flake fragments with orientation (proximal,medial,distal)	42	10		2				54	
	Indeterminate/Other		3			1			4	
Total		**103**	**25**		**4**	**2**			**134**	**98**

The 'Jocelyn' sample counts favor quartzite overall but there are more silcrete complete/almost complete specimens (n=26). There are a total of eight cores representing five different raw material types (Table 9), most of which (n=5) show small blade removals including one chert core with possible bipolar battering on both opposed platforms. There are few complete/almost complete cortical products (n=17) and non-cortical debitage is represented mainly by plain platform flakes and blades in non-quartzite materials and plain and facetted quartzite products. There is one complete facetted silcrete point (Appendix 4, Section 2- Find Number 176743).

Table 29. *ALBS* 'Jocelyn' artifact counts by raw material

Production Phase	Modified Geneste Techno-Typology	Quartzite	Silcrete	Quartz	Chert	Hornfels	Quartz Crystal	Other	Total	%
0	Manuport	1							1	3
	Primary Cortical (>60% cortex)	2	1	1	1				5	
1	Residual Cortical (<61% cortex)	1	6					1	8	4
2	Plain Platform Flakes	2	14	2	1				19	27
	Plain Platform Blade	4	4		1				9	
	Cortical point,flake, or blade with facetted platform		2		1				3	
	Facetted flake	1							1	
	Blade with facetted platform	3							3	
	Point with facetted platform		1						1	
	Core-edge or crested flake/blade	4							4	
	Thinning Flake		2						2	
	Discoid core				1	1			2	
	Single platform core	1	1						2	
	Change of orientation core				1				1	
	Core with opposed platforms		1	1					2	
	Other double platform core		1						1	
various	orientation	9	9	5	1	1			25	65
	Flake fragments with orientation (proximal,medial,distal)	24	53	1	3	2			83	
	Small Production Debris (<15mm max dimension)	1	3		1				5	
	Thermal Spall	1							1	
	Indeterminate/Other	2	1	1	2	1			7	
Total		**56**	**99**	**11**	**13**	**5**	**0**	**1**	**185**	**99**

'Erich' has less than half the sample size of the other ALBS samples (76 pieces) and consists mainly of silcrete lithics (Table 30). There are no cores and few complete/almost complete products (n=27) and only four cortical flakes, all of which are

silcrete. There are few 'Erich' debitage specimens that can be classified as blades or blade products (Table 31).

Table 30. *ALBS* 'Erich' artifact counts by raw material

Production Phase	Modified Geneste Techno-Typology	Quartzite	Silcrete	Quartz	Chert	Hornfels	Quartz Crystal	Other	Total	%
1	Residual Cortical (<61% cortex)		4						4	5
2	Plain Platform Flakes	4	3						7	30
	Plain Platform Blade	1	1						2	
	Cortical point,flake, or blade with facetted platform		1						1	
	Facetted flake	1							1	
	Core-edge or crested flake/blade		1						12	
various	Block shatter and flake fragments of indeterminate orientation	2	10						6	64
	Flake fragments with orientation (proximal,medial,distal)	11	30			1			42	
	Small Production Debris (<15mm max dimension)	1	5						1	
Total		**20**	**55**			**1**			**76**	**99**

The most compelling patterning within the *ALBS* is the shift in raw material use from quartzite in Conrad Series to silcrete in 'Erich'. Blade products are relatively scarce across these samples (Table 31), which is contradictory to the comparatively large sample of cores in 'Jocelyn' with blade removal scars. Flake scars in the *ALBS* are typically parallel and unidirectional (Tables 10-11) but complete/almost complete debitage mainly consists of non-cortical plain platform flakes. A Mann-Whitney test of length measurements on the small sample (n=21) of complete blade products across all *ALBS* samples shows significant differences in the medians between chert/silcrete versus quartzite blade debitage (Mann-Whitney U=17.5, exact p .0074)(Fig. 45). This suggests that in the *ALBS* there is already a significant size differentiation in blade production by raw material, a pattern that becomes very pronounced in the following *SADBS*.

Table 31. Simplified *ALBS* artifact counts including classified fragments by analytical sample

Sample	Raw Material	cortical	flake product	blade product	core	point	retouched blade	small flaking debris	indet. fragment	Total
Erich	silcrete	8	20	2				11	14	55
	hornfels		1							1
	quartzite	2	10	6				1	1	20
	total	*10*	*31*	*8*				*12*	*15*	*76*
Jocelyn	silcrete	7	14	7	2			7	18	55
	quartz	1	3		1				5	10
	chert	3	2	1	2			3		11
	hornfels		2		1				1	4
	quartzite	15	49	5	1	1	1	5	19	96
	other	1								1
	total	*27*	*70*	*13*	*7*	*1*	*1*	*15*	*43*	*177*
Conrad Series	silcrete	7	8	1	3			4	3	26
	chert		2	1				1		4
	hornfels				1					1
	quartzite	10	72	8					10	100
	total	*17*	*82*	*10*	*4*			*5*	*13*	*131*
Total		**54**	**183**	**31**	**11**	**1**	**1**	**32**	**71**	**384**

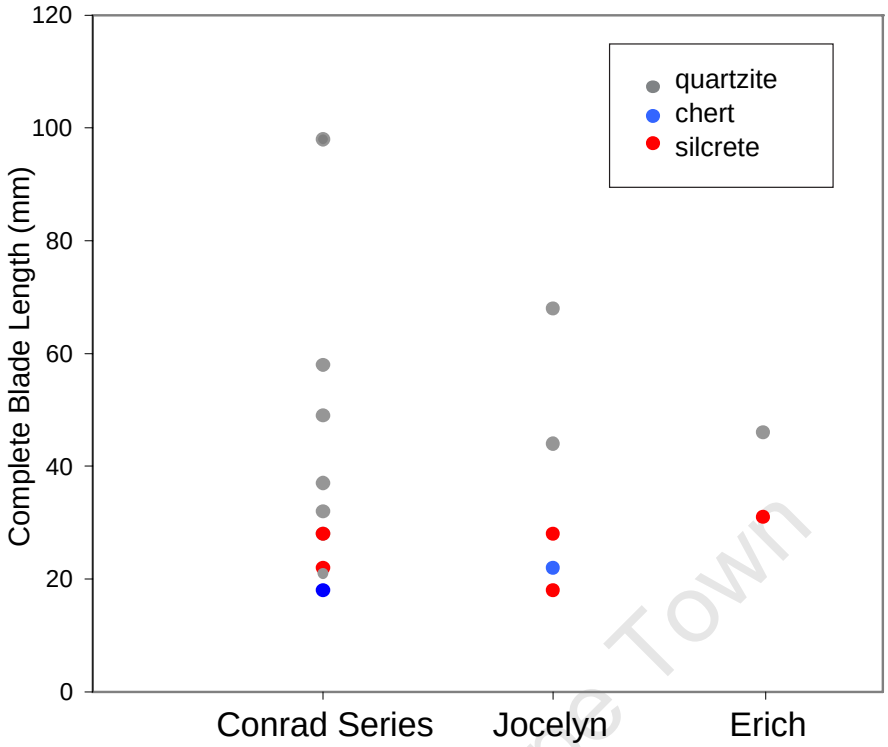

Figure 45. Plot of *ALBS* blade length by analytical sample

7.4 SADBS, SGS and DBCS

Three broadly similar but distinct small blade occurrences are recognized at PP5-6: 1) the *SADBS* which consists of very small bladelets and delicately made small backed pieces; 2) the *DBCS* which is more typical of the HP; and 3) the *SGS* which is summarized here but will be described in more detail after excavations in 2010-2011. The *SADBS* and *SGS* samples are separated by a thick dune (*OBS*) described in the following section. The *SADBS*, *SGS*, and *DBCS* are described together to facilitate direct comparison of technological attributes.

The *SADBS* occupation occurs within the primarily aeolian sediment input at PP5-6, which marks the transition from MIS 5 to MIS 4, and likely occurs within a narrow time period that has been OSL dated from 71-72 ± 3ka. Ages for the lower boundary are constrained by the *ALBS* at 76 ± 3ka and for the upper boundary of the *SADBS* by overlying *OBS* StratAgg with multiple OSL age estimates of 69 ± 3ka (Brown et al. 2009). The *OBS* dune, which caps the *SADBS*, is similar in chronology to the thick dune layer that marks the end of the SB sequence at Blombos Cave (Jacobs et al. 2003a, 2003b). The OSL ages for the *SADBS* (Brown et al. 2009) are approximately

contemporary with the age estimate of the SB determined by Jacobs et al. (2008). SB end products are carefully crafted bifacial foliate points (Goodwin and van Riet Lowe 1929).

The *SADBS* lithic assemblage is dominated by blade products (Fig. 46), and there are no associated bifaces or unambiguous biface production debitage. A summary of *SADBS* artifact counts can be found in Table 32. Most of the *SADBS* blades are short (24mm mean length), narrow (11 mm mean width), and are triangular or trapezoidal in cross-section (Figure 47). The blades are made predominantly on silcrete and other non-quartzite raw materials. Small bidirectional blade cores (Appendix 4, Section 1) support the characterization of the *SADBS* as a small blade focused assemblage. With a relatively low overall frequency of retouch (4% of tools show some form of modification), the *SADBS* assemblage does have segments (n=20) made from the small blades which will be discussed in more detail below. The *SADBS* is described here by comparison with the *DBCS* (HP) to which it shares some affinities. Comparisons with the smaller *SGS* sample are made when appropriate.

The *SGS* occurs stratigraphically between the *OBS* (69 ± 4ka) and *DBCS* (HP: 65-60ka). There is a very small sample count for the *SGS* (Table 33) due to the configuration of the excavated square along an erosional truncation. Excavations in 2009-2010 exposed a much larger area of the *SGS* for continued excavation in 2011-2012. The *SGS* lithic assemblage does have the second highest lithic density in terms of artifact count and third highest by weight (Table 3). Raw material percentages for the *SGS* overwhelmingly favor silcrete (55%) over quartzite (19%), a feature shared with the *SADBS* and *DBCS*. The *SGS* has more chert (13%) than the *DBCS* (9%) and *SADBS* (3%) and there is a visible concentration of chert within *SGS*-'Tamu' (inset-Fig. 28).

The *SGS* sample has two cores with blade scars (Find Number 138601-change of orientation; Find Number 168626-other double platform core) and two single platform cores. Complete and almost complete debitage consist mainly of plain platform flakes and blades. There are only 13 complete blades. Obviously this is a small blade sample for comparison but the mean values for the majority of the *SGS* blades (Fig. 47) are similar in size to those of the *SADBS* and *DBCS* with a few more elongated blades contributing to variability in length.

Table 32. *SADBS* artifact counts by raw material

Production Phase	Modified Geneste Techno-Typology	Quartzite	Silcrete	Quartz	Chert	Hornfels	Quartz Crystal	Other	Total	%
0	Manuport		1						1	2
	Primary Cortical (>60% cortex)	6	50		4				60	
1	Residual Cortical (<61% cortex)	14	141	1	5	1			162	5
	Naturally Backed Flake/Blade	2	11		2	1			16	
2	Plain Platform Flakes	55	174	6	4	2	1		242	17
	Plain Platform Blade	17	175	1	9		1		203	
	Cortical point,flake, or blade with facetted platform	2	12						14	
	Facetted flake	6	15		1				22	
	Blade with facetted platform		15		3				18	
	Point with facetted platform	5	3						8	
	Core-edge or crested flake/blade	7	41			1			49	
	Facetted core-edge flake/blade	3	2		1				6	
	Thinning Flake	2	26						28	
	Bipolar Flake	1							1	
	Discoid core	1	2	1	2				6	1
	Single platform core	2	3						5	
	Core on a flake		3						3	
	Minimal core		2						2	
	Change of orientation core		4						4	
	Core with opposed platforms	1	7				1		9	
	Other double platform core		2						2	
	Adjacent platform core	1	3						4	
3	Backed Blade	1	17	1	1				20	0.5
various	Block shatter and flake fragments of indeterminate orientation	123	755	44	26	2	7	5	962	75
	Flake fragments with orientation (proximal,medial,distal)	207	1190	23	31	3	9	2	1465	
	Small Production Debris (<15mm max dimension)	37	198	2	6		1		244	
Total		**493**	**2852**	**79**	**95**	**10**	**20**	**7**	**3556**	**100.5**

Table 33. *SGS* artifact counts by raw material

Production Phase	Modified Geneste Techno-Typology	Silcrete	Quartzite	Chert	Quartz	Hornfels	Crystal Quartz	CCS	Other	Total	%
0	Primary Cortical (>60% cortex)	2	1		1			1		**5**	**1%**
1	Residual Cortical (<61% cortex)	12	4	2	1					**19**	**5%**
	Naturally Backed Flake/Blade		2			2				**4**	
2	Plain platform flakes (non-cortical)	13	15	3	3				1	**35**	**16%**
	Plain platform blade (non-cortical)	14		4						**18**	
	Cortical point,flake, or blade with facetted platform			1						**1**	
	Flake with facetted platform	5			1					**6**	
	Blade with facetted platform	3								**3**	
	Point with facetted platform	1			1					**2**	
	Core-edge or crested flake/blade	3		1						**4**	
	Core with opposed platforms on same side			2						**2**	
	Other double platform core	1								**1**	
	Change of orientation core			1						**1**	
	Single platform core (fragment)	2								**2**	
	Thinning Flake	4		1						**5**	
various	Block shatter and flake fragments of indeterminate orientation	87	25	15	25	2			1	**155**	**77%**
	Flake fragments with orientation (proximal,medial,distal)	109	48	29	12	3	1	6		**208**	
	Small Production Debris (<15mm max dimension)	18	1	5	2					**26**	
	Hammerstone Spall								1	**1**	
	Thermal Spall	3		2						**5**	
3	Backed Blade	5		2						**7**	**1%**
Total		**282**	**96**	**68**	**46**	**7**	**1**	**7**	**3**	**510**	**100%**

Table 34. *DBCS* artifact counts by raw material

Production Phase	Modified Geneste Techno-Typology	Silcrete	Quartzite	Chert	Quartz	Hornfels	Crystal Quartz	CCS	Other	Total	%
0	Primary Cortical (>60% cortex)	3	5	2		1		1		**12**	**5%**
	Residual Cortical (<61% cortex)	32	8	4		3		2	1	**50**	
1	Naturally Backed Flake/Blade	1								**1**	**6%**
	Plain platform flakes (non-cortical)	45	24	3	4		1	1		**78**	
2	Plain platform blade (non-cortical)	21		10				1		**32**	**9%**
	Cortical point,flake, or blade with facetted platform	4	3	1		1				**9**	
	Flake with facetted platform	10	3	2						**15**	
	Blade with facetted platform	6						1		**7**	
	Point with facetted platform		4					1		**5**	
	Core-edge or crested flake/blade	4	2	5				1		**12**	
	Facetted core-edge flake/blade	1		1						**2**	
	Thinning Flake	10		1		1				**12**	
	Discoid core	2	2	1						**5**	
	Single platform core	2		1						**3**	
	Core with opposed platforms on same and opposite sides	3		1						**4**	
	Double platform core	1		1						**2**	
	Core on a flake	5	1							**6**	
	Minimal core	1								**1**	
	Indeterminate core fragment	1								**1**	
	Bipolar Flake	1								**1**	
various	Block shatter and flake fragments of indeterminate orientation	322	40	29	19	3	3	3		**419**	**80%**
	Small Production Debris (<15mm max dimension)	384	101	40	13	6	6	7	1	**558**	
	Flake fragments with orientation (proximal,medial,distal)	73	4	11		1	1	1		**91**	
	Thermal Spall	15								**15**	
3	Backed Blade	11		3						**14**	**1%**
	Notched Blade	1								**1**	
Total		**959**	**197**	**116**	**36**	**16**	**11**	**19**	**2**	**1356**	**100%**

The *DBCS* is located stratigraphically above the *SGS* and is OSL dated to 60-65 ± 3ka (Brown et al. 2009). *DBCS* summary artifact counts are presented in Table 34. The ages for the *DBCS* are consistent with those of a host of other HP occurrences in southern Africa (Jacobs et al. 2008). *DBCS* core reduction was focused on the production of small blades (mean length 27.1mm) as end products (Fig. 47). Some of the blades were retouched into backed blade segments and notched pieces (Appendix 4, Sections 3-4).

A major difference in core organization between the quartzite-dominant *LBSR* and silcrete-rich *SADBS*, and *DBCS* is the presence of opposed (double) platform blade cores (Table 35). The *LBSR* cores were typically discarded as either single platform or more opportunistically flaked change of orientation or discoid forms. In the *SADBS* in particular, blade cores continued to be flaked from single and double platform cores down to a very small size (Table 36) with less reorganization of core surface and flaking direction in later stages than cores in the *LBSR*. The *SADBS* and *DBCS* silcrete blade cores were discarded at a similar size with *SADBS* blade cores being slightly thicker. Core dimensions for other raw materials and core types are found in Appendix 4, Section 1. The *SADBS* and *DBCS* flake dorsal scar directionality shows a corresponding increase toward bidirectionality from cortical to non-cortical debitage (Table 11).

Table 35. Core type comparison for the *LBSR*, *DBCS*, and *SADBS* StratAggs

StratAgg	single platform		adjacent platform		opposed platform		other double platform core		change of orientation		core on a flake		discoid		minimal		Total
	n	%	n	%	n	%	n	%	n	%	n	%	n	%	n	%	
DBCS	3	*10*			4	*19*	2	*9*			6	*29*	5	*24*	1	*5*	21
SADBS	5	*14*	4	*11*	10	*28*	2	*6*	4	*11*	3	*8*	6	*17*	2	*6*	36
LBSR	3	*17*							2	*11*	3	*17*	7	*39*	3	*17*	18
Grand Total	**11**		**4**		**14**		**4**		**6**		**12**		**18**		**6**		**75**

Table 36. Summary statistics for *SADBS* and *DBCS* silcrete blade cores

Silcrete Blade Cores		SADBS	DBCS
Length	Mean	29.3	30.3
	SD	8.8	4.3
	Count	8	6
Width	Mean	18.6	19.7
	SD	5.8	6.9
	Count	8	6
Thickness	Mean	13.5	10.2
	SD	2.4	3.1
	Count	8	6

SADBS and *DBCS* blades are almost all made from non-quartzite raw materials (84% and 76%, respectively) and have more parallel flake scars and more debitage with dimensions that are consistent with the standard definition of blades (length of at least two times width). The *SADBS* is noteworthy for having the highest percentage of debitage with L/W ratio ≥ 2.0 (21%), which is even higher (23%) when fragmentary debitage is included. In other words, almost 1 out of every 4 excavated *SADBS* lithics qualifies as a blade compared to 1 in 6.6 for the *DBCS* and 1 in 10 for the *LBSR* (Fig. 48).

SADBS complete debitage has plain (n=256, 53%), punctiform (n=43, 9%), or crushed platforms (n=69, 8%), compared to a smaller percentage of facetted platforms (n=112, 16%). The *DBCS* sample exhibits similar percentages of plain (n=76, 46%), punctiform (n=13, 7%), crushed (n=13, 7%), and facetted (n=40, 24%) platforms (Table 13). The *SADBS* and *DBCS* debitage samples more commonly show evidence for core edge preparation in the form of platform abrasion, which is the process of strengthening

the core edge and creating proximal core surface convexity by grinding or the removal of very small trimming flakes at the intersection of the platform and flaking surface (Soriano et al. 2007). Some degree of platform abrasion occurs on 40% (n=274) of *SADBS* complete debitage pieces and 63 specimens (41%) of the *DBCS*, and is most common on non-cortical debitage (Table 14). Platform abrasion is less common in *LBSR* debitage (n=42, 13%).

Figure 46. Characteristic *SADBS* Lithics: a) blades, b) backed pieces c) blade cores, d) points (additional images in Appendix 4)

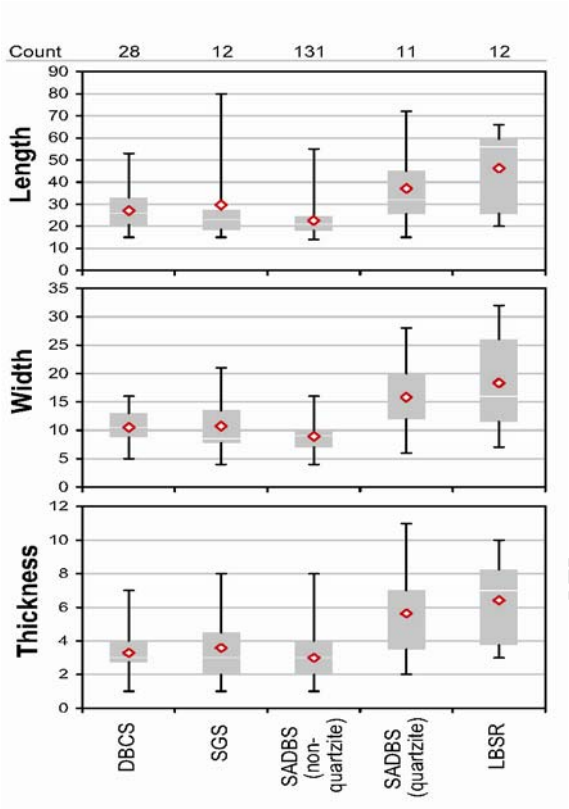

Figure 47. Box plots of length, midpoint width and thickness for *LBSR*, *SADBS*, *SGS*, and *DBCS* complete plain platform and facetted blades. *LBSR* blades are all quartzite, *SGS* and *DBCS* blades are all made on non-quartzite materials.

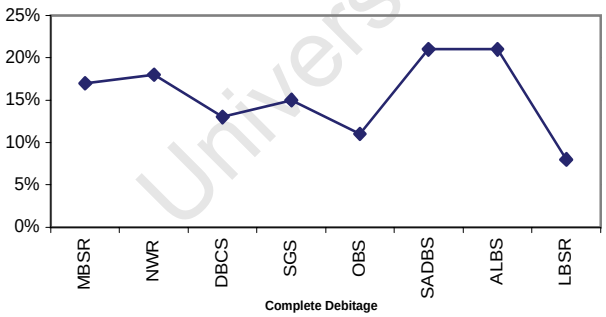

L/W >2.0	All Debitage		Complete Debitage	
	Count	All Lithics	Count	All Lithics
MBSR	122	19.0%	47	17%
NWR	201	20.0%	73	18%
DBCS	846	15.0%	242	13%
SGS	308	15%	100	15%
OBS	310	14.0%	134	11%
SADBS	2390	23.0%	849	21%
ALBS	228	21%	102	21%
LBSR	831	10%	381	8%

Figure 48. Percentage of debitage with length/width ≥ 2.0 for PP5-6 StratAggs.

The *SADBS* and *DBCS* non-cortical debitage typically exhibits parallel flake scars (*SADBS* n=215, 57%; *DBCS* n=48, 59%) (Table 11). The *SADBS* non-cortical sample shows a slightly higher percentage of convergent flake scars (n=93, 25%) than the *DBCS* (n=17, 21%). Convergent flaking and the production of points (n=8) is a feature of the *SADBS* that is less common in the PP5-6 *DBCS* (n=2) and Klasies River HP (Wurz 2000). The *SADBS* points (Appendix 4, Section 2), which are made on both quartzite (n=4) and

silcrete (n=3), are shorter (mean length=40.3) than those of the *LBSR* (mean length=50.3). Although the sample sizes are very small, the continued production of points and larger quartzite blades implies some level of technological continuity between the *LBSR* and the *SADBS* samples despite the apparent change in emphasis to small silcrete blades in the *SADBS*.

HP assemblages have a higher percentage of retouch than MSA occurrences that precede or follow (Wurz 1999). The HP type assemblage, excavated by P. Stapleton and John Hewitt in 1926, was distinguished by the presence of a number retouched tool implements, including burins, gravers, large crescents, trapezoids, obliquely pointed blades, trimmed points, and chisel-like scrapers (Stapleton and Hewitt 1927; 1928). They differentiated their collection from the LSA Wilton by the absence in the HP of smaller-sized Wilton lunates, triangles, or scalenes. The large HP assemblage at Klasies River contrasts with the type collection from Howiesons Poort Rockshelter by a near absence of points (unifacial or unretouched forms) (J. Deacon 1995). The most common retouched tools in the Klasies River HP are backed and notched blades (Singer and Wymer 1982; Wurz 1999).

Backed blades in the PP5-6 *SADBS*, *SGS* and *DBCS* are typically crescent-shaped with only a few trapezes (Appendix 4, Section 3) and are made most commonly from silcrete and chert (Table 37). Sample sizes are obviously not large enough at present for compelling statistical comparison between the *SADBS*, *SGS* and *DBCS*, but temporal changes in length, width, and thickness may be evident between the three largest stratigraphic samples of segments (Table 38, Fig. 49). Complete *SADBS* backed blades (n=14) are shorter, narrower, and thinner than *DBCS* blades. The *SGS* backed blades have the shortest mean length (24mm), and they are the least variable in terms of length and width, despite having the lowest count.

Table 37. PP5-6 backed blade counts by StratAgg and raw material

StratAgg	silcrete	chert	quartz	quartzite	Total	Excavated Sediment (m^3)	Estimated Density/m3
MBSR	3				3	0.06	50
NWR	1	1			2	0.19	11
DBCS	8	3			11	0.16	69
SGS	3	2	1		6	0.03	200
OBS	3				3	0.62	5
SADBS	17	1	1	1	20	0.49	41
Total	35	7	2	1	45	1.55	

Table 38. Backed blade dimensions from PP5-6 *SADBS*, *SGS*, and *DBCS* StratAggs

Backed Blades		PP5-6 (All)	DBCS	SGS	SADBS
Length	Mean	28.1	32.9	23.8	27
	SD	8.1	10.3	3.6	6.8
	95% CI	3	7.2	3.2	3.6
	Count	27	8	5	14
Width	Mean	10.4	15	12.4	8.9
	SD	5	3.4	1.3	2.6
	95% CI	1.9	2.36	1.1	1.36
	Count	27	8	5	14
Thickness	Mean	4.2	3.75	2.6	3.21
	SD	2.2	1.04	0.9	1.29
	95% CI	0.8	0.83	0.8	0.68
	Count	27	8	5	14

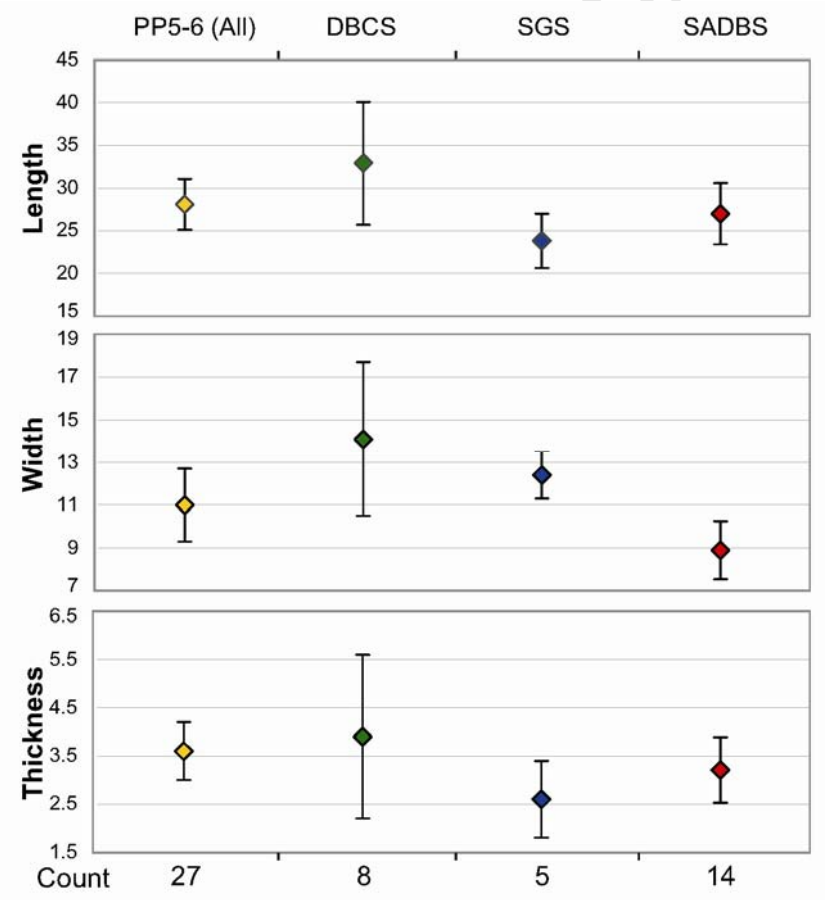

Figure 49. Comparison of length width and thickness for PP5-6 complete segments by StratAgg with 95% confidence interval of the means

Notched pieces are a common retouched tool form in the Klasies River HP (Singer and Wymer 1982; Wurz 2000) and in Diepkloof layer Jeff (Porraz et al. 2008). The term 'notched' is often used to describe invasive edge damage that creates small isolated concavities on tool edges. Notching on HP tools is more deliberate and involves the removal of a series of small parallel retouch flakes to create a carefully formed indentation or semi-circular tool edge. Similar tools are often termed "spokeshaves" in North American assemblages with an implied use for carving or dressing arrow shafts. Wurz (2000) noted a similarity in retouch between HP tools with wide, steep notches and LSA woodworking tools ("adzes"). This interpretation is interesting given recent research that promotes the use of HP backed pieces as armaments (Lombard 2011; Lombard and Phillipson 2010; but see Villa et al. 2010 for opposing view). This interpretation remains to be tested with use-wear analysis and experimental notched tool use.

A total of 11 notched pieces have been plotted at PP5-6 (Table 39; Appendix 4, Section 4). Ten were made from silcrete, with one chert specimen (162365), and most come from the upper layers of the *DBCS* (SubAgg 'Miller'). All are made on debitage that is now fragmentary. It is not always clear whether the notches were made on debitage fragments or whether the recovered notched tools were originally part of a larger tool. There is only one notched blade in the *SADBS* (Table 39). The rarity of *SADBS* notched pieces may be another characteristic that distinguishes this assemblage from the HP.

The majority of informally retouched tools at PP5-6 come from the *SADBS* (n=143) and *DBCS* (n=98) (Table 19) and most were made from silcrete (n=231, 64%). Single flake notches (n=61) appear to be the result of use or post-depositional damage rather than as deliberate retouch to create a working edge (Table 20). Pieces with abrasion (n=22) or blunting (n=24) do not have the systematic and regular modification exhibited by typical backed pieces such as segments. There are four burins, 10 denticulates and 47 pieces with steep scraper-like retouch. Steeply retouched pieces come primarily from the *SADBS* (n=22) and *DBCS* (n=10). The majority of the modification occurs on flake dorsal laterals and favors the left margin (n=86) over the right (n=59), and can be characterized as irregular modification that is assumed to occur as the result of use rather than deliberate retouch (Table 21).

Table 39. PP5-6 notched pieces by StratAgg, raw material, and artifact density

Agg	silcrete	chert	Total	Excavated Sediment (m^3)	Estimated Density/m3
DBCS	8		8	0.16	50
SGS	1	1	2	0.03	67
SADBS	1		1	0.49	2
Total	**10**	**1**	**11**	**0.68**	

SADBS, *SGS*, and *DBCS* Summary

The two features most commonly identified with the HP include: 1) a shift to the utilization of more fine-grained raw materials; 2) an increase in the percentage of retouched tools commonly in the form of backed and notched pieces. It has been recently demonstrated that 3) HP lithic assemblages across southern Africa date to between 60 and 65ka. The HP represents one of two "marker horizons" in the southern African MSA (Jacobs et al. 2008). The other marker horizon is the SB at ~71ka. The PP5-6 *DBCS* has a much smaller sample size than the Klasies River HP, but meets criteria 1-3. In the *DBCS*, silcrete and chert are favored for the production of all debitage, especially for the production of both formal and informal retouched tools. Quartzite lithics occur, but as with the Klasies River HP, there are few points. The *DBCS* has a sample of backed blades and notched pieces consistent with other HP sites.

The *SADBS* also meets criterion 1 in preference for the use of non-quartzite raw material. In fact, non-quartzite raw material counts, and particularly silcrete, peak in the *SADBS*. This demonstrates that at Pinnacle Point, as with Klasies River and Diepkloof Layer Jeff, the pattern in use of fine-grained raw material was actually established prior to the identified HP levels at all three sites. The *SADBS* satisfies criterion 2 in having a sample of backed pieces made from very small silcrete and chert blades. These backed pieces are similar in form to those of the *DBCS* and Klasies River HP, but they are narrower as are the blade blanks from which they were made. The *SADBS* has only a single notched piece.

The most interesting feature of the *SADBS* that makes it unique from the *DBCS* and HP is that it dates perhaps 6 to 7ka earlier (Brown et al. 2009). In fact, the OSL ages for the *SADBS* place this stratigraphic sample as being approximately contemporary with the SB, which occurs only 90km along the coastline to the west (Brown et al. 2011). The

SADBS and SB are both capped by dune formation that occurred at ~69ka. The SADBS and SB are technologically distinct. The SADBS has very small blades from blade cores, and the SB is defined by the presence of bifacial tools.

The *SADBS* also differs from the HP by the continued production of quartzite blades and points. The *SADBS* is dominated by silcrete products. Because the *SADBS* has such a large debitage sample size in comparison to the other silcrete-rich layers at PP5-6, it also has a moderate sample of quartzite debitage. At least some quartzite reduction in the *SADBS* appears to have been aimed at making larger facetted blades and points in comparison to the much smaller plain platform blades made on silcrete and chert. The *SADBS* facetted points are smaller than those of the LBSR and may represent a continuation in the point length reduction pattern noted by Wurz (2002, 2003) for the Klasies River MSA I and II. It is possible that some of the factors influencing the strategy or choice in production of the small fine-grained blades in the middle Long Section occupations may also be driving a reduction in size of quartzite points. The continued presence of facetted points and blades throughout the PP5-6 sequence suggests that there is a measure of technological continuity in how quartzite was used. Quartzite point and blade production may exist as a parallel technological strategy alongside small blades made on silcrete and chert.

The *SGS* requires additional excavation to create a larger sample size and to properly define its stratigraphic relationship with the *OBS* and *DBCS*. A recently exposed archaeological profile adjacent to the excavated SGS sample indicates that this layer is separated from both the *SADBS* and *DBCS* by aeolian dune sand, which has evidence for occupation (*OBS*-discussed below). The *SGS* has a small but dense sample of lithics with backed pieces and two irregular notched specimens.

The recently described Diepkloof Rockshelter 'Jeff' layer (Porraz et al. 2008) may offer the best chronological (but not necessarily typological) comparative sample for the *SGS*. Jeff is a high-density (>7000 pieces) 10-15cm thick layer that is sedimentologically differentiated from the overlying HP at Diepkloof and occurs stratigraphically above the Diepkloof SB. Like the PP5-6 SGS, Jeff exhibits a preference for silcrete use in the production of unidirectional and bidirectional blades. In the SGS there are 7 backed blades from a sample of 510 artifacts and only a single notched piece, but in Jeff there are only two truncated pieces in approximately 7000 artifacts but numerous notched and strangulated pieces.

7.5 OBS

The *OBS* is a thick layer of dune sand that occurs between the silcrete-rich *SADBS* and *SGS* layers. The *OBS* has higher artifact counts than many of the smaller occupation layer samples discussed in this dissertation (particularly from the *LBSR*) but because the artifacts were excavated from a larger volume of sediment than any other aggregate ($0.74m^3$), the artifact density is low at an estimated 657 lithics/m^3 (Table 3). The *OBS* stands out alongside the other upper Long Section StratAggs as having higher quartz (n=150) and quartzite (n=146) counts than silcrete (n=107). Artifact counts appear to over represent quartz which is highly fragmentary (124 out of 150 pieces are incomplete). Raw material percentages calculated by total mass favor quartzite in all *OBS* SubAggs (Table 40) and quartz over silcrete in the upper *OBS* ('Lizelle' and 'Peter').

Table 40. Sum of weight for each *OBS* SubAgg by raw material

Material	quartzite	silcrete	quartz	chert	crystal quartz	hornfels	other	Total
Lizelle	191.7	28.6	31.5	9.9	4.8	3.7	4.1	274.3
Peter	376.5	74.5	84.74	61	6.8			603.54
Celeste	535.2	517.5	171.3	17.14	6.7		4.1	1251.94
OBS total	1103.4	620.6	287.54	88.04	18.3	3.7	8.2	2129.78

Artifact counts for the *OBS* are provided in Table 41. The complete and almost complete quartz specimens can be characterized as non-cortical plain platform flakes (n=16). Three of four quartz cores show minimal preparation (two change of orientation cores and one discoid). There is one opposed platform quartz core to go along with two quartz plain platform blades. There is one quartz bipolar flake. Only one quartz medial fragment (Find Number 153406) shows any sign of edge modification in the form of a small notch on one lateral margin. The *OBS* quartzite debitage consists mainly of non-diagnostic plain platform flakes (n=38) and blades (n=6) along with 11 facetted products including one incomplete point. There is one quartzite change of orientation core. There are four pieces of quartzite debitage with steep retouch and one simple notched flake. Silcrete and chert debitage includes several cortical pieces (n=13) in addition to plain and facetted platform flakes and blades. There are a variety of silcrete (n=3) and chert (n=2) core types and one quartz crystal bipolar core.

The total sample of *OBS* debitage is organized according to generalized flake and blade categories in Table 42. In terms of the proportion of blade products, including two

small crescents, *OBS*-'Celeste' looks more like a lower-density continuation of the underlying *SADBS*. The well-formed backed pieces are similar in size and shape to those of the upper *SADBS* in 'Betina' and 'Joanne' (Appendix 4, Section 3). Many of the debitage blade products are associated with silcrete in *OBS*-'Celeste'. Blade debitage products are reduced in count as the percentage of silcrete diminishes in *OBS*-'Peter' and 'Lizelle' although cores with blade scars occur in greater frequency in the 'Peter' and 'Lizelle' SubAggs.

It will be demonstrated in the more detailed technological analyses to follow that the *OBS* stands out against the *SADBS* and *SGS* samples that precede and follow. The *OBS* shows an increased reliance on quartz and a decrease in acquisition of primary outcrop raw materials in comparison to the *SADBS* and *SGS*. The *OBS* occurs at a time when the Site Context Model predicts greater reliance on primary context raw materials but the *OBS* does not seem to follow this pattern although there are some blade products and backed pieces that show continuity between the *OBS* and the *SADBS* and *SGS*.

Table 41. *OBS* artifact counts by raw material

Production Phase	Modified Geneste Techno-Typology	Quartzite	Silcrete	Quartz	Chert	Hornfels	Quartz Crystal	Other	Total	%
0	Manuport		1						1	1
	Primary Cortical (>60% cortex)		3						3	
1	Residual Cortical (<61% cortex)	8	8	1	2			1	20	5
	Naturally Backed Flake/Blade	2	1						3	
2	Plain Platform Flakes	38	4	16	8		2		68	23
	Plain Platform Blade	6	3	2	2				13	
	Cortical point,flake, or blade with facetted platform		3						3	
	Facetted flake	8	3	2					13	
	Blade with facetted platform	1	1		1				3	
	Point with facetted platform	1							1	
	Core-edge or crested flake/blade	2	4		1				7	
	Facetted core-edge flake/blade	1	1						2	
	Thinning Flake	1	2						3	
	Bipolar Flake			1					1	
	Discoid core			1					1	2
	Single platform core				2				2	
	Core on a flake		1						1	
	Bipolar core						1		1	
	Change of orientation core	1	1	2					4	
	Core with opposed platforms		1	1					2	
various	Thermal Spall		2						2	68
	Block shatter and flake fragments of indeterminate orientation	15	13	67	19		3	1	118	
	Flake fragments with orientation (proximal,medial,distal)	60	44	52	23	1	2	1	183	
	Small Production Debris (<15mm max dimension)	2	8	5	12		1		28	
3	Backed Blade		3						3	1
Total		**146**	**107**	**150**	**70**	**1**	**9**	**3**	**486**	**100**

Table 42. Generalized complete and fragmentary artifact counts by *OBS* SubAgg

Sub Aggregate	Raw Material	Flake	Blade	Blade Cores	Other Cores	Point Fragment	Core Edge	Crescent	Indeterminate Fragments	Grand Total
Lizelle	quartzite	11	6						5	22
	silcrete	5	2		1				3	10
	quartz	4	2						11	17
	chert	1	3	1					2	6
	hornfels								1	1
	crystal quartz			1						
	other	1								1
	Total	*22*	*13*	*2*	*1*				*22*	*57*
Peter	quartzite	36	6		1	3			8	53
	silcrete	13	7	1					5	25
	quartz	16	1	1	1				25	42
	chert	12	8	2					2	22
	crystal quartz	1								1
	Total	*78*	*22*	*4*	*2*	*3*			*40*	*143*
Celeste	quartzite	46	9		2	3	1		11	70
	silcrete	19	32	1				2	15	68
	quartz	36	11						40	87
	chert	24							16	40
	crystal quartz	3	1						3	7
	other	1							1	2
	Total	*129*	*53*	*1*	*2*	*3*	*1*	*2*	*86*	*274*
Grand Total		**229**	**88**	**7**	**5**	**6**	**1**	**2**	**148**	**474**

7.6 NWR

The *NWR* is located on the northern boundary of PP5-6 and is not stratigraphically connected to the Long Section at present. This sample is of interest because OSL dates place this MSA deposit at ~59ka, later than the PP5-6 HP. The *NWR* lithic sample is relatively small (n=313), and slightly more than half of the sample (51%) is made from quartzite (Table 43). The lithic assemblage is characterized by a return to larger facetted points (n=7) and blades (n=5) more similar to those of the *LBSR* (Fig. 50), but produced using a greater percentage of silcrete: 8 points and blades are made from quartzite and 4 on silcrete. The assemblage has few primary (n=3) and residual cortical (n=14) products in comparison to non-cortical debitage (n=64). Complete debitage has mainly parallel (n=29) and convergent (n=13) flake scars initiated from a single platform (n=24) or opposed platforms (n=18) (Tables. 10-11).

The *NWR* has two quartzite opposed platform cores, one quartzite core on a flake and one silcrete single platform core. End products are characterized by a return to larger unretouched quartzite flakes and blades consistent with other post-HP assemblages. The presence of two backed blade segments (Appendix 4, Section 3, Find Numbers 103225 and 105221) also indicate some continuity with the *DBCS*. Specimen 10225 is a small

chert crescent with a burination scar that has removed the cutting edge. Specimen 105221 is obliquely backed blade with retouch on the right proximal lateral margin. The *NWR* rests directly on orange dune sand with age estimates similar to the *OBS* (~69ka), so it is unlikely that any mixing would occur from the *DBCS* (HP).

Figure 50. Sample of characteristic Northwest Remnant lithics

Table 43. *NWR* artifact counts by raw material

Production Phase	Modified Geneste Techno-Typology	Quartzite	Silcrete	Quartz	Chert	Hornfels	Quartz Crystal	Total	%
0	Primary Cortical (>60% cortex)	2		1				3	1%
1	Residual Cortical (<61% cortex)	5	5					10	4%
	Naturally Backed Flake/Blade	2						2	
2	Plain Platform Flakes	15	14	1				30	47%
	Plain Platform Blade	3	4		1			8	
	Cortical point,flake, or blade with facetted platform	2						2	
	Facetted flake	2	4					6	
	Blade with facetted platform	4	1					5	
	Point with facetted platform	4	3					7	
	Core-edge or crested flake/blade	1	4					5	
	Facetted core-edge flake/blade	1	1					2	
	Thinning Flake	1						1	
	Block shatter and flake fragments of indeterminate orientation	44	30	5	1	1		81	
	Single platform core		1					1	1%
	Core on a flake	1						1	
	Opposed platform core	2						2	
3	Backed Blade		1		1			2	0.60%
various	Flake fragments with orientation (proximal,medial,distal)	69	54	3	2			128	46%
	Small Production Debris (<15mm max dimension)	2	14				1	17	
Total		**160**	**136**	**10**	**5**	**1**	**1**	**313**	**100%**

7.7 Takis

Takis is an occupation horizon that occurs within the *MBSR* StratAgg, dating from approximately 47-49 ± 3ka, pending additional OSL dates (Brown et al 2009). Takis has a small lithic sample (n=187 pieces) made primarily from fine-grained raw materials, including silcrete (n= 82) and chert (n=29), but quartzite was used as well (n=53) (Table 44). Cores are well represented (n=7), given the size of the total sample. The majority of cores can be characterized as opposed platform blade cores made from quartzite and silcrete. The sample of complete and almost complete debitage (n=48) consists mainly of plain platform flakes (n=24) and blades (n=12). The few facetted products are larger quartzite flake and blades. Non-cortical debitage flake scars are mainly parallel (n=30, 77%) and unidirectional in orientation (n=28, 76%). One complete wide quartzite point (Appendix 4, Section 2; Find Number 153674) and one probable point base (153670) are present. Retouched tools of note include a burin (105437) made on a long silcrete blade and a thick ovate biface (Fig. 51), that could also be a small exhausted discoid core, and two backed blades (Appendix 4, Section 3, Find Numbers 153565 and 153977).

The RSP layer of Sibudu Cave is dated to 53.4 ± 3.2ka (Villa et al. 2005) and may be the closest in age of southern African MSA sites for comparison to the Takis sample. The large RSP lithic sample (c. 14,000 pieces) is described in detail by Villa et al. (2005) and summarized here. Sibudu Cave lithics are made of a different suite of raw materials than those of PP5-6, including more course-grained igneous dolerite and finer-grained hornfels. The RSP assemblage is variable having both flakes and blades noted to have been produced in a range of sizes. Twenty-three cores, six of which were classified as bladelet cores, are surmised to represent a final stage of core reduction. Bladelets (defined as blades less than 8mm in width) are argued to be opportunist removals. Flakes typically have unidirectional and bidirectional scars with narrow plain platforms, and they are variable and irregular in shape. Villa et al. (2005) noted that blades are usually either thin and wide or thick and come from a wider core flaking surface. Pointed forms, which consist of unifacial and unretouched points as well as two bifacial points, make up the largest category of formal tools in the RSP layer. This layer also includes broken point tips, scrapers, burins, scaled pieces, denticulates, and other miscellaneous forms.

The comparison between PP5-6 Takis and Sibudu RSP layers is not very relevant, given the very different sample sizes, differences in raw materials, and distance between the sites. It does, however, highlight the paucity of other sites with material dated to this period, with the possible other exception of Diepkloof (Jacobs et al. 2008). The main feature shared by these layers is the variable nature of the flake and blade samples. The majority of Takis cores are opposed platform small blade cores, but most of the debitage has scars from a single direction. Like the RSP layers, the blade cores may represent a final opportunistic attempt to recover cutting edge before core discard. The Takis blades are typically irregular in shape and size. Future excavation should expand the available Takis sample.

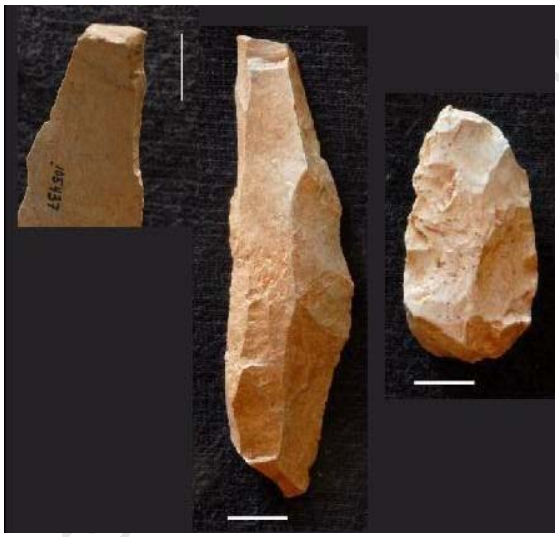

Figure 51. *MBSR* Takis: burin (Find Number 105437 close-up left and center) and thick biface (Find Number 120722 at right). Line segments represent 1cm.

Table 44. *MBSR* Takis artifact counts by raw material

Production Phase	Modified Geneste Techno-Typology	Silcrete	Quartzite	Chert	Quartz	Hornfels	CCS	Other	Total	%
0	Primary Cortical (>60% cortex)	2	1	1			1		**5**	**3%**
1	Residual Cortical (<61% cortex)	4	4	2			1		**11**	**6%**
2	Plain platform flakes (non-cortical)	6	10	3	2	3			**24**	**29%**
	Plain platform blade (non-cortical)	6	3	3					**12**	
	Flake with facetted platform	1	1			1			**3**	
	Blade with facetted platform	1							**1**	
	Point with facetted platform		1	1					**2**	
	Core-edge or crested flake/blade	3							**3**	
	Facetted core-edge flake/blade			1					**1**	
	Thinning Flake	2							**2**	
	Discoid core	1							**1**	
	Adjacent platform core	1							**1**	
	Opposed platform core	1		3					**4**	
	Other double platform core			1					**1**	
various	Hammerstone Spall		1						**1**	**60%**
	Block shatter and flake fragments of indeterminate orientatio	13	9	6	2	1	1	1	**33**	
	Flake fragments with orientation (proximal,medial,distal)	30	23	7	1	4	4		**69**	
	Small Production Debris (<15mm max dimension)	7		1		1			**9**	
3	Backed Blade	3							**3**	**2%**
	Burination Spall	1							**1**	
Total		**82**	**53**	**29**	**5**	**10**	**7**	**1**	**187**	**100%**

7.8 Comparison with Klasies River Sequence

The Klasies River main site's recognized status as the yardstick sequence for the southern Cape MSA, its coastal setting, and large and well-studied lithic assemblage make it the ideal comparative sample for the PP5-6 lithic sequence. The background and description for the Klasies River sequence was presented in Chapter 2.3 and is briefly summarized here. Quartzite raw material use in the LBS and SAS members at Klasies River is synonymous with large facetted flake and blade production and low percentages of retouch in the MSA I and MSA II (Wurz 2002). Non-quartzite raw material use occurs most frequently within the HP and is associated with smaller blades and backed and notched pieces. The Klasies River terminology for the cultural technological substages of the sequence implies a level of continuity through the MSA I and III (Thackeray and Kelly 1988; Wurz 1999). Variation in core reduction strategy at Klasies River has been differentiated by flake metrics and core morphology, all of which is punctuated by the HP, which was once considered to be "intrusive" (Goodwin and van Riet Lowe 1929; Singer and Wymer 1982).

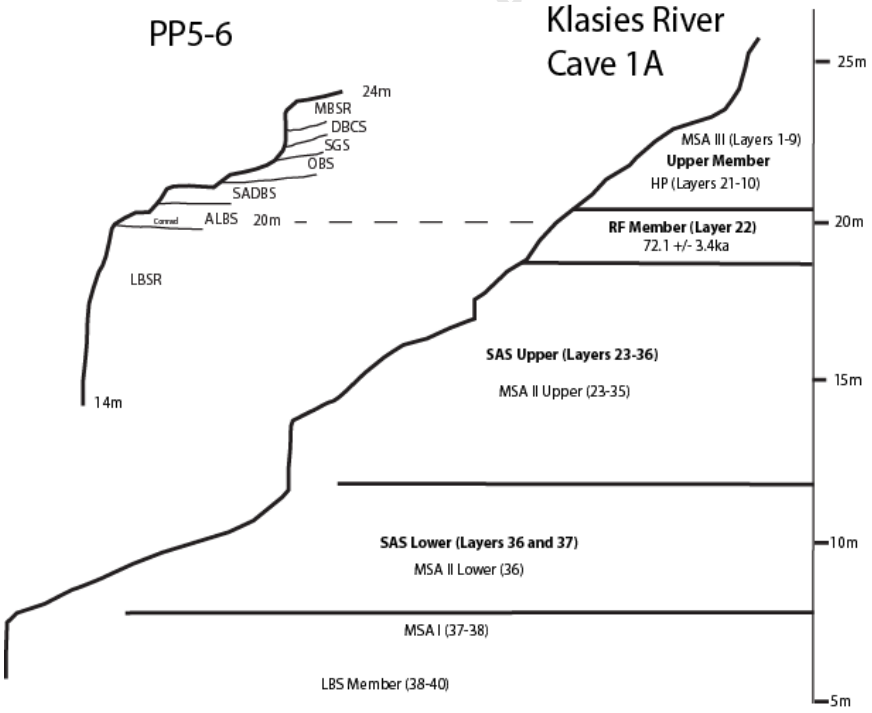

Figure 52. Schematic comparison of PP5-6 and Klasies River Cave 1A Sections. Klasies River Cave 1A stratigraphy redrawn from Deacon and Geleijnse (1988). RF Member age from Jacobs et al. (2008)

The PP5-6 sequence is broadly similar to that of Klasies River (Fig. 52). Lithics from the base of the excavated sequence were typically made on quartzite with an emphasis on the production of facetted point blanks. As with Klasies River, a shift occurs at PP5-6 in the use of non-quartzite stone for the production of small blades, some of which are retouched into repetitive backed and notched forms. Similar to the Klasies River transition from the HP to the MSA III, an increase or return to quartzite use occurs after the PP5-6 *DBCS* (HP) to the *NWR*. The PP5-6 sequence differs from Klasies River in the amplified non-quartzite raw material percentages throughout the sequence, higher chrono-stratigraphic resolution, and the presence of pre-HP MSA occurrences at the c. 72 to 76ka transition from the quartzite to non-quartzite-dominated samples. The trade-off in the PP5-6 sequence is that the higher resolution is at the expense of smaller sample sizes and less horizontal exposure. The analysis of nearby PP13B has demonstrated significant technological variability between artifacts recovered from contemporary layers in different areas of the cave (Thompson et al. 2010). This type of analysis is not currently possible at PP5-6.

Raw Materials

Thackeray (1989) and Wurz (2000) both presented raw material proportions from the Deacon excavations (D-Sample) at Klasies River as the percentage of non-quartzite raw materials present in each layer. These non-quartzite raw materials include quartz, silcrete, and chert. The non-quartzite raw materials for PP5-6 are the same as those at Klasies River but with the addition of trace amounts of quartz crystal. Figure 53 shows a comparison of the Klasies River and PP5-6 sequences based on non-quartzite raw materials. The 'anchor points' between the two graphs are tentative and are based on the Jacobs et al. (2008) OSL dates for the RF and Upper members, which provide linking points with PP5-6 at c. 72 and 58ka. The PP5-6 *LBSR* sequence extends beyond 90ka. The Klasies River SAS Upper Member, which is probably contemporary with the PP5-6 *LBSR,* is estimated to date between 80-100ka (Deacon and Geleijnse 1988; Grün et al. 1990) but there are no age estimates of sufficient resolution to link the older portions of the raw material graphs. These graphs also present the two sequences as being continuous, but systematic OSL dating has demonstrated that significant and repetitive occupation gaps exist in many MSA sequences that may complicate direct comparison (Jacobs and Roberts 2008). Such occupation gaps will need to be considered if absolute dates from the Klasies River SAS member become available.

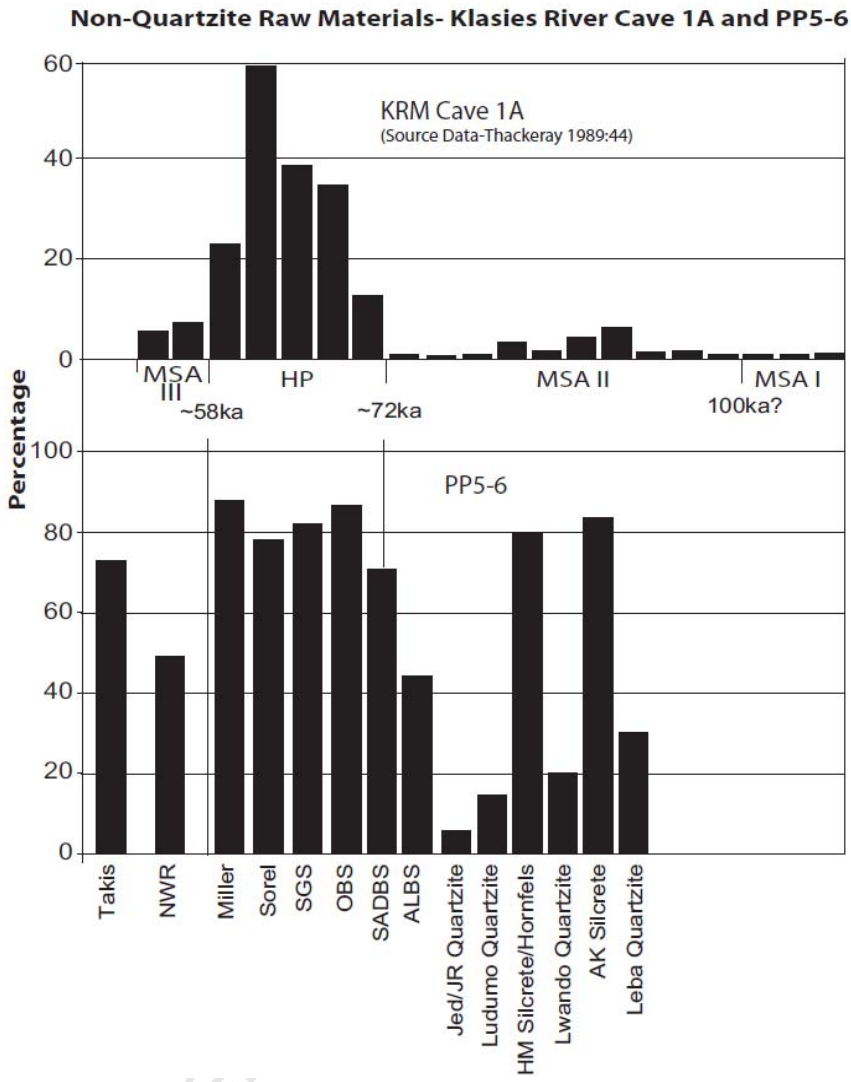

Figure 53. Percentage of non-quartzite raw materials at Klasies River compared with PP5-6 analytical samples. Klasies River raw materials from Thackeray (1989)

The Klasies River Cave 1A raw material graph shows two modal peaks in non-quartzite raw material use: 1) a low peak in the Middle of the SAS Upper member (MSA II); and 2) a significant high peak within the Cave 1A HP, which decreases measurably in the following MSA III (top of the Upper Member). The sequence from PP5-6 has a similar but more exaggerated trend in raw material use. Non-quartzite raw materials are well represented in analytical samples from the c. 82-86ka layers of the PP5-6 *LBSR*, but these stratigraphic layers currently have relatively few excavated artifacts available for analysis. At PP5-6, quartzite use peaks at 79ka and then non-quartzite raw materials become predominant from c. 72 to 76ka until approximately 59 to 60ka when non-quartzite materials drop to ~50% of the sample in the *NWR*.

PP5-6 LBSR and MSA II

The *LBSR* may be compared favorably with the Klasies River MSA II because the stratigraphic layers from which the samples were excavated are approximately contemporary, and they are quartzite-dominated lithic assemblages made from quartzite cobbles. The preferential blank or end products at both sites include points and blades from single platform cores typically with faceting platform preparation. PP5-6 has a relatively small sample size of points and blades with dimensions that are consequently more variable than those from the Klasies River MSA II (Fig. 54). The *LBSR* points are on average, smaller and thicker than their Klasies River counterparts (Table 45).
Most of the MSA II cores from Klasies River show convergent scars indicative of point removal as the final stage of core life (Wurz 2002). The PP5-6 *LBSR* cores were typically flaked centripetally before discard and were more likely to be abandoned in a smaller size (Table 46) and in discoid form. The *LBSR* complete cores are, on average, c. 75% smaller than Klasies River MSA II cores for which data are available (Table 46), and this size difference may reflect more intensive utilization of *LBSR* core volume. This creates a situation in the total *LBSR* StratAgg sample, for example, where there are 17 points but only 3 cores out of 13 have convergent flake scars.

Table 45. Comparison of Klasies River and PP5-6 *SADBS* and *DBCS* blade and point mean dimensions. 95% Confidence interval of mean was calculated from published mean, SD, and sample count presented in Wurz (2000; 2002)

	KRM End Product Dimensions										PP5-6					
	MSA I		MSAII Lower		MSA II Upper		HP		MSA III		LBSR		SADBS		DBCS (HP)	
	Points	Blades	Points	Blades	Points	Blades	Points	Blades	Points	Blades	Points	Blades	Points	Blades	Points	Blades
Mean Length	70.6	80.9	65.4	75.9	58.8	67.9	-	43.9	64.2	77.8	50.3	58.2	40.3	23.6	-	27.1
SD	15.9	23.5	16.6	23.3	15.8	22.8	-	12.8	18.4	31.4	15.7	7.6	7.9	8.7	-	8.6
count	60	83	413	455	246	218	-	75	11	23	17	6	7	145	-	28
95% CI	4.0	5.1	1.6	2.1	2.0	3.0	-	2.9	10.9	12.8	7.5	6.1	5.9	1.4	-	3.2
Mean Width	33.6	28.3	34.7	30.2	31.6	26.9	-	18.8	34.0	25.7	32	26.2	26.6	10.9	-	12.6
SD	6.1	8.2	7.7	8.8	7.2	8.5	-	5.7	7.2	9.0	6.4	3.8	3.7	3.7	-	3.8
count	71	472	545	1792	298	1037	-	714	15	259	17	6	7	145	-	28
95% CI	1.4	0.7	0.7	0.4	0.8	0.5	-	0.4	3.6	1.1	3.0	3	2.7	0.6	-	1.4
Mean Thickness	9.3	8.3	11.0	9.6	10.3	8.7	-	4.9	10.2	7.7	11.4	8.0	7.8	3.2	-	3.3
SD	2.3	3.4	3.9	3.7	2.9	3.4	-	2.0	2.3	4.1	3.3	2.1	1	1.6	-	1.4
count	71	472	545	1972	298	1073	-	714	15	259	17	6	7	145	-	28
95% CI	0.5	0.3	0.3	0.2	0.3	0.2	-	0.2	1.2	0.5	1.6	1.7	0.7	0.3	-	0.5

KRM Date from Wurz (2000, 2002)

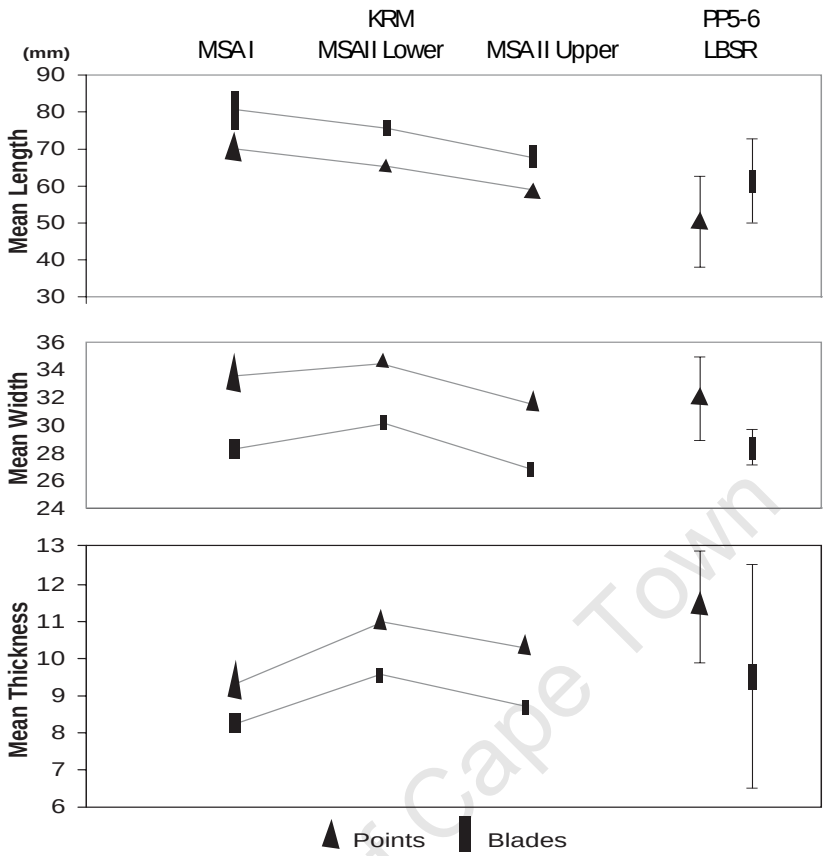

Figure 54. Comparison of Klasies River MSA and PP5-6 *LBSR* end product dimensions. The error bars for the PP5-6 *LBSR* blades and points represent 95% confidence intervals of the mean and are large due to smaller sample sizes. The Klasies River 95% confidence interval of the mean is depicted by the height of the point and blade symbols

Table 46. Comparison of PP5-6 *LBSR* and Klasies River MSA II core size

		LBSR (all)	MSA II Lower (point)	MSA II Lower (blade)	MSA II Upper (point)	MSA II Upper (blade)
Length	Mean	49.5	65.1	59.8	59.8	61
	SD	18.0	14.7	14.3	14.3	17.5
	Count	15	67	11	13	5
Width	Mean	45.7	62.6	58.3	58.3	62.6
	SD	18.9	11.9	8.2	8.2	26.1
	Count	15	67	11	13	5
Thickness	Mean	21.8	28.5	27.7	27.7	27.6
	SD	6.7	8.2	7.4	7.4	8.8
	Count	15	67	11	13	5

KRM Source Data: Wurz (2000):182-3

PP5-6 DBCS and SADBS and Klasies River HP

The Klasies River sequence shows an increase of up to 33% in the use of non-quartzite fine-grained raw material in the HP (Wurz 2002). The majority of the PP5-6 *SADBS* (86%) and *DBCS* (85%) assemblages are made from non-quartzite raw materials. Klasies River HP cores exhibit blade removals, typically from a single platform although some cores also have opposed platforms. Opposed platform cores are more common in the *SADBS* and *DBCS* than single platform cores. The majority of Klasies River HP blades have plain and sometimes punctiform small platforms in comparison to the MSA II which have larger platforms prepared by faceting with no evidence for the trimming or abrasion of the platform adjacent to the flaking surface (Wurz 2002). Platform abrasion is the most common form of preparation on PP5-6 *SADBS* and *DBCS* debitage. The PP5-6 *SADBS* and *DBCS* blades have mean lengths that are smaller than those found in the Klasies River HP (Table 45).

Wurz (2002) argued that KRM HP blade production was very similar to the strategy employed much earlier in the MSA I. Blades were commonly struck from pyramidal or flat blade cores that were initially prepared centripetally. Lateral convexity was maintained by laminar core edge border flakes and not by crested blade removal. The *SADBS* is noteworthy for being the only PP5-6 sample where crested blades are also well represented alongside core edge flakes and blades. There are 14 blades showing deliberate perpendicular versant scars, many of which appear to have been intended to modify the convexity of a natural cortical ridge for the first blade removal. There are only two crested blade specimens from the *DBCS* (150707, 182201) which may suggest that *DBCS* blade production was more like that of the KRM HP or may be reflective of a lower overall sample size and recovery rate.

Backed or truncated blades are present in all post-ALBS samples at PP5-6 (Appendix 4, Section 3), but they occur at highest density in the SGS, and highest frequency in the PP5-6 *SADBS* and *DBCS*. The small backed blade sample size is a function of the low sediment volumes excavated to present in the upper PP5-6 Long Section. The Singer and Wymer excavations of Klasies River Cave 1A yielded 1,327 “crescents and allied forms” from excavations in the HP measuring approximately 3 x 3.5 x 1m or 10.5m^3 (estimated from plan and profile section drawings in Singer and Wymer 1982). Klasies River therefore has an estimated backed piece density of ~125 pieces/m^3, which is midway between the estimates for the *SGS* and *DBCS* (Table 37). Segment size

is compared between the *SADBS* and a number of other MSA, LSA, and more recent sites in Chapter 12.

The HP is the only identified backed blade occurrence in the Klasies River sequence. At PP5-6 there are at least two backed blade entities that occur between the *LBSR* (suggested to be similar to the MSA II) and the *NWR* (proposed to be similar to the MSA III). The *SADBS* is older than the *DBCS* by approximately 5-7ka and is separated from the *DBCS* by a thick dune. The *SADBS* has narrow backed blades and a sample of larger points but only one notched piece. The *DBCS* is similar in age to the Klasies River HP and has both backed blades and notched pieces. The relationship between the *SGS*, *DBCS*, and *OBS* remains to be determined with future excavations.

PP5-6 NWR and Klasies River MSA III

The PP5-6 *NWR* shares similarities with the Klasies River MSA III (Wurz 2002). Both samples have relatively small sample sizes, which limit statistical comparison with previous layers. Both samples show a decrease in the use of non-quartzite raw materials in comparison to the HP, but not a complete return to the percentages typical of the LBSR and MSA II, respectively (Villa et al. 2010). The *NWR* and MSA III have points and blades that are larger than those found in the preceding HP at each site, and double platform cores. An MSA III feature that may also be present in the *NWR* is a small sample (n=12 at Klasies River) of unifacially retouched points termed "knives," which are described as being unstandardized in size but having continuous "flat" retouch along the entirety of at least one lateral margin (Wurz 2000:101). In other typologies, "knives" may be termed "sidescrapers" (Villa et al. 2005). The *NWR* has two specimens that are similar to this description (Fig. 55). Find Number 103892 is a medial blade fragment that has continuous irregular retouch along the entire right margin. Find Number 105536 is a proximal blade fragment that has parallel blunting or steep retouch on both laterals.

Figure 55. Potential *NWR* "knives." Find Numbers 103892 (left) and 105536 (right). White line is 1cm scale.

8.0 Raw Material Preparation- Heat Treatment

Silcrete is traditionally viewed as non-local, fine-grained raw material that is highly workable in its natural state (Ambrose & Lorenz 1990; McBrearty & Brooks 2000; McCall 2007). A silcrete heat treatment study was initiated at Pinnacle Point after unsuccessful attempts at locating silcrete of similar appearance to what was found in the PP5-6 archaeological record, and of sufficient flaking quality for experimental replications. It was found in actuality that silcrete stone gathered from some of the more homogeneous primary deposits in the southern Cape is typically tough and difficult to flake predictably. In Australia, where silcrete was extensively utilized for tool production by at least 20ka, indigenous knappers subjected silcrete to heat treatment to improve the flaking quality of the material (Flenniken & White 1983; Hanckel 1985).

Controlled and systematic experiments with heat treatment were then conducted at Pinnacle Point to produce experimental samples which could be used to quantify the changes observed in the heated silcrete and to develop a nondestructive method for identifying heat treatment in the PP5-6 archaeological assemblage. It was found that after heat treatment, south coast silcrete is significantly more workable, and bifaces are easy to flake with higher success rates. The improvements noted in the biface study presented here were also documented in mechanical testing of southern Cape silcrete (Brown et al. 2009 and Ch. 8.3). Silcrete heat treatment is central to the research questions addressed in this thesis because heat treatment requires a level of planning and preparation inconsistent with models that portray silcrete procurement as being strictly encounter-based. The following chapter details this author's contribution to a larger interdisciplinary study of silcrete heat treatment at Pinnacle Point (Brown et al. 2009). The initial published results are updated here with data from larger analyzed samples.

8.1 Heat Treatment Background

Heat treatment is defined as the deliberate alteration of lithic materials to bring about an improvement in the flaking quality of the stone (Luedtke 1992). "Thermal alteration" refers to silcrete that has been heated without reference to intentionality. Archaeologists were slow to recognize heat treatment products in their collections for two reasons. First, early ethnographers may have been confused by what they were

witnessing. Second, until recently, few archaeologists conducted controlled experiments to replicate stone tools found in their collections.

Archaeologists became aware of heat treatment from the publication of a paper by Crabtree and Butler (1964), which summarized experiments with North American chert from Flintridge, Ohio. Crabtree and Butler found that the heat treatment of their stone materials caused improvements beneficial to biface production. They noted that the flaking difference between treated and untreated materials could be demonstrated by the longer length of the pressure flakes that could be made on heated material. Also noteworthy are Crabtree's observations of a "greasy luster" and that thin blanks were more amenable to treatment than thicker blanks. To explain the improvement, he believed that the crystals in the heat-treated stone had become smaller during the treatment process.

Crabtree and Butler's (1964) publication spurred a review of ethnographic literature aimed at identifying eyewitness accounts of heat treatment by Native Americans (Hester 1972). Though observations are sparse, a number of examples are cited where Native American knappers would either directly or indirectly subject their lithic materials to heat. Heat treatment was conducted to improve the quality of the material or to reduce large pieces of material into core-size nodules either at the quarry site or at a reduction area. Binford and O'Connell observed quarrying activities by the Alyawara in central Australia where large stone boulders were levered out of the ground with wood poles and then fire was used to crack the blocks into manageable sizes (Binford and O'Connell 1984).

With the acceptance of the validity of lithic heat treatment came the need to properly identify this technique in an archaeological context. Collins and Fenwick (1974) divided the effects of thermal alteration on materials into visually observable changes and effects that are only detectable with the aid of an instrument. Potential visual changes include an increase in gloss after heating, color alteration, heat damage (potlidding and crazing), and the acceleration of patination. Changes potentially detectable by instrumentation include energy (light) loss through the use of a TL suitability test, the obliteration of fission tracks, hydration loss, changes in compressive and tensile qualities, and changes in the crystalline structure after heating, which is potentially detectable by X-ray diffraction (XRD).

The choice of technique for the detection of heat treatment is complicated by the ongoing debate over the actual physical changes that occur within the stone during

heating. Three primary models have been proposed to explain the structural changes that occur within silica-based stone as the result of heat treatment. This research is largely based on SEM and XRD studies (Domanski and Webb 1992; Luedtke 1992). The silica fusion model postulates that impurities in the stone melt at relatively low temperatures and act as flux to bind the crystalline structure more tightly, and fractures therefore propagate across or through internal structures rather than around them (Purdy and Brooks 1971). The micro cracking model holds that heat treatment creates very small fractures in the material causing the heated stone to be more brittle and consequently more easily flaked (Flenniken and Garrison 1975). The recrystallization model, which currently has the most support, suggests that the fabric structure of silicates is reorganized during heating so that fractures form more easily along realigned quartz crystal surfaces (Domanski and Webb 1992).

Resolution of this debate has important implications for the development of multiple non-destructive laboratory techniques for identifying heat treatment on archaeological specimens. This issue is complicated by the fact that some lithologies may show extreme heterogeneity within material from a single source or even across the flaked surface of an individual specimen (Flenniken and White 1983). Also problematic is that identification of heat treatment in archaeological samples requires the ability to detect deliberate heat treatment versus unintentionally heated lithics. Lithic materials can be burned in cooking fires or by naturally occurring fires in organic-rich cave sediments or from bush fires. Ethnographic evidence suggests that some heat treatment was aimed at breaking up larger blocks of material in a quarry context (Binford and O'Connell 1984). Some of this material will be thermally altered but not necessarily to improve flaking qualities (Gregg and Grybush 1976).

8.2 Silcrete Collection and Experimental Heat Treatment Methods

The analysis of cortex on PP5-6 lithics (Ch. 6) demonstrated that silcrete nodules used by MSA knappers at PP5-6 were collected mainly from primary sources. The collection strategy for experimental materials focused on primary sources within a 25km radius centered on Pinnacle Point (Appendix 1, Fig. 3). Some material was collected outside of this radius because more distant sources at Albertinia and Riversdale provided larger sized nodules necessary to mechanically cut uniform blanks for the biface experiments. The collection of samples beyond the Mossel Bay area also demonstrates

that heat treatment is effective on silcrete materials from other locations in the southern Cape (Olfontein near Cape Town, for example). Secondary context silcrete beach cobbles were sampled at two locations (Dana Bay and Rheebok).

Silcrete used in the experiments have a similar general appearance to the microcrystalline archaeological samples from PP5-6, based on characteristic luster, color, texture, and conchoidal fracture when examined under a hand lens (D.R. Roberts, pers. comm.). Thin sectioning of the artifacts would have required the destructive analysis of a larger sample of artifacts and was deemed unnecessary because all the sampled silcrete in the study area proved to be amenable to alteration by heat treatment. A geochemical raw material source study has not yet been conducted at Pinnacle Point, but the sampled locations were clearly utilized by prehistoric tool makers who left surface scatters of lithic debris surrounding the sampled outcrops. No archaeological materials were disturbed during silcrete collection.

Two methods were employed to heat treat experimental silcrete samples. In the first method, raw material and a thermocouple probe (type K) were placed within a sand bath approximately 2 to 3 cm below the surface. A fire was then built over the sand containing the silcrete. The temperature of the silcrete was slowly built up to approximately 350º C during a period of about five hours and then gradually cooled to ambient temperature (usually overnight) before the blanks were removed from the sand. Temperature was monitored and recorded using a J-Kem HHM-40 handheld temperature meter and data logger. Fires required approximately 20 kg of dried hardwood per 3 kg of stone.

The second heating method involved stacking samples in the open chamber of a Gallenkamp muffle furnace fitted with an external J-Kem programmable temperature controller (Model 360/Timer-K). It was not necessary to use a sand bath in the kiln because the wrap-around element distributes heat evenly throughout the oven. The controller was programmed to slowly ramp the temperature of the furnace to 350ºC over five hours. This temperature was held constant for 10-12 hours and then dropped slowly to 40º C before the blanks were removed from the kiln. The failure rates are quite low (<6%) for each treatment method and many failures were not catastrophic in that the spalls could still be used for flaking (Table 47).

Table 47. Total nodule failure rate during heating across 10 different treatment experiments. Many of these heat treatment trials were not part of the biface experiments described here

Treatment Method	Sample Count	Catastrophic Failures	Partial Failures	Total	Failure %
Fire	89	3	2	5	6%
Kiln	56	0	2	2	4%
Total	145	3	4	7	5%

8.3 Rebound Hardness

Rebound Hardness is a mechanical test that measures the relative stiffness of a lithic raw material sample (Noll 2000). Rebound Hardness is considered to be an objective measurement of the flaking quality of lithic raw materials (Braun et al. 2009). The following analysis was conducted in order to quantify the potential flaking benefits conferred to south coast silcrete by heat treatment. This analysis was performed as part of a larger heat treatment study (Brown et al. 2009) in collaboration with one of this author's supervisors, (David Braun). The Rebound Hardness study is included in this dissertation in order to develop the theoretical basis for understanding why heat treatment, a costly technological innovation, was adopted in the MSA at PP5-6. This author contributed to the Rebound Hardness study by collecting and preparing the silcrete samples. Braun tested the samples and performed the statistical analysis.

The silcrete samples were prepared using a large angle grinder to provide paired heated and unheated blocks from the same parent nodule, each with two parallel flat surfaces at least 10cm apart. One surface rests against a thick plate metal base and the other act as the test surface. Due to their large size, the heated samples were treated in the muffle furnace. The Rebound Hardness test is a measure of homogeneity of raw material and is sensitive to impurities. Silcrete samples that had observable cracks and large inclusions or voids were excluded.

Rebound Hardness tests were conducted using a Schmidt Hammer, which is a handheld instrument that has a metal plunger with a calibrated spring. When the plunger is released it rebounds off the surface of the sample measuring the reaction of the rock to a dynamic load in hardness values ranging between 5 and 80. The Schmidt hammer is used so that the plunger is exactly vertical otherwise the measurements must be corrected

for trace amounts of friction on the sides of the plunger. Because numerous factors can affect Schmidt Hammer Values (e.g. slipping of the plunger on the sample; mechanical failure of the specimen) each specimen is tested 20 times. These twenty values are then ranked from the highest to the lowest. The top five values and bottom five values are then removed from the analysis. An average is taken of the middle 10 values. Rebound Hardness values are provided in Table 48.

The significance of the change in Rebound Hardness after heat treatment (2 dependent samples) was tested using the non-parametric Wilcoxon matched pairs test because of the small sample size (n=26 pairs). The calculation of *p* values were based on randomization and used a 1-tailed distribution because it was assumed that heat treated samples would higher values than their unheated control. The results of the analysis show that heat-treated samples do have significantly higher Rebound Hardness values than their paired untreated samples (Wilcoxon matched pairs test; z = 2.512; p =.004, Fig. 56. The south coast silcrete samples tested in this study show a significant improvement in flaking quality after heat treatment.

Figure 56. Box and whisker plot comparison of Rebound Hardness values from Schmidt Hammer tests on paired experimental samples of unheated (grey) and heated (red) silcrete. Y-axis provides Schmidt Hammer H-values

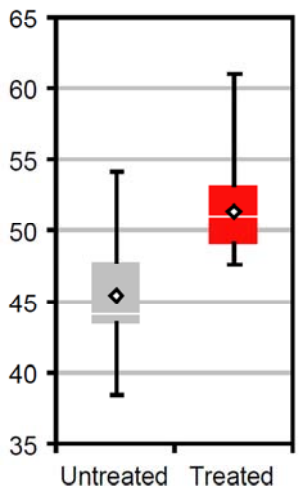

Table 48. Rebound hardness values for experimentally heat treated silcrete. Samples ALB-A47, ALB-A55, and R-A11 were not included in the statistical analysis due to visible flaws in the material. ZU and ZU2 were collected from a naturally burned outcrop and were included for comparison but were not used for statistical analysis because control samples were not available.

Sample	Rebound Hardness (Untreated)	Rebound Hardness (Treated)	Sample Count	Comment
ALB.A46	43.6	50.3	2	
ALB.A47	32	51.4	1	removed-failed during testing
ALB.A48	38.4	48.2	1	
ALB.A49	44.1	47.6	1	
ALB.A50	43.2	51	1	
ALB.A51	43.7	52	1	
ALB.A52	48	50	1	
ALB.A53	54.1	61	1	
ALB.A54	44.1	51.6	1	
ALB.A55	43.2	40.8	1	removed because of unlevel surface and cracks
ALB.A60	46.6	53.6	1	
ALB.A63	43.5	52.8	1	
ALB.A64	48	51	1	
R.A11	40.2	32.1	1	removed because of cracks in sample
R.A13	49.8	52.6	1	
R.A14	48.4	49.4	1	
R.A15	40.3	48.9	1	
R.A16	44	47.8	1	
R.A17	43.6	54.4	1	
R.A19	47.4	53.2	1	
R.A2	42.2	47.8	1	
R.A3	47	47.8	1	
R.A4	45.8	53.4	1	
R.A8	50.2	55	1	
R.A9	42.4	49.4	1	
ZU	41.1		1	naturally heated sample- brush fire
ZU2	47.9		1	naturally heated sample- brush fire

8.4 Timed Biface Reduction Experiments

The timed bifacial tool replication experiments presented here were designed to represent an actualistic complement to the laboratory rebound hardness tests described above. Blade replications may have been a more appropriate choice if these studies were limited to the findings from PP5-6, but the interdisciplinary study of silcrete heat treatment from which this chapter derives, focused on the role of silcrete heat treatment in both the HP and SB MSA of southern Africa (Brown et al. 2009). The archaeological samples selected for gloss and destructive analyses were not limited to blade production debitage at PP5-6 but also included an SB biface from Blombos Sands contributed to the study by Iziko Museum. The results of the analysis were discussed in context with

technological advances in both MSA blade and biface production (Brown et al. 2009). Further, the replication experiments described here were performed at a relatively early phase of research at PP5-6 when there was still an expectation of identifying an SB occupation based on the depth and chronology of the deposit which includes occupations that overlap temporally with the SB (Brown et al. 2011) and the identification of a biface found on the scree deposit at the base of the site. Planned experiments by this author will investigate and quantify specific costs and benefits of heat treatment on silcrete small blade production.

The results of the experiments were evaluated by comparing the width to thickness ratio (W/T) of bifaces knapped from heat-treated and untreated silcrete. This measurement has often been used to evaluate the production stage or craftsmanship exhibited in bifacial tools (Callahan 1979). Finished or more carefully crafted bifacial tools have higher width to thickness ratios than those produced more expediently. Variants of the W/T measurement have also been shown to correlate with projectile point function and ballistics (Shea 2006; Shea and Sisk 2009).

A total of 176 nodules or blanks were prepared from samples collected at two different silcrete collection sources ("Riversdale A" and "Albertinia A"). All Riversdale samples came from a single large boulder ("A4"). Albertinia samples were prepared from 16 nodules with similar texture and appearance (numbered "A30-A45"). Three different blank sets were created, including two sets of mechanically shaped standardized tabular nodules (Appendix 1, Fig. 4), and a set of more realistic flake blanks that ranged in size and morphology. Each set of blanks was entered and ranked on a spreadsheet by blank configuration and weight. Alternating blanks were selected for heat treatment, which eventually provided paired dependent samples for statistical analysis. Paired samples derived from the same nodules of parent raw material in order to control for variability in raw material homogeneity. Each side of the mechanically cut flake blanks was then painted a different color to aid in the eventual analysis of the production debris and to make the manipulation of the blank more visible on the video record. Two blanks failed during treatment.

After treatment, each blank was bifacially flaked (on two opposed surfaces). For consistency, a maximum of 14 minutes was allocated for each reduction (15-minute video discs were used) with the goal to maximize W/T in the final product. All reductions were video recorded and were performed by this author using sandstone percussors (3-8cm diameter). Some reductions were shorter than 14 minutes due either to blank failure

or diminished ability to detach flakes. A reduction was stopped if failure reduced the remaining fragments to less than half the length of the original biface blank.

The replication experiments resulted in the production of 50 surviving pairs of bifaces made from untreated and treated silcrete (Fig. 57). Maximum width and maximum thickness values were measured for each replicated artifact (Fig. 58), and the results were compared using one-tailed Related Sample t-Test. The results of the test ($t(49) = 8.11$ $p < .001$) are highly significant, and it is concluded that heated bifaces have significantly higher W/T values than unheated bifaces. Summary information for the experimental biface dataset is included in Appendix 1, Table 1.

The test W/T values are not currently published for archaeological SB bifaces, but a related measurement, artifact midpoint width, and midpoint thickness have been reported for bifacial artifacts from a number of sites in the southern Cape (Minichillo 2005). A box and whisker plot of midpoint width/midpoint thickness shows that the values of the heated samples closely match those of the archaeological specimens (Fig. 59), but the unheated specimens fall below that range. The results of the experiment demonstrate that heat-treated silcrete allows for greater control and has improved flaking properties when compared with unheated silcrete. A significantly thinner biface can be produced in the same amount of time using heated silcrete biface blanks. The flaking of heated biface blanks also resulted in fewer large step fractures (stepped flake scar width greater than 1cm) in comparison to the unheated biface blank reductions (Appendix 1, Fig. 5).

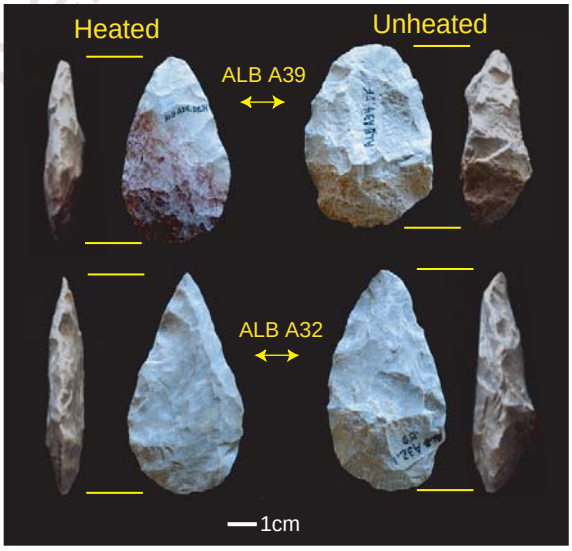

Figure 57. Two paired biface samples made from the same parent silcrete nodules. Heated material is on the left, unheated on the right

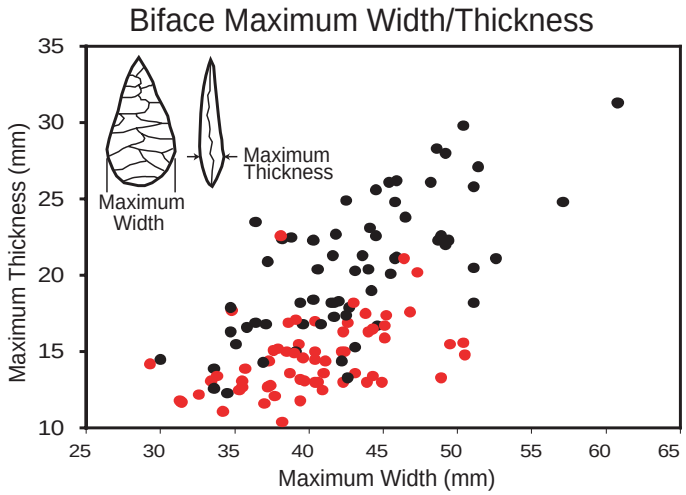

Figure 58. Scatter plot of biface maximum width and thickness for experimentally knapped unheated (black) and heated (red) bifaces

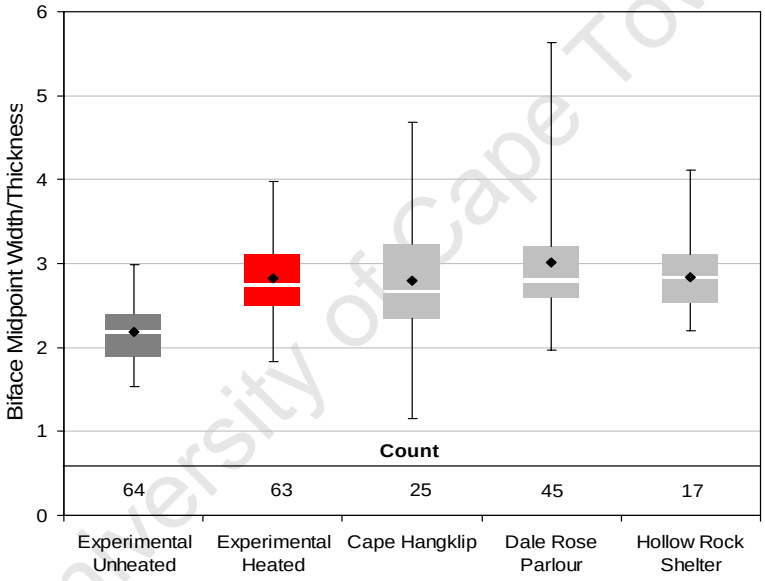

Figure 59. Comparison of midpoint width to thickness ratio (mpW/T) of experimental and archaeological bifaces. Data are from sites in Minichillo (2005) with biface sample size greater than 15 specimens

8.5 Gloss Analysis

"Gloss" and "luster" are terms regularly used in archeological literature to describe the surface reflectivity of heat-treated stone (Luedtke 1992). The most practical and efficient non-destructive way of identifying heat treatment is to look for patterned changes in gloss during lithic analysis because the higher gloss produced during treatment is visible only *after* heated material is flaked (Collins and Fenwick 1974). For many materials, including silcrete, the changes are obvious in that successfully treated

materials have increased gloss in comparison to the rougher pre-treatment surface (Fig. 60a), and they are often more reddish in color (for silcrete) in comparison to the untreated parent material.

Fifty silcrete nodules were selected for gloss analysis from a range of collection locations to demonstrate the suitability of using gloss measurements to track silcrete heat treatment. Each nodule was subdivided to supply three experimental datasets: 1) an original unheated flaked control sample; 2) a sample that was experimentally heated but was not flaked after heat treatment to simulate unintentional or post-depositional burning; and 3) a sample that was experimentally heated and then flaked after treatment to represent deliberate heat treatment. Samples were heated using the previously described methods.

Gloss was quantified with a desktop Rhopoint Novo-Curve instrument, which measures the reflectivity on flat and convex surfaces. The instrument is not designed to be used on concave surfaces and therefore the target region needs to be selected with care. Ventral flake surfaces are ideal. The instrument was used in continuous reading mode where the sample is manipulated over the light-reflecting orifice until a maximum gloss (MG) value, measured in gloss units (or GU), is achieved. Samples of less than 15mm in maximum diameter were generally not measured due to the difficulty in manipulating the object over the measurement orifice. All readings were taken in a darkroom setting because the instrument is sensitive to incidental light.

A maximum gloss value for each specimen set is provided in Appendix 1, Table 2. In almost every nodule set, related samples show an increase in gloss from the unheated flaked and heated flaked samples. The critical observation for establishing the intentionality of heat treatment is that a significant increase in gloss occurs only on samples that were flaked *after* they were heat-treated. Figure 60(b1) is the histogram of maximum gloss measurements on the 50 unheated specimens. The unheated samples range from 1.2 to 2.7 GU. Figure 60(b2) are samples from the same nodules that were heat-treated but were not yet flaked. Interestingly, the heated but unflaked sample control set actually exhibits a slight decrease in gloss from the unheated control sample set. In other words, heating alone does not create an increase in surface gloss. Figure 60(b3) is the set which was heat-treated and then flaked. Gloss measurements were taken on the freshly flaked surfaces. Heated and flaked samples ranged from 2.2 to 5.7 GU.

The significance of the increase in maximum gloss values from the unheated and heated/flaked samples was tested using the related sample t-test. The samples are related

because each tested sample pair originates from the same parent stone nodule. A normal distribution is assumed because of the large sample size (50 pairs). The flaked surfaces of heated experimental samples have significantly higher maximum gloss (MG) unit measurements than the unheated control samples (one-tailed related samples t- test: $t(49) = 14.71$ $p < .001$).

The experimental gloss data were then used to interpret the gloss measurements of the archaeological samples. Figure 60(c1) displays overlapped histograms for the MG values of all unheated (in black) and experimentally heated samples (red). Taking overlap into account, values below 2.0 (the lowest MG value of the experimental dataset) are attributed solely to unheated silcrete, and values above 2.7 occur only with silcrete that has been heat treated. Figure 60(c2) is a histogram with all experimental MG data grouped together, simulating an assemblage with equal proportions of heated and unheated silcrete artifacts. In Figure 60(c3), 37 unheated samples were randomly removed from the distribution, creating a hypothetical assemblage that has 80% heated silcrete. Conversely, in Figure 60(c4), 37 heated samples were randomly removed from the sample set and the histogram simulates an assemblage that is 80% unheated.

Gloss analysis on archaeological silcrete from PP5-6 included all silcrete artifacts that had been catalogued by May 1, 2009, but was limited to individual items greater than 15mm in maximum diameter having flat to convex surfaces suitable for gloss measurement. All specimens were cleaned, as described in Chapter 7.1, except for lot numbers set aside for residue and microwear analysis, including samples from *DBCS* 'Sorel' and 'Quinn', and *SGS* 'Jinga' and 'Zuri'. Some stratigraphic samples (particularly from the *LBSR* with low frequencies of lithics and silcrete) have few artifacts, but the results are presented along with artifact counts. Many samples retained a non-lustrous pre-heat treatment surface (Fig. 60a), which was also measured for maximum gloss in a second field (MG2). The pre-heat treatment surfaces are easily identified and are diagnostic because artifacts exhibiting different degrees of gloss on pre- and post-heat treatment surfaces are unquestionably heat-treated.

The results of the gloss analysis are presented according to the sample cutoff for heated and unheated histograms, which are identified in the experimental gloss analysis in Figure 60d; individual sample histograms with MG2 values are provided in Appendix 1, Figure 6. Most of the silcrete-rich archaeological samples exhibit gloss distributions similar to the 80% heated and 100% heated experimental datasets, but sample sizes decrease markedly in samples that occur stratigraphically below the *SADBS*. The *NWR*

stands out as being similar to the 50% heated/unheated experimental sample. 'Jocelyn' falls between the 50% and 80% heated distributions and 'Erich' stands out as having almost all silcrete with MG above 2.7 GU. Jed/JR Quartzite has only eight pieces suitable for the study of gloss and no values above the 2.7 GU threshold for identification of heated samples. The AK Silcrete and HM Silcrete/Hornfels samples both contain heated silcrete, including an example of MG2 pre-treatment gloss. The MG2 values fall largely within the experimental maximum gloss range documented for unheated silcrete.

All samples, with the exception of Jed/JR Quartzite, show some degree of heat treatment. Gloss distributions indicate the practice of heat treatment in all stratigraphic samples that are high in silcrete ('Erich', *SADBS*, *SGS*, and 'Miller'). The converse is not always true. 'Jocelyn' and *OBS* have very little silcrete but most samples appear to have been heat treated. Just over 50% of *NWR* lithics are quartzite, and the gloss distributions for silcrete are similar to the 50% heated/unheated experimental dataset. The Takis assemblage, which is stratigraphically above the *NWR*, exhibits heat treatment gloss for close to 80% of the analysed specimens. The Jed/JR Quartzite, 'Jocelyn', and *NWR* samples exhibit the highest frequencies of unheated silcrete.

The AK Silcrete and HM Silcrete/Hornfels samples demonstrate that heat treatment was practiced at PP5-6 prior to the major raw material shift that occurs in the *ALBS*, even though those earlier layers seem to reflect low intensity artifact manufacture where it might be expected to see more expedient tool making practiced. These findings are in agreement with conclusions reached from the gloss analysis of the small PP13B *LCMSA-Lower* silcrete sample dated to 164ka (Marean et al. 2007) that identified 6 out 22 sampled specimens with MG greater than 2.7 GU (Brown et al. 2009).

The three samples with the lowest percentage of heated silcrete are also the samples modeled to be closest to the coastline. Sample size is obviously a limiting factor with Jed/JR Quartzite (n=8) and HM Silcrete/Hornfels (n=13). The very low percentage of silcrete in Jed/JR Quartzite (2%) may validate the lack of heat treatment seen in the gloss sample. Perhaps this indicates that silcrete was used in a similar manner as the other Jed/JR Quartzite raw materials. The *NWR* sample is noteworthy because both the proportions of quartzite versus silcrete raw material percentages and the proportion of heated versus unheated silcrete are approximately equal.

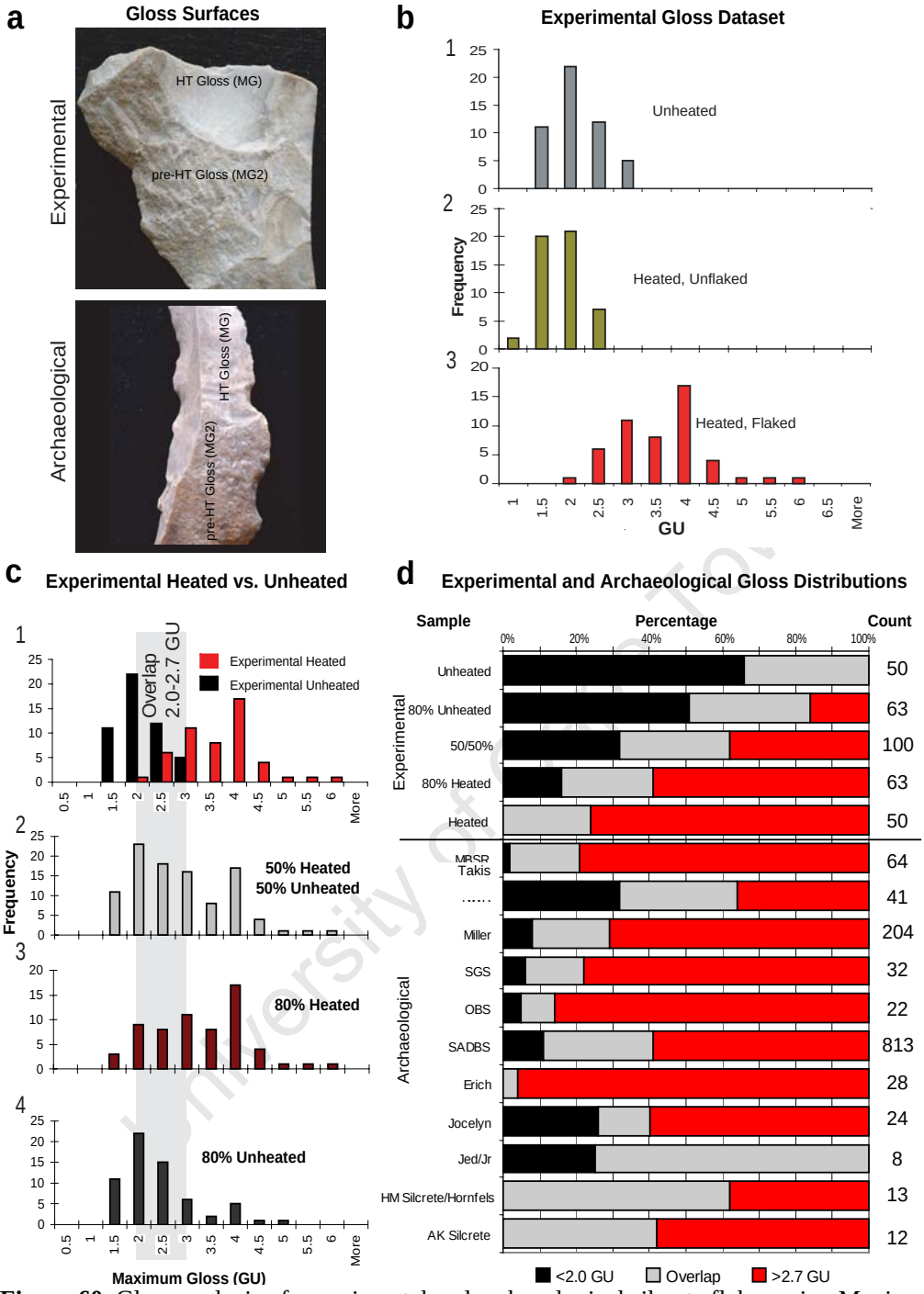

Figure 60. Gloss analysis of experimental and archaeological silcrete flakes using Maximum Gloss (GU) as the unit of measurement: a) Images of typical heat treatment gloss from an experimentally treated silcrete flake (top) and an archaeological specimen (bottom). The rougher surface represents the pre-treatment texture of the stone surface, and the smooth rippled surface represents the post-heat-treatment fracture plane; b) histograms of maximum gloss for experimental and archaeological silcrete. Experimental paired silcrete samples (n=50) are displayed in three datasets; b1) freshly flaked unheated surface; b2) experimentally heated silcrete not flaked after heat treatment; b3), experimentally heated silcrete flaked after heating; c) experimental data used to create hypothetical assemblages with varied percentages of heated versus unheated debitage; d) comparison of experimental dataset and PP5-6 analytical samples

8.6 Heat Treatment Analysis Summary

The majority of silcrete was obtained from primary sources (Chapter 6.4), and the gloss analysis shows that most silcrete was then heat-treated prior to flaking (Fig. 60d). The opposite pattern is demonstrated in Jed/JR Quartzite, which had only eight silcrete specimens suitable for gloss analysis, none of which yield MG values indicative of heat treatment. The frequency of specimens with heat-treatment gloss drops in stratigraphic samples where quartzite cobble cortex is most common. Jed/JR Quartzite, 'Jocelyn', and *NWR* show the highest frequencies of unheated silcrete specimens, i.e. with low gloss values. The *OBS* and *SGS* samples are also dominated by secondary context quartz, quartzite, and chert, but these stratigraphic samples have some of the highest frequencies of heated silcrete. This pattern emphasizes the continued investment in silcrete during the *OBS* and *SGS*, even though it was not the predominant raw material used for flaking. It is possible that restrictions on silcrete access may have led to the collection of secondary context quartz and chert as functional alternatives.

There does appear to be some correlation with silcrete heat treatment and the intensity of anthropogenic burning in the PP5-6 stratigraphic column. This evidence is the subject of a forthcoming PP5-6 publication, but it is possible to say at present that the *SADBS* and *SGS* have elevated percentages of heat treated silcrete and also some of the highest ash content in the entire PP5-6 sequence. In contrast however, the *OBS* and *DBCS* also show some of the highest percentage of heated silcrete lithics but there is little direct visual evidence for in-situ burning in these StratAggs layers. This lack of ash may be due to less favorable conditions for the preservation of ash and organics in the case of the *DBCS* StratAgg which would likely have been exposed to more leaching from groundwater in the upper layers of the sequence. The *OBS* appears to show only ephemeral occupation within the relatively rapid buildup of sand. Silcrete generally occurs in low frequency in the *LBSR* where occupations have discrete hearths but little evidence for multiple burning episodes within layers (P. Karkanas, pers comm.). It is also possible that heat treatment was occurring off-site and closer to fuel sources.

Silcrete heat treatment is most common during a time interval between approximately 75 and 60ka in which C4 vegetation is modeled to be a feature of the landscape (Bar-Matthews et al. 2010). Heat treatment peaks at the maximum distance modeled in the coastline curve (Fisher et al. 2010) (Fig. 61a,f). The implications of this patterning are discussed in Chapter 12, but some of the technological changes observed at

PP5-6 during MIS 4 can arguably be associated with landscape change and probably have less to do with harsh climates or colder temperatures.

Through mechanical testing and an experimental replication study of bifaces, it was found that south coast silcrete in raw quarried form is difficult to flake. After heat treatment, silcrete is significantly more workable, and bifaces are easier to flake with higher success rates. It is expected that similar improvements in blade production can also be demonstrated. The flaking properties of silcrete can be significantly improved through heat treatment but these improvements require an investment in preparation time and fuel acquisition. In this study, bifacial tools with dimensions similar to those found in the archaeological record could be produced in less than 15 minutes once materials had been collected and prepared. The short production time can be contrasted with perhaps a day-long round trip to collect the raw stone (unless scheduled with other activities) and fuel required for heat treatment, and then an additional 12 to 20 hours required for constructing and monitoring the heat-treatment fire. The effort required for the actual flaking of silcrete tools is probably a poor measure of how much total energy was invested in that technology (Bamforth and Bleed 1997).

The identification of heat treatment in the MSA record of the southern Cape (Brown et al. 2009) creates an additional step in the production path for silcrete tool making. The costs and benefits of silcrete heat treatment must have been an important consideration alongside the transport costs associated with bringing silcrete to the site from primary outcrops. Heat treatment is not congruent with models that portray raw material selection as a function of mobility-based procurement because the majority of silcrete at PP5-6 was not used in raw form. The collection and preparation of silcrete would have required significant advanced planning and forward investment prior to the actual flaking effort.

Heat Treatment and the Site Context Model

It has been proposed that the systematic use of silcrete on the south coast is usually accompanied by heat treatment preparation (Brown et al. 2009). Analytical samples that have high percentages of silcrete are expected to show higher frequencies of heat treatment as tracked by gloss analysis. It is also predicted that silcrete collected from cobble beaches might have been used more like the other raw materials collected from the beach, including hornfels and quartzite, which are not amenable to heat treatment. Gloss distributions from occupations where beaches are proposed to be a major source of raw materials are expected to display lower frequencies of heat-treatment gloss than those occupations where primary outcrop silcrete is the predominant raw material used.

There is a weak and insignificant positive relationship between mean maximum gloss values and distance to coastline (Kendall's Tau 0.29, p 0.32). The Jed/JR Quartzite, *ALBS* and *NWR* mean sample values deviate the most from the trendline (Fig. 62a). Similar to the raw material patterning, gloss values are too high in the *ALBS* sample for what is expected for an occupation that is still near to the coastline. The *NWR* represents an occupation that occurs during a coastal transgression and the values are lower than expected.

Mean maximum gloss values are compared against the ratio of quartzite to non-quartzite (Q/NQ) raw materials for all assemblages in Figure 62b. Gloss and Q/NQ variables were log transformed to adjust for different scales of measurement. A constant (1.0) was added to Q/NQ to avoid the calculation of an undefined logarithm of zero. Gloss values for the quartzite-rich Jed J/R Quartzite and *NWR* samples are low (Fig. 62b). The remaining assemblages all cluster with similar high values of gloss. The *OBS* is especially noteworthy because although it shows the lowest artifact counts and weight of silcrete in all of the MIS 4 samples, the *OBS* shows the highest percentage of heat-treated silcrete within that silcrete sample. The correlation between mean gloss and the ratio of Q/NQ is not significant (Kandall's Tau -0.21, p 0.458).

An important conclusion from the gloss analysis is that assemblages that have more than 10 pieces of silcrete (all but Jed/JR Quartzite) show at least a 50% heated gloss distribution (including AK Silcrete and HM Silcrete/Hornfels) and most assemblages are consistent with an 80-90% heated gloss distribution in comparison to the experimental samples (Fig. 60d). In other words, heat treatment at PP5-6 is not dependent on predictions of distance to coastline or the proportion of raw materials in an assemblage.

When silcrete artifacts are present in more than trace amounts, heat treatment occurs in at least half and usually in the majority of artifacts.

- Raw Material Preparation Expectations:

    1. Samples with high percentages of silcrete are expected to show higher frequencies of heat treatment tracked by gloss analysis.
    2. Gloss distributions from occupations where beaches are proposed to be a major source of raw materials are expected to have lower frequencies of heat-treatment gloss than those occupations where primary outcrop silcrete is the predominant raw material used.

- Analysis Results:

    1. Stratigraphic samples that have greater than 50% silcrete generally show the highest frequencies of gloss consistent with heat treatment (Fig. 60). Results are consistent with expectations but the statistical comparison is not significant because the *NWR* and Takis samples have higher than expected values (Fig. 61a).
    2. Jed/JR Quartzite, HM Silcrete/Hornfels, and the *NWR* have lower frequencies of heat-treatment gloss and higher frequencies of cobble cortex. *OBS*, *SGS*, and Takis all have less primary silcrete outcrop material than *SADBS* and *DBCS*, but most of that is heated. The gloss distributions did not match expectations for all samples that have higher percentages of cobble cortex and the correlation is not significant (Fig. 61b).

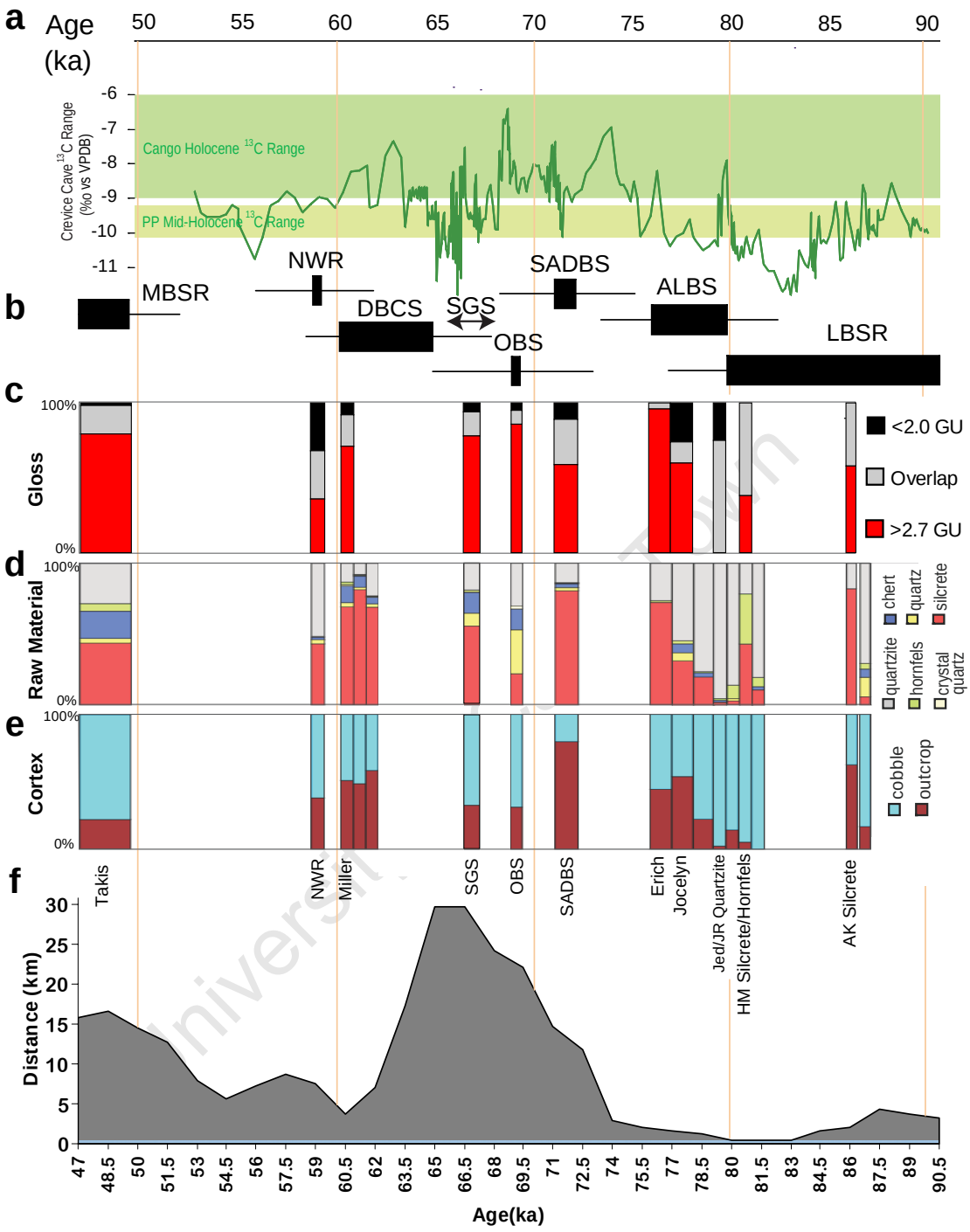

Figure 61. Gloss results compared with other PP5-6 contextual data. a) Crevice Cave $\delta^{13}C$ record from Bar-Matthews et al. 2010; b) OSL ages from Brown et al. 2010; c) heat treatment gloss analysis results by analytical sample; d) raw material; e) cortex; f) distance to the coastline from Fisher et al. 2010

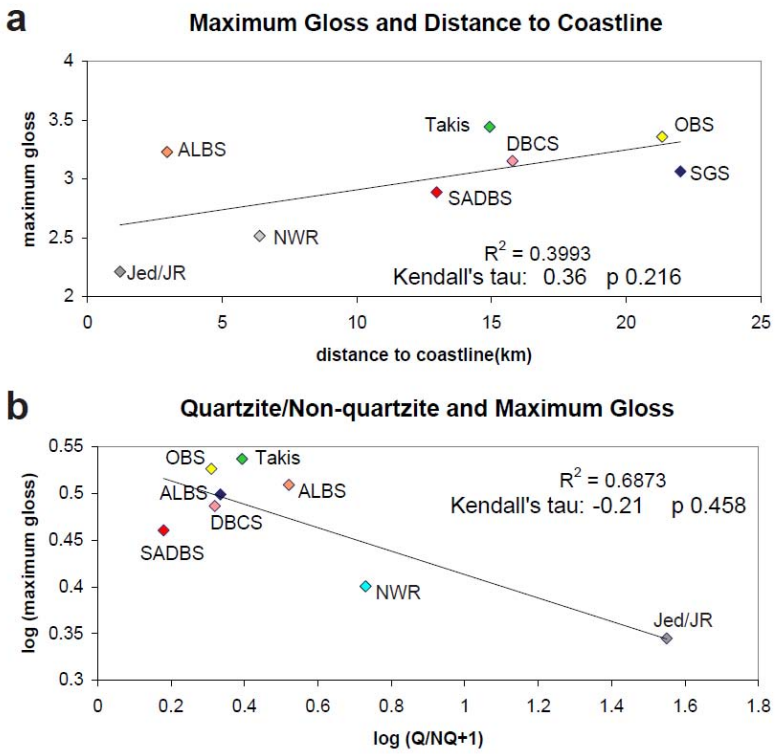

Figure 62. a) correlation of mean maximum gloss values and distance to coastline; b) mean maximum gloss values compared against the log transformed ratio of quartzite to non-quartzite (Q/NQ) raw materials.

9.0 Core Primary Form and Flake Metrics

The shift toward the use of more fine-grained raw materials at PP5-6, Klasies River, and other coastal sites is associated with the production of smaller blades (Fig. 5), especially in the HP. It has been argued that blade production in the HP is not technologically different from that of the quartzite-based blade and point assemblages that came before (Wurz 2000). The smaller blades and debitage have been attributed to differences in available nodule size across raw materials (Singer and Wymer 1982; Thackeray and Kelly 1988, Soriano et al. 2007), and not necessarily to functional requirements for smaller end products. An estimation of the original package form and size of the raw material nodules, which were selected for transport and core reduction for each sample, can help determine whether or not changes in mean debitage size can be tied primarily to raw material nodule size and will aid in the analysis of cortex to follow.

The Site Context Model predicts that weight would have been a consideration in transporting lithic raw materials to the site from inland sources. It is expected that nodules of lithic raw materials transported over longer distances will be smaller and lighter than those available in the immediate vicinity of the site. It is also anticipated that nodule size would be a limiting factor in the eventual size of the flaking products. Therefore, larger complete debitage is expected from Jed/JR where cobble sources are near to the site. Smaller debitage is expected from samples where the majority of raw materials are transported to the site from greater distances.

The estimation of original core primary form is challenging because PP5-6 cores were often reduced to the point of exhaustion (Appendix 4, Section 1) and some larger cortical by-products might not be present at the site due either to differential transport or prior reduction of tools at other locations on the landscape (Dibble et al. 2005). The majority of quartzite cores (15 of 23) retain cortex consistent with beach cobbles as the original raw material package. Leba Quartzite has one quartzite core made from a tabular primary context nodule. Two cores from the *NWR* and one core from Takis were made from larger quartzite debitage.

The majority of silcrete cores (36 of 56) are made on a primary form that represents an intermediate stage because most of these cores have been reduced to a small size. Primary form could be determined for 20 silcrete cores. Fourteen were made from large silcrete flake blanks, and half exhibit primary outcrop cortex. Two silcrete cores

from the *SADBS* and one core from *DBCS*-'Miller' were made from tabular nodules, and individual silcrete cores from *ALBS* and Takis have cobble cortex.

Complete debitage makes up a small percentage of the total analyzed lithic sample (18%). Complete flake measurements compared here include technological length, width at flake midpoint, thickness at flake midpoint, and weight for flakes with length ≥ 15mm. The analysis of flake upper quartile and maximum dimension includes all complete flakes with maximum dimension ≥15mm and thus the sample counts vary slightly. The 15mm cutoff for complete flakes in Chapters 9, 10, and 11 follows Mackay (2008a). Many of the *SADBS* bladelets and informally retouched pieces are less than 20mm in maximum length suggesting that at least some of the desired end products were very small. It is possible that the following analyses included some lithics that could be considered core preparation flakes. It is expected that MSA knappers were rational actors and would have sought to conserve raw materials in all aspects of core reduction and thus their potential inclusion would not violate the assumptions of these analyses. It is very unlikely that debitage resulting from retouch was included as these byproducts would be limited to very small backing and notching flakes that would have only been captured in the 3mm sieves (material not analyzed here).

Figure 63 provides complete flake mean length, midpoint width, midpoint thickness and weight with 95% confidence levels showing the differences between quartzite and silcrete flake attributes for each analytical sample. Sample variance is affected by low sample sizes in many of the analytical samples, particularly in the *NWR* and Takis (Table 49), but the most obvious patterning is that quartzite flake mean dimensions are always larger when compared against silcrete. Table 50 provides a statistical comparison of flake metrics for the entire PP5-6 sample of complete flakes using the Kruskal-Wallis non-parametric test for differences in sample medians. Silcrete flakes are significantly smaller than quartzite flakes in every tested variable. It is interesting that silcrete and chert flakes are not statistically different for any of the tested metric variables (Table 50). Mean quartz dimensions fall between those of silcrete and quartzite, and are significantly different for all comparisons except for silcrete flake length.

The graphs and confidence intervals presented in Figure 63 show that mean flake dimensions do not show much significant variation between analytical samples across raw material categories except for a few notable comparisons. When confidence intervals are considered, mean flake length is not significantly different between any two quartzite

samples except for the extremes of the relatively long *NWR* flakes in comparison to the much shorter *SADBS* quartzite flakes. Silcrete mean flake length is significantly shorter for *SADBS* flakes when compared between the *OBS* and *DBCS* samples.

The only significant difference observed in quartzite flake width is the reduction that occurs in the *ALBS* and *SADBS* samples between the wider flakes of the preceding Jed/JR and following *OBS* occupations. There is a similar decrease in mean flake width for the *SADBS* and *ALBS* silcrete flakes. *SADBS* silcrete flakes are significantly narrower than all other samples but those of the *ALBS*. Flake thickness and weight have statistically similar mean values across both raw material categories. *SADBS* silcrete and quartzite flakes are significantly thinner than those of Jed/JR. Jed/JR quartzite flakes are significantly heavier than quartzite flakes of the *SADBS*.

Given that there are relatively few statistically significant differences in flake metrics when examining the PP5-6 analytical samples across the two predominant raw material categories, it is informative to look at what happens when values from all raw materials are combined for each analytical sample (Figure 64). Here, mean flake measurements and mass vary consistently from sample to sample. Jed/JR Quartzite and the *SADBS* represent the two extremes of the PP5-6 debitage size variability. Jed/JR Quartzite flakes are significantly longer than those found in the *SADBS*, *SGS*, and Takis samples. Jed/JR Quartzite flakes are significantly wider and thicker than all other samples and *SADBS* flakes are significantly narrower and thinner. Jed/JR flakes are heavier than all other samples with the exception of the *NWR* (which has a very wide confidence interval), and *SADBS* flakes are thinner than all other samples except for the *SGS*.

Complete flake mean dimensions mimic the raw material percentages across the analyzed samples (Fig. 64), suggesting that mean flake size is a function of the proportion of the raw materials in each assemblage. In other words, samples rich in silcrete and chert tend to have the smallest debitage and conversely, samples that favor quartzite have larger mean debitage dimensions. In fact, the percentage of quartzite within each analytical sample is highly correlated with assemblage mean flake length (Spearman's r_s .93, p .002) as are the other dimensions analyzed here (Table 51). This association is highly significant without even considering variability in the composition of the complete flake assemblage. On the surface, this association between debitage size and raw material proportions tends to support the argument that reduction in debitage size in the HP may be explained primarily by the mobility-dependent selection of raw materials (Ambrose and Lorenz 1990).

Raw material package size may be an important factor in consideration of the debitage size differences observed between raw materials. Is flake size limited by the small size of available silcrete and chert raw material nodules as argued by Thackeray and Kelly (1988), or are small nodules deliberately selected for other benefits such as reduced weight and decrease in transportation costs? Potential differences in nodule size are investigated here by comparing the upper range of flake and core maximum dimensions for each analytical sample by predominant raw material type.

The upper quartile and maximum range for flake maximum dimension (MD) are provided in Fig. 65 for complete quartzite and silcrete flake analytical samples with counts greater than 30, and also for *SADBS* chert (n=21), *SGS* chert (n=10) and *OBS* quartz (n=14) for comparison. Core maximum length is also provided. The upper range of MD provides a minimum estimate for core size (in terms of core maximum length), which is required to produce the upper quartile flakes in each sample. This is because the core must have been larger in maximum dimension than the debitage to accommodate platform setup and preparation.

The MD values are similar among the *SADBS* quartzite (78mm), *SGS* silcrete (80mm), *DBCS* silcrete (76mm), and *NWR* quartzite (84mm) samples. The Jed/JR Quartzite and *ALBS* quartzite samples have the highest MD ranges (93 and 100mm, respectively). These quartzite samples may represent a willingness to carry larger cobbles (or possibly larger flake blanks) to the site, given that the coastline is modeled to be near PP5-6 at this time (Fisher et al. 2010). The *SADBS* MD values are small (55mm) in comparison to quartzite and the other silcrete-rich samples (*SGS* and *DBCS*). *SADBS* silcrete nodules seem to have been smaller, and this is not a function of assemblage sample size (n=461). The chert and quartz MD values are interesting because they would predict a small nodule size for quartz (44mm) and for chert (*SADBS*=28mm, *SGS*=32mm). The analysis in Chapter 6 indicates that *SGS* chert and quartz were collected as pebbles.

Nodule size appears to have played some role in determining length of complete silcrete flakes in the *SADBS* when compared with *DBCS*. The *SADBS* complete flakes are significantly shorter than those of *DBCS* (one-tailed t-test assuming unequal variances: $t(184) = 4.14$ $p < .01$). Even when silcrete flakes are compared across two silcrete rich samples, *SADBS* values are consistently and significantly smaller. In theory though, the same nodule sizes should have been available to tool makers in the *SADBS* and *DBCS* given that silcrete in both occupations came from primary sources.

The analysis of mean flake metrics demonstrates that flake length, midpoint width, thickness, and mass are all significantly larger for quartzite debitage when compared with silcrete. Chert mean dimensions are not significantly different than those of silcrete, which suggests that these materials may have been functionally equivalent. Even though there are few significant differences in flake dimensions between raw materials across the analytical samples, Jed/JR debitage is typically on the larger range of mean flake size and SADBS flakes are on the low range.

The analysis of cortex type (Fig. 33) demonstrates that in silcrete-rich layers the material originated mainly from primary outcrops. The analysis of core primary form shows that silcrete was collected as tabular nodules and flakes. It seems reasonable to assume that the same silcrete outcrops would have been available to tool makers in the *SADBS*, *SGS*, and *DBCS* occupations as previously noted. Thus a reasonable conclusion is that the size range of the hypothetical raw material nodule or package available for transport should have been the same across the silcrete-rich assemblages. Smaller nodules however, appear to have been selected during the *SADBS* occupations in comparison to those of the *SGS* and *DBCS* (Fig. 65b) and this is consistent with the relatively small size of *SADBS* complete flakes of both raw materials. Mean assemblage debitage size at PP5-6 is statistically correlated with raw material proportions. The raw material proportions at PP5-6 are not random (Ch. 6). The purpose of the Site Context Model is to determine how much influence raw material availability has on determining raw material proportions and perhaps debitage size as a consequence.

Flake Metrics and the Site Context Model

It is expected that flake and nodule weight would have been a consideration in evaluating the costs of transporting materials to the site and that materials transported over longer distances would be smaller than those available in the immediate vicinity of the site (Kuhn 1994; Morrow 1996). Smaller size should be reflected in the transported core primary form and thus in the eventual products of core reduction (Nelson 1991). Flake size was compared against distance to coastline using mean weight (Fig. 66) for complete flakes of at least 15mm in length. The fitted line shows a general trend of decreasing flake weight with increasing distance to coastline although the correlation is not significant using Kendall's Tau, a non-parametric test of correlation (Kendall's Tau -0.14, p 0.621). The same test was performed using flake length with similar results

(Kendall's Tau -0.35, p 0.216). It can be concluded that there is no significant relationship between distance to coastline and flake size.

Summary of Findings

- Debitage Metrics Expectations: Flakes made from raw materials transported over longer distances are expected to be smaller and lighter than those made in assemblages where raw materials were available in the immediate vicinity of the site.

  Analysis Results: Flake metrics are correlated with the proportions of predominant raw material types in each assemblage. The Jed/JR Quartzite sample is modeled to be closest to the coastline and has the largest mean and maximum dimensions for complete debitage but also has the highest percentages of quartzite. The smallest mean and maximum dimensions are from the SADBS which has the lowest percentage of quartzite and highest percentage of silcrete in the complete flake assemblage. Flake weight and mass do not correlate with distance to coastline. Post-hoc analysis failed to find any combination of samples that provided significance to support the expectations of the Site Context Model.

Table 49. Count of complete flakes (≥15mm length) by analytical sample and raw material

Sample	Quartzite	Silcrete	Chert	Quartz	Hornfels	Crystal Quartz	Other	Total
Takis	10	21	9	2	3			45
NWR	26	24	1	1				52
DBCS	32	92	21	2	3	1		151
SGS	14	37	8	6	2		1	68
OBS	42	22	8	10		1	1	84
SADBS	81	409	18	6	1	1		516
ALBS	47	22	4	2			1	76
Jed/JR	210	6	2		2			220
Total	462	633	71	29	11	3	3	1212

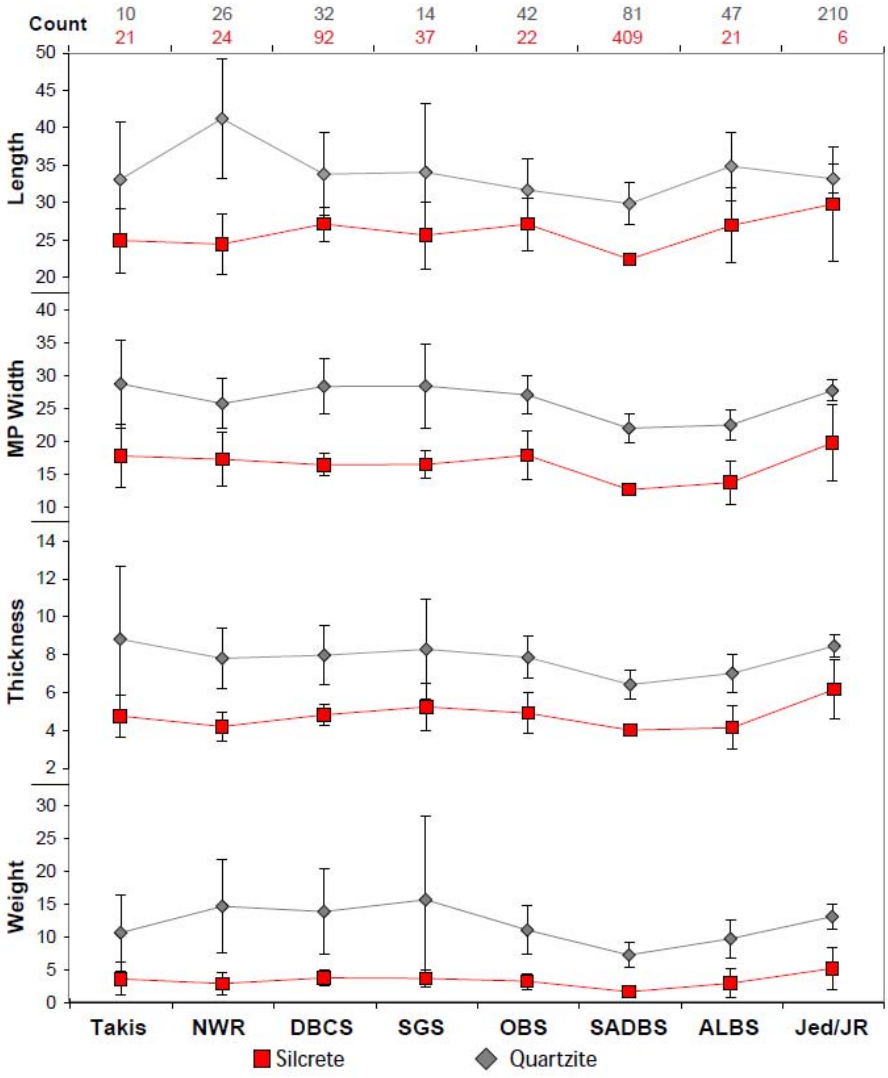

Figure 63. Complete flake (≥15mm) mean length, width, thickness and weight (with 95% CL) showing difference in attributes by quartzite and silcrete

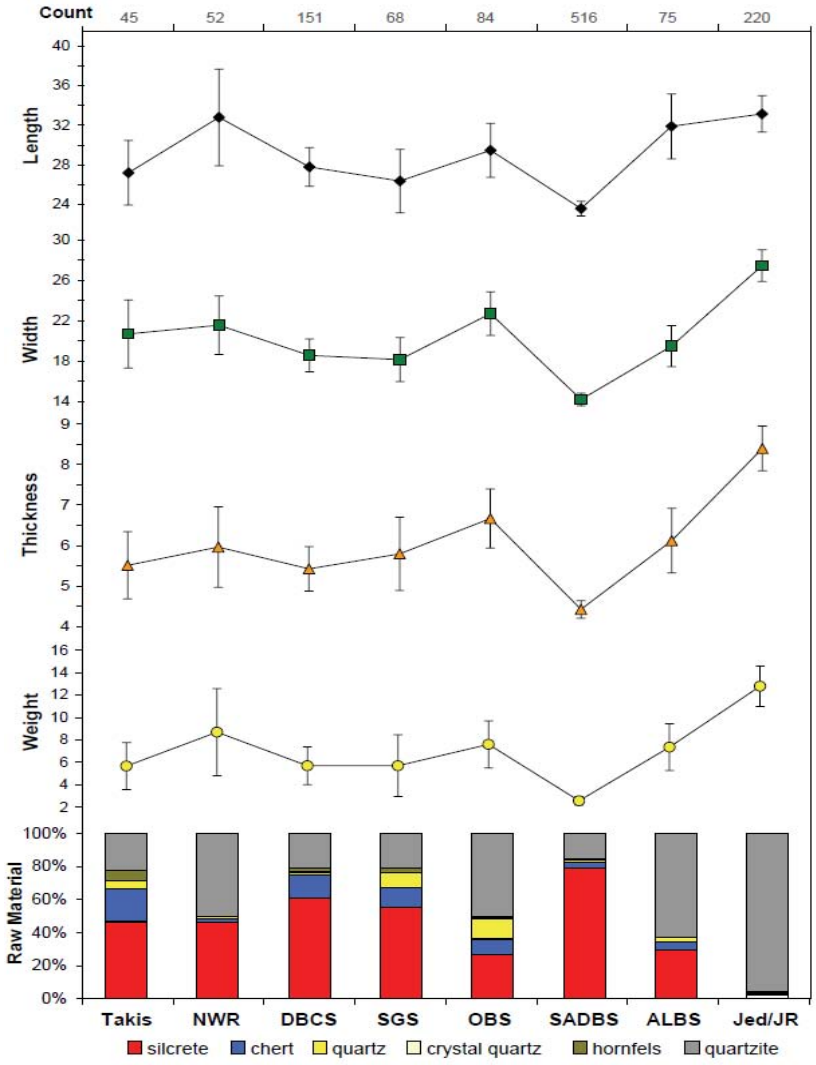

Figure 64. Complete flake (≥15mm) mean length, width, thickness and weight (with 95% CL) displayed with raw material percentage for PP5-6 analytical samples with counts greater than 30 specimens

Table 50. Kruskal-Wallis test results for comparison of PP5-6 complete flake dimensions for quartzite, silcrete, chert, and quartz. P-values in italics are Bonforroni corrected and those in blue identify sample comparisons that are not significantly different

Length	Quartzite	Silcrete	Chert	Quartz
Quartzite		p <.001	p <.001	p <.001
Silcrete	*p <.001*		0.5407	0.8189
Chert	*p <.001*	*1*		0.8853
Quartz	*p <.001*	*1*	*1*	
H_c 161.3 p <.001				

Width	Quartzite	Silcrete	Chert	Quartz
Quartzite		p <.001	p <.001	p <.001
Silcrete	*p <.001*		0.2088	0.0018
Chert	*p <.001*	*1*		p <.001
Quartz	*p <.001*	*0.01094*	*0.00568*	
H_c 445.4 p <.001				

Thickness	Quartzite	Silcrete	Chert	Quartz
Quartzite		p <.001	p <.001	0.0917
Silcrete	*p <.001*		0.7194	p <.001
Chert	*p <.001*	*1*		p <.001
Quartz	*0.5499*	*p <.001*	*0.00136*	
H_c 315.2 p <.001				

Weight	Quartzite	Silcrete	Chert	Quartz
Quartzite		p <.001	p <.001	p <.001
Silcrete	*p <.001*		0.517	p <.001
Chert	*p <.001*	*1*		p <.001
Quartz	*p <.001*	*0.0012*	*0.0032*	
H_c 438.5 p <.001				

Table 51. Results of Spearman's correlation between the percentage of quartzite and complete flake dimensions for each analytical sample.

Quartzite % and:	*rs*	*p*
Length	0.9341	0.002
MP Width	0.8503	0.011
MP Thickness	0.8862	0.006
Weight	0.8264	0.016

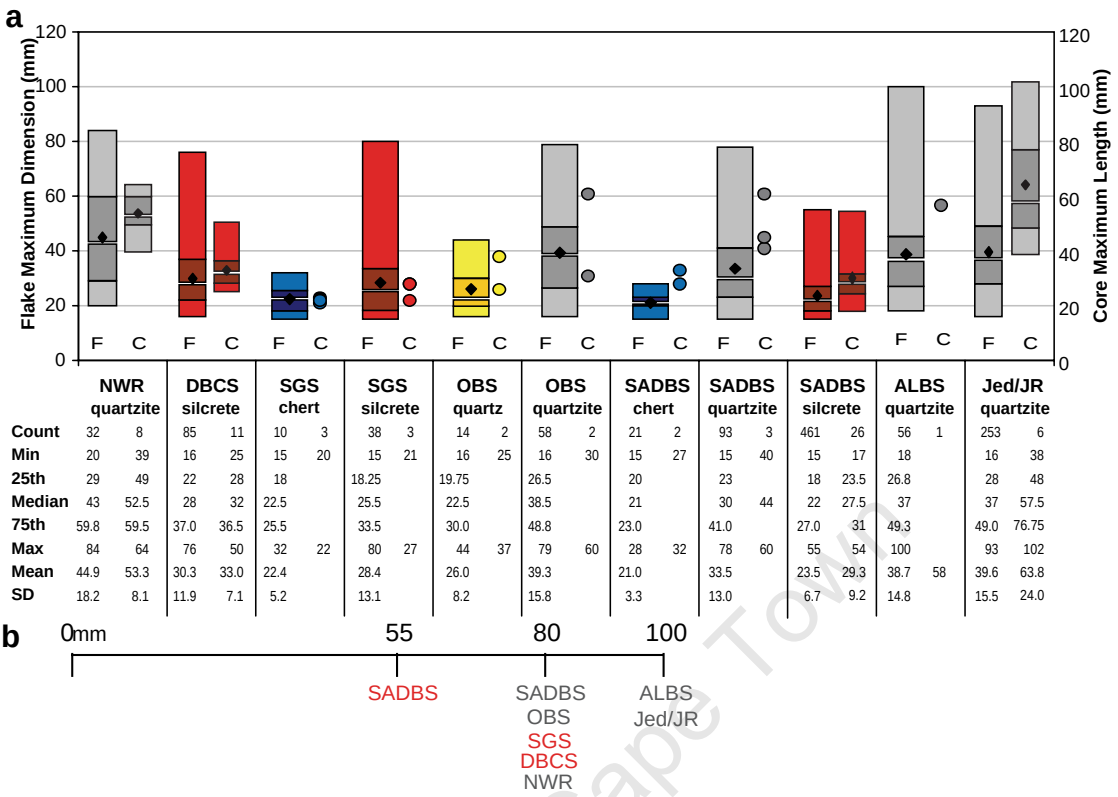

Figure 65. a) Box plots of complete flake maximum dimension (F) and core maximum length (C) for stratigraphic samples, with silcrete (red) and quartzite (grey) count more than 30 pieces. *OBS* quartz (yellow) and *SGS* chert (blue) have lower counts, but are provided for comparison. Individual core values are plotted for analytical samples with three or fewer total cores; b) scale bar showing actual size differences between materials and samples. An expanded version of this figure with additional analytical samples and raw materials may be found in Appendix 1, Figure 7.

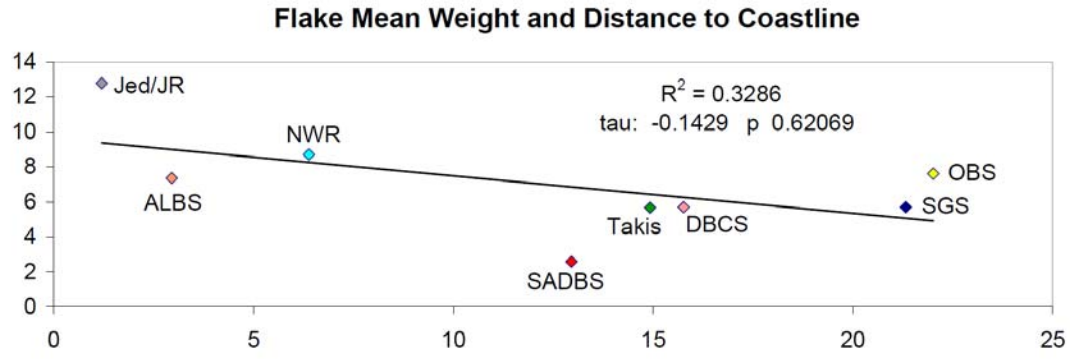

Figure 66. Plot of distance to coastline and mean flake weight for PP5-6 analytical samples. The fitted trendline shows the expected reduction in flake weigh with increased distance to coastline but the association is not significant using Kendall's Tau, a non-parametric test of correlation.

10.0 Cortex Abundance

Cortex abundance has often been used to model which stages of the core reduction process are represented for a given assemblage (Magne and Pokotylo 1981; Ahler 1989; Shott 1994; Marwick 2008). A problem in making behavioral inferences from the amount of cortical materials present in an assemblage is that it can be difficult to assess: a) how much cortical material should be represented, b) the original nodule size and morphology, and c) how many nodules were reduced on site (Dibble et al. 2005). The method for quantifying and comparing cortex abundance for this study is an archaeological application of an experimental approach developed by Dibble et al. (2005) and further refined by Lin et al. (2010).

Dibble et al. (2005) used surface area, volume, and weight measurements for 33 experimental cores of varying morphologies to test how well surface area formulas for a variety of geometric solids predicted the actual core surface area. They used this data to estimate the amount of cortical surface area that should be present for the experimental core reduction. The goodness of fit between the actual and predicted cortical surface area of an assemblage was assessed by Dibble et al. (2005) using an index called the Cortex Ratio. The Cortex Ratio is the total observed cortical surface area divided by the predicted or expected cortical surface area. Assemblages that retain all of their original cortical elements should have a Cortex Ratio value close to 1.0.

Dibble et al. (2005) demonstrated that the Cortex Ratio is not affected by the intensity of reduction because any given nodule will have a finite amount of cortical surface. They suggest that the Cortex Ratio can be a robust method for quantifying cortex abundance in experimental assemblages, even when the input variables are estimated. Dibble et al (2005) note that an over-estimation of original nodule size by 30% increases the Cortex Ratio by less than 10%. Underestimating nodule size by 30% reduces the Cortex Ratio by over 10%, thus it is better to overestimate original nodule size. The Cortex Ratio is affected by more than 10% when the estimated number of cores is approximately 30% above or below the actual number

Dibble et al. (2005) observed that the surface area formula for a sphere yielded the best overall results for estimating cortical surface area for a variety of core morphologies when the original nodule configuration was unknown. They cautioned however, that the application of the surface area formula for a sphere on flatter geometric

solids (including tabular blocks and flakes) yielded the most imprecise Cortex Ratio values. The surface area of flatter solids tends to increase at a faster rate than core volume when compared with cubes, spheres and cylinders. Therefore, core surface formulas more appropriate for tabular nodules and flakes should be applied to assemblages (such as at PP5-6) where flatter nodules were used for core reduction.

The Cortex Ratio will be used in this chapter to quantify cortical surface area for comparison across the PP5-6 sequence. Analytical samples are subdivided by predominant raw material type because the calculation of expected values requires different formulas for each raw material. Only analytical samples with more than 200grams of total lithic mass are evaluated for the analysis of cortex abundance, although data for other samples is provided in Tables 52 and 54.

It is expected that lithics from the PP5-6 stratigraphic samples where the coastline is modeled to provide abundant local raw materials will have higher Cortex Ratios than samples where raw materials are expected to have been transported to site from greater distances. This is essentially a distance-decay argument (Renfrew 1969; Blumenschine et al. 2008 for a recent review) based on the assumption that tool makers would have been more likely to have carried the entire cobble to the site for core reduction when raw material sources were close to site. Weight was probably a consideration for materials that were carried over greater distances (Kuhn 1994) and in these cases it is expected that more cortex would have been removed at the quarry or collection source. The removal of cortical materials off-site should be reflected in the archaeological assemblage by lower Cortex Ratio values.

Calculation of the Cortex Ratio requires the estimation of a series of variables including; total cortical surface area and mass from the archaeological samples, original core nodule shape, original core nodule size, and the number of reduced nodules (Dibble et al. 2005). It is acknowledged that each successive calculation presented for this analysis produced a sometimes unknown amount of cumulative error. Additional experimental research is required to establish a true margin of error for the results. Cortical surface area was estimated on cortical debitage (whole or fragmentary) during lithic analysis as a percentage category (1%-20%, 21%-40%, 41%-60%, 61%-80%, 81%-99%, and 100%). No debitage size cutoff was imposed for tabulating cortical surface area (as opposed to the 2cm cutoff of Dibble at al.) because the analysis was not dependent on completeness and it was important to try and capture as much of the original core primary form surface area as possible. Cortex coverage was obviously limited to the dorsal and

platform surfaces. Debitage cortical surface area was then quantified for each complete and fragmentary cortical artifact by taking the mid-range of the cortex percentage category coded during analysis (10%, or .10 for the 1%-20% category) and multiplying by an estimate of flake surface area. Surface area was calculated by multiplying technological length by midpoint width for complete specimens and multiplying maximum length by maximum width for fragments. Cortical surface area on flake platforms was estimated by multiplying platform width by platform thickness.

Cortical surface area on cores was recorded during lithics analysis as a percentage of the entire core surface. The PP5-6 cores tend to be relatively small, biconvex, and have cortex concentrated on a single face (Appendix 4, Section 1). To quantify cortex area from the estimated percentage, a formula was derived that treats each core as a composite of two domes placed base-to-base (Fig. 67).

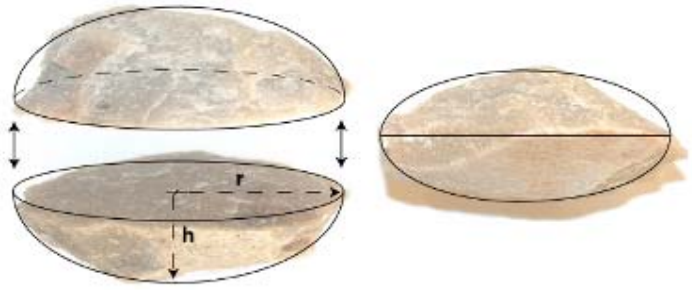

Figure 67. Inverted and stacked domes used to estimate discoid core surface area

The surface area for a dome is 2(πrh) square units. When the formula is applied to cores, radius (r) represents the mean of core maximum length and width (gives diameter) divided by two (to get the radius). Height (h) represents half of core maximum thickness. Then the output of the formula is doubled to generate the surface area for both dome halves to simulate the entire core. The tabulated cortical surface area for debitage and cores were then summed for each stratigraphic sample by raw material (Table 52).

Core nodule shape was estimated by analyzing cores for evidence of primary form as discussed in Chapter 9. PP5-6 silcrete cores appear to have been made most commonly from cortical flakes and more rarely from tabular nodules, whereas quartzite cores were usually made from beach cobbles. Therefore, in order to estimate expected cortical surface area from assemblage mass, it is necessary to arrive at different formulas to approximate the shape and size of the solids used for silcrete and quartzite core reduction for each sample in the PP5-6 sequence.

Quartzite cobbles are typically sub-spherical or ellipsoid in shape. Graham et al. (1988) provide a modified spheroid formula which is used in this analysis for estimating the surface area of water-rounded cobbles based on length (L), width (W), and height (H) measurements; surface area = 1.15(LW+LH+WH). They report a mean percentage error of approximately 4% for this method of estimation.

Table 52. Cortical surface area for each PP5-6 analytical sample

Sample	Location	Raw Material						Total
		quartzite	silcrete	quartz	hornfels	chert	other	
Takis	Dorsal	25.3	10.2	1.5	0.1	20.2		57.4
	Platform	46.3	2.3		2.7			51.2
	Core		0.5			0.3		0.8
	Total	*71.6*	*13.0*	*1.5*	*2.8*	*20.5*		*109.4*
NWR	Dorsal	97.5	15.4	1.7				114.6
	Platform	6.5	2.6					9.1
	Core	4.5	0.7					5.2
	Total	*108.5*	*18.7*	*1.7*				*128.9*
DBCS	Dorsal	160.6	108.368	3.5	5.438	11.645	1.583	291.134
	Platform	65.1	4.91		4.07	4.51		78.59
	Core	1.945	1.336			0.227		3.508
	Total	*227.645*	*114.614*	*3.5*	*9.508*	*16.382*	*1.583*	*373.232*
SGS	Dorsal	65.7	62.2	9.0	2.7	13.2	2.1	154.7
	Platform	46.3	3.3	0.3				49.9
	Core	1.3	0.6			0.1		2.0
	Total	*113.2*	*66.1*	*9.3*	*2.7*	*13.3*	*2.1*	*206.7*
OBS	Dorsal	67.8	31.5	6.9	1.8	8.2	1.8	118.0
	Platform	39.2	1.2			0.5		40.8
	Core	0.1	0.2	0.6		0.1		1.0
	Total	*107.1*	*32.9*	*7.5*	*1.8*	*8.8*	*1.8*	*159.8*
SADBS	Dorsal	136.4	532.1	3.7	10.9	15.3		698.4
	Platform	30.7	35.8		1.4	1.4		69.3
	Core	0.9	2.7	0.1		0.1		3.9
	Total	*168.0*	*570.7*	*3.8*	*12.3*	*16.9*		*771.6*
ALBS	Dorsal	86.4	36.8	13.7		1.9	1.3	140.0
	Platform	39.7	0.2		1.5		0.7	42.1
	Core	0.6	1.0	0.2	0.5	0.2		2.6
	Total	*126.7*	*38.0*	*13.8*	*2.0*	*2.1*	*2.0*	*184.6*
Jed/Jr	Dorsal	954.8	5.3		20.1	6.9		987.1
	Platform	86.1			7.1	1.0		94.2
	Core	6.4				0.1		6.5
	Total	*1047.3*	*5.3*		*27.2*	*8.0*		*1087.8*
Ludumo Quartzite	Dorsal	26.6			4.0			30.6
	Platform	0.7						0.7
	Total	*27.2*			*4.0*			*31.2*
HM Silcrete/Hornfels	Dorsal	3.1	17.6		16.0			36.8
	Platform	3.4			5.6			9.0
	Core		0.2		0.0			0.2
	Total	*6.5*	*17.8*		*21.6*			*45.9*
Lwando Quartzite	Dorsal	18.2	11.0		2.1	1.1		32.5
	Platform	4.4			6.9			11.2
	Core	0.3						0.3
	Total	*22.9*	*11.0*		*9.0*	*1.1*		*44.0*
AK Silcrete	Dorsal	10.2	12.9					23.1
	Platform		0.2					0.2
	Core		0.1					0.1
	Total	*10.2*	*13.2*					*23.4*
Leba Quartzite	Dorsal	19.9	0.6	1.7				22.1
	Core	0.8						0.8
	Total	*20.6*	*0.6*	*1.7*				*22.9*
Total	**cm^2**	**2057.4**	**901.8**	**42.9**	**92.9**	**87.1**	**7.4**	**3189.5**

Most of the PP5-6 silcrete cores are small and were intensively exploited making it difficult to identify the original nodule configuration for each stratigraphic sample. Primary form was identified for 20 of 56 total silcrete cores from PP5-6 and only 5 of 27 cores from the *SADBS*. Flake blanks (n=14) and tabular nodules (n=3) were the most common identified forms in the total silcrete core sample (Ch. 9). Flake blank surface area was estimated by multiplying technological length by midpoint width as was performed on archaeological specimens.

Here, 'tabular' refers to silcrete nodules that are relatively flat and retain some cortex on both planar surfaces. Cortex on both sides distinguishes these from flake blanks which usually show some portion of the original bulb and can only have cortex on the remnant dorsal surface. Tabular silcrete nodules found by this author in modern contexts are irregular planar pieces that result from spalling of exposed boulders or weathered outcrops, or form pedogenically as flat globular pieces with rounded edges. There are three silcrete core specimens that were made from tabular silcrete but only one of these was abandoned prior to intensive flaking (*SADBS*-'Gert' Find No. 132445). This specimen has cortex on both faces but not on its sides where it appears to have been fragmented from a larger plate (Fig. 68). Assuming this specimen is representative of other flat silcrete nodules used at PP5-6, tabular surface area was estimated by summing the area of each planar side; surface area= 2(LW). In other assemblages, where tabular blocks have a regular rectangular prism shape and cortex on the perpendicular sides, the surface area formula may include up to six sides (Dibble et al. 2005).

Figure 68. Find No. 132445: Minimally flaked tabular silcrete nodule from SADBS-'Gert'. Photo grid is in 1cm increments

Modeling original nodule size for estimates of mean original nodule mass and surface area was accomplished using a comparative sample of representative core blanks (cobbles, tabular nodules and flakes) coupled with estimates of the maximum flake and core width for each analytical assemblage (Ch. 9, Fig. 65). A sample of 93 South African and North American quartzite, chert, and basalt beach cobbles were then collected, weighed, and measured. Surface area was calculated for each cobble using the Graham et al. (1988) formula given above. An attempt was made to collect a wide range of cobble sizes so that there would be a comparative sample appropriate for the projected size range of each stratigraphic sample.

Modeling silcrete nodule size and cortical surface area required a comparative sample of tabular nodules and flake blanks. The sample of tabular nodules includes the cut silcrete blanks used in the experimental biface heat treatment study (Ch. 8.3 and Appendix 1, Table 4) and an additional sample of 98 tabular Cretaceous (Great Complex) sandstone nodules (Graymer et al. 2002) collected from Crockett, California to provide a wide range of sizes (Fig. 69). The comparative sample of flake blanks included flakes used in the silcrete biface experiments and flake blanks knapped from northern California obsidian (Fig. 70). For the purposes of this analysis the cortical surface area was estimated as if each flake dorsal surface was entirely cortical.

It is important to note that the comparative samples were only used for providing reasonable estimates of weight and surface area for each core primary form shape and to sample some of the variability of these forms as they occur in nature. It is assumed here that the stone materials in the comparative samples have similar densities and are acceptable for use in estimating volume or mass. This assumption could be tested by the future collection and comparison of additional South African materials which were not available at the time of this analysis.

A scatterplot of weight and cortical surface area of the comparative nodules confirms the need for developing individual mean surface area and mass estimates for each primary form (Fig. 71). The plots show that the surface area of cobbles and tabular nodules increases more steeply than flake blanks which makes sense given that flake blanks have one predominant cortical surface (and sometimes a platform) but tabular nodules have two planar surfaces.

Figure 69. Sandstone nodules used to supplement the tabular blank comparative sample for estimating average mass and surface area

Figure 70. Obsidian (left) and silcrete (right) flake blanks used for estimating surface area and mass of flake blanks

One potential source of variation introduced into this model is the difficulty in estimating the original ratio of cortical surface area to mass for flake blanks versus tabular nodules. The proportions of these primary forms, which have different formulas and expected values (Fig. 71) have important implications for the interpretation of the results of this analysis. For this reason, separate calculations were made for flake blanks and tabular nodules in the silcrete samples in order to contrast the results. The final estimates of expected cortical surface area for evaluation of the Site Context Model are a weighted

average based on the actual percentage of silcrete flake blanks versus tabular nodules (3:1) in the analyzed PP5-6 silcrete assemblage.

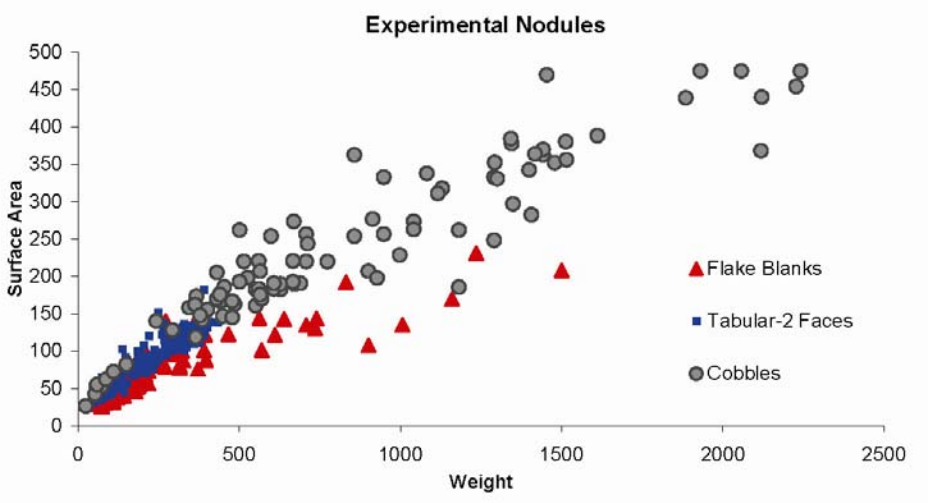

Figure 71. Scatterplot of weight(g) and cortical surface area(cm^2) for comparative tabular nodules (blue squares), beach cobbles (grey circles) and flake blanks (red triangles).

The calculation of expected cortical surface area requires mean estimates of original nodule surface area and weight. The estimation of original nodule size is problematic because there are few tested nodules that were abandoned on site and large cortical overshot flakes are rare at PP5-6. Original nodule size was estimated here by taking the maximum flake or core dimensions (whichever was larger) from each PP5-6 stratigraphic sample (Fig. 65, Ch. 9) as a starting reference (Table 53a). The idea was to develop an expectation of a nodule size that could account for the artifact maximum length observed in each sample. Width and thickness for most of the original nodules is unknown but it is assumed that the comparative samples capture some of the natural variability of these blanks. The original nodule size range for each sample was estimated by adding an additional 20% to the maximum flake or core length of each archaeological sample (Table 53a). The added length allows for some removal of the original nodule for platform preparation. The minimum original nodule length was estimated by subtracting 10%. Some of the original nodules were almost certainly smaller however, as Dibble et al. (2005) note, more accurate predictions of Cortex Ratio are achieved using an overestimate size when the original nodule size is unknown.

The minimum and maximum estimates of original nodule length were then used to select subsets of the comparative samples. The weight and surface area of each selected comparative nodule subsample were then averaged (values and sample counts are

presented in Table 53b). The observed total weight of each archaeological sample (Table 54) was divided by the mean nodule weight to provide an estimate of the number of nodules that were originally reduced (Table 53c). The estimated number of nodules was then multiplied by the estimated mean nodule surface area to arrive at the expected total cortical surface area for each archaeological sample (Table 53d). The observed cortical surface area for each archaeological sample was then divided by the expected cortical surface area to obtain the Cortex Ratio for each sample (Table 53f). Cortex Ratio values above 1.0 indicate more cortex than expected, and conversely values below 1.0 are suggestive of less overall cortex than expected.

Each silcrete sample has three expected cortical surface area estimates based on calculations made from; 1) only using the comparative flake blank sample; or 2) calculations based purely on the tabular blank formula; and 3) a weighted average that incorporates both formulas. A total of 12 out of 28 silcrete cores can be assigned to either flake (n=9) or tabular nodule (n=3) in a ratio of 3:1 respectively. The expected cortical surface area values for the flake/tabular sample was calculated in the same manner as the other stratigraphic samples except the estimated nodule mass and surface area were adjusted to average the mean values of three flake blanks and one tabular nodule for each analytical sample (Table 53d).

The observed and expected cortical surface area values are presented in Table 53 and Figure 72, which gives the silcrete values for the averaged flake/tabular nodule estimated surface area. Most of the analytical samples are at or below a Cortex Ratio of 1.0 including all of the quartzite assemblages. The only sample to exceed the Cortex Ratio is the *SADBS* silcrete sample calculated using the flake blank/tabular estimate (Cortex Ratio=1.1).

The expectation of the Site Context Model was that stratigraphic samples from coastal occupations where quartzite cobbles were available nearby should have higher Cortex Ratios than non-coastal occupations where raw materials of all types were transported to site. It was expected that some cortical reduction would occur elsewhere to reduce the weight of the transported nodule. The Jed/JR Quartzite sample is the largest in terms of mass and may be the only analyzed occupation less than 2km from the coastline. Jed/JR Quartzite has a Cortex Ratio of 0.88 and represents the sample by which all others may be compared for the purposes of evaluating the expectations of the Site Context Model. Figure 73 shows Cortex Ratio plotted against distance to coastline. The *ALBS* quartzite, *NWR* quartzite, and *DBCS* silcrete all have lower Cortex Ratio values than

Jed/JR quartzite and fit the expectation of the Site Context Model as all are modeled to be occupations where coastline is regressing.

Contra to the predictions of the Site Context Model, the three highest Cortex Ratio values are from samples that are modeled to occur at maximum distance from coastline (*OBS* quartzite, *SGS* silcrete, and *SADBS* silcrete) with values around 1.0 indicating that cortical materials are abundant and are close to what would be expected if most of the flake blank was reduced on-site at PP5-6. The results of the analysis of cortex abundance as a whole do not support the predictions of the Site Context Model. The correlation between Cortex Ratio values and distance to coastline is not significant for the entire analyzed assemblage using a non-parametric test of correlation (Kendall's Tau 0.32, p 0.26) or compared by raw material samples (quartzite samples and distance to coastline: Kendall's Tau 0.20, p 0.62; silcrete samples and distance to coastline: Kendall's Tau -0.33, p 0.60)(Fig. 73).

Table 53. Estimated variables used for calculating the Cortex Ratio by analytical sample

Calculation		NWR Quartzite	DBCS Silcrete	SGS Silcrete	OBS Quartzite	SADBS Quartzite	SADBS Silcrete	ALBS Quartzite	Jed/JR Quartzite
a	**Nodule Size Estimate**								
	Nodule Min (Flake/Core Max-10%)	75.6	68.4	72	71.1	70.2	49.5	90	91.8
	Flake Max	84	76	80	79	78	55	100	102
	Nodule Max (Flake/Core Max+20%)	100.8	91.2	96	94.8	93.6	66	120	122.4
b	**Experimental Nodule Mean Values**								
	Cobble Mass	442.8			392.8	392.8		683.1	707.3
	Tabular Nodule Mass		202.9	226.6			100.1		
	Flake Mass		152.0	155.2			86.6		
	Flake/Tabular Mass*		164.7	173.0			90.0		
	Cobble Surface Area	167.0			154.0	154.0		220.4	221.8
	Tabular Nodule Surface Area		86.76	93.2			54.6		
	Flake Surface Area		51.3	52.2			31.9		
	Flake/Tabular Surface Area*		60.2	62.5			37.7		
	Cobble Count	21			15	15		42	45
	Tabular Nodule Count		60	64			37		
	Flake Count		40	37			9		
c	**Expected Number of Reduced Nodules**								
	Cobbles	1.9			0.6	1.3		0.9	5.4
	Tabular Nodules		2.8	0.8			12.6		
	Flakes		3.8	1.2			14.6		
	Flakes/Tabular Nodule*		3.5	1.1			14.0		
	Actual Number of Cores	3	14	1	1	5	27		6
d	**Expected Cortical Surface Area**								
	Cobbles	313.4			98.5	193.4		187.4	1187.3
	Tabular Nodules		244.1	76.7			689.0		
	Flakes		192.7	62.7			465.1		
	Flakes/Tabular Nodule*		208.6	67.3			528.9		
e	**Observed Sample Values**								
	Total Mass	830.7	570.7	186.4	251.2	493.3	1262.7	580.9	3785.5
	Total Cortical Surface Area	108.5	114.6	66.1	107.1	168.0	570.7	126.7	1047.3
f	**Cortex Ratio**								
	Cobbles	**0.3**			**1.1**	**0.9**		**0.7**	**0.9**
	Tabular Nodules		**0.5**	**0.9**			**0.8**		
	Flakes		**0.6**	**1.1**			**1.2**		
	Flakes/Tabular Nodule*		**0.5**	**1.0**			**1.1**		

Table 54. Total mass (in grams) of cores and debitage by analytical sample and raw material

Sample	quartzite	silcrete	quartz	hornfels	chert	crystal quartz	other	Total
Takis	121.6	130.4	4.4	5.3	52.6			314.3
NWR	830.7	124	0.6					955.3
DBCS	793.9	570.71	2.9	21.9	65.1	0.2	2	1456.71
SGS	342.9	186.4	11	5.4	33		7.5	586.2
OBS	251.2	102.4	75.9	3.7	28.7	4.8	5.8	472.5
SADBS	493.25	1262.7	17.9	38.6	45.2	4.9		1862.55
ALBS	580.9	381	36.2	51	30.7		1.2	1081
Jed/Jr Quartzite	3785.5	18.5		68.9	55.9			3928.8
Ludumo Quartzite	52.7			2.1				54.8
HM Silcrete/Hornfels	34.3	66.1		102.3				202.7
Lwando Quartzite	133.5	13.8		3.8	9.7			160.8
AK Silcrete	31	43.4						74.4
Leba Quartzite	124.9	2.4	2.7					130
Total	**7576.35**	**2901.81**	**151.6**	**303**	**320.9**	**9.9**	**16.5**	**11280.06**

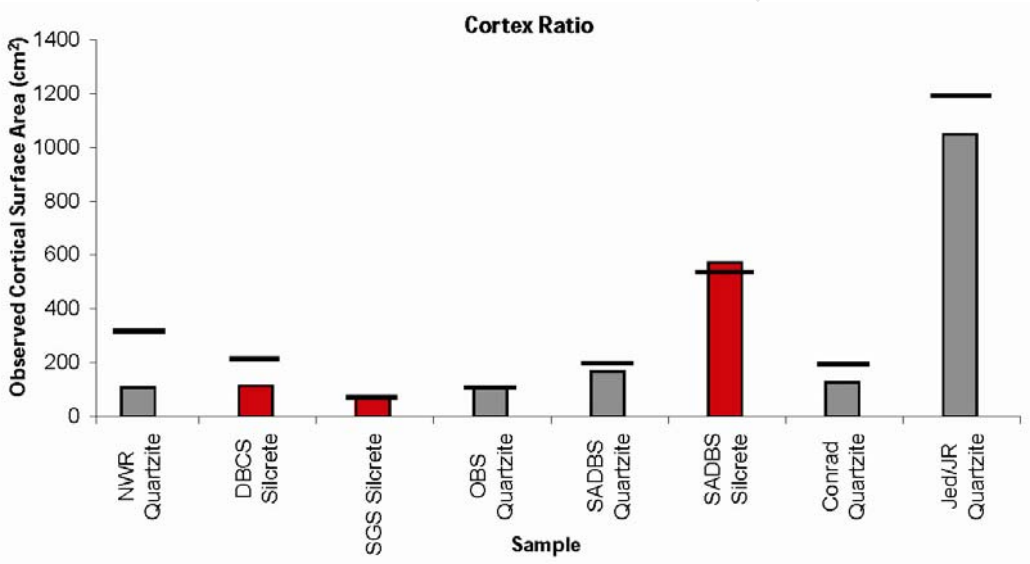

Figure 72. Cortex Ratio for PP5-6 analytical samples in stratigraphic order subdivided by quartzite (grey) and silcrete (red) raw materials. Vertical bars show observed cortex surface area (cm^2). Solid horizontal lines show the estimated cortical surface area based on cobbles (quartzite) or flake/tabular blanks (silcrete)

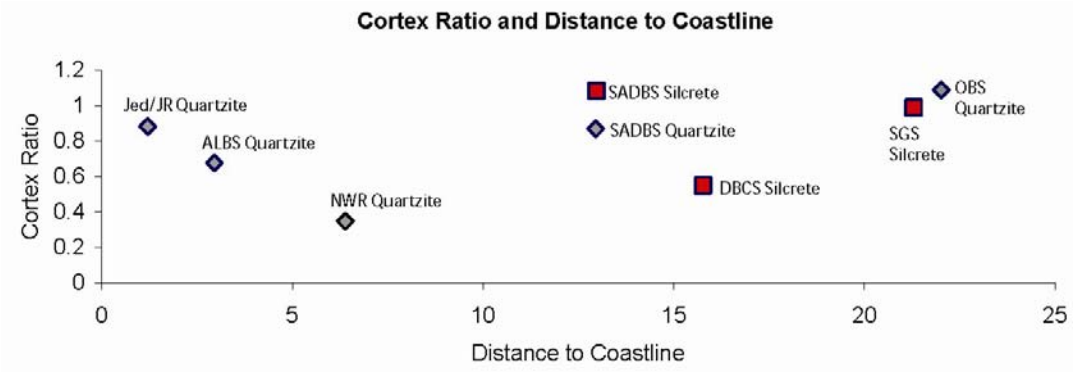

Figure 73. Plot of Distance to coastline and Cortex Ratio for PP5-6 analytical samples.

Dibble et al. (2005) caution that their methodology is most applicable to assemblages with primary core morphologies that can be estimated using a single formula for all samples. The PP5-6 results support this limitation on the Cortex Ratio and show that there are important methodological implications for studying assemblages where flake blanks were used alongside other nodule morphologies for core reduction. The quantification of cortical abundance in archaeological assemblages where variability in shape and the proportion of primary forms used for each stratigraphic sample is unknown may be uninformative beyond a simple presence/absence approach. The estimates of cortical surface area for silcrete nodules have been shown to vary according to which model is used, particularly in the *SADBS* silcrete sample where values range from 0.8 for estimates based on flakes to 1.2 for estimates based on tabular nodules. These results would be improved by developing better methods for identifying the original nodule morphology during analysis of cores so that more accurate predictions of the proportion of flake blanks to tabular nodules can be considered in the Cortex Ratio calculations. This approach would work very well on southern African assemblages where the majority of all raw materials derive from water-rounded cobbles.

Dibble et al. (2005) also caution that the expected surface area to volume ratio may increase if more than one core is made from each nodule. This may be an explanation for the differences in predicted versus observed core counts for the SADBS and DBCS silcrete samples and the relatively high values of the SADBS Silcrete Cortex Ratio. It is not known whether the discrepancies in number of predicted nodules versus the actual core count (Table 53c) is a reflection of an inaccurate estimate of core size or bias by the small horizontal areas excavated at PP5-6.

Jed/JR Quartzite is the only quartzite-rich assemblage with enough total mass to account for more than two cores. In fact, the expected number of reduced nodules (5.4) is very close to the actual number of cores (n=6). All other quartzite samples may be representative of a small number of core reductions. A minimum analytical nodule (MAN) analysis (Larson and Kornfeld 1997) of the PP5-6 samples would make an interesting comparison to the estimated number of nodules identified in this analysis of cortical abundance (Dibble et al. 2005; Douglass et al. 2008). The scarcity of cores from some samples and the difficulty in assessing the relative contribution of flakes and tabular nodules precluded the possibility of attempting to model expected cortex using the number of cores in an assemblage as a proxy measure for the number of original nodules present in the assemblage. This alternative approach proposed by Dibble et al. (2005) was tested with some success by Douglass et al. (2008) who were able to use a single surface area shape model (sphere) for their archaeological and experimental assemblages.

Summary of Findings

- Expectations for Cortical Product Abundance: It was anticipated that lithics from PP5-6 stratigraphic samples where the coastline is modeled to provide abundant local raw materials (Jed/JR Quartzite, *ALBS, and NWR*) would have higher Cortex Ratios than samples where raw materials are expected to have been transported to site from greater distances (*SADBS, OBS, SGS, DBCS*).

  Analysis Results: The *ALBS* quartzite, *NWR* quartzite, and *DBCS* silcrete samples have Cortex Ratios that are lower than those of Jed/JR Quartzite which supports the prediction of the Site Context Model. The highest Cortex Ratio values, however, are from assemblages that occur at the greatest distance from the coastline where it was expected that there would be a significant reduction in the amount of cortex present. Overall, the results of the analysis of cortex abundance do not support the predictions of the Site Context Model

11.0 Raw Material Conservation

A classic synthesis of flake attributes by Dibble (1997) provides a foundation for the evaluation of raw material conservation during core reduction. Dibble was interested in predicting original flake size on retouched specimens but he also demonstrated a clear association between decisions related to core preparation and the morphometric outcome of the end product. Knappers can vary flake surface area and thickness by altering the exterior platform angle and by controlling the flake platform area. Dibble's methodology has been extensively tested through experimental research (Davis and Shea 1998; Pelcin 1998; Dibble and Rezek 2009). These flake attributes can be measured, quantified, and statistically tested. Dibble's (1997) experimental methodology also allows for the comparison of aspects of raw material economy and flake production among typologically distinct assemblages.

The following description of flake attribute relationships is summarized from Dibble (1997). A tool maker who wishes to control the intended flake size has several core preparation options. Altering the width and thickness of the platform (consequently changing the total platform area), as well as increasing the exterior platform angle (EPA), which is the angle formed by the flake platform and the dorsal surface of the flake), will determine flake mass. However, the way in which a flintknapper controls these two variables has important implications for core maintenance and thus raw material economy.

Increasing the platform area produces a larger flake, but, from a raw material conservation perspective, this strategy has two disadvantages. First, holding other variables constant, a large platform area means that a greater volume of material has been removed from the core's striking platform, which limits core life. Second, a larger platform produces a flake that is thicker overall, especially near the butt of the flake. Increasing the platform area increases the size of the flake in terms of weight, but it does not necessarily provide more utilizable surface area or cutting edge.

Increasing the EPA also results in the production of a larger flake when other variables are held constant. Increasing the exterior platform angle has a distinct advantage: The resulting blanks have larger flake dimensions in relationship to the platform size. More utilizable volume is therefore contained within the flake. Core life is

prolonged by conservation of the core platform. The disadvantage associated with increasing the exterior platform angle is that it puts more force behind a smaller platform area which can result in the destruction of the desired flake blank during manufacture.

The EPA measurement is extremely useful for modeling production strategies and raw material conservation, but it can be very difficult to measure, depending on flake curvature and morphology. Results are notoriously inconsistent (Andrefsky 1998). Problems with measuring EPA has led some researchers to find more easily quantified expressions of the tool maker's conscious or intuitive ability to manipulate flake morphology. The ratio of cutting edge to flake mass is a readily measurable test variable that has been argued to monitor one of the eventual outcomes of manipulating flake platform area and platform thickness (Braun 2005; Mackay 2008a). This measurement has been referred to as the "Conservation Index" (CI)(Braun 2005), "edge length/mass" or "EL/M" (Mackay 2008a), and "cutting edge/mass" or "CE/M" (Brown 1999). These measurements are similar indexes.

The amount of flake cutting edge produced from a given mass of stone can be effectively managed because the knapper can deliberately control the potential flake surface area and flake thickness by altering the exterior platform angle and platform morphology (Braun 2005). It is expected that the casual or less conservation-minded exploitation of a nodule of stone will produce less cutting edge per mass unit of raw material than a strategy that seeks to maximize cutting edge by producing thin flakes or blades with greater surface area. The ratio of flake surface area to flake thickness can be maximized in two ways: increasing the exterior platform angle and increasing the ratio of flake width to flake thickness. The optimal strategy for producing large thin flakes, while still maintaining core striking platform involves increasing the exterior platform angle while minimizing the ratio of platform width to platform thickness. A potential criticism of this approach is that debitage with highest edge length to mass values may have been preferentially transported away from site. However, the same constraints acting to maximize the recovery of workable edge from finished tool blanks should apply to the entire core reduction sequence and also be reflected in other debitage (Braun 2005).

Edge conservation methodologies are particularly applicable to the coastal southern African MSA where assemblages are typically dominated by blades and elongated flakes, with very low percentages of retouch (Wurz 2000). Unlike many European and southwest Asian Middle Paleolithic assemblages, which are based on the production of large flake blanks for curated or transported tools (Kuhn 1992), southern

African MSA knappers appear to have adopted a strategy for producing what amounts to disposable blade technology that is discarded after use rather than maintained. Many southern Cape MSA retouched tools appear to have been made to facilitate hafting (Wadley and Mohapi 2008) rather than for prolonging use-life. In this sense, CE/M in many coastal southern African MSA assemblages represents a scenario where the emphasis is on producing fresh utilizable cutting edges rather than artifacts designed for extended use through resharpening (Kuhn 1994; Dibble 1995). SB bifaces are a notable exception to this pattern, and they may represent curated or maintained technology (Kelly 1988). A conservation strategy for maintaining blade core use-life would require blades to be thin and elongated with minimal platform area. Since the blades are typically not retouched, less need exists to create thicker or wider blades with maintainable volume that will stand up to prolonged use.

Mackay (2008a) applied a modified version of Braun's (2005) CI as a measure for estimating the conservation of fine-grained raw materials in the MSA at Diepkloof and Klein Kliphuis. Mackay (2008a) calculated the EL/M ratio (for specimens greater than 15mm in maximum dimension) by summing the flake length, maximum width, and maximum dimension measurements and then dividing by flake mass. He investigated EL/M values from the SB to HP transition at Diepkloof and the late-HP to Post-HP sequence at Klein Kliphuis to quantify flaking efficiency in the use of non-local raw materials. He found that the EL/M values at Diepkloof increased rapidly after the bifacial SB, and then peaked in the Late-HP. The Klein Kliphuis sequence shows a subsequent decline in EL/M in the post-HP.

Mackay (2008a) then compared upper limits of EL/M for the three predominant raw material classes at Diepkloof and Klein Kliphuis, and found that EL/M is consistently higher for silcrete and quartz when compared with quartzite. The EL/M mass values for all raw materials are statistically higher in the HP across the Diepkloof and Klein Kliphuis assemblages. Mackay (2008a) then argued that silcrete and quartz may have been selected because these raw materials allowed for the production of thinner flakes, and were thus more amenable to the conservation of raw material during core reduction. Mackay (2008a) calculated that from an equivalent mass of raw material, approximately twice as much cutting edge could be produced from silcrete than quartzite. He argued that despite poor fracture predictability, quartz may have been selected for the conservation of cutting edge at times when flaking efficiency was emphasized.

Mackay (2008a) argued that climatic conditions during MIS 4 pressured knappers to maximize the economic recovery of edge length from a given mass of raw material. Early humans gradually intensified their efforts to locate raw materials that would satisfy the need for flake production that maximized cutting edge and reduced mass. As the selective pressures eased toward the end of OIS 4, the requirements for fine-grained raw materials diminished. Importantly, Mackay argues that raw material conservation is not a function of distance to source.

The cutting edge to mass variable presented here is considered to be a similar measurement to Braun's CI and Mackay's (2008a) EL/M, and is a useful method of estimating conservation across raw material categories and between samples. The cutting edge analysis in this section tests the simple assumption that there would have been less pressure during coastline occupations to maximize cutting edge and conserve core volume when raw material was plentiful near site. Jed/JR Quartzite is currently the only sampled occupation from PP5-6 where the coastline was likely to be directly adjacent to the caves. This proximity to cobble beaches would have provided MSA knappers access to abundant quartzite and enough silcrete to account for the few Jed/JR Quartzite specimens potentially collected as beach cobbles. During the remainder of the excavated site occupations, PP5-6 was located several kilometers from the active beaches requiring greater conservation of materials. In the SADBS there is a clear shift away from quartzite beach cobbles to primary outcrop acquisition of silcrete. Silcrete is estimated to come from a distance of at least 8.5km. The Site Context Model predicts that cutting edge values relative to mass would increase when the site was located at greater distances to the coastline and when raw materials were then transported to the site from more than a few kilometers away.

Cutting edge was recorded for all complete PP5-6 debitage by 'rolling' flakes along a flexible plastic ruler. Flake platform and relict edges were not included as cutting edge. The analysis here follows Mackay (2008a) in using a size cutoff of 15mm in maximum dimension for sampled debitage. Cutting edge is a linear function of flake perimeter and mass is a function of volume. Dibble and Rezek (2009) identified a methodological problem in comparing log-linear variables. In effect, the uncorrected mass and cutting edge variables increase at different rates creating a curvilinear relationship (Fig. 74a). The effect of using the uncorrected cutting edge to mass ratio (CE/M) is that the untransformed variable is negatively correlated with flake size (log transformed length and uncorrected CE/M: r -0.68, $p < .001$). It has already been

demonstrated that there are significant differences in mean flake dimensions between raw materials (Ch. 9). The CE/M values should be reflective of shape changes in the debitage and not allometric effects of large and small flakes.

The CE/M ratio was corrected by dividing cutting edge values by the cube root of mass which results in a linear relationship between the two variables, thus facilitating statistical analysis (Fig 74b). The transformed $CE/M^{1/3}$ test variable does not correlate with flake size (length and $CE/M^{1/3}$: r 0.02, p 0.59). Thus the $CE/M^{1/3}$ test variable evaluates the effects of change in flake shape, rather than size, in controlling flake perimeter and cutting edge. $CE/M^{1/3}$ is significantly correlated with the ratio of length/width (L/W) in the sample of complete flakes from PP5-6 (r 0.64, p <.001). Not surprisingly, flakes that are more elongated have correspondingly more cutting edge than those with a lower ratio of L/W, holding weight constant. The increase in cutting edge yield per mass unit has long been an advantage associated with blade technology (Leroi-Gourhan 1957). The $CE/M^{1/3}$ basically quantifies the laminar nature of debitage from each PP5-6 analytical sample.

Figure 75(a) provides mean $CE/M^{1/3}$ values with 95% confidence levels for complete flakes from each analyzed analytical sample. The $CE/M^{1/3}$ values for Jed/JR Quartzite flakes are lowest. $CE/M^{1/3}$ values peak in the *ALBS* and *SADBS*. The difference in $CE/M^{1/3}$ means between the low point of the pattern in Jed/JR Quartzite and the peak in the *SADBS* is significant. $CE/M^{1/3}$ then drops in the *OBS* and *SGS*. The falloff in $CE/M^{1/3}$ values between the *SADBS* and *OBS* is also significant. The $CE/M^{1/3}$ mean values do not differ significantly between the *ALBS*, *SADBS*, *DBCS*, *NWR* and Takis complete flake samples.

The $CE/M^{1/3}$ and L/W line graphs are similar for each analytical sample with the exception of the small and variable Takis sample (Fig. 75a,b). The correlation of the L/W and $CE/M^{1/3}$ ratios for each sample is significant in a non-parametric test of correlation (Kendall's Tau 0.72, p 0.02) if the small and variable Takis sample is excluded. Thus samples that have more elongated flakes also tend to have higher cutting edge values. Figure 75c shows the percentage of both complete and fragmentary debitage that has L/W values greater than 2.0, the standard cutoff often used for the definition of blade products (Bar-Yosef and Kuhn 1999). The $CE/M^{1/3}$ and L/W ratios and blade product percentages all show high bimodal peaks in the *SADBS* and *NWR* and low values in the Jed/JR Quartzite and *OBS* samples.

Mean $CE/M^{1/3}$ and L/W values and 95% confidence level are plotted for each analytical sample by silcrete and quartzite in Figure 75. $CE/M^{1/3}$ and L/W values are always higher for silcrete over quartzite with the exception of L/W for the *NWR*. Table 55 provides a statistical comparison of $CE/M^{1/3}$ and L/W values for the combined PP5-6 sample of complete flakes using the Kruskal-Wallis non-parametric test for differences in sample medians. Silcrete flakes have significantly higher $CE/M^{1/3}$ and L/W values than quartzite flakes. Similar to the pattern observed in flake dimensions (Ch. 9) silcrete and chert flakes are not significantly different in $CE/M^{1/3}$ and L/W. Quartz $CE/M^{1/3}$ is closest to quartzite and L/W values are significantly different between quartzite and quartz. These results show that silcrete and chert flakes have significantly more cutting edge per mass unit of raw material than quartzite and quartz. Silcrete and chert flakes are significantly more elongated than quartzite or quartz flakes.

The mean $CE/M^{1/3}$ values for silcrete are not significantly different when compared between analytical samples, except that the small sample of Jed/JR silcrete flakes have lower $CE/M^{1/3}$ values than those from the *SADBS*. Quartzite $CE/M^{1/3}$ mean values have highest peaks in the *SADBS* and *NWR*. *SADBS* quartzite $CE/M^{1/3}$ is significantly higher than *DBCS* and *SGS* quartzite flakes. The L/W silcrete and quartzite patterning is similar to that described for $CE/M^{1/3}$. The most elongated silcrete flakes are found in the *SADBS*, *ALBS* and *DBCS*. *SADBS* silcrete L/W values are significantly higher than those for the small Jed/JR silcrete flake sample. The *ALBS*, *SADBS* and *NWR* have the highest quartzite L/W means but these differences are only significant between the ALBS and Jed/JR quartzite flakes.

The highest overall $CE/M^{1/3}$ values (Fig. 75c) occur in samples that are rich in silcrete and chert (*SADBS*, *DBCS*)(Fig. 75d) and/or where both quartzite and silcrete flake products are relatively elongated (*SADBS*, *ALBS* and *NWR*). In fact, there is a strong significant correlation with complete flake mean $CE/M^{1/3}$ values compared with the combined percentages of silcrete and chert for each analytical sample (Spearman's r_s .86, p .007). The *SGS* stands out as having relatively low overall $CE/M^{1/3}$ values and this may be due in part to the contribution of quartz flakes and relatively low L/W ratios for quartzite flakes.

Raw Material Conservation and the Site Context Model

In the comparison of $CE/M^{1/3}$ with distance to coastline (Fig. 77b) it can be seen that Jed/JR Quartzite has the lowest $CE/M^{1/3}$ mean values as predicted by the Site Context Model for an occupation close to abundant raw materials. The *SADBS* and *ALBS* have higher than expected $CE/M^{1/3}$ values that peak well before the climax in coastline regression. The *OBS* and *SGS* have unexpectedly low values close to the peak of the MIS 4 coastline transgression where it would be expected that transportation costs would be highest and raw material conservation would be maximized. It was also expected that $CE/M^{1/3}$ might drop in the MIS 4/3 transgression when cobble beaches were again closer to PP5-6, but $CE/M^{1/3}$ is not statistically different in the *DBCS*, *NWR* and Takis samples when compared with the *SADBS* and *ALBS*.

In a general sense, the predictions of the Site Context Model are met in that the lowest $CE/M^{1/3}$ values do occur when the coastline is modeled to be closest to site. Counter to what was predicted though, the lowest values of $CE/M^{1/3}$ occur in occupations at both the minimum (Jed/JR) and maximum distances to coastline (*OBS* and *SGS*), and the $CE/M^{1/3}$ high points occur in transgressive and regressive phases. A Kendall's Tau non-parametric test of correlation (Tau 0.0 p 1.0)(Fig. 77c) shows no association between mean $CE/M^{1/3}$ and distance to coastline. The predictions of the Site Context Model are not entirely supported for the $CE/M^{1/3}$ test variable.

Discussion

The lack of significant differences in $CE/M^{1/3}$ across the silcrete samples (with exception of Jed/JR) may point to a shortcoming in the assumptions of the Site Context Model. It is noted in Chapter 5.4 that the decision to collect silcrete is modeled to be dependent on the relative costs of acquiring secondary context quartzite, the availability of which was expected to change with coastline movement. The results of the $CE/M^{1/3}$ analysis suggest that conservation behavior of silcrete remains relatively constant with no significant differences between silcrete samples (with the exception of the small Jed/JR sample). This may result in part from the large error bars due to small sample sizes, but if silcrete availability is viewed independently of quartzite, the actual distance to silcrete sources from PP5-6 does not change with fluctuations in sea level. Thus if transport costs (without factoring in mobility and site use) for silcrete were same throughout the PP5-6

sequence then there may have been similar requirements for conservation as reflected in the $CE/M^{1/3}$ analysis of silcrete.

The comparison of $CE/M^{1/3}$ values by raw material may provide other reasons to view raw materials independently. The $CE/M^{1/3}$ analysis of PP5-6 complete flakes supports the findings of Mackay's (2008) EL/M analysis at Diepkloof and Klein Kliphuis. Mackay used differences in edge length in a large sample of complete flakes to show how some of the design parameters for each raw material may be gained by looking at the upper range of values for EL/M and lower range of values for thickness. Although the EL/M calculations used by Mackay do not account for allometric variation, the $CE/M^{1/3}$ results are similar when compared across the raw materials used at PP5-6. Silcrete has the highest $CE/M^{1/3}$ potential as measured by upper quartile and maximum values followed closely by chert (Fig. 78) with quartzite and quartz showing the lowest upper range of values. If flaking efficiency is a critical objective than it makes sense to select chert and silcrete rather than quartzite.

The *OBS* stands out as being the only analytical sample where quartz is dominant. Quartz and chert take the place of silcrete in raw material proportions in the *OBS* and *SGS* samples (Ch. 6). These occupations may occur in context with rapid climate fluctuation from c. 65 to 67ka. Extreme fluctuations in climate change (as expressed in the $\delta^{13}C$), may cause a breakdown in raw material supply, or pulses in dune formation (particularly at 69ka) may have created impediments to movement inland. It was hypothesized in Chapter 6 that quartz could have been a secondary raw material option when silcrete availability was restricted. Mackay (2008a) noted high overall EL/M values for quartz at Diepkloof and Klein Kliphuis, but the $CE/M^{1/3}$ mean values from the small sample (n=32) of complete quartz flakes in the PP5-6 assemblage is on the very low range of values for all PP5-6 raw materials (mean 39.13)(Fig. 78). Quartz at PP5-6 may have been selected for other properties like sharpness of edge rather than for the potential of producing elongated flake products that maximize cutting edge.

Quartzite $CE/M^{1/3}$ values fluctuate more than silcrete, but again there are relatively high confidence levels associated with some small sample sizes. In the two significant drops in quartzite $CE/M^{1/3}$ values (Jed/JR and *OBS*) the contribution of blade products may be the major source of variability in the quartzite samples. Elongated flakes have already been demonstrated to have the highest $CE/M^{1/3}$ values. This is true for both quartzite and silcrete where plain and facetted platform blades have the highest mean

$CE/M^{1/3}$ in comparison to other predominant flake types (Table 56). Quartzite blade counts and percentages are low in comparison to silcrete in most analytical samples with the exception of the *NWR* and Takis (Fig. 79) a feature that drives up the overall $CE/M^{1/3}$ value in these two samples (Fig. 75a). $CE/M^{1/3}$ may be sensitive to the removal of blades tools from site.

Mackay (2008a) found that mean EL/M values increased in HP layers with backed blades and concluded that this was a response to the need for conserving raw material during periods of deteriorating climate. The same pattern does not occur at PP5-6 where there are three analytical samples in which segments are common; the *SADBS*, *SGS*, and *DBCS*. The *SGS* has significantly lower $CE/M^{1/3}$ values than the *SADBS* when all raw materials are considered. When silcrete values are compared, *SADBS*, *SGS*, and *DBCS* are not significantly different than other layers where backed blades are few or absent. While the potential for raw material conservation was undoubtedly an important factor in selection of stone, variability in $CE/M^{1/3}$ between raw material classes and between analytical samples may also relate to the morphology of the desired end product and potential design constraints imposed upon their use.

In most fine-grained dominant samples, small blades are considered to be the desired end product. In the *SADBS*, *SGS*, and *DBCS*, many of these small blades are retouched into backed pieces. The morphology of the backed pieces differs by stratigraphic sample. *SGS* segments are relatively short and wide in comparison to those of the *SADBS* and *DBCS*. *SADBS* segments are significantly narrower than those of the *DBCS* and *SGS*. *SADBS* segments have the highest mean L/W ratio and this is reflected in the higher $CE/M^{1/3}$ values for *SADBS* complete flakes made from fine-grained raw materials (Table 57). *SGS* segments have the lowest L/W ratio and correspondingly lower $CE/M^{1/3}$ in debitage for the raw materials used to make segments. Subtle differences in $CE/M^{1/3}$ between analytical layers may be related to the production of different blank morphologies intended for composite tools rather than reduced need for flaking efficiency.

Mackay (2008a) argues that an advantage of using fine-grained raw materials is that they allow for the production of tools with more surface area and cutting edge while minimizing thickness, which serves to keep weight down and maximizes flaking efficiency. If retouched and unmodified small blades are replaceable inserts in compound tools, than presumably the ability to more readily control thickness would also be an important design constraint for standardized hafting. Flake mass, when transformed by

taking the cube root, is strongly correlated with thickness (r 0.90, $p < .001$). PP5-6 silcrete and chert flakes are significantly thinner than those of quartzite (Ch. 9) with lower minimum values and lower quartile range (Table 58). The consistency in $CE/M^{1/3}$ values across fine-grained materials may be imposed by design constraints for hafting as much as to conserve mass.

The analysis of quartzite debitage (Ch. 7) indicates that facetted flakes, points, and blades were often an end product of quartzite core reduction, with many cores showing evidence for continued centripetal or multidirectional reduction. What is interesting is that quartzite facetted flakes and points actually have values on the low range of $CE/M^{1/3}$ for debitage in comparison to quartzite blades (Table 56) which are relatively uncommon throughout the sequence. As a consequence, some of the most common quartzite tool forms found throughout the PP5-6 sequence were probably not produced with flaking efficiency as the primary objective.

The results of this analysis did not support the Site Context Model; the highest $CE/M^{1/3}$ values occur on the regressive (*SADBS*) and transgressive (*DBCS*) slopes of the MIS 4 coastline curve but not on the peak. The same pattern was observed with silcrete proportions (Ch. 6). Low $CE/M^{1/3}$ values can be at least partially attributed to reduced percentages of quartzite blade products in Jed/JR Quartzite, *OBS*, and *SGS*. Although the requirements for raw material conservation should be observed in all phases of tool production, $CE/M^{1/3}$ values may be sensitive to the transport of highest $CE/M^{1/3}$ value blade products away from site. This analysis also demonstrates that $CE/M^{1/3}$ values are significantly higher for silcrete and chert when compared with quartzite, a relationship that supports Mackay's (2008a) contention that fine-grained raw materials were selected based on their suitability to satisfy design constraints. Fine-grained raw materials allow for the production of thinner, more elongated debitage products (Mackay 2008a), which in turn allows for increased exploitation of cutting edge during core reduction.

Raw material conservation was undoubtedly an important consideration for silcrete and other raw materials with higher handling costs at PP5-6, but there few significant differences in silcrete $CE/M^{1/3}$ when compared between layers. It may be the case that conservation of silcrete was always an objective given that the primary sources of silcrete were never closer than 8.5km from site. Silcrete may also have been preferentially selected at PP5-6 when there were requirements for raw materials amenable for the production of thin elongated blades. This parameter would be important

in the production of standardized inserts for compound tools, regardless of whether they were modified by backing prior to hafting.

Summary of Findings

- Conservation Expectations: Materials with higher transportation and processing costs are more likely to have been conserved in comparison to raw materials available in the vicinity of the site. It is expected that materials transported over longer distances would have higher cutting edge/mass values than locally available materials.

  Analysis Results- The mean $CE/M^{1/3}$ values for Jed/JR Quartzite are the lowest and fit the expectations of the Site Context Model for a site close to lithic resources. $CE/M^{1/3}$ values are highest on either side of the MIS 4 maximum distance to coastline and drop at the peak of coastline regression in the *OBS* and *SGS* samples. The $CE/M^{1/3}$ analysis does not support all of the stated predictions of the Site Context Model.

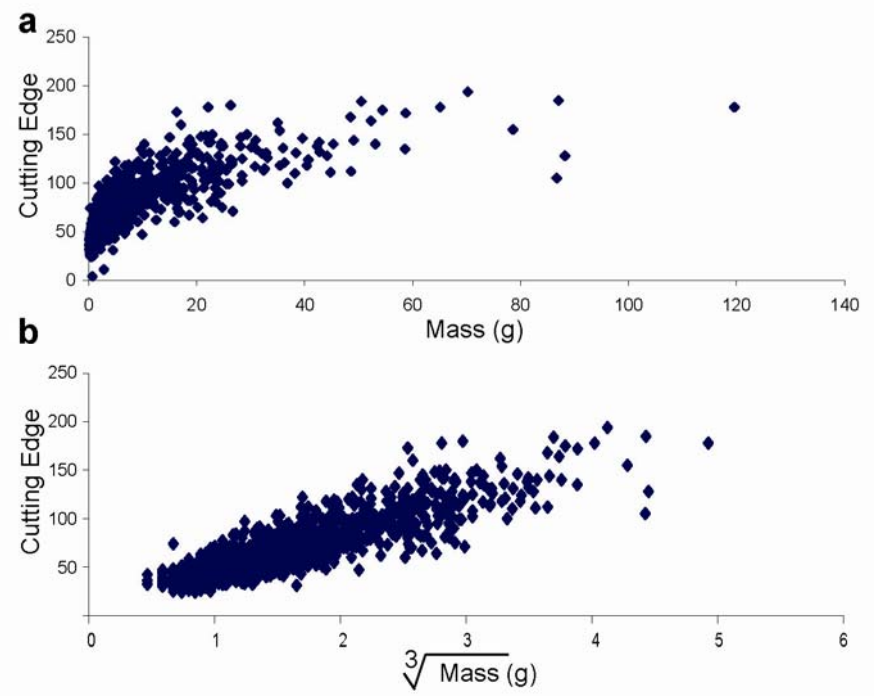

Figure 74. a) Comparison of log-linear relationship between untransformed cutting edge and mass variables, and (b) linear relationship after taking the cube root of mass.

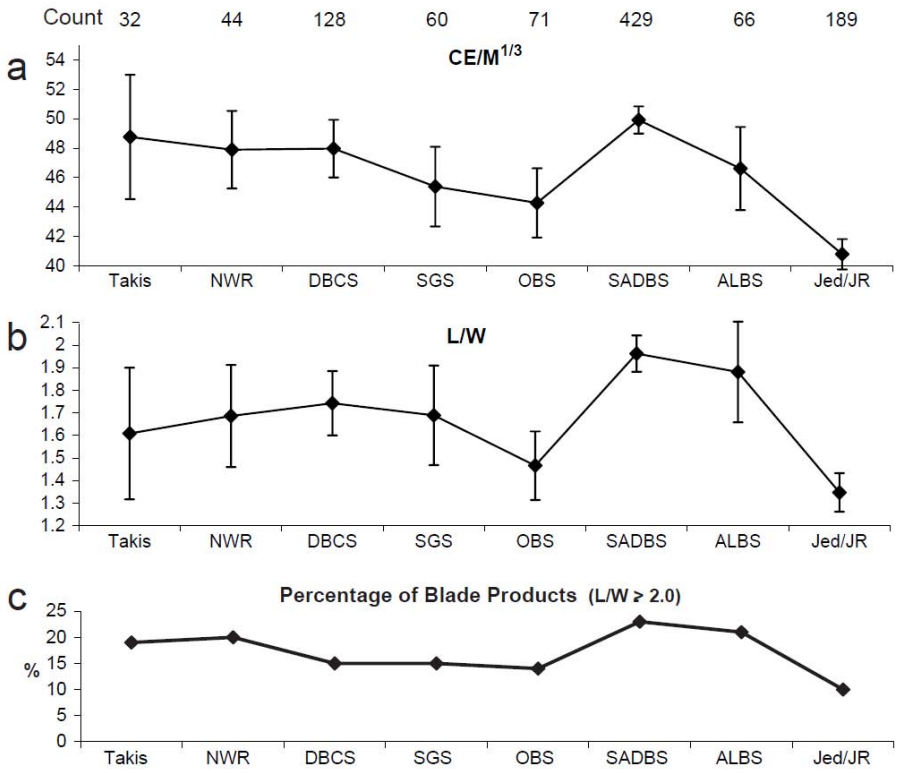

Figure 75. a) Mean CE/M1/3 values for PP5-6 analytical samples with 95% CI; b) mean length to width ratio (L/W) and 95% CI; d) percentage of complete and fragmentary debitage with L/W ≥ 2.0 for each analytical sample.

Table 55. Kruskal-Wallis test results for comparison of PP5-6 complete flake $CE/M^{1/3}$ and L/W attributes for quartzite, silcrete, chert, and quartz. P-values in italics are Bonforroni corrected and those in blue identify sample comparisons that are not significantly different

$CE/M^{1/3}$	Quartzite	Silcrete	Chert	Quartz
Quartzite		p <.001	p <.001	0.0117
Silcrete	*p <.001*		0.5788	p <.001
Chert	*p <.001*	*1*		p <.001
Quartz	*p <.001*	*p <.001*	*p <.001*	
H_c 196.8 p <.001				

L/W	Quartzite	Silcrete	Chert	Quartz
Quartzite		p <.001	p <.001	0.6828
Silcrete	*p <.001*		0.5308	0.0001
Chert	*p <.001*	*1*		0.0003
Quartz	*1*	*p <.001*	*0.0020*	
H_c 148.1 p <.001				

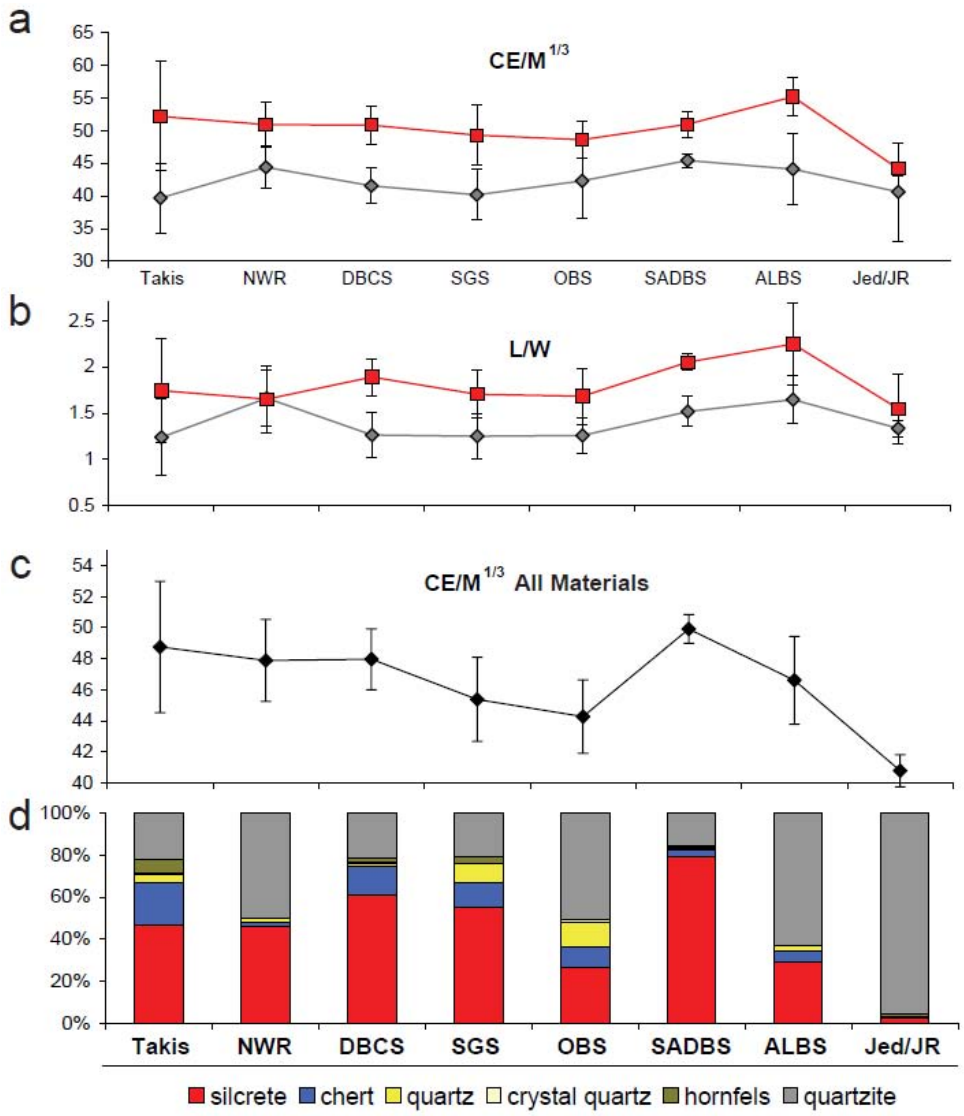

Figure 76. a) Mean CE/M1/3 values for PP5-6 analytical samples with 95% CI for complete silcrete (red) and quartzite (grey) flakes; b) Mean length to width ratio (L/W) and 95% CI by silcrete and quartzite; c) mean $CE/M^{1/3}$ values for all raw materials for comparison; d) complete flake raw material percentages by raw material

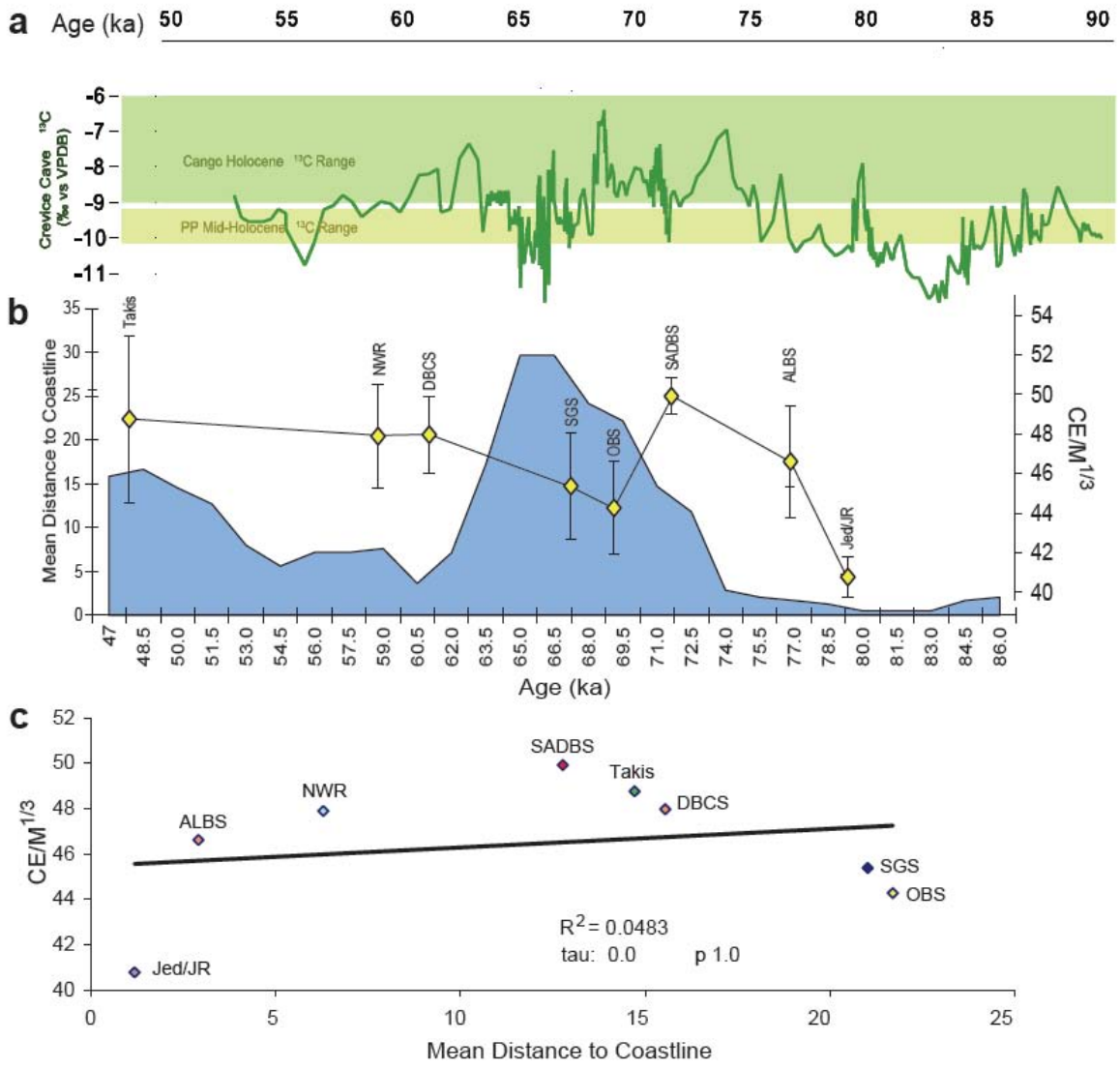

Figure 77. CE/M$^{1/3}$ values and 95% confidence level displayed with: a) Crevice Cave $\delta^{13}C$ record from Bar-Matthews et al. (2010) and b) CE/M$^{1/3}$ values and 95% confidence level for complete debitage by analytical sample and distance to coastline from Fisher et al. (2010); c) graph of mean CE/M$^{1/3}$ values plotted against mean distance to coastline from Fisher et al. (2010). There is no statistical correlation between CE/M$^{1/3}$ and distance to coastline.

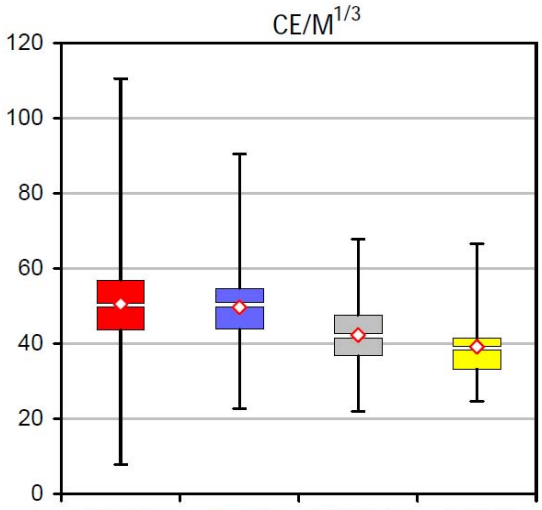

	Silcrete	Chert	Quartzite	Quartz
Count	542	63	463	32
Upper Quartile	56.81	54.78	47.58	41.44
Mean	50.57	49.65	42.31	39.13
SD	10.28	11.73	8.06	8.44
Max	110.54	90.49	67.84	66.69

Figure 78. Box plot distribution of CE/M1/3 for complete flakes by raw material. Table provides summary statistics for the upper range of the sample distributions to show the potential maximum limit for each raw material

Table 56. Predominant debitage type for complete flakes by raw material and mean $CE/M^{1/3}$ values

Debitage Type	Silcrete		Quartzite		Total	
	$CEM^{1/3}$	n	$CEM^{1/3}$	n	$CEM^{1/3}$	n
Point with facetted platform	42.4	3	42.8	36	42.8	39
Primary Cortical (>60% cortex)	48.1	27	38.2	30	42.9	57
Plain Platform Flakes	45.5	161	41.3	216	43.1	377
Residual Cortical (<61% cortex)	46.9	89	40.1	90	43.5	179
Facetted flake	48.6	18	42.0	17	45.4	35
Plain Platform Blade	56.9	108	53.8	27	56.3	135
Blade with facetted platform	57.7	19	52.0	9	55.9	28

Table 57. L/W values for complete segments from the SADBS, SGS, and DBCS compared with L/W and $CE/M^{1/3}$ for complete silcrete, quartz, and chert flakes

Sample	Segments	Complete Debitage	
	L/W	L/W	$CE/M^{1/3}$
DBCS	2.7	1.7	47.5
SADBS	3.03	1.9	48.9
SGS	1.91	1.7	46.6

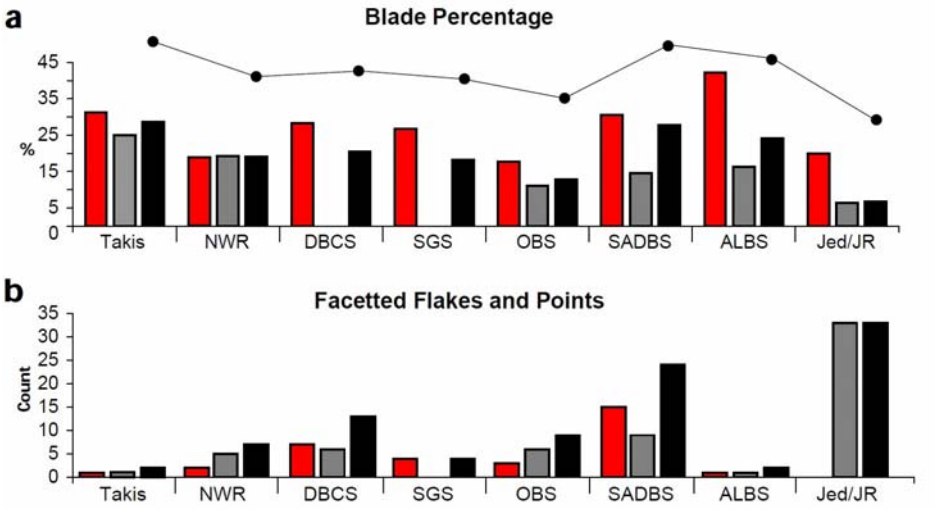

Figure 79. a) Percentage of plain and facetted platform blades for PP5-6 analytical samples by silcrete (red), quartzite (grey) and combined silcrete and quartzite sample (black). The line diagram shows the curve created by the linked totals; b) combined counts of facetted flakes and points by analytical sample

Table 58. Lower quartile and minimum thickness values for complete flakes by raw material

Material	Count	Mean	Lower Quartile	Minimum
Silcrete	633	4.3	3	1
Chert	71	4.3	3	1
Quartz	29	6.5	4	2
Quartzite	462	7.8	5	2

12.0 Summary of Results and Discussion

The archaeological record at PP5-6 shows a very clear shift from the predominant use of quartzite to silcrete that occurs between 72-76ka. This change is associated with a reduction in debitage size and the production of small blades and segments. A similar pattern has been observed at other coastal MSA sites in the Southern and Western Cape region of South Africa (Singer and Wymer 1982; Wurz 2002; Thackeray 2000; Porraz 2008). The models summarized in Chapter 3 attempt to explain aspects of the Cape Raw Material Pattern, and particularly the association of fine-grained raw materials and the appearance of the HP MSA. These prior models resorted to a climate-based catalyst for raw material variation and technological diversity. There is no consensus view of how the MIS 4 climate change is expressed in terms of rainfall, mean annual temperature, or vegetation (Chase 2010; Bar-Matthews et al. 2010) or whether climate would have been 'cold', or 'harsh' as is often speculated. It is clear, however, that at certain periods in MIS 4, climate was extremely variable (Bar-Matthews et al. 2010).

The Site Context Model presented and evaluated in this dissertation has also adopted and tested a climate-based explanation for observed technological variability and changes in raw material use at PP5-6. The goal for this study was to examine the potential effects of one expression of Pleistocene glaciation that unquestionably resulted in major changes to the southern coast paleo-landscape (Hendey and Volman 1986; Van Andel 1989). The Site Context Model presented in Chapter 3.2 and briefly summarized here hypothesizes that sea level changes modeled to occur between MIS 5 and MIS 3 (Fisher et al. 2010) would have influenced the availability of quartzite, one of the major classes of raw materials at PP5-6 which, is argued to have been collected from active sources of cobble beaches in the past. Cobble beaches retreated away from PP5-6 during periods of coastline regression. The distance from PP5-6 to primary sources of silcrete, which occur in abundance today at a minimum of 8.5km inland from Pinnacle Point, are not expected to have been affected by coastline change. At times when the coastline was far away, silcrete sources may have been closer to access from PP5-6 than active cobble beaches, and in those situations it is argued that silcrete was more likely to have been selected for tool use if cost of acquisition and transport was the main factor in choice of raw material.

The increase in post-HP quartzite use at PP5-6 is argued to coincide with a coastline transgression that occurs briefly between MIS 4 and MIS 3. The Site Context Model was offered in this study as an explanation for the apparent synchronous raw material shift from quartzite to more fine-grained raw materials at MSA sites on the south coast. The evaluation of the Site Context Model hypothesis can be seen as a test of how much of the fluctuating raw material proportions in the PP5-6 sequence could be explained by changing availability of stone imposed by natural processes, versus the deliberate selection of raw materials for functional reasons. It is important to emphasize that the Site Context Model was not proposed as a direct explanation for the appearance and disappearance of the SB and HP, which occur at a number of sites where raw material availability would not have been directly affected by coastline movement.

12.1 The Site Context Model

Test hypotheses were presented in Chapter 3.3 in order to associate technological variability in raw material use with the data derived from the Fisher et al. (2010) coastline model (in km. from Pinnacle Point). The results of the Site Context Model test attributes are summarized below with data from the analyses of raw material and cortex (Ch. 6), heat treatment (Ch. 8), flake metrics (Ch. 9), cortex abundance (Ch. 10), and raw material conservation (Ch. 11). The Site Context Model is then evaluated with respect to these results. Key features of the PP5-6 assemblage identified in this study are then summarized from the base to the top of the analyzed sequence. The broader behavioral implications for the findings from the PP5-6 lithic analysis are first discussed in consideration of the paleoenvironmental context of Pinnacle Point, and then with respect to models proposed for explaining technological variability and raw material use in the Cape and elsewhere.

Table 59. Summary of Site Context Model analysis test expectations

Analysis	**Expected Result for PP5-6 Paleolandscape Context Model**	
	Coastline Near	***Coastline Far Away***
Raw Material	Greater use of local quartzite	Increase in materials from inland
Cortex	More beach cobble cortex	More primary cortex
Heat Treatment	Lower percentage of heated silcrete	Higher percentage of heated silcrete
Cortical Reduction	More cortical products	Less cortical products
Debitage Metrics	Larger products	Smaller products
Cutting Edge/Mass	Lower ratio of cutting edge to mass	Higher ratio of cutting edge to mass

Raw Material

The Site Context Model predicted that quartzite use would be more common when the coastline was near and, silcrete use to be more frequent when the coastline was farther away (Table 59). This prediction was tested by comparing the ratio of quartzite to silcrete (based on weight) for each assemblage against distance to coastline. This comparison shows the expected relationship of lower quartzite to silcrete ratios with increased distance to coastline but the correlation is not significant (Kendall's Tau -0.5, p .083) because the *ALBS* and *SADBS* values are higher than expected and consequently the silcrete raw material use peaks well before the MIS 4 peak in distance to coastline (Fig. 80d). When the *SADBS* and *ALBS* are removed, there is a significant correlation in the quartzite to silcrete ratio (Kendall's Tau -0.73, p .039).

The post-hoc analysis of raw material identified two significant relationships. The comparison of the ratio of quartzite to non-quartzite raw materials is significantly correlated with distance to coastline (Kendall's Tau -0.57, p .048). The percentage of silcrete in each analytical sample is highly correlated with δ^{13}C (Kendall's Tau 1.0, p .002).

Cortex Type

The comparison of the ratio of Cobble/Outcrop cortex with distance to coastline is one of the least significant correlations observed in this analysis (Kendall's Tau -0.07, p .80). The plots show that the *SADBS* and *ALBS* have ratios of Cobble/Outcrop cortex that are too low for samples that occur during regression prior to the peak distance in coastline (Fig. 80e). The opposite is true of the *OBS*, *SGS*, and Takis samples which have higher cobble ratios than would be expected for the coastline peak. This is associated with the increased use of quartz and chert in these three samples (Ch. 6, Fig. 33). *OBS*, *SGS*, and Takis chert and quartz were collected as very small pebbles in comparison to quartzite (Ch. 9) and are most common in assemblages stratigraphically above the SADBS (Ch. 6, Figs 27-28).

A post-hoc analysis demonstrates that the log transformed Cobble/Outcrop ratio is significantly correlated with δ^{13}C (Kendall's Tau -0.71 p .02).

Heat Treatment

There is a weak and insignificant positive relationship between mean maximum gloss values and distance to coastline (Kendall's Tau 0.29, p 0.32). The Jed/JR Quartzite sets the baseline of the pattern with no samples having gloss values greater than 2.7 which are taken to be clearly indicative of heat treatment. *ALBS* and *NWR* mean sample values deviate the most from the trendline. Gloss values are too high in the *ALBS* sample for what is expected for an occupation that is still near to the coastline. The *NWR* represents an occupation that occurs during a coastal transgression and values are lower than expected.

When mean maximum gloss values are compared against the ratio of quartzite to non-quartzite raw materials for all assemblages, gloss values for the quartzite-rich Jed J/R Quartzite and *NWR* samples are low. The remaining assemblages all cluster with similar high values of gloss. The *OBS* is especially noteworthy because although it shows the lowest artifact counts and weight of silcrete in all of the MIS 4 samples, the *OBS* shows the highest percentage of heat-treated silcrete within that silcrete sample (Fig.80c). Heat treatment at PP5-6 is not dependent on predictions of distance to coastline or the proportion of raw materials in an assemblage. With the exception of silcrete from Jed/JR, heat treatment occurs in at least half and usually in the majority of silcrete artifacts from each PP5-6 assemblage.

Flake Metrics

Flake size was compared against distance to coastline using mean weight and mean length for complete flakes of at least 15mm in length. The Jed/JR Quartzite sample is modeled to be closest to the coastline and has the largest mean and maximum dimensions for complete debitage but also has the highest percentages of quartzite (Fig. 80g). The smallest mean and maximum dimensions are from the *SADBS* which has the lowest percentage of quartzite and highest percentage of silcrete in the complete flake assemblage. Flake weight (Kendall's Tau -0.14, p 0.621) and length (Kendall's Tau -0.35, p 0.216) do not correlate with distance to coastline. Post-hoc analysis failed to find any combination of samples that provided significance to support the expectations of the Site Context Model.

PP5-6 complete quartzite flakes are significantly longer, wider, thicker, and heavier when compared with silcrete flakes (Ch. 9, Table 50). As a consequence all flake metrics are significantly correlated with the proportions of predominant raw material

types in each assemblage (Ch. 9, Table 51). Silcrete and chert flakes are not statistically different for any of the tested metric variables (Ch. 9, Table 50).

Cortex Abundance

Cortex abundance was quantified using the ratio of expected versus observed values of cortical surface area (Cortex Ratio). The three highest Cortex Ratio values are from samples that are modeled to occur at maximum distance from coastline (*OBS* quartzite, *SGS* silcrete, and *SADBS* silcrete) with values around 1.0 indicating that cortical materials are abundant and are close to what would be expected if most of the flake blank was reduced on-site at PP5-6. The correlation between Cortex Ratio values and distance to coastline is not significant for the entire analyzed assemblage using a non-parametric test of correlation (Kendall's Tau 0.32, p 0.26) or compared by raw material samples (quartzite samples and distance to coastline: Kendall's Tau 0.20, p 0.62; silcrete samples and distance to coastline: Kendall's Tau -0.33, p 0.60). The results of the analysis of cortex abundance as a whole do not support the predictions of the Site Context Model.

Raw Material Conservation

Jed/JR Quartzite fits the expectations of the Site Context Model with the lowest $CE/M^{1/3}$ mean values for an occupation modeled to have abundant raw materials. The *SADBS* and *ALBS* have higher than expected $CE/M^{1/3}$ values when compared to mean distance to coastline (Fig 80f). Counter to expectations, the *OBS* and *SGS* have unexpectedly low values close to the peak of the MIS 4 coastline transgression. It was also expected that $CE/M^{1/3}$ might drop in the MIS 4/3 transgression when cobble beaches were again closer to PP5-6, but $CE/M^{1/3}$ is not statistically different between the *DBCS*, *NWR*, *SADBS*, *ALBS* and Takis samples. In a general sense, the predictions of the Site Context Model are met in that the lowest $CE/M^{1/3}$ values do occur when the coastline is modeled to be closest to site but there is no correlation between mean $CE/M^{1/3}$ and distance to coastline. The predictions of the Site Context Model are not supported for the $CE/M^{1/3}$ test variable.

The analysis demonstrated that $CE/M^{1/3}$ is significantly correlated with the ratio of length/width (L/W). Samples that are more laminar have higher $CE/M^{1/3}$ mean values. There is a strong significant correlation between mean $CE/M^{1/3}$ values and the combined

percentages of silcrete and chert for each analytical sample. Silcrete and chert flakes have significantly higher CE/M$^{1/3}$ and L/W values than quartzite flakes.

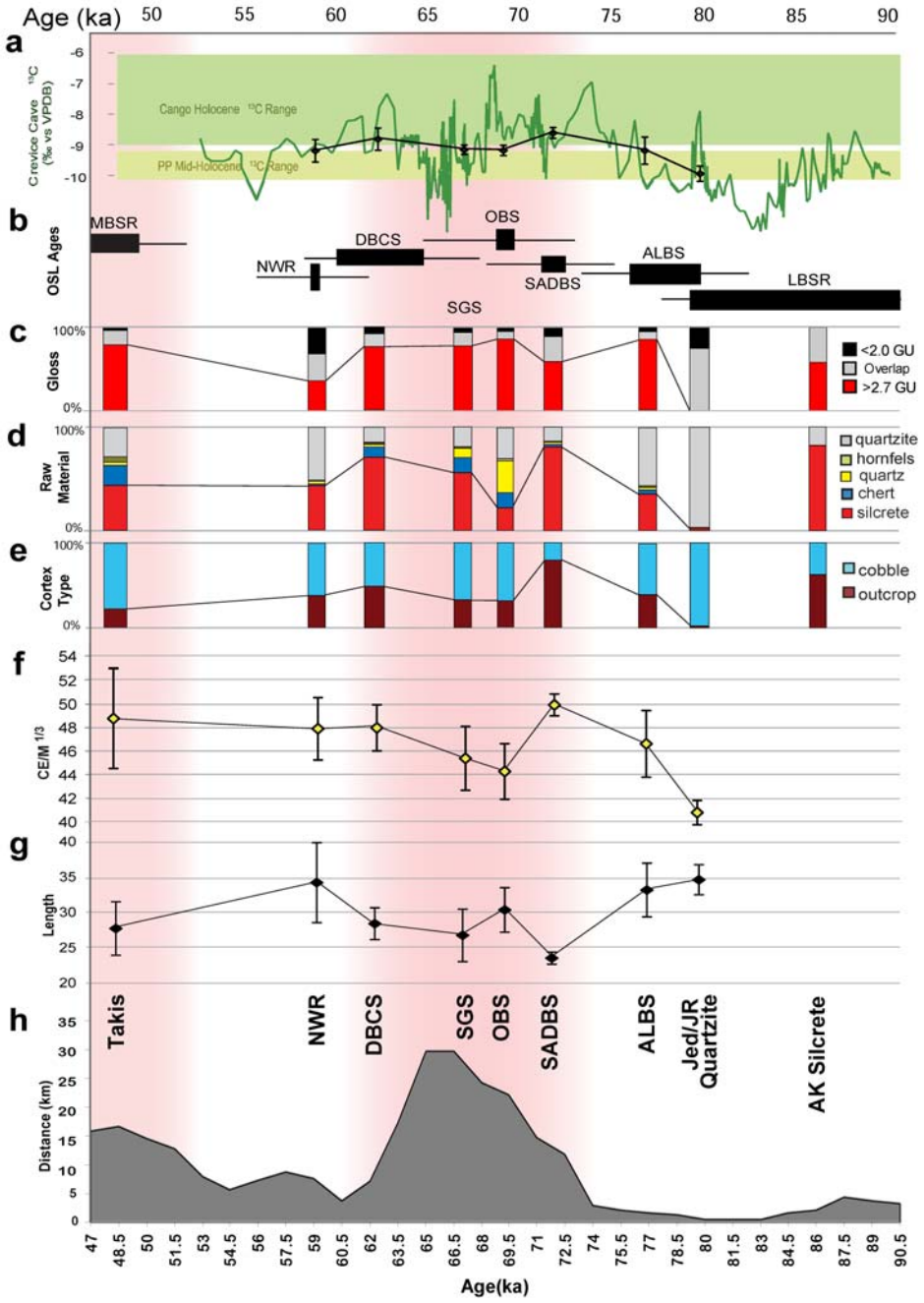

Figure 80. Visual comparison of test variables analyzed in Chapters 8-11 and paleoenvironmental contextual data for most of the PP5-6 analytical samples: a) Crevice Cave $\delta^{13}C$ Curve from Bar-Matthews et al. (2010) with mean values and 95% confidence level for the OSL range of each analytical sample overlain in black; b) PP5-6 StratAgg chronology based on OSL ages (Brown et al. 2009); c) silcrete maximum gloss analysis; d) raw material percentage by analytical sample; e) percentage cortex type; f) CE/M$^{1/3}$; g) mean flake length; f) mean distance to the coastline from Fisher et al. (2010). The red shading in the background shows where the peak values in silcrete proportions, primary outcrop cortex, and CE/M$^{1/3}$ were predicted for the Site Context Model.

Summary of Results and Evaluation of the Site Context Model

The results of the analyses presented in this dissertation demonstrate significant technological differences in how raw materials were used at PP5-6. The expectations of the Site Context Model are supported in many of the analyzed PP5-6 assemblages (Table 60) and would be more strongly supported if only the two largest PP5-6 lithic assemblages (in terms of weight and artifact count) were compared. Jed/JR Quartzite and the *SADBS* have been shown in this study to be significantly different from each other in almost every test variable examined. The Jed JR/Quartzite sample is from occupation layers where the coastline is modeled to have been close to PP5-6 (1.2km mean distance). The *SADBS* occupation is modeled to be associated with coastline regression (c.13km mean distance).

There are four assemblages with variables that consistently differ from the expected values predicted in the Site Context Model. These assemblages include the *ALBS, SADBS, OBS, and SGS*. The patterns can be visualized in reference to Figure 80. The *SADBS* and Jed/JR Quartzite samples represent the opposite extremes in values of most variables. The *ALBS* and *SADBS* have tested mean values that typically peak prior the maximum MIS regression (Fig. 80d-f,h). Values for the *OBS* are usually contrary to what was predicted for the MIS 4 coastline maximum distance. The exception for the *OBS* is that gloss values remain high even though silcrete percentages are low in comparison to contiguous StratAggs (Fig. 80c).

It was noted in Chapter 3.2 that the Fisher et al. (2010) coastline model is not yet orbitally tuned so that it is likely that there will be some adjustment to the model based on new data. Similarly, an additional set of OSL ages will soon be available for PP5-6. The coastline curve and the plotted analyzed variables in Figure 80 would be in better agreement if the *SADBS* peak lined up with the peak of the coastline model. This scenario would require an adjustment of up to 5000 years which seems very unlikely. The presence of shellfish in the assemblage from the present base of the *LBSR* through the *SGS* would probably not support a distance to coastline peak in the *SADBS*.

Table 60. Summary of results for comparison of PP5-6 analytical sample variables with distance to coastline. The presence of a 'y' indicates variables that fit the expectations of the Site Context Model, and an 'n' indicates predictions that were not met.

Sample	Test Variables					
	Raw Material	Cortex Type	Heat Treatment	Cortex Abundance	Flake Size	CE/M$^{1/3}$
Takis	y	n	y	n	n	n
NWR	y	y	n	n	n	n
DBCS	y	y	y	n	n	n
SGS	y	n	y	n	n	n
OBS	y	n	y	n	n	n
SADBS	n	n	y	n	n	n
ALBS	n	n	n	n	n	n
Jed/JR Quartzite	y	y	y	n	y	y

The Site Context Model is not strongly supported when technological variables from all PP5-6 stratigraphic samples are compared together (Figs. 80c-h; Table 60). The Jed/JR Quartzite sample sets the pattern expected from a coastal occupation with an assemblage made predominantly from quartzite cobbles. Major changes in technological patterning at PP5-6 begin in the *ALBS* and then peak in the *SADBS* prior to the maximum distance to coastline predicted by the Fisher et al. (2010) model. The *OBS* assemblage is estimated to occur temporally near the climax of the MIS 4 coastline regression but the *OBS* assemblage looks different than what was predicted by the Site Context Model in terms of raw material proportions, cortex, flake size, and CE/M$^{1/3}$.

The Site Context Model may be viewed as a version of a distance-decay model (Renfrew 1969; Blumenschine 2008) where constraints on raw material availability were expected to contribute to the conservation of raw materials and the manner in which nodules were prepared and transported to site. In contrast to most models that have examined the effects of raw material availability on technological variability (Bamforth 1990; Kuhn 1991; Andrefsky 1994), here it is argued that quartzite and potentially other secondary source raw materials can be seen as moving targets on the landscape during fluctuations in coastline and no explicit argument was invoked for changes in human mobility or settlement. Like some of the other studies investigating the effects of raw material availability summarized in Chapter 2.0 (Kuhn 1991; Milliken 1998), many of the variables investigated in this study did not fit the predicted patterns. In this study, 17 comparisons of test variables and distance to coastline matched the expected predictions and 31 did not fit the expectations of the Site Context Model (Table 60).

Some of the data presented in this study are subject to revision based on larger samples of lithics, and updates to the coastline model, site stratigraphy and OSL

chronology. Based on the present data, the Site Context Model shows a significant relationship between the ratio of quartzite to non-quartzite raw material and distance to coastline but did not show dependence with the other technological variables tested from PP5-6. The results of the PP5-6 analyses presented in this dissertation can however contribute to previously proposed models for understanding the Cape MSA Raw Material Pattern.

12.2 Key Findings-PP5-6 Lithic Assemblage

The analysis of PP5-6 lithics has identified a number of important and significant relationships in the use of raw material between c. 50-85ka. The sequence is summarized here highlighting the timing of technological change identified in the sequence, and key points are bulleted with significant relationships presented in Table 61. The summary begins in the *LBSR* at the base of the analyzed PP5-6 sequence.

Excavations on the PP5-6 *LBSR* are ongoing and the base of the excavated deposit now extends several meters below the assemblage described here. The analyzed PP5-6 *LBSR* sequence spans from approximately 79-86ka. There are a number of thin occupation horizons that were described in Chapters 7.2.2 - 7.2.6 that are rich in shellfish but have relatively small lithic samples that do not yet offer the possibility for detailed technological comparison. The largest *LBSR* lithic sample analyzed in this study is Jed/JR Quartzite which delineates the top of the *LBSR* sequence. The *LBSR* occupations, and particularly those of Leba Quartzite (~90ka) and Jed/JR Quartzite (~79ka), appear to have been focused on the production of quartzite points (Fig. 81). The *LBSR* as a whole is dominated by quartzite debitage made almost exclusively from beach cobbles based on the analysis of cortical products.

- The association of quartzite raw materials and beach cobble cortex is a significant pattern that occurs throughout the *LBSR* and most of the PP5-6 sequence.

Two thin layers identified in the lower portion of the analyzed *LBSR* sequence are of interest because the proportion of non-quartzite raw materials is much higher than in the surrounding layers. AK Silcrete (Ch.7.2.3) has a low sample count but has a raw material distribution that strongly favors silcrete (80%) and is represented by at least five different nodules. Cortical pieces demonstrate that silcrete derives from primary outcrops

and not beach cobbles like the majority of materials from surrounding stratigraphic samples. Specimens analyzed for gloss (7 of 12) had maximum gloss values indicative of heat treatment (Ch. 8.4). Thus the small AK Silcrete sample (c. 86ka) shares technological features with both the *LBSR* and also the later *SADBS*. The HM Silcrete/Hornfels assemblage (~83ka) shows a similar pattern in the flaking of non-quartzite raw materials. Refitting shows that many of the hornfels artifacts can be attributed to cortical reduction of perhaps two nodules. Several HM Silcrete/Hornfels silcrete cortical flakes have cobble cortex and one of these has clear heat treatment gloss along with four other non-cortical flakes with maximum gloss that overlaps with the heated experimental sample.

- The AK Silcrete and HM Silcrete/Hornfels samples show that even in thin layers that may have resulted from very short occupations, when silcrete was collected it was usually heat treated prior to flaking. The significance of this observation is discussed in more detail below.

The largest sample from the *LBSR* in terms of artifact counts and weight is the Jed/JR Quartzite assemblage at c. 79ka. Evidence for raw material procurement suggests a strategy based on the collection of quartzite cobbles from secondary contexts. The coastline model predicts that these cobbles may have been available from beaches that were located at a maximum of 1-2 kilometers from site. The analysis of core primary form indicates that the size of the cobble selected in Jed/JR Quartzite may have been larger than in the other assemblages. There are low percentages of non-quartzite raw materials (5%) and only 19 total pieces of silcrete, none of which show gloss with values that can be clearly attributed to heat treatment. The analysis of cortex abundance (Ch. 10) demonstrated that most of the Jed/JR Quartzite cortical products are present on site (Cortex Ratio 0.88) probably indicating that most of the cobbles were flaked on site.

Quartzite cobbles were reduced using a prepared core method for the production of quartzite points and a few blades, but cores were further reduced centripetally prior to abandonment. Some of the quartzite end products, including facetted flakes and points have $CE/M^{1/3}$values on the lower end of the scale when compared to blades and suggests that raw material conservation was not necessarily a primary consideration in quartzite point production. The Jed/JR complete flakes (all raw materials) are the largest in terms of length, width, thickness and weight and have the lowest $CE/M^{1/3}$ mean values of any other analyzed sample (Fig 80f) which is a function of the extremely high percentage of

quartzite debitage. The few complete silcrete flakes from Jed/JR (n=5) are shorter and are significantly narrow, thinner, and lighter than the Jed/JR quartzite complete flakes.

- In the sample of complete flakes from PP5-6, mean flake dimensions are always longer, wider, thicker, and heavier for quartzite flakes compared to silcrete flakes. This holds true in comparisons of quartzite and silcrete between analytical samples as well, where most differences are significant.

The Jed/JR Quartzite assemblage was one of the few analytical samples that consistently met the predictions of the Site Context Model. The Jed/JR Quartzite assemblage is interpreted to come from a coastal occupation where quartzite cobbles were collected from beaches near to site.

The transition away from the predominant use of quartzite at PP5-6 occurs within the *ALBS* (mean distance to coastline of approximately 3km). The lower *ALBS* Conrad Series SubAggs show very low density tool production still focused on quartzite cobbles. 'Jocelyn' shows increased use of silcrete from primary contexts, chert, and quartz. The 'Erich' assemblage consists mainly of primary outcrop silcrete. The gloss analysis shows that the majority of the *ALBS* silcrete is heat treated (c. 85%). Overall, there are few complete debitage products in the *ALBS* but there is a small sample of chert and silcrete blades that are significantly shorter than those made on quartzite. The sample of complete *ALBS* flakes demonstrates that both silcrete and quartzite flakes are narrow and more elongated in comparison to those from Jed/JR and there is a corresponding significant increase in $CE/M^{1/3}$ values in the *ALBS* when compared to Jed/JR (Fig. 80f). There are also a few small *ALBS* points (Fig 81).

- The unexpectedly high values of silcrete raw material, primary outcrop cortex, and maximum gloss values for the *ALBS* demonstrate that the change in raw material properties observed between the *SADBS* and Jed/JR Quartzite occurs in the *ALBS* when the coastline has only retreated by only a few kilometers. The differences between quartzite and silcrete size and $CE/M^{1/3}$ between silcrete and quartzite are accentuated in the *ALBS*. The Crevice Cave carbon isotopes show that the technological transition occurs during an interval with increasing contribution of C4 vegetation and gradual regression of the coastline.

The *SADBS* completes a transition which began in the *ALBS* from the use of predominantly secondary context raw materials in Jed/JR Quartzite (Fig. 80e) to an almost complete reliance on primary context silcrete which is available today 8.5km from

site and becomes very abundant at 20km. The majority of the silcrete was heat treated. Quartz, quartz crystal and chert appear in low frequencies in the upper *SADBS*. The *SADBS* raw material procurement strategy is argued to be very different than what was observed in the Jed/JR Quartzite assemblage.

- The *SADBS* shows a strategy of reliance on silcrete from primary outcrops which was then heated prior to flaking. This co-association between primary outcrop acquisition and heat treatment, which was observed as early as 86ka in the small *LBSR*-AK Silcrete sample, is argued to represent a strategy that required a level of forward investment in planning and energy expenditure that is inconsistent with models that view silcrete procurement as opportunistic.

The *SADBS* lithic assemblage is dominated by blade products that would fit many published definitions for microlithic and bladelet technology (Bar-Yosef and Kuhn 1999; Straus 2002). *SADBS* blades (mean length- 24mm, mean width- 11mm) are made predominantly from silcrete and chert and have plain platforms typically with abrasion on the platform edge adjacent to the flaking surface. Most of the *SADBS* silcrete was heat treated prior to flaking. Crested blades and small unidirectional and bidirectional blade cores support the characterization of the *SADBS* as a small blade focused assemblage although quartzite reduction in the *SADBS* appears to have been secondary parallel strategy aimed at making larger blades and small facetted points. The points are smaller than those of the PP5-6 *LBSR*. *SADBS* blades are shorter and narrower than those of the PP5-6 *DBCS* and Klasies River HP.

The very small *SADBS* debitage size range as a whole occurs alongside the highest $CE/M^{1/3}$ values of any analyzed PP5-6 assemblage (Fig. 80f). Silcrete complete flake metrics are not consistently different across most of the analytical samples. *SADBS* Silcrete flakes are significantly shorter than those of the *OBS* and *DBCS* (HP), and significantly narrower than all other silcrete samples except for the *ALBS*. *SADBS* silcrete and quartzite flake metrics fall on the low range of values when compared to most other samples. *SADBS* complete flakes have the highest $CE/M^{1/3}$ mean value which is a function of having high mean L/W values (more elongated flakes products) for both silcrete and quartzite but also raw material proportions that are dominated by silcrete.

- In the sample of complete flakes from PP5-6, mean $CE/M^{1/3}$ and L/W values are significantly higher for silcrete and chert versus quartzite flakes. Silcrete and chert flakes are more elongated and have more cutting edge per mass unit.

- Flake metrics and $CE/M^{1/3}$ do not show much significant variation when comparisons are made between the same raw materials across analytical samples. When all raw materials are considered, variability in flake metrics and $CE/M^{1/3}$ are significantly correlated with raw material percentages within the analytical samples.

- An exception is that *SADBS* and Jed/JR debitage often represent the minimum and maximum endpoints of many of the examined attributes and do show significant differences in many test variables.

The analysis of core primary form and maximum debitage and core dimensions (Ch. 9) demonstrate that the *SADBS* silcrete artifacts have the lowest mean flake dimensions with no silcrete products greater than 55mm in over 3500 analyzed artifacts. It is unlikely that the reduction in *SADBS* debitage size is entirely the result of smaller available nodule size because the same primary silcrete sources and materials should have been available relatively close to site during all PP5-6 occupations. The *SADBS* has the highest Cortex Ratio of all samples suggesting that decortification probably occurred on site. *SADBS* tool makers may have been deliberately selecting smaller nodules for the production of smaller tools to reduce handling costs which ultimately contributes to the small size of the debitage and retouched tools.

SADBS formal tools are segments made from small silcrete and chert blades. Unlike most HP assemblages, there are few notched blades in the *SADBS*. The *SADBS* segments, which are discussed in more detail later in this chapter, are similar in form to those of the PP5-6 and Klasies River HP, but they are typically shorter and are significantly narrower. At PP5-6 segments make their first appearance in the *SADBS* approximately 5ka earlier than the HP.

- At PP5-6, the transition to silcrete use in the *ALBS* is followed relatively soon after by backed blade segments in the *SADBS.* At PP5-6 segments make their first appearance when vegetation is characterized by a shift to environments with more C4 grasses (Fig. 80a).

- The *SADBS* and its sample of small segments likely overlaps in age with the SB which represents a very different technological strategy found only 90km west along the southern Cape coastline at Blombos Cave.

The *OBS* caps the *SADBS* and in many ways represents a dramatic departure from what comes before and after. The environmental context of the time period marked by the

OBS dune formation is critical for understanding MSA technological variability because similar appearing dunes that are statistically synchronous effectively terminate occupations at PP5-6 and Blombos Cave that appear to represent the peak of technological complexity at each site.

The *OBS* assemblage was modeled to occur near the peak regression of the coastline model but the sample of lithics shows patterning inconsistent with what was expected from the Site Context Model. The assemblage has a low density of finds due to the volume of excavated dune sand (which may have built up over a relatively short period of time) so the observed patterning needs to be viewed with caution. Quartz is the most common raw material by sample count and quartzite makes up the majority when calculated by sample mass. There are elevated percentages of quartz and chert (compared to the *SADBS*) which seem to replace silcrete in the overall proportions of raw material. Silcrete still had some importance, as gloss analysis demonstrates that the *OBS* has the highest percentages of heated silcrete of the StratAgg assemblages. The majority of all non-silcrete raw materials have cobble cortex showing that most materials came from secondary sources.

OBS silcrete and quartzite debitage have mean flake metrics values that are not significantly different than most of the other analytical samples but the contribution of quartzite and quartz flakes (which are relatively wide and thick), brings down the mean $CE/M^{1/3}$ values. There are a few carefully made segments at the base of the *OBS* at the interface with the *SADBS* but no other backed pieces occur in the *OBS* sequence (Fig. 81). There is only one quartzite point. It is possible that the increased use of quartz is a substitute for the silcrete and backed blades that precede and follow this sample.

A similar shift to quartz and quartzite use was noted by Cochrane (2006) in three stratigraphic layers that occur between the HP and Post-HP assemblages at Sibudu Cave. Cochrane interpreted raw material selection in these layers as a disruption in "the normal pattern of raw material usage" (p. 86). It is not known how far inland the dune pulse at c. 69ka extended at Pinnacle Point, but it is possible that dune fields functioned as a barrier temporarily restricting access to some of the silcrete outcrops that occur inland from PP5-6. In the *OBS,* quartz may have been valued for its sharp edges at the cost of predictable fracture and could have been hafted in mastic without shaping by retouch. At Sibudu Cave, however, quartz use in the early HP is associated with the production of small segments so it is clearly possible to make standardized retouched tools on quartz (Wadley and Mohapi 2008).

The *SGS* assemblage shows a return to mainly silcrete use and small blade production. There are still inflated proportions of chert (especially in 'Tamu') and quartz with cobble cortex.

- Complete chert flakes have length, width, thickness, weight, $CE/M^{1/3}$ and L/W attributes that are not significantly different than silcrete flakes. Chert and silcrete flakes also show a similar potential for high $CE/M^{1/3}$ values and low thickness values. Silcrete and chert were both used to produce small blades and segments and may be considered functionally equivalent raw materials in how they were used at PP5-6. Silcrete was typically acquired from primary outcrops but most chert has pebble cortex

SGS chert and quartzite debitage have slightly larger mean dimensions than flakes in the SADBS with less elongated products and higher percentages of quartzite and quartz which result in relatively low $CE/M^{1/3}$ when compared to other silcrete-rich assemblages. The *SGS* has a small sample of segments (Fig 81) which are shorter than those of the *DBCS* and wider than segments from the *SADBS*. The *SGS* requires additional OSL ages and continued excavation to clarify its stratigraphic relationship with the *DBCS* and *OBS*. The *SGS* results presented here are preliminary and will not be discussed in more detail until publication.

The *DBCS* is considered to be an HP occurrence at PP5-6 based on backed and notched pieces and ages of 60-65ka (Brown et al. 2009). The technological variables analyzed for the *DBCS* look very much like those of the *SADBS* but there is a slight falloff in most of the technological patterning which can be seen to have peaked in the *SADBS* (Fig. 79). *DBCS* raw material percentages favor silcrete although there are still elevated percentages of chert in comparison to the *SADBS* which inflates the percentage of cobble cortex in comparison to primary outcrop cortex. The gloss analysis shows that the majority of the *DBCS* silcrete was heat treated. The DBCS has larger mean debitage size and lower mean $CE/M^{1/3}$ values in comparison to the *SADBS*. The *DBCS* has segments and notched tools. The segments are wider and more variable than those of the *SADBS*.

- The PP5-6 *DBCS* (HP) segments occur at 60-65ka during a period that, like the *SADBS* occupation, can be characterized as having a strong C4 vegetation signal.

The PP5-6 *NWR* (~59ka) can be characterized as a typical Post-HP or MSA III assemblage in terms of raw material use. There is a noticeable decrease in the percentage of silcrete although the raw material proportions do not approach the quartzite dominant patterns observed in Jed/JR Quartzite. There is a corresponding increase in the percentage of cobble cortex which can be associated with the increase in quartzite use. Silcrete debitage metrics are not significantly different than silcrete from any other analytical sample. *NWR* quartzite flakes have the highest mean flake length but are extremely variable. What is interesting about the *NWR* is that quartzite and silcrete raw material proportions are similar and there is overlap in mean L/W between silcrete and quartzite flakes which results in a relatively high $CE/M^{1/3}$ mean value for the total sample. The percentage of silcrete drops below 50% but unlike the *OBS* sample, the *NWR* shows a corresponding decrease in the frequency of artifacts with gloss indicative of heat treatment, approximating the experimental 50% heated histogram (Ch. 8.4). There are few retouched tools in the *NWR* with the exception of a single segment and one obliquely truncated blade. The quartzite was used in the *NWR* to produce larger points (Figs. 50,81) and blades similar to those of the LBSR. The *NWR* occupation is associated with a decrease in C4 vegetation in comparison to the preceding *DBCS*.

The Takis sample (~48ka) shows a slight increase in silcrete use in comparison to the *NWR* and has the highest percentage of chert. Takis is the only sample where silcrete cortical debitage shows an even proportion of cobble and outcrop cortex (8 specimens each). Consequently, the total ratio of cobble to outcrop cortex is lowest in this assemblage. Takis has a variable mixture of flakes and blades but overall the mean metric values of debitage are smaller than those of the *NWR* and the $CE/M^{1/3}$ ratio is marginally higher due to the increased percentage of silcrete in Takis compared to the *NWR*.

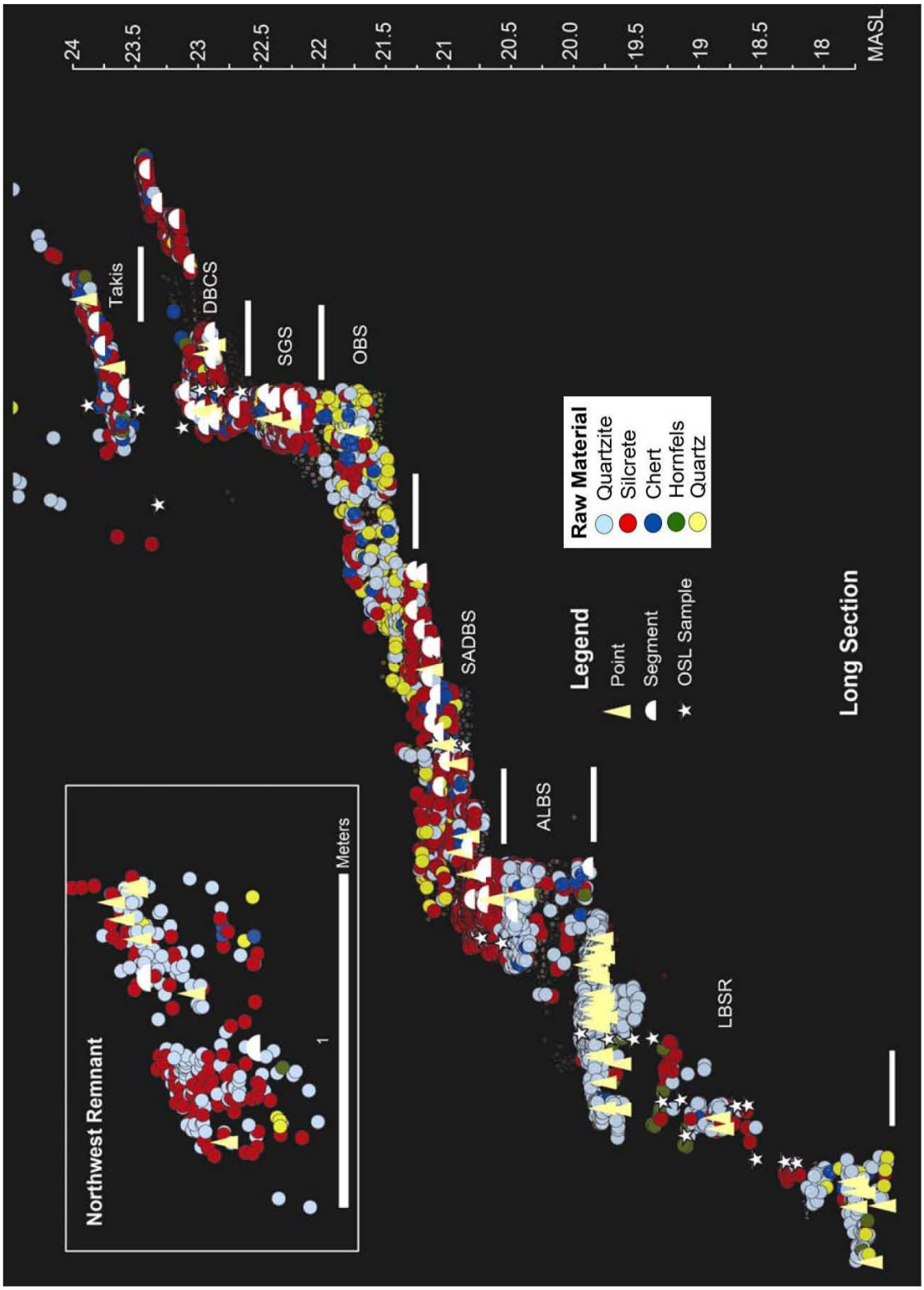

Figure 81. The distribution of complete and fragmentary points and segments superimposed on raw material plots from the PP5-6 StratAgg sequence

PP5-6 Summary of Technological Patterns

The PP5-6 sequence is best summarized by examining the relationship between the test variables compared above in Chapter 12.1 and itemized below in Table 61. Cortex type, mean debitage dimensions, and $CE/M^{1/3}$ can be significantly correlated with the choice of raw material. The ratio of quartzite to non-quartzite raw material is significantly correlated with distance to coastline. Silcrete percentages and cortex type are not correlated with distance to coastline but are instead significantly correlated with $\delta^{13}C$ from Crevice Cave. The two samples with highest percentage of silcrete (*SADBS* and *DBCS*) have the highest mean $\delta^{13}C$ measurements from Crevice Cave (Table 3).

There is a strong relationship that has been developed in this study between raw material use and cortex type. Specifically, silcrete is associated with primary outcrop cortex. Quartzite, chert, and quartz are associated with cobble cortex. Thus for assemblages where silcrete is the predominant raw material (*SADBS*, *SGS*, and *DBCS*), most silcrete came from primary sources, often in the form of flake blanks. Quartzite, hornfels, chert and quartz most commonly came from secondary sources as water worn pebbles or cobbles regardless of the modeled distance to coastline.

Flake metrics and $CE/M^{1/3}$ are each significantly correlated with the proportion of silcrete and chert versus quartzite in the analytical samples. Quartzite flakes are significantly larger than silcrete flakes (length, midpoint width, midpoint thickness and weight) and therefore samples with higher percentages of quartzite will have larger mean flake dimensions than samples where silcrete is the predominant raw material. $CE/M^{1/3}$ is significantly higher for silcrete versus quartzite complete flakes. Higher $CE/M^{1/3}$ in silcrete and chert is the result of complete flakes from these raw materials being more elongated and thinner than flakes made from quartz and quartzite. $CE/M^{1/3}$ is significantly correlated with the percentage of silcrete and chert in the analytical samples. With the exception of some variables in the *SADBS* and Jed/JR Quartzite, flake metrics and $CE/M^{1/3}$ do not vary significantly when comparing mean values from the same raw materials between analytical samples; this is partially due to low sample sizes that create wide confidence levels.

Heat treatment is obviously also associated with the choice of raw material. Unambiguously heated silcrete (based on the analysis of gloss histograms) occurs in every PP5-6 assemblage except for Jed/JR Quartzite where there are only 12 silcrete artifacts. Thin occupation layers in the lower *LBSR* sequence (c. 86-83ka) dominated by

non-quartzite raw materials have examples of heat-treated silcrete. Heat-treated silcrete occurs in the PP5-6 sequence in the *LBSR* and *ALBS* prior to the silcrete dominated *SADBS*.

The Jed/JR Quartzite and the *SADBS* samples illustrate the range of technological variability in the PP5-6 assemblage. The Jed/JR Quartzite occupation is modeled to occur near the coastline and has a strong C3 signature. The lithic assemblage is dominated by cores and debitage made almost exclusively from quartzite cobbles. Debitage size is variable and the sample has low mean $CE/M^{1/3}$. Jed/JR end products are quartzite points and also flakes made from opportunistically flaked cores. The *SADBS* is modeled to be more of an inland occupation with increased contribution of C4 vegetation. Raw material use was focused on silcrete from primary sources, the majority of which was heat treated. *SADBS* silcrete and quartzite debitage stand out as being relatively short, narrow, elongated and thin in comparison to most other samples and has the highest mean $CE/M^{1/3}$. Silcrete in the *SADBS* appears to have come from very small nodules. End products are small blades and segments made from silcrete and a few examples on chert. *SADBS* quartzite end products include blades and small points that are larger than those made on silcrete but smaller than those of the preceding Jed/JR and *ALBS* samples.

Table 61. Summary of statistically significant results by analysis

Signficant Results	
Raw Material	Ratio of Quartzite to Non-quartzite raw materials and distance to coastline signficant for all samples
	Silcrete percentages significantly correlated with δ13C for all tested samples
Cortex Type	Covariance between silcrete with primary outcrop cortex and quartzite with cobble cortex is significant
	Ratio of Cobble/Outcrop cortex significantly correlated with δ13C for all tested samples
Flake Size	Quartzite flakes significantly larger than silcrete flakes
	Silcrete and chert flakes are not significantly different in size
	Flake metrics signficantly correlated with the percentage of silcrete and chert in each sample
$CE/M^{1/3}$	$CE/M^{1/3}$ signficantly higher for silcrete and chert compared with quartzite
	$CE/M^{1/3}$ signficantly correlated with ratio of Length to Width (L/W)
	$CE/M^{1/3}$ signficantly correlated with combined percentage of silcrete and chert for each sample

12.3 Discussion

The Site Context Model was deliberately proposed as a null hypothesis to investigate the effects of distance to source on the PP5-6 lithic sequence as a necessary first step in understanding behavioral variability in raw material selection at PP5-6. The Site Context Model was based on the premise that raw materials were chosen according to distance as a proxy measure for cost of procurement. The estimates of distance were calculated as if PP5-6 was the center of settlement and mobility and that procurement would require logistical forays to access resources. It should also be emphasized that the Site Context Model linked the selection of silcrete with changes in the distance to secondary sources of quartzite. The distance to primary sources of silcrete is not expected to have changed with movement of the coastline. The decision to collect silcrete was modeled to be dependent on the relative costs of acquiring secondary context quartzite, which were demonstrated in Chapter 6 to vary significantly with changes in the position of the coastline from global climate change.

It has been demonstrated in this study that at PP5-6 there are significant technological differences in attributes associated with silcrete and quartzite lithics including patterns of procurement, raw material preparation, debitage size, recovery of cutting edge, and the production of formal retouched tools. There are three innovations that occur early at PP5-6 that offer clues to the potential differences in the roles of the major classes of raw materials at PP5-6. First, heat treatment technology and its associated costs appear well before the prominent shift in raw material use in the *ALBS* and *SADBS*. Silcrete use and its clear association at PP5-6 with the exploitation of primary outcrop materials is the second innovation to consider, and third is the adoption of small blades and segments made from fine-grained raw materials. Each innovation represents a choice to invest in more time intensive technologies and each has a different chronology for appearance at PP5-6.

An important point for consideration in modeling technological investment is the question of whether there is the replacement of one technology with another, or whether there are parallel “classes” of technologies that perform different roles within a larger resource procurement system (Bettinger et al. 2006: 540). Despite the apparent investment in technological innovation associated with the proliferation of silcrete use, both silcrete and quartzite are consistently represented throughout the PP5-6 assemblage and this study has demonstrated that there is continuity (with some inter-sample variation)

in many of the examined attributes for each of these raw materials that can be tracked across the entire PP5-6 assemblage. Silcrete was almost always heat treated even when it wasn't used to make backed blades. Silcrete flakes from each analytical sample have mean dimensions that are always smaller than quartzite. Silcrete consistently yields more cutting edge per mass unit of stone than quartzite. These differences are significant for most of the analytical samples. Even though small blade production on silcrete and chert becomes common after the *ALBS*, silcrete was still used to make small tools, relative to quartzite in the *LBSR*. Quartzite use and point production peaks in the Jed/JR sample but in the more recent occupations where the proportion of silcrete is dramatically higher, quartzite was still preferentially selected for the production of larger points and blades.

The Site Context Model was unable to predict all of the details of hominin technological investment because the costs and benefits of raw material selection need to consider more than just distance to source. Here it is useful to revisit the Chapter 2 discussion of why certain raw materials may have been selected with attention to the two major types of stone used at PP5-6. This discussion will show that the choice in selection of silcrete and quartzite (and often other PP5-6 raw materials) should be viewed independently and in an expanded context that considers distance to source in addition to human mobility and site use patterns on a dynamic paleolandscape.

At Pinnacle Point it is difficult to separate the technological decisions for the use of silcrete and adoption of heat treatment because almost all of the silcrete tested from the combined PP13B and PP5-6 sequences has been heat treated (Brown et al. 2009 and Ch. 8). Heated silcrete occurs in low frequencies even in quartzite-rich layers well before the prominent shift in raw material use in the *SADBS*, and also before the appearance of segments in the PP5-6 sequence. It is important to understand why silcrete was not typically used in its raw form at Pinnacle Point and why this investment in heat treatment occurs even in layers where silcrete artifacts are few.

Almost every study involving heat treatment of lithic raw materials, including this dissertation, has cited improvements in flaking quality as being the principal benefit (Bordes 1969; Crabtree and Butler 1964; Inizan et al. 1992; Luedtke 1992; Mandeville and Flenniken 1974; Schindler et al. 1982; Brown et al. 2009; Mourre et al. 2010; Rick and Chappell 1983; Wilke et al. 1991; Flenniken and White 1983). Studies of mechanical properties associated with heat treatment of lithic materials have consistently recorded changes in physical properties that track flaking quality in lithologies that respond to heat treatment. Studies commonly document a reduction in fracture toughness and an increase

in Young's Modulus after heating (Beauchamp and Purdy 1986; Domanski et al. 1994). These properties have been positively correlated with ease of fracture, and an increase in the modulus of elasticity (or Young' Modulus) which tracks material stiffness or rigidity.

Actualistic and mechanical flaking studies of siliceous raw materials have demonstrated an improvement in the ability to detach longer, thinner flakes after heat treatment due to changes in the rigidity of the material caused by heating (Crabtree and Butler 1967; Rick 1978; Bleed and Meier 1980). Material stiffness has been argued to be important in blade production (Webb and Domanski 1992) as stiffness-controlled fracture propagation is essentially responsible for the ability to create long, thin flakes (Cotterel et al. 1985) regardless of the technology employed. Heat treatment has been cited as being beneficial to blade production to make "less preferred materials" more brittle (Flenniken 1987:118), and to improve the flaking quality of transported blade cores (Lea 2005). Heat treatment is beneficial in biface reduction because thinning flakes travel further across the bifacial core allowing for removal of more mass with less effort (Mandeville and Flenniken 1974). Flenniken and White (1983) note that heat treatment of silcrete allows the raw material to "…be used for purposes it would be unsuitable in its original state"(p.45), and that in Australia, even when core reduction appears to have been relatively simple and static, heat treatment was often applied at various stages of the reduction sequence.

The potential benefits of heat treatment are not limited to improvements in the flaking performance of a material. Other advantages include an increase in the sharpness of cutting edge (Rick and Chappell 1983), and reduction in raw material search costs when inferior local materials are improved (Flenniken and White 1983). The flaking of heat treated materials also results in fewer step fractures during manufacture in comparison to unheated stone (Mandeville and Flenniken 1974; Appendix 1, Fig. 5, this study). Changes in color or luster may also have been desirable.

The foremost disadvantage of heat treatment is that it has associated costs in energy and time. Heat treatment fires require the collection of wood fuels to sustain the heat necessary to anneal the raw material, usually a temperature of 300-500°C over a period of 12 to 24 hours (Luedtke 1992). In addition to the collection of necessary materials (wood fuel and stone), the process would also require the scheduling of other activities around the preparation and maintenance of the fire. Managing the fire potentially takes time away from the ability to perform other critical tasks. The decision whether to heat a raw material obviously first rests on the requirements of the intended

tool use, and specifically if these activities require a raw material that maximizes flaking qualities and/or sharpness of cutting edge. Second, the choice to heat treat a raw material is dependent upon whether there are other lower cost options available with acceptable flaking and edge-sharpness properties in their raw form.

Silcrete composition, fabric, and homogeneity are extremely variable, and this is true between samples from the same source area (Roberts 2003; Corkill 1999), or even from either end of the same flake (Rowney and White 1997). The physical properties of silcrete and it suitability for knapping are controlled in part by contributions of grains and inclusions from the weathering profile of the parent geology that make up its fabric (Summerfield 1983; Domanski et al. 1994). Australian silcrete in raw form has mechanical properties that are variable, typically ranging between those of quartzite and chert (Cotterell and Kamminga 1990; Rowney and White 1997).

The improvements in flaking properties after heat treatment have been extensively researched on Australian silcretes (Domanski et al. 1994; Hanckel 1985; Flenniken and White 1983). Heat treatment of the South African silcretes tested in collaboration with this author's supervisor have been demonstrated to bring the flaking quality of raw silcrete (which has Young's Modulus values lower than unheated Australian silcrete) in-line with the tested properties of chert and silcrete samples from Australia (Brown et al. 2009). Thus heat treatment is a means for making the flaking quality of silcrete nodules better and more predictable. If treated silcrete is more like chert than quartzite, the question then becomes, what are the advantages of selecting fine-grained heated silcrete, chert, or quartz versus the more coarse-grained quartzite? The answer likely has to do with differences in the range of mechanical properties for these materials and the intended use of the finished tools.

Published fracture toughness values for quartzites vary but generally range between 2.0-4.0 MPa m $^{1/2}$ (Sevillano 1997) and are on average higher than those of chert at 1.2-1.8 MPa m $^{1/2}$ (Sevillano 1997); unheated silcrete 2.5-2.0 MPa $m^{1/2}$ (Domanski et al. 1994), heated silcrete 1.8-1.4 MPa $m^{1/2}$ (Domanski et al. 1994) and quartz at 0.3 to 2.1 MPa $m^{1/2}$ (Atkinson 1984). These values provide a relative scale of flaking quality for most of the materials discussed in this paper (Fig. 82), although it is acknowledged that the lithologies used at Pinnacle Point may differ to some degree once tested. The fracture toughness values indicate that unheated silcrete may overlap in flaking performance with quartzite but the heating of silcrete brings its flaking qualities closer to chert, which is much less abundant than silcrete in the Mossel Bay Region.

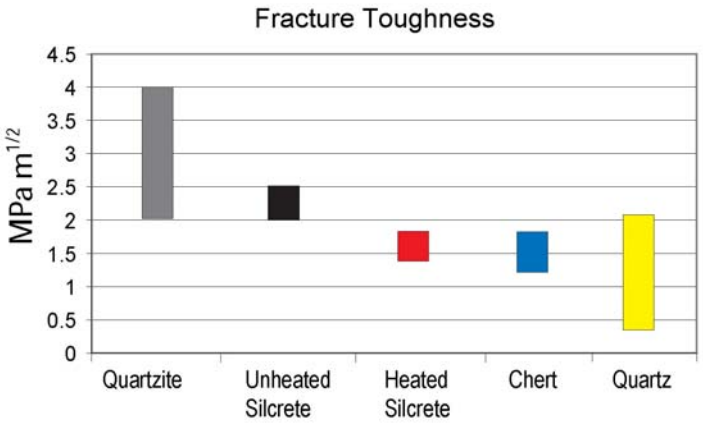

Figure 82. Fracture toughness values for the major classes of raw materials discussed in this study. Quartzite, chert and quartz from Sevillano (1997), silcrete values interpolated from Domanski et al. (1994: Fig.9).

On average, quartzite is more difficult to flake than silcrete chert and quartz. Other researchers have noted that coarse granular raw materials are less desirable for small blade manufacture because they are susceptible to step fracture terminations and limit the potential for reshaping or retouch (Webb and Domanski 2008, Kuhn 1990). However, the higher fracture toughness values may point to advantages in quartzite use. McCormick (1985) demonstrated a correlation between critical strain (strain where catastrophic fracture occurs), fracture toughness, Young's Modulus, and edge toughness. Edge toughness increases with critical strain, which is correlated with fracture toughness and Young's Modulus. This means that materials with relatively high fracture toughness values and lower overall Young's Modulus values will have edges that are more resistant to wear. Edge toughness is also positively correlated with edge angle and conversely, sharp or acute-angled edges are weakest (McCormick and Almond 1990). Edge strength is one advantage quartzite should have over heated silcrete, chert and quartz.

Sharpness of edge however, is dependent on the grain size of the material (McCormick and Almond 1990). The sharpest edges occur in the finest grained materials, which are more brittle, and less resistant to strain induced fracture (McCormick and Almond 1990). Since most siliceous materials show a decrease in fracture toughness and/or an increase in Young's Modulus after heating (Purdy and Beauchamp 1986; Domanski et al. 1994; Brown et al. 2009), in effect, heat treatment of silcrete should reduce edge toughness but create sharper more brittle edges (Crabtree 1967; Wilke et al. 1991).

The discussion above has developed some design perimeters for selecting specific raw materials, even if their sources occur at greater distances to site. Quartzite may have higher fracture toughness values making flaking more difficult but the toughness provides a more durable edge, observations also noted by Jones (1979) and Noll (2000) for ESA handaxes made on quartzite. Silcrete, once heated, becomes a higher quality flaking material on par with cherts from other parts of the world and has potentially sharper cutting edge, but at the expense of wood fuel and acquisition costs.

Would the expense of heat treatment be prohibitive? Heat treatment experiments performed by this author typically used 20kg of hardwood to heat an average of about 3kg of silcrete per trial with a very low rate of failure. For perspective, the entire SADBS assemblage consisting of 3556 silcrete pieces has a total mass of about ½ kg (Ch. 10, Table 53). By extrapolation, one experimental heat treatment session produced enough heated silcrete to account for the mass of archaeological specimens that might be expected in almost 5 cubic meters of SADBS deposit. Heat treatment costs may have been reduced by batch processing of heated blanks, collection of required materials during other activities, and maintaining a flaking strategy that produces more cutting edge per mass unit of stone. Heat treatment is a costly activity but there are ways of offsetting these costs.

Heat treatment improves the flaking quality of silcrete (Brown et al. 2009), but would this improvement have significantly benefited the production of small blades and segments? Throughout the PP5-6 sequence, silcrete (n=41) and chert (n=8) were preferentially selected for the production of backed pieces over quartz (n=2) and quartzite (n=1). Backed blades can be made from quartzite, but chert and heated silcrete have been demonstrated to allow for the greater control of thickness and production of longer blanks. Controlling thickness is important in the conservation of raw material (Mackay 2008; Ch. 11 this study) but should also be of concern in the standardized production of inserts for composite tools. The greater potential for higher overall cutting edge per mass unit made possible with silcrete and chert may also be a factor in the design of composite tools where a portion of the effective cutting edge is lost in the haft. It is not impossible to make backed blades on quartzite but at every site where backed blades occur, tool makers sought out the types of raw materials that provide more control over flaking (Ch. 3, Fig. 6) and especially allow for control of thickness which is suggested to be an important aspect of hafting.

Although many of the analyses presented in this study have focused on silcrete, data presented in Chapters 9 and 11 have demonstrated that heated silcrete and chert at PP5-6 were flaked in similar ways and can be considered functionally equivalent at PP5-6. Complete silcrete and chert flakes have mean dimensions, weight and $CE/M^{1/3}$ values that are not significantly different. Both show potential for the production of very thin elongated flakes. Both were used for the production of backed pieces. Quartz occurs in low density at PP5-6 and is found mainly in the *OBS* and *SGS*. At PP5-6 quartz mean flake dimensions are between those of silcrete and quartzite. Mackay (2008a) found relatively high edge length to mass unit (EL/M) values for quartz but PP5-6 quartz has the lowest mean $CE/M^{1/3}$. Undoubtedly quartz properties vary by region but PP5-6 quartz may have been selected for its potential for sharp cutting edge rather than predictable fracture and edge conservation.

Given the similarities in mechanical properties and flake attributes of heated silcrete and chert, consideration of distance to source may still be an effective way of explaining why it was worth the investment to heat treat silcrete when high quality or sharp-edged flaking materials were required. Chert occurs in the wider Mossel Bay region in primary context in the Ecca Group and has been found as pebbles on Kanon Beach, suggesting that it may also have been available from the Gouritz drainage (Ch. 5). Primary context Ecca Group chert could hypothetically provide a predictable supply of high quality raw material, but it occurs approximately 130km from Pinnacle Point, located on the backside of the Outeniqua Range (Fig. 83). Secondary context chert is located at a minimum distance of 30km from Pinnacle Point and that distance increases with travel up the Gouritz drainage. Secondary context chert would also require additional 'beach-combing' search costs at the collection locations to differentiate chert pebbles from less desirable raw materials. The sources for crystalline quartz are currently unknown but will likely be found at the interface between the Cape Granite Suite and TMS (Ferré and Améglio 2000) at a minimum distance of 35km from site.

Silcrete is predictable and abundant inland from Pinnacle Point (Fig. 83). From approximately 275° degrees W to 15° NNE or approximately ¼ of the distance around the compass it would be very difficult for a hunter gatherer not to encounter silcrete deposits when travelling away from site (Fig. 84). Approximately 4% of the ground surface geology (31 of $722km^2$) consists of silcrete within the NW quadrant of a 30km radius from Pinnacle Point (interpolated using ArcGIS polygon areas from digitized silcrete deposits on CGS maps).

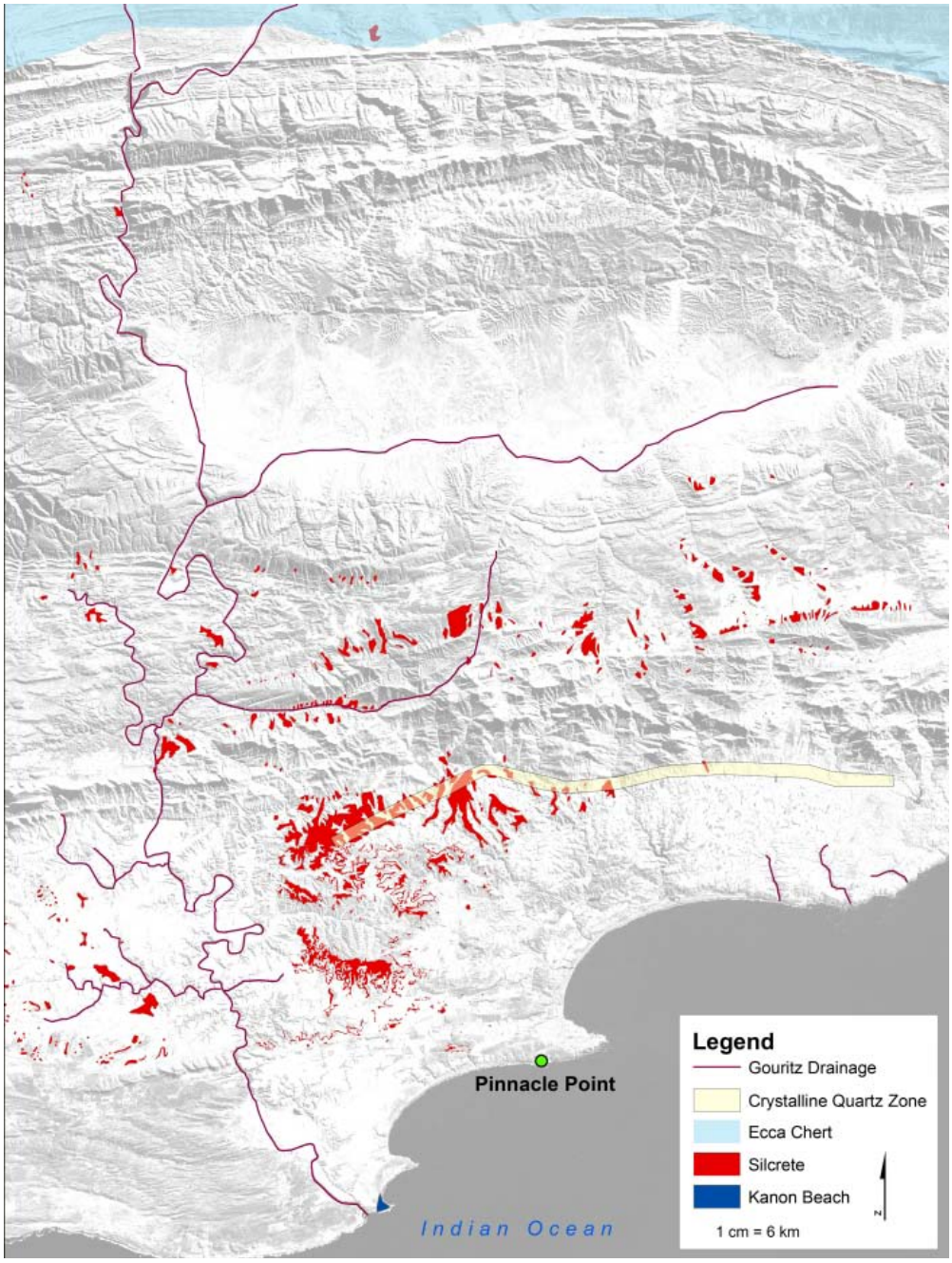

Figure 83. Map showing proximity of silcrete (red) in comparison to potential sources of chert (blue and Gouritz drainage) and crystalline quartz (yellow).

Hunter-gatherers should choose the least cost raw materials that meet their needs (Torrence 1989, 2001). It would make sense to collect raw materials of desired flaking quality without using heat treatment any time they were encountered on the landscape. If a predictable and abundant supply of raw material was required, it could be less costly to

invest in the heat treatment of silcrete. This is determined by both availability and design constraints. In situations where there was a technological requirement for raw materials of good flaking quality or ability to yield sharp edges, the heat treatment of silcrete would reduce the search costs for those materials (Flenniken and White 1983).

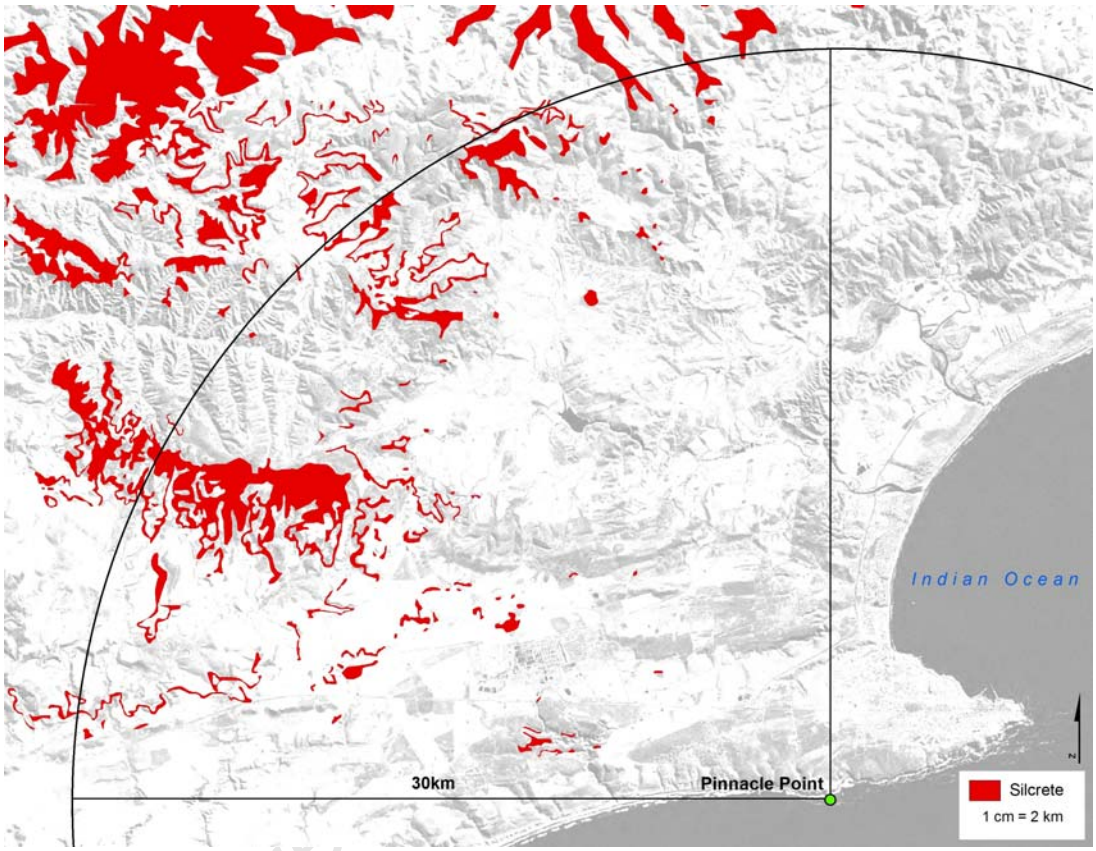

Figure 84. Distribution of primary silcrete sources in the Mossel Bay Region with 30km radius centered on Pinnacle Point. Perpendicular lines delineate how movement beyond 8.5km from Pinnacle Point in a northwesterly direction would inevitably result in a high encounter rate with silcrete sources

The costs associated with investment in silcrete and heat treatment may also be reduced by changes in provisioning strategy based on intensity of occupation, and mobility strategies that bring hunter-gatherers in greater contact with silcrete outcrops and the fuels required for heat treatment. Marean (2010b) has argued that the reliance on coastal ecosystems present logistical challenges to mobile hunter-gatherers. The return rate on shellfish is highest during spring low tides which occur approximately twice a month. During neap tide, the food yield from plant and animal resources would be maximized by placing residential camps further inland to get the best return rate on

terrestrial food resources (Marean 2010b). Thus the relative position of PP5-6 with respect to the paleocoastline would be expected to influence the character of resources exploited during occupations, the density of occupation, and also in modeling the movement of lithic materials tools to and from site. These observations are pertinent because all analytical samples with the exception of the *DBCS*, *NWR*, and Takis have abundant shellfish remains so PP5-6 resource structure is almost always tied to visits to the coastline.

Total plotted find density for each of the PP5-6 analytical samples is presented in Figure 85(c) as a proxy measure for intensity of site occupation. Find density was calculated by dividing plotted find counts by sediment volume (Table 3) which provides an estimate of the number of finds that would be expected in a cubic meter of sediment (and not the actual number of recovered artifacts). Sediment volume calculations are based on the cutoff date of the analyzed sample and will be updated after inclusion of data from the 2010-2012 excavation seasons. The analytical samples with the highest density of plotted finds include AK Silcrete, Jed/JR Quartzite, *SADBS*, *SGS*, and *DBCS*. The density of lithic artifacts (Fig. 85d) peaks in the Jed/JR, *SADBS*, *SGS*, and *DBCS* samples. A notable difference between the plotted find and lithic density graphs is that most of the *LBSR* samples show very low lithic density until the Jed/JR Quartzite occupation. This contrasts with the graph of total plotted finds which shows high artifact densities for Leba Quartzite and AK Silcrete, and this is almost certainly a function of high shellfish counts in these layers in comparison to the small excavated sediment volume. Plotted find and lithic densities are relatively low in the *ALBS*, *OBS*, *NWR*, and Takis samples and are subject to bias from a limited number of estimated core reductions (Ch. 10), which may partially explain why these samples often had test variables that contrasted sharply with those of contiguous samples.

The lighter density LBSR occupations between Leba Quartzite and Ludumo Quartzite occur within approximately 1-4km range of distance to coastline and the Crevice Cave stable carbon isotopes support a strong contribution from C3 vegetation. Site use may have been focused on short visits for the purpose of collecting shellfish during spring low tides (Marean 2010b). The low density lithic assemblages were made on locally available cobbles (as in the refitted hornfels cobbles from HM Silcrete/Hornfels) and could be considered an expedient strategy in the sense of Nelson (1991) where relatively simple tool production is intended for activities that occur near known sources of raw materials. In this scenario, a few cobbles may have been selected

during the collection of shellfish, and both shellfish and lithic raw materials were transported an estimated 1-4km to site for processing. A similar conclusion was reached for the quartzite-dominant MIS5-6 assemblage at nearby PP13B (Thompson et al. 2010).

Why was heat-treated silcrete present in these lower density *LBSR* occupations? This question is complicated by the lack of formal retouched tools or repetitive tool forms on silcrete found in the lower *LBSR* samples. There was probably always a requirement in the MSA for raw material with predictable fracture and very sharp cutting edges for some specialized activities to go along with the more durable-edged quartzite, even in layers where there are few formal retouched tools (Thompson et al. 2010). This is true for quartz, silcrete, and chert/opaline in non-HP layers at Klasies River (0.2-6.1%: Wurz 2000), PP13B (2.4-12.6%: Thompson et al. 2010), Nelson Bay Cave (0.7-1.6%: Volman 1981), and Border Cave (c. 3-19%: Beaumont 1979). All show a small but consistent percentage of quartz and fine-grained materials used in non-HP layers.

Given that raw silcrete has properties that are similar to quartzite, it would be less costly to use the more locally available quartzite from beach cobbles unless heated silcrete provided an edge quality that was not obtainable with quartzite. If there was alternating residential movement between the coastline and the coastal plain, the heat-treated silcrete lithics in the lower *LBSR* samples may have represented a strategy of provisioning people (Kuhn 2004) with relatively small and lightweight tools. Silcrete flakes and cores may have originated from inland residential locations closer to silcrete sources where the cost of silcrete preparation could have been partially offset by the collection of stone while performing other activities on the landscape. At other times, silcrete may have occasionally been collected when encountered in cobble form during the acquisition of other raw materials at cobble beaches, as was the case in HM Silcrete/Hornfels where some silcrete lithics have cobble cortex.

The Jed/JR Quartzite assemblage is from a dense occupation where the coastline is close to the MIS5/4 minimum. PP5-6 was close enough to the shoreline for this occupation or series of occupations to have had overlap between two critical resources directly adjacent to site; Jed/JR is rich in both shellfish and lithics. Quartzite density is highest in Jed/JR Quartzite (Figure 85e) and lithic reduction was focused on the production of points, blades, and flakes made from quartzite beach cobbles. Points are at their highest density in the Jed/JR Quartzite assemblage (Fig. 85g). Use-wear analysis of quartzite points discarded at PP13B has demonstrated that the majority of these artifacts have patterned edge-damage consistent with use as knives rather than hunting weapons

(Schoville 2010). The points and blades from PP5-6 are currently being studied by Ben Schoville for use-wear. If the same use-wear patterning holds at PP5-6, quartzite points and blades may have been produced during coastal occupations as knives with long durable cutting edges. During the Jed/JR quartzite occupation, PP5-6 may have functioned as a quarry location for the transport of quartzite points and blades to residential sites located further inland. The discarded debitage at Jed/JR has the lowest mean $CE/M^{1/3}$ values for quartzite and this may have been in response for less need to conserve the locally abundant raw materials, but it may also be the case that the more elongated blades with highest $CE/M^{1/3}$ values may have been transported away from site (as discussed in Ch. 11), effectively lowering the cutting edge to mass ratio for the remaining assemblage. There are few silcrete lithics in Jed/JR and only 5 complete flakes. This is the only analytical sample where there are no gloss values clearly indicative of heat treatment, although 6 out of 8 samples have values between 2.0 and 2.7GU which show overlap in experimental heated/unheated distributions (Ch. 8.5). Like the other analytical samples, Jed/JR silcrete lithics are smaller than those of quartzite with higher $CE/M^{1/3}$ values suggesting that there is continuity in the presence of small silcrete cutting tools throughout the *LBSR*.

The most significant pattern of technological variability associated with changes in raw material percentages at PP5-6 is the reduction in tool size and increase in both silcrete and quartzite $CE/M^{1/3}$ mean values that occur between the quartzite-dominant *LBSR* and silcrete-rich *SADBS*. The *ALBS* analytical sample is a low-density occupation that occurs between Jed/JR and the *LBSR*, and has an assemblage that is very small in terms of artifact counts that shows variability in debitage size and morphology. $CE/M^{1/3}$ mean values are higher than in the underlying Jed/JR Quartzite sample and there is also a trend in the *ALBS* to smaller and more lightweight tools prior to the climax in small tool size and high $CE/M^{1/3}$ values in the *SADBS*. A similar pattern was observed by Mackay (2008a) for the EL/M values leading up to the HP at Diepkloof and Klein Kliphuis. The coastline is modeled to be in regression and the $\delta^{13}C$ from Crevice Cave shows an increasing contribution from C4 vegetation, a pattern that is discussed in more detail below. The *ALBS* also shows an increase in acquisition of silcrete from primary sources and secondary context chert use in comparison to the *LBSR*, which may be indicative of increased mobility on the landscape if the present day distribution of chert was similar in the past (Ch. 5). The increase in chert in MIS 4 samples, which was collected in

secondary contexts may explain in part why the ratio of Cobble/Outcrop cortex is correlated with increased C4 vegetation.

The *SADBS* is modeled to occur during coastline regression and the *SGS* is near the MIS 4 maximum coastline distance. These occupations may show such high artifact densities and intensity of occupation because the site may have been ideally situated on the paleolandscape to access both coastal and interior resources as shellfish remains are still abundant in these layers. This may also be true of the *DBCS* but it is not clear yet whether the paucity of shellfish in these stratigraphic layers are the result of the coastline being too distant for the transport of coastal resources, or whether shellfish remains have decalcified due to increased groundwater flow from exposure after the cliff retreat in the upper Long Section. Alternatively, with the regression of coastline, the *DBCS* occupations may intersect different populations of hunter-gatherers in the interior, particularly if the carrying capacity of the coastline pushed an expanding population away from the coastline (Marean 2010b). The *OBS* is stratigraphically between the *SADBS* and SGS and is also modeled to occur near the peak of the coastline regression, but the *OBS* has one of the lowest find and lithic densities of any of the analyzed samples which may partially explain why this sample consistently failed to meet the predictions of the Site Context Model and looked so different from the samples that preceded and followed it. The small OBS sample may only be representative of what was brought into the cave by a limited number of individuals over a short period of time.

At PP5-6 silcrete raw material use first proliferates and small blades and segments first appear in the assemblage during the *SADBS* when the Crevice Cave $\delta^{18}O$ and $\delta^{13}C$ measurements are interpreted to represent increased summer rainfall and a shift to environments with more C4 grasses (Bar-Matthews et al. 2010). There is ongoing debate concerning what effects glacial cycling would have had on south and west coast vegetation and faunal communities in South Africa. Changes in the relative contribution of C3 and C4 vegetation in the Pleistocene and Holocene have been linked to a combination of paleoclimatic variables including the partial pressure of atmospheric carbon dioxide, temperature, soil and aspect, and seasonality of rainfall (Cowling 1983; Talma and Vogel 1992; Scott 2002; Huang et al. 2001).

Klein (1972, 1983) has argued that Pleistocene fauna, particularly between MIS3-5, is indicative of an expanded grassland ecosystem prior to the Holocene expression of fynbos vegetation, which supports mainly small browsers. In looking at large mammal

communities, Rector and Reed (2010) and Rector and Verelli (2010) argue that there is little change in the proportion of grazers and browsers between glacial and interglacial periods. They argue that Pleistocene faunal communities do not show a simple correlation between C3 shrubby vegetation with interglacial periods and C4 grassland vegetation with glacial periods. They instead suggest that glacial cycling may have produced a sometimes unpredictable succession of habitats or a mosaic of habitats that could have made animal prey and plant foods unpredictable during rapid climate change. Faith (2011) argues that the presence/absence approach is sensitive to assemblage sample size and finds, contra to Rector and Verelli (2010), that in larger Pleistocene fauna samples there was greater diversity of grazers, many of which went extinct in the Holocene, supporting more open grassland habitat as predicted by the Bar-Matthews et al. (2010) Crevice Cave isotopic record for MIS 4-3.

Marean (2010a) and Marean and Rector (2011) have recently proposed that the exposed Agulhas coastal plain with increased C4 grasses and shrubby vegetation could have supported a migratory ecosystem for large herd animals to move across the now submerged Agulhas platform following the distribution of winter and summer rains. The Pinnacle Point caves may have been ideally positioned to take advantage of the hunting opportunities offered by the grassy Agulhas plain, or mixed grassland/shrub ecosystem in addition to the coastal resources most commonly accessed during spring low tides (Marean 2010b).

Even if conditions with more C4 vegetation are characterized as a mixed mosaic of grassland and fynbos (Rector and Verelli 2010), it is likely that the more open environments at Pinnacle Point during MIS 4 would have resulted in the increased mobility of hunter-gatherers that targeted large-bodied open habitat grazers. This would have had the effect of bringing mobile hunter-gatherers in greater contact with silcrete sources. Second, the extreme climate variability at c. 72ka (Bar-Matthews et al. 2010) and potential rapid succession of vegetation and resources could have imposed risk and pressure to invest in composite technology with a higher degree of maintainability (Nelson 1991) such as hafted backed blades as projectiles that could have increased the success rate when less predictable but higher yield animal resources were encountered.

Research on MSA technology has increasingly focused on the potential use of backed blades as evidence for composite projectile technology (Brooks et al. 2006; Lombard and Pargeter 2008; Wadley and Mohapi 2008; Shea and Sisk 2010; Lombard 2011). Most of the evidence is based on the presence of characteristic diagnostic impact

fractures or 'DIF's' (Fischer et al. 1984; Lombard and Pargeter 2008; Yaroshevich et al. 2010), segment size (Wadley and Mohapi 2008) in comparison to ethnographic hunting weapons and North American arrow points (Shea 2006), and the presence of haft traces and bone and blood residues (Lombard 2007; 2008; 2011). There are also surviving analogous archaeological examples of microblades still attached to slotted hafts from sites in the European Magdallenian as evidence for use of bladelets in composite hunting technology (Petillon et al. 2011).

Use-wear studies on PP5-6 backed blades are ongoing but the preliminary analysis of macro-fractures in comparison to a dataset of test-fired experimentally replicated backed pieces has identified potential DIF's on some SADBS segments (Schoville et al. 2011). The *SADBS* backed blades (and perhaps those of the *SGS* and *DBCS*) may represent early investment in composite hunting technology as a strategy for obtaining high yield but less predictable food resources in more open but extremely dynamic environments. In this explanation, it is argued that the climate variability observed in the Crevice Cave isotopic record (Bar-Matthews et al. 2010) might have optimized the opportunities for MSA hunters to have taken advantage of higher ranked but less predictable resources available during the more open MIS 4 environments. In this hypothesis, technological innovation is seen less in response to the stress of 'cold' and 'harsh' climates, and is more in line with the expectations of Fitzhugh (2001) who suggested that, "change in foraging technology should occur first, if at all, in technologies for capturing large, high-utility species and then shift to more sustainable r-selected species" (p145).

Scheduling conflicts between the harvesting of shellfish during spring low tide (Marean 2010b) and the intercept hunting of migratory game may have occurred during the SADBS occupations in particular where shellfish remains are present (Torrence 1983). Time constraints and risk of raw material supply failure (Bamforth and Bleed 1997) may have created pressure for a procurement strategy focused on the collection of more expensive but predictably located primary outcrop silcrete and the provisioning of PP5-6 with silcrete (Kuhn's 2004 provisioning of places) to make sure that there was always a supply of raw material. Heat-treated silcrete was also amenable to conservation by the production of thin elongated blade tools with higher $CE/M^{1/3}$ ratios.

If there was increased mobility due to more open environments during inland residential occupations, silcrete sources would likely have been encountered more frequently. Collection of silcrete and fuel during other activities would have reduced

potential acquisition costs as a factor in the decision to use silcrete. The analysis of core primary form and core and flake maximum dimensions show that silcrete was typically collected from primary outcrops as small flakes and occasionally tabular nodules which could have been carried with less effort while performing other activities on the landscape. Merciera and Hiscock (2008) hypothesize that silcrete heat treatment may not have required as much fuel if small pieces were heated directly in the fire or wrapped in a buffer material such as clay. It is possible that a side-benefit of the reduction in blanks size observed in the silcrete-rich assemblages is in response to the need to reduce the amount of fuel used for heating to lower the costs of treatment. Smaller blanks may also have allowed for the batch processing of a larger number of pieces per treatment.

Bousman (2005) has made the point that evaluating the risk of failure in many parts of southern Africa is difficult because there is a diversity of resources, particularly plant foods and shellfish that can be relied upon if higher-ranking food resources are not procured. With the concept of intercept hunting on the Agulhas plain, risk might take the form of failure to obtain resources during temporally constrained availability of prey during seasonal migrations, and also the use of hunting weapons in proximity to dangerous animals such as buffalo. The investment in hunting technology would have required reliability (Bleed 1986) so that tools didn't fail at times when seasonal game was available. Elston and Brantingham (2002) also conclude that composite projectiles would be most appropriate in situations where the cost of failure is high.

The predictions for the use of backed blades as projectiles during periods characterized by more C4 conditions run contra to the expectations of Bousman (2005) who proposed that the use of LSA Wilton segments at Blydefontein occurred during times of stress and represented a flexible technology for the diversification of diet similar to what was proposed by Kuhn (2002) for the Proto-Aurignacian. Bousman notes though, that the early predictions of H.J. Deacon (1972) were that higher frequencies of Wilton backed blades in Zambia may have been associated with game in more open environments. Bousman (1993) also predicted however, that narrower diets would be expected where more expensive technological strategies would increase the handling costs of obtaining food resources. The expenses associated with the procurement and heat treatment of silcrete, and the costs of creating complex mastics for hafting (Wadley et al. 2009) could also support the prediction of narrower diet breadth in the SADBS.

Wadley (2010) has argued for expansion of diet breadth in the HP based on the results of faunal analysis at Sibudu Cave (Clark and Plug 2008) which shows an

increased representation of small game more typical of forests and decreased representation of larger species like buffalo wildebeest and roan antelope which are more common along with zebra in the post-HP at Sibudu. These smaller species may have been captured with traps or snares rather than by hunting with projectiles (Wadley 2010). Perhaps the diversification in HP segment size noted by Wadley and Mohapi (2008) may in fact represent increased flexibility in technological approach alongside other hunting technology, and may be consistent with the, "…shift to more sustainable r-selected species" (p.145) as predicted by Fitzhugh (2001).

The association between silcrete use and segments with more open environments characterized by increased input of C4 vegetation is compelling but speculative at this point. Additional use-wear analysis and the results of ongoing experimental research are required to more rigorously test the suitability of *SADBS*, *SGS*, and *DBCS* backed blades for use as projectiles. The forthcoming faunal and shellfish analyses from PP5-6 should provide critical additional information for a potential link between technological variability and changes in the faunal remains and diet breadth identified in the PP5-6 sequence.

Backed blades do not entirely disappear from the PP5-6 sequence after the *DBCS* (Fig. 81). The *NWR* and Takis analytical samples following the *DBCS* are characterized by very low density lithic finds as well as total plotted finds possibly indicating that these are short duration occupations. The low artifact densities are due in part to an almost complete absence of shellfish in these layers. Micromorphology may help determine whether the scarcity of shellfish is a preservation issue as the coastline model shows a transgression to between 5-10ka from site within the OSL sigma of the *NWR*. The *NWR* shows a corresponding increase in the use of quartzite which was used to make larger blades and points similar to those of Jed/JR. Crevice Cave $\delta^{13}C$ record shows a return to more C3 conditions and there is a corresponding drop in silcrete use. The *NWR* and Takis samples each have a few examples of backed blades on fine-grained material and quartzite points. Silcrete debitage has similar mean dimensions and $CE/M^{1/3}$ values as the preceding *DBCS*, but quartzite debitage is more variable.

Beyond Pinnacle Point-PP5-6 Lithics in Larger Context

The *SADBS*, *SGS*, and *DBCS* lithic assemblages are dense occupations dominated by small blade products and segments that fit many published definitions for microlithic and bladelet technology (Tixier 1974; Straus 2002). Most researchers consider microlithic assemblages to consist predominantly of standardized blanks or retouched tool forms that are too small to have been used without hafting (Kuhn 2002, but see Close 2002). Microlithic assemblages are significant because they represent widespread evidence for the adoption of composite technology by the Late Pleistocene through mid-Holocene in most parts of the world (Bar-Yosef and Kuhn 1999; Kuhn and Elston 2002).

Belfer-Cohen and Goring-Morris (2002) posited that the shift to backing of blades represents the assembly of composite tools with hafting along the long axis of the tool. Retouching of blanks into standardized forms allows for more flexibility in the morphology of the blank produced from the core. A similar observation was made by Mackay (2008b) who observed the blanks selected for HP blades at Diepkloof were variable in size and included flakes as well. Blade production in the PP5-6 *SADBS* does appear to have been relatively unstructured and flexible in terms of core preparation, with the initial removal often aligned along a natural cortical ridge.

Ambrose (2002) argued that early microliths and backed blades in East Africa arose from the increased access to fine-grained raw materials that allowed for the production of smaller blades. Ambrose (2002) argued that tool specialization, trade, and capacity for information exchange were at the root of microlithization and used this to argue that continuity in tool forms from the MSA to LSA in East Africa indicates that these populations may have had an advantage in the colonizing of new areas outside of Africa.

In the Ambrose (2002) model, use of fine-grained raw material came first through access to sources from increased mobility. Access to non-local fine-grained materials allow for the production of smaller blades. These smaller blades are argued to represent lightweight tool kits for unpredictable resources. The reduction in mobility and switch away from lithic raw material as exchange goods led to the conservation of costly non-local raw materials and the increasingly smaller size of the tools (Ambrose 2002). Once adopted, microlithic technology continued in East Africa as a strategy through the late Pleistocene and Early Holocene. Ambrose (2002) contrasted the East African record with southern Africa and noted that HP technology, which he also considered to be made on

fine-grained non-local raw materials (Ambrose and Lorenz 1990), does not show continuity between the MSA and LSA. Microlithic tools only appear again in southern Africa at approximately 20ka in the Robberg and segments in the Wilton around 8ka.

At PP5-6, the change in predominant raw material use begins in the ALBS prior to the peak in production of smaller tools in the SADBS, which tends to supports the Ambrose (2002) model for the use of fine-grained raw material occurring first prior to the appearance of segments. The increased use of silcrete in the ALBS also corresponds to an increase in C4 vegetation which may also support the Ambrose and Lorenz (1990) claim for more open environments during the initial shift towards the use of fine-grained raw materials.

Contra to the Ambrose (1990) and (2002) models for adoption of HP and microlithic technology, at Pinnacle Point, raw materials cannot be viewed as being non-local in origin (Minichillo 2006; and Ch. 5 of this thesis), and this has also been noted to be the case at Sibudu Cave (Wadley and Mohapi 2008). It is also unnecessary to argue for restrictions on trade as being the root cause for raw material conservation leading to smaller tools. Silcrete occurs within 10km of PP5-6 and there should have been few restrictions (except potentially during dune formation at ~69ka) to direct access to primary sources. It can also be demonstrated at PP5-6 (contra to Ambrose 2002) that the smallest blades and segments occur first in the *SADBS* and the trend to the *DBCS* (HP) is for larger blanks and segments.

The mobility-based strategy for the procurement of fine-grained raw materials which is a key feature of both the Ambrose and Lorenz (1990) model for the appearance and decline of the HP, as well as the Ambrose (2002) model for the origins of microlithic technology, is not entirely supported by the data from PP5-6. First, the early appearance of a low-density silcrete-dominant layer (AK Silcrete) dated to approximately 86ka suggests that MSA tool makers knew about silcrete and were probably aware of where to find it based on the presence of primary outcrop cortex in this early layer. Second, as noted earlier, silcrete was rarely used in the PP5-6 sequence in its raw form. However, if increased mobility leads to a greater encounter rate of silcrete when finer-grained raw materials were desired, then the reduction of search and travel time for locating silcrete and wood fuel, if packaged with other activities (Binford 1979), may have reduced some of the costs of procurement and heat treatment.

Ambrose (2002) argued for continuity in the use of microlithic and backed blade technology across the MSA and LSA of East Africa and suggested that complex behavior

associated with social networking and raw material exchange may have facilitated the dispersal of modern human populations out of East Africa during the last glacial period. Backed blade technology in southern Africa may appear very early depending on the age and context of segments in the Lupemban (Barham 2002; Clark and Brown 2001). The Howiesons Poort has been described as an 'anomalous' and 'exceptional' occurrence of early microlithic technology (Bar-Yosef and Kuhn 1999). The HP has been argued to represent early evidence for hafting and use of complex mastics (Wadley et al. 2009); lithic pyrotechnology (Brown et al. 2009); projectile armatures and perhaps even early arrow tips (Wadley and Mohapi 2008; Lombard and Phillipson 2010; Lombard 2011); and symbolic behavior and reciprocity (Deacon 1989; Wurz 1999; Texier et al. 2010).

Research on the origins of modern human technological variability typically highlights the recursive or sporadic appearance of HP early backed blade MSA technology in southern Africa. The disappearance of the HP has been suggested to represent a regression or loss of complexity in the late coastal southern African MSA in comparison to the East African record (J. Deacon 1984; Powell et al. 2009). The pattern of HP replacement by assemblages more typical of what came before has confounded the understanding of the contribution of the HP with respect to the origins of technological behavioural variability (Shea 2011).

Even though microlithic technology seems to become so widespread in the Late Pleistocene, researchers in other parts of the world have noted a similar lack of continuity in the use of microlithic technology as a strategy in more recent contexts (Kuhn 2002). Microlithic technology is often preceded, followed, or even occurs alongside what might be considered macrolithic technology (Neeley 2002). The consistent size differences between raw materials observed throughout the PP5-6 sequence supports a smaller tool technology on finer-grained raw materials that occurs at low frequency in the *LBSR* but proliferates in the *SADBS*, *SGS*, and *DBCS*, and then falls off somewhat in the *NWR* and Takis samples. This small tool component on silcrete and chert occurs alongside what might be termed a macrolithic component based on the production of significantly larger quartzite flakes, points and blades. At PP5-6, silcrete and chert may have been selected for superior flaking quality and sharp edges whereas quartzite may have been chosen for edge durability.

Microlithic technology may be independently reinvented as a viable technological strategy (Straus 2002) and thus its appearance or disappearance, particularly in contexts like the Holocene LSA in southern Africa (Orton 2008) does not necessarily mean a loss

of behavioral complexity. Kuhn (2002) observed that microlithic technology comes and goes in the early European Upper Paleolithic, noting that, "the advantages afforded by microlithic technologies, however great, are nonetheless limited and context specific" (p.88). Kuhn (2002) took exception to the assumption that microliths proliferate in the Late Pleistocene because they are more efficient. He argued that microlithization in the Proto-Aurignacian may be associated with an increase in diet breadth and thus composite tools may offer a flexible way to create a range of specialized tools for the acquisition of new food resources. This observation is supported by use-wear analysis of bladelets from Middle Woodland assemblage in North America that indicate a range of potential uses for small bladelets (Odell 1994).

Elston and Brantingham (2002) argued for the appearance of microlithic technology in northern Asia in response to the cool, dry and variable climate after the Last Glacial Maximum at 17 to 18ka. They proposed that microliths could have been used as inserts in projectile weapons in the intensification of large game hunting to help cope with seasonal variance and unpredictability of key resources. Hiscock (2002) proposed that the proliferation of backed artifacts (which are no longer considered microlithic) between 4-1500BP in Australia were associated with changes in climate. Drier and more variable climate associated with El Niño weather patterns produced less predictable resources which stimulated the development of more reliable, maintainable and versatile technology. Similar to Kuhn (2002), Hiscock (2002) proposed an expansion of diet breadth citing evidence of ground stone for plant processing and the adoption of mollusks that are more tolerant of climate fluctuation and depletion by humans. Interestingly, Hiscock (2002) noted that the increased production of backed artifacts is contemporary with a similar increase in bifacial production in northern Australia which he interpreted as representing parallel technological adaptations to similar environmental stress.

It was noted previously that the *SADBS* and SB may have been contemporary technologies. There is precedence in more recent assemblages for the co-occurrence of backed blade and bifacial technology. Backed bladelets occur with the Solutrean in some sites in France between c. 20-28ka (Geneste and Plisson 1993), and in Australia in the Mid-Holocene (Hiscock 2002). The presence of two distinct technologies in close chronological and geographical proximity suggests that technological strategies in the MSA may have been locally specific and adapted to regional conditions or constraints imposed on resources by the changing paleolandscape.

The *SADBS* occurs earlier than the HP and has segments with dimensions that fall between the HP and Wilton at many sites and are similar in size to those found in the Late Pleistocene and Holocene of East Africa (Fig 86). The very small size of these segments is a strong argument that they do represent inserts for composite tools. Bar-Yosef and Kuhn (1999) propose that an important implication for early occurrences of composite tools is that they demonstrate the ability for advanced planning and a significant forward investment of energy or "frontloading" (p.332) ahead of tool use. Regardless of the function of segments in the *SADBS* and *DBCS*, the direct procurement of silcrete, heat treatment, and the production of small standardized blades and backed pieces from PP5-6 demonstrates that the cognitive ability for the production of composite technologies was in place at least by 70ka in the *SADBS* and may in fact make multiple appearances throughout the duration of the southern African MSA (Wadley and Mohapi 2008).

Long-chain composite technology includes a series of linked steps or processes that may occur at different points on the landscape and require planning and scheduling to integrate into a single finished product (Fig. 87). The *SADBS* is argued to be an early expression of a number of traits associated with advanced planning and behavioral complexity including the use of primary context fine-grained raw materials, lithic heat treatment to improve the flaking and perhaps edge-quality of silcrete, and segment production for composite tools. This production process would also require the collection of wood fuels for heat treatment fires, organic materials for handles or projectile shafts, and resin or binding agents to join the components together.

Composite technology represents a significant investment over simple hand-held tools but many of the costs may be offset by the scheduling of resource collection embedded in other activities. It is not clear when systematic hafting begins, but at PP5-6 there is evidence for heat treatment as early as c. 86ka and small segments that are argued to be inserts in composite tools that occur prior to the HP at c. 70-72ka. Evidence for complex resin-based mastics has been proposed for the HP at Sibudu Cave from c.60-65ka (Wadley et al. 2009).

The Site Context Model was proposed in this thesis as an explanation for the MIS 4 increase in use of silcrete and other fine-grained raw materials observed at PP5-6 and perhaps other southern Cape MSA sites. This model was based on an assumption of reduced availability of quartzite due to the movement of cobble beaches during MIS 4 coastline regression. The model failed to explain much of the technological variability

observed beyond the proportions of quartzite versus non-quartzite raw materials in each analyzed sample. The Site Context Model only included distance to source as a reason to select raw materials, but the results from this dissertation indicate that there are important technological differences that occur in time between the use of quartzite and non-quartzite raw materials. The raw material selection at PP5-6 may be viewed as a parallel strategy where quartzite and silcrete use and tool production vary according to opportunities or constraints imposed by the changing landscape and the design parameters and requirements of tool use. At PP5-6, point production occurs throughout the sequence, but is especially common in the quartzite rich assemblages (Fig. 81). Small blade and segment production typically occurs in the silcrete-rich assemblages of MIS 4. Both points and segments occur in the *SADBS*.

The differential use of raw material tends to support functional interpretations (i.e. Mackay 2008a) for the increased use of fine-grained raw material in the MSA. Patterns in raw material selection observed throughout the analyzed sequence have been demonstrated to occur in proportions that cannot be explained by chance, particularly in the transition from the *LBSR* to the *SADBS* which also corresponds to changes in procurement patterns from secondary to primary sources. The results presented here support the view that the increased use of fine-grained raw material in MIS 4 is primarily deliberate, although the significant relationship between the ratio of quartzite to non-quartzite raw materials with coastline distance (Fisher et al. 2010), and the percentage of silcrete with the Crevice Cave $\delta^{13}C$ record (Bar-Matthews et al. 2010) indicate that landscape change may have caused some changes in availability of lithic raw materials that contributes to the differential patterning in raw material use observed between coastal and inland sites (Henshilwood 2008).

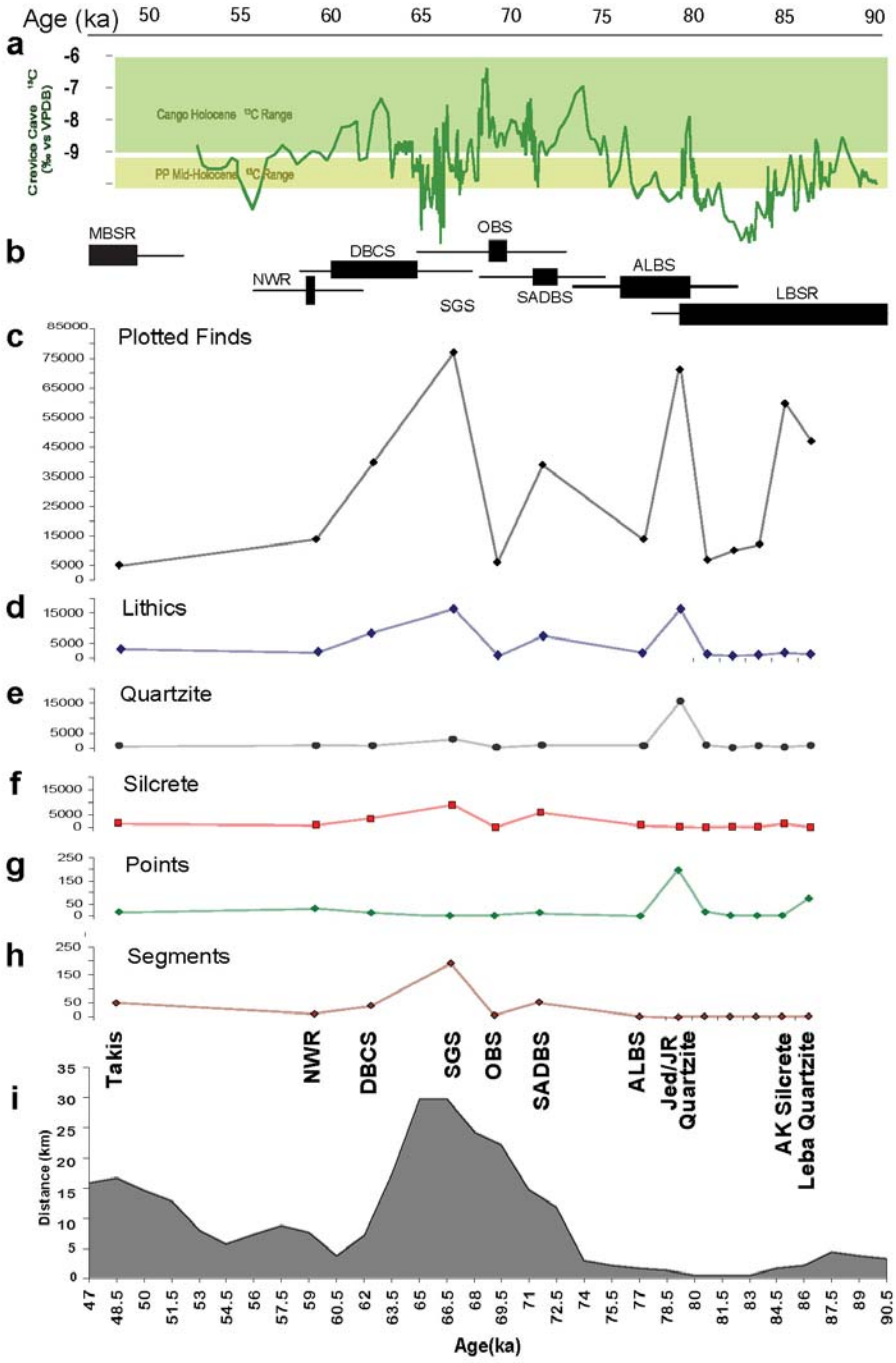

Figure 85. Find density graph (n/m3) by analytical sample. a) Bar-Matthews et al. Crevice Cave isotopic record; b) OSL ages (Z. Jacobs); c.) all plotted finds; d). lithic finds; e) quartzite; f) silcrete; g) points; and h) segments; i) Fisher et al. coastline model.

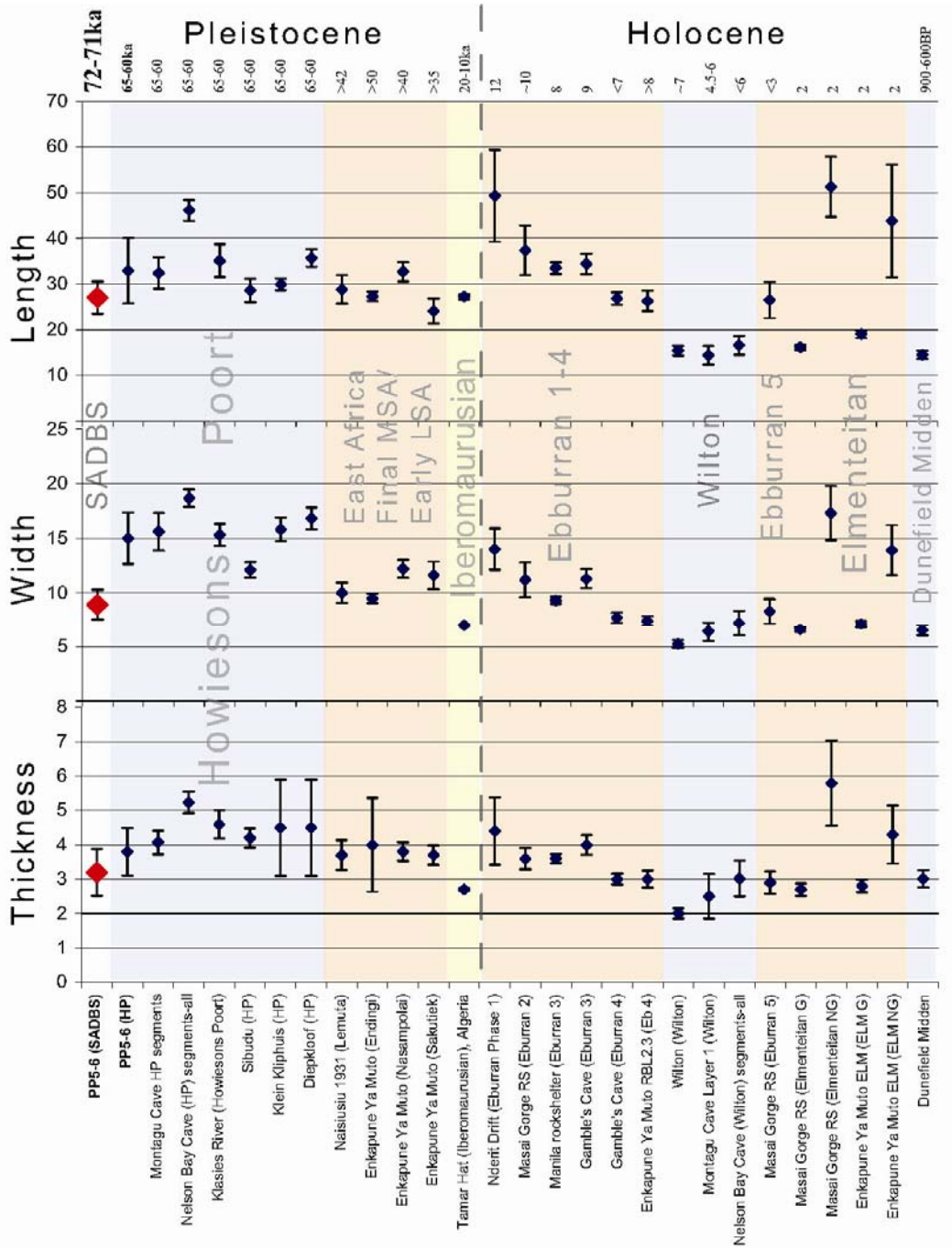

Figure 86. Comparison of SADBS segment metrics against those from a range of other African assemblages from the MSA through the Holocene. SADBS segments are on the low range for length and thickness when compared to the HP but fall well below the HP means for width and approach the upper range of means for width and thickness of Later Stone Age Wilton segments. SADBS segment dimensions also fit well within the 95% confidence interval of the mean values for segments from many of the Pleistocene and Holocene East African assemblages. Sources: Ambrose (2002); Close (2002); J. Deacon (1972); Inskeep (1978); Keller (1973); Mackay (2009); Orton (2002); Volman (1981); Wurz (1999); Wadley and Mohapi (2008)

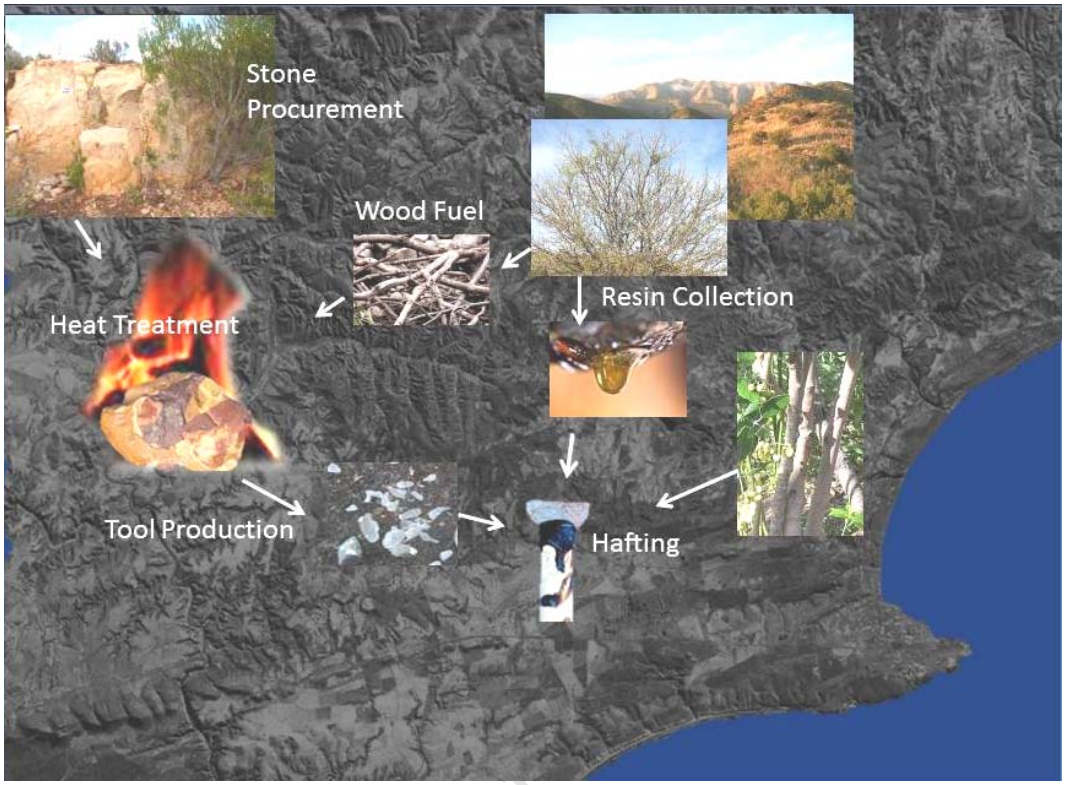

Figure 87. Potential components required for assembly of 'long-chain' composite technologies at PP5-6.

13.0 Conclusions

The results of six excavation seasons at PP5-6 near Mossel Bay, South Africa have revealed a deep, stratified and rich archaeological sequence that is well-dated and can be linked to the high-resolution study of paleoenvironment, climate change and coastline modeling at Pinnacle Point (Bar-Matthews et al 2010, Fisher et al 2010). The major contribution of the PP5-6 site is the high-resolution vertical distribution of the plotted artifact samples. The sample sizes for occupation layers at PP5-6 are small in comparison to other MSA sites due to the pace of the excavation strategy and efforts to conserve the bulk of the remaining sequence. The challenge of the lithic analysis has been to extract the maximum amount of information from the small but well-stratified and dated samples.

New paleoenvironmental contextual data has been used to evaluate existing published models on the Cape MSA Raw Material Pattern and the Site Context Model proposed in this thesis. The Site Context Model posited that availability of lithic resources, particularly from secondary sources, would fluctuate with changes in the distance between site and coastline. The Site Context model is partially effective in explaining the exaggerated pattern of raw material change at PP5-6, but there are occupations (particularly the *ALBS*, *SADBS* and *OBS*) that do not fit predicted patterns. A series of hypotheses and assumptions concerning raw material availability and the costs and benefits of their selection have also been presented which can be tested in the next phase of analysis and research at PP5-6 and at other MSA sites.

The association between technological change at PP5-6 and fluctuations in the Crevice Cave isotopic record (Bar-Matthews et al. 2010) suggests that the frequency of paleoenvironmental change may be important in modeling EMH technological adaptations. Extreme changes over a short time span would place a premium not only on the retention and transmission of knowledge (Fitzhugh 2001; Hill et al. 2009), but on the continued advancement of existing ideas such as silcrete heat treatment. The ability to recall and improve upon stored knowledge sets modern humans apart, and this ability may have allowed them to cope not only with generation-level extreme climate change, but with environmental conditions in places to which early modern humans eventually migrated.

The HP has been described as an "exception and an anomaly" (Bar-Yosef and Kuhn 1999: 333) and "precocious" (Butzer 1978:150). The growing number of small blade entities in southern Africa including Diepkloof Layer Jeff (Porraz et al. 2008), Die Kelders Cave I (Thackeray 2000), and the PP5-6 *SADBS* suggests that these terms no longer apply. Instead, small blade and backed blade technology may come and go as a viable technological strategy (Kuhn 2002), but the cognitive capacity for the long-chain production of composite technology manifests early in southern Africa (Wadley and Mohapi 2008).

The *SADBS*, SB, and HP in the southern Cape all appear to be associated with shifts to the increasing contribution of summer rainfall and C4 grasses in MIS 4 (Bar-Matthews et al. 2010). The rise and decline of these advanced looking entities may be associated with either risk presented by variable MIS 4 climates, or alternatively may be in response to opportunities brought by changes in paleoclimate and landscape rather than shifts in cognitive ability (Ambrose 2002). Here it has been argued that the *SADBS* backed pieces may represent composite hunting weapons, but this doesn't rule out other potential uses. One of the advantages of composite blade technology is flexibility in haft arrangement. It is also possible that similar technologies are adapted by other groups through social transmission particularly when population size increases (Powell et al. 2009) and the designs may be emulated and applied for other purposes (Bettinger and Eerkens 1999).

Some of the observed technological variability at PP5-6, particularly between the *SADBS*, *SGS*, and *DBCS*, may result from the influences environmental context, raw material mechanical properties, intensity of occupation, and mobility. It is also possible that we are beginning to see the type of regional differentiation more common in Holocene hunter gatherer assemblages across the globe (Clark 1988). Microlithization and backed blade technology may come and go as a viable technological strategy as it does in other parts of the world in more recent assemblages, but the cognitive capacity for the multi-step production of composite technology exists early in southern Africa (Brown et al. 2009; Wadley et al. 2009).

Variability observed at the micro-stratigraphic level in the LBSR at PP5-6 indicates that more subtle expressions of technological variability may be identified from examining cave sequences from occupation to occupation rather than from one stratigraphic block to the next (Thompson et al. 2010). The seemingly static nature of the

MIS 6-5 MSA may partially result from the lumping of large stratigraphic samples and the limited sampling of non-coastal occupations at sites in the southern Cape.

The recent systematic OSL dating program by Jacobs et al. (2008) has the potential to change the way the MSA is viewed. Well-dated occupations can be placed on a time line and viewed as a continuum rather than as replacement (e.g., MSA I replaced by MSA II, which is replaced by the HP, and so forth)(Fig. 88). If occupations can be defined by chronology rather than by name, there is infinite space to place newly discovered technological variability rather than trying to eliminate diversity by fitting the patterning of one site into another (Thompson et al. 2010). Obviously, this type of approach requires that all sites be systematically and carefully excavated and dated by comparable techniques. Occupation gaps must also be considered (Jacobs et al. 2008).

The stone artifacts from the site of PP5-6 represent one of the most comprehensive records of human technological change on the southern coast of South Africa in the Middle to Late Pleistocene. The technological analysis of the ~50-85ka sequence has identified a previously unknown stage in the MSA reduction sequence in the heat treatment of silcrete and one of the earliest occurrences of backed blade composite technology. While gaps in occupation certainly exist, excavations have continued to expose a rich and near continuous record of human behavior that extends beyond 100ka, and there are already hints from recent excavations that the technological complexity observed in the MIS 4 record of PP5-6 may extend deep into the earliest occupations of the sequence.

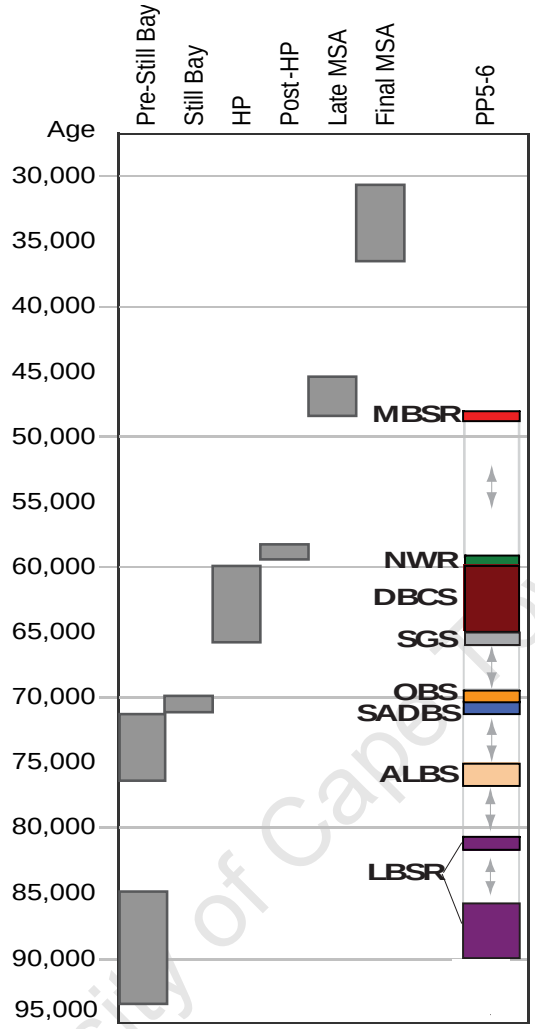

Figure 88. The PP5-6 StratAgg sequence compared with the chrono-stratigraphic sequence presented in Jacobs et al. (2008) with potential gaps in occupation indicated by diverging arrows.

14.0 References

Ahler, S.A. (1989). Mass analysis of flaking debris: studying the forest rather than the tree. In: D.O. Henry, G.H. Odell (Eds.), Alternative Approaches to Lithic Analysis. *Archaeological Papers of the American Anthropological Association* 1, 85-118.

Allan, J.C., R. Hart, J.V. Tranquili (2006). The use of Passive Integrated Transponder (PIT) tags to trace cobble transport in a mixed sand and gravel beach on the high-energy Oregon coast, USA. *Marine Geology* 232, 63-86.

Ambrose, S.H. (2001). Paleolithic technology and human evolution. *Science* 291, 1748-1753.

Ambrose, S.H. (2002). Small things remembered: origins of early microlithic industries in Sub-saharan Africa. In: R. Elston, S. Kuhn (Eds.), Thinking Small: Global Perspectives on Microlithic Technologies. *Archaeological Papers of the American Anthropological Association* 12, 9-29.

Ambrose, S.H., Lorenz, K.G. (1990). Social and ecological models for the Middle Stone Age in southern Africa. In: P. Mellars (Ed.), The Emergence of Modern Humans: An Archaeological Perspective. Edinburgh University Press, Edinburgh, 3-33.

Andrefsky,W. Jr. (1994). Raw material availability and the organization of technology. *American Antiquity* 59, 21-34.

Andrefsky, W. Jr. (1998). Lithics: Macroscopic Approaches to Analysis. Cambridge: Cambridge University Press.

Arthur, K.W. (2010). Feminine knowledge and skill reconsidered: women and flaked stone tools. *American Anthropologist* 112, 228-243.

Atkinson, B.K. (1984). Subcritical crack growth in geological materials. *Journal of Geophysical Research* 89, 4077-4114.

Avery, G., D. Halkett, J. Orton, T. Steele, M. Tusenius, R. Klein (2008). The Ysterfontein 1 Middle Stone Age Rock Shelter and the evolution of coastal foraging. *South African Archaeological Society Goodwin Series* 10, 66-89.

Avery, G., K. Cruz-Uribe, P. Goldberg, F.E. Grine, R.G. Klein, M.J. Lenardi, C.W. Marean, W.J. Rink, H.P. Schwarcz, A.I., Thackeray, M.L. Wilson, (1997). The 1992-1993 excavations at the Die Kelders Middle and Later Stone Age Cave Site, South Africa, *Journal of Field Archaeology* 24, 263-291.

Bamforth, D.B. (1990). Settlement, raw material, and lithic procurement in the central Mojave Desert, *Journal of Anthropological Archaeology* 9, 70-104.

Bamforth, D.B. (1986). Technological efficiency and tool curation. *American Antiquity* 51, 38-50.

Bamforth, D. B., P. Bleed (1997). Technology, flaked stone technology, and risk. *Archeological Papers of the American Anthropological Association* 7, 109–139.Barut, S. (1994). Middle and Later Stone Age lithic technology and land use in East African savannas. *African Archaeological Review* 12, 43-72.

Barham, L. (2002). Backed tools in Middle Pleistocene central Africa and their evolutionary significance. *Journal of Human Evolution* 43, 585-603.

Bar-Matthews, M., C.W. Marean, Z. Jacobs, P. Karkanas, E.C. Fisher, A.I.R. Herries, K.S. Brown, H.M. Williams, J. Bernatchez, A. Ayalon, P. J. Nilssen (2010). A high resolution and continuous isotopic speleothem record of paleoclimate and paleoenvironment from 90 to 53 ka from Pinnacle Point on the south coast of South Africa. *Quaternary Science Reviews* 29, 2131-2145.

Bar-Yosef and Kuhn (1999). The Big Deal about Blades: Laminar Technologies and Human Evolution. *American Anthropologist* 101, 322-338.

Barut, S. (1994). Middle and Later Stone Age lithic technology and land use in East African savannas. *African Archaeological Review* 12, 43-72.

Beauchamp, E. K., B.A. Purdy (1986). Decrease in fracture toughness of chert by heat treatment. *Journal of Materials Science* 21, 1963-1966.

Beaumont, P. (1979). The stone age cultural stratigraphy of Border Cave. Report presented at the Southern African Association of Archaeologists Workshop held at Stellenbosch at the end of June 1979- Towards a Better Understanding of the Upper Pleistocene in Sub-Saharan Africa.

Beaumont, P., H. de Villiers, J.C. Vogel (1978). Modern man in sub-Saharan Africa prior to 49,000 B.P.: a review and evaluation with particular reference to Border Cave. *South African Journal of Science* 74, 409-419.

Belfer-Cohen, A., N. Goring-Morris (2002). Why microliths? microlithization in the Levant. In: R.G. Elston, S.L. Kuhn (Eds.), Thinking Small: Global Perspectives on Microlithization, 57-68.

Bernatchez, J. (2010). Taphonomic implications of orientation of plotted finds from Pinnacle Point 13B (Mossel Bay, Western Cape Province, South Africa). *Journal of Human Evolution* 59, 274-288.

Bernatchez, J. (2008). Geochemical characterization of archaeological ochre at Nelson Bay Cave (Western Cape Province), South Africa. *South African Archaeological Bulletin* 63, 3-11.

Bernatchez, J., K. Brown, C. Marean, Z. Jacobs (2008). A continuous archaeological sequence from MIS 3 to 5: Preliminary results from the Middle Stone deposits at Pinnacle Point Site 5-6, Mossel Bay, Southern Cape, South Africa. Paper presented at the 2008 Paleoanthropology Society Meetings, Vancouver Canada.

Bettinger, R.L., B. Winterhalder, R. McElreath (2006). A simple model of technological intensification. Journal of Archaeological Science 33,538-545.

Bettinger, R. L., J. Eerkens (1999). Point typologies, cultural transmission, and the spread of bow-and-arrow technology in the prehistoric Great Basin. *American Antiquity* 64, 231–242.

Binford, L.R. (1980). Willow smoke and dogs' tails: hunter-gatherer settlement systems and archaeological site formation. *American Antiquity* 45, 4-20.

Binford, L.R. (1979). Organization and formation processes: looking at curated technologies. *Journal of Anthropological Research* 35, 255-273.

Binford, L.R., (1977). Forty-seven trips: A case study in the character of archaeological formation processes. In*:* R.V.S. Wright (Ed.), Stone Tools as Cultural Markers: Change, Evolution and Complexity. Australian Institute of Aboriginal Studies: Canberra, 24-36.

Binford, L.R., N.M. Stone (1985). "Righteous Rocks" and Richard Gould: some observations on misguided "debate." *American Antiquity* 50, 151-153.

Binford, L.R., J.F. O'Connell (1984). An Alyawara Day: the stone quarry. *Journal of Anthropological Research* 40, 406-432.

Bird, C., T. Minichillo, C. W. Marean (2007). Edge damage distribution at the assemblage level on Middle Stone Age lithics: an image-based GIS approach. *Journal of Archaeological Science* 34, 771-780.

Bleed, P. (2002). Cheap, regular, and reliable: implications of design variation in Late Pleistocene Japanese microblade technology. In: R.G. Elston, S.L. Kuhn (Eds.), Thinking Small: Global Perspectives on Microlithization, 95-102.

Bleed, P. (1986). The optimal design of hunting weapons: maintainability or reliability. *American Antiquity* 51, 737-747.

Bleed, P., M. Meier (1980). An objective test of the effects of heat treatment of flakeable stone. *American Antiquity* 45, 502-507.

Blumenschine, R.J., F.T. Masao, J.C. Tactikos, J.I. Ebert (2008). Effects of distance from stone source on landscape-scale variation in Oldowan artifact assemblages in the Paleo-Olduvai Basin, Tanzania. *Journal of Archaeological Science 35*, 76-86.

Bordes, F. (1969). Reflections on typology and techniques in the Palaeolithic. *Arctic Anthropology* 6, 1-29

Bousman, C. B. (2005). Coping with risk: Later Stone Age technological strategies at Blydefontein Rock Shelter, South Africa, *Journal of Anthropological Archaeology* 24, 193-226.

Bousman, C.B (1993). Hunter-gatherer adaptations, economic risk and tool design. *Lithic Technology* 18, 59-86.

Brantingham, P.J. (2003). Neutral model of stone raw material procurement. *American Antiquity* 68, 487-509.

Brantingham, P.J., J.W. Olsen, J.A. Rech, A.I. Krivoshapkin (2000). Raw material quality and prepared core technologies in Northeast Asia. *Journal of Archaeological Science* 27, 255–271.

Braun, D.R. (2005). Examining flake production strategies: examples from the Middle Paleolithic of Southwest Asia. *Lithic Technology* 30, 107-125.

Braun, D.R., T. Plummer, J.V. Ferraro, P. Ditchfield, L.C. Bishop (2009). Raw material quality and Oldowan hominin toolstone preferences: evidence from Kanjera South, Kenya. *Journal of Archaeological Science* 36, 1605–1614.

Braun, D.R., T. Plummer, P. Ditchfield, J.V. Ferraro, D. Maina, L. C. Bishop, R. Potts (2008). Oldowan behavior and raw material transport: perspectives from the Kanjera Formation. *Journal of Archaeological Science* 35, 2329-2345.

Brooks, A.S., L. Nevell, J. Yellen, G. Hartman (2006). Projectile technologies of the African MSA: implications for Modern Human Origins. In: E. Hovers, S. Kuhn (Eds.), Transitions Before the Transition: Evolution and Stability in the Middle Paleolithic and Middle Stone Age. Springer: New York, 233-255.

Brooks, A.S., D.M. Helgren, J.S. Cramer, A. Franklin, W. Hornyak, J.M. Keating, R.G. Klein, W.J. Rink, H. Schwarcz, J.N. Leigh-Smith, K. Stewart, N.E. Todd, J. Verniers, J. E.Yellen (1995). Dating and context of three Middle Stone Age sites with bone points in the Upper Semliki Valley, Zaire. *Science* 268, 548-553.

Brown, K. (1999). Raw Material Selection and Flake Production in the Middle Stone Age of Southern Africa: Die Kelders Cave I and Montagu Cave. Unpublished M.A. thesis. SUNY Stony Brook.

Brown, K.S., C.W. Marean, Z. Jacobs, J. Bernatchez, P. Karkanas, S. Oestmo, B. Schoville (2011). A Pre-Howiesons Poort small backed blade MSA occurrence at Pinnacle Point. Abstracts of the PaleoAnthropology Society 2011 Meetings. *PaleoAnthropology* 2011

Brown, K.S, C. W. Marean (2010). Wood fuel availability for heat treatment drives the rise and fall of silcrete as a raw material in the Middle Stone Age of South Africa. Abstracts of the PaleoAnthropology Society 2010 Meetings. *PaleoAnthropology* 2010:A0006.

Brown, K.S., C. Marean, A.I.R. Herries, D. Braun, C. Tribolo, D. Roberts, Z. Jacobs, M. Myer, J. Bernatchez (2009). Fire as an engineering tool of early modern humans in coastal South Africa. *Science* 325, 859-862.

Butzer, K. W. (1973). Geology of Nelson Bay Cave, Robberg, South Africa. *South African Archaeological Bulletin* 29, 97-110.

Butzer, K.W. (1984). Late Quaternary environments in South Africa. In: (J.C. Vogel (Ed.), Late Cainozoic Palaeoclimates of the Southern Hemisphere. Balkema: Rotterdam, 235-264.

Butzer, K.W. (1978). Sediment stratigraphy of the Middle Stone Age sequence at Klasies River Mouth, Tsitsikama Coast, South Africa. *The South African Archaeological Bulletin* 33, 141-151.

Butzer, K.W., P. B. Beaumont, J. C. Vogel (1978). Lithostratigraphy of Border Cave, KwaZulu, South Africa: a Middle Stone Age sequence beginning c. 195,000 b.p. *Journal of Archaeological Science* 5, 317-341.

Callahan, E. (1979). The basics of biface knapping in the eastern fluted point tradition: a manual for flint-knappers and lithic analysts. *Archaeology of Eastern North America* **7**, 1-180.

Catuneanu, O., H. Wopfner, P.G. Eriksson, B. Cairncross, B.S. Rubidge, R.M.H. Smith, P.J. Hancox (2005). The Karoo basins of south-central Africa. *Journal of African Earth Sciences* 43, 211-253.

Chase, B.M. (2010). South African paleoenvironments during marine oxygen isotope stage 4: a context for the Howiesons Poort and Still Bay Industries. *Journal of Archaeological Science* 37, 1359-1366.

Clark, J.D. (1992). African and Asian perspectives on the origins of modern humans. *Philosophical Transactions: Biological Sciences* 337, 201-215.

Clark, J. Desmond (1988). The Middle Stone Age of East Africa and the beginnings of regional identity. *Journal of World Prehistory* 2, 235-305.

Clark, J. D. (1982). The cultures of the Middle Paleolithic/Middle Stone Age. In: J. D. Clark (Ed.), The Cambridge History of Africa. Cambridge University Press: Cambridge , 249-341.

Clark, J.D. (1980). Raw material and African lithic technology. *Man and Environment* 4, 44-55.

Clark, J.D. (1959). The Prehistory of Southern Africa. Pelican Books: London.

Clark, J.D., K.S. Brown (2001). The Twin Rivers Kopje, Zambia: stratigraphy, fauna, and artefact assemblages from the 1954 and 1956 Excavations. *Journal of Archaeological Science* 28, 305–330.

Clark, J.D., H. Kurashina (1979). An analysis of Earlier Stone Age bifaces from Gadeb (Locality 8E), Northern Bale Highlands, Ethiopia. *South African Archaeological Bulletin*, 34, 93-109.

Clark, J.L., I. Plug (2008). Animal exploitation strategies during the South African Middle Stone Age: Howiesons Poort and post-Howiesons Poort fauna from Sibudu Cave. *Journal of Human Evolution* 54, 886–898.

Close, A.E. (2002). Backed bladelets are a foreign country. In: R.G. Elston, S.L. Kuhn (Eds.), Thinking Small: Global Perspectives on Microlithization, 31-44.

Cochrane, G.W. (2006). An analysis of lithic artefacts from the ~60ka layers of Sibudu Cave. *Southern African Humanities* 18, 69-88.

Collins, M.B., J.M. Fenwick (1974). Heat treating of chert: methods of interpretation and their application. *Plains Anthropologist* 19, 134-145.

Corkill, T. (1999). Here and there: links between stone sources and Aboriginal archaeological sites in Sydney, Australia. M.P. Thesis, University of Sydney.

Cotterell, B., Kamminga, J. (1990). Mechanics of Pre-industrial Technology: an Introduction to the Mechanics of Ancient and Traditional Material Culture. Cambridge University Press: Cambridge.

Cotterell, B., J.Kamminga, F.P. Dickson (1985). The essential mechanics of conchoidal flaking. *International Journal of Fracture* 29, 205-221.

Cowling, R.M. (1983). The occurrence of C3 and C4 grasses in fynbos and allied shrublands in the South Eastern Cape, South Africa. *Oecologia* 58, 121-127.

Crabtree, D. (1967). Notes on experiments in flintknapping: 3, the flintknapper's raw materials. *Tebiwa* 10, 8-25.

Crabtree, D.E., B.R. Butler (1964). Notes on experiment in flint knapping: 1, Heat treatment of silica materials. *Tebiwa* **7**, 1-6.

Davis, Z.J., J. J. Shea (1998). Quantifying lithic curation: An experimental test of Dibble and Pelcin's original flake-tool mass predictor. *Journal of Archaeological Science* 25, 603-610.

Deacon, H.J. (1995). Two Late Pleistocene-Holocene Archaeological Depositories from the Southern Cape, South Africa. *South African Archaeological Bulletin* 50, 121-131.

Deacon, H.J. (1989). Late Pleistocene palaeoecology and archaeology in the southern Cape, South Africa. In: P. Mellars, C. Stringer (Eds.), The Human Revolution. Princeton University Press: Princeton, 547-564.

Deacon, H.J. (1983). Another look at the Pleistocene climates of South Africa. *South African Journal of Science* 79, 325-328.

Deacon, H.J. (1972). A review of the Post-Pleistocene in South Africa. *Goodwin Series* 1, 26-45.

Deacon, H.J., J. Deacon (1999). Human Beginnings in South Africa: Uncovering the Secrets of the Stone Age. Cape Town: David Philip Publishers.

Deacon, H. J., V.B. Geleijnse (1988). The stratigraphy and sedimentology of the main site sequence, Klasies River, South Africa. *South African Archaeological Bulletin* 43, 5–14.

Deacon, J. (1995). An unsolved mystery at the Howiesons Poort name site. *South African Archaeology Bulletin* 50, 110-120.

Deacon, J. (1984). The Later Stone Age of Southernmost Africa. BAR Cambridge Monographs in African Archaeology 12:Oxford.

Deacon, J. (1978). Changing Patterns in the Late Pleistocene/Early Holocene prehistory of Southern Africa as seen from the Nelson Bay Cave stone artefact sequence. *Quaternary Research* 10, 84-111.

Deacon, J. (1972). Wilton: an assessment after fifty years. *South African Archaeological Bulletin* 27, 10-48.

Delagnes, A., L. Wadley, P. Villa, M. Lombard (2006). Crystal quartz backed tools from the Howiesons Poort at Sibudu Cave. *Southern African Humanities* 18, 43-56.

Delagnes, A., H. Roche (2005). Late Pliocene hominid knapping skills: the case of Lokalalei 2C, West Turkana, Kenya. *Journal of Human Evolution* 48, 435-472.

Dibble, H.L. (1997). Platform variability and flake morphology: A comparison of experimental and archaeological data and implications for interpreting prehistoric lithic technological strategies. *Lithic Technology* 22, 150-170.

Dibble, H.L. (1995). Middle Paleolithic Scraper Reduction: Background, Clarification, and Review of the Evidence. *Journal of Archaeological Method and Theory* 2, 299-368.

Dibble, H.L., Z. Rezik (2009). Introducing a new experimental design for controlled studies of flake formation: results for exterior platform angle, platform depth, angle of blow, velocity, and force. *Journal of Archaeological Science* 36, 1945–1954.

Dibble, H.L., U.A. Schurmans, R.P. Iovita, M.V. McLaughlin (2005). The measurement and interpretation of cortex in lithic assemblages. *American Antiquity* 70, 545-560.

Domanski, M., Webb, J. A. (2007). A review of heat treatment research. *Lithic Technology* 32, 153-194.

Domanski, M., J.A. Webb, J. Boland (1994). Mechanical properties of stone artefact materials and the effect of heat treatment. *Archaeometry* 36, 177-208.

Domanski, M., J.A. Webb (1992). Effect of heat treatment on siliceous rocks used in prehistoric lithic technology. *Journal of Archaeological Science* 19, 601-614.

Douglass, M.J., S. J. Holdaway, P. C. Fanning, J.I. Shiner (2008). An assessment and archaeological application of cortex measurement in lithic assemblages. *American Antiquity* 73, 513-526.

Duke, C., J. Steele (2010). Geology and lithic procurement in Upper Palaeolithic Europe: a weights-of-evidence based GIS model of lithic resource potential. *Journal of Archaeological Science* 37, 813-824.

d'Errico, F., C.S. Henshilwood (2007). Additional evidence for bone technology in the southern African Middle Stone Age. *Journal of Human Evolution* 52,142-163.

Ellis, G.J. (1997). Factors influencing the use of stone projectile tips. In: H. Knecht (Ed.), Projectile Technology. Plenum Press: New York, 37-74.

Elston, R.G., P.J. Brantingham (2002). Microlithic technology in northern Asia: A risk-minimizing strategy of the Late Paleolithic and Early Holocene. In: R.G. Elston, S.L. Kuhn (Eds.), Thinking Small: Global Perspectives on Microlithization,103-116.

Evans, A.A., R.E. Donahue (2005). The elemental chemistry of lithic microwear: an experiment. *Journal of Archaeological Science* 32, 1733-1740.

Faith, J.T. (2011). Ungulate community richness, grazer extinctions, and human subsistence behavior in southern Africa's Cape Floral Region. *Palaeogeography, Palaeoclimatology, Palaeoecology* 306, 219–227.

Fischer, A., P. Vemming Hansen, P. Rasmussen (1984). Macro and micro wear traces on lithic projectile points: experimental results and prehistoric examples. *Journal of Danish Archaeology* 3, 19-46.

Fisher, E.C., M. Bar-Matthews, A. Jerardino, C.W. Marean (2010). Middle and Late Pleistocene paleoscape modeling along the southern coast of South Africa. *Quaternary Science Reviews* 29, 1382-1398.

Féblot-Augustins, J. (1997). Middle and Upper Paleolithic transfers in western and central Europe: assessing the pace of change. *Journal of Middle Atlantic Archaeology* 13, 57-90.

Ferré, E.C., L. Améglio (2000). Preserved magnetic fabrics vs. annealed microstructures in the syntectonic recrystallized George granite, South Africa. *Journal of Structural Geology* 22, 1199-1219.

Fitzhugh, B. (2001). Risk and invention in human technological evolution. *Journal of Anthropological Archaeology* 20, 125-167.

Flenniken, J.J. (1987). The Paleolithic Dyuktai Pressure Blade Technique of Siberia. *Arctic Anthropology* 24, 117-132.

Flenniken, J.J., J. P. White, (1983). Heat treatment of siliceous rocks and its implications for Australian prehistory. *Australian Aboriginal Studies* 1, 43-48.

Flenniken, J.J. and E.G. Garrison (1975). Thermally altered Novaculite and Stone Tool Manufacturing Techniques. *Journal of Field Archaeology* 2, 125-131.

Foley, R., M.M. Lahr (2003). On Stony Ground: Lithic Technology, Human Evolution, and the Emergence of Culture. *Evolutionary Anthropology* 12,109–122.

Frankel, J.J. (1952). Silcrete near Albertinia, Cape Province. *South African Journal of Science* 49, 173-182.

Geneste, J.-M (1985). Analyze lithique d'industries mousteriennes du Perigord: Une aproche technologique du comportement des groupes humains au Paloelithique moyen. PhD Dissertation, University of Bordeaux.

Geneste, J.- M, H. Plisson (1993). Hunting technologies and human behavior: lithic analysis of Solutrean shouldered points. In: H. Knecht, A. Pike-Tay, R. White (Eds.), Before Lascaux. The complex record of the Early Upper Paleolithic. : CRC Press: London, 117-135.

Goldman-Neuman, T., E. Hovers (2009). Methodological considerations in the study of Oldowan raw material selectivity: insights from A. L. 894 (Hadar, Ethiopia). In: E. Hovers, D.R. Braun (Eds.), Interdisciplinary Approaches to the Oldowan. Springer: Netherlands Reference, 71-84.

Goodman, M.E. (1944). The physical properties of stone tool materials. *American Antiquity* 9, 415-433.

Goodwin, A.J.H., C. van Riet Lowe (1929). The Stone Age Cultures of South Africa. *Annals of the South African Museum* 27, 95-145.

Goodyear, A.C. (1989). A hypothesis for the use of cryptocrystalline raw materials among the paleoindian groups of North America. In: C. Ellis, J. Lathrop (Eds.), Eastern Paleoindian Lithic Resource Use. Westview Press: Boulder, 1-9.

Goudie, A. (2006). The Schmidt Hammer in geomorphological research. *Progress in Physical Geography* 30, 703–718.

Gould, R.A. (1985). The empiricist strikes back: reply to Binford. *American Antiquity* 50, 638-644.

Gould, R.A., J.E. Yellen (1991). Misreading the past: a reply to Binford concerning hunter-gatherer site structure. *Journal of Anthropological Archaeology* 10, 283-298.

Gould, R. A.,S. Saggers (1985). Lithic procurement in central Australia: a closer look at Binford's idea of embeddedness in archaeology. *American Antiquity* 50, 117-136.

Gould, R.A., D.A. Koster, A.H.L. Sontz (1971). The lithic assemblage of the Western Desert Aborigines of Australia. *American Antiquity* 36, 149-169.

Graham, A.A., D.J. McCaughan, F.S. McKee (1988). Measurement of surface area of stones. *Hydrobiologia* 157, 85-87.

Graymer, R.W., Jones, D.L., Brabb, E.E. (2002). Geologic map and map database of northeastern San Francisco Bay region, California; Most of Solano County and parts of

Napa, Marin, Contra Costa, San Joaquin, Sacramento, Yolo, and Sonoma Counties: U.S. Geological Survey Miscellaneous Field Studies Map MF-2403, U.S. Geological Survey, Menlo Park, CA.

Gregg, M.L., R.J. Grybush, (1976). Thermally altered siliceous stone from prehistoric contexts: intentional versus unintentional alteration. *American Antiquity* 41, 189-192.

Grine, F.E., R. G. Klein, T. Volman (1991). Dating, archaeology and human fossils from the Middle Stone Age levels of Die Kelders, South Africa. *Journal of Human Evolution* 21, 363-395.

Grün, R., P. Beaumont (2001). Border Cave revisited: a revised ESR Chronology. *Journal of Human Evolution* 40, 467–482.

Grün, R., N.J. Shackleton, H.J. Deacon (1990) Electron-Spin-Resonance dating of tooth enamel from Klasies River Mouth Cave. *Current Anthropology* 31, 427-432.

Hanckel, M. (1985). Hot rock: heat treatment at Burrill Lake and Curarong, New South Wales. *Archaeology in Oceania* 20, 98-102.

Harmand, S. (2009). Variability in raw material selectivity at the Late Pliocene sites of Lokalalei, West Turkana, Kenya. In: E. Hovers, D.R. Braun (Eds.), Interdisciplinary Approaches to the Oldowan. Springer: Netherlands, 85-97.

Heider, K.G. (1967) Archaeological assumptions and ethnographical facts: a cautionary tale from New Guinea. *Southwestern Journal of Anthropology* 23, 52-64.

Hendey, Q.B., T.P. Volman (1986). Last interglacial sea levels and coastal caves in the Cape Province, South Africa. *Quaternary Research* 2, 189–198.

Henry, D. O. (1989). Correlations between reduction strategies and settlement patterns. *Archeological Papers of the American Anthropological Association* 1, 139–155.

Henshilwood, C.S. (2008). Winds of change: palaeoenvironments, material culture and human behaviour in the Late Pleistocene (~77ka-48ka ago) in the Western Cape Province, South Africa. *South African Archaeoogical Society Goodwin Series* 10, 35-51.

Henshilwood, C., J. Sealy (1997). Bone artefacts from the Middle Stone Age at Blombos Cave, Southern Cape, South Africa. *Current Anthropology* 38, 890-895.

Henshilwood, C.S., F. d'Errico, M. Vanhaeren, K. Van Niekerk, Z. Jacobs, (2004). Middle Stone Age shell beads from South Africa. *Science* 304, 404.

Henshilwood, C.S., F. d'Errico, R. Yates, Z. Jacobs, C. Tribolo, G.A.T. Duller, N. Mercier, J.C. Sealy, H. Valladas, I. Watts, A.G. Wintle. (2002). Emergence of modern human behaviour: Middle Stone Age engravings from South Africa. *Science* 295, 1278-1280.

Henshilwood,C.S., F. d'Errico,C.W. Marean, R.G. Milo,R.J. Yates (2001a). An early bone tool industry from the Middle Stone Age, Blombos Cave, South Africa:

implications for the origins of modern human behaviour, symbolism and language. *Journal of Human Evolution* 41, 631-678.

Henshilwood, C.S., J. C. Sealy, R. Yates, K. Cruz-Uribe, P. Goldberg, F. E. Grine, R. G. Klein, C. Poggenpoel, K. van Niekerk, I. Watts (2001b). Blombos Cave, Southern Cape, South Africa: preliminary report on the 1992–1999 excavations of the Middle Stone Age levels. *Journal of Archaeological Science* 28, 421–448.

Herries, A.I.R. E. C. Fisher (2010). Multidimensional GIS modeling of magnetic mineralogy as a proxy for fire use and spatial patterning: evidence from the Middle Stone Age bearing sea cave of Pinnacle Point 13B (Western Cape, South Africa). *Journal of Human Evolution* 59, 306-320.

Hester, T.R. (1972). Ethnographic evidence of thermal alteration of siliceous stone. *Tebiwa* 15, 63-65.

Hiscock, P. (2002). Pattern and context in the Holocene proliferation of backed artifacts in Australia. In: R.G. Elston, S.L. Kuhn (Eds.), Thinking Small: Global Perspectives on Microlithization,163-178.

Hiscock, P., A. Turq, J.-P Faivre, L. Bourguignon (2009) Quina procurement and tool production. In: B. Adams, B.S. Blades (Eds.), Lithic Materials and Paleolithic Societies. Wiley-Blackwell: Oxford, 232-246.

Howell, D.C. (1999). Fundamental Statistics for the Behavioral Sciences. Brooks/Cole Publishing Company: Pacific Grove.

Huang, Y., F.A. Street-Perrott, S.E. Metcalfe, M. Brenner, M. Moreland, K.H. Freeman (2001). Climate change as the dominant control on glacial-interglacial variations in C3 and C4 plant abundance. *Science* 293, 1647–1651.

Inizan, M.-L., H. Roche, J. Tixier (1992). Technology of Knapped Stone. Cercle de Recherches et d'Etudes Prehistoriques C.N.R.S. -1, Meudon, France.

Inskeep, R.R. (1987). Nelson Bay Cave, Cape Province, South Africa : the Holocene levels. BAR Cambridge Monographs in African Archaeology 357:Oxford.

Isaac, G.L. (1986). Foundation stones; early artifacts as indicators of activities and abilities. In: G.N. Bailey, P. Callow (Eds.). Stone Age Prehistory: Studies in Memory of Charles McBurney. Cambridge University Press: Cambridge, 221-242.

Isaac, G.L., (1981). Emergence of human behavior patterns. Archaeological tests of alternative models of early hominid behaviour: excavations and experiments. *Philisophical Transactions of the Royal Society, London* 292, 177-188.

Isaac, G.L. (1975). Middle Pleistocene stratigraphy and cultural patterns in East Africa. In: K.W. Butzer and G.L. Isaac (Eds.), After the Australopithecines: Stratigraphy, Ecology, and Culture Change in the Middle Pleistocene. Mouton: The Hague, 495-542.

Jacobs, Z. R.G. Roberts, R. F. Galbraith, H. J. Deacon, R. Grün, A. Mackay, P. Mitchell, R. Vogelsang, L. Wadley (2008). Ages for the Middle Stone Age of Southern Africa: implications for human behavior and dispersal. *Science* 322, 733-735.

Jacobs, Z., R.G. Roberts (2008). Testing times: old and new chronologies for the Howieson's Poort and Still Bay Industries in environmental context. *South African Archaeological Society Goodwin Series* 10, 9-34.

Jacobs, Z., A.G. Wintle, G.A.T. Duller (2003a). Optical dating of dune sand from Blombos Cave, South Africa: I-Multiple grain data. *Journal of Human Evolution* 44, 599-612.

Jacobs, Z., A.G. Wintle, G.A.T. Duller (2003b). Optical dating of dune sand from Blombos Cave, South Africa: II Single grain data. *Journal of Human Evolution* 44, 613-625.

Jerardino, A. (2007). Excavations at a Hunter-Gatherer Site Know as 'Grootrif G' Shell Midden, Lamberts Bay, Western Cape Province. *South African Archaeological Bulletin* 62, 162-170.

Jeske, R. (1989). Economies in raw material use by prehistoric hunter-gatherers. In: R. Torrence (Ed.), Time, Energy and Stone Tools. Cambridge University Press:Cambridge, 34-45.

Johnson, M.R., C.J. van Vuuran, J.N.J. Visser, D.I. Cole, H. de V. Wickens, A.D.M. Christie, D.L. Roberts, G. Brandle (2006). Sedimentary rocks of the Karoo Supergroup In: B. Thomas (Ed.), The Geology of South Africa. Geological Society of South Africa: Johannesburg, 461-500.

Johnson, M.R., C.J. Van Vuuren, W.F. Hegenberger, R. Key, U. Show (1996). Stratigraphy of the Karoo Supergroup in southern Africa: an overview. *Journal of African Earth Sciences* 23, 3-15.

Jolly, K. (1948). The development of the Cape Middle Stone Age in the Skildergat Cave, Fish Hoek. *South African Archaeological Bulletin* 3, 106-107.

Jones, P.R. (1979). Effects of raw materials on biface manufacture. *Science* 204, 835-836.

Kahraman, S. M. Fener (2007). Predicting the Los Angeles abrasion loss of rock aggregates from the uniaxial compressive strength. *Materials Letters* 61, 4861-4865.

Karkanas, P., P. Goldberg (2010). Site formation processes at Pinnacle Point Cave 13B (Mossel Bay, Western Cape Province, South Africa): resolving stratigraphic and depositional complexities with micromorphology. *Journal of Human Evolution* 59, 256-273.

Keeley, L. and N. Toth (1981). Microwear Polishes on early stone tools from Koobi Fora, Kenya. *Nature* 293, 464-465.

Keller, C.M. (1973). Montagu Cave in Prehistory. University of California Press: Berkeley.

Kelly, R.L. (1995). The Foraging Spectrum. Smithsonian Institution Press:Washington D.C.

Kelly, R. L. (1992). Mobility/sedentism: concepts, archaeological measures, and effects. *Annual Review of Anthropology* 21, 43-66.

Kelly, R. L. (1988). The three sides of a biface. *American Antiquity* 53, 717-734.

Kim, H, M. Barton, A.M. Hurtado (2009). The emergence of human uniqueness: Characters underlying behavioral modernity. *Evolutionary Anthropology* 18,187-200.

King, L.C. (1948). On the ages of African land-surfaces. *Journal of the Geological Society* 104, 439-459.

Klein, R.G. (2008). Out of Africa and the evolution of human behavior. *Evolutionary Anthropology* 17, 267–281.

Klein, R.G. (2000). The Earlier Stone Age of Southern Africa. *South African Archaeological Bulletin* 55, 107-122.

Klein, R.G., 1972. The Late Quaternary mammalian fauna of Nelson Bay Cave (Cape Province, South Africa): its implications for megafaunal extinctions and environmental and cultural change. *Quaternary Research* 2, 135-142.

Klein, R.G., 1983. Palaeoenvironmental implications of Quaternary large mammals in the fynbos region. In: H.J. Deacon, Q.B. Hendey, J.J.N. Lambrechts, J.J.N. (Eds.), Fynbos Palaeoecology: A Preliminary Synthesis. South African National Scientific Programmes Report No. 75. Mills Litho, Cape Town, pp. 116-138.

Klein, R.G., G. Avery, K. Cruz-Uribe, D. Halkett, T.Hart, R.G. Milo, T. P. Volman (1999). Duinefontein 2: an Acheulean Site in the Western Cape Province of South Africa. *Journal of Human Evolution* 37, 153-190.

Knecht, H. (1997). Projectile points of bone, antler and stone: experimental explorations of manufacture and use. In: H. Knecht (Ed.), Projectile Technology. Plenum Press: New York, 191-212.

Kuhn, S.L. (2004). Upper Paleolithic raw material economies at Űçağızlı cave, Turkey. *Journal of Anthropological Archaeology* 23, 431–448.

Kuhn, S.L. (2002). Pioneers of microlithization: the "Proto-Aurignacian" of southern Europe. In: R.G. Elston, S.L. Kuhn (Eds.), Thinking Small: Global Perspectives on Microlithization, 83-94.

Kuhn, S. L. (1994). A Formal Approach to the Design and Assembly of Mobile Toolkits. *American Antiquity* 59, 426-442.

Kuhn, S. L. (1992). Blank form and reduction as determinants of Mousterian scraper morphology. *American Antiquity* 57, 115–28.

Kuhn, S. L. (1991). 'Unpacking' reduction: lithic raw material economy in the Mousterian of west-central Italy. *Journal of Anthropological Archaeology* 10,76-106,

Kuhn, S. L. and R. G. Elston (2002). Introduction: Thinking Small Globally. *Archeological Papers of the American Anthropological Association* 12, 1–7.

Kuman, K. (1994). The archaeology of Sterkfontein-past and present. *Journal of Human Evolution* 27, 471-495.

Larson, M., Kornfeld, M. (1997). Chipped stone nodules: theory, method and examples. *Lithic Technology* 22, 4-18.

Lavrenov, I.V. (1998). The wave energy concentration at the Agulhas current off South Africa. *Natural Hazards* 17, 117-127.

Lea, V. (2005). Raw, pre-heated or ready to use: discovering specialist supply systems for flint industries in mid-Neolithic (Chassey culture) communities in southern France. *Antiquity* 79, 51-65.

Leakey, M.D. (1971). Olduvai Gorge Vol. 3. Cambridge University Press: Cambridge.

Leroi-Gourhan, A. (1957). Prehistoric Man. Philisophical Library: New York.

Lin, S.C.H., M. J. Douglass, S. J. Holdaway, B. Floyd (2010). The application of 3D laser scanning technology to the assessment of ordinal and mechanical cortex quantification in lithic analysis. *Journal of Archaeological Science* 37, 694-702.

Lombard, M. (2011). Quartz-tipped arrows older than 60 ka: further use-trace evidence from Sibudu, Kwazulu-Natal, South Africa, *Journal of Archaeological Science* 28, 1918-1930.

Lombard, M., (2006). First impressions of the functions and hafting technology of Still Bay pointed artefacts from Sibudu Cave. *Southern African Humanities* 18, 27-41.

Lombard, M. (2005). Evidence of hunting and hafting during the Middle Stone Age at Sibudu Cave, KwaZulu-Natal, South Africa: a multianalytical approach. *Journal of Human Evolution* 48, 279-300.

Lombard, M., L. Phillipson (2010). Indications of bow and stone-tipped arrow use 64,000 years ago in KwaZulu-Natal, South Africa. *Antiquity* 84, 635-648.

Lombard, M., J. Pargeter (2008). Hunting with Howiesons Poort segments: pilot experimental study and the functional interpretation of archaeological tools. *Journal of Archaeological Science* 35, 2523–2531.

Lowe, D.R. (1999). Petrology and sedimentology of cherts and related silicified sedimentary rocks in the Swaziland Supergroup In: D.R. Lowe, G.R. Byerly (Eds.),

Geologic Evolution of the Barberton Greenstone Belt, South Africa, Geological Society of America Special Papers 329, 83-114.

Lowe, D.R., B.W. Nocita (1999). Foreland basin sedimentation in the Mapepe Formation, southern-facies Fig Tree Group. In: D.R. Lowe, G.R. Byerly (Eds.), Geologic Evolution of the Barberton Greenstone Belt, South Africa, Geological Society of America Special Papers 329, 233-258.

Luedtke, B. E. (1992). An archaeologist's guide to chert and flint. *Archaeological Research Tools 7*. Institute of Archaeology, University of California, Los Angeles: Los Angeles.

Mackay, A. (2011). Potentially stylistic differences between backed artefacts from two nearby sites occupied ~60,000 years before present in South Africa. *Journal of Anthropological Archaeology* 30, 235-245.

Mackay, A. (2008a). A method for estimating edge length from flake dimensions: use and implications for technological change in the southern African MSA. *Journal of Archaeological Science* 35, 614-622.

Mackay, A. (2008b). On the production of blades and its relationship to backed artefacts in the Howiesons Poort at Diepkloof, South Africa. *Lithic Technology* 33, 87-99.

Mackay, A., J. Orton, S. Schwortz, T.E. Steele (2010). Soutfontein (SFT)-001: preliminary report on an open-air site rich in bifacial points, Southern Namaqualand, South Africa. *South African Archaeological Bulletin* 65, 84-95.

Magne, M.P. (2001). Debitage analysis as a scientific tool for archaeological analysis. In: W. Andrefsky (Ed.), Lithic Debitage Context Form Meaning. University of Utah Press: Salt Lake City, 21-30.

Magne, M.P., D. Pokotylo (1981). A pilot study in bifacial lithic reduction sequences. *Lithic Technology* 10, 34-47.

Malan, B.D. (1949). Magosian and Howieson's Poort. *South African Archaeological Bulletin* 4, 34-36.

Malan, J., J. Viljoen (2008). Southern Cape Geology: Evolution of a Rifted Margin. Field Excursion FT07 Guidebook. Prepared for the American Association of Petroleum Geologists International Conference and Exhibition, 26-29th of October, 2008, Cape Town, South Africa.

Mandeville, M.D., J. J. Flenniken (1974). A comparison of the flaking qualities Nehawka Chert before and after thermal pretreatment. *Plains Anthropologist* 19, 146-148.

Marean, C. W. (2010a). Pinnacle Point Cave 13B (Western Cape Province, South Africa) in context: The Cape Floral Kingdom, shellfish, and modern human origins. *Journal of Human Evolution* 59, 425-443.

Marean, C. W. (2010b). When the Sea Saved Humanity. *Scientific American*. August 2010, 54-61.

Marean, C.W., M. Bar-Matthews, J. Bernatchez, E. Fisher, P. Goldberg, A. I. R. Herries, Z. Jacobs, A. Jerardino, P. Karkanas, T. Minichillo, P. J. Nilssen, E. Thompson, I. Watts, H.M. Williams (2007). Early human use of marine resources and pigment in South Africa during the Middle Pleistocene. *Nature* 449, 905-908.

Marean, C.W., Assefa, Z. (2005). The Middle and Upper Pleistocene African record for the biological and behavioral origins of modern humans. In: B. Stahl (Ed.), African Archaeology. Blackwell: New York, 93-129.

Marean, C.W., P.J. Nilssen, K. Brown, A. Jerardino, D. Stynder (2004). Paleoanthropological investigations of Middle Stone Age sites at Pinnacle Point, Mossel Bay (South Africa): Archaeology and hominid remains from the 2000 Field Season. *PaleoAnthropology* 83, 14-83.

Marean, C.W., P. Goldberg, G. Avery, F.E. Grine, R.G. Klein (2000). Middle Stone Age stratigraphy and excavations at Die Kelders Cave 1: results of the 1992, 1993, and 1995 field seasons. *Journal of Human Evolution* 38, 7-42.

Marker, M.E., M.J. McFarlane (1997). Cartographic analysis of the African surface complex between Albertinia and Mossel Bay, Southern Cape, South Africa. *South African Journal of Geology* 100, 185-194.

Marks, A.E., J. Shokler, J. Zilhão (1991). Raw material usage in the Paleolithic: the effects of local availability on selection and economy. In: A. Montet-White, S. Holen (Eds.), Raw Material Economies among Prehistoric Hunter-Gatherers. University of Kansas:Lawrence, 127-129.

Martini, J.E.J. (1974). On the presence of ash beds and volcanic fragments in the Southern Cape Province (South Africa). *Transactions of the Geological Society of South Africa* 77, 113- 116.

Martinson, D.G., N.G. Pisias, J.D. Hays, J. Imbrie, T.C. Moore, Jr, N.J. Shackleton (1987). Age dating and the orbital theory of the ice ages: Development of a high-resolution 0 to 300,000-year chronostratigraphy. *Quaternary Research* 27, 1-29.

Marwick, B. (2008). What attributes are important for the measurement of assemblage reduction intensity? Results from an experimental stone artifact assemblage with relevance to the Hoabinhian of mainland Southeast Asia. *Journal of Archaeological Science* 35, 1189-1200.

McBrearty, S., A. S. Brooks (2000). The revolution that wasn't: a new interpretation of the origin of modern human behavior. *Journal of Human Evolution* 39, 453-563.

McCall, G.S. (2006). Multivariate perspectives on change and continuity in the Middle Stone Age lithics from Klasies River Mouth, South Africa. *Journal of Human Evolution* 51, 429-439.

McCall, G.S. (2007). Behavioral ecological models of lithic technological change during the later Middle Stone Age of South Africa. *Journal of Archaeological Science* 34, 1738-1751.

McCormick,N.J. (1985). Edge flaking as a measure of material performance. *Metals and Materials* 8, 154-156.

McCormick, N.J., and E.A. Almond (1990). Edge flaking of brittle materials. *Journal of Hard Materials* 1, 25-52.

Mellars P. (1989). Major issues in the emergence of modern humans. *Current Anthropology* 30, 349-385.

Mercieca, A., P. Hiscock (2008). Experimental insights into alternative strategies of lithic heat treatment. *Journal of Archaeological Science* 35, 2634–2639.

Milliken, S. (1998). The role of raw material availability in technological organization: a case study from the southeast Italian Late Palaeolithic. In: S. Milliken (Ed.), The Organization of Lithic Technology in Late Glacial and Early Postglacial Europe. British Archaeological Reports 700:Oxford, 63-82.

Minichillo, T. (2006). Raw material use and behavioral modernity: Howiesons Poort lithic foraging strategies. *Journal of Human Evolution* 50, 359-364.

Minichillo,T. (2005). Middle Stone Age Lithic Study, South Africa: An Examination of Modern Human Origins. Unpublished PhD dissertation, University of Washington.

Mitchell, P. J. (2002). The Archaeology of Southern Africa. Cambridge: Cambridge University Press.

Mitchell, P. J. (1996). The archaeological landscape at Sehonghong, a hunter-gatherer site in the Lesotho highlands, southern Africa. *Antiquity* 70, 623-638.

Mitchell, P. J. (1995). Revisiting the Robberg: New Results and a Revision of Old Ideas at Sehonghong Rock Shelter. *South African Archaeological Bulletin* 50, 28-38.

Morrow, T.A. (1996). Bigger is better: comments on Kuhn's formal approach to mobile tool kits. *American Antiquity* 61, 581-590.

Mourre,V., P. Villa, C.S. Henshilwood (2010). Early use of pressure flaking on lithic artifacts at Blombos Cave, South Africa. *Science* 330, 659-662.

Neeley, M.P. (2002). Going microlithic: a Levantine perspective on the adoption of microlithic technologies. In: R.G. Elston, S.L. Kuhn (Eds.), Thinking Small: Global Perspectives on Microlithization,45-56.

Neeley, M.P., C.M. Barton (1994). A new approach to interpreting late Pleistocene microlith industries in southwest Asia. *Antiquity* 68, 275-288.

Nelson, M.C. (1991). The study of technological organization. *Archaeological Method and Theory* 3, 57-100.

Nelson, N.C. (1916). Flint working by Ishi. In: R.F. Heizer, T. Kroeber (Eds.), Ishi the Last Yahi A Documentary History. University of California Press: Berkeley,168-172.

Noll, M.P. (2000). Components of Acheulean Lithic Assemblage Variability at Olorgesaile, Kenya. PhD Dissertation, University of Illinois at Urbana-Champaign.

O'Brien, E.M. (1993). Climatic gradients in woody plant species richness: towards an explanation based on an analysis of southern Africa's woody flora. *Journal of Biogeography* 20,181-198.

Odell, G.H. (1994). The role of stone bladelets in Middle Woodland society. *American Antiquity* 59, 102-120.

Orton, J. (2008). A useful measure of the desirability of different raw materials for retouch within and between assemblages: the raw material retouch index (RMRI). *Journal of Archaeological Science* 35, 1090-1094.

Orton, J (2002). Patterns in stone: the lithic assemblage from Dunefield Midden, Western Cape, South Africa. South African Archaeological Bulletin 57, 31-37.

Oswalt, W. (1973). Habitat and Technology. Holt, Rinehart and Winston:New York.

Parkington, J.E. (1989). A critique of the consensus view of the age of Howieson's Poort assemblages in South Africa In: P.Mellars, C. Stringer (Eds.), The Human Revolution. Edinburgh University Press: Edinburgh, 34-55.

Partridge, T.C., G.A. Botha, I.G. Haddon (2006). Cenozoic deposits of the interior. In: B. Thomas (Ed.), The Geology of South Africa. Geological Society of South Africa:Johannesburg, 585-604.

Partridge, T.C. and R.R. Maud (1987). Geomorphic evolution of southern Africa since the Mesozoic. *Transactions of the Geological Society of South Africa* 90, 179-208.

Pelcin, A. W. (1998). The threshold effect of platform width: A reply to Davis and Shea, *Journal of Archaeological Science* 25, 615-620.

Pelcin, A. W. (1997). The effect of core surface morphology on flake attributes: evidence from a controlled experiment. *Journal of Archaeological Science* 24, 749-756.

Petillon,J-M, O. Bignon, P. Bodu, P. Cattelain, G. Debout, M. Langlais, V. Laroulandie, H. Plisson, B. Valentin (2011). Hard core and cutting edge: experimental manufacture and use of Magdalenian composite projectile tips. *Journal of Archaeological Science*, 38, 1266-1283.

Porraz, G., P-J. Texier, J-P. Rigaud, J. Parkington, C. Poggenpoel, D.L. Roberts (2008). Preliminary characterization of a Middle Stone Age lithic assemblage preceding the

'Classic' Howieson's Poort Complex at Diepkloof Rock Shelter, Western Cape Province, South Africa. *South African Archaeological Society Goodwin Series* 10, 105-121.

Potts, R. (1991). Why the Oldowan? Plio-Pleistocene tool making and the transport of resources, *Journal of Anthropological Research* 47, 153-176.

Powell, A., S., Shennan, M. G., Thomas (2009). Late Pleistocene demography and the appearance of modern human behavior, *Science* 324, 1298-1301.

Purdy, B, H.K. Brooks (1971). Thermal alteration of silica minerals: an archeological approach. *Science* 173, 322-325.

Rector, A. L., C.W. Marean (2011). Community paleoecology and habitat variability during Middle Stone Age occupation of the Cape Floral Region, South Africa. Abstracts of the PaleoAnthropology Society 2011 Meetings. *PaleoAnthropology* 2011

Rector, A.L., K.E. Reed (2010) Middle and Late Pleistocene faunas of Pinnacle Point and their paleoecological implications. *Journal of Human Evolution* 59 (2010) 340-357.

Rector, A.L., B.C. Verrelli (2010). Glacial cycling, large mammal community composition, and trophic adaptations in the Western Cape, South Africa. *Journal of Human Evolution* 58, 90-102.

Renfrew, C. (1969). Trade and Culture Process in European Prehistory. *Current Anthropology 10*, 151-169.

Rick, J.W. (1978). Heat-Altered Cherts of the Lower Illinois Valley: An Experimental Study in Prehistoric Technology. *Northwestern University Archaeological Program Prehistoric Records* 2. Evanston: Northwestern University.

Rick, J.W., S. Chappell (1983). Thermal alteration of silica materials in technological and functional perspective. *Lithic Technology* 12, 69-80.

Roberts, D.L., G.A. Botha, R.R. Maud, and J. Pether (2006). Coastal Cenozoic Deposits In: B. Thomas (Ed.), The Geology of South Africa. Geological Society of South Africa: Johannesburg, 605-628.

Roberts, D. L. (2003) Age, Genesis and Significance of South African Coastal Belt Silcretes. *Memoir 95*. Council for Geoscience, Pretoria.

Roth, B, H.L. Dibble (1998). Production and transport of blanks and tools at the French Middle Paleolithic Site of Combe-Capelle Bas. *American Antiquity* 63, 47-62.

Rowney, M., J.P. White (1997). Detecting heat treatment on silcrete: Experiments with methods. *Journal of Archaeological Science* 24, 649–657.

Rudner, J. (1979). The use of stone artefacts and pottery among the Khoisan peoples in historic and protohistoric times. *South African Archaeological Bulletin* 34, 3–17.

Sackett, J.R. (1986). Style, function, and assemblage variability: a reply to Binford. *American Antiquity*, 51, 628-634.

Sackett, J.R. (1982). Approaches to style in lithic archaeology. *Journal of Anthropological Archaeology* 1, 59-112.

Sampson, C.G. (1974). The Stone Age Archaeology of Southern Africa. Academic Press: New York.

Schick, K.D., Toth, N. (1993). Making Silent Stones Speak: Human Evolution and the Dawn of Technology. Simon and Schuster: New York.

Schindler, D.L. J. W. Hatch, C. A. Hay, R.C. Bradt (1982). Aboriginal thermal alteration of a central Pennsylvania jasper: Analytical and behavioral implications. *American Antiquity* 47, 526-544.

Schoville, B.J. (2010). Frequency and distribution of edge damage on Middle Stone Age lithic points, Pinnacle Point 13B, South Africa. *Journal of Human Evolution* 59, 378-391.

Schoville, B.J., K. S. Brown, S. Oestmo, C.W. Marean (2011). The Potential of Pre-Howiesons Poort MSA Backed Blades from Pinnacle Point, South Africa as Projectile Armatures. Paper presented at the Stone Age Weaponry Workshop, 19-21 September, 2011. Mainz, Germany

Schoville, B.J., K. S. Brown (2010). Comparing lithic assemblage edge damage distributions: examples from the Late Pleistocene and preliminary experimental results. *Vis-à-vis: Explorations in Anthropology* 10, 34–49. vav.library.utoronto.ca.

Schrire, C., J. Deacon (1989). The indigenous artefacts from Oudepost I, a colonial outpost of the VOC at Saldanha Bay, Cape. *South African Archaeological Bulletin* 44, 105-113.

Schweitzer, F.R. (1979). Excavations at Die Kelders, Cape Province, South Africa: the Holocene deposits. *Annals of the South African Museum* 78, 101-233.

Scott, L., 2002. Grassland development under glacial and interglacial conditions in southern Africa: review of pollen, phytolith and isotope evidence. *Palaeogeography, Palaeoclimatology, Palaeoecology* 177, 47-57.

Sevillano, J.G. (1997) Lithic tool making by Amazonian palaeoindians: a case-study on materials selection. *Journal of Materials Science Letters* 16, 465–468.

Shackleton, N.J. (1982). Stratigraphy and chronology of the KRM deposits: oxygen isotope evidence in R. Singer and J. Wymer, The Middle Stone Age at Klasies River Mouth in South Africa. University of Chicago Press: Chicago, 194-199.

Shackleton, N.J., A. Berger, W. R. Peltier (1990). An alternative astronomical calibration of the lower Pleistocene timescale based on ODP Site 677. *Transactions of the Royal Society of Edinburgh: Earth Sciences* 81, 251-261.

Shackleton, N.J., N.D. Opdyke (1973). Oxygen isotope and palaeomagnetic stratigraphy of Equatorial Pacific core V28-238: Oxygen isotope temperatures and ice volumes on a 10^5 year and 10^6 year scale. *Quaternary Research* 3, 39-55.

Shackley, M.S. (1998). Gamma rays, X-rays and stone tools: some recent advances in archaeological geochemistry. *Journal of Archaeological Science* 25, 259-270.

Sharon, G. (2008). The impact of raw material on Acheulian large flake production. *Journal of Archaeological Science* 35, 1329-1344.

Shea, J.J. (2011). *Homo sapiens* is as *Homo sapiens* was. *Current Anthropology* 52, 1-35.

Shea, J.J. (2006). The origins of lithic projectile point technology: evidence from Africa, the Levant, and Europe. *Journal of Archaeological Science* 33, 823-846.

Shea, J.J., M. L. Sisk (2010). Complex projectile technology and Homo sapiens dispersal into Western Eurasia. *PaleoAnthropology* 2010,100−122.

Shea, J.J., Z. Davis, K. Brown (2001). Experimental tests of Middle Palaeolithic spear points using a calibrated crossbow. *Journal of Archaeological Science 28*, 807-816.

Shone, R.W. (2006). Onshore Post-Karoo Mesozoic Deposits In: B. Thomas (Ed.), The Geology of South Africa. Geological Society of South Africa:Johannesburg, 541-552.

Shott, M.J. (1994). Size and Form in the Analysis of Flake Debris: Review and Recent Approaches. *Journal of Archaeological Method and Theory* 1, 69-110.

Shott, M. J. 1986. Technological organization and settlement mobility: an ethnographic examination. *Journal of Anthropological Research* 42,15-51.

Singer, R, J. Wymer (1982). The Middle Stone Age at Klasies River Mouth in South Africa. University of Chicago Press: Chicago.

Sisk, M.L., J. J. Shea (2009). Experimental use and quantitative performance analysis of triangular flakes (Levallois points) used as arrowheads. *Journal of Archaeological Science* 36, 2039–2047.

Smith, A.B., K. Sadr, J. Gribble, R. Yates (1991). Excavations in the south-western Cape, South Africa, and the archaeological identity of prehistoric hunter-gatherers within the last 2000 Years. *South African Archaeological Bulletin* 46, 71-91.

Soriano, S., P. Villa, L. Wadley (2007). Blade technology and tool forms in the Middle Stone Age of South Africa: the Howiesons Poort and post-Howiesons Poort at Rose Cottage Cave. *Journal of Archaeological Science* 34, 681-703.

Stapleton, P., J. Hewitt (1927). Stone implements from a rock shelter at Howieson's Poort, near Grahamstown. *South African Journal of Science* 24, 574-587.

Stapleton, P., J. Hewitt (1928). Stone implements from Howieson's Poort, near Grahamstown. *South African Journal of Science* 25, 399-409.

Stout, D. (2002). Skill and cognition in stone tool production. *Current Anthropology* 43, 693-715.

Stout, D., J. Quade, S. Semaw, M.J. Rogers, N.E. Levin (2005). Raw material selectivity of the earliest stone toolmakers at Gona, Afar, Ethiopia. *Journal of Human Evolution* 48, 365-380.

Straus, L.G. (2002). Selecting small: microlithic musings for the Upper Paleolithic and Mesolithic of Western Europe. In: R.G. Elston, S.L. Kuhn (Eds.), Thinking Small: Global Perspectives on Microlithization, 69-82.

Summerfield, M.A. (1983). Silcrete as a palaeoclimatic indicator: evidence from southern Africa. *Palaeogeography, Palaeoclimatology, Palaeoecology* 41, 65-79.

Summerfield, M.A. (1981). The nature and occurrence of silcrete, southern Cape Province, South Africa. Report Number 28, School of Geography, University of Oxford, 1-36.

Sumner, P, W. Nel (2002). The effect of rock moisture on Schmidt hammer rebound: Tests on rock samples from Marion Island and South Africa. *Earth Surface Processes and Landforms* 27, 1137-1142.

Talma, A.S. and J.C. Vogel (1992). Late Quaternary paleotemperatures derived from a speleothem from Cango Caves, Cape Province, South Africa. *Quaternary Research* 37, 201-213.

Texier, P-J, G. Porraz, J. Parkington, J-P. Rigaud, C, Poggenpoel, C. Miller, C. Tribolo, C. Cartwright, A. Coudenneauf, R. Klein, T. Steele, C. Verna (2010). A Howiesons Poort tradition of engraving ostrich eggshell containers dated to 60,000 years ago at Diepkloof Rock Shelter, South Africa. *Proceedings of the National Academy of Science* 107, 6180-6185.

Tixier, J. (1974). Glossary for the description of stone tools with special reference to the Epipaleolithic of the Maghreb. Newsletter of Lithic Technology: Special Publication 1. Washington State University: Pullman.

Thamm, A.G., M.R. Johnson (2006). The Cape Supergroup In: B. Thomas (Ed.), The Geology of South Africa. Geological Society of South Africa: Johannesburg, 443-460.

Thackeray, A. I. (2000). Middle Stone Age artefacts from the 1993 and 1995 excavations at Die Kelders Cave I. *Journal of Human Evolution* 38, 147-168.

Thackeray, A.I. (1989). Changing fashions in the Middle Stone Age: the stone artefact sequence from Klasies River Main Site, South Africa. *African Archaeological Review* 7, 33-57.

Thackeray, A. I., A. J. Kelly (1988). A technological and typological analysis of Middle Stone Age assemblages antecedent to the Howieson's Poort at Klasies River Main Site. *South African Archaeological Bulletin* 43, 15-26.

Thompson, E., H.M. Williams, T. Minichillo (2010). Middle and late Pleistocene Middle Stone Age lithic technology from Pinnacle Point 13B (Mossel Bay, Western Cape Province, South Africa). *Journal of Human Evolution* 59, 358-377.

Thompson, E, and C.W. Marean (2008). The Mossel Bay lithic variant: 120 Years of Middle Stone Age research from Cape St Blaize Cave to Pinnacle Point. *South African Archaeological Society Goodwin Series* 10, 90-104.

Torrence, R. (1989). Retooling: towards a behavioral theory of stone tools. In: R. Torrence (Ed.) Time, Energy and Stone Tools. Cambridge University Press: Cambridge, 57-66.

Torrence, R. (1986). Production and Exchange of Stone Tools. Cambridge University Press: Cambridge.

Torrence, R. (1983). Time budgeting and hunter-gatherer technology. In: G. Bailey (Ed.), Hunter Gatherer Economy in Prehistory. Cambridge University Press: Cambridge, 11-22.

Toth, N. (1985). The Oldowan reassessed: a close look at early stone artifacts. *Journal of Archaeological Science* 12,101-120.

Tribolo, C., N. Mercier, H. Valladas, J.L. Joron, P. Guibert, Y. Lefrais, M. Selo, P.-J. Texier, J.-Ph. Rigaud, G. Porraz, C. Poggenpoel, J. Parkington, J.-P. Texier, A. Lenoble (2009). Thermoluminescence dating of a Stillbay–Howiesons Poort sequence at Diepkloof Rock Shelter (Western Cape, South Africa). *Journal of Archaeological Science* 36, 730–739

Ugan, A., J. Bright, A. Rogers (2003). When is technology worth the trouble? *Journal of Archaeological Science* 30, 1315–1329.

Van Andel, T.H. (1989). Late Pleistocene sea levels and the human exploitation of the shore and shelf of southern South Africa. *Journal of Field Archaeology* 16, 133–155.

Villa, P., S. Soriano (2010). Hunting weapons of Neanderthals and early modern humans in South Africa, similarities and differences. *Journal of Anthropological Research* 66, 5-38.

Villa, P., S. Soriano, N. Teyssandier, S. Wurz (2010). The Howiesons Poort and MSA III at Klasies River main site, Cave 1A. *Journal of Archaeological Science* 37, 630–655.

Villa, P., M. Soressi, C.S. Henshilwood, V. Mourre (2009). The Still Bay points of Blombos Cave (South Africa). *Journal of Archaeological Science* 36, 441–460.

Villa, P., A. Delagnes, L. Wadley (2005). A late Middle Stone Age artifact assemblage from Sibudu (KwaZulu-Natal): comparisons with the European Middle Paleolithic. *Journal of Archaeological Science* 32, 399-422.

Volman,T.P. (1984). Early prehistory of southern Africa. In: R.G. Klein (Ed.), *Southern African Prehistory and Paleoenvironments*. Balkema: Rotterdam, 169-220.

Volman, T.P. (1981). The Middle Stone Age in the Southern Cape. Unpublished PhD dissertation. University of Chicago: Chicago.

Vorster, C.J. (2003). Simplified Geology Map of South Africa, Lesotho and Swaziland. Republic of South Africa Council for Geoscience (CGS). Public access maps: http://www.geoscience.org.za/images/stories/rsageology.gif

Wadley, L. (2010). Were snares and traps used in the Middle Stone Age and does it matter? A review and a case study from Sibudu, South Africa. *Journal of Human Evolution* 58, 179-192.

Wadley, L. (2008). The Howieson's Poort Industry of Sibudu Cave. *South African Archaeological Society Goodwin Series* 10, 122-132.

Wadley, L. (2007). Announcing a Still Bay industry at Sibudu Cave, South Africa. *Journal of Human Evolution* 52, 681-689.

Wadley, L. (2005). A typological study of the Final Middle Stone Age stone tools from Sibudu Cave, KwaZulu-Natal. *South African Archaeological Bulletin* 60, 51-63.

Wadley, L. (2000). The Wilton and Pre-Ceramic Post-Classic Wilton Industries at Rose Cottage Cave and their context in the South African sequence. *South African Archaeological Bulletin* 55, 90-106.

Wadley, L. (1996). The Robberg Industry of Rose Cottage Cave, Eastern Free State: The technology, spatial patterns and environment. *South African Archaeological Bulletin* 51, 64-74.

Wadley, L., T. Hodgskiss, M. Grant (2009). Implications for complex cognition from the hafting of tools with compound adhesives in the Middle Stone Age, South Africa. *Proceedings of the National Academy of Sciences* 106, 9590-9594.

Wadley, L, M. Mohapi (2008). A segment is not a monolith: evidence from the Howiesons Poort of Sibudu, South Africa. *Journal of Archaeological Science* 35, 2594–2605.

Wadley, L., Z. Jacobs (2006). Sibudu Cave: background to the excavations, stratigraphy and dating. *Southern African Humanities* 18, 1-26.

Wadley, H., P. Harper (1989). Rose Cottage Cave revisited: Malan's Middle Stone Age collection. *South African Archaeological Bulletin* 44, 23-32.

Walker, F., M. Mathias (1946). The petrology of two granite-slate contacts at Cape Town, South Africa.*Quarterly Journal of the Geological Society* 102, 499-521.

Watts, I., (2002). Ochre in the Middle Stone Age of southern Africa: ritualized display or hide preservative? *South African Archaeological Bulletin* 57, 1-14.

Weedman, K.J. (2006). An ethnoarchaeological study of hafting and stone tool diversity among the Gamo of Ethiopia. *Journal of Archaeological Method and Theory* 13, 189-238.

Wendt, W.E. (1976). 'Art Mobilier' from the Apollo 11 Cave, South West Africa: Africa's Oldest Dated Works of Art. *South African Archaeological Bulletin* 31, 5-11.

Wilke, P. J., J.J. Flenniken, T.L. Ozbun (1991). Clovis Technology at the Anzick Site, Montana. *Journal of California and Great Basin Anthropology* 13, 242-272.

Wolff, E.W., J. Chappellaz, T. Blunier, S.O. Rasmussen, A. Svensson (2010) Millennial-scale variability during the last glacial: the ice core record. *Quaternary Science Reviews,* 29, 2828-2838.

Wurz, S. (1999). The Howiesons Poort backed artefacts from Klasies River: an argument for symbolic behavior. *South African Archaeological Bulletin* 54, 38-50.

Wurz, S. (2000). The Middle Stone Age at Klasies River, South Africa. Unpublished PhD dissertation. Stellenbosch, University of Stellenbosch.

Wurz, S. (2002). Variability in the Middle Stone Age lithic sequence, 115,000–60,000 years ago at Klasies River, South Africa. *Journal of Archaeological Science* 29, 1001–1015.

Wurz, S., N.J. le Roux, S. Gardner, H.J. Deacon (2003). Discriminating between the end products of the earlier Middle Stone Age sub-stages at Klasies River using biplot methodology. *Journal of Archaeological Science* 30, 1107-1126.

Yaroshevich, A, D. Kaufman, D. Nuzhnyy, O. Bar-Yosef, M.Weinstein-Evron (2010). Design and performance of microlith implemented projectiles during the Middle and the Late Epipaleolithic of the Levant: experimental and archaeological evidence. *Journal of Archaeological Science* 37, 368–388.

Yellen, J.E., A.S. Brooks, E. Cornelissen, M.J. Mehlman, K. Stewart (1995). A middle stone age worked bone industry from Katanda, Upper Semliki Valley, Zaire. *Science* 268, 553-556.

Appendix 1- Supplemental Figures and Tables

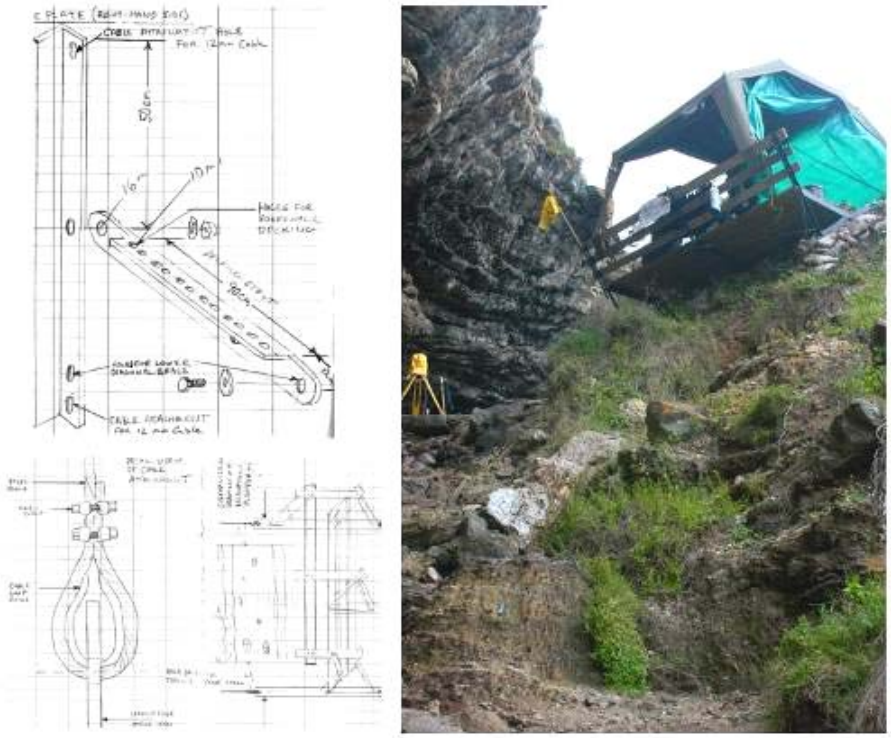

Figure 1. PP5-6 Excavation platform (2006-2007) and the unexcavated lower Long Section deposit

Figure 2. PP5-6 Sailcloth. A) as designed; B) installed 2007; C) PP5-6 view beneath sailcloth from south to north; D) PP5-6 upper Long Section view east

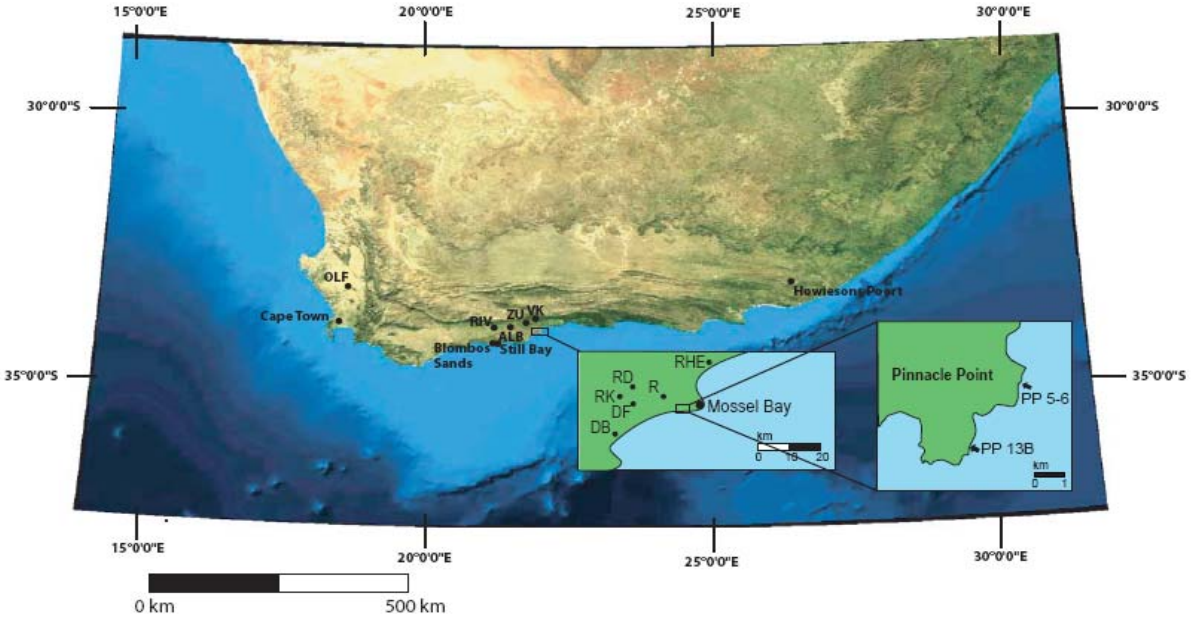

Figure 3. Silcrete sources used for the collection of modern experimental samples. OLF = Olfontein, RIV = Riversdale, ALB = Albertinia, ZU = Zuurvlagtke , VK = Vaalekraal, RD = Rooidebloom, RK = Rooikoppie, DF = Driefonteinen, R = Rietvlei, DB = Danabaai, RHE = Rheebok

Figure 4. Unheated Albertinia cut biface blanks

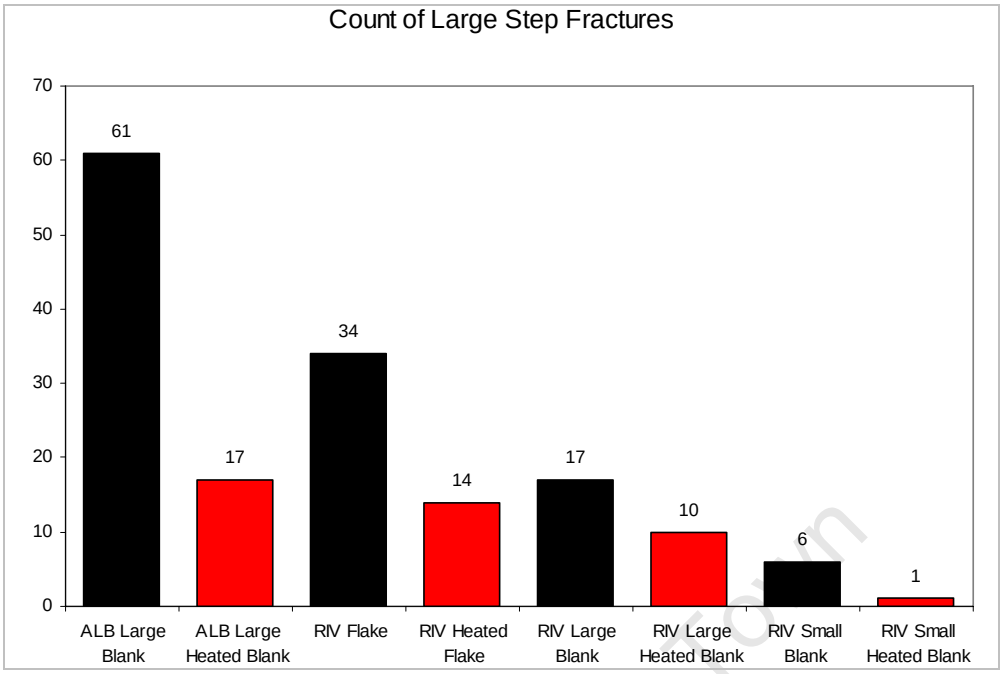

Figure 5. Number of large step fractures (> 1cm width) for each set of paired biface samples tabulated by original blank type

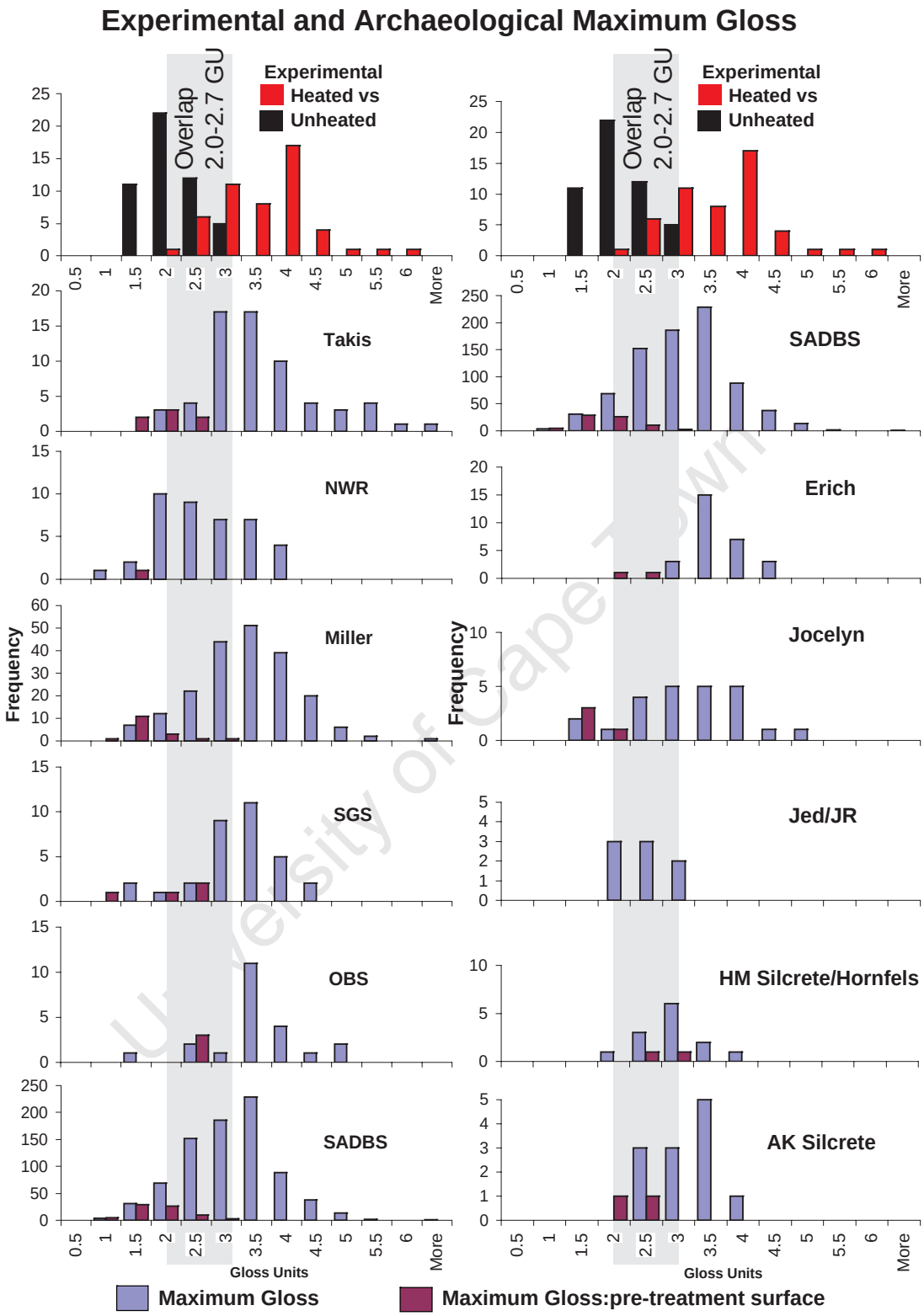

Figure 6. Experimental histograms for heated and unheated silcrete are compared with silcrete from archaeological samples

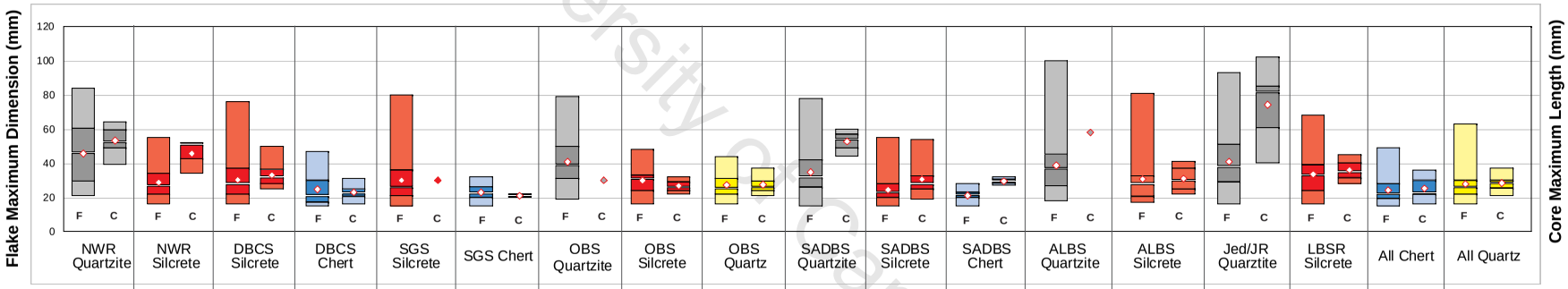

	NWR Quartzite		NWR Silcrete		DBCS Silcrete		DBCS Chert		SGS Silcrete		SGS Chert		OBS Quartzite		OBS Silcrete		OBS Quartz		SADBS Quartzite		SADBS Silcrete		SADBS Chert		ALBS Quartzite		ALBS Silcrete		Jed/JR Quarztite		LBSR Silcrete		All Chert		All Quartz	
Count	31	8	21	3	85	11	22	4	33	1	8	3	54	1	23	3	12	4	85	3	398	26	20	2	56	1	23	5	227	6	23	3	74	18	33	6
Min	21	39	16	34	16	25	15	16	15		15	20	19	30	16	22	16	21	15	44	15	19	15	27	18		17	22	16	40	16	28	15	16	16	21
25th	29.5	49	22	42.5	22	28	17.25	20.5	21		20	20.5	31	30	24	24	22	24	26	49	20	25	20	28.25	26.75		20.5	25	29	60.75	24	31.5	19.25	22	22	25.5
Median	46	52.5	27	51	28	32	21	22.5	26		22.5	21	39	30	31	26	25.5	26	32	54	23	28	21.5	29.5	37		28	30	38	81.5	33	35	22	22.5	26	28.5
75th	60.5	59.5	34	51.5	37	36.5	30	25	36		26.25	21.5	49.75	30	33	29	31	29.5	42	57	28	32.5	23	30.75	45.25		32.5	37	51	85	39	40	28	30	30	30
Max	84	64	55	52	76	50	47	31	80		32	22	79	30	48	32	44	37	78	60	55	54	28	32	100		81	41	93	102	68	45	49	36	63	37
Mean	45.7	53.3	28.7	45.7	30.3	33.0	24.7	23.0	30.0	30.0	22.9	21.0	40.9	30.0	29.8	26.7	27.3	27.5	34.8	52.7	24.4	30.6	21.1	29.5	38.7	58.0	30.7	31.0	40.9	74.2	33.5	36.0	24.2	25.3	27.8	28.3
SD	17.9	8.1	9.4	10.1	11.9	7.1	9.1	6.2	13.4		5.5	1.0	15.2		7.5	5.0	8.2	6.8	12.9	8.1	6.8	9.5	3.4	3.5	14.8		14.9	8.0	15.3	22.8	11.8	8.5	7.6	5.8	10.4	5.4

Figure 7. a) Box plots of complete flake maximum dimension (F) and core maximum length (C) for most of the PP5-6 StratAggs and raw materials.

Table 1. Experimental biface replication dataset. Fields include primary form, weight (Wt) and dimensions (mm) including (L), width (W), thickness (Thk). Maximum treatment temperature (Max-T, measured with thermocouple) and treatment type are provided for blanks that were selected for heat treatment. Mass and maximum and midpoint dimensions are provided for bifaces that did not fail during treatment or manufacture. The maximum width to thickness (W/Thk) and midpoint width to thickness (mpW/Thk) ratios used for statistical analysis are also tabulated.

Sample	Blank Type	Blank Wt(g)	Blank (L)	Blank (W)	Blank (Thk)	Max(T) °C	Treat Type	Failure Cause	Biface Wt(g)	Max (L)	Max (W)	Max (Thk)	MP (W)	MP (Thk)	W/Thk	MP W/Thk
ALB-A30.DM.H	Large Cut Blank	312.0	100	59	25	344	Fire		54.9	82.6	42.2	15.0	41.6	15.2	2.8	2.7
ALB-A30.DQ.H	Large Cut Blank	393.4	107	62	28	344	Fire		76.4	93.0	50.5	14.8	47.3	13.8	3.4	3.4
ALB-A30.EX	Large Cut Blank	372.7	113	60	28			Manufacture								
ALB-A30.FH	Large Cut Blank	339.3	105	59	27				85.8	73.1	45.9	26.2	42.9	25.7	1.8	1.7
ALB-A31.1.CT.H	Large Cut Blank	365.6	106	59	29	353	Kiln	Manufacture								
ALB-A31.1.CW	Large Cut Blank	357.1	106	62	27				102.9	81.2	51.4	27.1	47.4	25.0	1.9	1.9
ALB-A31.2.CX.H	Large Cut Blank	305.9	102	55	27	353	Kiln		37.9	60.8	42.3	13.0	41.6	12.2	3.3	3.4
ALB-A31.2.DU	Large Cut Blank	315.5	96	60	28				70.4	75.4	49.2	22.0	47.5	21.6	2.2	2.2
ALB-A31.3.CU	Large Cut Blank	338.1	102	59	29				78.1	76.1	45.8	24.8	41.4	24.3	1.8	1.7
ALB-A31.3.DY.H	Large Cut Blank	319.9	96	61	28	344	Fire		31.7	61.2	39.3	15.5	37.0	13.5	2.5	2.7
ALB-A31.4.EI	Large Cut Blank	316.6	93	58	28				77.9	64.1	46.5	23.8	46.2	22.8	2.0	2.0
ALB-A31.4.EJ	Large Cut Blank	308.0	100	61	25				99.7	64.4	57.1	24.8	54.6	25.3	2.3	2.2
ALB-A31.CS.H	Large Cut Blank	339.5	107	62	26	353	Kiln	Manufacture								
ALB-A31.DA.H	Large Cut Blank	316.2	106	62	25	353	Kiln	Manufacture								
ALB-A31.FS.H	Large Cut Blank	315.3	106	57	27	344	Fire		34.5	61.2	34.8	17.7	33.6	16.5	2.0	2.0
ALB-A32.1.CV	Large Cut Blank	353.5	101	59	28				87.1	84.8	51.1	18.2	47.8	17.3	2.8	2.8
ALB-A32.1.ED	Large Cut Blank	369.2	104	63	28				71.5	80.0	44.1	23.1	41.9	19.0	1.9	2.2
ALB-A32.2.EM.H	Large Cut Blank	348.6	100	62	28	353	Kiln	Manufacture								
ALB-A32.2.EN.H	Large Cut Blank	317.3	101	59	28	344	Fire		30.7	76.8	35.5	12.7	25.0	10.2	2.8	2.5
ALB-A32.3.EG	Large Cut Blank	312.5	101	61	27				59.5	70.5	44.5	22.6	41.9	22.6	2.0	1.9
ALB-A32.3.EO	Large Cut Blank	343.6	103	60	28				44.4	60.2	44.6	16.7	42.2	16.1	2.7	2.6
ALB-A32.4.EC.H	Large Cut Blank	355.2	106	55	31	344	Fire		53.9	90.3	43.9	13.0	43.0	13.1	3.4	3.3
ALB-A32.5.FO	Large Cut Blank	289.9	102	54	28			Manufacture								
ALB-A32.5.FQ.H	Large Cut Blank	299.1	104	57	27	353	Kiln		41.2	80.8	43.1	13.6	38.8	12.2	3.2	3.2
ALB-A33.1.EU.H	Large Cut Blank	375.8	101	55	31	344	Fire	Manufacture								
ALB-A33.1.FA	Large Cut Blank	357.5	97	60	30				78.4	69.6	48.2	26.1	45.7	23.2	1.8	2.0
ALB-A33.2.FD.H	Large Cut Blank	342.3	103	59	25	353	Kiln		25.6	52.6	39.4	11.8	38.4	12.0	3.3	3.2
ALB-A33.2.FE	Large Cut Blank	338.6	107	60	24				66.9	65.1	45.9	21.2	44.5	20.3	2.2	2.2
ALB-A33.EV	Large Cut Blank	328.8	95	53	32				34.9	53.6	41.7	18.2	38.6	17.6	2.3	2.2
ALB-A33.EZ.H	Large Cut Blank	329.1	105	61	26	344	Fire		40.9	66.9	40.4	17.0	35.6	14.0	2.4	2.5
ALB-A33.FT.H	Large Cut Blank	257.0	93	53	25				42.9	62.8	43.8	17.5	42.1	17.1	2.5	2.5
ALB-A34.10.DL.H	Large Cut Blank	331.6	102	58	29	353	Kiln		31.3	49.1	41.8	14.8	40.6	15.0	2.8	2.7
ALB-A34.10.DO	Large Cut Blank	310.1	100	58	28			Manufacture								
ALB-A34.11.DD	Large Cut Blank	288.6	100	55	27				50.9	61.8	43.6	21.3	42.1	21.1	2.0	2.0
ALB-A34.11.DR.H	Large Cut Blank	307.6	103	61	28	353	Kiln		47.8	78.4	45.1	16.7	36.6	13.7	2.7	2.7
ALB-A34.DF	Large Cut Blank	368.3	102	60	29				78.9	67.2	48.6	28.3	47.2	22.7	1.7	2.1
ALB-A34.DP	Large Cut Blank	344.8	98	59	31			Manufacture								
ALB-A34.DV.H	Large Cut Blank	353.8	103	55	31	344	Fire		46.5	84.2	37.3	14.4	36.2	13.2	2.6	2.7
ALB-A34.DZ.H	Large Cut Blank	313.1	102	60	29	344	Fire		38.4	69.1	41.0	13.6	38.3	13.8	3.0	2.8
ALB-A34.FN	Large Cut Blank	323.3	97	57	31				100.4	85.2	50.4	29.8	49.8	28.0	1.7	1.8
ALB-A35.CZ.H	Large Cut Blank	283.4	97	54	27	353	Kiln		32.4	61.1	37.9	15.2	37.7	14.4	2.5	2.6
ALB-A35.DG	Large Cut Blank	304.6	98	56	27				46.2	54.0	44.0	20.4	37.2	19.8	2.2	1.9
ALB-A35.FM.H	Large Cut Blank	350.7	105	64	29	344	Fire		65.9	91.8	49.5	15.5	46.2	12.7	3.2	3.6
ALB-A36.CR.H	Large Cut Blank	323.7	104	57	29	344	Fire		35.9	72.9	38.5	15.0	32.0	14.7	2.6	2.2
ALB-A36.DE.H	Large Cut Blank	352.5	103	60	30	353	Kiln		48.6	75.9	42.6	16.9	40.9	16.8	2.5	2.4
ALB-A36.DI.H	Large Cut Blank	356.3	101	60	30	344	Fire		49.0	84.7	39.4	13.2	38.1	12.2	3.0	3.1
ALB-A36.EH	Large Cut Blank	331.1	99	58	31				45.1	58.8	42.7	17.9	41.7	14.8	2.4	2.8
ALB-A36.EK	Large Cut Blank	355.0	106	54	29				58.5	67.3	43.1	20.3	42.5	18.2	2.1	2.3
ALB-A36.EL	Large Cut Blank	371.8	105	55	31			Manufacture								

Table 1. Continued.

Sample	Blank Type	Blank Wt(g)	Blank (L)	Blank (W)	Blank (Thk)	Max(T) °C	Treat Type	Failure Cause	Biface Wt(g)	Max (L)	Max (W)	Max (Thk)	MP (W)	MP (Thk)	W/Thk	MP W/Thk
ALB-A37.EF.H	Large Cut Blank	311.0	103	55	29	344	Fire		47.7	67.8	44.3	16.5	39.2	16.0	2.7	2.5
ALB-A37.FB	Large Cut Blank	335.2	104	55	29			Manufacture								
ALB-A37.FF	Large Cut Blank	374.8	108	60	30				71.8	66.6	49.2	28.0	48.5	26.8	1.8	1.8
ALB-A37.FJ.H	Large Cut Blank	358.3	102	60	31	353	Kiln		16.9	50.7	32.6	12.2	31.6	11.8	2.7	2.7
ALB-A38.EP	Large Cut Blank	391.2	106	57	32			Manufacture								
ALB-A38.FI.H	Large Cut Blank	334.4	105	53	28	353	Kiln		44.9	80.3	40.9	12.5	39.4	13.0	3.3	3.0
ALB-A38.FP.H	Large Cut Blank	292.4	92	60	26	344	Fire		25.1	49.7	40.6	13.0	37.0	12.9	3.1	2.9
ALB-A38.FR	Large Cut Blank	316.6	96	61	27				51.0	60.4	44.2	19.0	43.9	15.7	2.3	2.8
ALB-A39.1.FC	Large Cut Blank	333.2	98	57	29				49.0	60.0	38.8	22.5	35.0	21.3	1.7	1.6
ALB-A39.EQ.H	Large Cut Blank	327.0	108	61	25	353	Kiln		49.3	79.8	40.4	15.0	38.9	14.3	2.7	2.7
ALB-A39.ES.H	Large Cut Blank	292.3	96	52	27	344	Fire		37.3	70.9	38.7	13.6	36.5	13.6	2.8	2.7
ALB-A39.EY.H	Large Cut Blank	285.8	93	58	27	353	Kiln		50.0	75.4	48.9	13.3	47.7	12.0	3.7	4.0
ALB-A39.FG	Large Cut Blank	286.9	105	54	26				61.8	72.8	40.3	18.4	39.1	15.7	2.2	2.5
ALB-A39.FK	Large Cut Blank	318.9	99	58	28				66.9	75.0	41.8	22.7	36.6	21.9	1.8	1.7
ALB-A40.1.EW.H	Large Cut Blank	310.6	104	53	26	353	Kiln	Manufacture								
ALB-A40.2.ER	Large Cut Blank	275.0	96	59	23				30.6	50.7	39.6	16.8	37.8	16.2	2.4	2.3
ALB-A40.EE	Large Cut Blank	327.4	96	60	27			Manufacture								
ALB-A40.ET	Large Cut Blank	357.6	106	56	28				56.8	78.1	37.2	20.9	34.9	20.3	1.8	1.7
ALB-A40.FL.H	Large Cut Blank	332.5	102	60	27	344	Fire	Manufacture								
ALB-A41.DB.H	Large Cut Blank	311.1	104	57	25	344	Fire	Treatment								
ALB-A41.DK	Large Cut Blank	281.4	102	55	25				86.2	79.6	48.9	22.6	48.3	21.9	2.2	2.2
ALB-A42.DH	Large Cut Blank	270.9	101	54	25			Manufacture								
ALB-A42.DN.H	Large Cut Blank	303.7	107	54	25	353	Kiln		48.9	81.2	40.4	14.5	38.5	12.7	2.8	3.0
ALB-A43.DS.H	Large Cut Blank	269.3	103	56	24	353	Kiln		30.8	64.8	39.7	13.1	33.3	11.4	3.0	2.9
ALB-A43.DT.H	Large Cut Blank	313.9	103	59	25	344	Fire		36.8	64.3	39.1	17.1	36.0	16.9	2.3	2.1
ALB-A43.DW	Large Cut Blank	236.4	97	49	24				58.4	81.0	36.4	23.5	34.0	22.1	1.5	1.5
ALB-A43.DX	Large Cut Blank	275.6	107	56	22				53.2	63.7	41.6	21.3	39.5	21.4	2.0	1.8
ALB-A44.DC.H	Large Cut Blank	304.0	104	55	26	344	Fire		31.3	70.1	35.5	13.1	34.8	11.0	2.7	3.2
ALB-A45.CY.H	Large Cut Blank	284.5				344	Fire	Treatment								
ALB-A45.DJ.H	Large Cut Blank	312.7	100	56	28	353	Kiln	Manufacture								
ALB-A45.EA	Large Cut Blank	324.6	103	57	26				90.1	80.5	44.5	25.6	42.4	24.9	1.7	1.7
ALB-A45.EB	Large Cut Blank	286.8	99	57	25			Manufacture								
RIV-A4.A	Large Cut Blank	382.6	108	55	34				35.9	57.1	43.1	15.3	40.9	15.4	2.8	2.7
RIV-A4.AA	Small Cut Blank	175.9	71	47	26				30.3	54.3	42.2	14.4	40.1	14.4	2.9	2.8
RIV-A4.AB	Small Cut Blank	240.6	82	51	24			Manufacture								
RIV-A4.AC.H	Small Cut Blank	201.9	75	48	24	353	Kiln	Manufacture								
RIV-A4.AD.H	Small Cut Blank	229.5	82	56	25	353	Kiln		14.0	43.5	31.3	11.8	30.6	11.4	2.7	2.7
RIV-A4.AE	Small Cut Blank	310.4	87	64	28				22.5	50.3	33.6	13.9	32.7	13.5	2.4	2.4
RIV-A4.AF.H	Small Cut Blank	231.9	79	55	25	353	Kiln		25.5	55.3	35.7	13.9	32.6	11.8	2.6	2.8
RIV-A4.AG	Small Cut Blank	249.9	76	61	24				25.6	50.8	36.9	14.3	34.7	13.9	2.6	2.5
RIV-A4.AH	Small Cut Blank	206.3	69	58	23	353	Kiln		22.3	51.7	33.6	12.6	31.5	12.0	2.7	2.6
RIV-A4.AI.H	Small Cut Blank	243.3	84	55	24	353	Kiln	Manufacture								
RIV-A4.AJ.H	Small Cut Blank	212.3	74	56	23	353	Kiln		22.0	58.3	38.2	10.4	32.2	9.3	3.7	3.5
RIV-A4.AK.H	Small Cut Blank	174.4	73	48	23	353	Kiln		26.9	51.5	39.0	14.9	35.3	13.2	2.6	2.7
RIV-A4.AL	Small Cut Blank	227.7	78	58	24			Manufacture								
RIV-A4.AM.H	Small Cut Blank	337.4	89	59	30	353	Kiln		40.5	70.4	41.1	14.4	40.0	13.2	2.9	3.0
RIV-A4.AN	Small Cut Blank	215.0	72	55	24			Manufacture								
RIV-A4.AO	Small Cut Blank	268.7	82	57	27			Manufacture								
RIV-A4.AP	Small Cut Blank	230.8	83	55	25				27.2	52.7	34.7	17.9	31.7	17.6	1.9	1.8
RIV-A4.AQ.H	Small Cut Blank	262.6	83	57	29	353	Kiln		22.9	52.5	33.8	13.4	33.8	11.8	2.5	2.9
RIV-A4.AR	Large Cut Blank	268.3	94	59	26				31.6	56.6	37.1	16.8	33.2	17.3	2.2	1.9
RIV-A4.AS.H	Large Cut Blank	324.7	104	56	33	353	Kiln	Manufacture								
RIV-A4.AT.H	Small Cut Blank	206.7	70	53	25	353	Kiln		26.4	55.6	37.4	12.8	36.7	13.2	2.9	2.8
RIV-A4.AU	Small Cut Blank	209.0	73	55	28				21.9	42.8	34.7	16.3	34.8	12.9	2.1	2.7
RIV-A4.AV.H	Large Cut Blank	311.9	108	60	23	353	Kiln	Manufacture								
RIV-A4.AW	Flake	1235.2	165	140	35				148.1	80.5	60.8	31.3	59.1	31.1	1.9	1.9
RIV-A4.AX	Flake	1006.1	135	100	42			Manufacture								
RIV-A4.AY.H	Flake	740.2	125	115	45	367	Kiln		31.5	57.0	37.6	15.1	49.3	21.6	2.5	2.3
RIV-A4.AY	Flake	740.2	125	115	45				63.0	65.0	49.4	22.3	35.4	15.2	2.2	2.3
RIV-A4.AZ.H	Flake	735.4	145	90	35	367	Kiln		42.2	55.8	38.1	22.6	38.4	21.0	1.7	1.8
RIV-A4.B.H	Large Cut Blank	382.2	109	58	28				25.7	56.3	35.3	12.5	34.3	12.2	2.8	2.8
RIV-A4.BA.H	Flake	1500.0	160	130	60	367	Kiln	Manufacture								
RIV-A4.BB.H	Flake	1160.1	150	113	50	367	Kiln		51.8	73.3	46.8	17.6	46.8	17.5	2.7	2.7
RIV-A4.BC	Flake	466.3	120	102	30				102.6	94.2	51.1	20.5	47.0	20.1	2.5	2.3
RIV-A4.BD	Flake	610.6	135	90	35				78.7	70.9	51.1	25.8	47.2	25.4	2.0	1.9

Table 1. Continued.

Sample	Blank Type	Blank Wt(g)	Blank (L)	Blank (W)	Blank (Thk)	Max(T) °C	Treat Type	Failure Cause	Biface Wt(g)	Max (L)	Max (W)	Max (Thk)	MP (W)	MP (Thk)	W/Thk	MP W/Thk
RIV-A4.BE.H	Flake	639.2	114	125	35	367	Kiln	Manufacture								
RIV-A4.BF	Flake	359.7	130	105	25				71.3	71.0	52.6	21.1	51.9	20.6	2.5	2.5
RIV-A4.BG.H	Flake	357.9	145	80	30	367	Kiln	Manufacture								
RIV-A4.BH.H	Flake	391.1	135	75	35	367	Kiln	Manufacture								
RIV-A4.BI	Flake	707.8	150	90	45				47.7	62.4	41.5	18.2	40.7	18.4	2.3	2.2
RIV-A4.BJ.H	Flake	900.7	135	80	40	367	Kiln		56.3	68.9	46.4	21.1	45.9	21.2	2.2	2.2
RIV-A4.BK	Flake	394.0	143	85	35			Manufacture								
RIV-A4.BL.H	Flake	562.2	180	80	30	367	Kiln	Manufacture								
RIV-A4.BM	Flake	327.2	94	93	25				62.4	63.2	42.5	24.9	42.2	20.0	1.7	2.1
RIV-A4.BN.H	Flake	272.3	100	140	25	360	Kiln		45.9	66.7	43.0	18.2	41.0	15.1	2.4	2.7
RIV-A4.BO	Flake	372.2	80	95	30				68.7	69.0	48.7	22.3	47.6	20.2	2.2	2.4
RIV-A4.BP.H	Flake	322.2	125	80	30	367	Kiln		42.6	63.2	45.1	15.9	44.4	15.7	2.8	2.8
RIV-A4.BQ.H	Flake-chunk	425.5	120	80	35	360	Kiln		18.3	45.7	33.4	13.1	32.2	12.9	2.5	2.5
RIV-A4.BR.H	Flake-chunk	370.1	140	75	35	367	Kiln		75.3	87.3	47.3	20.2	46.3	20.4	2.3	2.3
RIV-A4.BS.H	Flake	287.9	80	120	25	360	Kiln		50.2	63.4	50.4	15.6	50.3	14.3	3.2	3.5
RIV-A4.BT	Flake	212.1	120	80	20				46.0	59.5	45.5	20.1	44.9	19.8	2.3	2.3
RIV-A4.BU	Flake	314.5	110	70	35				64.6	65.8	45.4	26.1	43.7	25.2	1.7	1.7
RIV-A4.BV	Flake	258.0	115	70	30				65.2	68.5	45.8	21.1	45.6	20.5	2.2	2.2
RIV-A4.BW	Flake	270.4	105	75	25				42.3	58.3	40.6	20.4	40.4	18.7	2.0	2.2
RIV-A4.BX.H	Flake	221.8	105	85	20	367	Kiln	Treatment								
RIV-A4.BY.H	Flake	198.2	110	55	25	367	Kiln	Manufacture								
RIV-A4.BZ	Flake	172.1	135	55	22				33.2	50.2	38.2	22.4	36.5	20.8	1.7	1.8
RIV-A4.C	Large Cut Blank	359.0	106	63	25				35.4	67.8	35.1	15.5	33.8	14.1	2.3	2.4
RIV-A4.CA	Flake	197.4	100	65	25				50.3	72.9	40.3	22.3	39.4	20.2	1.8	2.0
RIV-A4.CB.H	Flake	149.1	85	75	15	367	Kiln		40.7	67.6	44.3	13.4	43.8	13.3	3.3	3.3
RIV-A4.CC	Flake	150.1	90	65	20			Manufacture								
RIV-A4.CD.H	Flake	169.5	105	55	25	367	Kiln		35.0	60.6	42.4	15.0	39.4	11.8	2.8	3.3
RIV-A4.CE.H	Flake	124.5	85	55	20	367	Kiln		45.0	71.5	42.3	16.3	39.8	16.2	2.6	2.5
RIV-A4.CF	Flake	186.2	110	75	20				22.7	56.9	30.0	14.5	28.7	13.7	2.1	2.1
RIV-A4.CG	Flake	119.4	95	50	25				35.0	56.7	35.8	16.6	35.4	17.2	2.2	2.1
RIV-A4.CH.H	Flake	185.3	90	100	25	367	Kiln		27.5	63.2	37.0	11.6	34.7	11.2	3.2	3.1
RIV-A4.CI	Flake	110.3	80	45	17				34.5	59.6	36.4	16.9	35.3	16.6	2.2	2.1
RIV-A4.CJ.H	Flake	101.1	80	50	15	360	Kiln	Manufacture								
RIV-A4.CK.H	Flake	68.4	80	50	10	367	Kiln	Manufacture								
RIV-A4.CL	Flake	90.0	72	50	15			Manufacture								
RIV-A4.CM	Flake	75.9	85	42	13				21.4	51.1	34.5	12.3	30.2	10.1	2.8	3.0
RIV-A4.CN	Flake	147.3	100	50	25				36.7	68.9	39.1	15.0	36.3	13.4	2.6	2.7
RIV-A4.CO.H	Flake	85.9	75	55	17	367	Kiln		16.2	45.0	34.2	11.1	34.3	11.4	3.1	3.0
RIV-A4.CP.H	Flake	194.0	94	60	26	367	Kiln	Manufacture								
RIV-A4.CQ.H	Flake	114.5	75	55	20	367	Kiln		23.3	52.6	37.2	12.7	35.1	11.3	2.9	3.1
RIV-A4.D	Large Cut Blank	377.3	102	61	31				34.7	65.6	42.6	13.3	36.1	13.2	3.2	2.7
RIV-A4.E	Large Cut Blank	361.1	98	56	33			Manufacture								
RIV-A4.F.H	Large Cut Blank	337.5	100	56	28	353	Kiln		28.3	52.3	38.6	16.9	38.0	15.3	2.3	2.5
RIV-A4.G.H	Large Cut Blank	357.7	105	62	27	353	Kiln	Manufacture								
RIV-A4.H.H	Large Cut Blank	408.8	107	65	27	353	Kiln		57.9	78.9	44.0	16.3	43.3	16.2	2.7	2.7
RIV-A4.I	Large Cut Blank	338.3	100	62	27			Manufacture								
RIV-A4.J.H	Large Cut Blank	333.1	104	64	26	353	Kiln		41.3	79.3	39.6	14.6	37.1	12.9	2.7	2.9
RIV-A4.K	Large Cut Blank	433.9	108	64	32				33.0	51.1	42.0	18.3	40.2	15.6	2.3	2.6
RIV-A4.L	Large Cut Blank	381.5	109	63	28				76.8	99.8	40.8	16.8	38.5	16.2	2.4	2.4
RIV-A4.M.H	Large Cut Blank	361.6	115	59	27	353	Kiln		50.5	74.4	45.2	17.4	43.4	17.4	2.6	2.5
RIV-A4.N	Large Cut Blank	406.1	106	65	30			Manufacture								
RIV-A4.O.H	Large Cut Blank	378.8	104	61	30	353	Kiln		22.5	58.0	29.3	14.2	29.3	13.3	2.1	2.2
RIV-A4.P	Large Cut Blank	335.2	105	63	24				31.8	57.1	42.5	17.4	33.2	15.7	2.4	2.1
RIV-A4.Q	Large Cut Blank	348.3	106	62	26				47.6	67.8	39.4	18.2	39.5	18.1	2.2	2.2
RIV-A4.R.H	Large Cut Blank	401.2	106	62	30	353	Kiln		28.2	68.8	37.7	12.1	36.6	10.5	3.1	3.5
RIV-A4.S.H	Large Cut Blank	374.0	103	58	31	353	Kiln		33.9	67.2	44.9	13.0	44.1	12.9	3.5	3.4
RIV-A4.T.H	Large Cut Blank	345.1	105	62	24	353	Kiln	Manufacture								
RIV-A4.U.H	Large Cut Blank	360.1	104	60	27	353	Kiln		48.3	82.9	40.4	13.0	40.3	12.6	3.1	3.2
RIV-A4.V	Large Cut Blank	371.4	108	65	26				56.5	84.2	41.7	17.3	39.2	17.3	2.4	2.3
RIV-A4.W.H	Small Cut Blank	221.7	74	57	25	353	Kiln		22.3	52.3	31.4	11.7	30.9	12.4	2.7	2.5
RIV-A4.X.H	Small Cut Blank	272.0	78	60	26	353	Kiln	Manufacture								
RIV-A4.Y.H	Small Cut Blank	251.3	80	55	26	353	Kiln	Manufacture								
RIV-A4.Z	Small Cut Blank	252.7	83	56	24			Manufacture								

Table 2. Maximum Gloss (MG) values for experimental silcrete samples used in the analysis of luster. Each nodule was subdivided so that an unheated control was retained for measurement. Heated samples were measured for maximum gloss prior to and after flaking.

Sample	Context	Maximum Gloss		
		unheated	heated (unflaked)	heated (flaked)
alb-a25	experimental	2.2	1.4	2.8
alb-a65	experimental	2.6	2.0	4.0
alb-a66	experimental	2.6	1.7	4.3
alb-b11	experimental	1.6	1.2	4.6
alb-b14	experimental	1.3	1.4	2.2
alb-b15	experimental	1.9	1.8	3.7
alb-b18	experimental	1.8	1.6	3.8
alb-b20	experimental	1.6	1.4	3.7
alb-b21	experimental	1.5	1.3	3.4
alb-b22	experimental	1.9	1.4	3.6
db-a1	experimental	2.2	1.5	2.5
db-a2	experimental	1.4	1.1	3.2
df-a3	experimental	1.7	1.3	2.4
df-a6	experimental	1.6	1.8	2.7
df-a7	experimental	1.5	2.0	3.0
df-a8	experimental	1.7	1.0	2.2
olf-a23	experimental	1.5	1.8	3.3
r-a1	experimental	1.4	2.1	2.9
r-a18	experimental	2.7	1.5	3.2
r-a2	experimental	1.6	2.2	2.0
rhe-a1	experimental	2.1	1.5	2.7
riv-a3	experimental	2.6	2.0	4.3
riv-a4	experimental	2.5	1.8	3.6
vk-a10	experimental	1.8	1.9	3.6
vkb3	experimental	1.9	2.0	3.6
vk-b7	experimental	2.6	1.8	3.0
za-a11	experimental	1.5	1.0	2.4
zu-a10	experimental	1.5	2.0	2.2
zu-a5	experimental	2.2	1.4	2.7
zu-a7	experimental	2.2	2.2	5.7
zu-a9	experimental	2.1	1.8	4.3
riv-a5	experimental	2.2	1.8	2.6
df-a14	experimental	1.8	1.4	3.6
olf-a7	experimental	2.2	2.0	5.4
dfa10	experimental	1.6	1.4	3.1
alb-b23	experimental	1.9	1.6	3.7
r-a19	experimental	2.2	1.7	3.5
olf-a15	experimental	1.8	1.7	3.7
r-a11	experimental	1.8	1.6	4.1
rd-a1	experimental	1.9	1.8	3.7
df-b6	experimental	1.3	1.4	3.3
df-b3	experimental	1.2	1.1	2.6
rd-a1	experimental	2.3	2.2	3.6
df-b2	experimental	2.0	2.5	3.9
df-b1	experimental	2.2	2.1	3.6
df-b7	experimental	1.7	2.1	3.9
df-b4	experimental	1.6	1.5	3.0
df-b8	experimental	1.7	1.1	3.8
df-b5	experimental	1.6	1.4	2.9
alb-b13	experimental	1.4	1.1	3.1

Appendix 2- Key to Fields in PP5-6 Lithics Database

Note: The follosing describes fields in the database. Many of the following categories or variables were simplified or collapsed as necessary for analysis.

Flakes and Retouched Tools

Find No. - This is the unique id number given to each artifact plotted in the field.

Specimen Number – number given in the lab during cataloguing or the original plotted find number is often decimalized if it is found that multiple artifacts have been placed in a bag by the excavator or if an artifact is contained within sediment adhering to a different specimen (i.e. inside a shell).

Lot #- each StratUnit excavated is given a unique lot number per 50cm quadrant. All materials collected from a given StratUnit and quadrant are coded with the same lot number.

Description – informal classification of specimen to be used for sorting, query and cross checking of other variables. Drop down list includes most common but other descriptions are written in as needed (i.e. "backed blade").

Cortical flake

Small production debris

Indeterminate fragment

Core preparation

Split flake

Backed blade

Type- debitage categories

Flake

Blade

Bladelet - blades less than 10mm wide

Shatter – specimen that does not exhibit enough diagnostic flake attributes for coding completeness

Convergent blade – symmetric pointed flakes and blades

Geneste Type- This is a modified version of Geneste's (1985) techno-typology that classifies debitage according to technological phases of the reduction sequence. The major differences between the two (my own and Geneste's) are that I replace the word 'Levallois' with 'Prepared' and I also code fragments.

Modified Geneste Techno-Typology

Type No.	Description of Artifact-Type
0	Block of raw material ("tested" or unmodified)
1	Primary cortical flake (>50% cortex)
2	Residual cortical flake (<50% cortex)
3	Naturally backed flake (flake with cortical lateral margin)
4	Non-cortical complete flakes
5	Simple (plain platform) blade
6	Cortical point,flake, or blade with facetted platform
7	Facetted flake
8	Blade with facetted platform
9	Point with facetted platform
11	Discoid core
12	Various core types
13	Preferential removal core (Levallois flake core, point core)
15	Facetted core-edge flake
16	Core-edge flake, crested flake
17	Core fragment
20	Kombewa flake
22	Biface thinning flake
24	Block shatter and flake fragments of indeterminate orientation
26	Small flakes less than 15mm in length.

The advantage of using this system is that it allows one to characterize the entire assemblage according to reduction stage. These phases are organized with respect to tool manufacture in the following way:

Phase 0- Acquisition/Retrieval of Material

Phase 1- Initial Core Preparation

Phase 2- Core Reduction

Phase 3- Retouch/Resharpening

Raw Material Type-

Fine Quartzite – Typical fine textured quartzite

Coarse Quartzite – Coarse TMS similar to cave wall

Quartz

Crystalline Quartz

Silcrete – silcrete of indeterminate fabric type (Summerfield 1981)

Msilcrete- matrix dominated silcrete

Gsilcrete- grain dominated silcrete

Hornfels

Chert

Chalcedony/Opaline

Other

Maximum Gloss- Surface gloss of archaeological and experimental silcrete samples was quantified with the use of a desktop Rhopoint Novo-Curve instrument. The instrument was used in continuous reading mode where the sample is manipulated over the light reflecting orifice until a maximum gloss value, measured

in gloss units (or GU), is achieved. That value was recorded for most silcrete artifacts greater than 15mm in maximum dimension.

Maximum Gloss2- second value recorded on silcrete artifacts with pre- and post-heat treatment surfaces.

HT Luster – checkbox to record presence or absence of heat treatment luster on silcrete artifacts (more subjective as compared to gloss analysis).

Photo- The majority of lithic specimens were photographed with Nikon D70 (RAW format) fitted with a 60mm lens for most shots. Artifacts were photographed on a dark background printed with overlaid 1cm grid which was taped to the tray of the digital scale. This field was entered with date and time by pressing 'cntrl' + ';' (for date stamp) and then 'cntrl' + 'shift' + ';'(for time stamp) in rapid succession after pressing remote shutter on camera. The computer and camera clocks were synched in advance which allows the date and time stamp text to be screen captured and entered into the Access database as the unique identifier.

Weight- This is mass taken in grams. This is a required field and it is recorded for all specimens

Completeness- This field is used to record what portion of the original flake is still preserved.

Complete is a whole specimen.

Almost Complete indicates a flake that is missing an estimated 1-3mm of the distal tip.

proximal flakes preserve the flake platform and usually at least some portion of the bulb of percussion.

mid-section has neither the platform nor the distal end of the flake.

distal portion is the distal end of the flake.

laterals correspond to the remnants of a split flake, oriented with the proximal end facing the analyst.

Incomplete/unknown doesn't preserve enough attributes to determine its original orientation.

Maximum Dimension- recorded for all artifacts.

Length- technological length which is the distance from the point of percussion to the most distant point on the flake's ventral surface.

Maximum Width

Midpoint Width- the width of the flake measured perpendicular to the technological length at the midpoint of the technological length.

Midpoint Thickness- The thickness of the flake measured at the intersection of technological length and midpoint width. The purpose of measuring at the midpoint is to avoid the influence of the bulbar thickness.

Platform Width- the distance between the two points at which the striking platform intersects with the ventral surface.

Platform Thickness- the distance between the point of percussion and the nearest point on the edge of the striking platform and the flake dorsal surface.

Comment- This field is for anything noteworthy about the artifact including additional description of raw material and retouch.

Cutting Edge- The total length of the feather edge on a flake's circumference. This does not include the platform, any relict edge, or the distance across a step or hinge fracture. The measurement is taken by rolling a flake on a ruler and reporting the value in mm.

Cutting edge is used in conjunction with mass to assemble a measurement of cutting edge/mass (CE/M) that is believed to monitor the efficiency by which a quantity of cutting edge is recovered from a given mass of raw material. Because the knapper can deliberately control the potential flake surface area and flake thickness by altering the exterior platform angle and platform morphology (Dibble 1997), the knapper can also control the amount of flake cutting edge produced from a nodule of stone.

Exterior Platform Angle- Dibble (1997). Platform angle is very difficult to measure consistently and was only recorded on flakes with a high confidence of accuracy.

Dorsal Cortex1- This field codes for the amount of cortex found on the dorsal surface of flakes, blades, and flake fragments. For block shatter/chunks, the cortex percentage is coded according to how much cortex exists on the entire surface of the artifact (as opposed to just the dorsal surface of flakes and blades).

1-20%

21-40%

41-60%

61-80%

81-99%

100%

Platform Cortex1-checkbox to record presence or absence of cortex on platform

Cortex Type1- These cortex types were derived from comparative observation of cortex type on raw material samples collected in the Mossel Bay area and beyond. Cobble cortex is smooth and round like beach or river cobbles. Outcrop cortex is irregular and often jagged and coarse. Rind cortex is the chalky matrix that often surrounds silcrete nodules. Pre-HT indicates silcrete artifacts that have pre-heat treatment non-glossy surfaces. Indet samples could not be assigned to type.

Cortex Location1- where cortex occurs on the flake.

Proximal

Distal

Right Lateral

Left Lateral

Mid

Dorsal- for primary flakes

Dorsal Cortex2, Platform Cortex2, Cortex Type2, **Cortex Location2**- Same as above but for artifacts that show pre-ht gloss surfaces in addition to cortex.

Flake Termination- This is the state of the distal edge of the flake or blade.

feather edge is a smooth cutting edge.

Hinge fractures result from incomplete fracture propagation.

Step/Snap fractures are usually indistinguishable from step fractures and the types are combined.

Burinated are flakes that show a scar down a lateral margin that initiated from the distal end, either as retouch or as edge damage.

Retouch is for flakes that have been modified by retouch at the distal end.

Overpassed is a flake that preserves core relict edge or opposite platform at the distal end.

Scar Density- This is the number of flake scars on the dorsal surface that are greater than 10mm in maximum dimension or for lot numbers with very small debitage (such as those from the SADBS aggregate) it includes scars with a maximum dimension of c. greater than or equal to 20% of the technological length. This attribute can give some indication of the intensity of core reduction.

Scar Pattern- This codes for the direction of the scars on the flake dorsal surface. This can give some idea of the type of core reduction used in any given stage or phase of reduction.

unidirectional indeterminate- The scars all go in the same direction though it is not possible to determine whether they are parallel or convergent.

unidirectional parallel- The scars all go in one direction and they are aligned parallel to one another (as in a single platform blade core).

unidirectional convergent- The scars all go in one direction and the trend toward converging at the distal end. This type of flaking usually produces points.

centripetal flaking- scars come from multiple directions from the outer flake circumference and converge near the center. Disc cores will produce this kind of scar pattern.

bidirectional-opposed (0-180 degrees) Flake scars are parallel and originate from opposite ends of the flake.

bidirectional opposed (0-90) flake scars come from two directions and are perpendicular to one another. These usually come from cores that have two platforms on adjacent core edges

bidirectional convergent scars originate from opposed cores but create triangular shape scar usually for prepared core point removal.

parallel indeterminate- Flake scars are parallel but it is not possible to determine from which direction they are struck.

cortical- Flake dorsal surface is almost completely covered with cortex.

No Scars- no dorsal scars

convergent indeterminate- dorsal scars converge but it is not possible to tell the direction of the removals.

Indeterminate

Location of Maximum Width. Maximum width is reported as occurring in 1 of 5 equal-length theoretical divisions along the technological length of the artifact. Proximal = 1 and Distal = 5.

Platform Lipping- checkbox for presence or absence of lipping (see Pelcin 1997 for list of references for discussion and references for platform lipping).

Percussion Mark- checkbox for presence or absence of hammerstone percussion mark (a very small divot or fissure that will also occasionally mark the initiation of an incompletely propagated flake splitting crack when artifact is held up to the light.

Platform Preparation (Flaking Surface)- See Soriano et al 2007 for detailed description and illustration.

Platform Abrasion- See Soriano et al 2007 for detailed description and illustration.

Platform Preparation

none- plain platform flake

bruising- platform has been prepared by abrasion or crushing down the core edge (as opposed to along the dorsal surface for the Platform Abrasion attribute above)

single flake – intended point of percussion prepared by one faceting flake

multiple flakes- prepared by multiple faceting flake

stepped flake

multiple stepped flakes

indeterminate

Platform Type (modified from Thackeray and Kelly 1988)

plain- is a plain unmodified or unprepared striking platform

residual facetted- platform point of percussion isolated by prior flake removal scars (no evidence for initiation of faceting flake scars in the form of negative bulbs)

facetted- a platform with one or more faceting flake scars designed to isolate the point of percussion.

diffuse- platform is extremely small and thin. Attributes are very difficult to determine even with the aid of a low-power scope.

crushed/shattered- the majority of the platform broke off during the blow that created the flake.

cortex- flake has a completely cortical platform

Platform Shape-This refers to the plan view of the platform (modified from Thackeray and Kelly 1988).

flat- platform is straight with no concavity or convexity

concave- platform is rounded and curves inward toward the center of the flake.

convex- platform is rounded and curves away from the center of the flake

dihedral- the apex or ridge of two flake scars, forming a single triangular point on the platform

chapeau de gendarme- classic Levallois, 'police man's hat'shape.

peaked- irregular or generally asymmetric but deliberately created high point not covered by the other categories

indeterminate- shape not determined

no platform- flake is missing the platform

Soriano et al. (2007) Type- blade classification used for complete and almost complete blades and bladelets. Refer to Soriano et al 2007 for complete description and illustrations.

Fracture Initiation, Platform Delineation, Platform Fissure, Bulb Attributes, Platform Morphology- used for complete and almost complete blades and bladelets. Refer to Soriano et al 2007 for complete description and illustrations.

Edge Modification-presence/absence checkbox

Edge Modification Location

indeterminate

distal ventral

lateral right ventral

lateral right dorsal

lateral right bifacial

lateral left ventral

lateral left dorsal

lateral left bifacial

distal dorsal

distal bifacial

proximal dorsal

proximal bulbar

proximal bifacial

complete unifacial

complete bifacial

entire circumference (not including platform)

Modification Type

irregular marginal

backing

burination

acute short

acute long

acute invasive

steep short

steep long

Modification Angle This is the angle formed by the ventral surface of the flake and the retouched portion of the dorsal face. Measured in degrees using a goniometer. For reference see Dibble and Bernard 1980.

0-30%

31-60%

61-90%

90+%

indeterminate

Modification Length- This is similar to cutting edge, but only the cumulative length of the retouched portion(s) of the flake edge is recorded in mm.

Cores/Hammerstones

Find No., Specimen No., Lot Number, Raw Material, and Geneste Type- Refer to the section above. These field descriptions are the same for flakes and cores.

Hammerstone- checkbox ticked if artifact is a hammerstone

Typology- Core type was described according to Volman (1981). The abbreviated typology is spelled out in the comment section. The majority of PP5-6 cores are single platform and discoid cores.

Completeness-A core is either complete (1) or incomplete (2). Core fragments are coded but attribute values are not commonly included in any metrical analysis.

Number of Removals- This is a count of the total number of flake scars that are greater than 10mm in length.

Scar Pattern-This essentially follows the same description as given for flakes.

Weight- core mass in grams

Maximum length- If the core has an obvious primary flake release surface, maximum length is taken down the long axis of the core, parallel to that surface. Otherwise, maximum length corresponds to maximum dimension as in the case of disc cores.

Maximum width- Once maximum length has been taken, maximum width is the largest dimension that can be taken on the same plane, perpendicular to maximum length.

Maximum thickness- This is the maximum thickness of the core on a third plane of the artifact.

Cortex Type- same description fields as flake**.** Multiple cortex surfaces are described in comments.

Cortex- Cortex coverage percentage is coded according to what percentage of the entire core surface area is covered by cortex. Code values are the same as for flakes.

Photo- Same as flakes

Comment- In the comment field core typology is spelled out and any additional is added

Appendix 3- Debitage and Core Data Entry Forms

(MS Access screen captures)

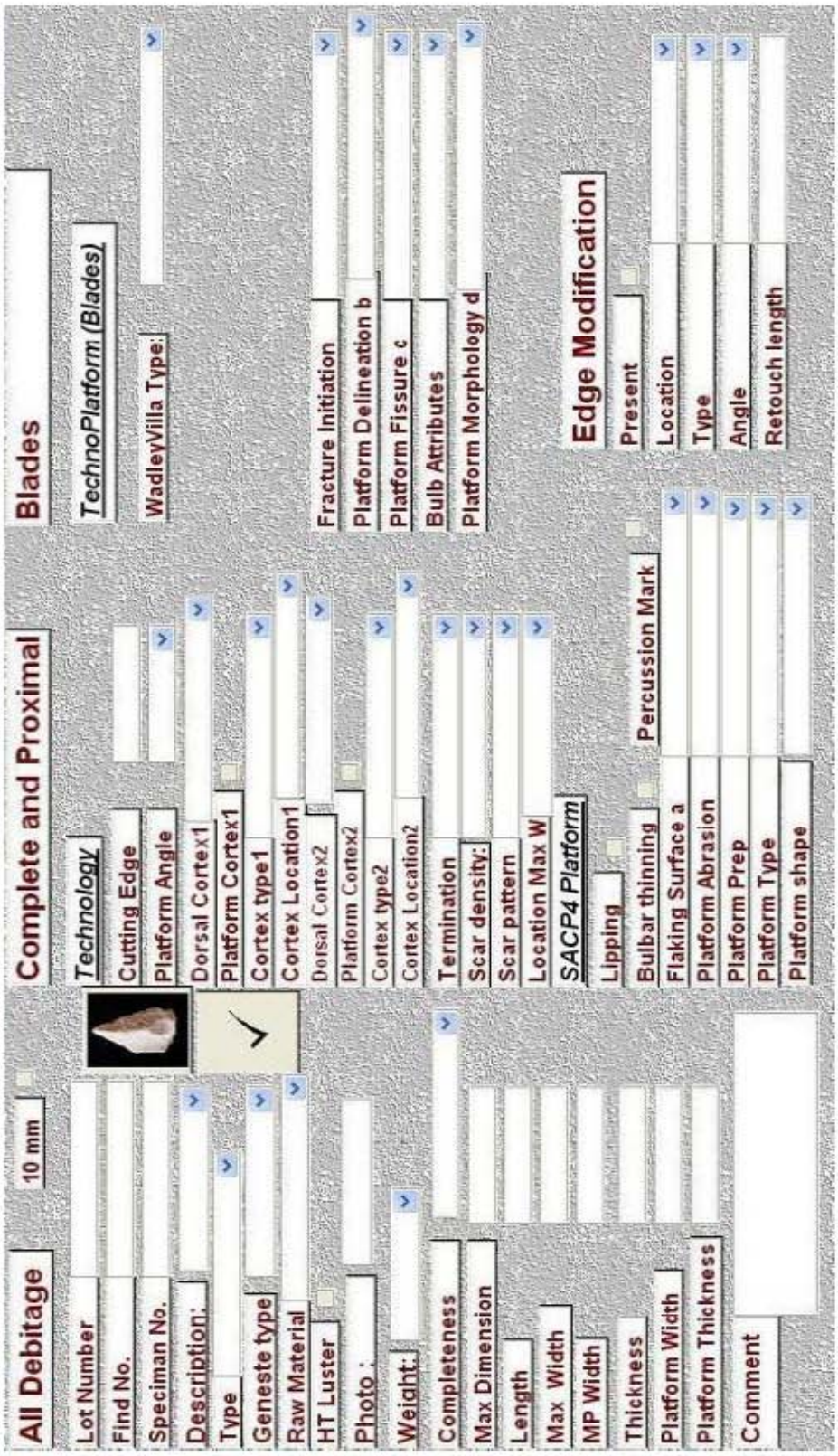

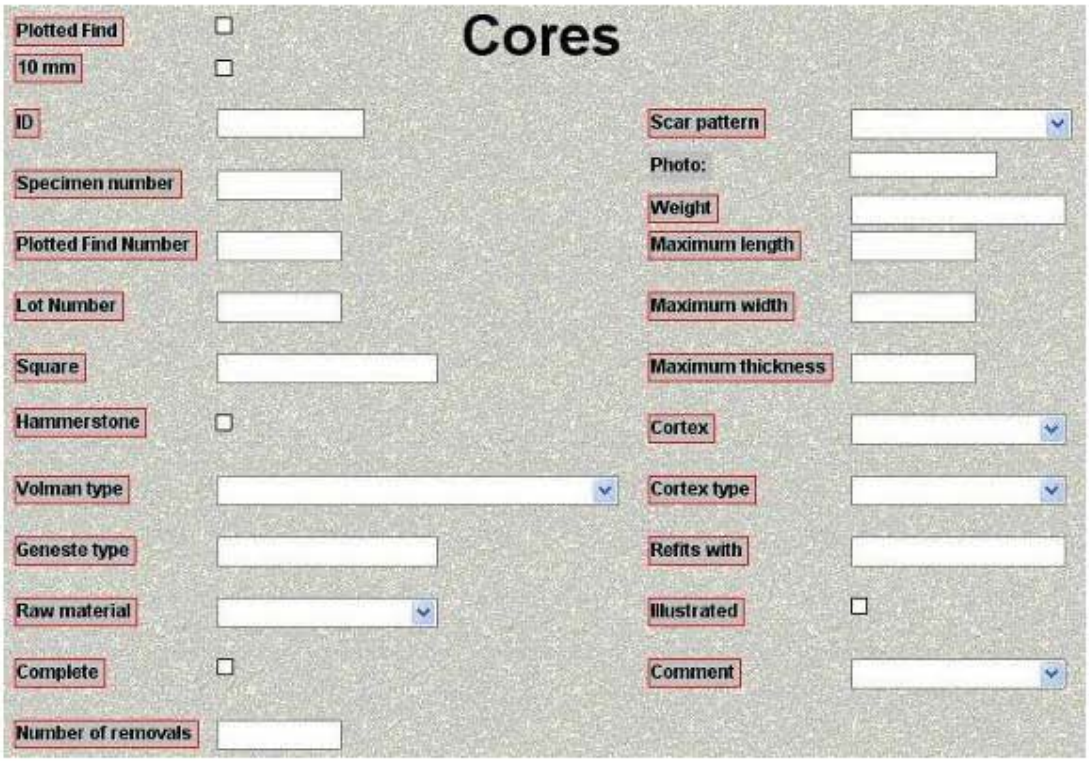
Cores
Plotted Find
10 mm
ID
Specimen number
Plotted Find Number
Lot Number
Square
Hammerstone
Volman type
Geneste type
Raw material
Complete
Number of removals
Scar pattern
Photo:
Weight
Maximum length
Maximum width
Maximum thickness
Cortex
Cortex type
Refits with
Illustrated
Comment

Appendix 4- Artifact Summary Tables and Images

Appendix 4: Section 1- Cores

Find No.	Agg	SubAggregate	Sample	Core Type	Scar pattern	Comment	Complete	Cortex %	Cortex type	Raw Material	Scar Count	Wt	L	W	Thk	MG	MG 2
152923	MBSR	Takis	Takis	other double platform core	unidirectional-parallel	chalcedony pebble with three attempted blade removal	complete	41-60	cobble	Chert	3	7.6	30	18	13		
153515	MBSR	Takis	Takis	opposed platform	bidirectional 0-180°	opposed platform blade core	complete	none		Chert	6	9	30	25	12		
153526	MBSR	Takis	Takis	opposed platform	bidirectional 0-180°	small bidirectional bladelet core	complete	41-60	cobble	Chert	6	9.5	26	25	13		
153538	MBSR	Takis	Takis	adjacent platform	bidirectional 0-90°	adjacent platform core. Not completely exhausted	complete	41-60	pre-treatment surface	Silcrete	7	23.5	35	32	22	3.3	1.9
153540	MBSR	Takis	Takis	opposed platform	unidirectional-parallel	small exhausted double platform bladelet core	complete	41-60	indet	Chert	3	1.4	22	11	6		
153960	MBSR	Takis	Takis	opposed platform	bidirectional 0-180°	bidirectional bladelet core made from an angular cobble fragment	complete	21-40	cobble	Silcrete	8	26.1	39	32	21	2.9	
153973	MBSR	Takis	Takis	discoid	radial/centripedal	minimally flaked discoid core	complete	none		Silcrete	4	4.6	26	22	10	2.2	
102429	NWR	DBSS	NWR	single platform	unidirectional-convergent	Has differential heat treatment luster. This core was made from a large untreated cortical flake that was then heat treated and flaked as a blade core	complete	1-20	outcrop	Silcrete	5	30	51	31	28	3.1	
102898	NWR	DBSS	NWR	opposed platform	bidirectional 0-180°	bidirectional core on large chunk/flake fragment	complete	none		Quartzite	2	36	49	32	24		
103491	NWR	DBSS	NWR	opposed platform	bidirectional 0-180°		complete	none		Quartzite	8	108	59	55	33		
104725	NWR	DBSS	NWR	core on a flake	bidirectional 0-180°	bidirectional 0-180 bladelet core on a flake or blade fragment	complete	1-20	outcrop	Quartzite	7	17	39	29	11		
107469	DBCS	Miller	Miller	other double platform core	bidirectional 0-180°	small expedient core on a tabular piece of silcrete	complete	21-40	outcrop	Silcrete	4	6.6	35	25	10	2	
107993	DBCS	Miller	Miller	discoid	radial/centripedal		complete	21-40	cobble	Quartzite	5	79	68	43	29		
119754	DBCS	Miller	Miller	other double platform core	bidirectional 0-90°	double platform core with flaking surfaces 90 opposed on opposite surfaces	complete	1-20	cobble	Chert	8	4.4	22	18	10		
120770	DBCS	Miller	Miller	discoid	radial/centripedal	cobble chunk with 4 discoid removals around the circumference	complete	41-60	cobble	Quartzite	4	99	71	59	24		
120918	DBCS	Miller	Miller	discoid	radial/centripedal	radial chalcedony core with a large incompletely propogated fracture down the center of the core	complete	21-40	rind	Chert	6	12.8	31	25	18		
121078	DBCS	Miller	Miller	opposed platform	bidirectional 0-180°	very small double platform 0-180 degrees on both surfaces. Both platforms are a little battered, possibly from bipolar flaking	complete	none		Chert	7	0.7	16	9	5		
121148	DBCS	Miller	Miller	core on a flake	unidirectional-parallel	sent for heat treatment analysis	complete	none		Silcrete	2	9.8	37	21	11		
121180	DBCS	Miller	Miller	opposed platform	bidirectional 0-180°	small double platform bladelet core made from a untreated silcrete flake. Largest flake scar is 20mm in length	complete	1-20	pretreatment	Silcrete	2	7.1	31	21	13	3.6	1.5

Find No.	Agg	SubAggregate	Sample	Core Type	Scar pattern	Comment	Complete	Cortex %	Cortex type	Raw Material	Scar Count	Wt	L	W	Thk	MG	MG 2
121204	DBCS	Miller	Miller	minimal	unidirectional-convergent	core made from what was originally an unheated cortical flake which was then heat treated and minimally flaked producing one small bladelet	complete	41-60	rind	Silcrete	3	3.7	26	16	10	3.1	1.5
121855	DBCS	Miller	Miller	single platform	unidirectional-convergent	small convergent single platform core	complete		pre-ht	Silcrete	5	12.1	36	23	18		
122715	DBCS	Miller	Miller	discoid	radial/centripedal	discoid core fragment with ht gloss and potlid scar	complete	none		Silcrete	7	9.8	38	23	15	2.7	
122776	DBCS	Miller	Miller	opposed platform	bidirectional 0-180°	exhausted opposed platform blade core. Three last scars all max dimension c. 27mm	complete	1-20	outcrop	Silcrete	7	7.1	33	23	8	3	1.3
129873	DBCS	Miller	Miller	opposed platform	bidirectional 0-180°	10% of surface is also pretreatment surface. This is a small nodule of silcrete with rind on most sides.	complete	61-80	rind	Silcrete	11	39.8	50	40	22	2.1	1.1
129883	DBCS	Miller/Sorel	Miller/Sorel	single platform	unidirectional-parallel	simple expedient single platform core with 2 parallel flake scars	complete	61-80	globular	Chert	2	4.8	23	23	10		
180743	DBCS	Miller/Sorel	Miller/Sorel	discoid	radial/centripedal	small discoid core half fragment. Smallest flake is 10mm in length	fragment	none		Silcrete	3	2.1	20	10	13		
181703	DBCS	Miller/Sorel	Miller/Sorel	core on a flake	unidirectional-parallel	minimal bladelet core made on the edge of a larger distal flake/blade silcrete fragment. The removals were taken on the thick split break as a sort of burin blow. It appears there was one succesful removal and then then two small step fragments damaged the core platform	complete	none		Silcrete	2	7.8	37	22	9		
182196	DBCS	Miller/Sorel	Miller/Sorel	core on a flake	unidirectional-parallel	bladelet core made from a larger quartzite cortical flake. The proximal snap is used as the platform and the lateral edges as the flake release surfaces. There is some modification on the distal end of the core to create distal convexity	complete	21-40	outcrop	Quartzite	4	16.5	35	30	12		
246339	DBCS	Miller/Sorel	Miller/Sorel	core on a flake	bidirectional 0-180°	silcrete flake with small bidrectional bladelet removals along one margin. There are some small notches on the opposite margin	complete	none		Silcrete	5	2.9	29	6	15		
250610	DBCS	Miller/Sorel	Miller/Sorel	single platform	unidirectional-parallel		complete	41-60	outcrop	Silcrete	6	9.8	32	30	11		
132366	DBCS	Sorel/Coco	Sorel/Coco	core on a flake	unidirectional-convergent	small bladelet core on distal end of a flake	complete	1-20	pre-ht surface on right lateral and platform	Silcrete	5	5.8	25	25	9		
133993	DBCS	Sorel/Coco	Sorel/Coco	core on a flake	bidirectional 0-180°	small bidirectional blade core on a flake. There is a single blade removal on the ventral surface. Not cleaned for measuring gloss.	complete	none		Silcrete	6	5.1	27	21	7		

Find No.	Agg	SubAggregate	Sample	Core Type	Scar pattern	Comment	Complete	Cortex %	Cortex type	Raw Material	Scar Count	Wt	L	W	Thk	MG	MG 2
167066	SGS	Jinga	SGS	opposed platform	bidirectional 0-180°	small exhausted bladelet core with removals primarily on one side. Max length of largest removal is 21mm	complete	none		Chert	5	2.5	22	15	6		
168626	SGS	Jinga	SGS	other double platform core	bidirectional 0-90°	core with parallel scars on each side arranged 0-90 with respect to each other. 22mm max length on largest final scar	complete	none		Silcrete	13	14.6	27	30	20		
138601	SGS	Tamu	SGS	change of orientation	multidirectional	discoid style core with blade removals on one surface	complete	1-20	cobble	Chert	8	5.5	20	19	13		
138832	SGS	Tamu	SGS	opposed platform	bidirectional 0-180°	small "discoid" shaped core with opposed 0-180 flaking surface on each side. This is probably a pretty good model for how bladelets on small nodules are made. It is very opportunistic use of material.	complete	none		Chert	12	4.7	21	20	10		
105975	OBS	Celeste	OBS	opposed platform	unidirectional-parallel	sent for heat treatment analysis	complete	none		Silcrete	6	9.9	32	22	16		
139256	OBS	Celeste	OBS	change of orientation	multidirectional		complete	none		Quartz	5	8.7	25	20	14		
242689	OBS	Celeste	OBS	discoid	radial/centripedal	biconvex doscoid core with large border removal on one surface	complete	none		Quartz	6	35.9	37	36	28		
171009	OBS	Lizelle	OBS	single platform	unidirectional-convergent	small convergent core	complete	none		Chert	4	2.1	14	22	7		
171158	OBS	Lizelle	OBS	bipolar	bipolar	cobble wedge with battering on opposite ends	complete	41-60	cobble	Crystal Quartz	2	4.8	30	20	9		
172051	OBS	Lizelle	OBS	core on a flake	bidirectional 0-180°	proximal primary cortical flake with a few very small bidirectional scars initiated from the platform and from the distal ventral break. The largest final removal is 16mm in max dimension	complete	41-60	outcrop	Silcrete	4	5.1	22	22	9	3.5	
173477	OBS	Peter	OBS	single platform	unidirectional-parallel	small unidirectional parallel scars	complete	none		Chert	4	3	18	17	11		
181026	OBS	Peter	OBS	opposed platform	bidirectional 0-180°		complete	21-40	cobble	Quartz	3	10.7	27	25	16		
203945	OBS	Peter	OBS	change of orientation	multidirectional	small angular quartz core	complete	none		Quartz	4	3.9	21	18	13		
205804	OBS	Peter	OBS	change of orientation	radial/centripedal	irregular exhausted core with crushing on two adjacent sides bringing the sides together in a prominance	complete	1-20	rind	Silcrete	5	5.3	26	21	9		
208545	OBS	Peter	OBS	change of orientation	multidirectional	worked out exhausted core with heavy bifacial battering on both lateral margins and a burination on the wider end.	complete	none		Quartzite	4	7.5	30	26	8		
152683	SADBS	Betina	SADBS	single platform	unidirectional-indeterminate	small single platform silcrete core with only two removal scars from the platform. The core may have been abandoned due to the rind cortex around half the circumference. no convex surface for gloss	complete	21-40	rind	Silcrete	2	8.6	25	33	10		
153185	SADBS	Betina	SADBS	change of orientation	radial/centripedal	random orientation core	complete	none		Silcrete	9	9.9	3	25	15	3.2	

Find No.	Agg	SubAggregate	Sample	Core Type	Scar pattern	Comment	Complete	Cortex %	Cortex type	Raw Material	Scar Count	Wt	L	W	Thk	MG	MG 2
153417	SADBS	Betina	SADBS	opposed platform	bidirectional 0-180°	small double platform 0-180 bladelet core	complete	none		Silcrete	4	4	27	9	18	3	
153422	SADBS	Betina	SADBS	single platform	multidirectional	single platform core with preparation flakes around the margin to create a point core. Core abandoned prior to final desired remova	complete	21-40	cobble	Quartzite	5	44.2	40	54	23		
153927	SADBS	Enrico	SADBS	other double platform core	unidirectional-parallel	small core with two platforms and flaking surfaces. One surface shows convergent parallel flaking of small bladelet scars. The other platform shows unidirectional parallel flaking	complete	1-20	pre-ht	Silcrete	6	3.7	17	22	15	3	1.6
154909	SADBS	Enrico	SADBS	discoid	radial/centripedal	small exhausted discoid core for chalcedony	complete	41-60	rind	Chert	6	6.8	32	23	8		
156192	SADBS	Enrico	SADBS	discoid	radial/centripedal		complete	none		Chert	8	7.4	27	22	16		
160366	SADBS	Enrico	SADBS	opposed platform	bidirectional 0-180°	small silcrete blade core	complete	1-20	pre-ht surface	Silcrete	6	3.5	31	11	8		
120819	SADBS	Gert	SADBS	opposed platform	bidirectional 0-180°	small exhausted opposed platform core. Shows heat treatment gloss	complete	1-20	rind	Silcrete	4	6.3	25	17	12		
129974	SADBS	Gert	SADBS	discoid	radial/centripedal	typical small discoid core.	complete	none		Silcrete	5	4.9	22	19	13	3.5	2.6
132105	SADBS	Gert	SADBS	opposed platform	bidirectional 0-180°	no convex surface for gloss	complete	21-40	rind	Silcrete	5	3.9	17	20	9		
132445	SADBS	Gert	SADBS	minimal	multidirectional	tabular piece of silcrete with cortex on both sides and pretreatment cortex on one end. There are several small flake scars around the margin but the block appears to have been unsatisfactory for continued flaking	complete	61-80	outcrop	Silcrete	6	42.2	54	41	19	2.5	1.4
133225	SADBS	Gert	SADBS	change of orientation	radial/centripedal	worked out core	complete	none		Silcrete	3	2.9	22	15	9	3.3	
159133	SADBS	Gert	SADBS	opposed platform	bidirectional 0-180°	small informal opposed platform blade core	complete	41-60	rind	Quartzite	3	6.6	26	18	10		
119322	SADBS	Gert/Enrico/Pit Fill	SADBS	opposed platform	bidirectional 0-180°	double platform bladelet core	complete			Silcrete	7	23.3	39	26	18	5	
119863	SADBS	Gert/Enrico/Pit Fill	SADBS	single platform	unidirectional-parallel	single platform blade core. Preserves platform of cortical flake primary form	complete	1-20	cobble	Quartzite	6	45.3	44	43	21		
130450	SADBS	Gert/Pit Fill	SADBS	adjacent platform	bidirectional 0-180°	small adjacent platform bidirectional core made form a silcrete cobble cortical flake. Largest final removal was 29mm in length	complete	21-40	cobble	Quartzite	5	11	28	27	13		
131652	SADBS	Gert/Pit Fill	SADBS	adjacent platform	bidirectional 0-180°	void on opposite side filled with globular rind.	complete	none		Silcrete	4	8.6	29	23	11		
133823	SADBS	Holly	SADBS	change of orientation	multidirectional	small angular core with three removals.	complete	none		Silcrete	3	5.5	25	17	15	1.5	
133942	SADBS	Holly	SADBS	other double platform core	bidirectional 0-90°	cortex identicle to ALB D. Looks like cobble cortex but isn't. no convex surface for gloss	complete	21-40	outcrop	Silcrete	9	6.4	22	26	15		
106905	SADBS	Joanne	SADBS	opposed platform	bidirectional 0-180°	bidirectional scars on one surface of a proximal quartz crystal fragment	fragment	41-60	other	Crystal Quartz	4	4.8	24	16	12		

Find No.	Agg	SubAggregate	Sample	Core Type	Scar pattern	Comment	Complete	Cortex %	Cortex type	Raw Material	Scar Count	Wt	L	W	Thk	MG	MG 2
138508	SADBS	Joanne	SADBS	discoid	radial/centripedal	quartz discoid core	complete	none		Quartz	8	9.6	30	26	12		
140102	SADBS	Joanne	SADBS	core on a flake	bidirectional 0-180°	bidirectional core on a flake or blade fragment. Core is missing one of the opposite platforms. The existing platform has crushing that looks like bipolar battering	fragment	none		Silcrete	6	2.6	24	21	7	3	
149061	SADBS	Joanne	SADBS	change of orientation	multidirectional	multidirectional core	complete	1-20	outcrop	Silcrete	10	14.6	30	26	19	4	
150816	SADBS	Joanne	SADBS	core on a flake	unidirectional-parallel	larger distal flake fragment with three small bladelet removals on the distal end of the flake	fragment	61-80	pre-ht	Silcrete	3	15.5	46	22	14	2.6	1.6
228710	SADBS	Joanne	SADBS	opposed platform	bidirectional 0-180°	outille ecaille or exhausted core with battering on both sides. Small bladelet core	complete	none		Silcrete	6	4.9	23	21	10		
239673	SADBS	Joanne	SADBS	minimal	one scar	small angular nodule with one removal showing ht surface beneath	complete	41-60	outcrop	Silcrete	1	5.3	28	23	10		
243320	SADBS	Joanne	SADBS	opposed platform	bidirectional 0-180°	small wedge-shaped blade core with very small bladelet removals	complete	21-40	outcrop	Silcrete	9	3.6	29	12	14		
138060	SADBS	Sydney	SADBS	core on a flake	unidirectional-parallel	simple core on tabular piece of silcrete. May represent collection of tabular natural spalls or use as bladelet cores	complete	41-60	pre-ht	Silcrete	3	1.4	19	12	6	1.6	
138236	SADBS	Sydney	SADBS	adjacent platform	Multi-directional	flaking surfaces share common platfrom core give appearance of half a discoid core. Very similar to Rietvlei silcrete. Shows differential ht surfaces	complete	41-60	rind	Silcrete	10	48.8	39	52	30	1.7	
138647	SADBS	Sydney	SADBS	opposed platform	bidirectional 0-180°	double platform bladelet core	complete	61-80	outcrop	Silcrete	3	7.9	31	19	13	3.6	1.4
139512	SADBS	Sydney	SADBS	single platform	unidirectional-convergent	single platform convergent core	complete	21-40	outcrop	Silcrete	4	6.9	26	21	12	3.1	
154121	SADBS	Sydney	SADBS	single platform	unidirectional-parallel	single platform blade bladelet core made from what looks like a thermally spalled angular fragment which has a potlid on the opposite side.	complete	61-80	pre-ht	Silcrete	6	11.5	36	27	12	2.6	3.6
159113	SADBS	Thandesizwe	SADBS	adjacent platform	bidirectional 0-180°	three fragments of a thermally damaged blade core	fragment	21-40	rind	Silcrete	7	30.4	46	34	19		
174560	SADBS	Thandesizwe	SADBS	discoid	radial/centripedal	unifacial discoid core with cobble cortex on base. Cobble has some battering	complete	41-60	cobble	Quartzite	6	128	60	53	33		
208841	ALBS	Conrad	Conrad Series	single platform	unidirectional-convergent	very good example of bladelet core. Largest final removal is 26mm. Fits pattern of cortical debitage being heated and then flaked	complete	1-20	rind	Silcrete	6	13.6	37	25	18		
106312	ALBS	Conrad Cobble and Sand	Conrad Series	cylinder	unidirectional-parallel	small conical core with differential heat treatment luster and cortex	complete	1-20	cobble	Silcrete	7	7.4	22	25	15	3.6	
222695	ALBS	Conrad Shell	Conrad Series	single platform	unidirectional-parallel	split pebbles with parallel removals from most of the circumference. Some smaller stepped removals on one portion of the cortex may be a scraper edge	complete	41-60	cobble	Hornfels	7	21.9	37	31	18		

Find No.	Agg	SubAggregate	Sample	Core Type	Scar pattern	Comment	Complete	Cortex %	Cortex type	Raw Material	Scar Count	Wt	L	W	Thk	MG	MG 2
138423	ALBS	Jocelyn	Jocelyn	change of orientation	multidirectional	small intensively worked core	complete	1-20	rind	Chert	7	7.8	22	21	16		
173936	ALBS	Jocelyn	Jocelyn	opposed platform	bidirectional 0-180°	large bidirectional blade core on ht silcrete. battered platforms but no percussion marks	complete	none		Silcrete	9	50.1	41	36	37	3.2	
176802	ALBS	Jocelyn	Jocelyn	single platform	unidirectional-convergent		complete	none		Silcrete	3	16.3	30	30	22	3	1.1
177115	ALBS	Jocelyn	Jocelyn	single platform	unidirectional-parallel	wide unidirectional single platform blade core. Platform shows extensive preparation. Removals from core would have been facetted	complete	none		Quartzite	5	63.2	50	58	20		
177527	ALBS	Jocelyn	Jocelyn	discoid	radial/centripedal	largest final removal was 20mm in maximum length	complete	41-60	rind	Chert	6	13.6	35	29	16		
178509	ALBS	Jocelyn	Jocelyn	opposed platform	bidirectional 0-180°		complete	none		Quartz	6	17	30	21	26		
182999	ALBS	Jocelyn	Jocelyn	discoid	radial/centripedal	hornfels cobble fragment with 6 removals around the circumference	fragment	21-40	cobble	Hornfels	6	29.1	40	30	20		
183494	ALBS	Jocelyn	Jocelyn	other double platform core	bidirectional 0-180°	exhausted core probably made from a flake. One margin has preparation or retouch	complete	21-40	pretreatment cortex	Silcrete	3	5	25	24	7		
185101	LBSR	Aaron Shell		discoid	radial/centripedal		complete	21-40	rind	Silcrete	8	13.1	35	26	15		
134600	LBSR	Adrian Sand and Roofspall	AK Silcrete	change of orientation	multidirectional		complete	1-20	outcrop	Silcrete	6	10.8	28	21	19	2.6	2.1
164309	LBSR	Adrian Shell		discoid	radial/centripedal	discoid core	complete	none		Quartzite	9	52	53	39	30		
152991	LBSR	Bijou Sand and Roofspall		core on a flake	radial/centripedal	large quartzite cortical flake with several large removals and what might be retouch on the distal dorsal surface	complete	21-40	outcrop	Quartzite	5	113	90	71	27		
106548	LBSR	Jed	Jed/JR Quartzite	discoid	radial/centripedal	discoid core	complete	none		Quartzite	8	37.9	54	40	22		
107398	LBSR	Jed	Jed/JR Quartzite	single platform	unidirectional-convergent	simple convergent point core	complete	21-40	cobble	Quartzite	3	33.6	38	40	31		
107882	LBSR	Jed	Jed/JR Quartzite	change of orientation	multidirectional	core on an irregular cortical cobble fragment	complete	21-40	cobble	Quartzite	6	61.8	82	38	22		
156523	LBSR	Jed	Jed/JR Quartzite	single platform	unidirectional-convergent	cobble cortex on base of core.	complete	21-40	cobble	Quartzite	8	115	61	81	30		
156535	LBSR	Jed	Jed/JR Quartzite	core on a flake	unidirectional-parallel	secondary cortical flake with two small paralle removals on the ventral surface.	complete	41-60	rind	Chert	2	10.5	24	36	13		
157696	LBSR	Jed	Jed/JR Quartzite	minimal	bidirectional 0-180°	cobble fragment with 2 opposed flake removals on the flaking surface. The opposite side is cortical	fragment	41-60	cobble	Quartzite	6	242	102	65	35		
158317	LBSR	Jed	Jed/JR Quartzite	single platform	unidirectional-convergent	unidirectional convergent point core with basal cobble cortex. Final point removal was prepared but not removed	complete	61-80	cobble	Quartzite	7	70.1	46	86	17		
169177	LBSR	Leba Sand and Roofspall		minimal	multidirectional	small split quartz cobble with two random removals in addition to the split surface. This could be a split hammerstone but there is no obvious battering	complete	41-60	cobble	Quartz	3	37	48	35	29		

Find No.	Agg	SubAggregate	Sample	Core Type	Scar pattern	Comment	Complete	Cortex %	Cortex type	Raw Material	Scar Count	Wt	L	W	Thk	MG	MG 2
175691	LBSR	Leba Shell	Leba Quartzite	minimal	Indeterminate	core fragment on a tabular piece of quartzite. There are four non-patterned removals including two core edge blades on opposite sides of the core	complete	none		Quartzite	4	76.9	79	48	16		
120722	LBSR	Ludumo Sand and Roofspall	Ludumo Quartzite	discoid	radial/centripedal	discoid core fragment with cortical cobble base. Largest scar is 35mm in max length	fragment	41-60	cobble	Quartzite	6	62.1	63	57	19		
179483	LBSR	Lwando Shell	Lwando Quartzite	discoid	radial/centripedal	minimally worked discoid core with cobble cortex on one margin	complete	21-40	cobble	Quartzite	8	27	39	40	16		
130688	LBSR	Lwando Shell/Aaron Sand and Roofspall	Lwando Quartzite	discoid	radial/centripedal	irregular expedient core	complete	1-20	cobble	Quartzite	7	49.7	55	50	21		
131497	LBSR	Lwando Shell/Aaron Sand and Roofspall	Lwando Quartzite	discoid	radial/centripedal	cobble cortex on the base	complete	21-40	cobble	Quartzite	8	42.8	45	40	25		
119101	LBSR	Martin SR/ Hope Red/ Lwando SR	HM Silcrete Hornfels	core on a flake	Indeterminate	large unheated silcrete flake with three core preparation flakes on the left proximal margin and a single removal from the original dorsal surface.	complete	none		Silcrete	4	20.6	45	42	10	2	

1. MBSR- Takis

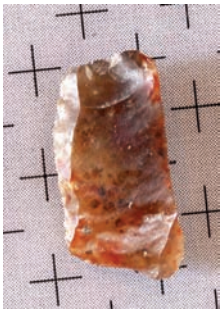

152923 (Lot 7938, LS8CD1). **Double platform core**- chert pebble with three attempted unidirectional parallel blade removals and cobble cortex.

153515 (Lot 7938, LS8CD1). **Core with opposed platforms on same side-** Opposed platform chert blade core with bidirectional 0-180° flake scars.

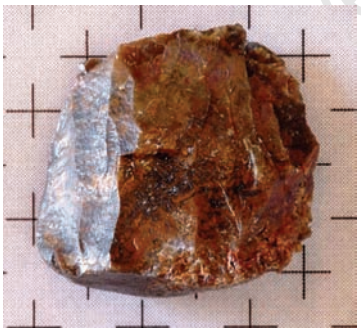

153526 (Lot 7941, LS8CD1). Core **with opposed platforms on same side-** small chert bidirectional bladelet core with cobble cortex.

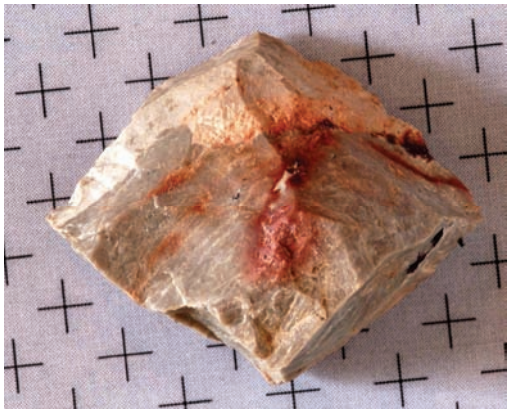

153538 (Lot 7938, LS8CD1). (Lot 7938, LS8CD1) **Adjacent platform core-** Incompletely exploited silcrete adjacent platform core. Surface exhibits bidirectional 0-90° scars and dull pre-heat treatment luster.

153540 (Lot 7938, LS8CD1) **Core with opposed platforms on same side-** small chert exhausted double platform bladelet core with unidirectional-parallel scars and cortex of indeterminate type.

153960 (Lot 7941, LS8CD1). **Core with opposed platforms on same side-** bidirectional 0-180° bladelet core made from an angular silcrete cobble fragment.

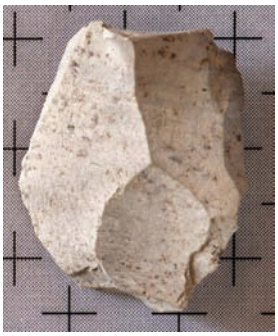

153973 (Lot 7938, LS8CD1). **Discoid core-** minimally flaked silcrete discoid core

103491 (Lot 3341, NWR6J). **Core with opposed platforms on same side-** quartzite bidirectional 0-180° core

2. Northwest Remnant

(no photo)

102429 (Lot 3322, NWR6C1). **Single platform core-** core made from a large untreated silcrete cortical flake (outcrop cortex) that was then heat treated and unidirectional-convergent flaked as a blade core. Core has both pre- and post-heat treatment dull and glossy surfaces.

104725 (Lot 3366, NWR6AK). **Core on a flake**- quartzite bidirectional 0-180° bladelet core on a cortical (primary outcrop cortex) flake or blade fragment.

102898 (Lot 3331, NWR6C2). **Core with opposed platforms on same side-** quartzite bidirectional 0-180° core made on a large chunk/flake fragment

3. DBCS-Miller

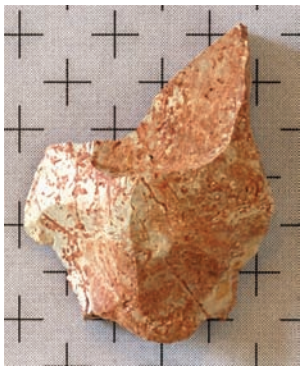

107469 (Lot 3245, LS7AA). **Double platform core**- small expedient silcrete core made from a tabular nodule. Core has bidirectional (0-180°) scars and primary outcrop cortex.

107993 (Lot 3245, LS7AA). **Discoid core**- Radial prepared quartzite core with cobble cortex.

119754 (Lot 3245, LS7AA). **Double platform core**- chert double platform core with flaking surfaces 0-90° opposed and located on opposite surfaces. Core has secondary context cobble cortex.

120770 (Lot 3296, LS7BO). **Discoid core**- Quartzite cobble chunk with four centripetal removals around the circumference and cobble cortex on the base.

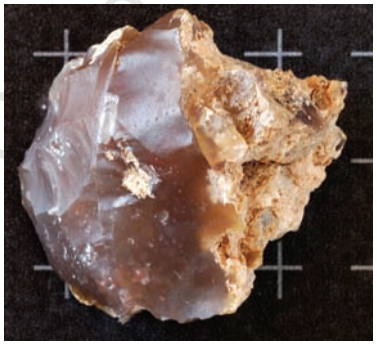

120918 (Lot 3296, LS7BO). **Discoid core**- radially prepared chert core with a large incompletely propogated crack down the center and rind cortex.

121078 (Lot 3296, LS7BO). **Core with opposed platforms on same and opposite sides-** very small double platform chert core with bidirectional 0-180° scars on both surfaces. Both platforms are slightly battered, possibly from bipolar flaking.

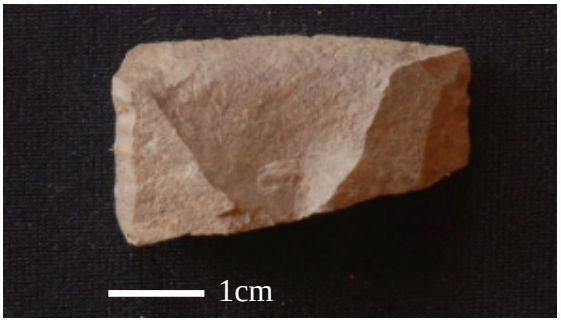

121148 (Lot 3296, LS7BO). **Core on a flake**- silcrete flake with unidirectional-parallel flake scars. Artifact was permanently exported for destructive TL and magnetics analysis in order to develop methodology for detecting lithic heat treatment.

121180 (Lot 3296, LS7BO). **Core with opposed platforms on same side-** Small double platform silcrete bladelet core with bidirectional 0-180° scars made from an unheated silcrete flake. Last largest flake scar is 20mm in length

121204 (Lot 3296, LS7BO). **Minimal core-** silcrete core made from what was originally an unheated cortical (rind) flake which was then subsequently heat treated and minimally unidirectional-convergent flaked producing one small bladelet.

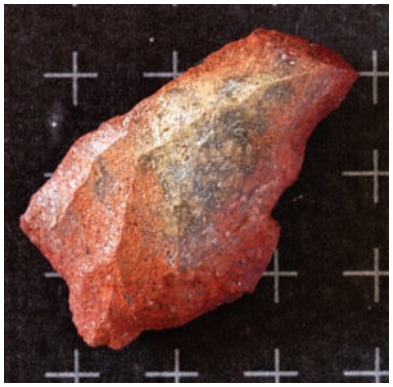

121855 (Lot 3296, LS7BO). **Single platform core**- small convergent single platform silcrete core with unidirectional-convergent flake and pre-heat treatment non-lustrous surface present.

122715 (Lot 3296, LS7BO). **Discoid core**- radially prepared core fragment with heat treatment gloss and potlid scars from thermal damage.

122776 (Lot 3296, LS7BO). **Core with opposed platforms on opposite sides-** silcrete exhausted opposed platform 0-180° blade core. Three last scars all have a maximum of dimension c. 27mm and there is primary outcrop cortex.

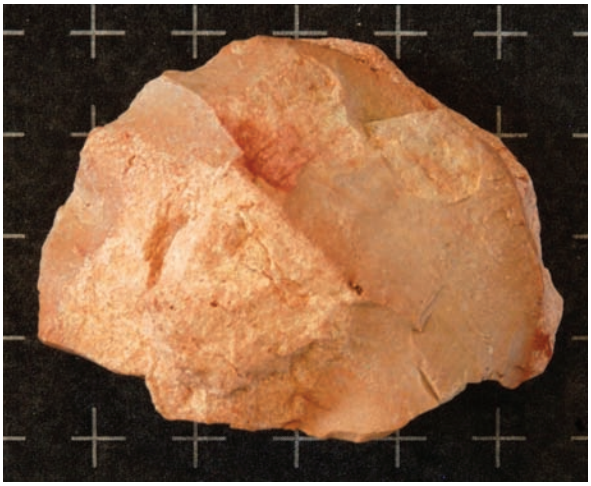

129873 (Lot 3454, LS7DS). **Core with opposed platforms on opposite sides-** Small nodule of silcrete with rind on most of the surface and with a small amount (c.10%) of pre-heat treatment surface. Bidirectional 0-180° flake scars.

181703 (Lot 8206, LS8LB). **Core on a flake**- minimal bladelet core made on the edge of a larger distal flake/blade silcrete fragment. The unidirectional-parallel removals were taken on the thick split break as a sort of burin blow. It appears there was one successful removal and then two small step fragments damaged the platform.

4. DBCS-Miller/Sorel

129883 (Lot 1148, LS7EV). **Single platform core-**chert simple and expedient single platform core with 2 unidirectional parallel flake scars.

182196 (Lot 8206, LS8LB). **Core on a flake**- Unidirectional-parallel flaked bladelet core made from a larger quartzite cortical flake. The proximal snap is used as the platform and the lateral edges as the flake release surfaces. There is some modification on the distal end of the core to create distal convexity. Surface exhibits primary outcrop cortex.

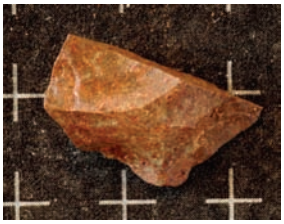

180743 (Lot 8206, LS8LB). **Discoid core-** small silcrete discoid core half fragment. Smallest flake is 10mm in length.

246339 (Lot 8430, LS9DI). **Core on a flake**- silcrete flake with small 0-180° bidirectional bladelet removals along one margin. There are some small notches on the opposite margin.

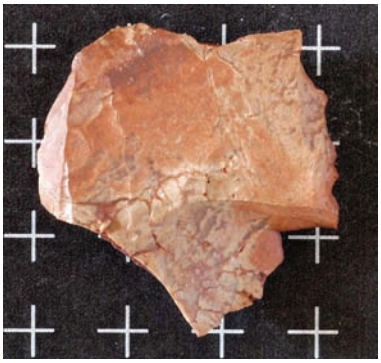

250610 (Lot 8430, LS9DI). **Single platform core**- Unidirectional-parallel flaked silcrete single platform core with outcrop cortex.

5. DBCS- Sorel/Coco

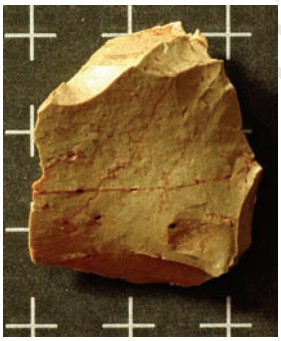

132366 (Lot 1169, LS7FM). **Core on a flake**- small bladelet core on the distal end of a silcrete flake with Unidirectional-convergent flake scars and dull, pre-heat treatment surface on the right lateral margin and platform.

133993 (Lot 1181, LS7FX). **Core on a flake-** small bidirectional 0-180° blade core made from a silcrete flake. There is a single blade removal on the ventral surface

.

6. SGS- Jinga

167066 (Lot 8038, LS8FT). **Core with opposed platforms on same side-** small exhausted chert bladelet core with bidirectional 0-180° removals primarily on one side. Maximum length of largest removal is 21mm.

168626 (Lot 8054, LS8GJ). **Double platform core**- silcrete core with parallel scars on each side arranged 0-90 with respect to each other. 22mm maximum length on largest final scar

7. SGS- Tamu

138601 (Lot 1283, LS7IH). **Change of orientation core**- discoid style chert core with multidirectional aligned blade removals on one surface and cobble cortex.

138832 (Lot 1283, LS7IH). **Core with opposed platforms on opposite sides**- small discoid shaped chert core with bidirectional opposed 0-180 flake scars from each side. This is probably a good example for how bladelets on small nodules are made. It shows very opportunistic use of material.

(no photo)

164821 (Lot 8037, LS8FS). **Single platform core (fragment)-** silcrete lateral core fragment with unidirectional-convergent flake scars and outcrop cortex.

8. OBS- Celeste

105975 (Lot 3205, LS7C). **Core with opposed platforms on same side-** Unidirectional parallel flaked silcrete core permanently exported for heat treatment destructive analysis.

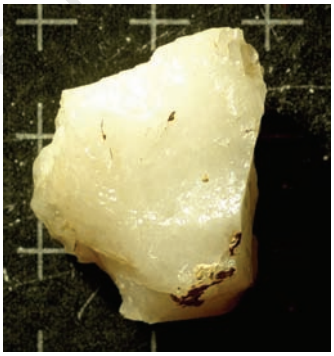

139256 (Lot 5206, LS7JB). C**hange of orientation core-**multi-directional flaked quartz core.

242689 (Lot 8563, LS9GU1). **Discoid core-** quartz biconvex discoid core with large border removal on one surface and radial flake scars.

9. OBS- Lizelle

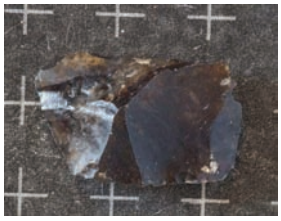

171009 (Lot 8099, LS8HL). **Single platform core**- small convergent chert core with unidirectional-convergent flake scars.

171158 (Lot 8092 LS8HL). **Bipolar core**- crystalline quartz cobble wedge with battering on opposite ends.

172051 (Lot 8103, LS8HY). **Core on a flake**- proximal primary cortical (outcrop cortex) silcrete flake with a few very small bidirectional 0-180° scars initiated from the platform and from the distal ventral break. The largest final removal is 16mm in max dimension.

10. OBS- Peter

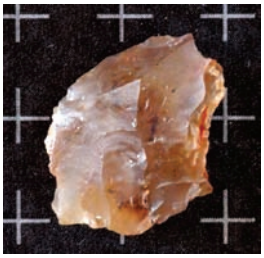

173477 (Lot 8115, LS8IK). **Single platform core**- chert core with small unidirectional parallel scars.

(no photo)

181026 (Lot 8200, LS8KW). **Core with opposed platforms on same side-** quartz bidirectional 0-180° core with cobble cortex.

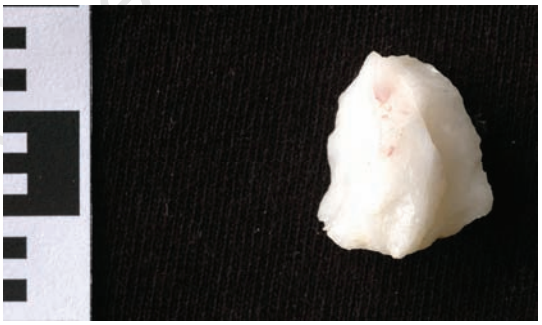

203945 (Lot 8273, LS9X). **Change of orientation core-** small angular quartz core with multi-directional flake scars.

205804 (Lot 8273, LS9X). **Change of orientation core-** irregular exhausted silcrete core with crushing on two adjacent sides bringing the sides together in a prominence. Radially flaked with rind cortex.

(no photo)

208545 (Lot 8328, LS9X1). **Change of orientation core-** quartzite exhausted core with heavy bifacial battering on both lateral margins and a burination on the wider end and multidirectional flake scars.

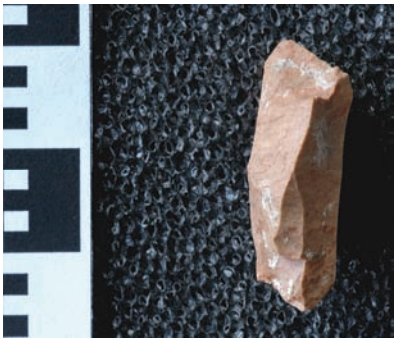

153417 (Lot 7927, LS8CB). **Core with opposed platforms on same side-** silcrete small double platform bladelet core with bidirectional 0-180° flake scars.

11. SADBS- Betina

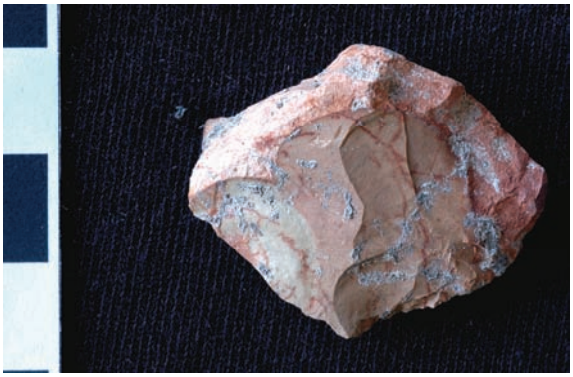

152683 (Lot 7927, LS8CB) S**ingle platform core-** small single platform silcrete core with only two removal scars from the one platform. The core may have been abandoned due to the rind cortex around half the circumference .

153422 (Lot 7927, LS8CB). **Single platform core-** preparation flakes around the margin create a quartzite point core. Core has cobble cortex and was abandoned prior to final prepared removal.

153185 (Lot 7927, LS8CB). **Change of orientation core**- silcrete core with flake scars of random orientation.

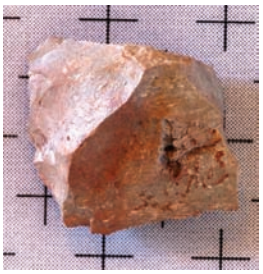

153927 (Lot 7944, LS8CM). **Double platform core-** small silcrete core with two platforms and flaking surfaces. One surface shows convergent parallel flaking of small bladelet scars. The other platform shows unidirectional parallel flaking. Core has dull pre-treatment luster on a small percentage of the surface.

12. SADBS Enrico

154909 (Lot 7974, LS8DM). **Discoid core-** small exhausted chert discoid core with chalky rind cortex.

156192 (Lot 7981, LS8DS). **Discoid core-** radially prepared chert core.

160366 (Lot 8014, LS8EV). **Core with opposed platforms on same side-** small silcrete blade core with bidirectional 0-180° flake scars and pre-heat treatment surface.

13. SADBS- Gert

120819 (Lot 3293, LS7BL). **Core with opposed platforms on same side-** small exhausted opposed platform silcrete core.

129974 (Lot 1154, LS7FA). **Discoid core-** small exhausted silcrete discoid core.

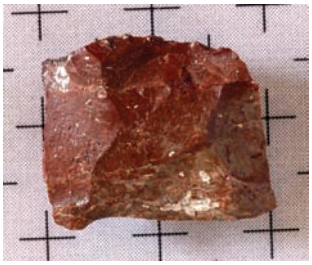

132105 (Lot 1159, LS7FE). **Core with opposed platforms on same side**- silcrete blade core with bidirectional 0-180° flake scars and cortical rind.

132445 (Lot 1153, LS7EX). **Minimal core**- tabular piece of silcrete with cortex (outcrop) on both sides and pre-heat treatment surface on one end. There are several small flake scars around the margin but the block appears to have been unsatisfactory for continued flaking.

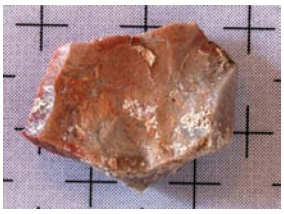

133225 (Lot 1168, LS7FL). **Change of orientation core**- silcrete exhausted core with radial flake scars.

159133 (Lot 8005, LS8EP). **Core with opposed platforms on same side**- small informal opposed platform silcrete blade core with 0-180° flake scars and cortical rind.

14. SADBS- Gert/Enrico/Pit Fill

119322 (Lot 3269, LS7AQ). **Core with opposed platforms on same side**. Double platform silcrete bladelet core.

119863 (Lot 3273, LS7AR). **Single platform core**-quartzite single platform blade core. Preserves platform of cortical flake primary form. Unidirectional-parallel flake scars and cobble cortex.

15. SADBS- Gert/Pit Fill

130450 (Lot 3461, LS7EA). **Adjacent platform core**- small adjacent platform bidirectional core made from a silcrete cobble cortical flake. Largest final removal was 29mm in length. Bidirectional 0-180° flake scars.

131652 (Lot 1149, LS7EW). **Adjacent platform core**- Silcrete core with bidirectional 180° scars. A void on the opposite face is filled with globular rind. Lithic material is similar to that found at collection location ALB-D (Appendix X).

16. SADBS- Holly

133823 (Lot 1180, LS7FW). **Change of orientation core**-small exhausted angular silcrete core with three unpatterned removals.

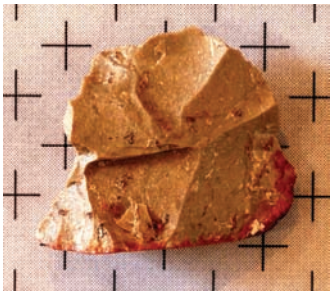

133942 (Lot 1180, LS7FW). **Double platform core**- silcrete core with bidirectional 0-90° scars. Outcrop cortex is identical to modern collected ALB D which looks like dripped and hardened wax.

17. SADBS- Joanne

106905 (Lot 3228, LS7L). **Core with opposed platforms on same side**- Crystalline quartz core with bidirectional 0-180° scars. One surface exhibits quartz crystalline plane.

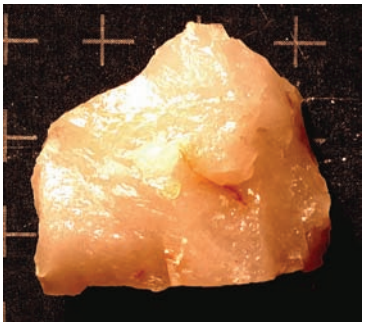

138508 (Lot 5202, LS7IY). **Discoid core.** Quartz discoid core.

140102 (Lot 5262, LS8AA). **Core on a flake-** silcrete bidirectional core on a flake or blade fragment. Core is missing one of the opposed platforms. The existing platform has crushing that looks like bipolar battering. Bidirectional 0-180° scars.

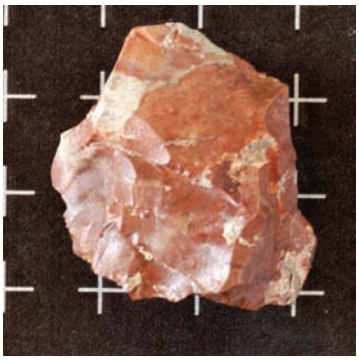

149061 (Lot 5262, LS8AA). **Change of orientation core-** multidirectional and radial flaked silcrete core with primary outcrop cortex.

150816 (Lot 5262, LS8AA). **Core on a flake-** large distal silcrete flake fragment with three small unidirectional bladelet removals on the very distal end of the flake and dull pre-heat treatment luster over most of the core surface.

228710 (Lot 8480, LS9EX). **Core with opposed platforms on opposite sides-** silcrete outille ecaille or exhausted small bladelet core with battering on both sides and bidirectional 0-180° flake scars.

239673 (Lot 8557, LS9HE). **Minimal core-** small angular silcrete nodule with one flake removal scar showing glossy heat treatment surface. Approximately 50% of the surface is covered with outcrop cortex.

243320 (Lot 8557, LS9HE). **Core with opposed platforms on same side- s**mall wedge-shaped silcrete blade core with very small bladelet removal scars of bidirectional 0-180° orientation and outcrop cortex.

18. SADBS- Sydney

138060 (Lot 1248, LS7GQ). **Core on a flake-** simple silcrete core on a tabular piece of silcrete. May represent collection of tabular natural spalls for use as bladelet cores. Core exhibits unidirectional-parallel flake scars and approximately 50% of the surface displays dull pre-heat treatment luster.

138236 (Lot 1248, LS7GQ). **Adjacent platform core-** Flaking surfaces share a common platform giving this silcrete core the appearance of a half discoid core. This material is very similar in appearance to the modern collected Rietvlei silcrete. The core exhibits differential pre- and post-heat treatment surfaces, multidirectional flake scars and cortical rind.

138647 (Lot 1248, LS7GQ). **Core with opposed platforms on same side-**silcrete double platform bladelet core with bidirectional 0-180° scars and outcrop cotex.

139512 (Lot 1248, LS7GQ). **Single platform core**-silcrete single platform unidirectional point core with convergent scars and primary outcrop cortex.

(no photo)
154121 (Lot 7928, LS8BB1). **Single platform core**- silcrete bladelet core made from what looks like a thermally-spalled angular fragment which has a potlid on the side opposite the flaking surface. Core has unidirectional-parallel scars and pre-heat treatment surface.

19. SADBS Thandesizwe

(no photo)
159113 (Lot 7983, LS8DU). **Adjacent platform core-** three fragments of a thermally damaged silcrete blade core. Bidirectional 0-180° scars and rind cortex.

174560 (Lot 8131, LS8IV). **Discoid core**- quartzite unifacial discoid core with cobble cortex on base. Cobble face exhibits some battering.

20. ALBS- Conrad

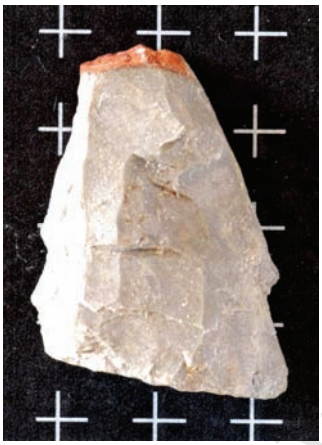

208841 (Lot 8313, LS9BG) **Single platform core**- bladelet core with unidirectional-convergent flake scars and silcrete rind cortex. The largest final removal is 26mm. Core fits pattern of cortical debitage as a common primary form which was first heated and then flaked.

21. ALBS- Conrad Cobble and Sand

(no photo)

106312 (Lot 3217, LS7G). **Cylinder core**- small silcrete conical cylindrical core with unidirectional-parallel flake scars. Surface shows differential luster from heat treatment luster and cobble cortex.

22. ALBS- Conrad Shell

(no photo)

222085 (Lot 8411, LS9DB). **Core fragment**- irregular silcrete cortical chunk fragment with multi-directional flake scars and cobble cortex.

222695 (Lot 8451, LS9DX). **Single platform core**. Hornfels split pebble (cobble cortex) with unidirectional-parallel removals originating from most of the circumference. Some smaller stepped removals on one portion of the cortex may have formed a scraper worked edge.

23. ALBS- Jocelyn

(no photo)

138423 (Lot 1289, LS7IM). **Change of orientation core**- small intensively worked chert core with multi-directional flake scars and silcrete rind cortex.

173936 (Lot 8123, LS8IT). **Core with opposed platforms on same side-** large bidirectional (0-180°) blade core on heat treated, matrix dominated silcrete. Opposed platform are battered but exhibit no percussion marks.

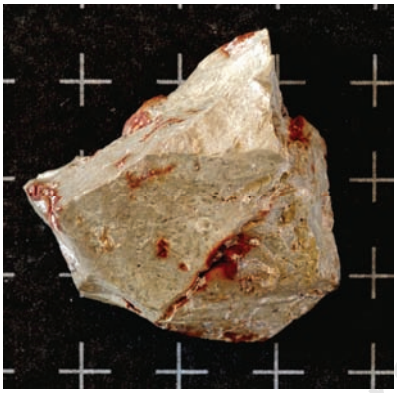

176802 (Lot 8156, LS8JQ). **Single platform core**- single platform silcrete core with unidirectional-convergent flake scars.

177115 (Lot 8156, LS8JQ). **Single platform core**- wide unidirectional single platform blade core. Platform shows extensive preparation. Removals from core would have been facetted. This quartzite core exhibits unidirectional-parallel flake scars and no cortical surface.

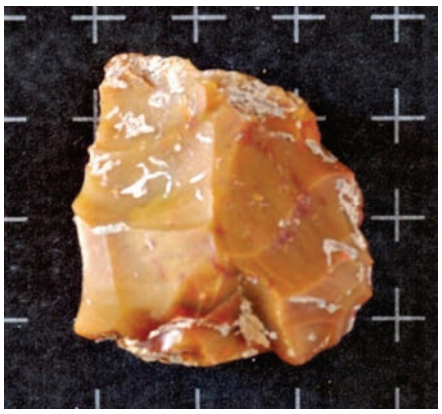

177527 (Lot 8172, LS8JZ). **Discoid core**- radial prepared chert core with chalky cortex. The largest final removal was 20mm in maximum length.

24. LBSR- Jed

178509 (Lot 8172, LS8JZ) **Core with opposed platforms on same side**-quartz core with bidirectional opposed (0-180°) flake scars from a single flake release surface.

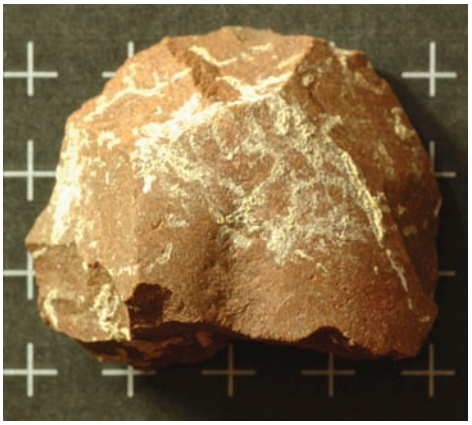

182998.95 (Lot 8212, LS8LF) **Discoid core**- hornfels cobble fragment with 6 removals originating from around its circumference.

183494 (Lot 8211, LS8LF) **Double platform core**- exhausted silcrete core probably made from a flake. The core exhibits bidirectional (0-180°) scars and pre-heat treatment non-lustrous surface. One margin has remnant platform preparation or retouch.

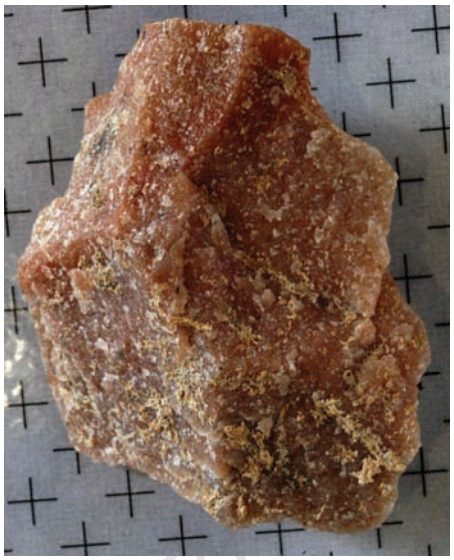

106548 (Lot 3226, LS7J). **Discoid core**- radial prepared quartzite discoid core.

107312 (Lot 3232, LS7N). **Indeterminate core fragment**- quartzite core fragment with radial flakes scars.

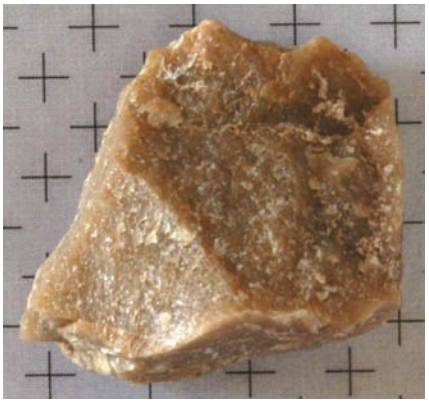

107398 (Lot 3232, LS7N). **Single platform core**. Simple quartzite convergent point core. Surface exhibits unidirectional-convergent flakes scars and cobble cortex.

156131 (Lot 7980, LS8DR). **Indeterminate core fragment-** indeterminate large quartzite core fragment with cobble cortex.

107882 (Lot 3232, LS7N). **Change of orientation core-** core on an irregular quartzite cortical cobble fragment. Flaking is a multi-directional and unpatterned.

156523 (Lot 7980, LS8DR). **Single platform core-** unidirectional convergent flaked quartzite cobble with cortex visible on base.

156535 (Lot 7980, LS8DR). **Core on a flake**- chalcedony secondary cortical flake with two small parallel removals on the ventral surface. Core is unidirectional-parallel flaked with rind cortex.

157696 (Lot 7980, LS8DR). **Minimal core**- quartzite cobble fragment with 2 opposed flake removals on the single flaking surface. The opposite surface is cortical (cobble surface).

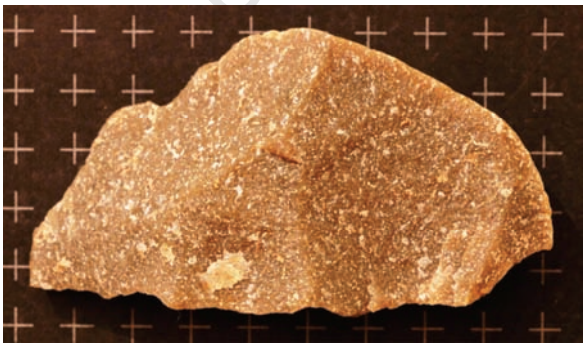

158317 (Lot 7980, LS8DR) **Single platform core**- unidirectional convergent quartzite point core with basal cobble cortex. Final point removal was prepared but not removed.

25. LBSR- Ludumo Sand and Roofspall

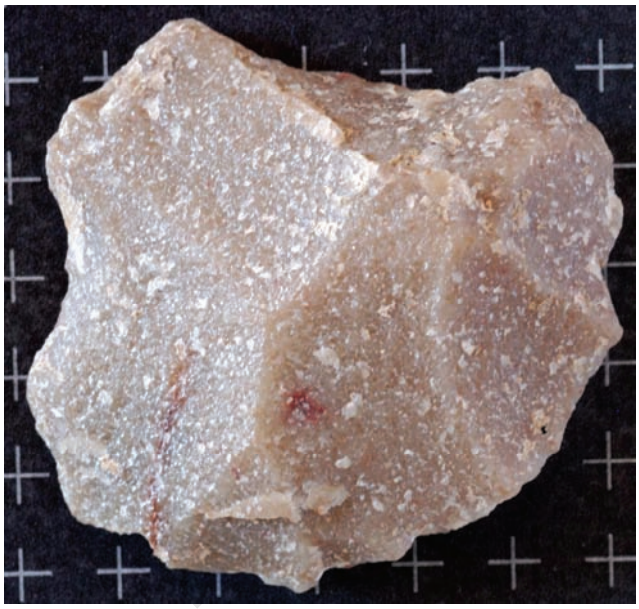

120722 (Lot 3427, LS7BT). **Discoid core**- quartzite discoid core fragment with cortical cobble base. Largest scar is 35mm in max length.

179483 (Lot 8183, LS8KH). **Discoid core**- quartzite minimally worked discoid core with cobble cortex on one margin and radial flake scars.

26. LBSR- Martin Red

(no photo)
245068 (Lot 8572, LS9HS).
Indeterminate core fragment- fine grained quartzite core fragment with indeterminate scar pattern and cobble cortex.

27. LBSR-Martin SR/Hope Red/Lwando SR

119101 (Lot 3262, LS7AK)- **Core on a flake-** large unheated silcrete flake with three core preparation flakes on the left proximal margin and a single removal from the original dorsal surface.

130688 (Lot 1147, LS7EU). **Discoid core-** quartzite irregular expedient core with radial flaking and cobble cortex.

131497 (Lot 1147, LS7EU). **Discoid core-** quartzite discoid core with cobble cortex on the base.

LBSR- Lwando Shell/Aaron Sand and Roofspall

LBSR- Aaron Shell

(no photo)

185101 (Lot 8279, LS9AC). **Discoid core-** centripetally prepared silcrete discoid core with rind cortex.

LBSR- Adrian Sand and Roofspall

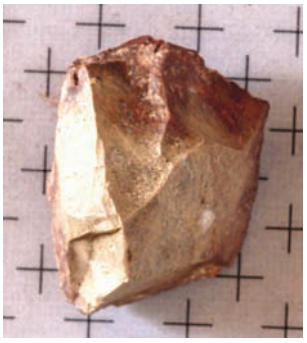

134600 (Lot 1182, LS7FY). **Change of orientation core**- Multidirectional patterned flake scars on silcrete nodule with outcrop cortex.

LBSR- Adrian Shell

164309 (Lot 7995, LS8EG). **Discoid core**- quartzite discoid core.

LBSR- Leba Sand and Roofspall

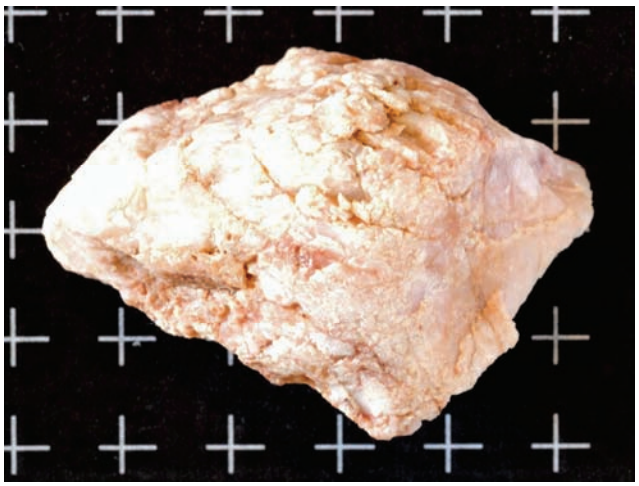

169177 (Lot 8063, LS8GS). **Minimal core**- small split quartz cobble with two random removals in addition to the split surface. This could be a split hammerstone but there is no obvious battering.

LBSR- Leba Shell

175691 (Lot 8108, LS8ID). **Minimal core**- quartzite core fragment on a tabular nodule. There are four non-patterned removals including two core edge blades on opposite margins of the core.

LBSR- Bijou Sand and Roofspall

(no photo)

152991 (Lot 7942, LS8CK). **Core on a flake**- large quartzite cortical flake (outcrop cortex) with several large radial removals and what might be retouch on the distal dorsal surface

Appendix 4: Section 2- Points

Find No.	Lot No.	Agg	Sub Agg	Sample	RM	Completeness	Scar pattern	Comment	max w	max thick	tcsa	Wt	Max Dim	L	Max Width	MP Width	MP Thk	Plat width	Plat thk	Plat angle
175674	**8108**	LBSR	Leba Shell	Leba Quartzite	quartzite	Complete	Convergent-indeterminate	large thick point, two notches on the left lateral side and a single notch on the proximal right corner	**37**	**15**	**277.5**	30.1	69	64	37	31	11	33	11	70
175958	**8108**	LBSR	Leba Shell	Leba Quartzite	quartzite	Complete	Convergent-indeterminate	long point with a single prominent notch on the distal right lateral margin				54.4	100	89	44	33	11	48	18	60
175960	**8108**	LBSR	Leba Shell	Leba Quartzite	quartzite	Complete	Unidirectional-convergent		**31**	**15**	**232.5**	11.2	39	33	31	24	8	32	13	57
206381	**8299**	LBSR	Leba Shell	LBSR	quartzite	Complete	Unidirectional-convergent	point with damaged lateral margins	**30**	**7**	**105**	9.2	51	46	30	27	6	25	8	60
243881	**8568**	LBSR	Cobus Shell		quartzite	Complete	Unidirectional-convergent	convergent point	**30**	**12**	**180**	13.6	58	53	30	24	7	30	9	72
201148	**8301**	LBSR	Aaron Shell		quartzite	Complete	Convergent-indeterminate	irregular damage on both laterals	**28**	**9**	**126**	11.1	48	47	28	26	7	28	8	75
119985	**3289**	LBSR	Ludumo Red	Ludumo Quartzite	quartzite	Complete	Convergent-indeterminate	symmetrical small point	**27**	**10**	**135**	12.7	52	49	27	27	7	24	10	61
107281	**3232**	LBSR	Jed	Jed/JR Quartzite	quartzite	Complete	Convergent-indeterminate		**23**	**7**	**80.5**	6	39	37	23	20	5	21	6	66
107439	**3232**	LBSR	Jed	Jed/JR Quartzite	quartzite	Complete	Bidirectional-180		**32**	**12**	**192**	17.2	55	48	32	30	9	28	10	70
149834	**5291**	LBSR	Jed	Jed/JR Quartzite	quartzite	Complete	Unidirectional-parallel	small single ridge convergent point	**23**	**9**	**103.5**	5.8	41	39	23	19	6	22	8	70
152456	**7903**	LBSR	Jed	Jed/JR Quartzite	quartzite	Complete	Convergent-indeterminate		**23**	**8**	**92**	5.1	37	34	23	16	6	23	8	65
152967	**7929**	LBSR	Jed	Jed/JR Quartzite	quartzite	Almost Complete	Convergent-indeterminate	missing distal tip, single ridge point	**37**	**14**	**259**	13	43	43	38	26	7	37	12	
154561	**7962**	LBSR	Jed	Jed/JR Quartzite	quartzite	Complete	Convergent-indeterminate	small symmetrical point	**32**	**13**	**208**	11.6	42	42	32	24	8	32	13	70
154574	**7962**	LBSR	Jed	Jed/JR Quartzite	quartzite	Almost Complete	Convergent-indeterminate	missing left lateral corner of the platform				34.9	84	84	40	37	10	24	16	85
158303	**7980**	LBSR	Jed	Jed/JR Quartzite	quartzite	Complete	Convergent-indeterminate	symmetric complete point.				22.8	61	57	33	31	11	31	10	78
158788	**7980**	LBSR	Jed	Jed/JR Quartzite	quartzite	Complete	Bidirectional-180	slightly snapped tip	**26**	**12**	**156**	11.8	45	42	26	25	8	22	9	70
154608	**7968**	LBSR	Jed Red	Jed/JR Quartzite	quartzite	Almost Complete	Convergent-indeterminate	21mm average diameter potlid scar on the proximal left center of the dorsal surface	**36**	**11**	**198**	12.1	46	44	36	31	7	33	11	68
154629	**7968**	LBSR	Jed Red	Jed/JR Quartzite	quartzite	Complete	Unidirectional-convergent	symmetric point	**33**	**8**	**132**	9.5	47	46	33	25	6	33	4	69
176743	**8157**	ALBS	Jocelyn	Jocelyn	quartzite	Complete	Unidirectional-parallel		**33**	**10**	**165**	12.6	49	48	34	29	8	29	10	78
156852	**7983**	SADBS	Thandesizwe	SADBS	silcrete	Complete	Unidirectional-convergent		**29**	**7**	**101.5**	6.8	33	32	30	22	5	30	4	75
133345	**1168**	SADBS	Gert	SADBS	quartzite	Complete	Unidirectional-convergent	convergent point missing last few distal mm's. one of several small quartzite convergent points from the SADBS	**20**	**7**	**70**	5.8	43	40	20	16	5	20	7	71

Find No.	Lot No.	Agg	Sub Agg	Sample	RM	Completeness	Scar pattern	Comment	max w	max thick	tcsa	Wt	Max Dim	L	Max Width	MP Width	MP Thk	Plat width	Plat thk	Plat angle
120206	**3285**	SADBS	Gert/Enrico/Pit Fill	SADBS	quartzite	Complete	Convergent-indeterminate	small symmetric point	**29**	**9**	**130.5**	9.7	48	47	26	23	6	26	9	76
107761	**3257**	SADBS	Enrico	SADBS	quartzite	Proximal	Convergent-indeterminate	proximal point				4.1	31	28	31		4	30	4	
107820	**3259**	SADBS	Enrico	SADBS	quartzite	Almost Complete	Unidirectional-convergent	point missing distal 10mm	**27**	**8**	**108**	11.5	50	49	27	24	8	17	5	82
157558	**7987**	SADBS	Enrico	SADBS	silcrete	Almost Complete	Unidirectional-convergent				**0**	7.5	47	46	24	24	7	15	5	84
240182	**8557**	SADBS	Joanne	SADBS	silcrete	Complete	Unidirectional-parallel	silcrete convergent flake	**27**	**9**	**121.5**	7.8	40	40	28	24	7	24	8	80
181161	**8206**	DBCS	Sorel	Sorel	quartzite	Complete	Convergent-indeterminate	point	**28**	**10**	**140**	11.7	53	50	30	24	7	30	10	61
107951	**3245**	DBCS	Miller	Miller	quartzite	Proximal	bidirectional convergent	point missing distal 10mm	**27**	**9**	**121.5**	10.8	46	45	27	27	6	23	7	85
102941	**3332**	NWR		NWR	silcrete	Almost Complete	Bidirectional-180	large silcrete point with burin scar down all the way down one lateral margin.				15.4	55	54		20	8	21	9	65
104001	**3342**	NWR		NWR	silcrete	Complete	Unidirectional-convergent	point	**22**	**5**	**55**	4.9	41	41	23	20	4	16	5	82
102970	**3333**	NWR	Dark Brown Silty Sand	NWR	quartzite	Complete	Unidirectional-convergent		**25**	**7**	**87.5**	4	31	31	25	17	6	21	6	70
102998	**3333**	NWR	Dark Brown Silty Sand	NWR	silcrete	Almost Complete	Unidirectional-convergent	convergent silcrete flake missing tip	**25**	**9**	**112.5**	6.7	37	35	25	19	5	24	8	68
103480	**3337**	NWR	Dark Brown Silty Sand	NWR	quartzite	Complete	Bidirectional-180	there is a very small patch of cortex on the proximal left corner of perhaps 0.5% of the surface	**37**	**12**	**222**	24.1	62	60	37	34	10	30	10	74
104662	**3363**	NWR	Dark Brown Silty Sand	NWR	quartzite	Complete	Convergent-indeterminate		**18**	**7**	**63**	6.7	46	44	19	18	6	13	6	80
153674	**7941**	MBSR	Takis	Takis	quartzite	Complete	Unidirectional-convergent		**37**	**14**	**259**	21.9	51	44	37	35	10	37	13	76

1. LBSR

175674 (Lot 8108) LBSR-Leba Shell-quartzite

175960 (Lot 8108) LBSR-Leba Shell-quartzite

206381 (Lot 8289) LBSR- Leba Shell-quartzite

175958 (Lot 8108) LBSR-Leba Shell-quartzite

243881 (Lot 8568) LBSR-Cobus Shell-quartzite

201148 (Lot 8301) LBSR-Aaron Shell-quartzite

152456 (Lot 7903) LBSR- Jed-quartzite

119985 (Lot 3289) LBSR- Ludumo Red-quartzite

152967 (Lot 7929) LBSR- Jed-quartzite

149834 (Lot 5291) LBSR- Jed-quartzite

154561 (Lot 7962) LBSR- Jed-quartzite

154574 (Lot 7962) LBSR- Jed-quartzite

158788 (Lot 7980) LBSR-Jed-quartzite

154608 (Lot 7968) LBSR- Jed Red-quartzite

158303 (Lot 7980) LBSR-Jed-quartzite

154629 (Lot 7968) LBSR- Jed Red-quartzite

176743 (Lot 8157) ALBS- Jocelyn-quartzite

120206 (Lot 3285) SADBS- Gert/Enrico/Pit Fill-quartzite

3. SADBS

156852 (Lot 7983) SADBS- Thandesizwe-silcrete

107761 (Lot 3257) SADBS- Enrico-quartzite

133345 (Lot 1168) SADBS- Gert-quartzite

107820 (Lot 3259) SADBS- Enrico-quartzite

240182 (Lot 8557) SADBS- Joanne-silcrete

107951 (Lot 3245) DBCS- Miller- quartzite

4. DBCS

181161 (Lot 8206) DBCS-Sorel- quartzite

5. NWR

102941 (Lot 3332) NWR- (no assigned SubAgg)-silcrete

104001 (Lot 3342) NWR- Point with facetted platform-silcrete

102970 (Lot 3333) NWR- Dark Brown Silty Sand-quartzite

104662 (Lot 3363) NWR- Dark Brown Silty Sand-quartzite

102998 (Lot 3333) NWR- Dark Brown Silty Sand-silcrete

153674 (Lot 7941) MBSR-Takis-quartzite

103480 (Lot 3337) NWR- Dark Brown Silty Sand-quartzite

Appendix 4: Section 3- Backed Blades

Find No.	Lot No.	Agg	SubAgg	Raw Material	Condition	Description	Comment	L	W	Thk	Wt	Scar Count	Scar pattern	Retouch Location	MG
156417	7983	SADBS	Thandesizwe	silcrete	Mid	crescent medial fragment	Crescent medial fragment	12	10	1	0.3	2	Unidirectional-parallel	lateral right dorsal	
156670	7983	SADBS	Thandesizwe	silcrete	Distal	crescent end fragment	Crescent end fragment	15	12	3	0.5	3	Indeterminate		
160170	7983	SADBS	Thandesizwe	silcrete	Proximal		2/3 of backed blade crescent made from the proximal end of a small thin bladelet. The bladelet was backed to remove the platform and most of the bulb. The distal end snapped along a flaw in the material.	23	8	3	0.5	5	Parallel-indeterminate	lateral left dorsal	
174910	8131	SADBS	Thandesizwe	silcrete	Complete	complete crescent	Backed blade with more intensive steep backing on proximal end of the blade where the bulb is still recognizable. The remainder of the left lateral margin was blunted by abrasion. The distal end is snapped, possibly by impact.	35	11	6	1.2	3	Unidirectional-parallel	lateral left dorsal	3.2
176324	8131	SADBS	Thandesizwe	quartzite	Almost Complete	end fragment	2/3 of a quartzite backed blade, backed from ventral and dorsal surface.	22	9	3	0.8	0	No scars	distal bifacial	
153912	7928	SADBS	Sydney	silcrete	Incomplete/Unknown	trapeze end fragment	Obliquely backed bladelet. Non-backed end shows a notch adjacent to the transverse break	19	9	3	0.6	3	Parallel-indeterminate	distal dorsal	2.5
155127	7928	SADBS	Sydney	silcrete	Complete	crescent	Crescent backed blade, retouch occurs over most of left lateral margin. Complete or proximal bladelet selected for tool making. There is parallel edge damage on the cutting edge opposite the backing that occurs only on the ventral side	30	10	2	0.7	2	Parallel-indeterminate	lateral left dorsal	
120974	3428	SADBS	Pit Fill	silcrete	Complete	complete crescent	Thick backed blade	41	14	4	3.1	4	Unidirectional-convergent	lateral left dorsal	
130317	3456	SADBS	Pit Fill	chert	Complete	complete crescent	Complete crescent	19	11	3	0.6	3	Unidirectional-indeterminate	lateral right dorsal	
	3428	SADBS	Pit Fill	silcrete	end fragment	triangle half fragment	Backed blade triangle. Missing one end. Piece is small but thick	17	11	4	0.6	2	Parallel-indeterminate	lateral left dorsal	
106912	3228	SADBS	Joanne	silcrete	Complete	complete crescent	Small complete crescent	18	8	2	0.3	3	Unidirectional-convergent	lateral right dorsal	3
219352	8402	SADBS	Joanne	quartz	Incomplete/Unknown	crescent half fragment	2/3 of a quartz backed blade-crescent	16	11	2	0.5	2	Unidirectional-parallel	lateral right dorsal	
243944	8571	SADBS	Joanne	silcrete	end fragment	crescent half fragment	Backed blade on silcrete bladelet with burination down the cutting edge initiated from the tip. There is also unifacial damage visible under magnification only on the ventral surface. There are small potlid spalls on both surfaces	21	8	3	0.6	2	Parallel-indeterminate	indeterminate	
248292	8571	SADBS	Joanne	silcrete	Complete	complete crescent	Irregular backed blade made from a thick blade segment	23	13	6	2	3	Bidirectional-180	lateral left dorsal	
259888	3238	SADBS	Joanne	silcrete	Complete	complete crescent	Small carefully made backed crescent on a residual cortical blade	22	5	2	0.2	2	Bidirectional-180	lateral left dorsal	
262162	5262	SADBS	Joanne	silcrete	end fragment	crescent end fragment	End fragment of small backed bladelet	10	7	2	0.1	2	unidirectional	lateral left dorsal	

Find No.	Lot No.	Agg	SubAgg	Raw Material	Condition	Description	Comment	L	W	Thk	Wt	Scar Count	Scar pattern	Retouch Location	MG
-	7901	SADBS	Joanne	silcrete	Almost Complete	complete crescent	small crescent. Distal end has slight snap.	27	8	3	0.7	2	Unidirectional-parallel	lateral left dorsal	
-	3228	SADBS	Joanne	silcrete	Complete	complete crescent	very small crescent. Retains portion of platform. Backing is on left lateral but there are two small notches on the right lateral. Distal left backing is parallel and from the ventral side. Proximal left is denticulated and from the dorsal side	19	6	2	0.3	2	Parallel-indeterminate	lateral left dorsal	
-	5248	SADBS	Joanne	silcrete	Complete	complete crescent	small narrow backed blade with backing retouch along the entire left margin	22	8	2	0.4	2	Indeterminate	lateral left dorsal	
131697	1149	SADBS	Gert/Pit Fill	silcrete	Distal	incomplete crescent	Crescent fragment with proximal blade end missing (c. 25% missing). Backing occurs on proximal and distal end of left lateral margins	21	10	1	0.4	3	Unidirectional-convergent	lateral left dorsal	
155421	7969	SADBS	Enrico	silcrete	Distal	crescent fragment	Trapeze 1/2 fragment	33	16	3	2.1	3	Parallel-indeterminate	lateral right dorsal	
107536	3249	SADBS	Betina/Unnamed	silcrete	Distal	complete crescent	Distal bladelet truncated and backed on one side. The opposite end is slightly burinated. The unbacked margins show slight damage visible under magnification.	29	8	3	0.6	3	Unidirectional-convergent	proximal dorsal	
-	3247	SADBS	Betina/Pit Fill	silcrete	Complete	complete crescent	small narrow blacked blade crescent. Symmetrical with backing on 2/3 of the left lateral margin, 1/3 on each end. Bulb is still visible. Most of the backing is from the ventral surface but there are a few small scars from the dorsal on the proximal end. There is no evidence for impact damage.	27	7	3	0.4	3	Bidirectional-Convergent	lateral left dorsal	
151511	7912	SADBS	Betina	silcrete	Complete	complete crescent	Narrow crescent with backing along the entire left lateral margin	29	7	4	0.8	3	Parallel-indeterminate	lateral left dorsal	
272915	8884	SADBS	Betina	silcrete	Complete	complete crescent	Small narrow crescent with backing on only the distal right end	32	8	3	0.8	2	Parallel-indeterminate	lateral left dorsal	
272915	8884	SADBS	Betina	silcrete	Complete	complete crescent	long narrow crescent . There is backing on the proximal left margin and then very small irregular bifacial edge damage on the cutting edge. The proximal has backing initiated from the cutting edge to form a peak or point.	32	8	3	0.8	1	Parallel-indeterminate	lateral left dorsal	
177975	8151	OBS	Celeste	silcrete	Complete	complete crescent	Narrow well-formed backed crescent. Careful parallel steep retouch from the ventral to dorsal surface. The cutting edge is ragged with marginal bifacial edge modification.	27	8	2	0.6		Unidirectional-parallel	lateral left dorsal	3.2
179167	8185	OBS	Celeste	silcrete	Almost Complete	crescent fragment	Crescent fragment	24	6	2	0.4	3	Unidirectional-parallel	lateral left dorsal	
206481	8309	OBS	Celeste	silcrete	end fragment	crescent half fragment	Distal bladelet with backing on left dorsal distal end. Ragged minute bifacial edge damage on right lateral margin opposite the backing	17	7	2	0.3	3	Unidirectional-parallel	lateral left dorsal	
164166	8033	SGS	Zuri	silcrete	Complete	complete crescent	Complete crescent	23	13	4	1	1	Indeterminate	lateral left dorsal	

Find No.	Lot No.	Agg	SubAgg	Raw Material	Condition	Description	Comment	L	W	Thk	Wt	Scar Count	Scar pattern	Retouch Location	MG
139022	1283	SGS	Tamu	chert	Mid	complete crescent	Crescent with backing over 70% of left lateral margin. There is only the slightest hint of bulb on the proximal end. Retouch starts out on the proximal end from the dorsal side and then switches to the ventral c. 10mm down the margin.	27	10	2	0.7	3	Bidirectional-180		
167693	8048	SGS	Jinga	silcrete	Complete	minimally backed	Minimally backed complete segment	28	13	2	1.2	5	Bidirectional-180	distal dorsal	
167695	8048	SGS	Jinga	quartz	Proximal	complete crescent	Complete crescent	21	13	3	1.1	2	Bidirectional-180	distal dorsal	
168271	8054	SGS	Jinga	silcrete	Incomplete/Unknown	crescent end fragment	Snapped backed blade appears to be a half crescent. There is a multiple flake notch on the cutting edge at the snap	20	17	3	1.1	4	Parallel-indeterminate	distal dorsal	
168598	8054	SGS	Jinga	chert	Complete	complete crescent	Crescent with minimal backing to create shape	20	13	2	0.8	3	Parallel-indeterminate	distal dorsal	
133878	1173	DBCS	Sorel/Coco	chert	Complete		Small crescent with slight abrasion on the cutting edge	24	14	3	1	4	Bidirectional-90	lateral left dorsal	
181256	8206	DBCS	Sorel	chert	Distal	end fragment	Distal fragment of a backed blade	9	10	3	0.3	2	Parallel-indeterminate	lateral left dorsal	
183327	8206	DBCS	Sorel	silcrete	Distal	crescent end fragment	Backed blade made from a distal blade fragment. There is also notching on the left lateral cutting edge side which could have facilitated hafting	15	11	2	0.4	3	Parallel-indeterminate	distal dorsal	
183972	8206	DBCS	Sorel	silcrete	Complete	complete crescent	Complete crescent	18	11	3	0.9	4	Bidirectional-180	lateral left dorsal	
121094	3296	DBCS	Miller	silcrete	Complete		Backed blade with a single notch on the cutting edge	43	19	4	4.1	4	Unidirectional-parallel	lateral right dorsal	3.2
121649	3296	DBCS	Miller	chert	Distal		Irregular shaped backed blade	16	8	3	0.5	3	Unidirectional-convergent	lateral left dorsal	
122719	3296	DBCS	Miller	silcrete	Incomplete/Unknown		Crescent, one side is crushed and snapped off creating cracks that extend into the remaining half. Good candidate for impact	31	18	4	2.3	3	Parallel-indeterminate	lateral left dorsal	3.6
266287	8783	DBCS	-	silcrete	Complete	complete crescent	Complete crescent. Bulb is visible	32	14	3	1.5	3	Unidirectional-parallel	lateral left dorsal	
266674	8783	DBCS	-	silcrete	Complete	complete crescent	Complete crescent with irregular protruding point on cutting edge.	34	17	4	2.9	4	Bidirectional-180	lateral left dorsal	
266888	8800	DBCS	-	silcrete	Complete	complete trapeze	Complete large crescent or trapeze with backing on both ends. Proximal end has backing that removed the platform but the bulb is still visible. Irregular bifacial edge damage on proximal cutting edge.	51	19	6	6.5	2	Unidirectional-parallel	lateral left dorsal	
266946	8800	DBCS	-	silcrete	Complete	complete crescent	Complete crescent with excurvate cutting edge. Potlid spall on dorsal surface.	32	16	4	1.8	4	bidirectional convergent	lateral left dorsal	
280295	8798	DBCS	-	chert	Complete	complete crescent	crescent with retouch along entire left lateral margin. A portion of the buld is still visible	29	10	3	1.1	3	Unidirectional-parallel	lateral left dorsal	

Find No.	Lot No.	Agg	SubAgg	Raw Material	Condition	Description	Comment	L	W	Thk	Wt	Scar Count	Scar pattern	Retouch Location	MG
103225	3339	NWR	Dark Brown Silty Sand	chert	Almost Complete	crescent fragment	Chert crescent with a burination spall that removed the cutting edge. Burination initiated from the distal end of the original flake. Like most backed pieces the backing is from the ventral surface.	20	10	3	0.6	2	Parallel-indeterminate	lateral left dorsal	
105221	3381	NWR	Compact Brown and Red Sands	silcrete	Complete	irregular crescent	Silcrete backed blade. Unlike many backed blades, this one is made from a complete blade, having a platform and distal end	26	13	3	1.1	4	Bidirectional-90		
152924	7938	MBSR	Takis	silcrete	Complete		Backed piece with retouch on right lateral distal and proximal ends. There is also a little retouch on the non-backed side	29	11	3	1.2	3	Bidirectional-180	lateral right dorsal	3.3
153565	7941	MBSR	Takis	silcrete	Complete	irregular crescent	Cutting edge of irregular crescent. Cutting edge has edge damage	31	17	5	2.7	3	Bidirectional-180	lateral right dorsal	3.5
153977	7938	MBSR	Takis	silcrete	Mid	truncated backed blade	Transverse backed prismatic blade segment. There is some edge damage on the distal right lateral margin	33	19	3	2.9	>5	Unidirectional-parallel	proximal dorsal	4.8

PP5-6 Backed Pieces

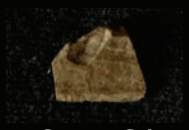

156417- SADBS
Thandesizwe

1cm

156670- SADBS
Thandesizwe

174910- SADBS
Thandesizwe

176324- SADBS
Thandesizwe

153912- SADBS
Sydney

155127- SADBS
Sydney

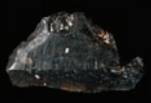

130317- SADBS Pit
Fill

131697- SADBS
Gert/Pit Fill

1cm

120974- SADBS-Pit
Fill

155421- SADBS
Enrico

107536- SADBS
Betina

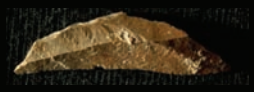

151511- SADBS
Betina

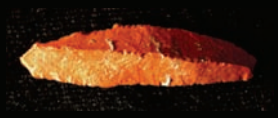

272915- SADBS
Betina

L-3247 (3mm)
Betina/Pit Fill

106912.1- SADBS
Joanne

219352- SADBS
Joanne

1cm

243944- SADBS
Joanne

L-5248 (3mm)
Joanne

L-7901 (3mm)
Joanne

L-3228 (3mm)
Joanne

248292- SADBS
Joanne

259888- SADBS
Joanne

261162- SADBS
Joanne

179167- OBS Celeste

177975- OBS Celeste

PP5-6 Backed Pieces

167693- SGS Jinga

167695- SGS Jinga

168271- SGS Jinga

168598- SGS Jinga

164166- SGS Zuri

139022- SGS-Tamu

1cm

133878- DBCS Sorel/Coco

181256- DBCS Sorel

183327- DBCS Sorel

183972- DBCS Sorel

1cm

121094- DBCS Miller

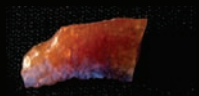

121649-DBCS Miller

122719- DBCS Miller

266888-DBCS

266287-DBCS

266674-DBCS

1cm

266946-DBCS

280295- DBCS

103225- NWR

105221- NWR

153565- MBSR Takis

153977- MBSR Takis

Appendix 4: Section 4- Notched Pieces

Find No.	Lot No.	Agg	Sub Agg	Deb Type	Raw Material	Condition	Retouch location	Comment	L	W	Thk	Wt	Retouch location	Retouch type	Retouch Angle	Retouch Length	MG
165696	**8038**	SGS	Jinga	Blade	silcrete	Mid	both laterals	Long parallel sided medial blade fragment with bending fracture on distal ventral end. There are multiple flake notches directly across from one another on opposite lateral sides creating a slightly strangulated blade	41	15	2	2	both laterals	notched	60	16	
162365	**8028**	SGS	Tamu	Flake	chert	Mid	both laterals	Multiple flake notches on opposite sides creating a strangulated fragment	26	20	5	3	both laterals	notched	61-90	24	
134566	**1194**	DBCS	Coco/Quinn	Blade	silcrete	Mid	both margins	Double notched medial blade fragment with distal outcrop cortex. Notches are carefully formed	17	19	4	1.5	both margins	notched	72	23	
130105	**1152**	DBCS	Miller/Sorel/ Coco	Indet	silcrete	Incomplete/ Unknown	entire circumference	Notched fragment with irregular steep retouch scars around the entire circumference	35	28	9	9.5	entire circumferen ce	notched	74	12	
246011	**8430**	DBCS	Miller/Sorel	Indet	silcrete	Distal	both laterals	Distal convergent tip with carefully made multiple flake notch on the left margin. There is abrasion or edge modification all along the right lateral dorsal margin	21	12	3	0.6	both laterals	notched	82	11	
119244	**3245**	DBCS	Miller	Blade	silcrete	Distal	both laterals	4 symmetric multiple flake notches, 2 on each side, directly opposite one another	37	17	4	2.4	both laterals	notched	72	42	4.1
121088	**3296**	DBCS	Miller	Blade	silcrete	Distal	lateral right dorsal	A single hinged flake and rounding on the distal end	43	21	7	7.4	lateral right dorsal	notched	85	11	
122711	**3296**	DBCS	Miller	Blade	silcrete	Mid	lateral left dorsal	V-shaped notch in a medial blade fragment	18	19	3	1.1	lateral left dorsal	notched	61-90	17	
122775	**3296**	DBCS	Miller	Blade	silcrete	Proximal	both laterals	4 notches. Blade snapped across 2 notches that created a narrow strangulation in the blade. Outcrop cortex on left lateral	38	19	6	5.7	both laterals	notched and abraded	60	75	3.6
129848	**3454**	DBCS	Miller	Flake	silcrete	Proximal	lateral right dorsal	Notched proximal wide blade fragment	32	28	3	3	lateral right dorsal	notched	48	10	4.1

PP5-6 Notched Pieces

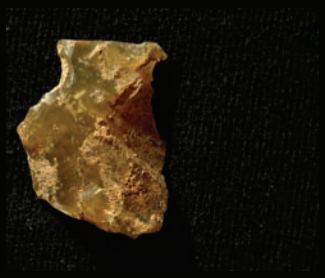

162365- SGS Tamu

1cm

122711- DBCS Miller

134566- DBCS Coco/Quinn

122718- DBCS Miller

246011- DBCS Miller/Sorel

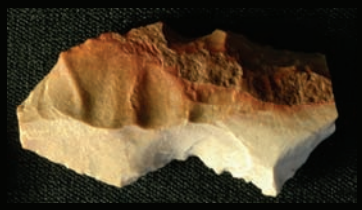

122775- DBCS Miller

119244- DBCS-Miller

129848- DBCS Miller

121088- DBCS Miller

1cm

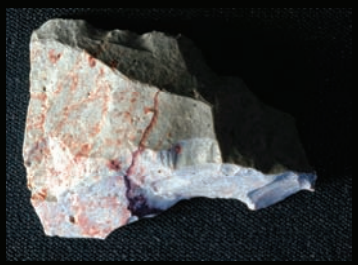

130105- DBCS Miller